# Halogen- and hydrogen bonding host structures for anion recognition

**Maria Luiza Bondilă**

St Cross College, University of Oxford




A thesis submitted for the degree of Doctor of Philosophy

Inorganic Chemistry Laboratory

University of Oxford

Trinity Term 2019

## Halogen- and hydrogen bonding host structures for anion recognition

Maria Luiza Bondilă, St Cross College, University of Oxford

Abstract of thesis submitted for the degree of D.Phil., Trinity Term 2019

This thesis describes the utilisation of acyclic and interlocked host molecules for anion recognition and sensing in organic media. Halogen bonding is primarily employed as the intermolecular interaction of choice for anion complexation, often assisted by hydrogen bonding.

**Chapter 1** introduces the field of supramolecular chemistry, with a particular emphasis on supramolecular anion recognition and non-covalent interactions, followed by an overview of mechanically interlocked molecules and their applications.

**Chapter 2** investigates the construction of amido-(iodo)triazole anion hosts. The synthesis and anion binding properties of a family of cationic and neutral [2]rotaxanes incorporating this motif are reported. In particular, a dramatic increase in iodide affinity upon introducing a halogen bond donor is reported.

**Chapter 3** explores the preparation and fine-tuning of (thio)urea-(iodo)triazole acyclic receptors, and the resulting anion binding trends are compared and contrasted. Attempts to construct analogous higher order structures are reported.

**Chapter 4** outlines the exploitation of covalently appended perfluoroaryl motifs for enhancing the anion binding properties of novel carbazole-(iodo)triazole structures. Their anion complexation equilibria are quantified through $^{1}$H NMR titration experiments and qualitatively assessed through UV-Vis and fluorescence spectroscopy.

**Chapter 5** provides a summary of the main conclusions of this thesis.

**Chapter 6** details the synthetic protocols employed in this work and includes the characterisation of novel and previously reported compounds in **Chapters 2** – **4**.

# ACKNOWLEDGMENTS

*"If I have seen further it is by standing on the shoulders of giants"* - Isaac Newton

It's been a fun ride.

When I first got my offer letter from Oxford, I was beyond ecstatic, and studying here has changed my life in ways I could not begin to imagine. For this, I would firstly like to thank Paul for accepting me into his research group. He was a calm and understanding supervisor throughout and I had a great time here.

My mentor and immediate supervisor in the lab was Dr. Asha Brown. I am grateful to her for sharing her expertise and knowledge of chemistry with me and putting up with me in my troublesome first year. Another beacon of knowledge and wisdom was Dr. Jason Lim, who may be one of the most intelligent people I have ever met. Similarly, I would like to thank Dr. Thanthapatra Bunchuay, also known as Valentine the SupraHero. He was always kind and friendly to me and encouraged me to break out of my shell.

This list would not be complete without some other lovely Beeries. Edward (TJ) Mitchell was always fun to be around in the lab, we share a love for memes and cute dogs and he was the one who inspired me to become a pescetarian and later a vegetarian. I also need to mention my fellow metalheads Arseni Borissov for his amazing skills and passion for chemistry and Robert Hein for his incredible self-confidence and critical thinking (I wish I had half your bravery!).

In this lab I have also met one of my best friends in the whole world, Xiaoxiong (George) Li. He was kind enough to proofread my thesis, along with Asha and Andrew Docker. He is funny, calm, and wise and I know that just like my fingers, I can always count on him. In these four years, he taught me the meaning of Eastern philosophy while I taught him British slang. I think it's a fair exchange. I know he will become an amazing chemist – if not, at least a chef at a Chinese restaurant!

A special thanks goes to another of my dear friends and my close confidant, Andrei Florea. He went out of his way to make me more sociable and has been a constant source of support, even when we were at odds. Thanks to him, I have become more confident and I have felt less alone. I have become a better person and I could never repay him enough.

Another dear friend of mine is Oscar Murcia, hailing from Sweden – probably one of the few people whose brand of weird matches mine. He was always there for me when I was upset, angry or I had just taken a picture of an adorable random bird and I absolutely had to show it to someone. *Ecavtoy,* mate!

I could not forget to acknowledge my therapist, Dr. Belinda Graham. She helped me overcome my social anxieties and panic attacks, which massively improved the quality of my life. She helped me break free of my mental chains and I will forever be indebted to her.

Soon after I moved here, I started doing cat sitting on the side. My sweet cat Newton crossed the rainbow bridge in 2015, a few months before I left for Oxford (I miss you, buddy) and this was a good chance to take care of other animals and save for a rainy day. My first cat sitting clients, the lovely Arshad and Wendy, welcomed me into their home with open arms and unbelievable kindness. They are some of the nicest people I have ever had the pleasure to meet.

They say to always keep the best for last. I need to thank my parents for their unconditional love and endless support, especially my powerhouse of a mother who worked hard to keep me here. They always encouraged me to be what I wanted to be, even though it meant being far away from them – and they love me with all my faults. I am lucky to be their daughter.

I also need to mention three amazing teachers I have had the luck to study with: Adriana Urdă (organic chemistry), Mihai Bălună (mathematics), and Monica Raicu (physics). Mrs. Raicu in particular is one of my role models. One of the most heartwarming moments of my life was when she told me I reminded her of herself when she was younger. And of course, the good friends I made in Romania: Paul Pătrăşcoiu (we share a birthday!), Camelia Alexandroaia, Ioana Pavel, Elena “Hei” Trofin, Diana Badea, Iacob Voichițoniu, Cristian Spînu.

My life has changed immensely since moving to Oxford and it feels like a whole new world full of possibilities has opened up for me.

I am alive and free.

Luiza Bondila

2019

*This thesis is dedicated to my friends from across the world. I am a better person thanks to your support, kindness, and understanding.*

*Thank you for caring.*

*“Don't walk behind me; I may not lead. Don't walk in front of me; I may not follow. Just walk beside me and be my friend.”*

*– Albert Camus*

# Abbreviations

| | |
|---|---|
| $\delta$ | chemical shift |
| $\Delta\delta$ | change in chemical shift |
| $\lambda$ | wavelength |
| $\lambda_{max}$ | maximum absorption wavelength |
| $\varepsilon$ | molar absorptivity coefficient |
| $\varepsilon_{max}$ | molar absorptivity coefficient at the maximum absorption wavelength |
| $\mu$ | micro |
| v | frequency |
| ° | degree |
| °C | degrees Celsius |
| 2D | two-dimensional |
| $A^-$ | anion |
| $AcO^-$ | acetate |
| ADP | adenosine diphosphate |
| AMT | active metal templation |
| aq. | aqueous |
| ATP | adenosine triphosphate |
| a.u. | arbitrary units |
| B | base |
| Boc | *tert*-butyloxy carbonyl |
| $Boc_2O$ | di-*tert*-butyl dicarbonate |
| br. | broad |
| Bu | butyl |
| cat. | catalytic |
| CDI | 1,1'-carbonyldiimidazole |
| CN | coordination number |
| CuAAC | copper(I)-catalysed azide–alkyne cycloaddition |
| d | doublet |
| dd | doublet of doublets |
| dt | doublet of triplets |
| DABCO | 1,4-diazabicyclo[2.2.2]octane |
| DBU | 1,8-diazabicyclo[5.4.0]undec-7-ene |
| DCC | *N,N*-dicyclohexylcarbodiimide |
| DIPEA | *N*,*N*-di-*iso*-propylethylamine |
| DMAP | 4-dimethylaminopyridine |
| DMF | *N*,*N*-dimethylformamide |
| DMSO | dimethyl sulfoxide |
| DNA | deoxyribonucleic acid |
| EDC | 1-ethyl-3-(3-dimethylaminopropyl)carbodiimide |
| eq., equiv. | equivalent |

| | |
|---|---|
| ESI | electrospray ionisation |
| Et | ethyl |
| $Et_2NH$ | diethylamine |
| $Et_3N$ | triethylamine |
| $Et_2O$ | diethyl ether |
| EtOAc | ethyl acetate |
| EtOH | ethanol |
| g | gram |
| h | Planck's constant |
| h. | hour |
| hν | light quanta |
| HB | hydrogen bonding |
| HRMS | high-resolution mass spectrometry |
| Hz | Hertz |
| IDA | indicator displacement assay |
| J | Joule |
| *J* | coupling constant |
| k | kilo |
| K | Kelvin |
| $K_a$ | association constant |
| $K_D$ | association constant for the D isomer |
| $K_L$ | association constant for the L isomer |
| L | litre |
| log | logarithm |
| m | mili, multiplet |
| M | molar, mega |
| mM | milimolar |
| *m/z* | mass-to-charge ratio |
| MALDI | matrix-assisted laser desorption/ionisation |
| Me | methyl |
| MeOH | methanol |
| MIM | mechanically interlocked molecule |
| min | minute |
| mol | mole |
| MOM | methoxymethyl |
| MS | mass spectrometry |
| Ms, mesyl | methanesulfonate |
| n-Bu | n-butyl |
| NB | not binding |
| NDI | naphthalene diimide |
| NMR | nuclear magnetic resonance |
| Oct | n-octyl |
| *p* | *para* |

| | |
|---|---|
| PBP | phosphate binding protein |
| pH | $-\log_{10}[H^+]$ |
| Ph | phenyl |
| $PhCOO^-$ | benzoate |
| p$K_a$ | $-\log_{10} K_a$ |
| $PPh_3$ | triphenylphosphine |
| ppm | parts per million |
| q | quartet |
| quant. | quantitative |
| quin. | quintet |
| R | chemical substituent |
| r.t. | room temperature |
| RNA | ribonucleic acid |
| ROESY | rotating-frame nuclear Overhauser effect correlation spectroscopy |
| s | singlet |
| $S_0$ | singlet ground state |
| $S_n$ | singlet $n^{th}$ excited state |
| SBP | sulfate binding protein |
| $S_N2$ | second order nucleophilic substitution |
| $S_NAr$ | aromatic nucleophilic substitution |
| t | triplet |
| *tert* | tertiary |
| $t_{1/2}$ | half life |
| TBA | tetrabutylammonium |
| TBTA | tris[(1-benzyl-1*H*-1,2,3-triazol-4-yl)methyl]amine |
| td | triplet of doublets |
| TEG | triethylene glycol monomethyl ether |
| TFA | trifluoroacetic acid |
| THF | tetrahydrofuran |
| TLC | thin layer chromatography |
| TMS | trimethylsilyl |
| Trz | triazole |
| Ts, tosyl | *para*-toluenesulfonate |
| TTF | tetrathiafulvalene |
| UV | ultra-violet |
| v/v | volume by volume |
| v/v/v | volume by volume by volume |
| vis. | visible |
| w/v | weight by volume |
| w/w | weight by weight |
| X | halogen atom |
| XB | halogen bonding |

# TABLE OF CONTENTS

**Abstract** i

**Acknowledgements** ii

**Abbreviations** vii

**Chapter 1: Introduction**

**1.1. The emergence of supramolecular chemistry as a research field** 1

**1.2. Anion recognition** 2

1.2.1. The importance of anions 2

1.2.2. The challenges of anion recognition 3

1.2.3. Biotic receptors 4

1.2.4. Non-covalent interactions for anion recognition 5

1.2.5. Abiotic receptors 11

1.2.5.1. Principles of anion receptor design 11

1.2.5.2. Examples of abiotic receptors 13

1.2.5.2.1. Cationic receptors 13

1.2.5.2.2. Neutral receptors 17

1.2.5.2.3. Halogen bonding anion receptors 24

**1.3. Anion sensing** 26

1.3.1. Optical anion sensing 27

**1.4. Mechanically interlocked molecules** 30

1.4.1. Historical developments 30

1.4.2. Strategies towards the synthesis of mechanically interlocked molecules 31

1.4.2.1. Template-directed syntheses 34

1.4.2.1.1. Cationic templates 34

1.4.2.1.2. Neutral templates 38

1.4.2.1.3. Anionic templates 39

1.4.3. Applications of interlocked structures 43

**1.5. Project aims** 49

**1.5. References** 50

**Chapter 2: Cationic and neutral amido-triazole [2]rotaxanes for anion binding** 59

**2.1. Introduction** 59

2.1.1. The 1,2,3-triazole, 1,2,3-iodotriazole and amidotriazole motifs in anion binding 59

**2.2. Chapter aims** 62

**2.3. Cationic HB/XB amido-triazolium [2]rotaxanes for anion recognition** 63

2.3.1. Design of target rotaxanes 63

2.3.2. Synthesis and anion recognition properties of cationic acyclic systems 64

2.3.2.1. Synthesis of amido-triazolium acyclic receptors 64

2.3.2.2. Preliminary anion binding studies 66

2.3.3. Synthesis and anion recognition properties of cationic interlocked systems 68

2.3.3.1. Synthesis and characterisation of amido-triazolium [2]rotaxanes 68

2.3.3.2. Anion binding studies of cationic HB rotaxane 78

**2.4. Neutral HB/XB amido-triazole [2]rotaxanes for anion recognition** 81

2.4.1. Design of target rotaxanes 81

2.4.2. Synthesis and anion recognition properties of neutral acyclic systems 83

2.4.2.1. Synthesis of amido-triazole acyclic receptors 83

2.4.2.2. Preliminary anion binding studies 85

2.4.3. Synthesis of a bis(iodotriazole) macrocycle 85

2.4.4. Synthesis and anion recognition properties of neutral rotaxane systems 87

2.4.4.1. Synthesis and characterisation of amido-triazole [2]rotaxanes 87

2.4.4.2. Anion binding studies of neutral HB/XB rotaxanes 94

2.4.5. Towards the synthesis of amido-iodotriazole [2]rotaxanes 98

2.4.5.1. Neutral XB rotaxanes 98

2.4.5.1.1. Anion binding studies of neutral XB rotaxane 102

**2.5. Conclusions and future work** 105

**2.6. References** 108

**Chapter 3: Urea and thiourea-based (iodo)triazole structures for anion binding** 111

**3.1. Introduction** 111

3.1.1. The (thio)urea-triazole motifs in anion binding 112

**3.2. Chapter aims** 113

**3.3. Acyclic HB/XB (thio)urea-triazole structures for anion recognition** 114

3.3.1. Design of target acyclic hosts 114

3.3.2. Flexible (thio)urea-triazole receptors 114

3.3.2.1. Synthesis of (thio)urea-monotriazole receptors incorporating a methylene spacer 114

3.3.2.2. Preliminary anion binding studies 117

3.3.2.3. Synthesis of (thio)urea-bistriazole receptors incorporating a methylene spacer 120

3.3.2.4. Preliminary anion binding studies 122

3.3.2.5. Towards cationic (thio)urea-triazole receptors 125

3.3.3. Rigid (thio)urea-triazole receptors 127

3.3.3.1. Synthesis of (thio)urea-triazole receptors incorporating a 1,2-phenylene spacer 127

3.3.3.2. Synthesis of urea-triazole receptors incorporating a 1,3-phenylene spacer 130

3.3.3.3. Preliminary chloride binding studies 132

3.3.3.4. Dicarboxylate binding studies 134

3.3.3.5. Towards a fluorescent dicarboxylate sensor based on the urea-triazole motif 137

**3.4. Interlocked HB/XB urea-triazole structures for anion recognition** 139

3.4.1. Neutral urea-monotriazole [2]rotaxanes incorporating a methylene spacer 139

3.4.1.1. Synthesis of a bis(triazole)-pyridyl macrocycle 140

3.4.1.2. Synthesis of an alkyne-appended stopper incorporating a urea motif 142

3.4.2. Neutral urea-bistriazole [2]rotaxanes incorporating a methylene spacer 145

3.4.2.1. Attempted synthesis of a [2]rotaxane 145

3.4.3. Cationic urea-bistriazolium [2]rotaxanes incorporating a methylene spacer 146

3.4.3.1. Synthesis of a cationic urea-bistriazolium axle 147

3.4.3.2. Attempted anion template synthesis of cationic [2]rotaxanes 149

3.4.3.3. Attempted synthesis of cationic [2]rotaxanes incorporating a neutral bistriazole-urea axle 150

3.4.4. Neutral urea-bistriazole [2]rotaxanes incorporating a 1,3-phenylene spacer 152

3.4.4.1. Attempted synthesis of a neutral [2]rotaxane 152

3.4.5. Cationic urea-bistriazolium [2]rotaxanes incorporating a 1,3-phenylene spacer 153

3.4.5.1. Attempted syntheses of cationic [2]rotaxanes 153

**3.5. Macrocyclic urea-triazole structures for anion recognition** 155

3.5.1. Attempted synthesis of a urea-triazole macrocycle 155

**3.6. Conclusions and future work** 156

**3.7. References** 158

**Chapter 4: Perfluoroaryl-based carbazole-(iodo)triazole structures for anion recognition** 161

**4.1. Introduction** 161

4.1.1. The carbazole-triazole motif in anion binding 162

**4.2. Chapter Aims** 163

**4.3. Acyclic HB/XB carbazole-triazole structures for anion recognition** 164

4.3.1. Design of target acyclic hosts 164

4.3.2. Carbazole-triazole receptors with octyl chains 165

4.3.2.1. Synthesis of HB/XB carbazole-triazole receptors with octyl chains 165

4.3.2.2. Preliminary anion binding studies 168

4.3.3. Carbazole-triazole receptors with perfluorobenzene motifs 170

4.3.3.1. Synthesis of HB/XB carbazole-triazole receptors with perfluorobenzene motifs 170

4.3.3.2. Preliminary anion binding studies 172

4.3.4. Optical properties 174

4.3.4.1. UV-Vis absorption studies 174

4.3.4.1. Fluorescence emission behaviour 178

**4.4. Towards macrocyclic HB/XB carbazole-triazole structures** 181

4.4.1. Design of initial target macrocyclic hosts 181

4.4.1.1. Synthetic attempts towards initial target macrocyclic hosts 181

4.4.2. Design of modified target macrocyclic hosts 184

4.4.1.1. Synthetic attempts towards novel target macrocyclic hosts 185

4.4.3. Attempts to increase the solubility of perfluoroaryl receptors 190

4.4.3.1. Synthetic attempts to introduce bulky groups 190

**4.5. Towards interlocked HB/XB carbazole-triazole [2]rotaxane structures** 193

**4.6. Conclusions and future work** 195

**4.7. References** 196

**Chapter 5: Conclusions** 199

**Chapter 6: Experimental** 205

# Chapter 1

Introduction

# Chapter 1: Introduction

## 1.1. The emergence of supramolecular chemistry as a research field

Throughout time, biological systems have adapted to their environment by continuously evolving highly selective and specific chemical recognition processes. [1] Specific examples include DNA replication, alkali metal transport, and enzyme catalysis. [2,3] For molecular recognition to function, reversibility is a crucial factor. The dynamic nature of biotic interactions is a direct consequence of the employment of arrays of convergent weak intermolecular forces. [4]

Whilst studying biological catalysis at the turn of the 20th century, Emil Fischer coined the *lock and key* metaphor to describe the mechanism of enzyme – substrate interactions. This principle states that a guest substrate must have geometric complementarity to the active site of the enzyme, in both size and shape. [5] It is now however more accurately described as an *induced fit*, wherein a host adapts its structure in order to accommodate the guest, thus leading to cooperativity. [6]

These early studies laid the basis for a more in-depth study of molecular recognition, which led to the development of supramolecular chemistry. This fast-growing field deals with complex entities that result from the assembly of two or more chemical species through non-covalent interactions, being often termed "chemistry beyond the molecule." [7] Supramolecular chemistry encompasses mainly two domains: 1) host-guest chemistry, which refers to the selective binding of a smaller chemical entity to a larger one [8] (**Figure 1.1.a**), and 2) self-assembly, which involves the spontaneous aggregation of two or more small molecules or ions to form complex higher-ordered structures [9] (**Figure 1.1.b**).

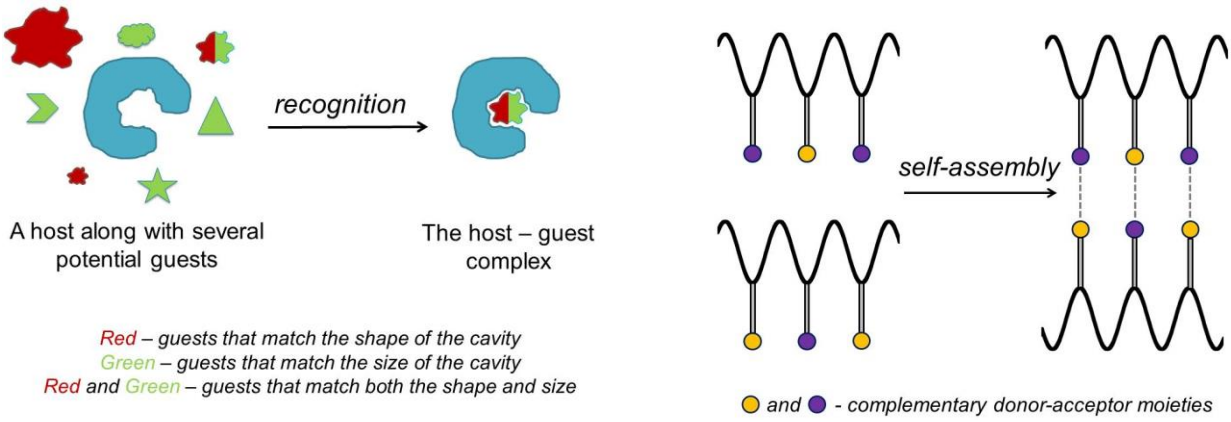



***Figure 1.1.*** *Cartoon illustrating the principles of a) host-guest interactions and b) self-assembly.*

In the late 1960s, Charles Pedersen serendipitously synthesized the cyclic polyether dibenzo[18]crown-6 and discovered that its solubility in methanol was greatly enhanced by the addition of $Na^+$ salts. [10] Further studies on similar crown ether species of different ring size revealed the existence of a direct link between the stability of an alkali metal cation – crown ether complex and the size ratio of the diameters of the individual components; this was termed an *optimal spatial fit*. [11] Subsequently, Jean-Marie Lehn and Donald Cram developed ingenuous three-dimensional hosts for group 1 and 2 metal cations such as cryptands and spherands, respectively. Together with Pedersen, their groundbreaking contributions opened the door to research into artificial receptors and resulted in the Nobel Prize for Chemistry being jointly bestowed upon the three aforementioned scientists in 1987. [7,12,13]

Since these seminal discoveries, supramolecular chemistry has flourished exponentially and has led to the synthesis of a wide breadth of host systems and self-assembled molecular architectures. Remarkable examples include exotic chemical topologies (e.g. trefoil knots or Borromean links), programmable molecular machines and even a four-wheeled molecular system that moves along a surface in response to light input [14–17]. The relevance of this body of research was acknowledged through the award of another Nobel Prize in 2016 to Fraser Stoddart, [18] Jean-Pierre Sauvage, [19] and Ben Feringa, [20] "for the design and synthesis of molecular machines."

This introductory chapter will focus on reviewing the underlying aspects and challenges of supramolecular anion host-guest chemistry, the theme of this thesis. Examples of natural anion receptors will be presented, followed by an outline of abiotic receptor design principles that were inspired by them, while concluding with an overview of anion sensing. Particular emphasis will be placed on halogen bonding and related non-covalent interactions employed in the supramolecular toolkit as well as on mechanically interlocked receptors for anion binding.

## 1.2. Anion recognition

### 1.2.1. The importance of anions

Charged chemical species are omnipresent in the biosphere and play a plethora of roles in nature. DNA and RNA are two essential macropolyanions for all forms of life and their roles include, but are not limited to, storing and conveying genetic information. [21] Another polyanion with relevance in biochemistry is ATP, a coenzyme which governs energy transfer in living cells. [3] Carboxylates such as malonate, fumarate, and succinate are important intermediates in the citric acid cycle, [22] while chloride plays an essential part in

regulating the pH balance of body fluids and transmitting nerve impulses, and its channel misregulation leads to the medical condition cystic fibrosis. [23] Fluoride is commonly added to public water supplies for dental health; however, abnormally high levels can cause skeletal fluorosis. [24] Anthropogenic activities including the widespread use of fertilisers have been linked to phosphate and nitrate contamination in soil water run-off, which has resulted in eutrophication in aquatic ecosystems. [25,26] Environmental concerns include the recovery of radioactive $^{99}TcO_4^-$ originating from low level nuclear waste, [27] cyanide employed in precious metals mining, [28] and azide playing the role of propellant in airbags. [29]

It is thus apparent that the synthesis of artificial receptors capable of the selective binding, sensing and sequestering of anions is a highly relevant topic of interest in modern supramolecular chemistry.

### 1.2.2. The challenges of anion recognition

Despite the obvious importance of anion recognition, the chemistry of anions is multi-faceted and their coordination is non-trivial due to their intrinsic characteristics, as outlined below.

Anions are typically larger than their isoelectronic cationic counterparts, [30] resulting in a small charge-to-radius ratio and relatively weaker electrostatic interactions with an anion host. [31] Secondly, anions display a wide breadth of geometries, as exemplified in **Figure 1.2**, which can be exploited in the design of an anion receptor of geometric shape complementarity to the targeted guest.

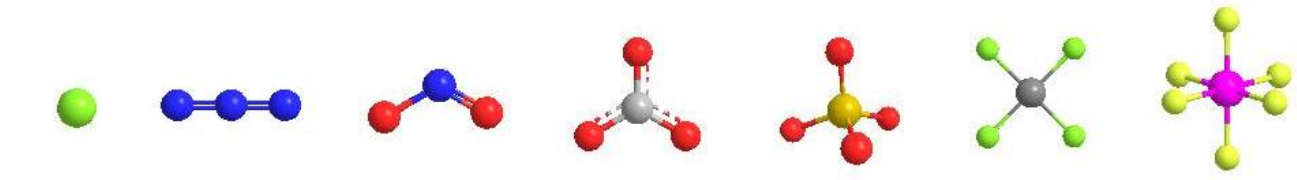



***Figure 1.2.*** *Representative examples highlighting the varying geometries adopted by anions.*

Additionally, most anions are pH-dependent and only exist within the confines of a certain pH window. The same is true of some receptors which only function upon protonation such as polyammonium host systems. [32] Hence, anion recognition only occurs in the pH region where the anion is deprotonated and the host is protonated.

Last but not least, negatively charged species display high free energies of solvation. [4] This aspect is relevant to their chemistry since, in order for the binding event to occur, the anion must be stripped of its solvation shell, which carries an enthalpic penalty. The extent of solvation is heavily solvent-dependent, i.e. anions are more heavily solvated in protic media, due to the formation of hydrogen bonding networks. [33] The relative degree of solvation in water for common anions is indicated by the Hofmeister series [34,35] (**Figure 1.3.**).

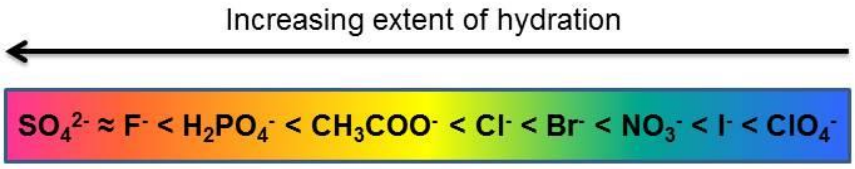



***Figure 1.3.*** *The Hofmeister series.*

Anions are weakly solvated in aprotic solvents; however, in this type of media, ion-pairing with the countercation is significant and becomes an additional factor which must be overcome for the anion complexation to occur. [36]

### 1.2.3. Biotic receptors

Nature has an unparalleled ability to selectively bind and transport anions, which has ultimately served as inspiration for chemists striving to mimic the same affinity and selectivity in synthetic receptors. Relevant examples are two bacterial proteins termed after the anions they transport, namely, sulfate binding protein (SBP) [37] and phosphate binding protein (PBP). [38]

Some features of their binding cavities can be discerned from **Figure 1.4.** Both SBP and PBP employ an array of convergent hydrogen bond donors inside a well-defined three-dimensional cavity. The former binds sulfate with the assistance of seven N – H donors, whereas the latter accommodates hydrogen phosphate by means of eight N – H donors, four O – H donors, and electrostatic interactions with a guanidinium motif. These features make both proteins highly selective for their respective oxoanion guests.

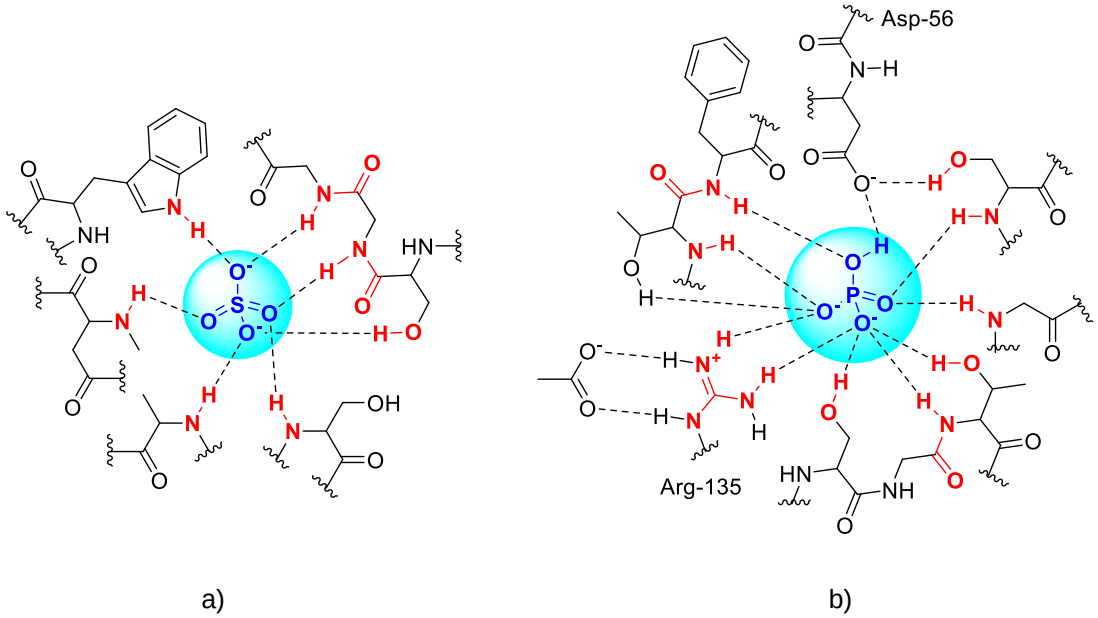



***Figure 1.4.*** *Two-dimensional projections of the anion binding pockets of two selected proteins selective for a) sulfate* [37] *and b) hydrogen phosphate.* [38]

### 1.2.4. Non-covalent interactions for anion recognition

As highlighted in the previous section, the utilisation of non-covalent interactions is quintessential for anion complexation. Their considerably weaker nature compared to that of covalent bonds imparts a degree of reversibility upon the host – guest association. [39] The synergistic effect of multiple weak intermolecular bonds can facilitate the affinity and selectivity of the anion recognition process. Several such interactions are discussed below, with particular emphasis on those relevant to this thesis.

**Electrostatic interactions:** These refer to Coulombic forces and they encompass ion-ion, ion-dipole, and dipole-dipole interactions, [40] as exemplified in **Figure 1.5.**

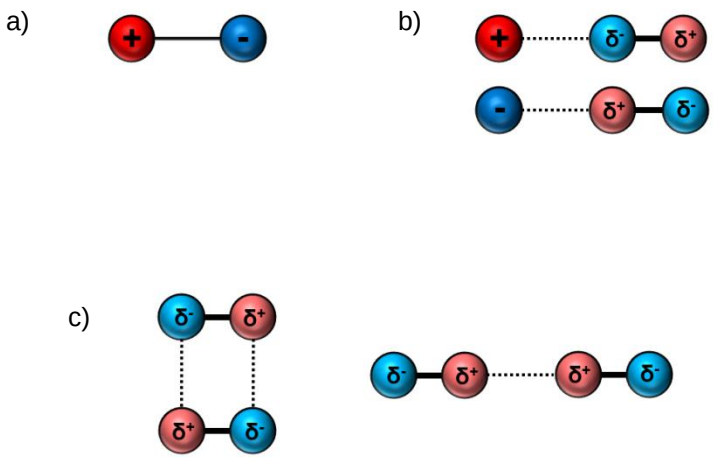



***Figure 1.5.*** *Cartoon representation of the main subtypes of electrostatic interactions: a) ion-ion; b) ion-dipole; c) dipole-dipole.*

Ion-ion interactions are highly isotropic and strong (200 – 300 kJ/mol), [31] while the latter two types of interactions have a degree of orientation dependence and are slightly weaker (in the range 50 – 200 kJ/mol for ion-dipole and 5 – 50 kJ/mol for dipole-dipole forces). [4] Electrostatic interactions are highly solvent-dependent and tend to be stronger in media with small dielectric constants.

**Hydrogen bonding (HB):** This can be considered a sub-type of dipole-dipole or ion-dipole interactions, which occurs between a hydrogen atom attached to an electronegative fragment and a Lewis base (either an anion or a neutral molecule with a lone pair of electrons). [41] These interactions are stronger than most typical intermolecular forces (typically 4 – 120 kJ/mol) [39] and somewhat directional, depending on the environment and the nature of the hydrogen bonding acceptor. Typical geometries are summarized in **Figure 1.6.**

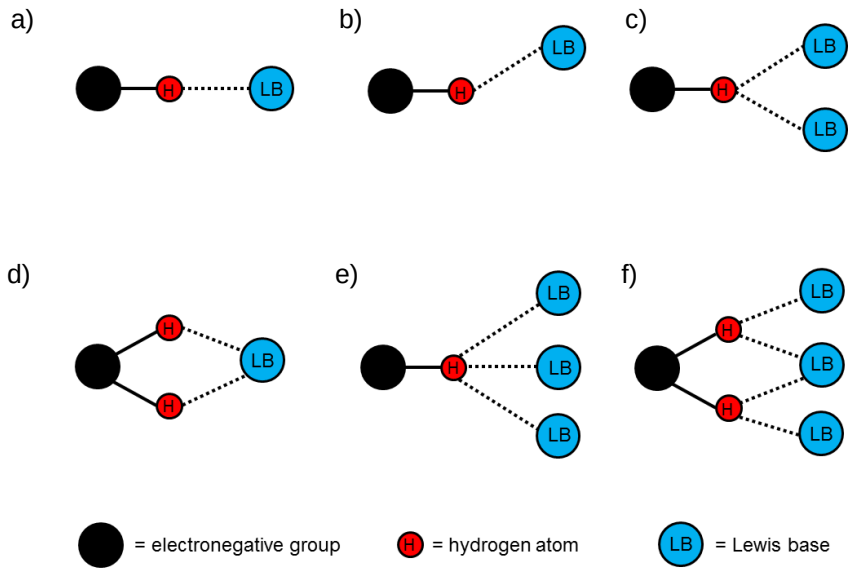



***Figure 1.6.*** *Types of hydrogen bonding geometries: a) linear; b) bent; c) donating bifurcated; d) accepting bifurcated; e) trifurcated; f) three-centre bifurcated.* [39]

Due to their strength and versatility, hydrogen bonds mediate anion binding in a broad range of receptor molecules (**Section 1.2.5.2**).

**Halogen bonding (XB):** Although the formation of adducts between halogenated molecules and Lewis bases in the solid state has been known since the 19$^{th}$ century, [42,43] it was not until Politzer's seminal computational studies on halomethanes that the origin of this interaction was elucidated. [44] In the case of halotrifluoromethanes, with progressively heavier halogens (labelled X) the electron density on the halogen atom becomes more anisotropically distributed, resulting in a circular belt of negative potential perpendicular to the C – X bond and a small area of increasing positive potential in the polar region of the halogen atom, termed the σ-hole (**Figure 1.7.a**). The interaction of this localised positive electrostatic potential with a Lewis base such as an anion is termed *halogen bonding* (XB).

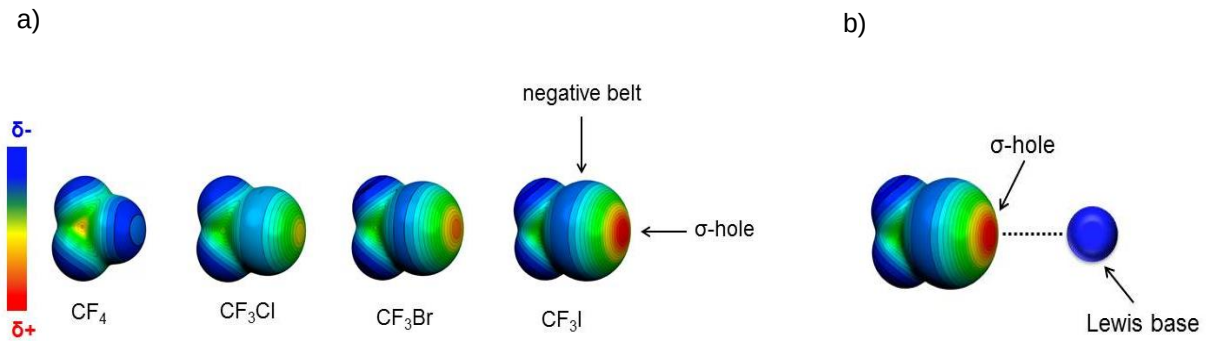



***Figure 1.7.*** *a) The molecular potential in Hartrees plotted at the 0.001 electrons Bohr$^{-3}$ isodensity surface of various halomethanes. Adapted from reference 44.* [44] *b) Cartoon representation of a generic halogen bonding interaction highlighting the importance of the positive potential of the σ-hole.*

The stringent directionality of the halogen bond resulting from the specific polar position of the σ-hole of the halogen atom leads to halogen bonding interactions being often highly linear (**Figure 1.7.b**) and of comparable strength to, if not stronger than, hydrogen bonding. [45] Their strength increases with decreasing electronegativity and increasing polarisability of the halogen atom X (F < Cl < Br < I). [46]

**Anion-π interactions:** In the case of electron-deficient arenes such as perfluorobenzene, the π system above and below the molecular plane is electron-poor while the molecular plane itself is electron-rich, such a species is labelled π-acidic, [40,47] which can interact with Lewis bases (**Figure 1.8.a**). This anion-π interaction has been shown to be predominantly electrostatic in nature, with contributions from anion-induced polarisation. [48,49] However, due to their relatively low strength and lack of directionality, they are mostly employed to complement other stronger interactions in anion receptors.

Anion-π interactions have been successfully exploited by Stoddart and co-workers, who demonstrated the encapsulation of a linear triiodide anion inside a prismatic cavity featuring electron-poor naphthalenediimide (NDI) motifs in $CD_2Cl_2$ (**Figure 1.8.b**). [50]

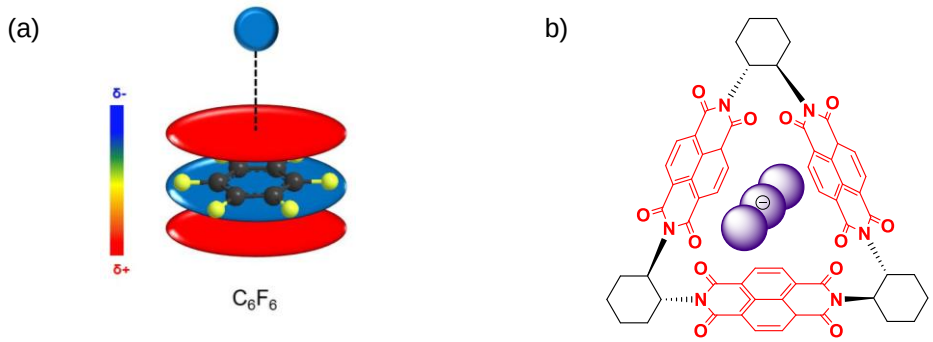



***Figure 1.8.*** *a) Cartoon representation of quadrupole moments in π-acidic hexafluorobenzene, showing its propensity to interact with anions.* [51] *b) Stoddart's NDI-based triangular prism binding triiodide.*

**Coordinate bond:** This type of interaction between a Lewis acid and a Lewis base such as an anion contains significant orbital overlap and is thus not strictly non-covalent. Commonly employed Lewis acidic elements are either neutral, such as boron, silicon, germanium, tin, antimony, and tellurium, or positively charged transition metal cations. [52,53] The use of coordinatively unsaturated metal cations in particular allows for exploitation of their stereochemical preferences in order to impart selectivity towards anions of a particular geometry. [54]

A remarkable example is a calix[4]arene derivative functionalised with two Lewis acidic boron centres, synthesised by Davidson and co-workers (**Figure 1.9.a**). [55] This rigid host exhibits strong $F^-$ binding in $CDCl_3$ (log $K_a$ = 6.3).

Another class of Lewis acid-based receptors is the so-called anticrowns, which derive their name from the analogy to crown ethers – the key difference being the incorporation of electron-deficient atoms such as Sn and Hg instead of the electron-rich oxygen. [4] A family of organotin cryptands synthesised by Newcomb and co-workers (**Figure 1.9.b**) is capable of encapsulating smaller halides such as $F^-$ and $Cl^-$ in $CDCl_3$. [56] Hawthorne's mercuracarborand featuring four Hg atoms and 4 carborane clusters is capable of binding chloride in the centre of its cavity in a 1:1 stoichiometry in acetone-$d_6$ (**Figure 1.9.c**). [57]

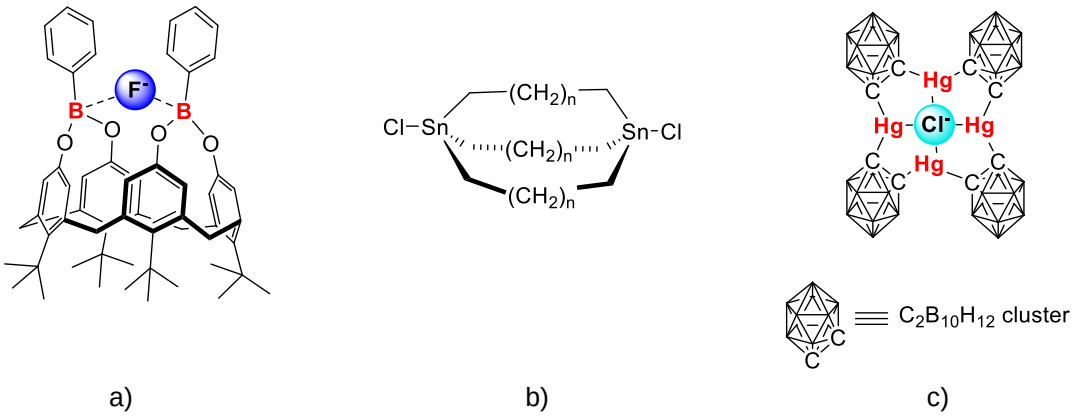



***Figure 1.9.*** *Examples of Lewis acidic anion receptors: a) Davidson's boron-based fluoride host; b) Newcomb's organotin cryptands that bind halides; c) Hawthorne's mercuracarborand that binds chloride.*

Fabbrizzi designed a bimetallic $Cu^{2+}$ cage (**Figure 1.10**) that was capable of selective recognition of $HCO_3^-$ in buffered aqueous media at neutral pH. [58]

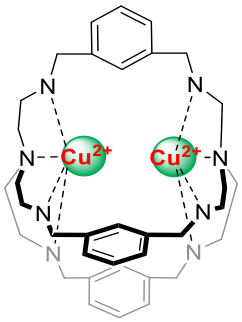



***Figure 1.10.*** *Fabbrizzi's Cu(II) cryptand binding bicarbonate in water.*

**Solvophobic effects:** Although not technically a single, non-covalent interaction, solvophobic effects are of high relevance in anion receptor design. They refer to the expulsion of solvent molecules from the cavity of a receptor upon anion guest inclusion which is typically entropically favourable. In protic solvents, the formation of hydrogen bond networks between the liberated solvent molecules and bulk solvent is also enthalpically favoured. [59,60] This is especially the case for anion recognition in water, where the overall process is referred to as "the hydrophobic effect". [61]

Related to solvophobic effects is the Hofmeister series (see **Section 1.2.2**), where weakly hydrated chaotropic anions such as $ClO_4^-$ are preferentially recognised by cage-like hydrophobic hosts such as bambus[6]uriles in water. [62,63]

More recently, the affinity of hydrophobic cavities for chaotropic anions has been exploited by Nau and co-workers, who reported the formation of exceptionally stable inclusion complexes in water between dodecaborate anionic clusters and γ-cyclodextrin (**Figure 1.11**). [64] The binding process was determined to be enthalpically driven with unfavourable entropy.

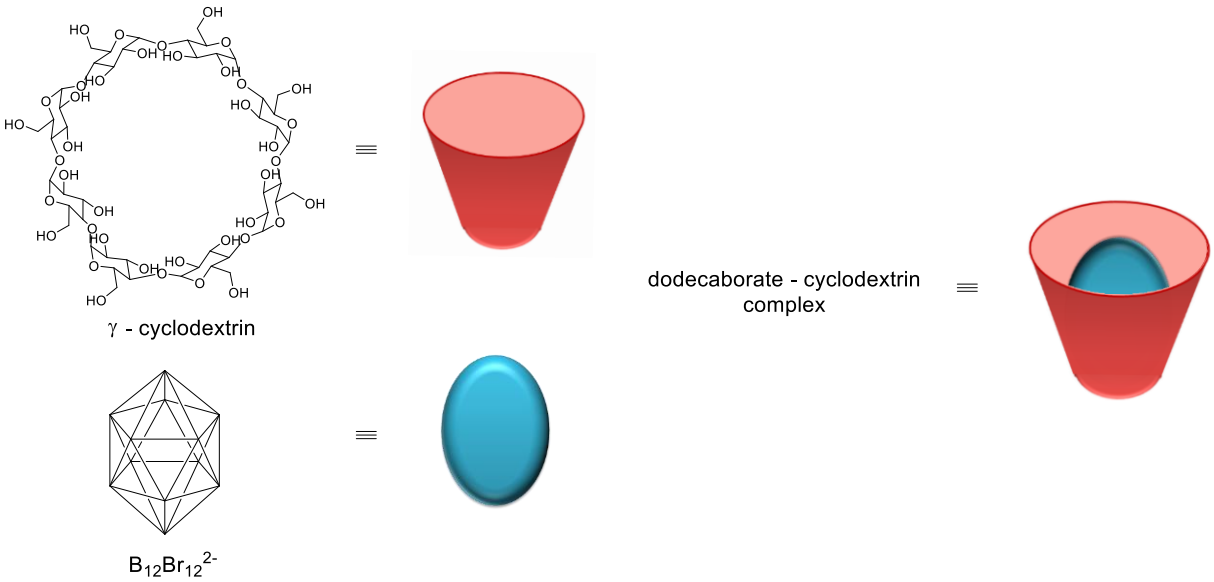



***Figure 1.11.*** *Cartoon representation of the inclusion complex formed between a γ-cyclodextrin host and a dodecaborate guest.*

### 1.2.5. Abiotic receptors

#### 1.2.5.1. Principles of anion receptor design

Preorganisation and the macrocyclic effect, concepts originating from cation host-guest supramolecular chemistry, have been commonly exploited in anion receptor design.

Cram's preorganisation concept was conceived from his work on the rigid spherand host systems for group 1 metal cations. Briefly, this states that a host that already exists in a favourable conformation prior to guest binding will exhibit a stronger affinity than a flexible host that changes conformation. [65] Hence fewer degrees of freedom are lost upon binding with a rigid, preorganised host system. By appending a hydroxyl group *ortho* to each amide group of a simple acyclic isophthalamide receptor, Gale and co-workers demonstrated the affinity for $Cl^-$ in $CD_3CN$ increased by more than twenty-fold (**Figure 1.12**). [66] The acidic hydrogen atoms of the phenolic groups engage in intramolecular hydrogen bonding with the

amide carbonyl motifs, which preorganises the amide NH donor groups in a favourable *syn-syn* conformation.

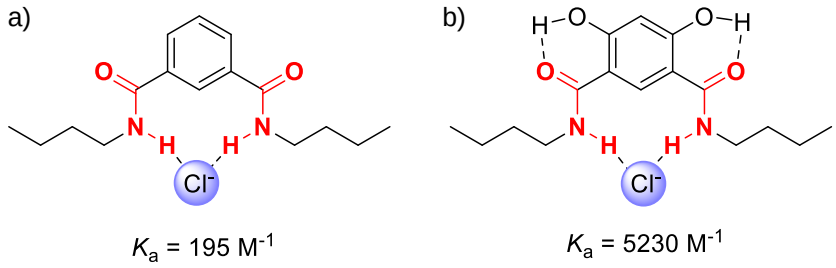



***Figure 1.12.*** *Stability constants ($K_a$) for the complexes formed between $Cl^-$ and (a) a simple isophthalamide host or (b) a more preorganised host featuring two intramolecular hydrogen bonds. Values determined in $CD_3CN$ at 298 K.*

An anion macrocyclic effect was demonstrated by Jurczak and co-workers (**Figure 1.13**). The cyclic polyamide macrocycle binds $F^-$ over 75 times more strongly than an acyclic analogue with the same number and arrangement of donors. [67] Therefore, rigid, preorganised macrocyclic hosts are highly sought after in anion receptor design.

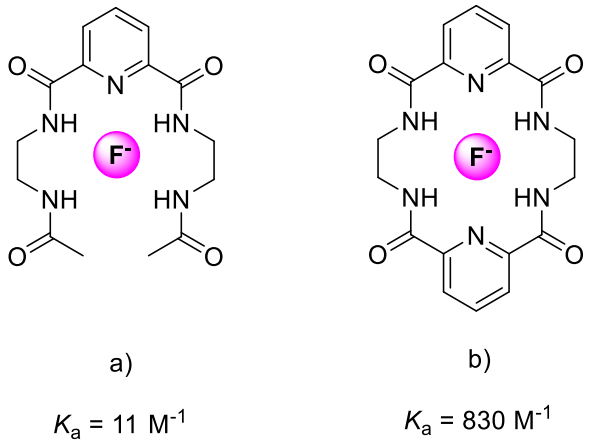



***Figure 1.13.*** *Stability constants ($K_a$) for the complexes formed between $F^-$ and a) an acyclic polyamide host or b) a macrocyclic polyamide host. Values determined in DMSO-$d_6$ at 298 K.*

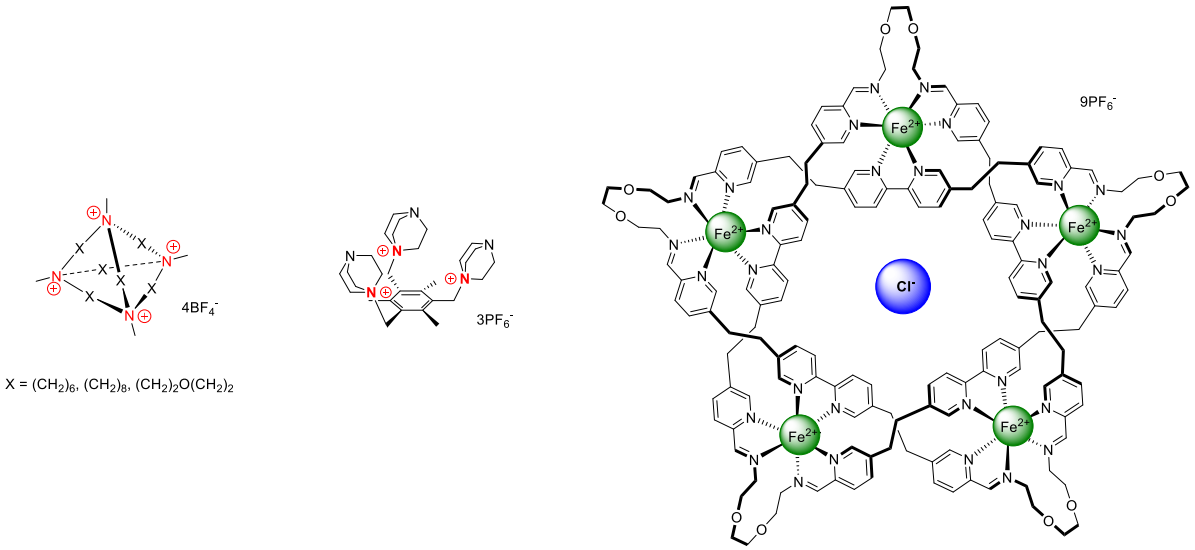
### 1.2.5.2. Examples of abiotic receptors

The following sections give an overview of synthetic anion receptors, which are classified by the types of non-covalent interactions that are commonly used in combination to mediate anion recognition. Cationic hosts are designed to function in aqueous media, whereas neutral hosts typically operate in polar organic media.

#### 1.2.5.2.1. Cationic receptors

- **Receptors exploiting electrostatic interactions**

In pioneering work, Schmidtchen and co-workers constructed pH-independent, quaternary ammonium tetrahedral cage hosts which bind halides in water (**Figure 1.14.a**). [68] By altering the methylene bridges chain length, halide discrimination was achieved on the basis of size complementarity. More recently, in 1997, a tripodal receptor based on three alkylated diazabicyclooctane (DABCO) motifs was reported by Malik and co-workers [69] to selectively recognise $[Fe(CN)_6]^{3-}$ over $[Fe(CN)_6]^{4-}$ in aqueous solution (**Figure 1.14.b**). A more recent example is Leigh's pentameric cyclic double helicate (**Figure 1.14.c**) exhibiting a 10+ charge. [70] The cavity in this remarkable Fe(II)-metallated knot turned out to be exceptionally selective for $Cl^-$ over heavier halides in $CD_3CN$.




a) b) c)

***Figure 1.14.*** *Examples of hosts that bind anions exclusively through electrostatic interactions: a) Schmidtchen's cage-like receptor; b) Malik's DABCO-based tripod; c) Leigh's multiply charged pentafoil knot.*

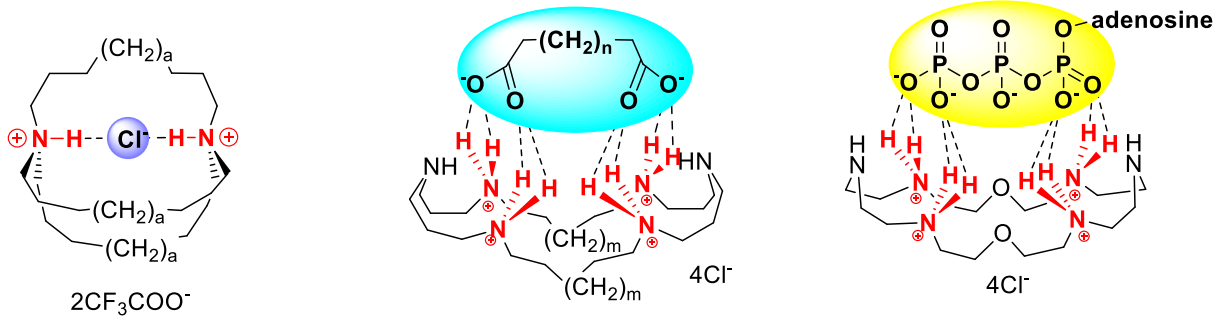
- **Cationic hydrogen bonding receptors**

Charge-assisted hydrogen bonding entwines the strength of electrostatic interactions and the directionality constraints of hydrogen bonding, and thus has been widely exploited in the design of anion receptors.

N – H hydrogen bond donors

*Polyammonium-based hosts*

Arguably the simplest positively charged hydrogen bond donor groups, protonated tertiary amines have found use in anion binding. Considered the first synthetic anion receptors, diazabicyclic hosts designed by Park and Simmons in 1968 (**Figure 1.15.a**) were found to encapsulate small halides in 50% deuteriotrifluoroacetic acid via two charge-assisted N – H hydrogen bonds. [71] Later, Lehn and co-workers demonstrated an elegant example of fine-tuning a receptor to a target anion (**Figure 1.15.b**). By varying the length of the alkyl spacer between the two propylene units of a cationic polyammonium macrocycle, selectivity for dicarboxylates of complementary chain length was achieved in aqueous solution. [72] Building on these results, Lehn extended the study of these pH-dependent polyammonium macrocycles for practical applications. A similar host, shown in **Figure 1.15.c**, bound ATP anion in water and catalysed its hydrolysis to ADP, thus mimicking the action of natural catalytic systems. [73]

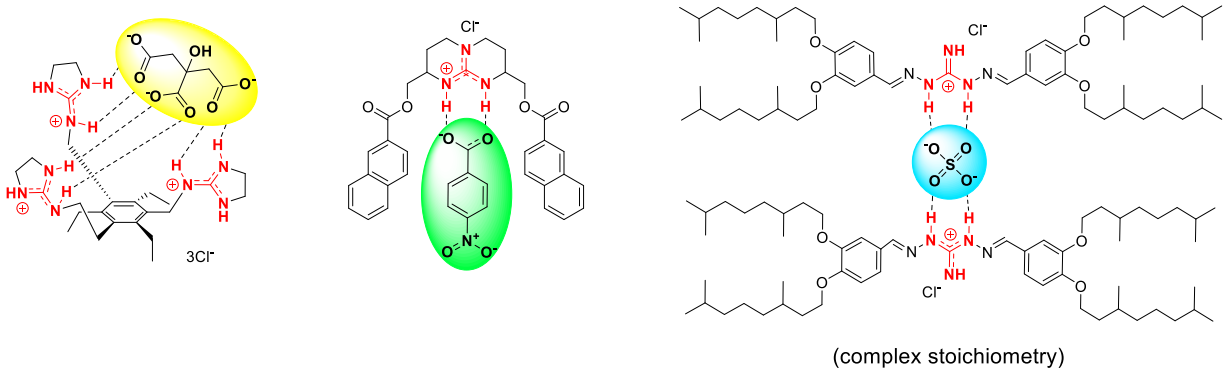



a) b) c)

***Figure 1.15.*** *Selected anion receptors employing cationic hydrogen bond-donating ammonium moieties: a) Park and Simmons' macrobicycle binding halides; b) Lehn's polyammonium macrocycles binding dicarboxylates; c) Lehn's ulterior polyammonium macrocycle binding ATP.*

*Guanidinium-based hosts*

The guanidinium functional group is a component of the natural amino acid arginine and is often employed by anion binding proteins, as illustrated in the case of PBP (**Section 1.2.3**). [4] Its high p$K_a$ value (13.6) resulting from charge delocalisation over three nitrogen atoms make it a valuable building block for anion recognition purposes over a large pH window. [74] Anslyn's tripodal host notably complexes citrate in $D_2O$ [75] with an association constant $K_a$ = 6.9 x $10^3$ $M^{-1}$ (**Figure 1.16.a**), whereas Lehn's receptor employs a rigid bicyclic guanidinium unit to quantitatively extract p-nitrobenzoate from water into chloroform (**Figure 1.16.b**) [76]. A more recent example is Moyer's amphiphilic receptor which encapsulates $SO_4^{2-}$ into micelles at the organic phase – water interface (**Figure 1.16.c**). [77]




a) b) c)

***Figure 1.16.*** *Anion receptors incorporating guanidinium units: a) Anslyn's tris(guanidinium) host for citrate; b) Lehn's 4-nitrobenzoate extractant; c) Moyer's micelle-forming sulfate extractant.*

C – H hydrogen bond donors

*Imidazolium-based hosts*

Typical examples of motifs containing charge-assisted C – H hydrogen bond donors are π-deficient heteroaromatic groups such as imidazolium, which present the advantage of pH independence. [78]

Lan and co-workers developed a chiral BINOL-based bis(imidazolium) macrocycle [79] which was significantly more selective for D-tryptophan over L-tryptophan in aqueous solution at physiological pH (**Figure 1.17.a**). Kang's receptor incorporating four imidazolium units linked by methylene bridges [80] (**Figure 1.17.b**) displayed selectivity for $I^-$ over the other

halides in 1:9 DMSO-$d_6$/$CD_3CN$ (*v/v*). A "molecular box" designed by Sessler and co-workers which also features imidazolium moieties (**Figure 1.17.c**) was shown to encapsulate carboxylate anions in DMSO-$d_6$. [81]

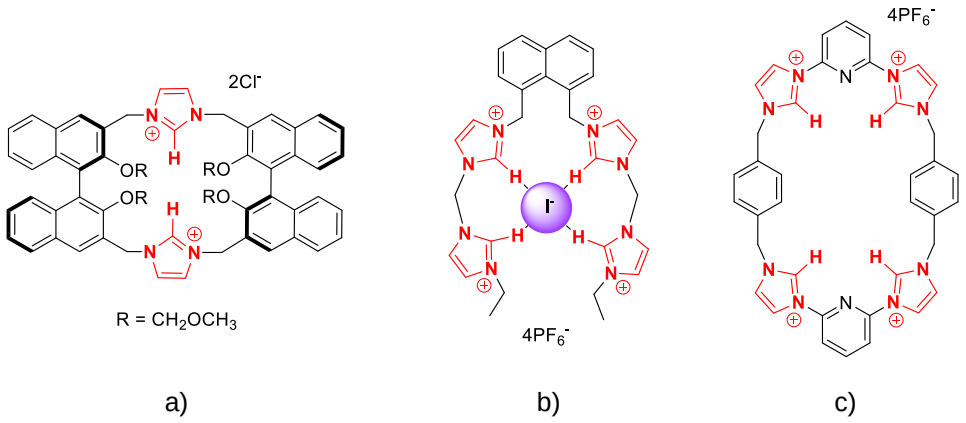



***Figure 1.17.*** *Imidazolium-based species for anion recognition: a) Lan's optically active macrocycle which performs chiral anion discrimination; b) Kang's tetrakis(imidazolium) receptor for iodide; c) Sessler's macrocycle which encapsulates monoterephthalate.*

*Triazolium-based hosts*

Due to its facile synthesis and ease of functionalisation, the 1,2,3-triazolium motif has been exploited for incorporation into anion receptors as a potent C – H hydrogen bond donor. [82] A seminal report by Pandey described a receptor based on three triazolium moieties appended onto a steroidal scaffold [83] which selectively bound $H_2PO_4^-$ in $CDCl_3$ over halide and acetate anions (**Figure 1.18.a**). In a more recent example, Schubert's acyclic mixed triazole-triazolium receptor (**Figure 1.18.b**) forms a complex with $SO_4^{2-}$ in $CD_3CN$ wherein the oxoanion is encapsulated between two mutually orthogonal host molecules. [84] In 2012, Beer and co-workers synthesised a simple tetratriazolium macrocycle [85] which proved capable of strongly binding $F^-$ and $Cl^-$ in the highly competitive solvent mixture 1:9 $D_2O$/DMSO-$d_6$ (*v/v*) (**Figure 1.18.c**).

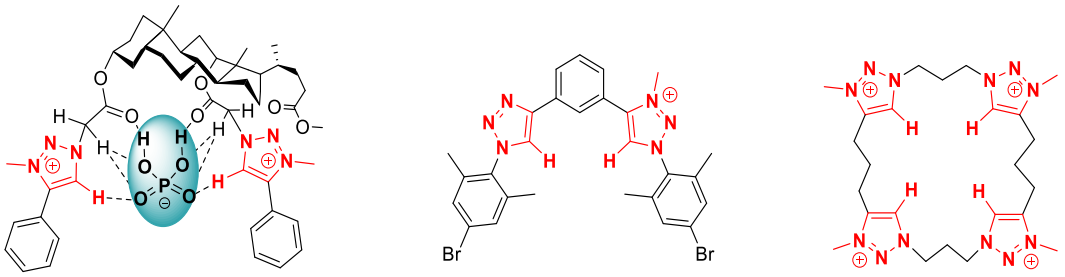



***Figure 1.18.*** *Anion receptors incorporating triazolium motifs: a) Pandey's bile acid-based receptor for dihydrogen phosphate; b) Schubert's acyclic mixed triazole-triazolium host that encapsulates $SO_4^{2-}$; c) Beer's tetratriazolium macrocycle binding halides.*

### 1.2.5.2.2. Neutral receptors

By employing an array of convergent, directional, neutral hydrogen bond donors into acyclic and cyclic structural frameworks, a range of highly selective anion receptors have been produced that mainly operate in organic media. [86]

N – H hydrogen bond donors

*Amide-based hosts*

The amide functional group is omnipresent in peptide and protein structures. [3] Its facile synthesis and propensity to form strong, directional hydrogen bonds makes it one of the most widely employed N – H donors in anion recognition. [82] The first anion receptor incorporating amide motifs was reported in 1986 by Pascal and co-workers, who designed a cage like tris-amide capable of $F^-$ complexation in DMSO-$d_6$ [87] (**Figure 1.19**).

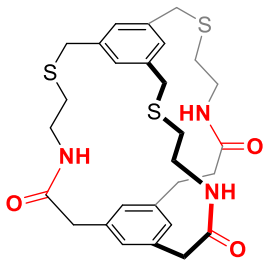


***Figure 1.19.*** *Pascal's seminal amide-based anion receptor.*

In 1997, Crabtree described a simple isophthalamide host (**Figure 1.20.a**) that bound $Cl^-$ in $CD_2Cl_2$ with an affinity almost an order of magnitude greater than that of $Br^-$ and two orders of magnitude larger than that of $I^-$. [88] More recently, Ghosh and co-workers investigated the binding properties of a receptor with six pendant arms, each incorporating one highly electron-withdrawing pentafluorophenyl unit appended to an amide motif. [89] This hexapodal host altered the relative orientation of its arms depending on the nature of the anionic guest in acetone-$d_6$ (**Figure 1.20.b**). For example, acetate was bound in an *aaabbb* conformational mode, while an alternate arrangement (*ababab*) resulted upon binding nitrate.

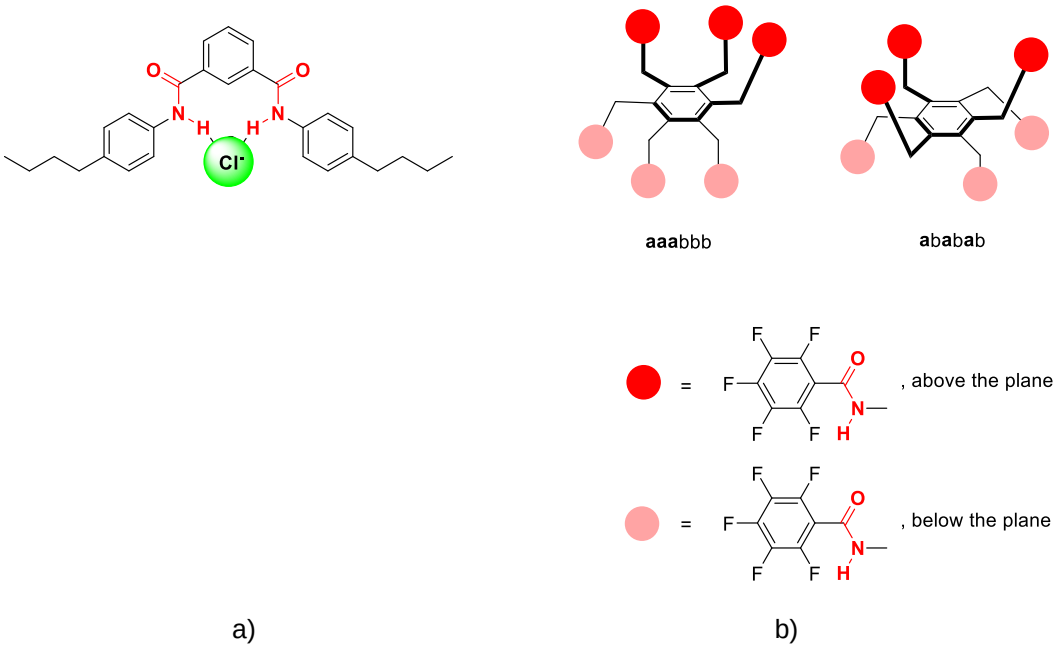
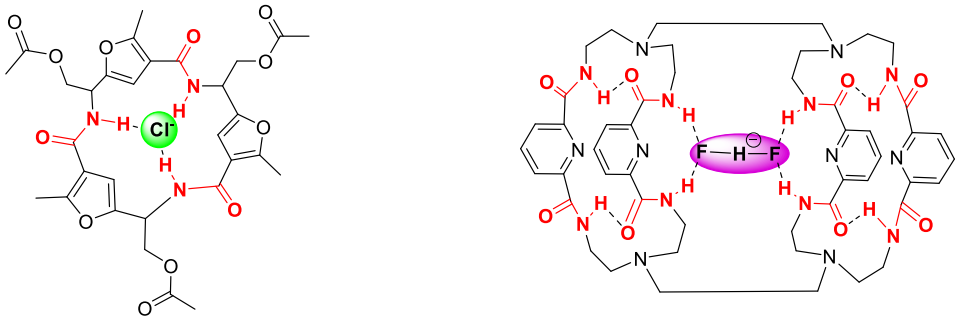



***Figure 1.20.*** *Amide-based anion receptors, from simple to complex: a) Crabtree's isophthalamide host selective for chloride; b) Ghosh's flexible hexapodal receptor for oxoanions.*

Robina reported a cyclic tripeptide platform (**Figure 1.21.a**) exhibiting selective complexation of chloride over more basic anions such as $AcO^-$ and $CN^-$ in $CD_3CN$. [90] In 2006, Bowman-James and co-workers described a cryptand consisting of two tetraamido-macrocycles linked by ethylene bridges (**Figure 1.21.b**). This cage-like receptor was demonstrated to encapsulate $HF_2^-$ in DMSO-$d_6$ by employing four of its eight available amide donors (two for each fluorine atom), while the other four participated in intramolecular hydrogen bonding. [91]

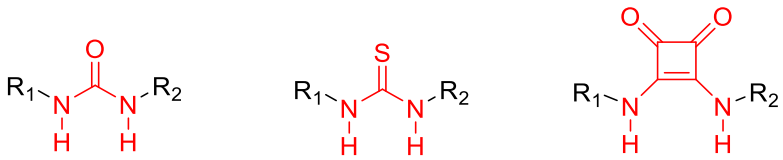


(a) (b)

***Figure 1.21.*** *Amide-based anion receptors: a) Robina's furan-based tripeptide that binds $Cl^-$; b) Bowman-James' cryptand that binds difluoride.*

*Urea, thiourea, and squaramide-based hosts*

N,N'-Disubstituted ureas can be considered symmetrical analogues of amides employing two parallel N – H hydrogen bond donors. An analogue bearing a thiocarbonyl group instead of a carbonyl group, termed a thiourea, has relatively more acidic N – H protons due to the greater ability of the sulfur atom to stabilise additional electron density. [92,93] Another closely related HB donor motif is squaramide, which employs two proximal electron-withdrawing carbonyl groups (**Figure 1.22**).



a) b) c)

***Figure 1.22.*** *Examples of hydrogen bond donor motifs: a) urea; b) thiourea; c) squaramide. $R_1$, $R_2$ = organic substituents.*

All the above HB donor motifs have been widely employed in the design of anion binding receptors, from the very simple to the incredibly complex. In 1992, Hamilton and co-workers reported that the association constant for the complexation of a bis(thiourea) host with glutarate in DMSO-$d_6$ was more than 15-fold that for its urea analogue (**Figure**

**1.23.a**). [94] More recently, Jurczak appended chiral peracetylated β-D-glucose units onto a rigid bis-urea framework (**Figure 1.23.b**), which led to significant enantiodiscrimination between D- and L-aminoacid carboxylate anions in 0.5:99.5 $H_2O$/DMSO-$d_6$ (*v/v*) (e.g. $K_D/K_L$ = 2.42 for valine anions). [95] A macrocyclic host incorporating three squaramide units synthesised by Jolliffe and co-workers (**Figure 1.23.c**) was found to display remarkable selectivity for sulfate in the highly competitive 1:2 $D_2O$/DMSO-$d_6$ (*v/v*) and in aqueous media mimicking nuclear waste. [96]

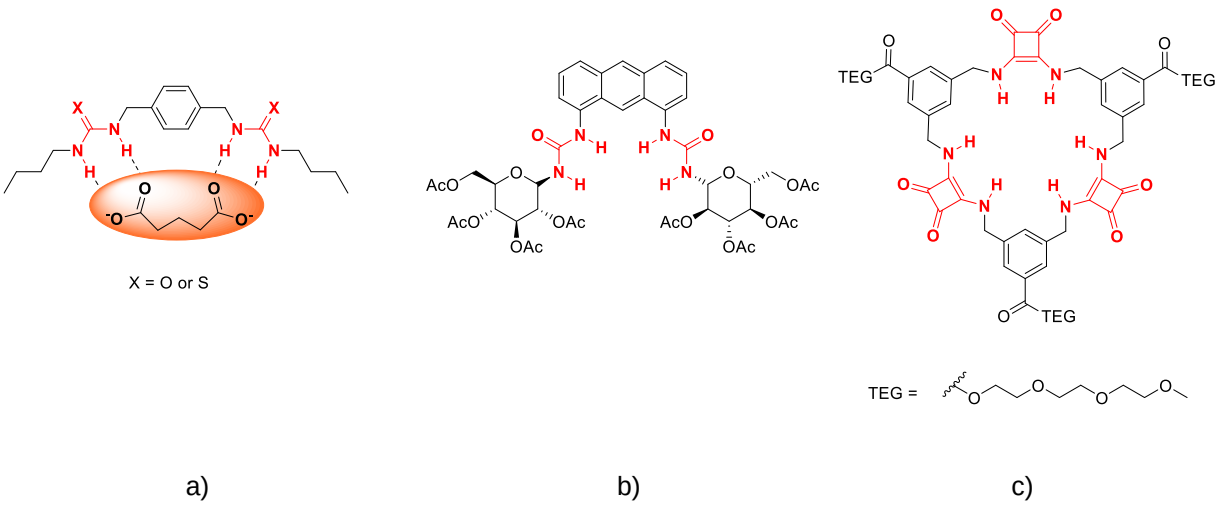



***Figure 1.23.*** *Examples of (thio)urea and/or squaramide-based anion receptors: a) Hamilton's (thio)urea host for glutarate; b) Jurczak's chiral urea-based host for enantiomer discrimination; c) Jolliffe's macrocyclic squaramide-based host for* $SO_4^{2-}$.

In an elegant example from 2016, Feringa designed a photoswitchable anion receptor based on a stilbene scaffold. Upon irradiating the (*E*) isomer with UV light (λ = 365 nm) and converting it to its (*Z*) counterpart, the affinity for $H_2PO_4^-$ increased drastically from $K_a$ = 77 $M^{-1}$ to $K_a$ = 2020 $M^{-1}$ in 0.5:99.5 $D_2O$/DMSO-$d_6$ (*v/v*) (**Figure 1.24**), demonstrating the cooperativity of the two urea functional groups. [97]

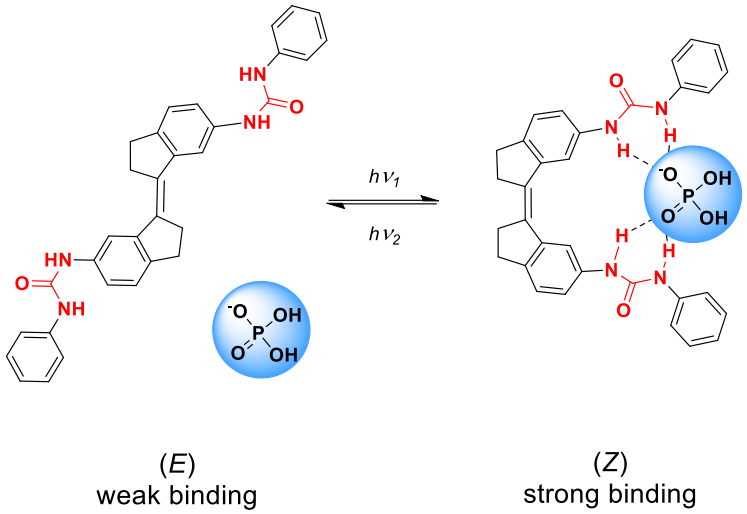



***Figure 1.24.*** *Enhanced anion binding caused by reversible photoinduced isomerisation of Feringa's urea-based molecular switch.*

*Pyrrole, indole, and carbazole-based hosts*

A disadvantage of integrating amides and ureas into an anion receptor is that they contain HB acceptors (the carbonyl group) concomitantly with HB donors, which makes them prone to self-aggregation. [98] Pyrrole is thus privileged as it lacks a hydrogen bond acceptor; the electron density on the acidic N – H proton can also be further depleted by conjugation of the pyrrole unit with one phenyl ring (indole) or two (carbazole) (**Figure 1.25**).

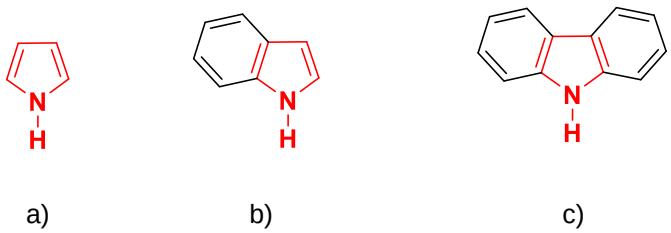
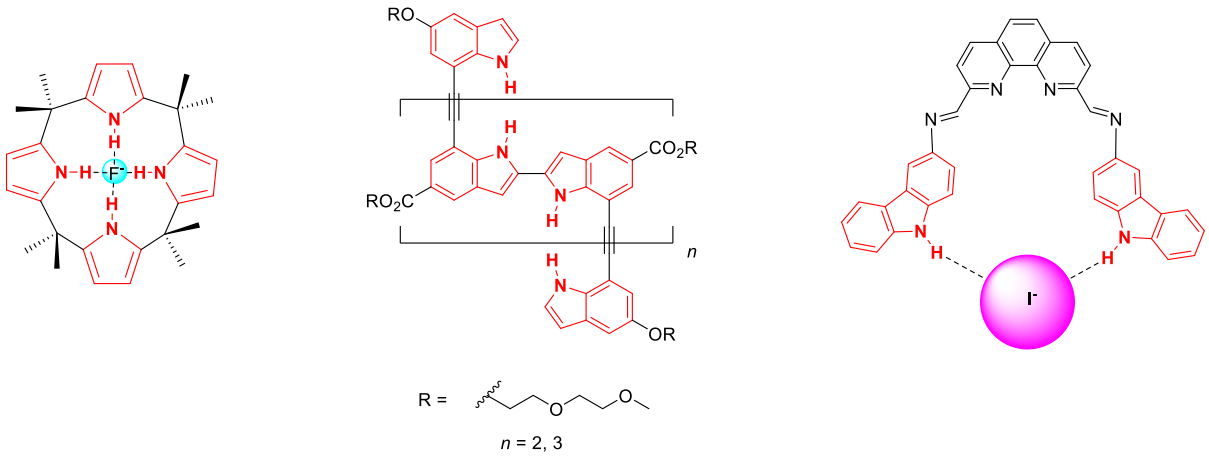



***Figure 1.25.*** *Examples of commonly employed pyrrole-based hydrogen donor motifs: a) 1*H*-pyrrole; b) 1*H*-indole; c) 9*H*-carbazole.*

In 1996, Sessler and co-workers determined that previously reported calix[4]pyrrole (**Figure 1.26.a**) had a strong affinity for $F^-$ (log $K_a$ > 4 in $CD_2Cl_2$). [99] Jeong's indole-based foldamer structure (**Figure 1.26.b**) encapsulates $Cl^-$ in $CD_3CN$ by adopting a helical conformation. [100] Lin and co-workers appended two convergent carbazole units onto a

phenanthroline scaffold (**Figure 1.26.c**) to produce a receptor that strongly complexes iodide ($K_a$ = 5 x $10^4$ $M^{-1}$) in DMF. [101]




a) b) c)

***Figure 1.16.*** *Examples of anion receptors incorporating a) pyrrole motifs; b) indole motifs; c) carbazole motifs.*

C – H hydrogen bond donors

Traditionally, hydrogen bond donors are directly linked to a more electronegative heteroatom such as N or O. However, if placed in a sufficiently electron – withdrawing environment, a proton can become highly charge–depleted and is thus able to function as a hydrogen bond donor, whose acidity is directly correlated to the strength of the resulting bond - as hypothesised by Hay in 2005. [102]

The seminal example of a non-classical HB donor was reported by Farham and co-workers in 1990, based on the serendipitous discovery that a perfluorinated macrocycle was capable of binding fluoride solely through the means of C – H ··· $F^-$ interactions in THF (**Figure 1.27**). [103]

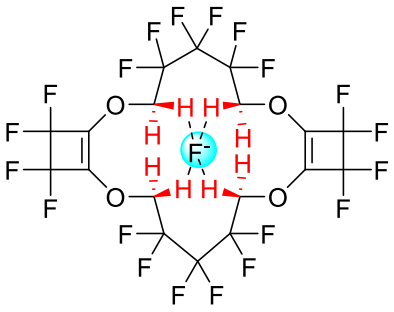
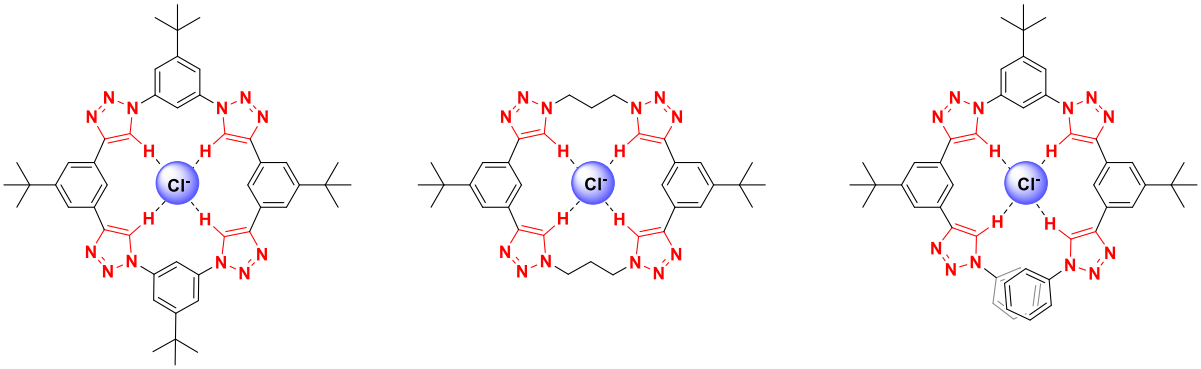


***Figure 1.27.*** *The structure of the complex formed between Farham's cyclic fluorinated ether and a fluoride anion.*

*Triazole-based hosts*

The use of 1,2,3-triazoles in anion binding is now widespread due to their synthetic accessibility and large dipole moment (approximately 5 Debye), leading to a highly polarised C – H bond even in the absence of charge assistance. [82] A remarkable example of an anion host incorporating convergent triazole motifs is Flood's preorganised macrocyclic triazolophane (**Figure 1.28.a**), which is capable of the strong binding of chloride in $CD_2Cl_2$. [104] Related more flexible cyclic and acyclic hosts displayed much weaker affinities for $Cl^-$ (**Figure 1.28.b** and **Figure 1.28.c**, respectively). [105]



$K_a$ = 5 x $10^6$ $M^{-1}$ $K_a$ = 1 x $10^3$ $M^{-1}$ $K_a$ = 1 x $10^2$ $M^{-1}$

a) b) c)

***Figure 1.28.*** *Examples of structurally similar polytriazole host structures that bind $Cl^-$. Association constants determined in $CD_2Cl_2$ at 298 K.*

The same group later synthesised an analogous macrocycle featuring alternating carbazole – triazole moieties (**Figure 1.29.a**). This host, termed *tricarb*, formed strong and

selective 2:1 host:guest stoichiometric sandwich complexes with $PF_6^-$ and $SbF_6^-$ in 1:4 $CD_3OD/CDCl_3$ (*v/v*), which are typically regarded as non-coordinating (**Figure 1.29.b**). [106]

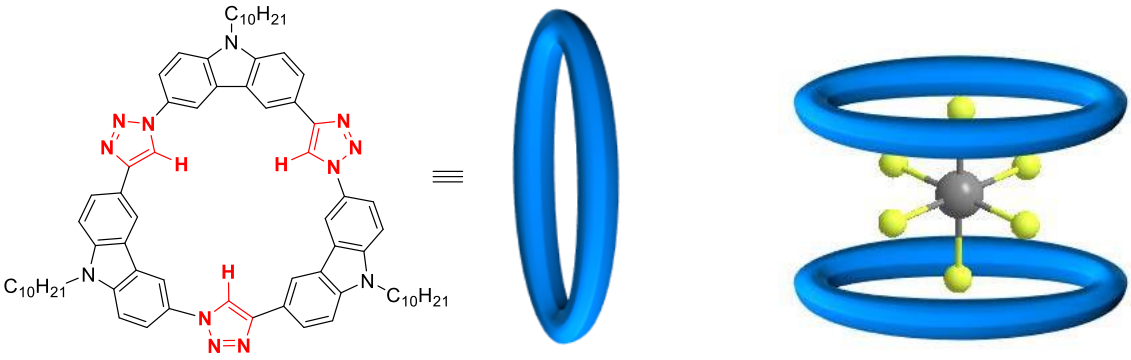



***Figure 1.29.*** *a) Two-dimensional structure of Flood's carbazole – triazole host* tricarb*; b) cartoon representation of the sandwich complex formed between* tricarb *and* $SbF_6^-$.

### 1.2.5.2.3. Halogen bonding anion receptors

Of particular relevance to the theme of this thesis are anion receptors incorporating halogen bonding (XB) donor motifs. The structures of the most commonly employed XB donors in anion recognition are outlined in **Figure 1.30**. They are derived from common hydrogen bond donor motifs, where the halogen atom (typically iodine or bromine) formally replaces the highly acidic C – H proton of a strongly electron-withdrawing functional group. [45]

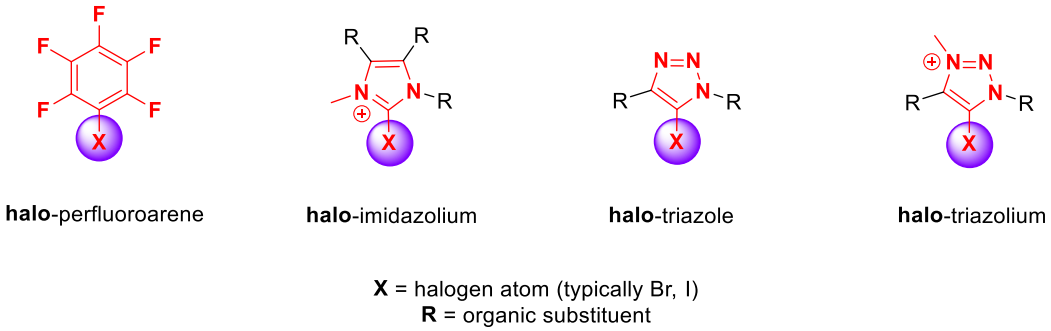
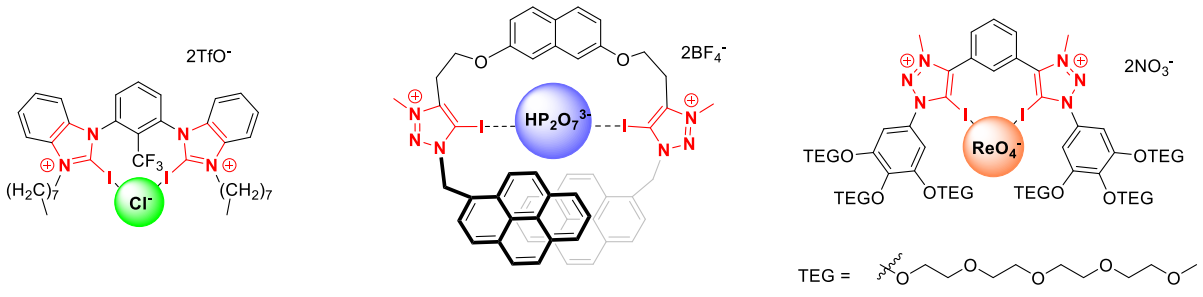



***Figure 1.30.*** *Common halogen bond donor motifs incorporated into anion receptors.*

It is only in the past decade or so that halogen bonding has begun to be exploited in anion recognition applications, which is reviewed in the following sections.

- **Cationic halogen bonding receptors**

Charge-assisted XB donors are most commonly derived from haloimidazolium or halo-1,2,3-triazolium. Among them, Huber's bidentate bis-iodoimidazolium receptor (**Figure 1.31.a**) exhibits a high affinity for chloride ($K_a$ = 3.5 x $10^6$ $M^{-1}$ in $CD_3CN$) and has been successfully employed as a catalyst in a halide abstraction reaction. [107] Molina and co-workers exploited the potency of cationic halogen bonding to achieve strong complexation of the biologically relevant $HP_2O_7^{3-}$ by a bis(iodotriazolium) host (**Figure 1.31.b**) in the competitive solvent mixture 9:1 $CD_3CN/CD_3OD$ (*v/v*). [108] Importantly, the all-hydrogen bonding and the mixed HB/XB analogues displayed markedly decreased affinities for this anion compared to the all-halogen bonding receptor. A more recent example designed by Beer and co-workers recognises perrhenate, which is a surrogate for radioactive $^{99}TcO_4$, in pure water (**Figure 1.31.c**). [109] Contrastingly, the HB analogue displayed no appreciable affinity for the oxoanion.




a) b) c)

***Figure 1.31.*** *Anion receptors incorporating cationic XB donors: a) Huber's iodoimidazolium-based catalyst that binds chloride; b) Molina's iodotriazolium host for hydrogen pyrophosphate; c) Beer's iodotriazolium receptor that complexes perrhenate.*

- **Neutral halogen bonding receptors**

Neutral XB donors typically comprise of perfluorinated arenes and halotriazoles. In 2010, Taylor and co-workers designed a family of mono-, bi-, and tridentate receptors that operate exclusively through halogen bonding interactions (**Figure 1.32**), which also served to highlight the importance of chelate cooperativity in anion binding. [110] The dipodal and tripodal host exhibited association constants for $Cl^-$ in acetone several orders of magnitude higher than a single XB donor receptor analogue.

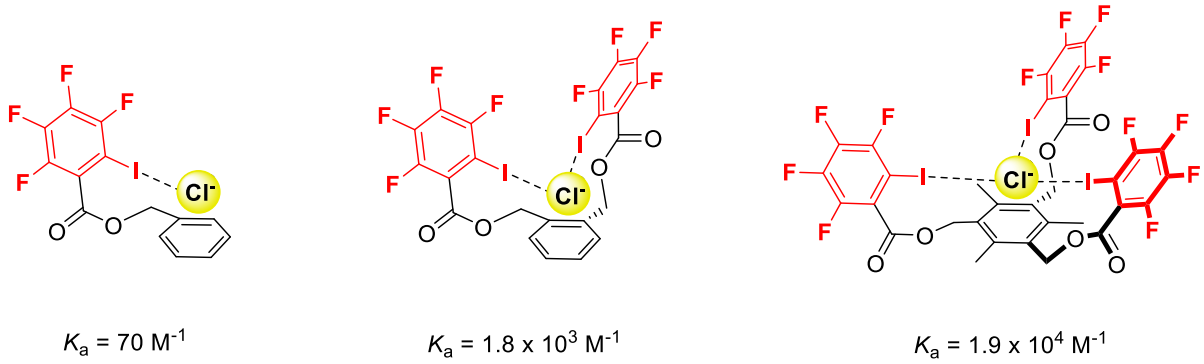



***Figure 1.32.*** *Taylor's perfluorobenzene-based receptors incorporating one, two, or three XB contacts to chloride. Association constants were determined in acetone-$d_6$ at 295 K.*

More recently, Kubik and co-workers exploited halogen bonding to achieve high selectivity for chloride. [200] A macrocyclic pseudopeptide incorporating three neutral iodotriazole XB donors (**Figure 1.33**) was found to bind chloride strongly (log $K_a$ = 3.28) in 1:39 $H_2O$/DMSO-$d_6$ (*v/v*) with an affinity more than twice that of bromide and thirteenfold that of iodide. This was attributed to the rigidity of the macrocycle and its complementary cavity size for smaller halides.

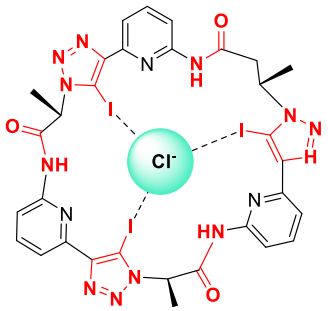



***Figure 1.33.*** *Kubik's tris(iodotriazole) macrocycle binding halides.*

### 1.3. Anion sensing

For sensing applications, the anion binding event can be coupled to the generation of a macroscopic, detectable response which can be colorimetric, fluorescent, or electrochemical. [111] Anion sensors are typically classed under one of three categories (**Figure 1.34**):

a) The anion undergoes an irreversible chemical reaction with the receptor and the resulting product exhibits different optical or redox properties to those of the starting material. Such a host molecule is termed a chemodosimeter.

b) The anion binds in proximity to an appended reporter group of the receptor, which perturbs its properties. This mechanism is termed receptor-reporter sensing.

c) The target anion displaces a weakly bound dye molecule from the receptor's host cavity. This approach is termed an indicator displacement assay (IDA).

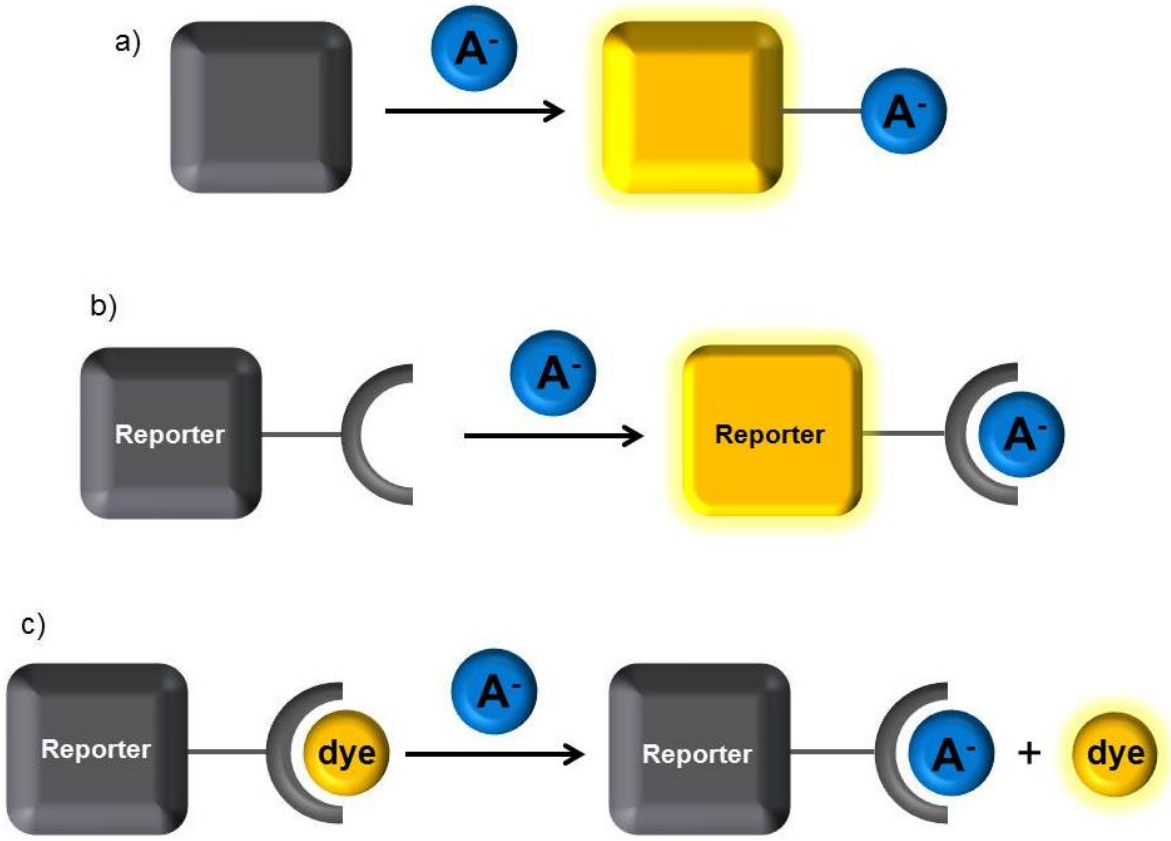



***Figure 1.34.*** *Cartoon representation of various anion sensing mechanisms: a) the chemodosimeter approach; b) receptor-reporter sensing; c) the indicator displacement assay approach. $A^-$ = anion.*

### 1.3.1. Optical anion sensing

Of particular relevance to this thesis are optical anion sensors. They are typically divided into colorimetric and fluorescent; the former allows for naked eye detection of anions, whereas the latter has the advantage of being highly sensitive.

Saha and Guha synthesised a naphthalenediimide (NDI)-based colorimetric sensor for fluoride (**Figure 1.35.a**). [112] Upon addition of $F^-$, the initially colourless host solution in DMSO-$d_6$ turned orange and then pink when adding increasing amounts of the halide anion, facilitating naked eye sensing. This was attributed to an initial binding of one fluoride anion between the two NDI moieties via anion-π and charge transfer interactions, which subsequently underwent $F^-$ - NDI electron transfer to generate orange NDI radical anions. Addition of a large excess of fluoride led to further reduction to produce pink NDI dianions. Impressively, this receptor detected fluoride in toothpaste samples containing NaF amounts as low as 0.24% (w/v).

Sessler and co-workers reported a calix[4]pyrrole receptor incorporating two benzimidazolium moieties that sensed $HCO_3^-$ in aqueous media via the indicator displacement assay mechanism. [113] Intermolecular charge transfer between the host and a chromenolate anionic dye quenched its fluorescence. Competitive complexation of bicarbonate displaced the dye, restoring its fluorescent emission (**Figure 1.35.b**). This sensor was also capable of quantifying $HCO_3^-$ levels in several commercial carbonated drinks.

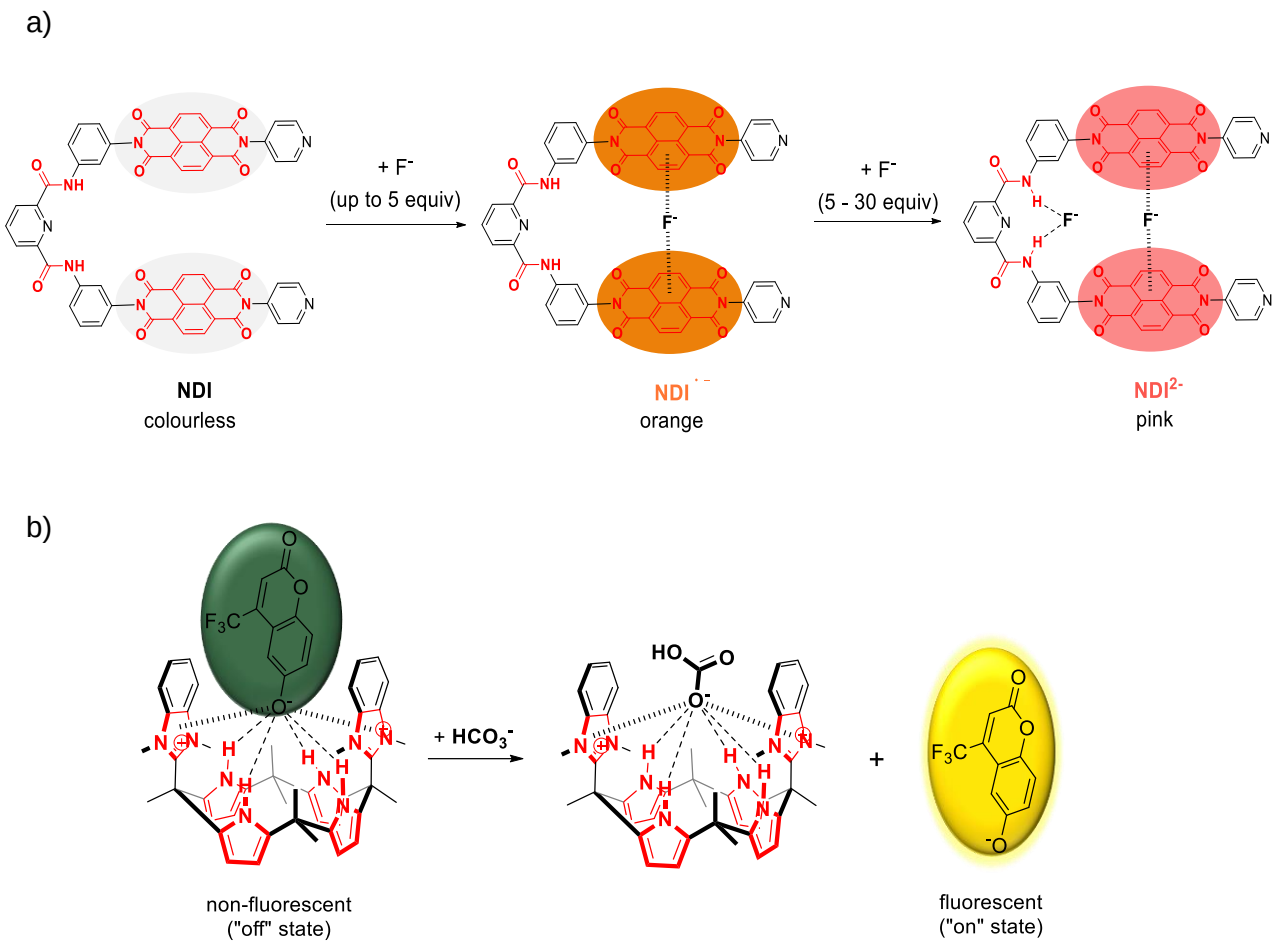



***Figure 1.35.*** *Selected examples of optical anion sensors: a) Saha and Guha's colourimetric fluoride sensor; b) Sessler's fluorescent bicarbonate sensor.*

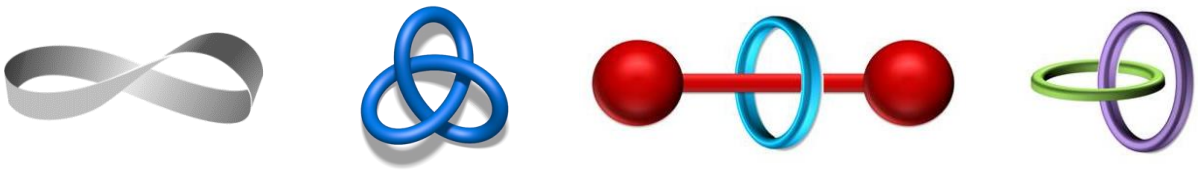
## 1.4. Mechanically interlocked molecules

### 1.4.1. Historical developments

The study of chemical bonding has led to the development of the concept of chemical topology, which was introduced in 1961 in a seminal paper by Frisch and Wasserman. [114] This field is solely concerned with the three-dimensional description of molecules derived from their connectivity patterns, while disregarding parameters such as bond lengths and bond angles. [40] A molecule whose topology is preserved through imaginary deformations such as compressing, stretching, or bending chemical bonds is termed topologically non-trivial (examples are Möbius strips and knots – see **Figure 1.36.a** below).

A closely related concept is the mechanical bond, which refers to a spatial entanglement between at least two distinct molecular components such that they cannot be separated without breaking or deforming covalent bonds [115] – an entity bearing mechanical bonds is termed a mechanomolecule. Quintessential examples are [n]catenanes, which consist of interlocked macrocyclic ring-shaped entities, and [n]rotaxanes, which comprise of one or more axle-shaped entities bearing bulky stopper groups threaded through one or more macrocycles; in both cases, [n] describes the total number of individual components (**Figure 1.36.b**).

The fields of mechanostereochemistry and chemical topology are overlapping but not identical; for example, both include catenanes, whereas a rotaxane contains a mechanical bond but is topologically trivial, as sufficient compressing of the stopper bonds would enable the macrocycle(s) to slip through. The more embracing term “mechanically interlocked molecules” (MIMs) has been introduced, encompassing all mechanomolecules as well as knot-like architectures, which are entangled but do not consist of distinguishable component parts.



Möbius strip Trefoil knot [2]Rotaxane [2]Catenane

a) b)

***Figure 1.36.*** *Cartoon exemplifying different types of molecular architectures: a) topologically non-trivial structures; b) mechanomolecules.*

While initially all these exotic topologies seemed to be of purely theoretical interest, they have since been discovered in a number of biological processes. DNA forms a biomolecular pseudorotaxane structure with λ-exonuclease, which accounts for the enzyme's high processivity, [116,117] while DNA catenanes[118] and knots[119] act as intermediates during replication and recombination. This intriguing paradigm inspired new research avenues in the synthesis of MIMs (**Section 1.4.2**); the potential for independent motion of their component parts as well as the presence of uniquely preorganised, shielded interior cavities led to the development of a wide breadth of applications, up to and including anion recognition and sensing (**Section 1.4.3**).

### 1.4.2. Strategies towards the synthesis of mechanically interlocked molecules

Typical routes employed to synthesise [2]catenanes are illustrated in **Figure 1.37** below. The most common protocol for catenane synthesis, termed "clipping", proceeds through the intramolecular ring-closing of an acyclic molecule which is threaded through the cavity of a macrocycle. A more challenging and hence less widely employed strategy is the so-called "double cyclisation", which involves the formation of a complex between two acyclic species arranged in a mutually orthogonal fashion, both of which undergo a ring-closing reaction.

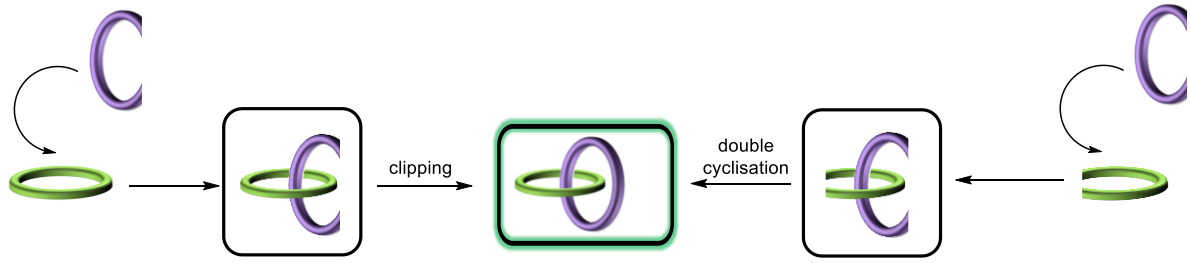



***Figure 1.37.*** *Schematic representation of the most common routes for synthesising [2]catenanes.*

Capitalising on their simpler topology, a wider variety of methods have been designed for the synthesis of [2]rotaxanes, as highlighted in **Figure 1.38.** The most common strategies include:

- stoppering [120] – an acyclic axle precursor threads through the annulus of a macrocycle (thus forming a "pseudorotaxane" complex) and subsequently its reactive

ends are covalently bound to bulky stopper groups to prevent the macrocycle from dethreading;

- clipping [121] – a macrocycle precursor wraps around a stoppered axle and its reactive ends are then clipped together;
- snapping [122] – two half-axle precursors become covalently linked through the cavity of a macrocycle.

Less common strategies involve preformed axles and macrocycles. Examples include:

- shrinkage [123] – an axle penetrates through a large macrocycle which is later chemically shrunk;
- swelling [124] – a macrocycle slips onto an axle with a smaller stopper group which is later chemically enlarged;
- slippage [125] – a macrocycle slips over the stopper groups of an axle at elevated temperatures, thus forming a [2]rotaxane that is kinetically inert at room temperature.

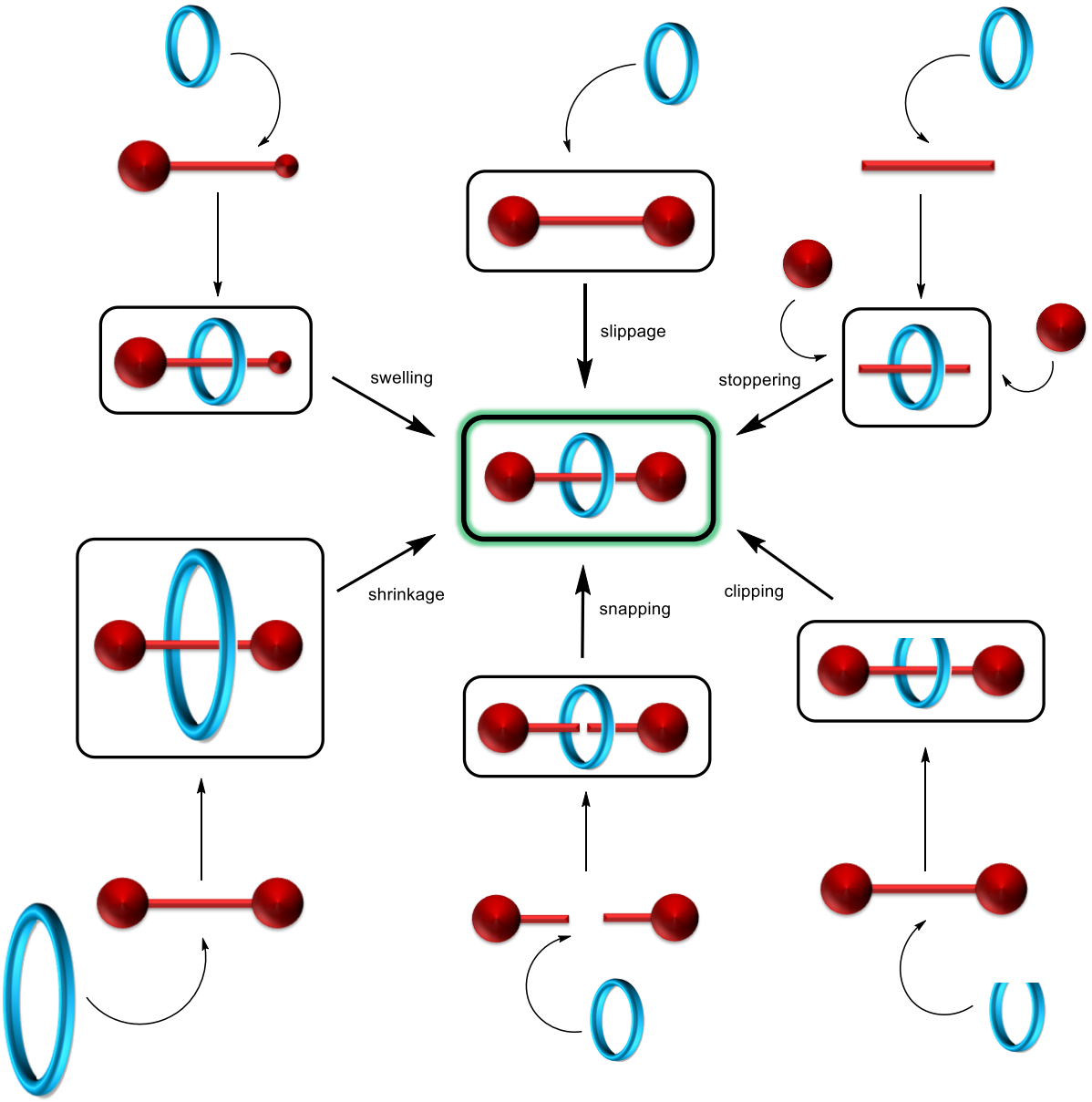


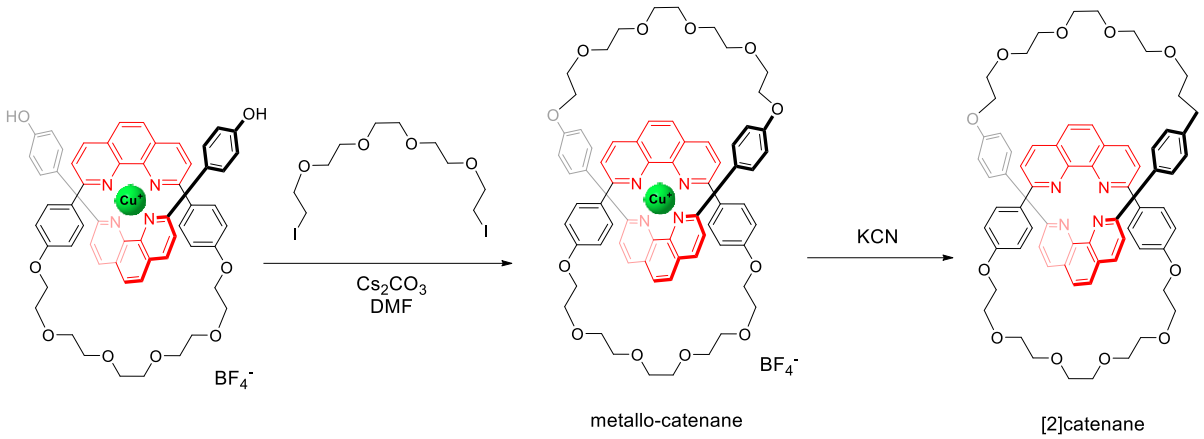

***Figure 1.38.*** *Schematic representation of the most common routes for synthesising [2]rotaxanes.*

Historically, the very first synthetic methodologies towards MIMs employed purely statistical methods, which relied on the serendipitous threading of an acyclic fragment through a macrocycle followed by clipping of its reactive ends to afford two interlocked rings. In 1962, Wasserman [126] provided evidence for the formation of an interlocked structure, a [2]catenane formed from a cycloalkane and a diester thread. Inevitably however, statistical limitations and challenging separation from oligomeric side-products led to an isolated yield of just 0.0001%.

These challenges made the synthesis of MIMs highly impractical and thus stimulated the development of alternative template-directed approaches, discussed in the following section.

### 1.4.2.1. Template-directed syntheses

It soon became apparent that the main obstacle that needed to be overcome for MIM synthesis was maximising the probability that the component precursors are entangled in a favourable relative arrangement for mechanical bond formation. This was first achieved by Sauvage and co-workers in 1983, who exploited the tetrahedral coordination preference of Cu(I) cations to preorganise two phenanthroline-based ligands in a mutually orthogonal fashion. Subsequently, a Williamson ether ring-closing reaction afforded a metallo-catenane in a then unprecedented 42% yield, which was later demetallated using KCN to obtain the free [2]catenane [127,128] (**Scheme 1.1**).




***Scheme 1.1.*** *Sauvage's seminal Cu(I) template-directed synthesis of a mechanically interlocked molecule.*

#### 1.4.2.1.1. Cationic templates

Sauvage's pioneering research rekindled interest in the synthesis of mechanically interlocked molecules by opening up a new research avenue – that of passive metal templation, in which the metal cation does not participate directly in the formation of the mechanical bond, but simply serves to preorganise the components. Since then, a wide

variety of transition metal cation templates have been employed to construct MIMs, with coordination geometries ranging from square planar ($Pd^{2+}$) [129] and tetrahedral ($Cu^{+}$) [130] to trigonal bipyramidal ($Cu^{2+}$, $Ni^{2+}$, $Zn^{2+}$), [131,132] octahedral ($Co^{3+}$, $Cd^{2+}$, $Fe^{2+}$, $Ni^{2+}$, $Ru^{2+}$) [133–135] and even linear ($Au^{+}$) [136] (**Figure 1.39**).

The versatility of this approach has enabled access to a range of higher order interlocked structures such as hetero[3]catenanes [137] and hetero[3]rotaxanes [138]. Another impressive example obtained via metal templation is Chiu's daisy chain polyrotaxane capable of performing muscle-like contractions. [139]

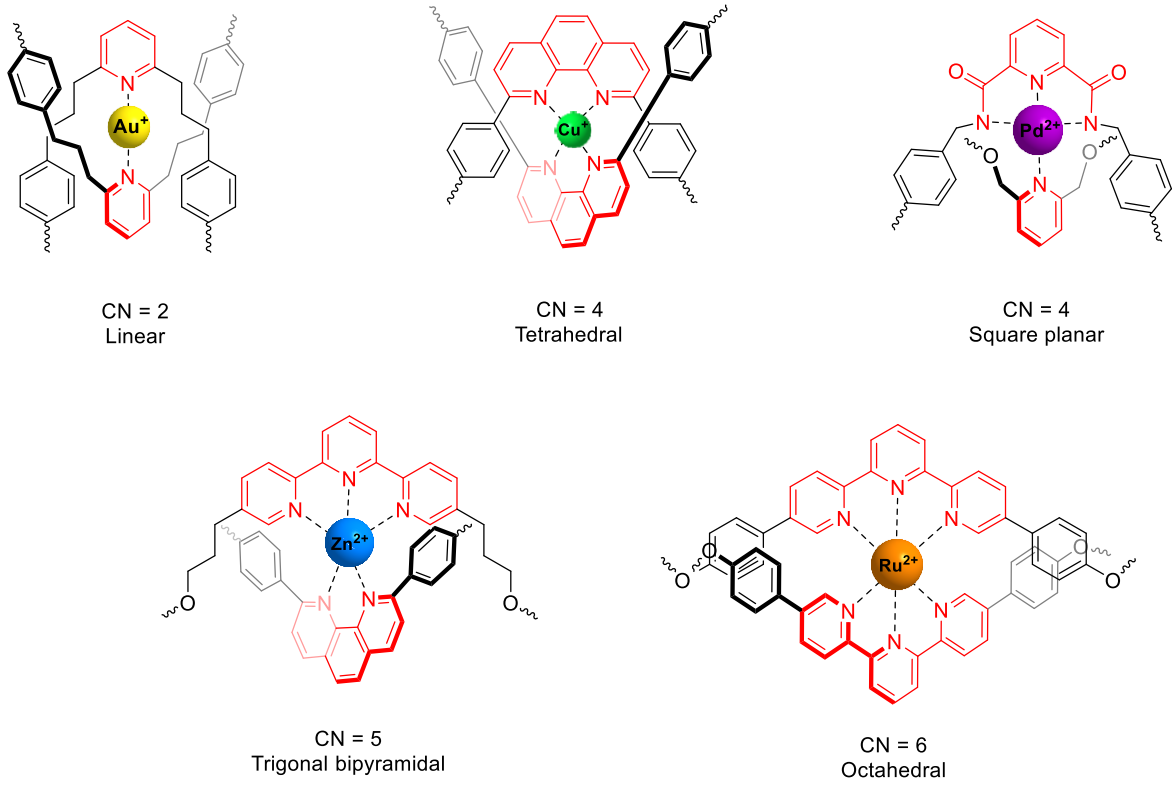
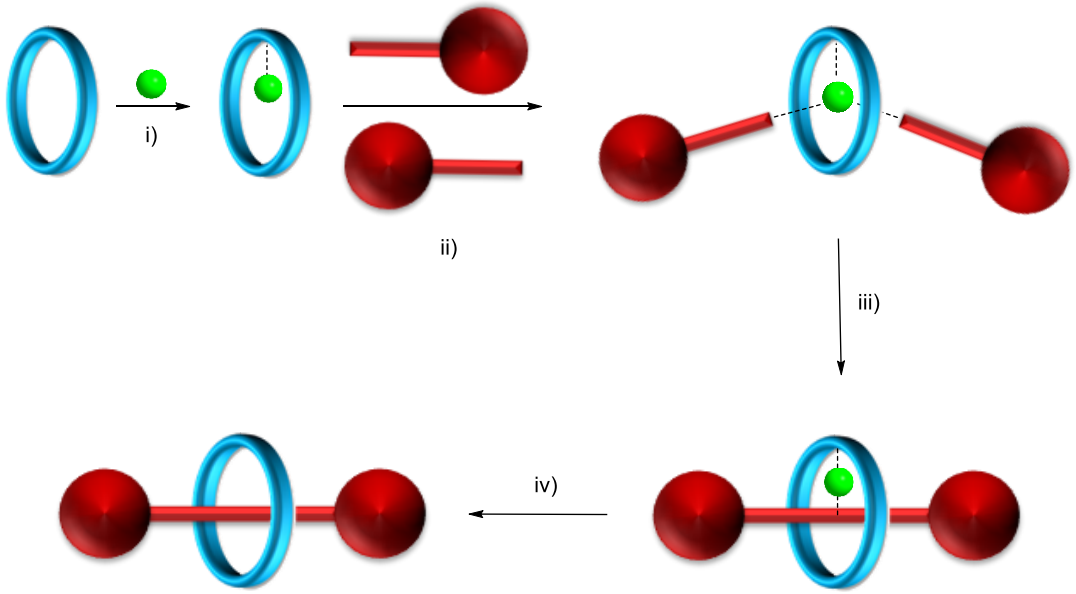



***Figure 1.39.*** *Examples of various coordination geometries employed in passive metal templation.*

Recent efforts have seen the passive metal templation approach expand to include alkali and alkali earth metal cations. The seminal example is Sauvage's $Li^{+}$ - templated doubly interlocked [2]catenane. [140] The favourable ion-dipole interactions between $Na^{+}$ and oligo(ethylene glycol) chains have been exploited by Chiu in the synthesis of a [2]catenane, [141] while Beer and co-workers employed $Ba^{2+}$ as a templating agent in the construction of a [2]rotaxane. [142]

In 2006, the groups of Saito [143] and Leigh [144] independently developed the method of active metal templation (AMT) for MIM synthesis, which relies on the metal cation playing a dual role of both template and catalyst (**Scheme 1.2**). Importantly, this elegant approach does not require the presence of permanent coordination sites built into each of the component parts and often, the template can be employed in sub-stoichiometric quantities. [145]




***Scheme 1.2.*** *Simplified scheme highlighting the steps of the AMT mechanism; i) endotopic coordination of the metal cation; ii) coordination of both half-axles to the metal cation; iii) mechanical bond formation; iv) decomplexation of the metal template.*

While the Cu(I)-catalysed azide-alkyne cycloaddition (CuAAC) is the most commonly employed reaction in the active metal template methodology, [146] this principle has been extended to include a wide array of bond forming reactions mediated by various metal ions such as $Cu^{+}$ (Glaser homocoupling of terminal alkynes [147]), $Pd^{2+}$ (Heck cross-coupling [148]), $Ni^{2+}$ ($sp^3$ – $sp^3$ haloalkane homocoupling [149]) and $Zn^{2+}$ ($Zn^{2+}$ – catalysed Diels-Alder reaction [150]). The AMT approach has proven to be amenable to the synthesis of challenging architectures such as a [4]catenane “molecular necklace” [151], a [3]rotaxane molecular sheaf [152] and a trefoil knot [153] (**Figure 1.40**).

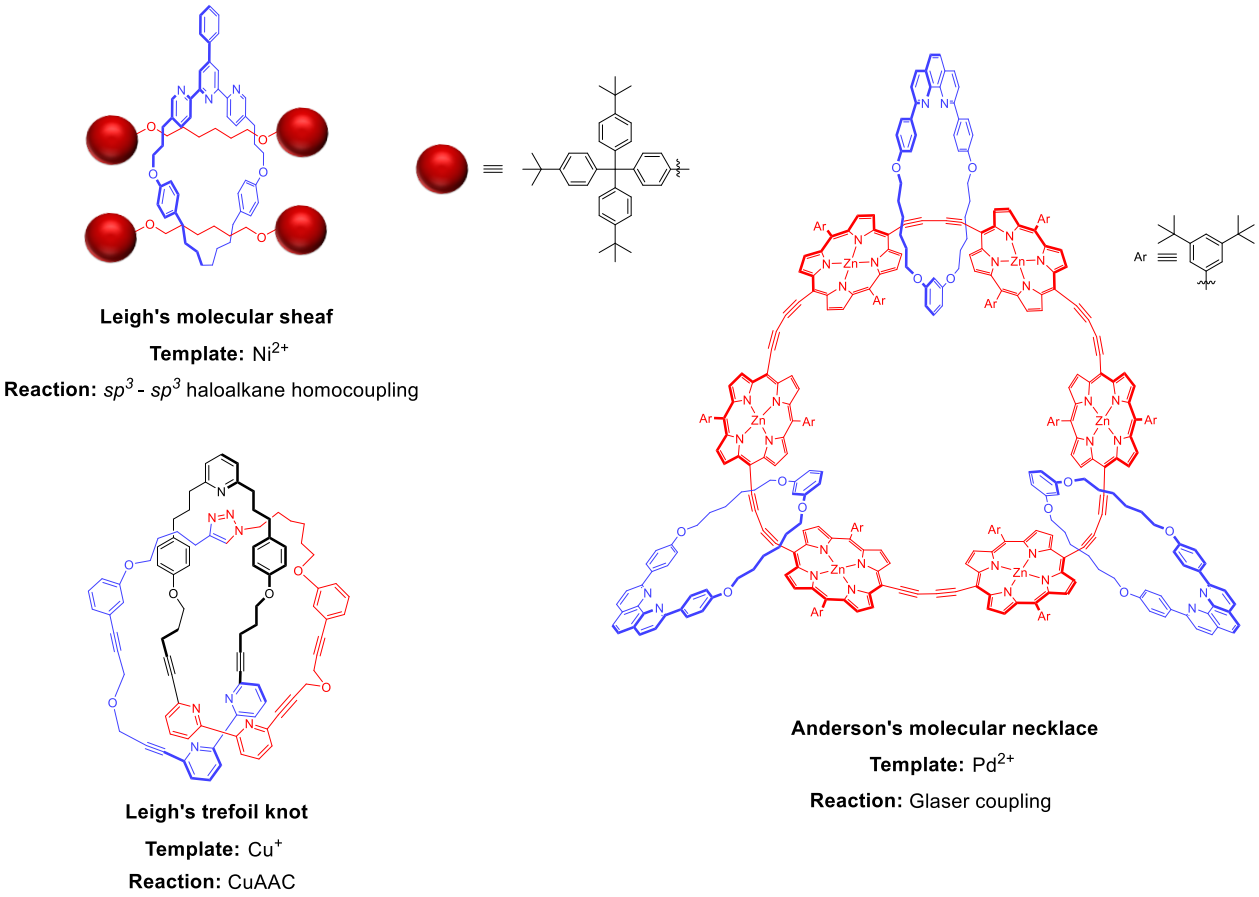



***Figure 1.40.*** *Examples of exotic interlocked structures obtained via the active metal template methodology.*

In parallel with metal templates, a number of organic cationic templating motifs have been developed [115] (**Figure 1.41.a**). Stoddart and co-workers have exploited 4,4'-bipyridinium cations in conjunction with aromatic electron-rich motifs to access challenging higher order structures such as oligocatenanes and oligorotaxanes, a remarkable example being a [5]catenane termed olympiadane (**Figure 1.41.b**). [154] In addition, secondary alkylammonium groups interpenetrate dibenzo-24-crown-8 derivatives to form assemblies stabilised by electrostatics and hydrogen bonding interactions for rotaxane [155–157] and catenane construction [158,159] **(Figure 1.41.c)**.

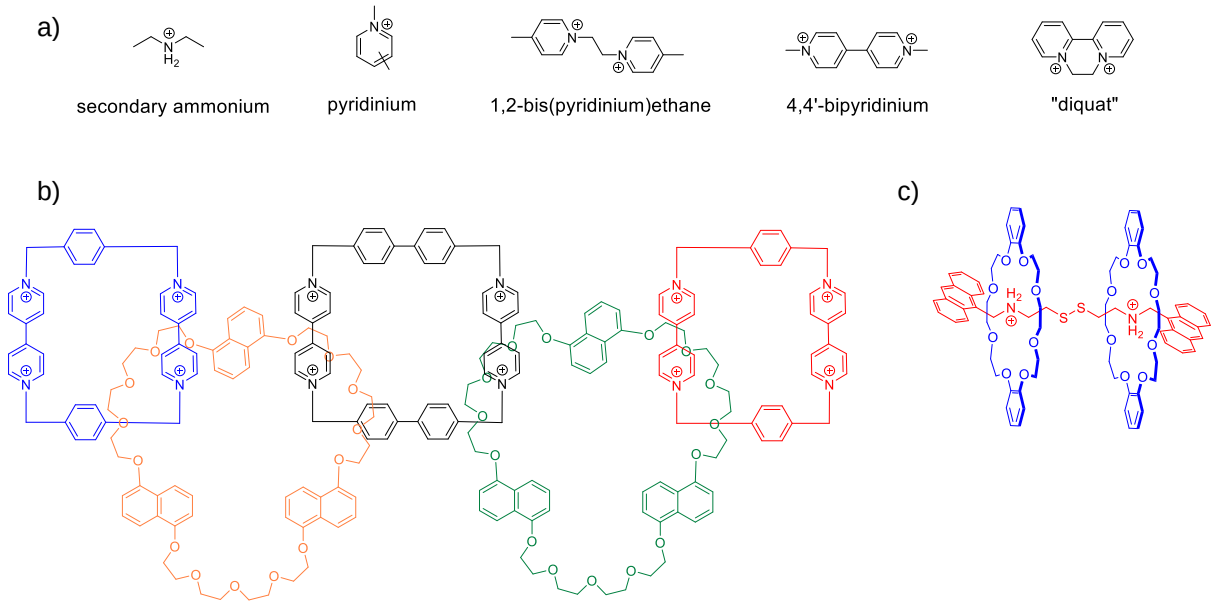
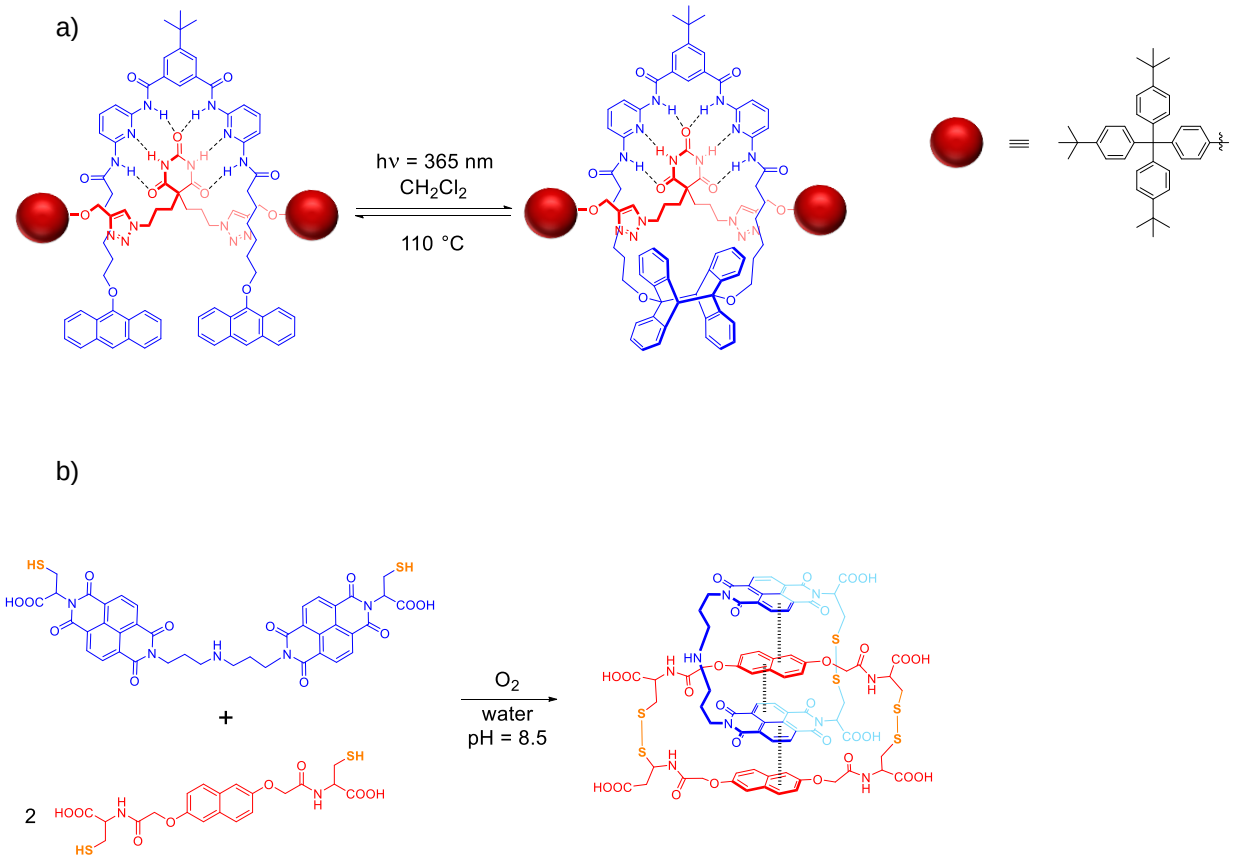



***Figure 1.41.*** *a) Examples of organic cations employed as templates for the construction of MIMs; b) Stoddart's [5]catenane, "olympiadane"; c) Busch's alkylammonium-based [3]rotaxane.* [160]

### 1.4.2.1.2. Neutral templates

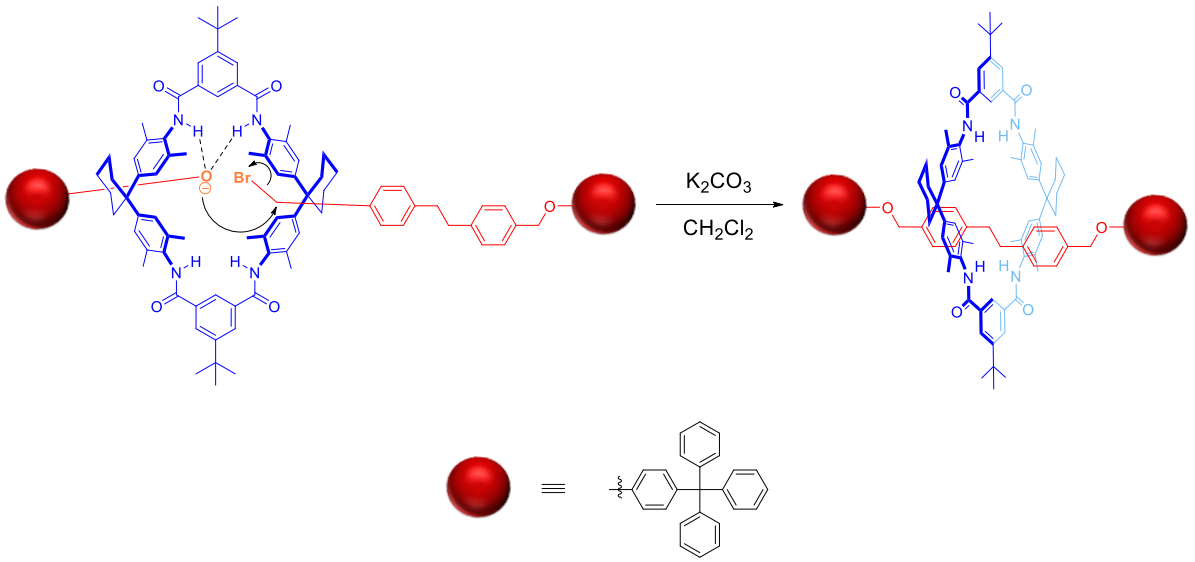
The formation of interlocked molecules can be achieved via hydrogen bonding, aromatic donor-acceptor interactions, or solvophobic effects. Seminal discoveries were made independently by Hunter [161] and Vögtle, [162] who serendipitously synthesised [2]catenanes via an acid chloride and amine condensation reaction. Extending early work on HB templation, McClenaghan synthesised a barbiturate-based [2]rotaxane through HB-mediated assembly followed by a photochemical clipping reaction (**Scheme 1.3.a**). [163] Aromatic donor-acceptor interactions and hydrophobic effects can drive the assembly of mechanomolecules, as exemplified by Pantoş' synthesis of a hetero[2]catenane starting from dialkoxynaphthalene and naphthalenediimide building blocks, in an impressive 93% yield in water (**Scheme 1.3.b**). [164]




***Scheme 1.3.*** *Mechanically interlocked architectures accessed via neutral templates: a) McClenaghan's [2]rotaxane templated by hydrogen bonding; b) Pantoş' [2]catenane templated by π-π interactions and hydrophobic effects.*

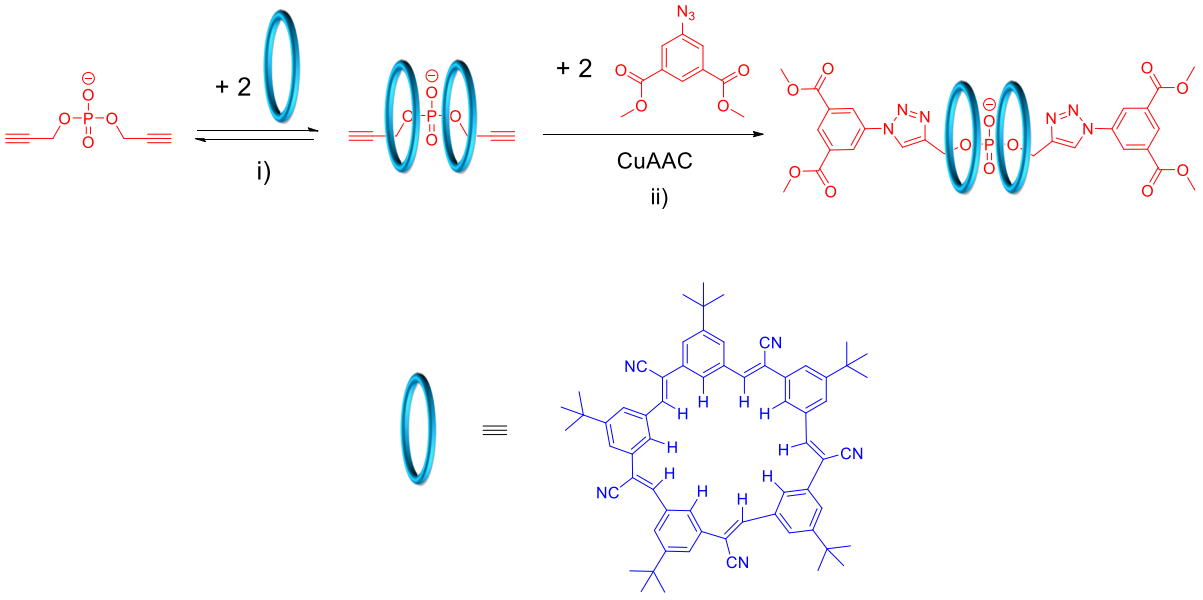
### 1.4.2.1.3. Anionic templates

The use of anions as templates for the assembly of mechanically interlocked molecules was pioneered by Vögtle and co-workers, who devised a 'snapping' procedure to bind a bulky phenoxide anion inside a tetralactam macrocycle, followed by capture via an $S_N2$ reaction with a bulky electrophile (**Scheme 1.4**). [122]



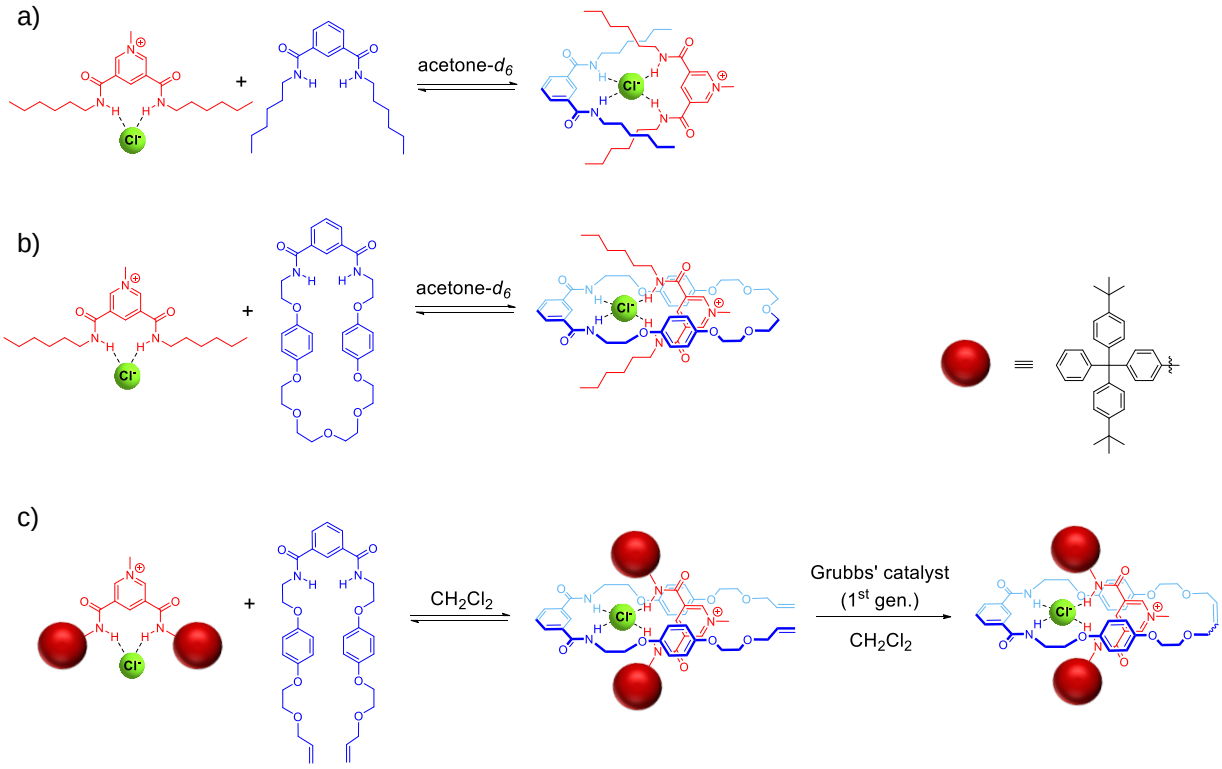

***Scheme 1.4.*** *Vögtle's seminal anion-templated synthesis of a [2]rotaxane.*

An alternative strategy was recently employed by Flood and co-workers, who capitalised on the tendency of a cyanostilbene macrocycle to form 2:1 stoichiometric host-guest complexes with dialkylphosphate anions. [165] Dipropargylphosphate was threaded through two such macrocycles, which was followed by reacting both alkyne termini with an azide-appended stopper component to afford a [3]rotaxane (**Scheme 1.5**).




***Scheme 1.5.*** *The synthesis of Flood's anion-templated [3]rotaxane based on dipropargylphosphate: i) formation of the pseudorotaxane sandwich complex; ii) stoppering via the CuAAC protocol.*

In the case of Vögtle's rotaxane, the anion template is consumed as the reaction progresses, whereas Flood's protocol integrates the anion into the interlocked structure. An alternative anion template strategy has been developed by Beer and co-workers, who conceptualised that a discrete anion could direct a mutually orthogonal assembly of ligands, akin to Sauvage's passive Cu(I) templation. This was realised through the chloride anion-templated assembly of an orthogonal complex between a pyridinium bis-amide and an isophthalamide acyclic component (**Scheme 1.6.a**). [166] A pseudorotaxane was formed between the pyridinium bis-amide chloride salt and a macrocyclic isophthalamide component that was in addition to the $Cl^-$ template further stabilised by additional aromatic donor-acceptor interactions between electron-rich hydroquinone groups in the macrocycle and the electron-poor pyridinium motif (**Scheme 1.6.b**). [167] This strategy was successfully extended to the synthesis of an interlocked structure via a ring-closing metathesis clipping method to afford a [2]rotaxane (**Scheme 1.6.c**). [168] Upon chloride template removal via salt metathesis with $AgPF_6$, the resulting vacant preorganised three-dimensional interlocked cavity was demonstrated to be highly selective for $Cl^-$ over acetate and dihydrogen phosphate anions.




***Scheme 1.6.*** *Formation of chloride-templated assemblies between pyridinium and isophthalamide motifs: a) two acyclic components; b) an acyclic and a macrocyclic component; c) an axle and an acyclic component, subsequently ring-closed to afford a [2]rotaxane.*

Since its inception, discrete anion templation has flourished and has proved a powerful avenue for assembling exotic MIMs such as "handcuff" catenane, [169] a Janus [2]rotaxane, [170] and a triply interlocked molecular capsule [171] (**Figure 1.42**). The scope of anion templates has also been expanded to include sulfate, [172] nitrite, [173] and even weakly coordinating nitrate. [174] More recently, halogen bonding-assisted anion templation methodologies have been employed in the construction of interlocked structures (**Scheme 1.7**). [175–177]

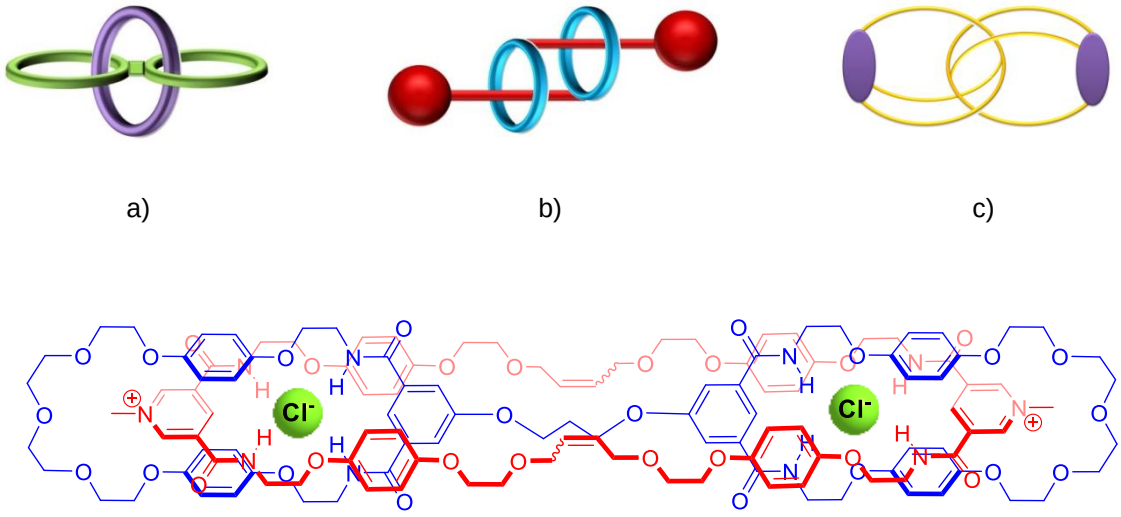
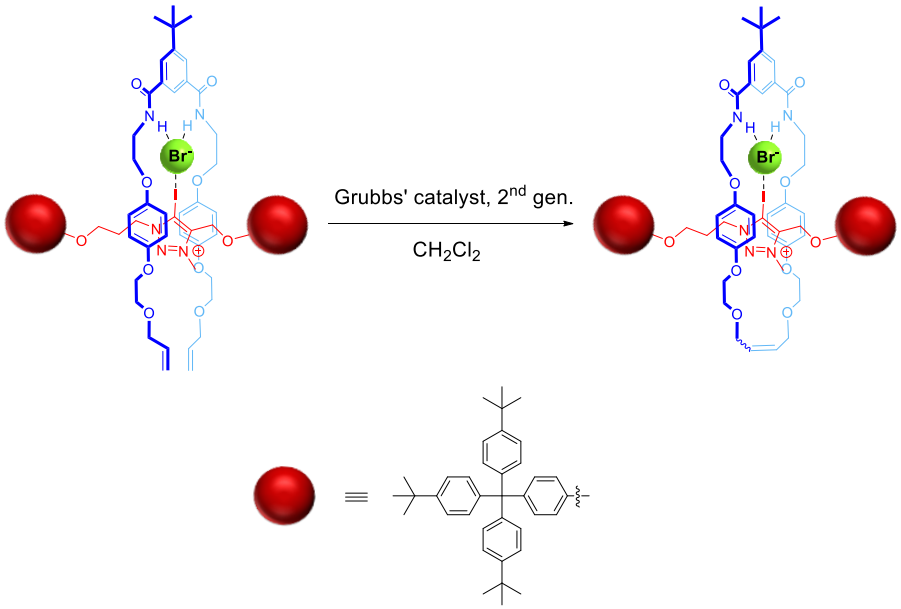



***Figure 1.42.*** *Top: Cartoon representations of mechanically interlocked structures synthesised using the passive metal templation approach: a) a handcuff catenane; b) a Janus rotaxane; c) a triply interlocked molecular capsule. Bottom: Structure of Beer's chloride-templated handcuff catenane.* [169]



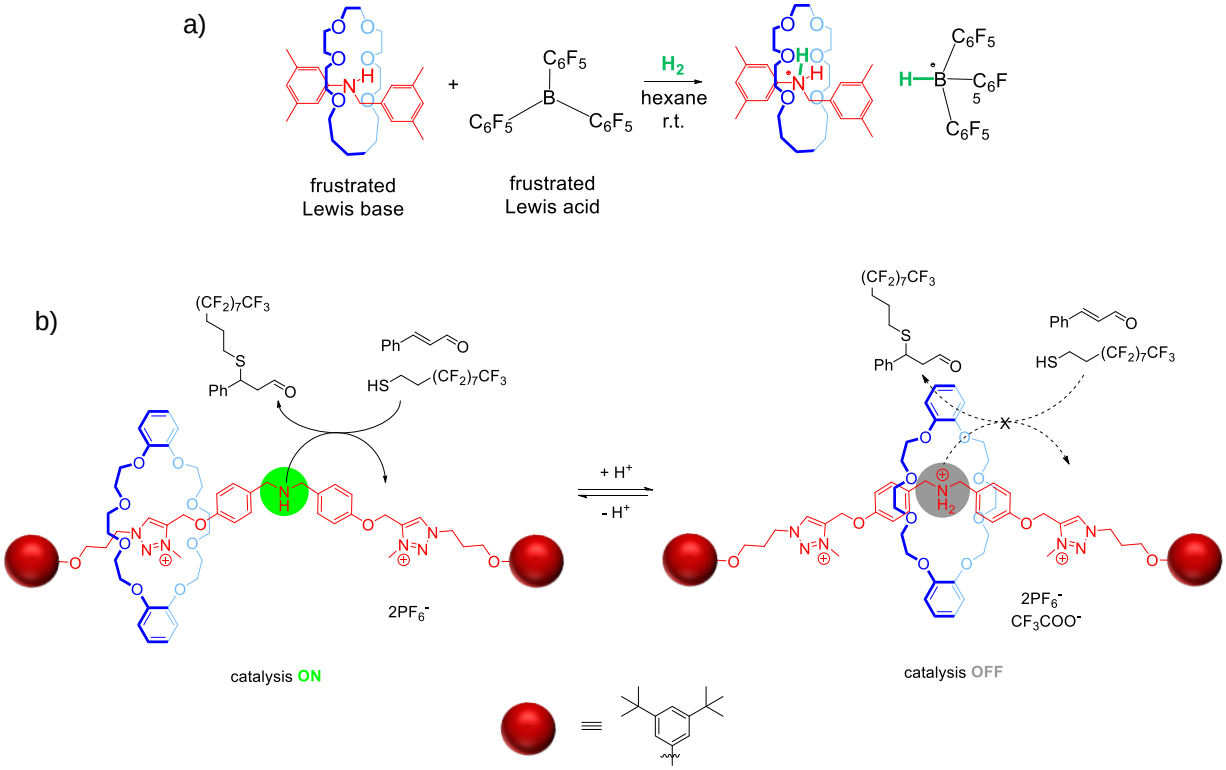

***Scheme 1.7.*** *Synthesis of a [2]rotaxane via XB-assisted bromide templation.* [175]

### 1.4.3. Applications of interlocked structures

As synthetic methods for the construction of mechanically interlocked molecules are being constantly developed and improved upon, their practical applications continue to expand to include analyte recognition and sensing, catalysis, information storage and drug delivery, among many others. [115,178,179]

Catalysis and reactivity

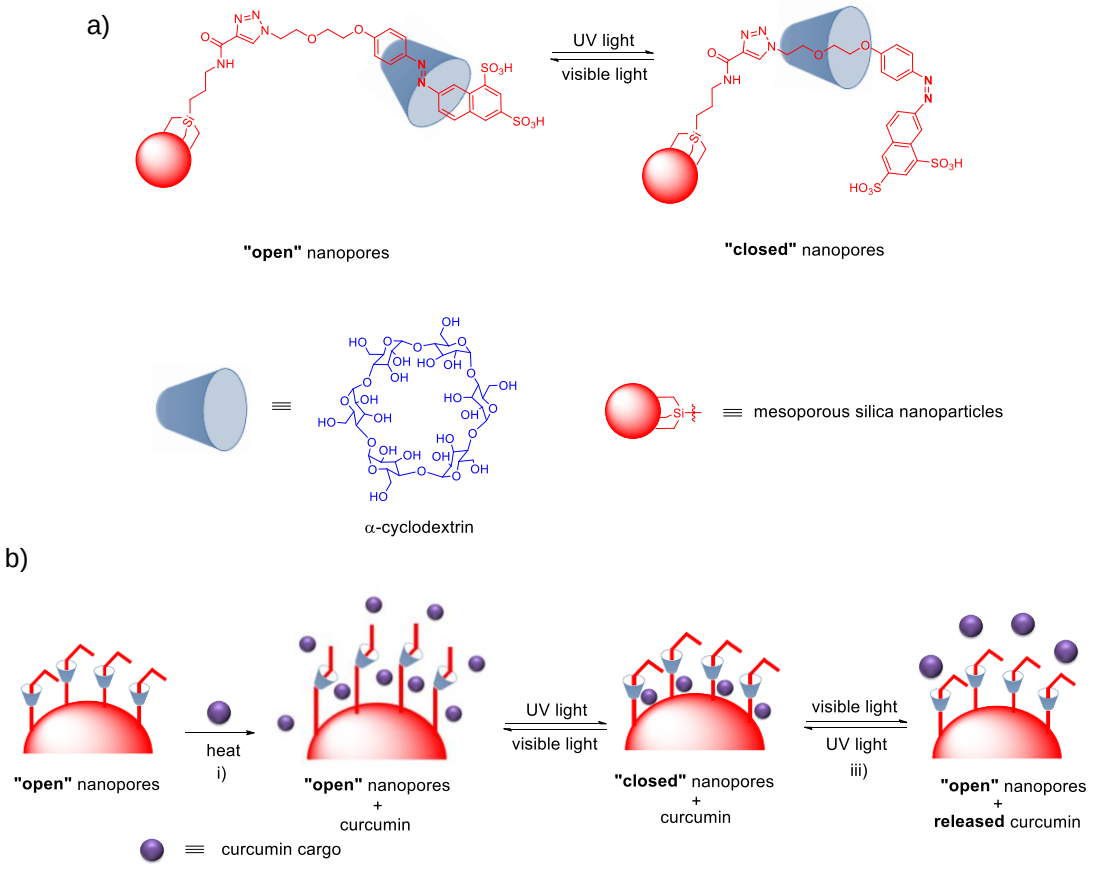
Interlocked structures have found applications as reagents and catalysts. [180,181] For example, Loeb, Stephan, and co-workers exploited the characteristic steric encumbrance of the mechanical bond to design a [2]rotaxane-based frustrated Lewis base which, along with a Lewis acid partner, mediated heterolytic cleavage of $H_2$ at room temperature (**Scheme 1.8.a**). [182] Leigh constructed a [2]rotaxane organocatalyst for a thio-Michael reaction; upon protonation of the secondary amine catalytic unit, the macrocycle shuttles to the middle of the axle, thus blocking access to the catalytic centre (**Scheme 1.8.b**). The process is reversible, implying that its catalytic properties can be tuned by applying simple acid-base stimuli. [183]




***Scheme 1.8.*** *a) Loeb's [2]rotaxane for activation of dihydrogen; b) Leigh's [2]rotaxane which acts as a switchable catalyst.*

Medicine

Exciting potential applications for MIMs in biochemistry and medicine have also been demonstrated. [184–189] Zhao and co-workers have exploited [2]rotaxanes for controlled drug delivery (**Scheme 1.9**). [190] A *trans*-azobenzene axle threading through an α-cyclodextrin macrocycle was attached to mesoporous silica nanoparticles, which were subsequently loaded with the drug curcumin. Irradiation with UV light induces *trans*-to-*cis* isomerisation of the azobenzene moiety, which causes the macrocycle to shuttle closer to the surface of the particles, physically blocking the nanopores and effectively trapping the curcumin molecules inside. Irradiation with visible light reverses the isomerisation process, opening the nanopores and releasing the molecular cargo. Importantly, this photochemically-controlled drug release process was replicated *in vivo* by injecting the nanoparticles into zebrafish larvae.



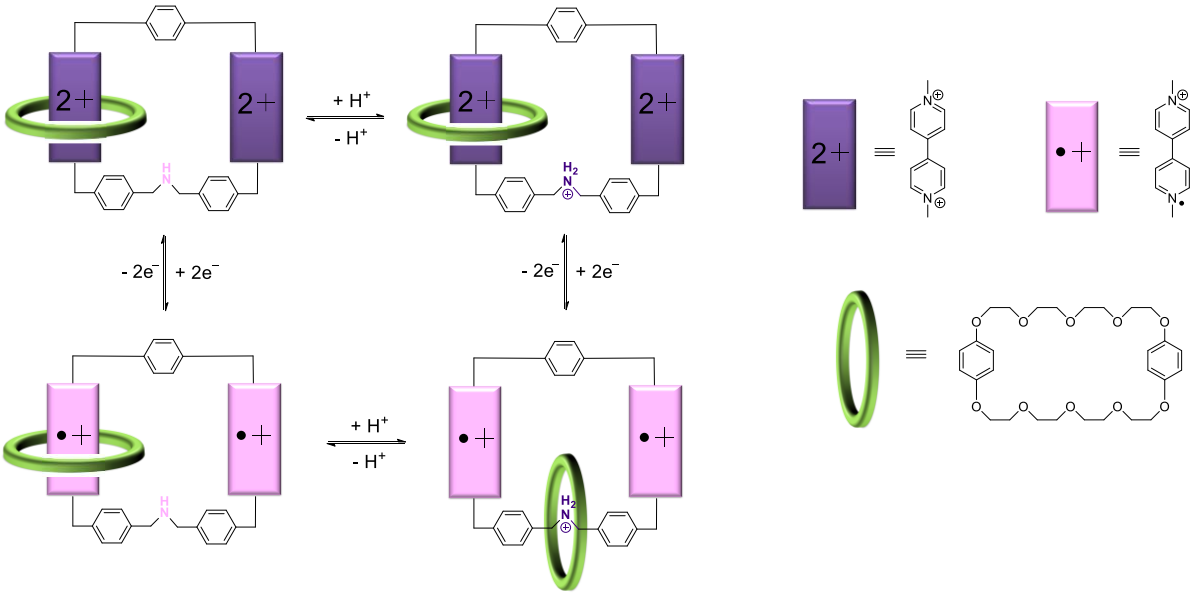

***Scheme 1.9.*** *a) Structure of the silica-appended [2]rotaxane, showing how isomerisation of the azobenzene unit enables shuttling of the cyclodextrin macrocycle along the axis, which controls the "open" or "closed" conformation of the nanopores.*

*b) Cartoon representation of the operating mechanism of photothermal drug release: i) loading of the curcumin cargo; ii) closing of the nanopores to trap the cargo inside; iii) opening of the nanopores to release the cargo.*

Information storage and processing

There is growing interest in employing mechanically interlocked structures for molecular computation owing to their versatility in responding to a wide variety of external stimuli and their nanoscale dimensions which could enable device miniaturisation. [115]

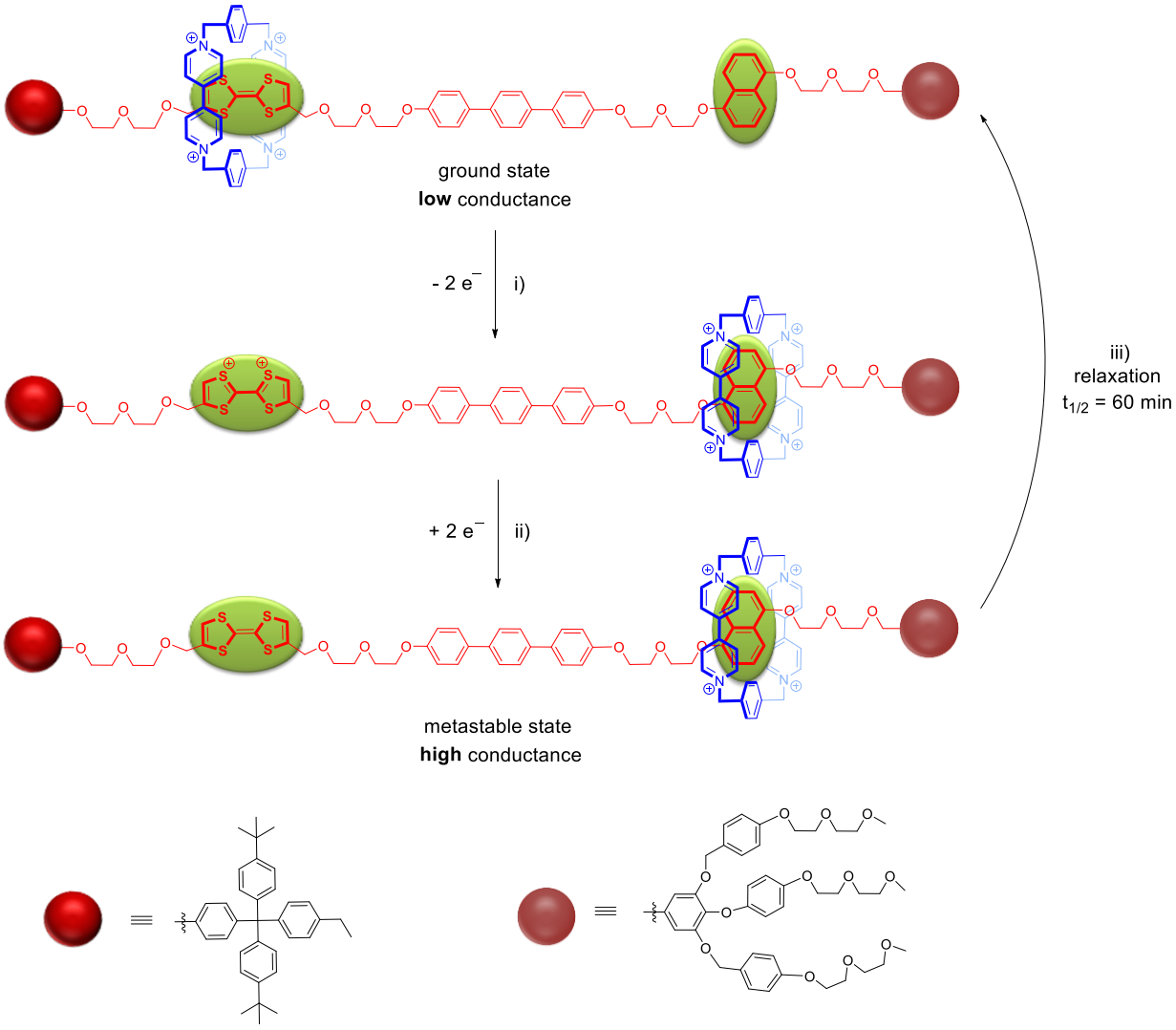
A logic gate produces a sole output, which is dependent on the input(s). In the case of logic gates based on mechanomolecules, the input is the applied stimulus, whereas the output is a structural change. A representative example is a [2]catenane designed by Stoddart and co-workers (**Scheme 1.10**). The system is susceptible to either redox stimuli via the bipyridinium units or acid-base stimuli via the ammonium moiety; however, the hydroquinone-based macrocycle encircles the latter solely in environments that are simultaneously acidic and reducing, which makes it a prototype *AND* logic gate. [191]




***Scheme 1.10.*** *Cartoon representation highlighting the* AND *logic exhibited by Stoddart's [2]catenane.*

The same group exploited interlocked structures for practical information processing applications. Previous research by Choi and co-workers showed a bistable [2]rotaxane could be switched from a co-conformation with low conductance to another with high conductance by applying redox stimuli, with the latter slowly relaxing to the former with a half-life of 60 minutes (**Scheme 1.11**). [192] Based on these observations, it was conceptualised that the [2]rotaxane could serve as a data storage element. This was achieved by incorporating a monolayer of switchable [2]rotaxane molecules into a memory circuit; the resulting device

had an unprecedented density of $10^{11}$ bits·cm$^{-2}$ and was capable of storing and reading small strings of information. [193]




***Scheme 1.11.*** *The molecular processes that enable Stoddart's memory circuit to function: i) oxidation of the tetrathiafulvalene (TTF) unit and translocation of the macrocycle to the naphthalene station; ii) reduction of the positively charged TTF unit; iii) relaxation of the metastable state to the ground state.*

## Guest recognition and sensing

Mechanically interlocked molecules often contain shielded and three-dimensional binding cavities, which makes them amenable to selective guest recognition processes. There are a number of examples of designed MIM host systems being used for recognition and sensing of charged and neutral guests. [194–197]

Of particular relevance to this thesis is the application of MIMs to anion recognition and sensing, as exemplified in **Figure 1.43**. Smith and co-workers designed a squaraine-based [2]rotaxane (**Figure 1.43.a**) which was found to selectively sense $Cl^-$ over heavier halides in acetone by producing a colorimetric and fluorescent response upon addition of TBACl. [198] Jeong and co-workers have exploited indolocarbazole motifs to synthesise a homo[2]catenane that was found to be selective for $Cl^-$ over more basic anions such as $AcO^-$, $H_2PO_4$, or $N_3^-$ in 1:99 $D_2O$/acetone-$d_6$ (*v/v*) (**Figure 1.43.b**). [172] Another impressive example is Beer's [3]rotaxane that functions as a naked-eye anion sensor in $CHCl_3$. (**Figure 1.43.c**). Upon addition of $NO_3^-$, the two macrocycles shuttle from the periphery of the axle towards the central XB donor sites to form a sandwich complex with the anion; the loss of the donor-acceptor interactions between the hydroquinone motifs on the macrocycles and the NDI moieties on the axle leads to a visible colour change from orange to colourless. [199]

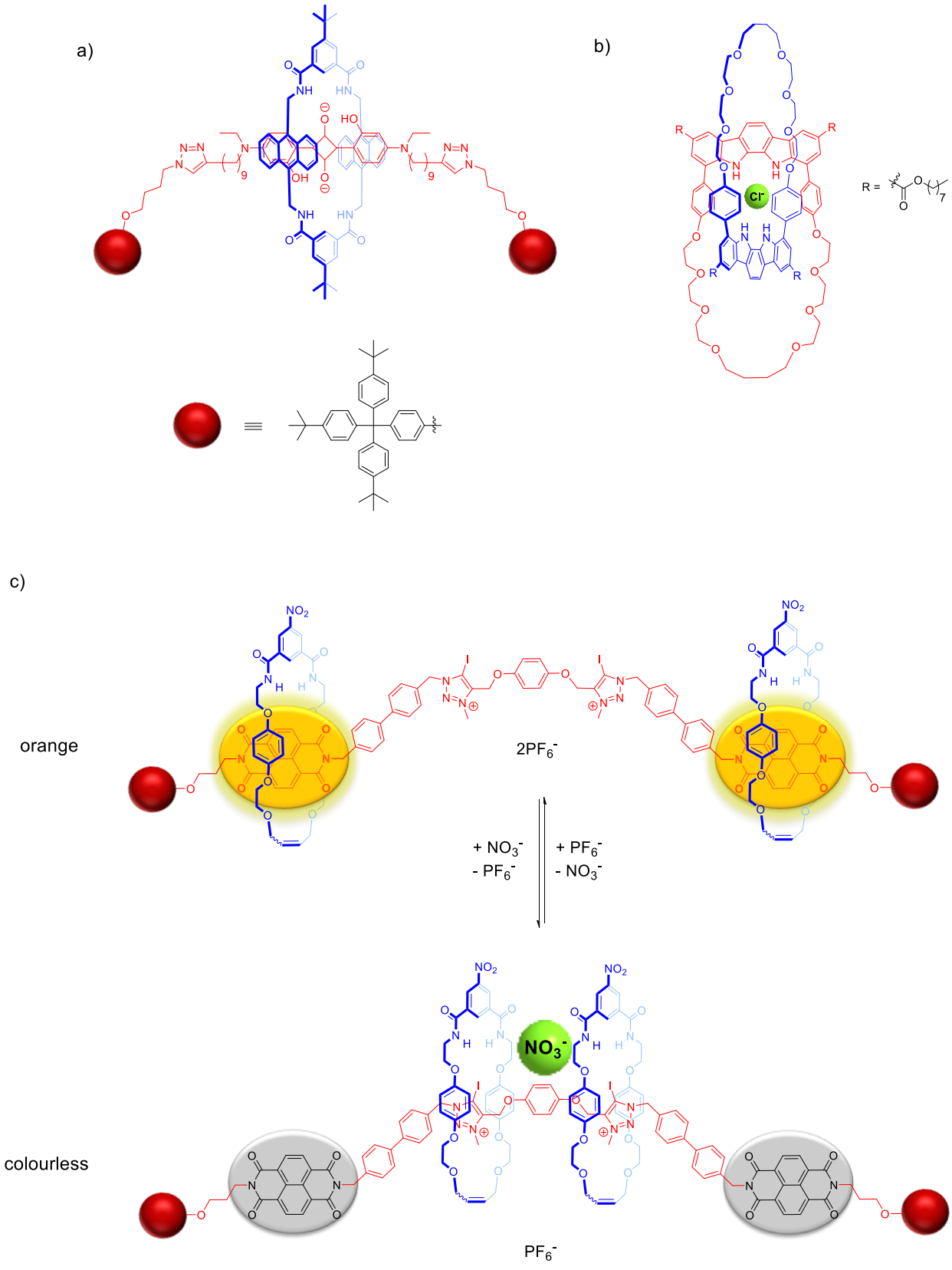



***Figure 1.43.*** *Representative examples of interlocked structures employed for anion recognition and sensing: a) a chiral [2]rotaxane for anion enantiodiscrimination; b) a [2]rotaxane for luminescent sensing of iodide in water; c) a [3]rotaxane molecular shuttle for naked-eye detection of nitrate.*

### 1.5. Project aims

XB hosts for anions are an emerging area of research in supramolecular chemistry. As previously illustrated in this chapter, receptors incorporating XB donors often display superior anion affinities compared to their HB analogues; however, such examples are relatively rare compared to HB receptors, especially those that function in competitive, protic media.

The objective of this thesis was to combine the XB 1,2,3-iodotriazole moiety and a variety of HB N – H donors into acyclic and MIM structural frameworks to produce novel host systems for anion recognition in protic and aprotic organic media. A wide variety of such hosts are synthesised and their anion binding trends elucidated, compared, and contrasted.

**Chapter 2** concerns the synthesis of a family of acyclic and interlocked XB/HB [2]rotaxane hosts incorporating the amido-triazole motif via either active metal or discrete anion templating methodologies. This allows for a detailed study and comparison of their anion binding behaviour. Thereafter, the effect of various parameters such as host charge, the presence of the mechanical bond, and solvent hydration on selectivity trends is elucidated.

**Chapter 3** focuses on the incorporation of one or more 1,2,3-(iodo)triazole motifs onto acyclic (thio)urea-based frameworks and its implications for halide and dicarboxylate binding strength and selectivity. Attempts to construct analogous macrocyclic and interlocked structures are also outlined.

**Chapter 4** investigates the use of perfluoroaryl motifs appended onto mixed carbazole-triazole scaffolds for anion recognition and sensing. Furthermore, attempts to extend these acyclic structures to macrocyclic and interlocked hosts are detailed.

### 1.6. References


1. A. L. Lehninger, D. L. Nelson and M. M. Cox, Lehninger principles of biochemistry, W.H. Freeman, New York, 4th ed., **2005**.
2. W. Wang, E. Y. Wu, H. W. Hellinga and L. S. Beese, *J. Biol. Chem.*, **2012**, 287, 28215–28226.
3. P. J. Cragg, Supramolecular chemistry: from biological inspiration to biomedical applications, Springer, Dordrecht ; New York, **2010**.
4. J. W. Steed and J. L. Atwood, Supramolecular chemistry, Wiley, Chichester, UK, 2nd ed., **2009**.
5. E. Fischer, *Berichte Dtsch. Chem. Ges.*, **1894**, 27, 2985–2993.
6. D. E. Koshland, *Angew. Chem. Int. Ed. Engl.*, **1995**, 33, 2375–2378.
7. J.-M. Lehn, *Angew. Chem. Int. Ed. Engl.*, **1988**, 27, 89–112.
8. E. P. Kyba, R. C. Helgeson, K. Madan, G. W. Gokel, T. L. Tarnowski, S. S. Moore and D. J. Cram, *J. Am. Chem. Soc.*, **1977**, 99, 2564–2571.
9. J.-M. Lehn, *Proc. Natl. Acad. Sci.*, **2002**, 99, 4763–4768.
10. C. J. Pedersen, *J. Am. Chem. Soc.*, **1967**, 89, 7017–7036.
11. H. K. Frensdorff, *J. Am. Chem. Soc.*, **1971**, 93, 600–606.
12. C. J. Pedersen, *Angew. Chem. Int. Ed. Engl.*, **1988**, 27, 1021–1027.
13. D. J. Cram, *Angew. Chem. Int. Ed. Engl.*, **1988**, 27, 1009–1020.
14. N. Ponnuswamy, F. B. L. Cougnon, J. M. Clough, G. D. Pantos and J. K. M. Sanders, *Science*, **2012**, 338, 783–785.
15. K. S. Chichak, *Science*, **2004**, 304, 1308–1312.
16. S. Kassem, A. T. L. Lee, D. A. Leigh, V. Marcos, L. I. Palmer and S. Pisano, *Nature*, **2017**, 549, 374–378.
17. T. Kudernac, N. Ruangsupapichat, M. Parschau, B. Maciá, N. Katsonis, S. R. Harutyunyan, K.-H. Ernst and B. L. Feringa, *Nature*, **2011**, 479, 208–211.
18. J. F. Stoddart, *Angew. Chem. Int. Ed.*, **2017**, 56, 11094–11125.
19. J.-P. Sauvage, *Angew. Chem. Int. Ed.*, **2017**, 56, 11080–11093.
20. B. L. Feringa, *Angew. Chem. Int. Ed.*, **2017**, 56, 11060–11078.
21. C. R. Calladine, Understanding DNA: the molecule & how it works, Elsevier Academic Press, San Diego, CA, **2004**.
22. H. A. Krebs, J. Kay and P. D. J. Weitzman, Eds., Krebs' citric acid cycle: half a century and still turning, Biochemical Society, London, **1987**.
23. M. Anderson, R. Gregory, S. Thompson, D. Souza, S. Paul, R. Mulligan, A. Smith and M. Welsh, *Science*, **1991**, 253, 202–205.
24. S. Ayoob and A. K. Gupta, *Crit. Rev. Environ. Sci. Technol.*, **2006**, 36, 433–487.
25. V. H. Smith and D. W. Schindler, *Trends Ecol. Evol.*, **2009**, 24, 201–207.
26. L. Keith and W. Telliard, *Environ. Sci. Technol.*, **1979**, 13, 416–423.
27. S. S. Suthersan, J. Horst, M. Schnobrich, N. Welty, J. McDonough, Remediation engineering: design concepts, CRC Press, 2nd ed., **2017**.
28. N. Kuyucak and A. Akcil, *Miner. Eng.*, **2013**, 50–51, 13–29.
29. E. A. Betterton, *Crit. Rev. Environ. Sci. Technol.*, **2003**, 33, 423–458.
30. R. D. Shannon, *Acta Crystallogr. Sect. A*, **1976**, 32, 751–767.
31. H.-J. Schneider, *Angew. Chem. Int. Ed.*, **2009**, 48, 3924–3977.
32. E. García-España, P. Díaz, J. M. Llinares and A. Bianchi, *Coord. Chem. Rev.*, **2006**, 250, 2952–2986.
33. J. Hormadaly and Y. Marcus, *J. Phys. Chem.*, **1979**, 83, 2843–2848.
34. F. Hofmeister, *Arch. Für Exp. Pathol. Pharmakol.*, **1888**, 24, 247–260.
35. K. D. Collins, *Biophys. Chem.*, **2006**, 119, 271–281.
36. U. Mayer, *Coord. Chem. Rev.*, **1976**, 21, 159–179.
37. J. W. Pflugrath and F. A. Quiocho, *J. Mol. Biol.*, **1988**, 200, 163–180.
38. H. Luecke and F. A. Quiocho, *Nature*, **1990**, 347, 402–406.
39. J. W. Steed, D. R. Turner and K. J. Wallace, Core concepts in supramolecular chemistry and nanochemistry, John Wiley, Chichester, England ; Hoboken, NJ, **2007**.

40. E. V. Anslyn and D. A. Dougherty, Modern physical organic chemistry, University Science, Sausalito, CA, **2006**.
41. J. J. Dannenberg, *J. Am. Chem. Soc.*, **1998**, 120, 5604–5604.
42. F. Guthrie, *J Chem Soc*, **1863**, 16, 239–244.
43. M. H. Kolář and P. Hobza, *Chem. Rev.*, **2016**, 116, 5155–5187.
44. T. Clark, M. Hennemann, J. S. Murray and P. Politzer, *J. Mol. Model.*, **2007**, 13, 291–296.
45. A. Brown and P. D. Beer, *Chem. Commun.*, **2016**, 52, 8645–8658.
46. D. J. R. Duarte, G. L. Sosa, N. M. Peruchena and I. Alkorta, *Phys. Chem. Chem. Phys.*, **2016**, 18, 7300–7309.
47. S. E. Wheeler and K. N. Houk, *J. Am. Chem. Soc.*, **2008**, 130, 10854–10855.
48. D. Quiñonero, C. Garau, A. Frontera, P. Ballester, A. Costa and P. M. Deyà, *Chem. Phys. Lett.*, **2002**, 359, 486–492.
49. C. Garau, A. Frontera, D. Quiñonero, P. Ballester, A. Costa and P. M. Deyà, *ChemPhysChem*, **2003**, 4, 1344–1348.
50. S. T. Schneebeli, M. Frasconi, Z. Liu, Y. Wu, D. M. Gardner, N. L. Strutt, C. Cheng, R. Carmieli, M. R. Wasielewski and J. F. Stoddart, *Angew. Chem. Int. Ed.*, **2013**, 52, 13100–13104.
51. C. R. Martinez and B. L. Iverson, *Chem. Sci.*, **2012**, 3, 2191.
52. J. D. Wuest, *Acc. Chem. Res.*, **1999**, 32, 81–89.
53. P. D. Beer and E. J. Hayes, *Coord. Chem. Rev.*, **2003**, 240, 167–189.
54. L. Fabbrizzi and A. Poggi, *Chem Soc Rev*, **2013**, 42, 1681–1699.
55. S. Arimori, M. G. Davidson, T. M. Fyles, T. G. Hibbert, T. D. James and G. I. Kociok-Köhn, *Chem Commun*, **2004**, 1640–1641.
56. M. Newcomb and M. T. Blanda, *Tetrahedron Lett.*, **1988**, 29, 4261–4264.
57. T. J. Wedge and M. F. Hawthorne, *Coord. Chem. Rev.*, **2003**, 240, 111–128.
58. L. Fabbrizzi, A. Leone and A. Taglietti, *Angew. Chem. Int. Ed.*, **2001**, 40, 3066–3069.
59. M. S. Cubberley and B. L. Iverson, *J. Am. Chem. Soc.*, **2001**, 123, 7560–7563.
60. M. Fernández-Vidal, S. H. White and A. S. Ladokhin, *J. Membr. Biol.*, **2011**, 239, 5–14.
61. N. T. Southall, K. A. Dill and A. D. J. Haymet, *J. Phys. Chem. B*, **2002**, 106, 521–533.
62. C. L. D. Gibb and B. C. Gibb, *J. Am. Chem. Soc.*, **2011**, 133, 7344–7347.
63. V. Havel, M. A. Yawer and V. Sindelar, *Chem. Commun.*, **2015**, 51, 4666–4669.
64. K. I. Assaf, M. S. Ural, F. Pan, T. Georgiev, S. Simova, K. Rissanen, D. Gabel and W. M. Nau, *Angew. Chem. Int. Ed.*, **2015**, 54, 6852–6856.
65. D. J. Cram, *Angew. Chem. Int. Ed. Engl.*, **1986**, 25, 1039–1057.
66. P. V. Santacroce, J. T. Davis, M. E. Light, P. A. Gale, J. C. Iglesias-Sánchez, P. Prados and R. Quesada, *J. Am. Chem. Soc.*, **2007**, 129, 1886–1887.
67. A. Szumna and J. Jurczak, *Eur. J. Org. Chem.*, **2001**, 2001, 4031–4039.
68. F. P. Schmidtchen, *Angew. Chem. Int. Ed. Engl.*, **1977**, 16, 720–721.
69. P. J. Garratt, A. J. Ibbett, J. E. Ladbury, R. O'Brien, M. B. Hursthouse and K. M. Abdul Malik, *Tetrahedron*, **1998**, 54, 949–968.
70. J.-F. Ayme, J. E. Beves, D. A. Leigh, R. T. McBurney, K. Rissanen and D. Schultz, *Nat. Chem.*, **2012**, 4, 15–20.
71. C. H. Park and H. E. Simmons, *J. Am. Chem. Soc.*, **1968**, 90, 2431–2432.
72. M. W. Hosseini and J.-M. Lehn, *Helv. Chim. Acta*, **1986**, 69, 587–603.
73. M. W. Hosseini, J.-M. Lehn and M. P. Mertes, *Helv. Chim. Acta*, **1983**, 66, 2454–2466.
74. P. Blondeau, M. Segura, R. Pérez-Fernández and J. de Mendoza, *Chem Soc Rev*, **2007**, 36, 198–210.
75. A. Metzger, V. M. Lynch and E. V. Anslyn, *Angew. Chem. Int. Ed. Engl.*, **1997**, 36, 862–865.
76. A. Echavarren, A. Galan, J. M. Lehn and J. De Mendoza, *J. Am. Chem. Soc.*, **1989**, 111, 4994–4995.
77. N. J. Williams, C. A. Seipp, K. A. Garrabrant, R. Custelcean, E. Holguin, J. K. Keum, R. J. Ellis and B. A. Moyer, *Chem. Commun.*, **2018**, 54, 10048–10051.
78. J. Yoon, S. K. Kim, N. J. Singh and K. S. Kim, *Chem. Soc. Rev.*, **2006**, 35, 355.
79. L. Yang, S. Qin, X. Su, F. Yang, J. You, C. Hu, R. Xie and J. Lan, *Org Biomol Chem*, **2010**, 8, 339–348.
80. H. Kim and J. Kang, *Tetrahedron Lett.*, **2005**, 46, 5443–5445.

81. H.-Y. Gong, B. M. Rambo, E. Karnas, V. M. Lynch and J. L. Sessler, *Nat. Chem.*, **2010**, 2, 406–409.
82. P. A. Gale and W. Dehaen, Eds., *Anion Recognition in Supramolecular Chemistry*, Springer Berlin Heidelberg, Berlin, Heidelberg, **2010**, vol. 24.
83. A. Kumar and P. S. Pandey, *Org. Lett.*, **2008**, 10, 165–168.
84. B. Schulze, C. Friebe, M. D. Hager, W. Günther, U. Köhn, B. O. Jahn, H. Görls and U. S. Schubert, *Org. Lett.*, **2010**, 12, 2710–2713.
85. N. G. White, S. Carvalho, V. Félix and P. D. Beer, *Org. Biomol. Chem.*, **2012**, 10, 6951.
86. M. M. G. Antonisse and D. N. Reinhoudt, *Chem. Commun.*, **1998**, 443–448.
87. R. A. Pascal, J. Spergel and D. Van Engen, *Tetrahedron Lett.*, **1986**, 27, 4099–4102.
88. K. Kavallieratos, S. R. de Gala, D. J. Austin and R. H. Crabtree, *J. Am. Chem. Soc.*, **1997**, 119, 2325–2326.
89. M. Arunachalam and P. Ghosh, *Org. Lett.*, **2010**, 12, 328–331.
90. L. Molina, E. Moreno-Clavijo, A. J. Moreno-Vargas, A. T. Carmona and I. Robina, *Eur. J. Org. Chem.*, **2010**, 2010, 4049–4055.
91. S. O. Kang, D. Powell, V. W. Day and K. Bowman-James, *Angew. Chem.*, **2006**, 118, 1955–1959.
92. Y. Suzuki, R. Yazaki, N. Kumagai and M. Shibasaki, *Angew. Chem. Int. Ed.*, **2009**, 48, 5026–5029.
93. K. B. Wiberg and D. J. Rush, *J. Am. Chem. Soc.*, **2001**, 123, 2038–2046.
94. E. Fan, S. A. Van Arman, S. Kincaid and A. D. Hamilton, *J. Am. Chem. Soc.*, **1993**, 115, 369–370.
95. P. Hamankiewicz, J. M. Granda and J. Jurczak, *Tetrahedron Lett.*, **2013**, 54, 5608–5611.
96. L. Qin, A. Hartley, P. Turner, R. B. P. Elmes and K. A. Jolliffe, *Chem. Sci.*, **2016**, 7, 4563–4572.
97. S. J. Wezenberg and B. L. Feringa, *Org. Lett.*, **2017**, 19, 324–327.
98. J. L. Sessler, S. Camiolo and P. A. Gale, *Coord. Chem. Rev.*, **2003**, 240, 17–55.
99. P. A. Gale, J. L. Sessler, V. Král and V. Lynch, *J. Am. Chem. Soc.*, **1996**, 118, 5140–5141.
100. K.-J. Chang, B.-N. Kang, M.-H. Lee and K.-S. Jeong, *J. Am. Chem. Soc.*, **2005**, 127, 12214–12215.
101. M. Yu, H. Lin and H. Lin, *Supramol. Chem.*, **2008**, 20, 357–361.
102. V. S. Bryantsev and B. P. Hay, *J. Am. Chem. Soc.*, **2005**, 127, 8282–8283.
103. W. B. Farnham, D. C. Roe, D. A. Dixon, J. C. Calabrese and R. L. Harlow, *J. Am. Chem. Soc.*, **1990**, 112, 7707–7718.
104. Y. Li and A. H. Flood, *Angew. Chem. Int. Ed.*, **2008**, 47, 2649–2652.
105. A. H. Flood, *Beilstein J. Org. Chem.*, **2016**, 12, 611–627.
106. S. Lee, B. E. Hirsch, Y. Liu, J. R. Dobscha, D. W. Burke, S. L. Tait and A. H. Flood, *Chem. - Eur. J.*, **2016**, 22, 560–569.
107. S. H. Jungbauer and S. M. Huber, *J. Am. Chem. Soc.*, **2015**, 137, 12110–12120.
108. F. Zapata, A. Caballero, P. Molina, I. Alkorta and J. Elguero, *J. Org. Chem.*, **2014**, 79, 6959–6969.
109. J. Y. C. Lim and P. D. Beer, *Chem. Commun.*, **2015**, 51, 3686–3688.
110. M. G. Sarwar, B. Dragisic, S. Sagoo and M. S. Taylor, *Angew. Chem. Int. Ed.*, **2010**, 49, 1674–1677.
111. N. H. Evans and P. D. Beer, *Angew. Chem. Int. Ed.*, **2014**, 53, 11716–11754.
112. S. Guha and S. Saha, *J. Am. Chem. Soc.*, **2010**, 132, 17674–17677.
113. E. Mulugeta, Q. He, D. Sareen, S.-J. Hong, J. H. Oh, V. M. Lynch, J. L. Sessler, S. K. Kim and C.-H. Lee, *Chem*, **2017**, 3, 1008–1020.
114. H. L. Frisch and E. Wasserman, *J. Am. Chem. Soc.*, **1961**, 83, 3789–3795.
115. C. J. Bruns and J. F. Stoddart, The nature of the mechanical bond: from molecules to machines, Wiley, Hoboken, New Jersey, **2017**.
116. R. Kovall, *Science*, **1997**, 277, 1824–1827.
117. K. Subramanian, *Nucleic Acids Res.*, **2003**, 31, 1585–1596.
118. B. Hudson and J. Vinograd, *Nature*, **1967**, 216, 647–652.
119. S. Spengler, A. Stasiak and N. Cozzarelli, *Cell*, **1985**, 42, 325–334.

120. S. J. Cantrill, D. A. Fulton, M. C. . Fyfe, J. F. Stoddart, A. J. . White and D. J. Williams, *Tetrahedron Lett.*, **1999**, 40, 3669–3672.
121. J. Wu, K. C.-F. Leung and J. F. Stoddart, *Proc. Natl. Acad. Sci.*, **2007**, 104, 17266–17271.
122. G. M. Hübner, J. Gläser, C. Seel and F. Vögtle, *Angew. Chem. Int. Ed.*, **1999**, 38, 383–386.
123. S.-Y. Hsueh, J.-L. Ko, C.-C. Lai, Y.-H. Liu, S.-M. Peng and S.-H. Chiu, *Angew. Chem. Int. Ed.*, **2011**, 50, 6643–6646.
124. C.-W. Chiu, C.-C. Lai and S.-H. Chiu, *J. Am. Chem. Soc.*, **2007**, 129, 3500–3501.
125. X. Huang, S. Huang, B. Zhai, Y. Zhang, Y. Xu and Q. Wang, *Tetrahedron Lett.*, **2012**, 53, 6414–6417.
126. E. Wasserman, *J. Am. Chem. Soc.*, **1960**, 82, 4433–4434.
127. C. Dietrich-Buchecker, J. . Sauvage and J. . Kintzinger, *Tetrahedron Lett.*, **1983**, 24, 5095–5098.
128. C. Dietrich-Buchecker and J.-P. Sauvage, *Tetrahedron*, **1990**, 46, 503–512.
129. A.-M. Fuller, D. A. Leigh, P. J. Lusby, I. D. H. Oswald, S. Parsons and D. B. Walker, *Angew. Chem. Int. Ed.*, **2004**, 43, 3914–3918.
130. C. Wu, P. R. Lecavalier, Y. X. Shen and H. W. Gibson, *Chem. Mater.*, **1991**, 3, 569–572.
131. S. Saha, S. Santra, B. Akhuli and P. Ghosh, *J. Org. Chem.*, **2014**, 79, 11170–11178.
132. C. Hamann, J.-M. Kern and J.-P. Sauvage, *Inorg. Chem.*, **2003**, 42, 1877–1883.
133. D. A. Leigh, P. J. Lusby, R. T. McBurney, A. Morelli, A. M. Z. Slawin, A. R. Thomson and D. B. Walker, *J. Am. Chem. Soc.*, **2009**, 131, 3762–3771.
134. D. A. Leigh, P. J. Lusby, S. J. Teat, A. J. Wilson and J. K. Y. Wong, *Angew. Chem. Int. Ed.*, **2001**, 40, 1538–1543.
135. J.-C. Chambron, J.-P. Collin, V. Heitz, D. Jouvenot, J.-M. Kern, P. Mobian, D. Pomeranc and J.-P. Sauvage, *Eur. J. Org. Chem.*, **2004**, 2004, 1627–1638.
136. S. M. Goldup, D. A. Leigh, P. J. Lusby, R. T. McBurney and A. M. Z. Slawin, *Angew. Chem. Int. Ed.*, **2008**, 47, 6999–7003.
137. J. D. Megiatto and D. I. Schuster, *Chem. - Eur. J.*, **2009**, 15, 5444–5448.
138. A.-M. L. Fuller, D. A. Leigh and P. J. Lusby, *J. Am. Chem. Soc.*, **2010**, 132, 4954–4959.
139. J.-C. Chang, S.-H. Tseng, C.-C. Lai, Y.-H. Liu, S.-M. Peng and S.-H. Chiu, *Nat. Chem.*, **2017**, 9, 128–134.
140. C. Dietrich-Buchecker and J.-P. Sauvage, *Chem. Commun.*, **1999**, 615–616.
141. S.-T. Tung, C.-C. Lai, Y.-H. Liu, S.-M. Peng and S.-H. Chiu, *Angew. Chem. Int. Ed.*, **2013**, 52, 13269–13272.
142. L. M. Hancock and P. D. Beer, *Chem. Commun.*, **2011**, 47, 6012.
143. S. Saito, E. Takahashi and K. Nakazono, *Org. Lett.*, **2006**, 8, 5133–5136.
144. V. Aucagne, K. D. Hänni, D. A. Leigh, P. J. Lusby and D. B. Walker, *J. Am. Chem. Soc.*, **2006**, 128, 2186–2187.
145. J. D. Crowley, S. M. Goldup, A.-L. Lee, D. A. Leigh and R. T. McBurney, *Chem. Soc. Rev.*, **2009**, 38, 1530.
146. K. D. Hänni and D. A. Leigh, *Chem Soc Rev*, **2010**, 39, 1240–1251.
147. Y. Sato, R. Yamasaki and S. Saito, *Angew. Chem. Int. Ed.*, **2009**, 48, 504–507.
148. J. D. Crowley, K. D. Hänni, A.-L. Lee and D. A. Leigh, *J. Am. Chem. Soc.*, **2007**, 129, 12092–12093.
149. S. M. Goldup, D. A. Leigh, R. T. McBurney, P. R. McGonigal and A. Plant, *Chem. Sci.*, **2010**, 1, 383.
150. J. D. Crowley, K. D. Hänni, D. A. Leigh and A. M. Z. Slawin, *J. Am. Chem. Soc.*, **2010**, 132, 5309–5314.
151. M. J. Langton, J. D. Matichak, A. L. Thompson and H. L. Anderson, *Chem. Sci.*, **2011**, 2, 1897.
152. H. M. Cheng, D. A. Leigh, F. Maffei, P. R. McGonigal, A. M. Z. Slawin and J. Wu, *J. Am. Chem. Soc.*, **2011**, 133, 12298–12303.
153. P. E. Barran, H. L. Cole, S. M. Goldup, D. A. Leigh, P. R. McGonigal, M. D. Symes, J. Wu and M. Zengerle, *Angew. Chem. Int. Ed.*, **2011**, 50, 12280–12284.
154. L. Fang, M. A. Olson, D. Benítez, E. Tkatchouk, W. A. Goddard III and J. F. Stoddart, *Chem Soc Rev*, **2010**, 39, 17–29.
155. Y. Tachibana, N. Kihara, Y. Ohga and T. Takata, *Chem. Lett.*, **2000**, 29, 806–807.

156. J. Cao, M. C. T. Fyfe, J. F. Stoddart, G. R. L. Cousins and P. T. Glink, *J. Org. Chem.*, **2000**, 65, 1937–1946.
157. P. T. Glink, A. I. Oliva, J. F. Stoddart, A. J. P. White and D. J. Williams, *Angew. Chem. Int. Ed.*, **2001**, 40, 1870–1875.
158. M. C. T. Fyfe and J. F. Stoddart, *Acc. Chem. Res.*, **1997**, 30, 393–401.
159. P. R. Ashton, P. J. Campbell, P. T. Glink, D. Philp, N. Spencer, J. F. Stoddart, E. J. T. Chrystal, S. Menzer, D. J. Williams and P. A. Tasker, *Angew. Chem. Int. Ed. Engl.*, **1995**, 34, 1865–1869.
160. A. G. Kolchinski, R. A. Roesner, D. H. Busch and N. W. Alcock, *Chem. Commun.*, **1998**, 1437–1438.
161. C. A. Hunter, *J. Am. Chem. Soc.*, **1992**, 114, 5303–5311.
162. F. Vögtle, S. Meier and R. Hoss, *Angew. Chem. Int. Ed. Engl.*, **1992**, 31, 1619–1622.
163. A. Tron, P. J. Thornton, C. Lincheneau, J.-P. Desvergne, N. Spencer, J. H. R. Tucker and N. D. McClenaghan, *J. Org. Chem.*, **2015**, 80, 988–996.
164. M. E. Dehkordi, V. Luxami and G. D. Pantoş, *J. Org. Chem.*, **2018**, 83, 11654–11660.
165. S. Lee, C.-H. Chen and A. H. Flood, *Nat. Chem.*, **2013**, 5, 704–710.
166. J. A. Wisner, P. D. Beer and M. G. B. Drew, *Angew. Chem. Int. Ed.*, **2001**, 40, 3606.
167. J. A. Wisner, P. D. Beer, N. G. Berry and B. Tomapatanaget, *Proc. Natl. Acad. Sci.*, **2002**, 99, 4983–4986.
168. J. A. Wisner, P. D. Beer, M. G. B. Drew and M. R. Sambrook, *J. Am. Chem. Soc.*, **2002**, 124, 12469–12476.
169. N. H. Evans, C. J. Serpell and P. D. Beer, *Angew. Chem. Int. Ed.*, **2011**, 50, 2507–2510.
170. N. H. Evans and P. D. Beer, *Chem. - Eur. J.*, **2011**, 17, 10542–10546.
171. Y. Li, K. M. Mullen, T. D. W. Claridge, P. J. Costa, V. Felix and P. D. Beer, *Chem. Commun.*, **2009**, 7134.
172. M. K. Chae, J. Suk and K.-S. Jeong, *Tetrahedron Lett.*, **2010**, 51, 4240–4242.
173. M. J. Langton, O. A. Blackburn, T. Lang, S. Faulkner and P. D. Beer, *Angew. Chem. Int. Ed.*, **2014**, 53, 11463–11466.
174. M. J. Langton and P. D. Beer, *Chem Commun*, **2014**, 50, 8124–8127.
175. N. L. Kilah, M. D. Wise, C. J. Serpell, A. L. Thompson, N. G. White, K. E. Christensen and P. D. Beer, *J. Am. Chem. Soc.*, **2010**, 132, 11893–11895.
176. B. R. Mullaney, A. L. Thompson and P. D. Beer, *Angew. Chem. Int. Ed.*, **2014**, 53, 11458–11462.
177. S. W. Robinson, C. L. Mustoe, N. G. White, A. Brown, A. L. Thompson, P. Kennepohl and P. D. Beer, *J. Am. Chem. Soc.*, **2015**, 137, 499–507.
178. M. J. Langton and P. D. Beer, *Acc. Chem. Res.*, **2014**, 47, 1935–1949.
179. J. E. M. Lewis, M. Galli and S. M. Goldup, *Chem. Commun.*, **2017**, 53, 298–312.
180. M. Galli, J. E. M. Lewis and S. M. Goldup, *Angew. Chem. Int. Ed.*, **2015**, 54, 13545–13549.
181. J. Berná, M. Alajarín and R.-A. Orenes, *J. Am. Chem. Soc.*, **2010**, 132, 10741–10747.
182. C. B. Caputo, K. Zhu, V. N. Vukotic, S. J. Loeb and D. W. Stephan, *Angew. Chem. Int. Ed.*, **2013**, 52, 960–963.
183. V. Blanco, A. Carlone, K. D. Hänni, D. A. Leigh and B. Lewandowski, *Angew. Chem. Int. Ed.*, **2012**, 51, 5166–5169.
184. C. Chhun, J. Richard-Daniel, J. Kempf and A. R. Schmitzer, *Org. Biomol. Chem.*, **2013**, 11, 6023.
185. D. B. Smithrud, X. Wang, P. Tarapore and S. Ho, *ACS Med. Chem. Lett.*, **2013**, 4, 27–31.
186. J. M. Baumes, J. J. Gassensmith, J. Giblin, J.-J. Lee, A. G. White, W. J. Culligan, W. M. Leevy, M. Kuno and B. D. Smith, *Nat. Chem.*, **2010**, 2, 1025–1030.
187. A. Fernandes, A. Viterisi, F. Coutrot, S. Potok, D. A. Leigh, V. Aucagne and S. Papot, *Angew. Chem. Int. Ed.*, **2009**, 48, 6443–6447.
188. R. Barat, T. Legigan, I. Tranoy-Opalinski, B. Renoux, E. Péraudeau, J. Clarhaut, P. Poinot, A. E. Fernandes, V. Aucagne, D. A. Leigh and S. Papot, *Chem. Sci.*, **2015**, 6, 2608–2613.
189. S. Chen, Y. Wang, T. Nie, C. Bao, C. Wang, T. Xu, Q. Lin, D.-H. Qu, X. Gong, Y. Yang, L. Zhu and H. Tian, *J. Am. Chem. Soc.*, **2018**, 140, 17992–17998.
190. H. Yan, C. Teh, S. Sreejith, L. Zhu, A. Kwok, W. Fang, X. Ma, K. T. Nguyen, V. Korzh and Y. Zhao, *Angew. Chem. Int. Ed.*, **2012**, 51, 8373–8377.

191. P. R. Ashton, V. Baldoni, V. Balzani, A. Credi, H. D. A. Hoffmann, M.-V. Martínez-Díaz, F. M. Raymo, J. F. Stoddart and M. Venturi, *Chem. - Eur. J.*, **2001**, 7, 3482.
192. J. W. Choi, A. H. Flood, D. W. Steuerman, S. Nygaard, A. B. Braunschweig, N. N. P. Moonen, B. W. Laursen, Y. Luo, E. DeIonno, A. J. Peters, J. O. Jeppesen, K. Xu, J. F. Stoddart and J. R. Heath, *Chem. - Eur. J.*, **2006**, 12, 261–279.
193. J. E. Green, J. Wook Choi, A. Boukai, Y. Bunimovich, E. Johnston-Halperin, E. DeIonno, Y. Luo, B. A. Sheriff, K. Xu, Y. Shik Shin, H.-R. Tseng, J. F. Stoddart and J. R. Heath, *Nature*, **2007**, 445, 414–417.
194. R. Shukla, M. J. Deetz and B. D. Smith, *Chem. Commun.*, **2000**, 2397–2398.
195. R. T. S. Lam, A. Belenguer, S. L. Roberts, C. Naumann, T. Jarrosson, S. Otto, J. K. Sanders, *Science*, **2005**, 308, 667–669.
196. K. N. Houk, S. Menzer, S. P. Newton, F. M. Raymo, J. F. Stoddart and D. J. Williams, *J. Am. Chem. Soc.*, **1999**, 121, 1479–1487.
197. T. Ogoshi, T. Akutsu and T. Yamagishi, *Beilstein J. Org. Chem.*, **2018**, 14, 1937–1943.
198. C. G. Collins, E. M. Peck, P. J. Kramer and B. D. Smith, *Chem. Sci.*, **2013**, 4, 2557.
199. T. A. Barendt, A. Docker, I. Marques, V. Félix and P. D. Beer, *Angew. Chem. Int. Ed.*, **2016**, 55, 11069–11076.
200. M. R. Krause, R. Goddard, S. Kubik, *J. Org. Chem.*, **2011**, 76, 17, 7084-7095.

# Chapter 2

## Cationic and neutral amido-triazole [2]rotaxanes for anion binding

# Chapter 2: Cationic and neutral amido-triazole [2]rotaxanes for anion binding

## 2.1. Introduction

The development of synthetic host systems which display high binding affinity and selectivity for a target guest anion is an important goal of modern supramolecular chemistry. [1] These properties can be fine-tuned by careful modification of a synthetic host structure through changing the number or type of donors, the degree of flexibility, or the cavity size. For example, building on previous results, [2] Sessler and co-workers demonstrated that slight modifications in the structure of a pyridine-2,6-dicarboxamide dipyrromethane macrocycle afford dramatic changes in anion selectivity trends (**Figure 2.1**). [3]

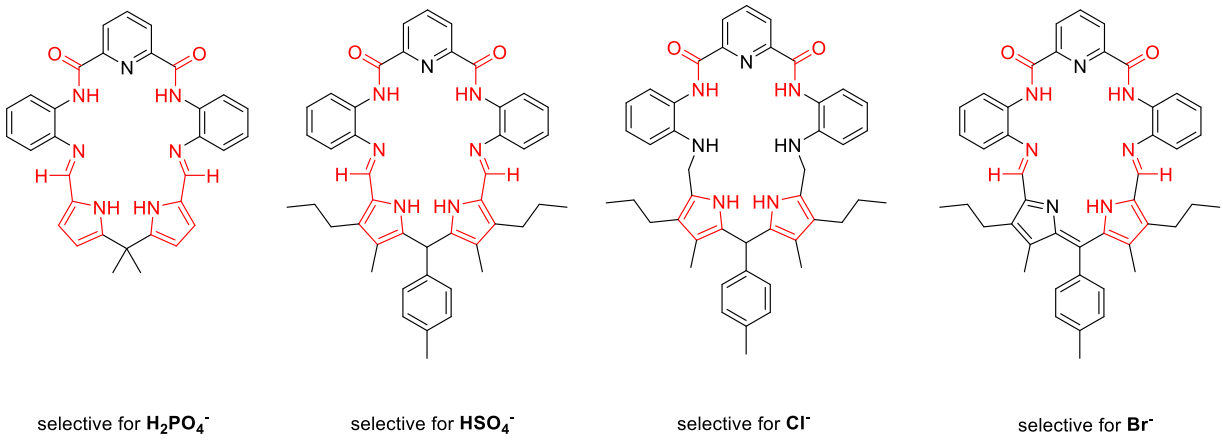
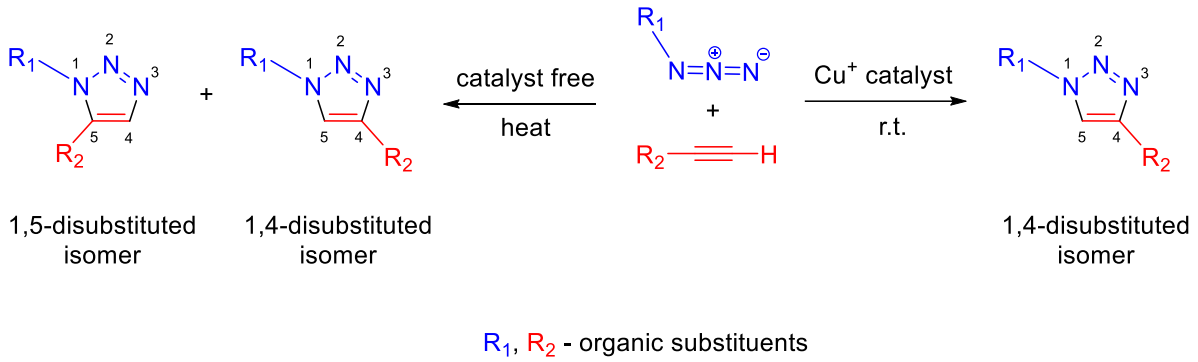



***Figure 2.1.*** *A family of structurally related pyridine-2,6-dicarboxamide macrocycles exhibiting different anion selectivity patterns ($CH_3CN$, 296 K).*

### 2.1.1. The 1,2,3-triazole, 1,2,3-iodotriazole and amidotriazole motifs in anion binding

In 1967, Huisgen first reported the 1,3-dipolar cycloaddition between an azide and a terminal alkyne to afford substituted 1,2,3-triazoles. [4] The synthetic methodology was significantly improved later, when Sharpless [5] and Meldal [6] independently discovered the Cu(I)-catalysed azide-alkyne cycloaddition reaction (CuAAC), which exhibited complete regioselectivity for 1,4-disubstituted triazole formation (**Scheme 2.1**). The CuAAC protocol is

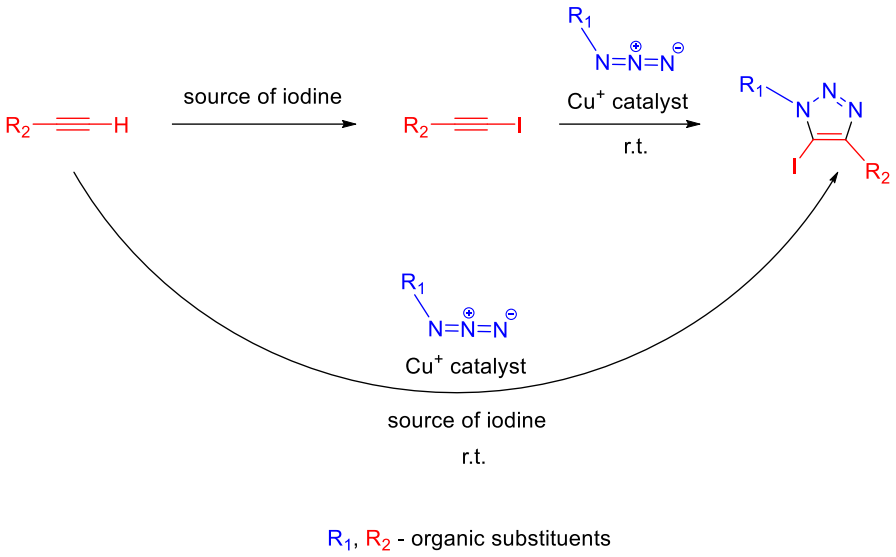
also typically mild, highly efficient, and compatible with numerous functional groups and solvents.




***Scheme 2.1.*** *The outcomes of catalysed and non-catalysed azide-alkyne cycloadditions, respectively.*

The 1,2,3-triazole motif is an attractive functional motif for incorporation in anion receptor molecules. Besides its ease of synthesis, it also features a favourable electronic structure (see **Chapter 1, Section 1.2.5.2.2**) – the electron-withdrawing character of the three adjacent nitrogen atoms provides a large dipole moment of approximately 5 Debye (thus polarising the $C_5$ – H bond). The electron-deficient triazole proton is hence a potent hydrogen bond donor for anions.

Its interaction with negatively charged species can be tuned by further reducing the electron density on the $C_5$ proton through alkylation of the triazole ring or introduction of electron deficient functional groups. Alternatively, the $C_5$ proton can be replaced by an iodine atom in order to make use of halogen bonding. Several versatile CuAAC methodologies for the synthesis of 1,2,3-iodotriazoles have been developed, allowing for the parent 1-iodoalkyne to be either synthesised [7] or generated in situ from the analogous protoalkyne with an electrophilic iodine source [8] (**Scheme 2.2**).




***Scheme 2.2.*** *Common synthetic pathways towards 1,2,3-iodotriazoles.*

By exploiting the properties of amide N – H donors (see **Chapter 1, Section 1.2.5.2.2**) in conjunction with 1,2,3-(iodo)triazole motifs, the anion binding properties can be further enhanced and fine-tuned. Kumar and co-workers designed a simple acyclic structure (**Figure 2.2.a**) which changes colour upon $F^-$ binding in 2:98 DMSO-$d_6$ / $CDCl_3$ (*v/v*). [9] Li and co-workers appended amide and triazole motifs onto a 1,3,5-triethylbenzene scaffold to yield a receptor that bind $SO_4^{2-}$ strongly and selectively in 0.5:99.5 DMSO-$d_6$ / acetone-$d_6$ (*v/v*) (**Figure 2.2.b**). [10] Jiang's host incorporating one triazole and two amide motifs was found to be selective for $Cl^-$ over heavier halides in pyridine-$d_5$ (**Figure 2.2.c**). [11]

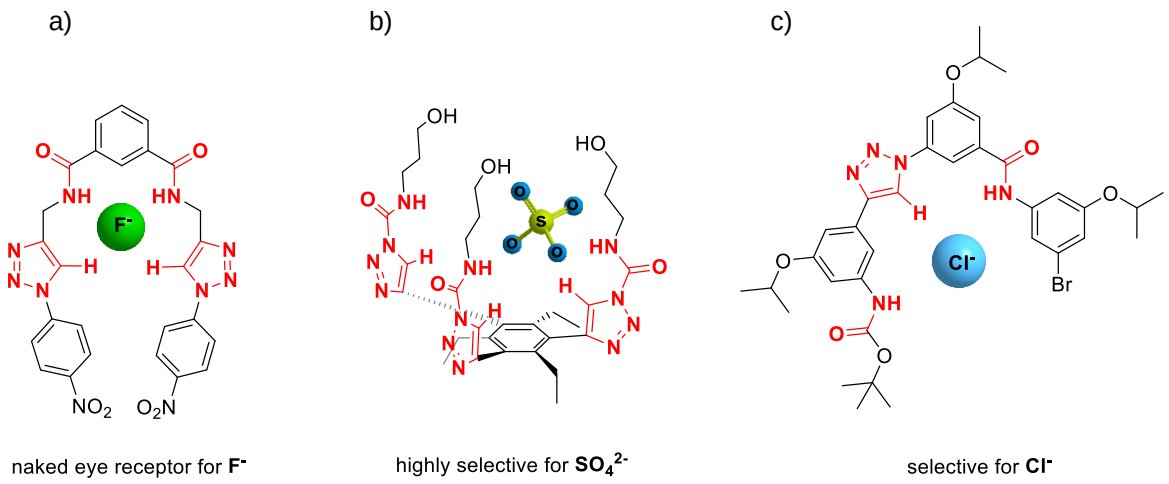
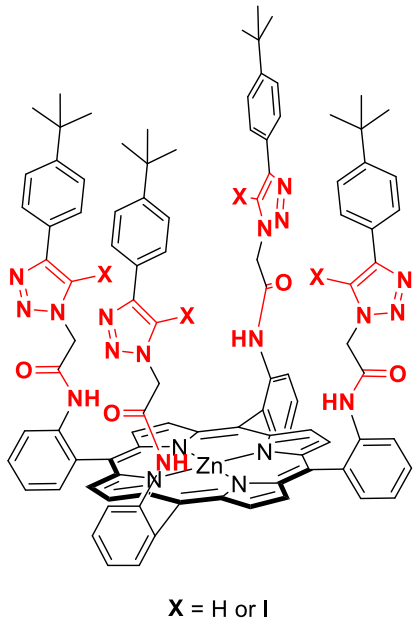



***Figure 2.2.*** *Examples of anion receptors incorporating both triazole and amide motifs: a) Kumar's chromogenic $F^-$ sensor; b) Li's tripodal sulfate host; c) Jiang's chloride-selective receptor.*

In order to enhance the anion binding strength of amido-triazole receptors, efforts to incorporate halogen bond donors in these systems have been undertaken. To this extent, Beer and co-workers designed a tetrapodal receptor based on a metalloporphyrin scaffold decorated with amide and iodotriazole motifs, which was shown to bind halides more strongly than its all-HB analogue (**Table 2.1**). [12]




| Anion | Association constants for receptor | |
|---|---|---|
| | **X** = I | **X** = H |
| $Cl^-$ | 272144 | 34626 |
| $Br^-$ | 13589 | 4494 |
| $I^-$ | 656 | 396 |

***Table 2.1.*** *Anion binding constants ($K_a$/ $M^{-1}$) of XB/HB amide-triazole functionalised porphyrin hosts with halides in $CH_3CN$ at 293 K. Inset: Generic structure of the two receptors.*

## 2.2. Chapter aims

The work described in this chapter focuses on the synthesis and anion binding properties of mixed HB/XB [2]rotaxane structures. Building on previous results, two main research avenues are undertaken:

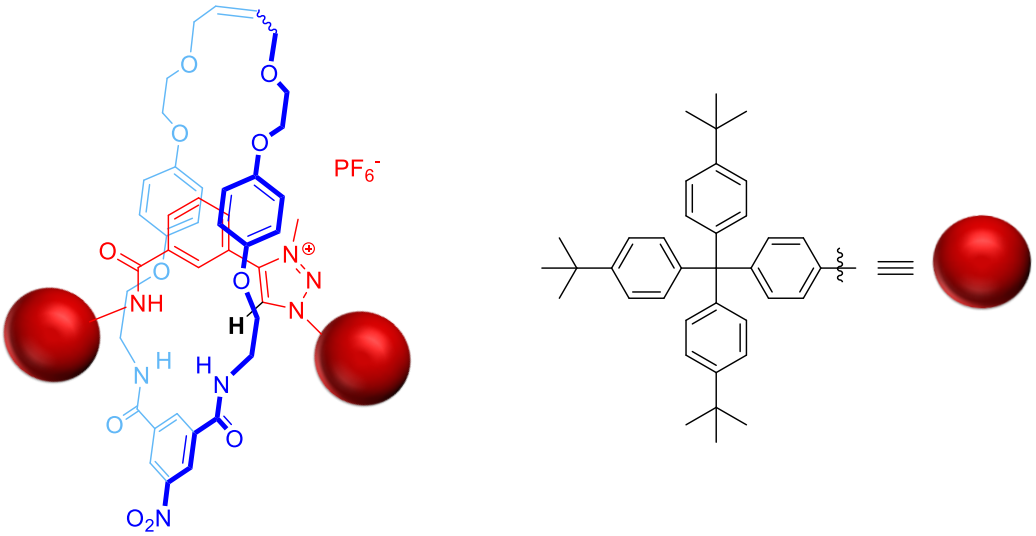
1) A series of acyclic and interlocked hosts incorporating the amido-triazolium motif are synthesised using a discrete anion templation methodology and their anion binding properties are compared and contrasted to those of an analogous, more preorganised structure.

2) Neutral mixed HB/XB [2]rotaxanes centered around the triazole motif are constructed employing an active metal templation protocol and their anion binding properties correlated to structural differences.

## 2.3. Cationic HB/XB amido-triazolium [2]rotaxanes for anion recognition

### 2.3.1. Design of target rotaxanes

In previous work, Beer and co-workers reported a [2]rotaxane incorporating a 3-amido-phenyl-triazolium motif which was proven to strongly and selectively bind chloride and bromide in the competitive 1:1 $CD_3OD/CDCl_3$ (*v/v*) solvent mixture, with no evidence of iodide, acetate, and dihydrogen phosphate binding (**Figure 2.3**). [13]




**2.19.HB$^+$PF$_6^-$**

***Figure 2.3.*** *Structure of previously reported amido-triazolium rotaxane* ***2.19.HB$^+$PF$_6^-$****.*

In an effort to fine-tune the selectivity towards larger, more polarisable anions, a XB iodo-triazolium donor was incorporated into the axle component of the rotaxane structural framework (**Figure 2.4**). The following sections describe the synthesis and anion binding properties of new HB/XB amido-triazolium rotaxane host structures.

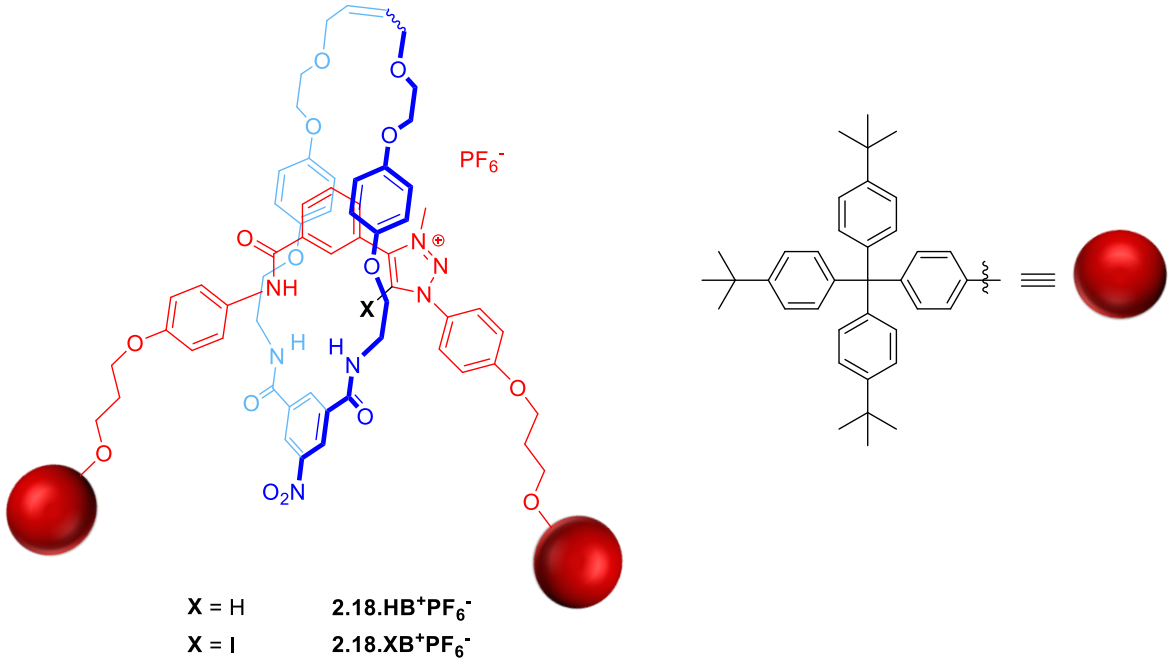
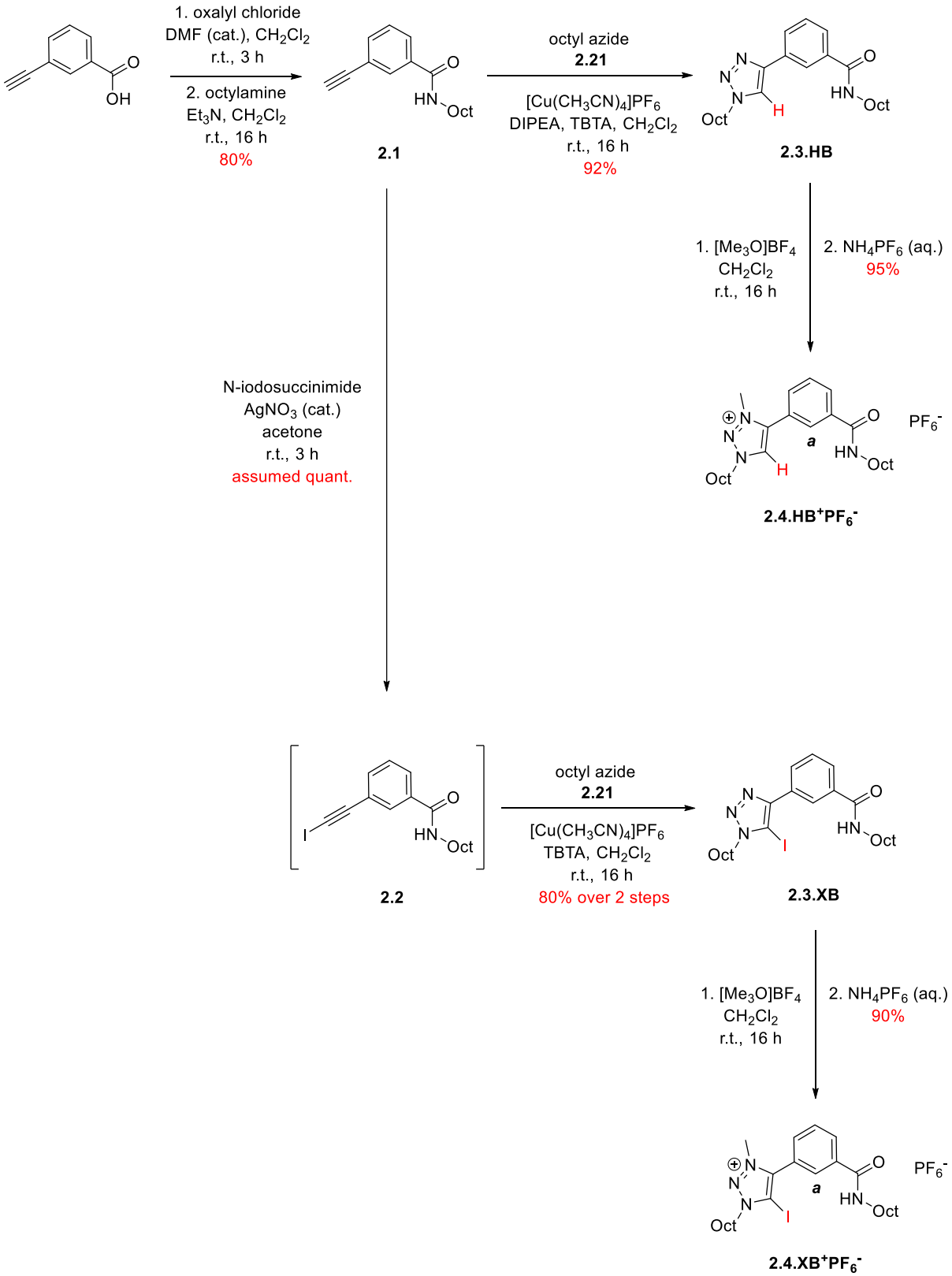



***Figure 2.4.*** *Structures of the target novel amido-triazolium HB/XB rotaxanes.*

### 2.3.2. Synthesis and anion recognition properties of cationic acyclic systems

#### 2.3.2.1. Synthesis of amido-triazolium acyclic receptors

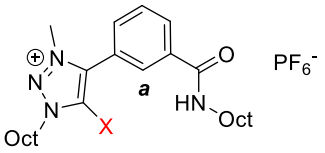
Initially, two model acyclic receptors incorporating the amido-triazolium moiety were synthesised and their preliminary anion binding properties investigated (**Scheme 2.3**). Commercially available 3-ethynylbenzoic acid was converted to its acyl chloride and immediately condensed with octyl amine to afford alkyne **2.1**. A CuAAC reaction of **2.1** with octyl azide afforded the triazole derivative **2.3.HB**, which was subsequently alkylated with trimethyloxonium tetrafluoroborate**.** Anion exchange was achieved by repeated washing with aqueous $NH_4PF_6$ to afford receptor **2.4.HB$^+$PF$_6^-$**. In order to obtain the analogous XB receptor **2.4.XB$^+$PF$_6^-$**, the alkyne synthon **2.1** was first iodinated with *N*-iodosuccinimide to produce **2.2** in situ and then a CuAAC reaction with octyl azide gave the iodotriazole derivative **2.3.XB**. Methylation followed by anion exchange afforded **2.4.XB$^+$PF$_6^-$** (**Scheme 2.3**).




***Scheme 2.3.*** *Synthesis of model acyclic monocationic HB and XB receptors (oct = n-$C_8H_{17}$).*

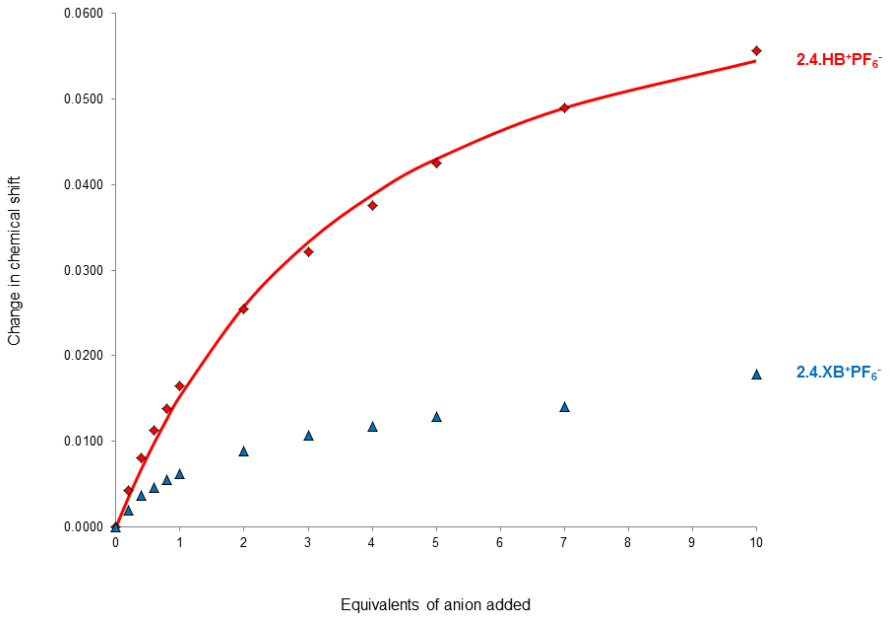
### 2.3.2.2. Preliminary anion binding studies

The affinity of each receptor towards several anions was probed via $^{1}$H NMR titration experiments in the solvent system 1:1 $CD_3OD/CDCl_3$ (*v/v*) by monitoring the chemical shift of the aromatic proton flanked by the (iodo)triazolium and amide groups (labelled ***a*** in **Scheme 2.3**). Solutions of the tetrabutylammonium (TBA) salts of a range of halides and oxoanions were titrated into a 1 mM solution of the receptor and the anion-induced shifts were plotted against the equivalents of anion added (**Figure 2.5**). The signals corresponding to the triazole proton and inner aromatic proton ***a*** were found to shift significantly downfield, indicating that the anions were binding in the vicinity of the receptor cleft. Anion binding was observed to be fast on the NMR timescale; the resulting 1:1 stoichiometric host-guest association constants were determined via BindFit [14,15] analysis of the binding isotherms and are presented in **Table 2.2**.




**X = H** **2.4.HB$^+$PF$_6^-$**
**X = I** **2.4.XB$^+$PF$_6^-$**

a)




b)

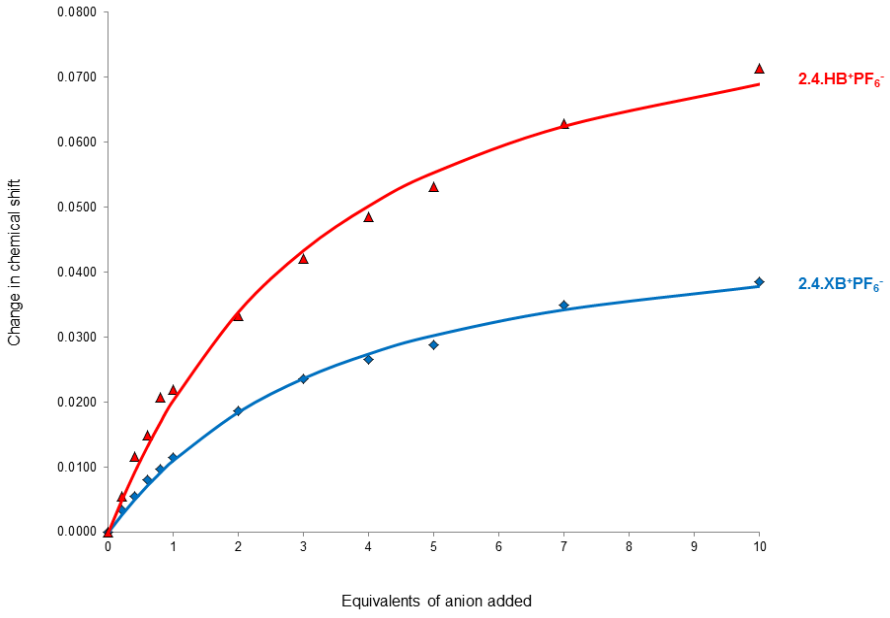



***Figure 2.5.*** *Comparative plots of the change in chemical shift of the proton* ***a*** *(ppm) against equivalents of anion added (a – acetate, b - chloride) for the acyclic amido-triazolium receptors* ***2.4.HB$^+$PF$_6^-$*** *and* ***2.4.XB$^+$PF$_6^-$*** *(1:1 $CD_3OD/CDCl_3$ (v/v), 298 K). Observed data is represented as solid points, whereas fitted isotherms are represented as lines. Inset: Structure of receptors* ***2.4.HB$^+$PF$_6^-$*** *and* ***2.4.XB$^+$PF$_6^-$****.*

***Table 2.2.*** *Anion association constants ($K_a$/ $M^{-1}$) of acyclic amido-triazolium receptors* ***2.4.HB$^+$PF$_6^-$*** *and* ***2.4.XB$^+$PF$_6^-$*** *in 1:1 $CD_3OD/CDCl_3$ (v/v) at 298 K*

| Anion[a] | Association constants ($K_a$/ $M^{-1}$) [b] | |
|---|---|---|
| | **2.4.HB$^+$PF$_6^-$** | **2.4.XB$^+$PF$_6^-$** |
| $Cl^-$ | 343 | 335 |
| $Br^-$ | 298 | — [c] |
| $I^-$ | 385 | 401 |
| $AcO^-$ | 300 | NB [d] |
| $H_2PO_4^-$ | 158 | NB [d] |

*[a] Anions were added as their tetrabutylammonium (TBA) salts. [b] Calculated using BindFit [14,15] by monitoring the change in the chemical shift of the internal aromatic proton (labelled* ***a*** *in* ***Scheme 2.3****). Errors < 10%. [c] Precipitation occurred during the titration. [d] NB = no binding. In all cases, the perturbations of the chemical shift were very small (Δδ ≤ 0.05 ppm), which indicates that the receptor does not interact significantly with the guest anion.*

Despite the competitiveness of the solvent, both acyclic receptors **2.4.HB$^+$PF$_6^-$** and **2.4.XB$^+$PF$_6^-$** show significant anion affinities. However, it is apparent that the amido-triazolium receptor **2.4.HB$^+$PF$_6^-$** does not discriminate between anions with the exception of dihydrogen phosphate, which it binds more weakly, whereas its halogen-bonding analogue **2.4.XB$^+$PF$_6^-$** displays impressive selectivity for halides over oxoanions, in particular for iodide. Notably, XB receptors commonly exhibit selectivity for the heavier halide in protic media due to the soft anion being relatively less solvated in comparison to harder oxoanions.

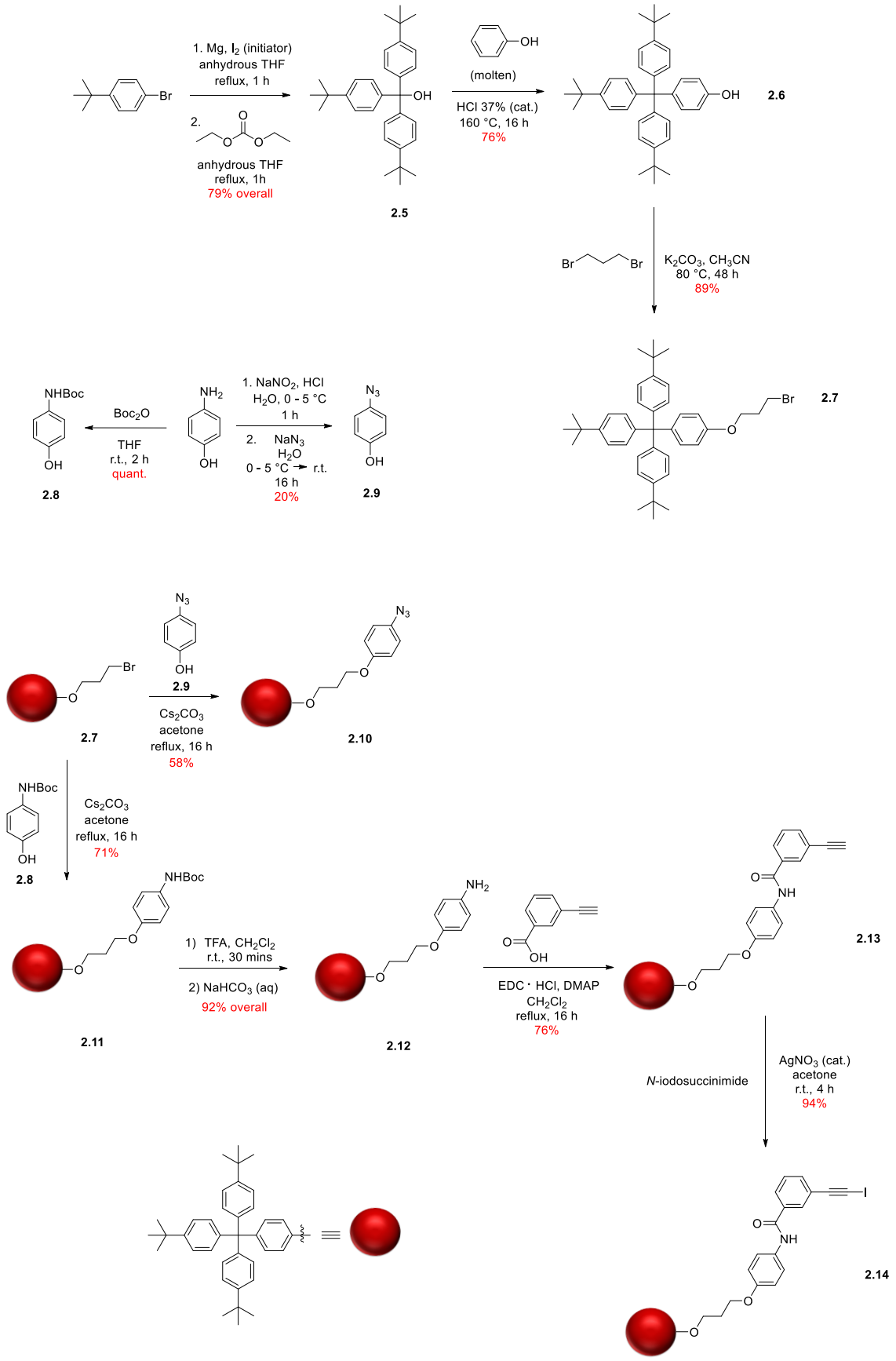
### 2.3.3. Synthesis and anion recognition properties of cationic interlocked systems

#### 2.3.3.1. Synthesis and characterisation of amido-triazolium [2]rotaxanes

Having studied the anion complexation properties of the acyclic receptors, these mixed HB/XB motifs were incorporated into [2]rotaxane frameworks. The multi-step approach used to prepare the required axle precursors is outlined in **Scheme 2.4.**

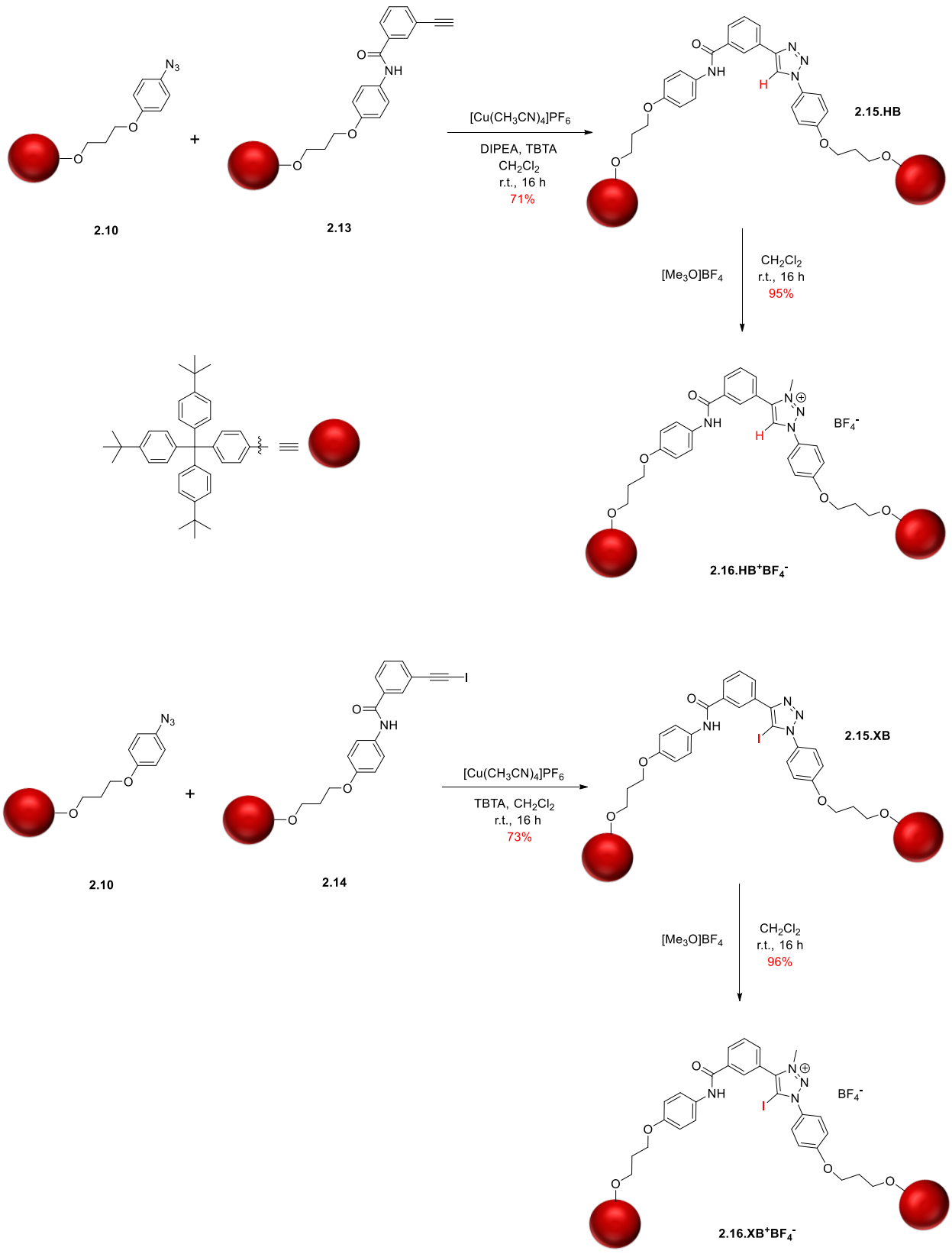
Firstly, the Grignard reagent of commercially available 4-tert-butylbromobenzene was reacted with diethyl carbonate to afford tertiary alcohol **2.5**, [16] which was subsequently condensed with phenol via acid catalysis to form the phenol-appended stopper **2.6.** [16] An $S_N2$ reaction between **2.6** and 1,3-dibromopropane, which was used in large excess, provided the versatile stopper bromide **2.7**. [17] Separately, 4-aminophenol was employed to synthesise both Boc-protected aniline **2.8** through acylation with $Boc_2O$ [18] and aromatic

azide **2.9** through the reaction of $NaN_3$ with the intermediate diazonium salt. [19] Stopper bromide **2.7** was reacted separately under basic conditions in refluxing acetone with azide **2.9** to afford the azide-appended half-axle **2.10** in 58% yield, and with *N*-Boc protected aniline **2.8** to produce stopper **2.11** in 71% yield. [20] Following deprotection with trifluoroacetic acid, the aromatic amine group of **2.12** was subjected to EDC·HCl-mediated amide coupling with 3-ethynylbenzoic acid, resulting in the formation of alkyne-appended half-axle **2.13** in 76% yield. The terminal alkyne proton was exchanged for iodine using *N*-iodosuccinimide in the presence of a catalytic amount of $AgNO_3$ to give the iodo-alkyne **2.14** in near-quantitative yield.



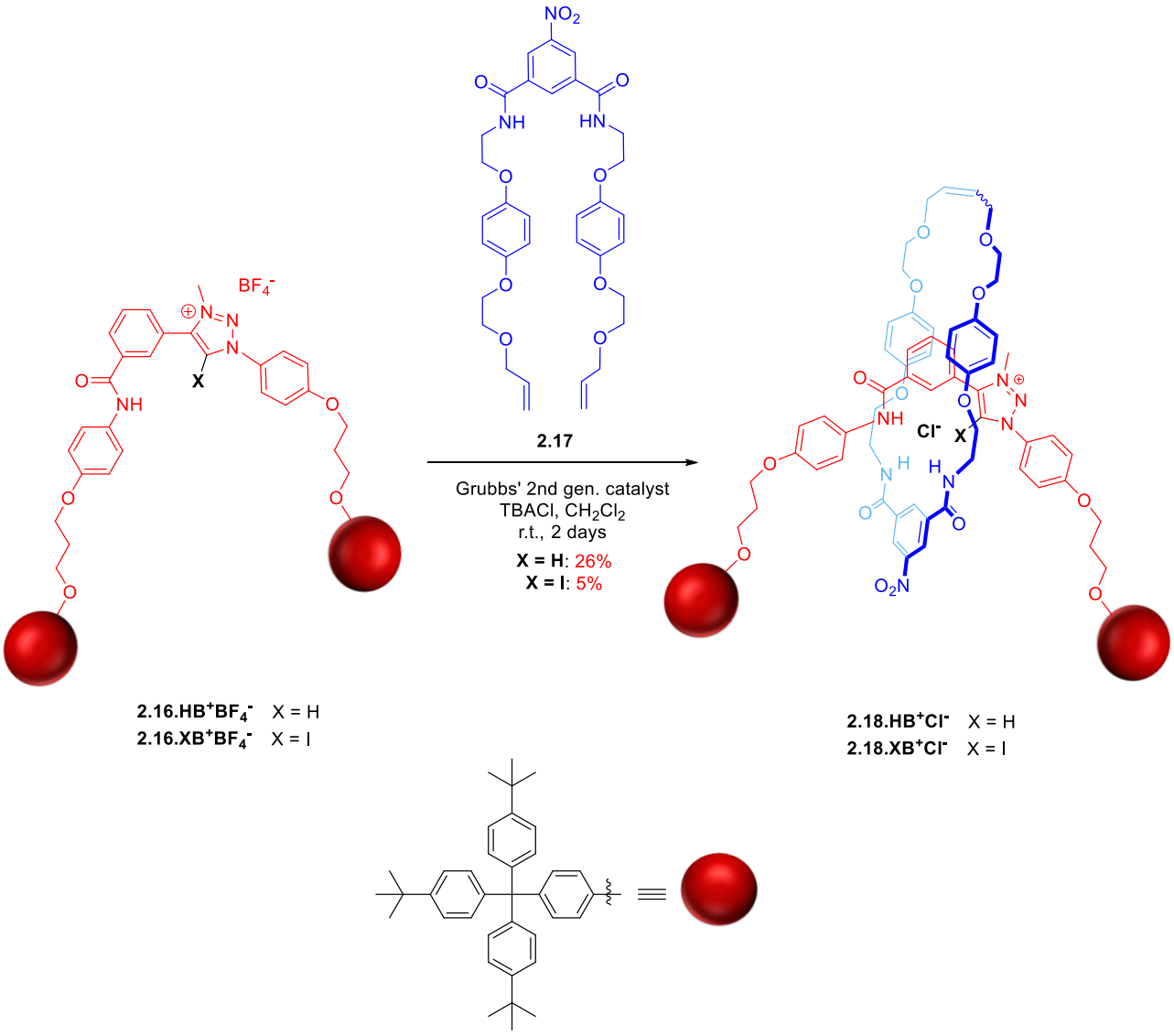

***Scheme 2.4.*** *Synthesis of stoppers and half-axles later employed in the construction of amido-triazole [2]rotaxanes.*

These half-axles were subsequently combined as shown in **Scheme 2.5** below. Stopper azide **2.10** was reacted with proto-alkyne **2.13** via the CuAAC protocol to give neutral axle **2.15.HB** in 71% yield**,** which was then methylated in the presence of $[Me_3O]BF_4$ to give the monocationic axle **2.16.HB$^+$BF$_4^-$**. Surprisingly, the reaction of **2.10** with **2.14** proved to be highly challenging, as typical CuAAC conditions failed to afford any product. However, through optimisation of the reaction conditions, the desired product **2.15.XB** was formed under high reactant concentrations and with large Cu(I) catalyst loadings. Subsequent alkylation of **2.15.XB** under similar conditions as its HB analogue gave axle **2.16.XB$^+$BF$_4^-$**.




***Scheme 2.5.*** *Synthesis of cationic amido-triazolium HB and XB axles* ***2.16.HB$^+$BF$_4^-$*** *and* ***2.16.XB$^+$BF$_4^-$***

A discrete anion templation strategy was then employed to synthesise the target amido-triazolium rotaxanes (**Scheme 2.6**). Bis-alkene precursor **2.17** prepared by a literature procedure [21] (kindly donated by Dr. Asha Brown) was first assembled around an amido-triazolium axle (**2.16.HB$^+$BF$_4^-$** or **2.16.XB$^+$BF$_4^-$**, respectively) in the presence of chloride as a templating anion, after which ring-closing metathesis using Grubbs' 2$^{nd}$ generation catalyst afforded rotaxanes **2.18.HB$^+$Cl$^-$** and **2.18.XB$^+$Cl$^-$** in 26% and 5% isolated yields, respectively, after preparative TLC purification. The poor yield in the latter case is attributed to significant decomposition in the reaction mixture and could not be improved upon despite numerous attempts at optimisation. Both rotaxanes were characterised by $^1$H NMR, $^{13}$C NMR spectroscopy, and high resolution mass spectrometry.




***Scheme 2.6.*** *Synthesis of cationic amido-triazolium [2]rotaxanes* ***2.18.HB$^+$Cl$^-$*** *and* ***2.18.XB$^+$Cl$^-$***.

Comparing the $^1$H NMR spectrum of **2.18.HB$^+$Cl$^-$** to the spectra of the free axle **2.16.HB$^+$BF$_4^-$** and macrocycle **2.17.B** which was isolated as a side-product of the rotaxane synthesis reaction (**Figure 2.6**) revealed some important features. Upon incorporation into an interlocked structure and exchange of the counteranion to chloride, the inner axle protons (***f***, ***g***, and ***k***) undergo downfield shifts, along with the macrocyclic amide protons ***3*** which show significant perturbation (> 3 ppm), suggesting that they co-operate to bind Cl$^-$ inside the rotaxane cavity. Importantly, the macrocycle component hydroquinone signals ***6*** and ***7*** split and shift upfield, arising from aromatic donor-acceptor interactions with the electron-deficient triazolium axle motif, which is a characteristic feature of rotaxane formation.

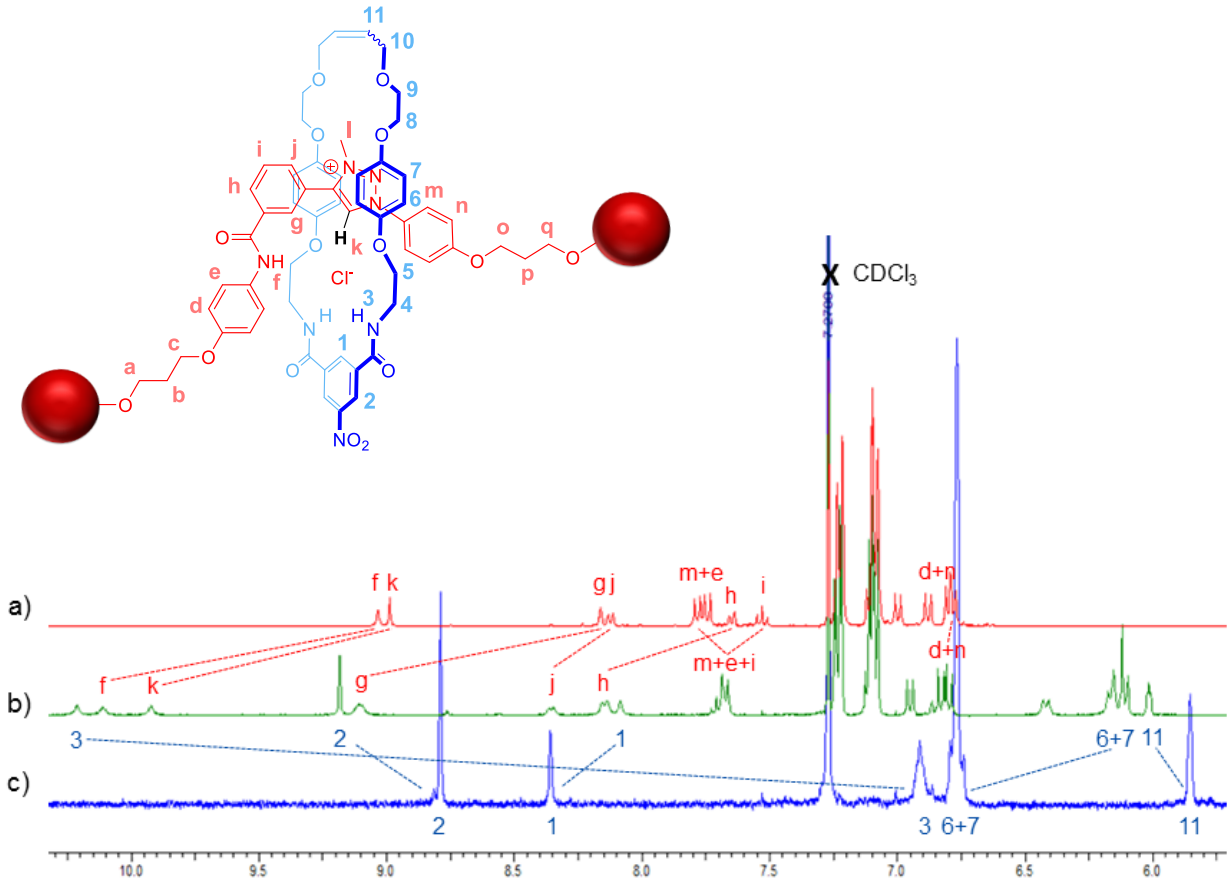



***Figure 2.6.*** *Overlay of truncated $^1$H NMR spectra of a) amido-triazolium HB axle* ***2.16.HB$^+$BF$_4^-$****, b) amido-triazolium HB rotaxane* ***2.18.HB$^+$Cl$^-$*** *and c) non-interlocked macrocycle* ***2.17.B*** *(CDCl$_3$, 298 K, 400 MHz). Inset: the structure of* ***2.18.HB$^+$Cl$^-$*** *with relevant protons labelled.*

To enable the study of anion binding properties, the chloride counteranion was exchanged for the non-coordinating hexafluorophosphate by repeated washing with

aqueous $NH_4PF_6$ (**Figure 2.7**). After the counteranion exchange, all peaks in the $^1$H NMR spectrum became broad, presumably due to the presence of strong intercomponent hydrogen bonds, which slows the rotation of the components. Upon addition of $CD_3OD$ the signals sharpened again, as the protic solvent presumably disrupts the hydrogen bond network.

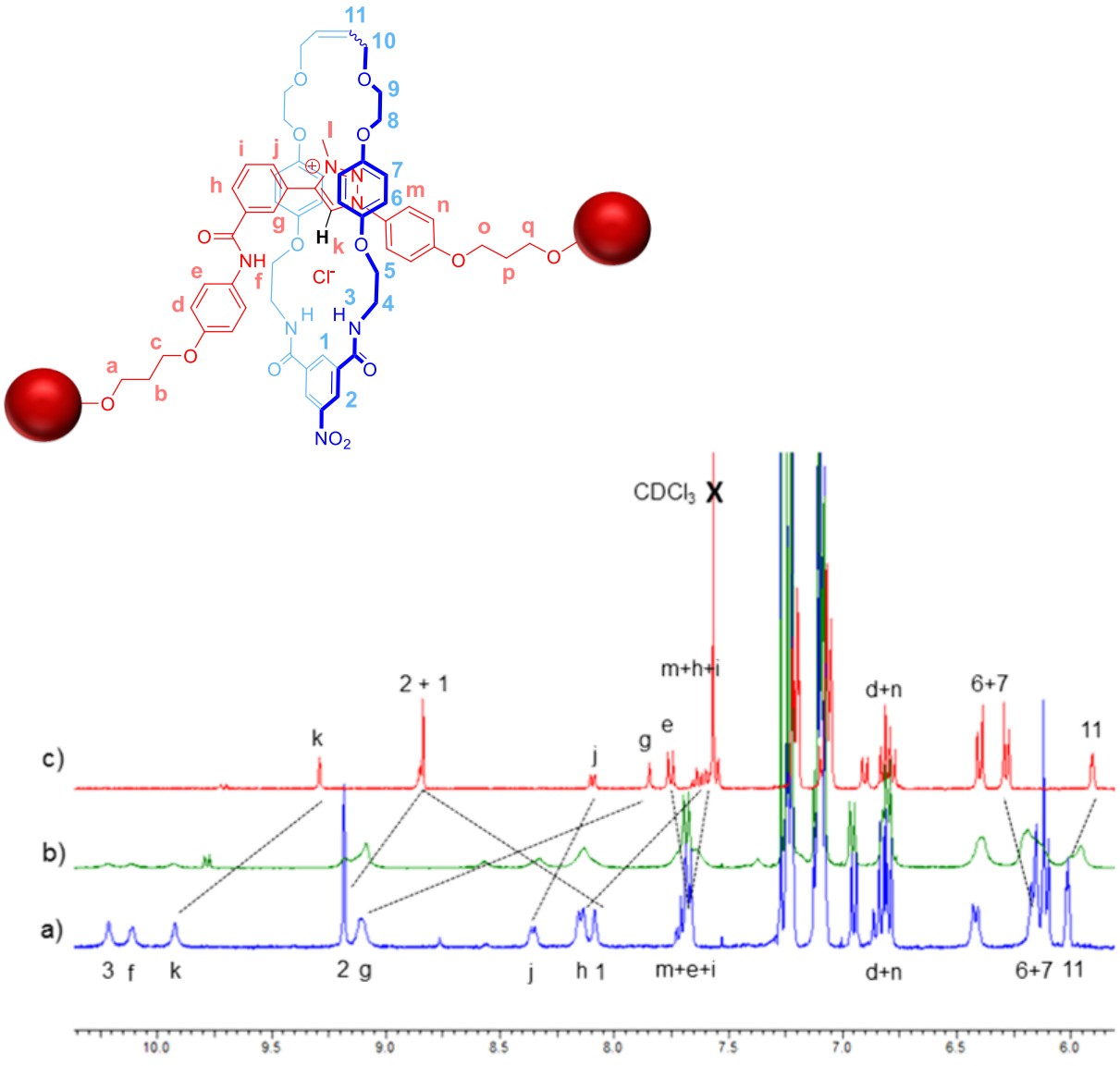



***Figure 2.7.*** *Overlay of truncated $^1$H NMR spectra of amido-triazolium HB rotaxane: a)* ***2.18.HB$^+$Cl$^-$****, $CDCl_3$; b)* ***2.18.HB$^+$PF$_6^-$****, $CDCl_3$; c)* ***2.18.HB$^+$PF$_6^-$****, 1:1 $CD_3OD/CDCl_3$ (v/v).*

Further unequivocal evidence of the interlocked nature of **2.18.HB$^+$PF$_6^-$** was obtained by $^1$H–$^1$H ROESY experiments (**Figure 2.8**), which showed several through-space interactions between axle and macrocycle protons. The cross-coupling between macrocyclic

alkenyl protons ***11*** and the triazolium methyl group ***l*** correlates with the slight downfield shift of macrocyclic alkenyl protons ***11*** upon rotaxane formation. This indicates that the macrocycle resides predominantly at the triazolium ring, with the isophthalamide moiety forming an anion binding cavity with the amido-triazolium motif and the pseudo-crown ether moiety stabilising the positive charge via ion-dipole interactions.

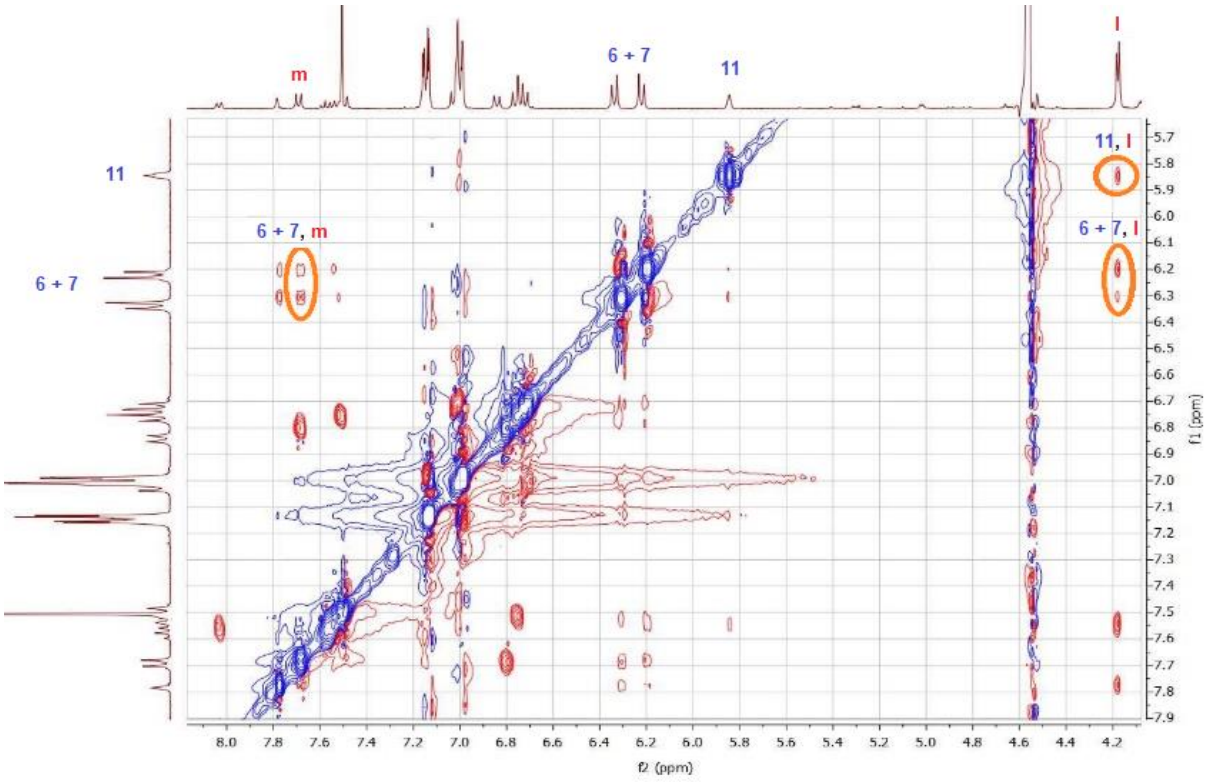



***Figure 2.8.*** *Truncated 2D ROESY spectrum of rotaxane* ***2.18.HB$^+$PF$_6^-$****, showing relevant inter-component couplings (1:1 $CD_3OD/CDCl_3$ (v/v), 298 K).*

In the case of the halogen bonding analogue **2.18.XB$^+$Cl$^-$**, comparison of the $^1$H NMR spectra of the rotaxane, axle, and macrocycle (**Figure 2.9**) revealed that upon mechanical bond formation, the aromatic C – H signals ***g*** and ***1*** shift downfield, along with the macrocyclic amide protons ***3***. Interestingly, the axle amide protons ***f*** shift significantly upfield. As in the case of **2.18.HB$^+$Cl$^-$**, the hydroquinone signals shift upfield, however, the split is considerably larger (≈0.2 ppm in contrast with ≈0.05 ppm for the HB rotaxane).

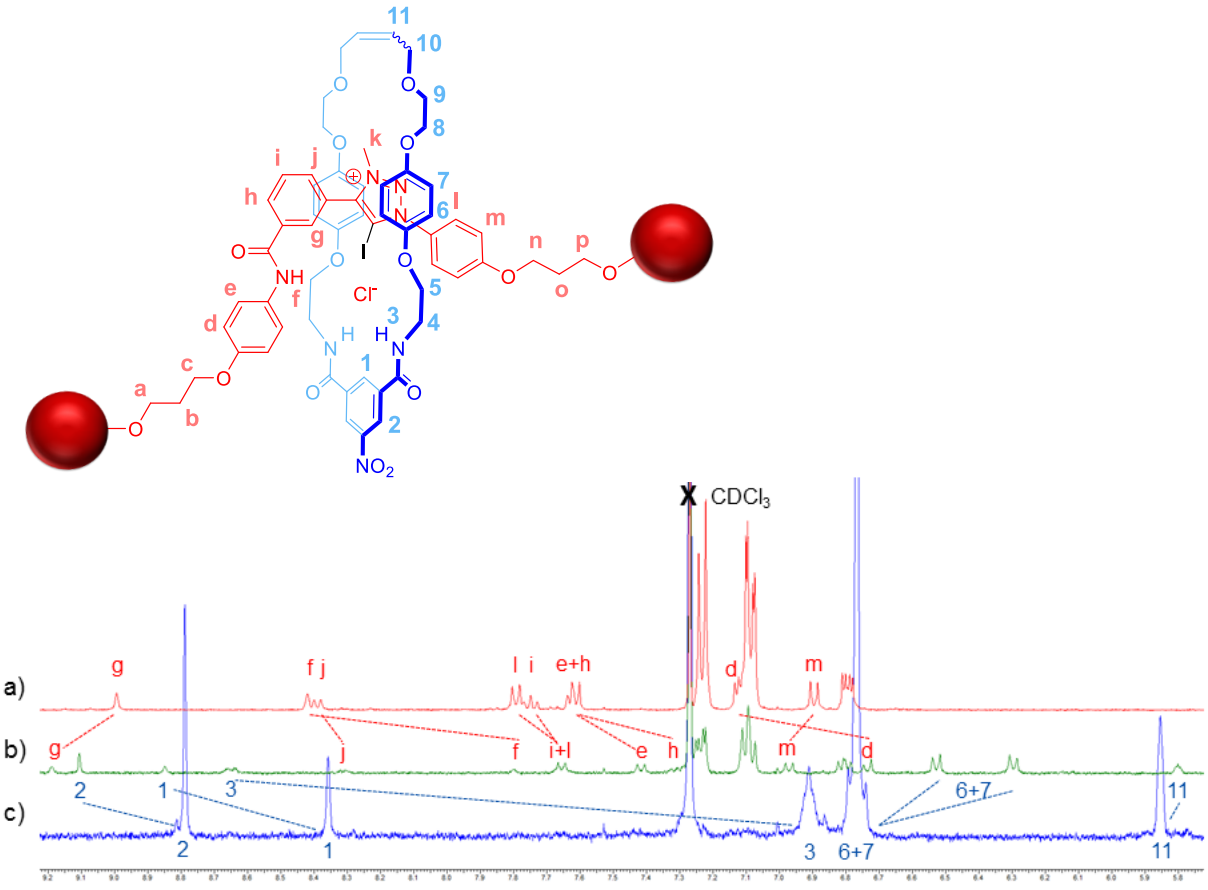



***Figure 2.9.*** *Overlay of truncated $^{1}$H NMR spectra of a) amido-triazolium HB axle* ***2.16.XB$^{+}$BF$_4^{-}$****, b) amido-triazolium HB rotaxane* ***2.18.XB$^{+}$Cl$^{-}$*** *and c) non-interlocked macrocycle* ***2.17.B*** *(CDCl$_3$, 298 K, 400 MHz).*

**2.18.XB$^{+}$Cl$^{-}$** was subjected to a similar anion metathesis procedure as its HB analogue. Disappointingly, no hexafluorophosphate salt could be obtained; even after copious washing with aqueous $NH_4PF_6$ and employing alternative anion exchange methods such as heating with aqueous $NH_4PF_6$ or precipitating from a concentrated solution, the $^{1}$H NMR spectrum of the product remained identical to that of the initial chloride salt and no signal could be detected in the $^{19}$F NMR spectrum. Henceforth, a $^{1}$H–$^{1}$H ROESY spectrum of the chloride salt was obtained which demonstrated the existence of through-space cross-couplings between axle and macrocycle components and further confirmed the interlocked nature of the product (**Figure 2.10**).

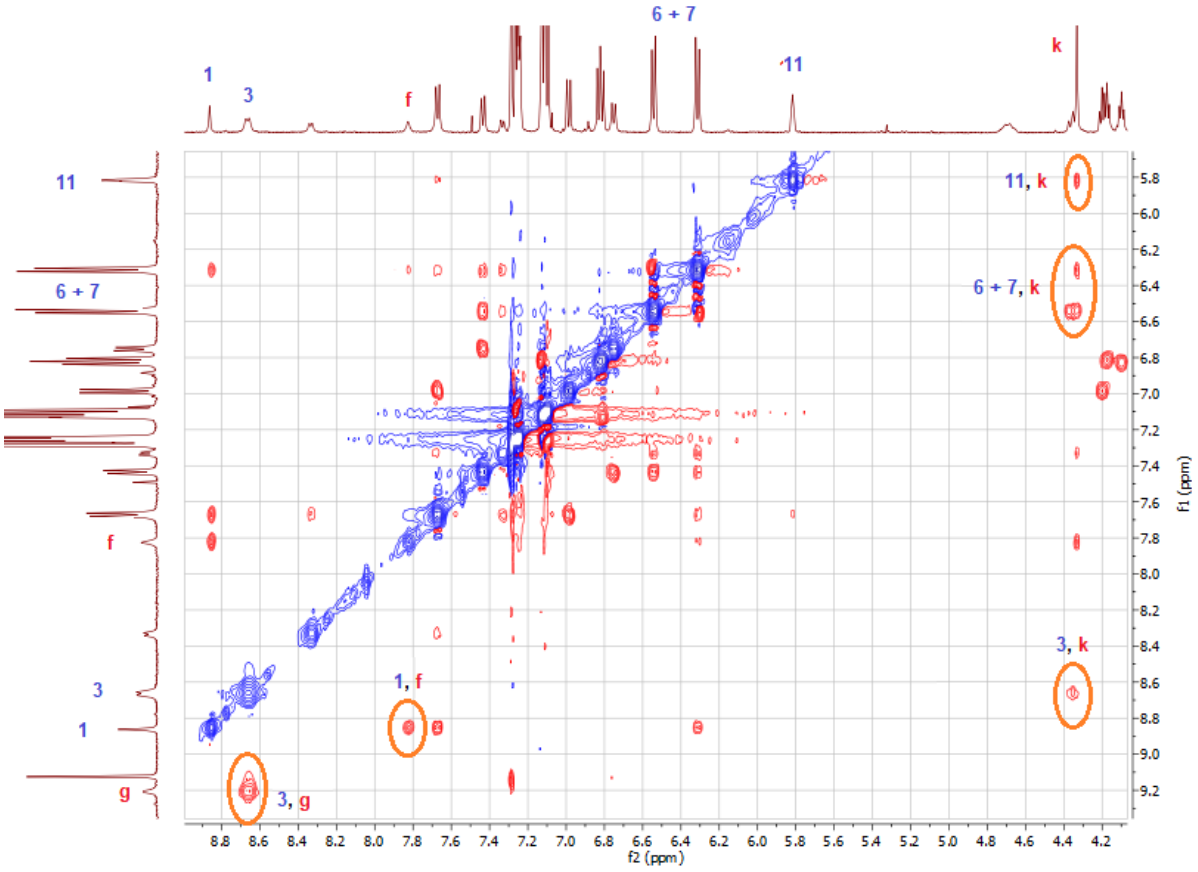


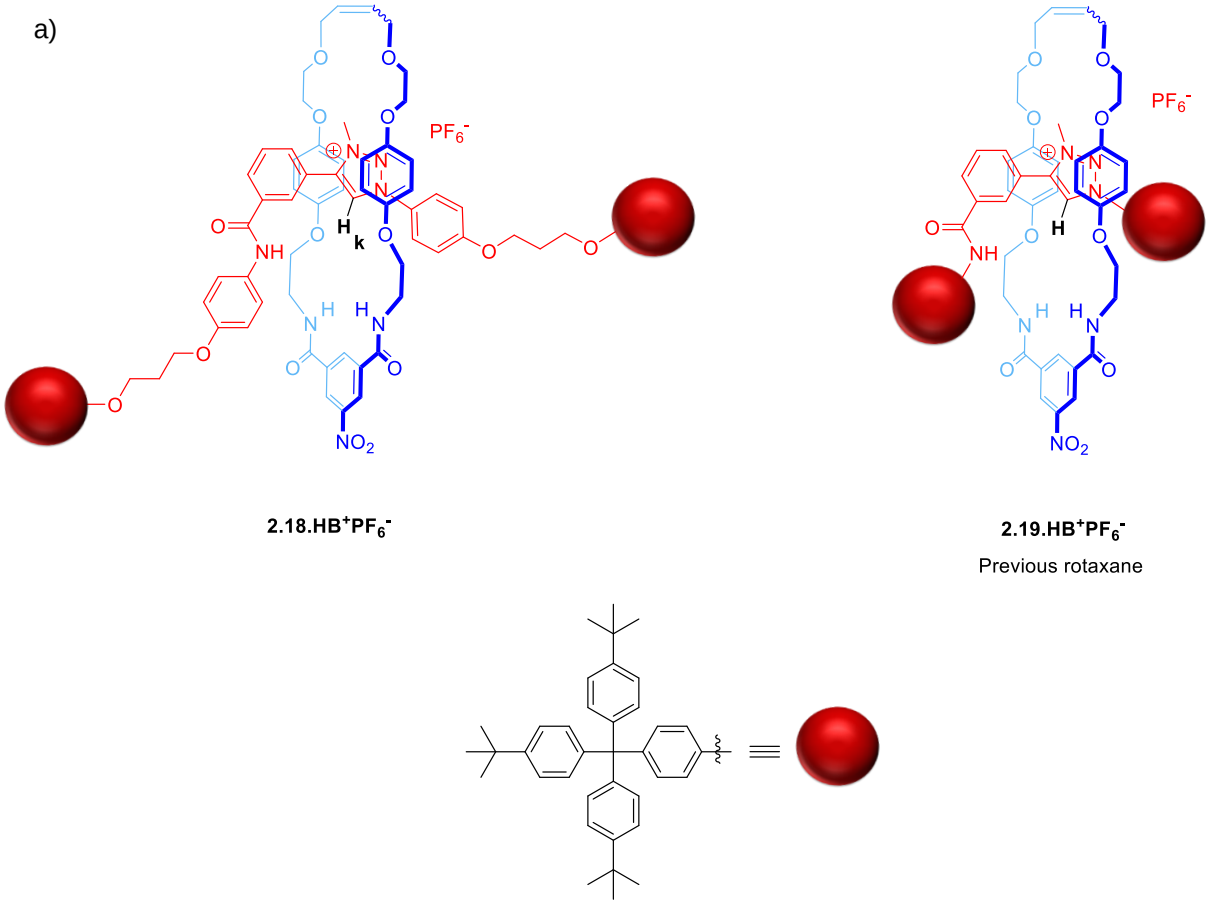

***Figure 2.10.*** *Truncated 2D ROESY spectrum of rotaxane* ***2.18.XB$^+$Cl$^-$*** *showing relevant inter-component couplings ($CDCl_3$, 298 K).*

These experimental observations imply that **2.18.XB$^+$** binds chloride very strongly; however, the problematic exchange to $PF_6^-$ coupled with the low yield of formation negated any further investigations with the halogen-bonding rotaxane.

### 2.3.3.2. Anion binding studies of cationic HB rotaxane

The anion recognition properties of **2.18.HB$^+$PF$_6^-$** were determined *via* $^1$H NMR titration experiments in the competitive solvent system 45:45:10 $CDCl_3$/$CD_3OD$/$D_2O$ (*v/v/v*). Upon addition of TBAX (X = Cl, Br or I), most aromatic resonances shifted downfield, with the largest change in chemical shift observed for the axle triazolium proton (0.72 ppm for $Cl^-$, 0.67 ppm for $Br^-$ and 0.36 ppm for $I^-$). In contrast, addition of oxoanions acetate and dihydrogen phosphate led to small upfield shifts of these resonances (around 0.05 ppm), suggesting weak binding.

Monitoring the axle triazolium proton (labelled ***k*** in **Figure 2.11**), BindFit [14,15] analysis of the titration data gave the 1:1 stoichiometric host:guest association constants summarized in **Table 2.3**, which were compared to those obtained for the acyclic receptor **2.4.HB$^+$PF$_6^-$** and for the structurally similar, more preorganised rotaxane **2.19.HB$^+$PF$_6^-$** previously synthesised in the group (**Figure 2.11**). [13]





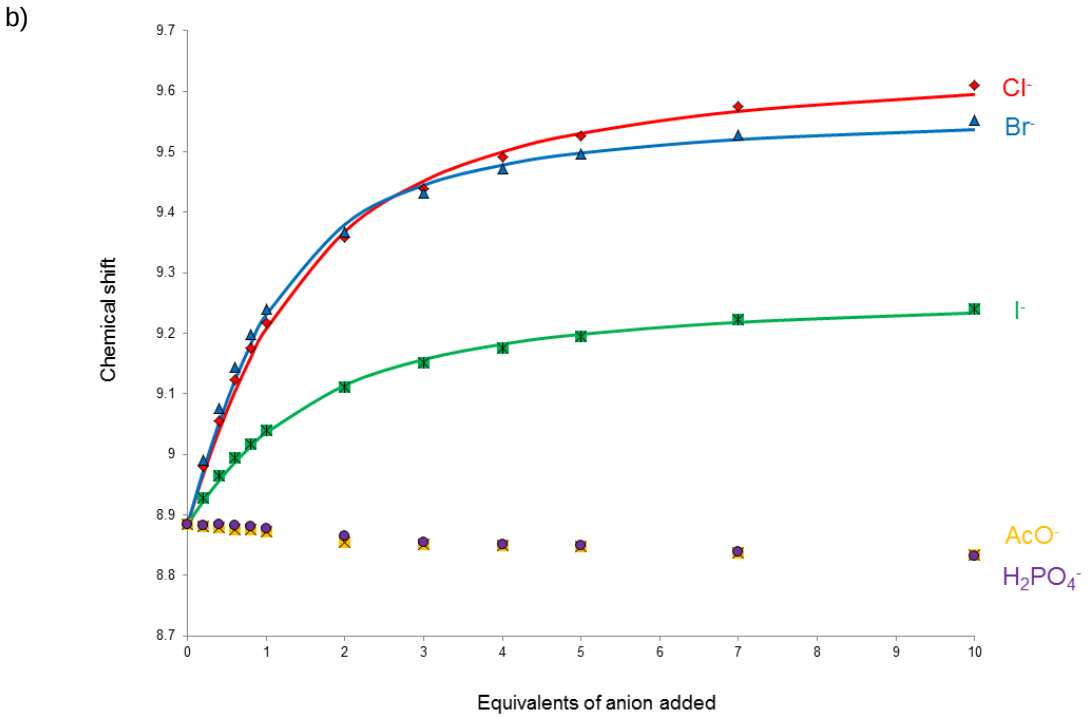




***Figure 2.11.*** *a) Structures of rotaxane* ***2.18.HB⁺PF₆⁻*** *(left) and previously synthesised rotaxane* ***2.19.HB⁺PF₆⁻*** *(right); b) Binding isotherms obtained by monitoring the chemical shifts of proton* ***k*** *with increasing quantities of various anions (45:45:10 $CDCl_3$/$CD_3OD$/$D_2O$ (v/v/v), 298 K).*

***Table 2.3.*** *Anion association constants ($K_a$/ $M^{-1}$) for acyclic and interlocked amido-triazolium receptors at 298 K.*

| Anion[a] | Association constants ($K_a$/ $M^{-1}$) [b] | | |
|---|---|---|---|
| | Acyclic | Rotaxanes | |
| | **2.4.HB$^+$PF$_6^-$** [c] | **2.18.HB$^+$PF$_6^-$** [d] | **2.19.HB$^+$PF$_6^-$** [c] |
| $Cl^-$ | 343 | 2003 | 2035 |
| $Br^-$ | 298 | 1175 | 1948 |
| $I^-$ | 385 | 1012 | NB [e] |
| $AcO^-$ | 300 | NB [e] | NB [e] |
| $H_2PO_4^-$ | 158 | NB [e] | NB [e] |

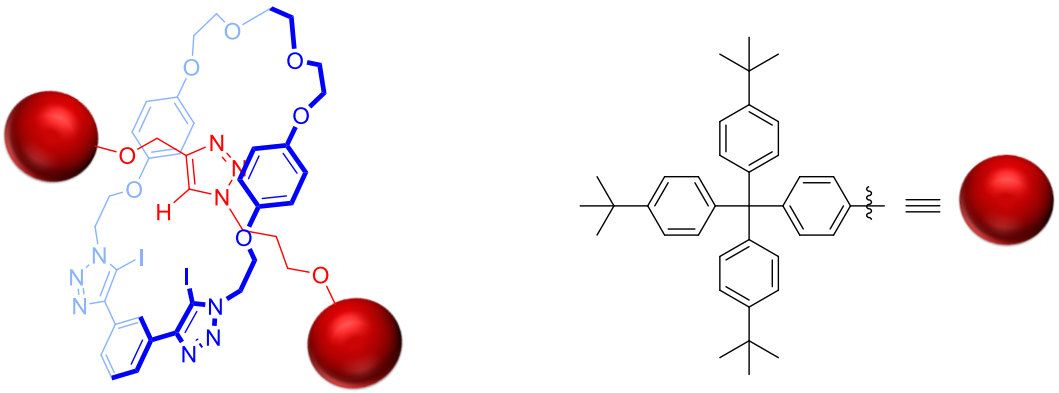
*[a] Anions were added as their tetrabutylammonium (TBA) salts. [b] Calculated using BindFit [14,15] by monitoring the change in the chemical shift of the triazolium proton (labelled **k** in **Figure 2.11**). Errors < 10%. [c] Titrations were conducted in 1:1 $CDCl_3$/$CD_3OD$ (v/v). [d] Titrations were conducted in 45:45:10 $CDCl_3$/$CD_3OD$/$D_2O$ (v/v/v). [e] NB = no binding. In all cases, the perturbations of the chemical shift were very small (Δδ ≤ 0.05 ppm), which indicates that the receptor does not interact significantly with the guest anion.*

Not surprisingly, both rotaxanes are superior hosts than the acyclic system **2.4.HB$^+$PF$_6^-$** due to the presence of an interlocked binding cavity, forming strong and selective complexes with chloride and bromide. Notably, the rotaxanes do not bind the larger oxoanions, which do not fit in the three-dimensional cavity of the interlocked receptor and thus bind weakly on the periphery, as indicated by the very small upfield shift of the axle triazolium proton. The novel rotaxane **2.18.HB$^+$PF$_6^-$** binds chloride as well as the previously reported rotaxane, notably in a more competitive aqueous – organic solvent mixture. Surprisingly, it also binds iodide strongly, unlike its more rigid counterpart – presumably, the binding pocket of **2.18.HB$^+$PF$_6^-$** is less sterically hindered and thus can accommodate the larger iodide anion. Moreover, an additional solvophobic driving force is present in the $CDCl_3$/$CD_3OD$/$D_2O$ solvent system.

## 2.4. Neutral HB/XB amido-triazole [2]rotaxanes for anion recognition

### 2.4.1. Design of target rotaxanes

In previous work, Beer and co-workers reported a neutral mixed HB/XB [2]rotaxane incorporating a simple triazole donor motif on the axle, which displayed modest halide affinities in 2:98 $D_2O$/acetone-$d_6$ (*v/v*) (**Figure 2.12**). [22]



**2.40**

***Figure 2.12.*** *Structure of previously reported mixed HB/XB rotaxane* ***2.40****.*

In an effort to enhance the anion binding strength and selectivity properties of **2.40**, a series of novel neutral HB/XB [2]rotaxanes were targeted by exploiting the same XB macrocycle component, while the nature of the axle component HB triazole donor was varied (**Figure 2.13**).

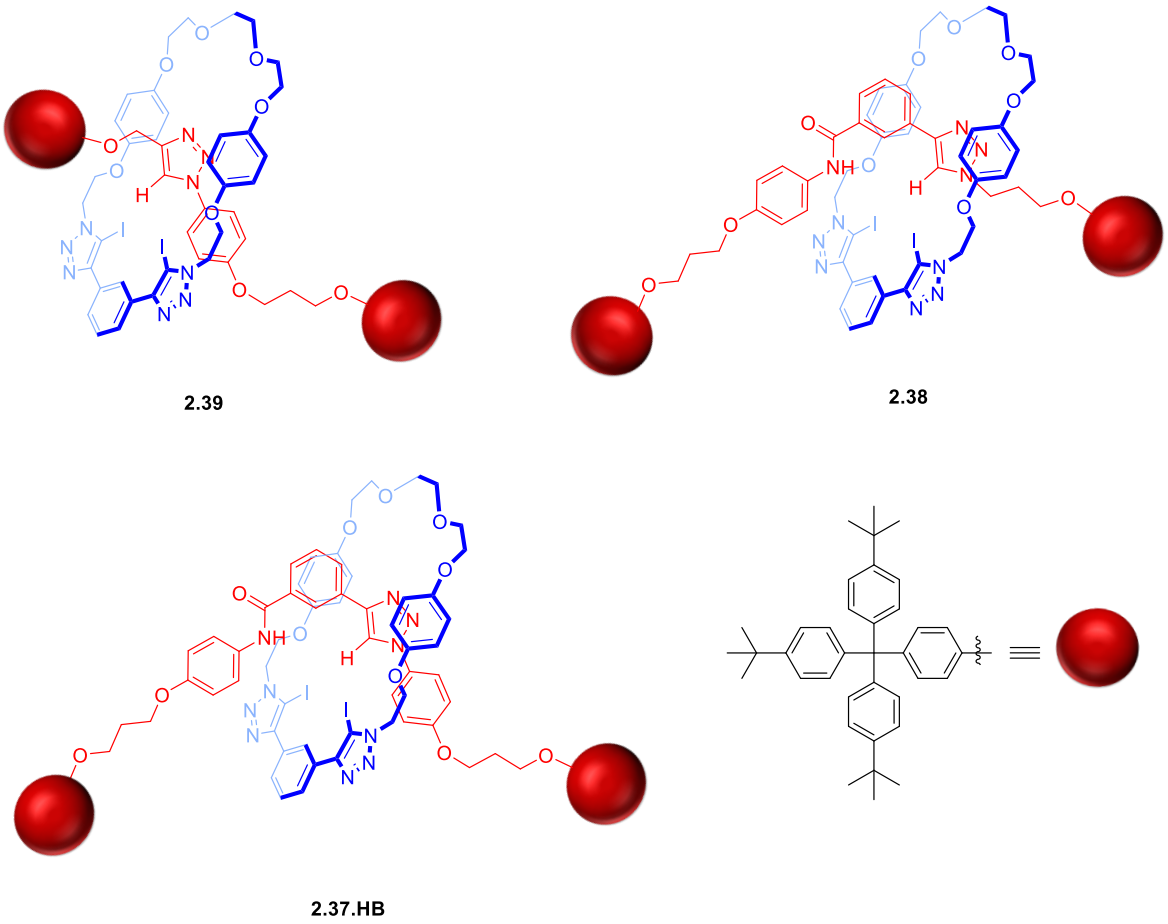



***Figure 2.13.*** *Structures of the target novel neutral HB/XB rotaxanes* ***2.37.HB – 2.39****.*

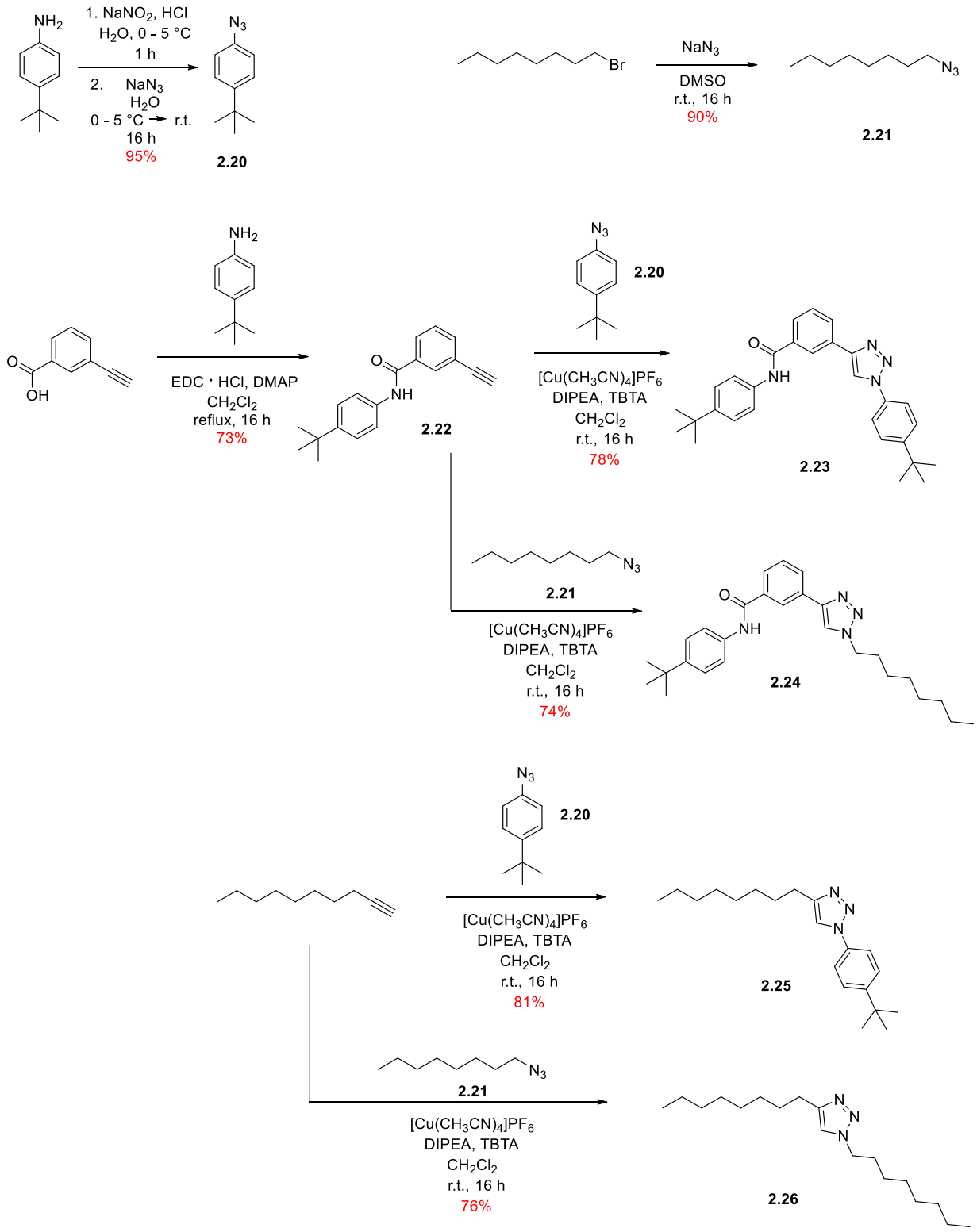
### 2.4.2. Synthesis and anion recognition properties of neutral acyclic systems

#### 2.4.2.1. Synthesis of amido-triazole acyclic receptors

Initially, four model acyclic receptors each bearing the same anion recognition motifs as the axles of the target rotaxanes were synthesised and their preliminary anion binding properties investigated (**Scheme 2.7**).

Firstly, aromatic azide **2.20** was synthesised through the diazotisation of 4-(tert-butyl)aniline followed by substitution with $NaN_3$ in an overall yield of 95%, [23] while aliphatic azide **2.21** was obtained in a 90% yield through an $S_N2$ reaction of 1-bromooctane with $NaN_3$ in DMSO. [24] EDC-mediated amide condensation of 3-ethynylbenzoic acid with 4-(tert-butyl)aniline afforded aromatic alkyne **2.22** in a 73% yield. Subsequently, each of the azides **2.20** and **2.21** was subjected to a CuAAC reaction with the alkynes **2.22** and

commercially available 1-decyne, thus affording a library of the acyclic triazole-based receptors **2.23** – **2.26** in reasonable yields.




***Scheme 2.7.*** *Synthesis of model acyclic neutral receptors* ***2.23*** *–* ***2.26****.*

### 2.4.2.2. Preliminary anion binding studies

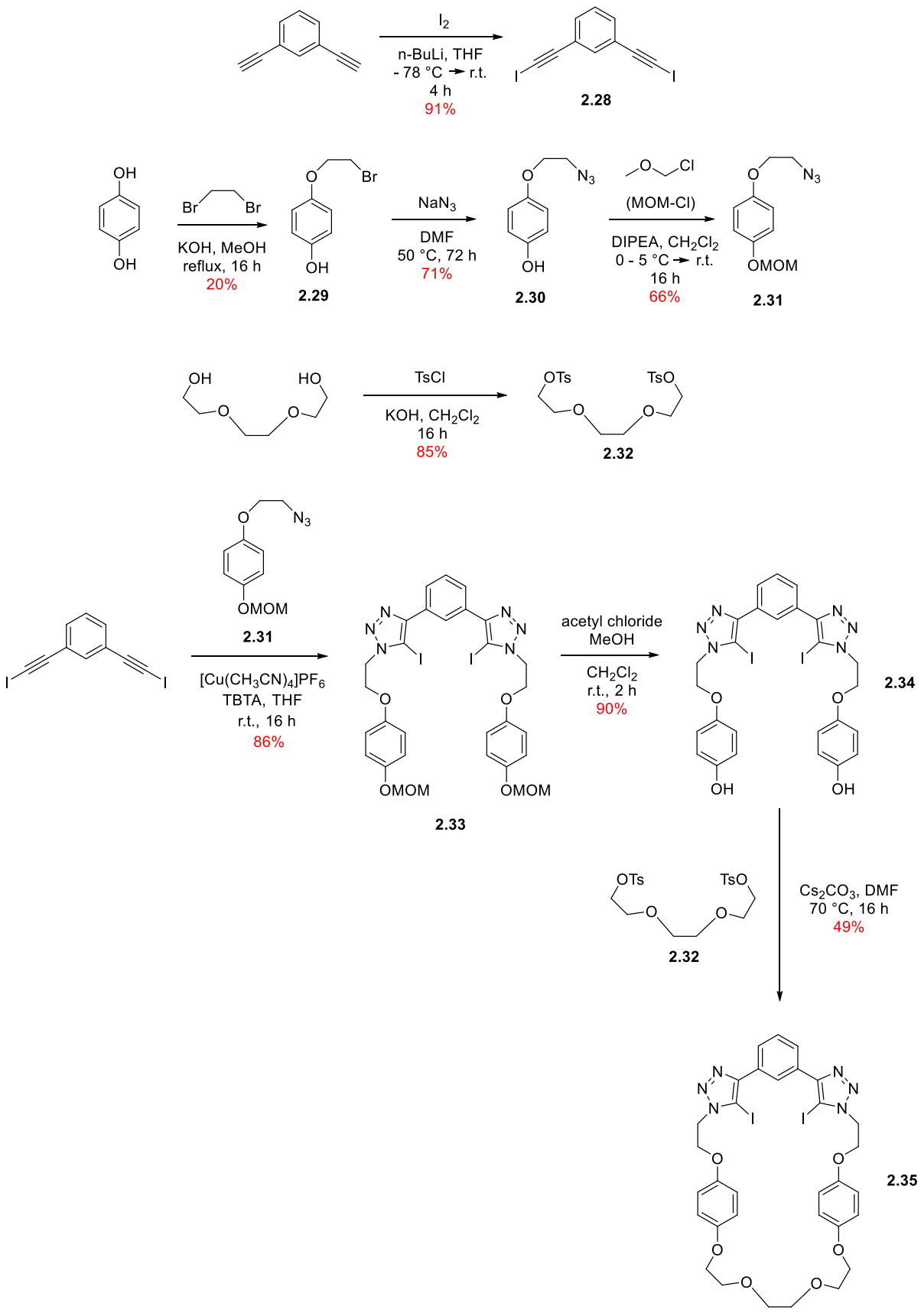
The affinity of each receptor towards several anions was probed via $^1$H NMR titration experiments in the mildly competitive solvent system 2:98 $D_2O$/acetone-$d_6$ (*v/v*) by monitoring the chemical shift of the triazole proton. The anion-induced shifts were plotted against the equivalents of anion added and the resulting isotherms were analysed using BindFit [14,15].

Unfortunately, the observed shift (Δδ) in the triazole C – H proton even after addition of 10 equivalents of anion was less than 0.05 ppm for **2.25** and **2.26**, which suggests weak binding. Δδ was more significant for the amido-triazole receptors **2.23** and **2.24** (0.06 – 0.48 ppm), however, the experimental binding isotherms did not show sufficient curvature to allow accurate determination of $K_a$ values over the anion concentration range covered, and in most cases it was only possible to estimate an upper limit of $K_a \leq 50$ M$^{-1}$. The sole exception was **2.23**, which weakly bound chloride with a 1:1 host:guest stoichiometry ($K_a$ = 65 M$^{-1}$). The limited anion binding capabilities of receptors **2.23** – **2.26** in $D_2O$/acetone-$d_6$ were rationalised in terms of their neutrality and provision of only one or two HB donor groups.

It was anticipated that incorporation of these motifs into multivalent rotaxane systems with more preorganised and solvent-shielded binding cavities decorated with convergent HB and XB donor groups would lead to greatly improved anion binding.

### 2.4.3. Synthesis of a bis(iodotriazole) macrocycle

The bis(iodotriazole) macrocycle **2.35** has been shown to coordinate a $Cu^+$ cation endotopically, thus favouring AMT synthesis of neutral rotaxanes. [22] The macrocycle was synthesised according to established procedures (**Scheme 2.8**). [22,25–27] Commercially available 1,4-hydroquinone was monoalkylated with 1,2-dibromoethane to afford bromo-appended phenol **2.29**, which was subsequently reacted with $NaN_3$ in an $S_N2$ reaction to give the organic azide **2.30** in a 71% yield after column chromatography. The phenol moiety was then protected with chloromethyl methyl ether (MOM chloride) to give MOM-protected azide **2.31**. A CuAAC reaction of **2.31** with bis(iodoalkyne) **2.28** derived from 1,3-diethynylbenzene afforded bis(iodotriazole) **2.33** which was subsequently deprotected with acetyl chloride. The resulting bisphenol **2.34** was subjected to a Williamson ether cyclisation with bis(tosylate) **2.32** derived from triethylene glycol to afford the desired macrocycle **2.35** in 25% yield after iterative preparative TLC purification. The yield was improved to 49% by alternatively employing silica column chromatography as a purification method.



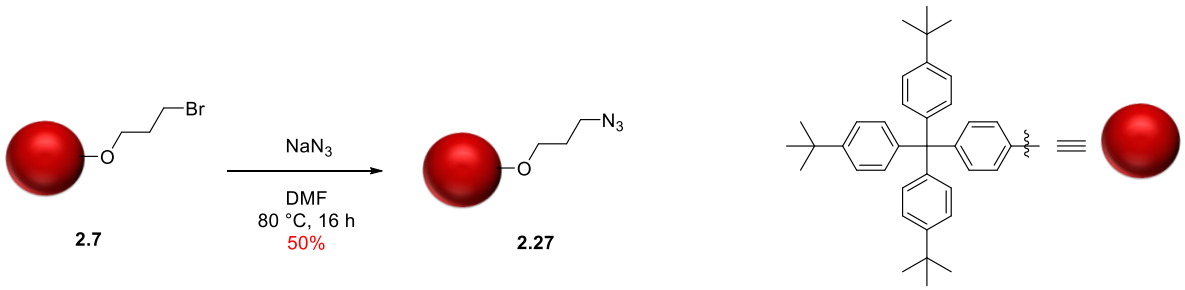

***Scheme 2.8.*** *Synthesis of bis(iodotriazole)macrocycle* ***2.35****.*

### 2.4.4. Synthesis and anion recognition properties of neutral rotaxane systems

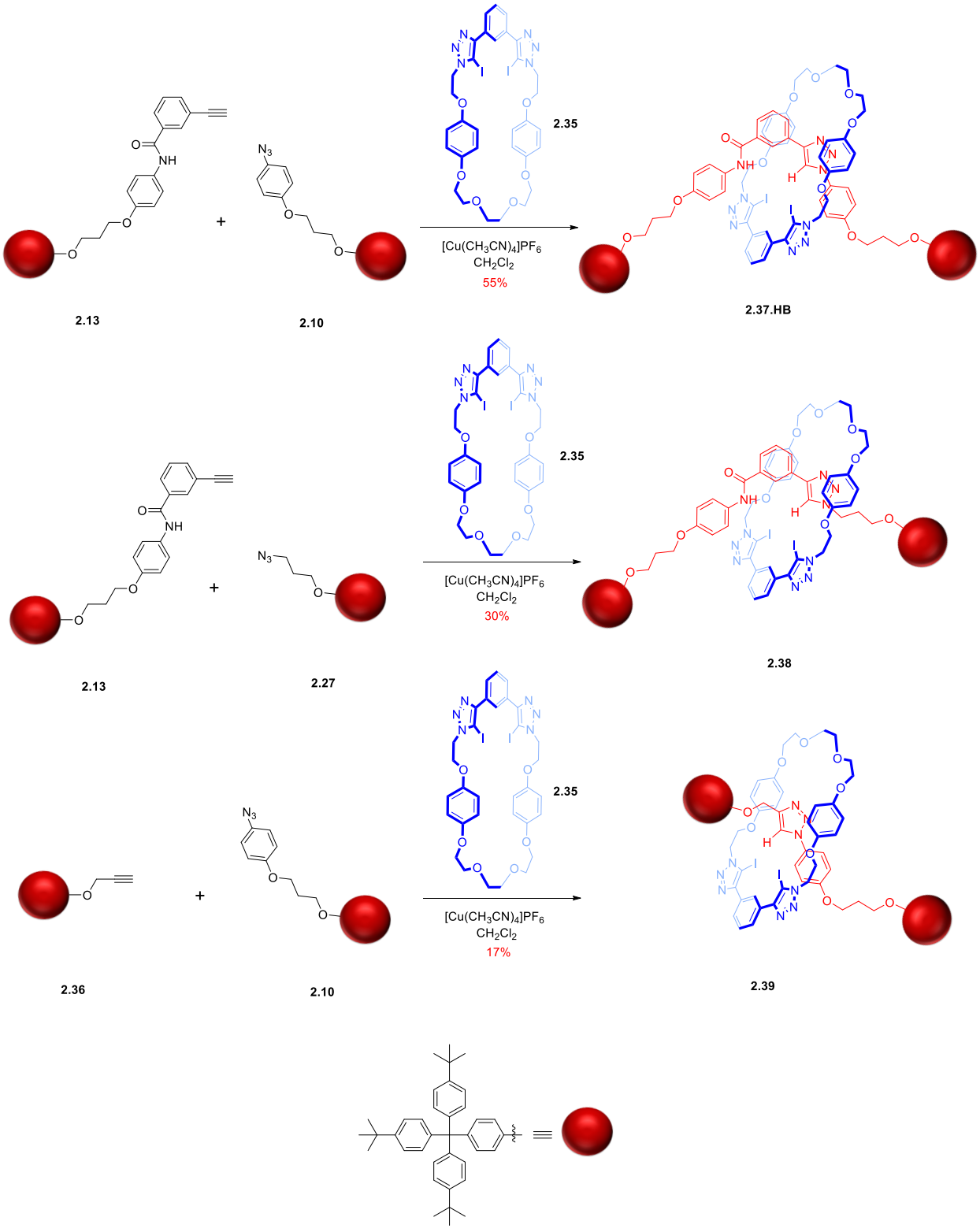
#### 2.4.4.1. Synthesis and characterisation of amido-triazole [2]rotaxanes

An active metal templation strategy was employed to synthesise the target neutral rotaxanes. This necessitated the preparation of appropriate azide- and alkyne-functionalised stopper derivatives. Aromatic azide **2.10** and aromatic alkyne **2.13** were synthesised as shown in **Scheme 2.4**. Aliphatic azide **2.27** was prepared via an $S_N2$ reaction of stopper bromide **2.7** with $NaN_3$ in DMF [17] (**Scheme 2.9**) and aliphatic alkyne **2.36** was prepared by a literature procedure [28] and kindly donated by Dr. Asha Brown.

Three equivalents of alkyne-appended half-axle and three equivalents of azide-appended half-axle were added to an equimolar $CH_2Cl_2$ mixture of macrocycle **2.35** and $[Cu(CH_3CN)_4]PF_6$ and stirred at room temperature for 3 days to afford [2]rotaxanes **2.37.HB**, **2.38**, and **2.39** (**Scheme 2.10**).




***Scheme 2.9.*** *Synthesis of aliphatic azide-appended half-axle* ***2.27****.*




***Scheme 2.10.*** *Active metal template synthesis of the family of neutral rotaxanes* ***2.37 – 2.39.***

The desired rotaxane **2.37.HB** was isolated in 55% yield after iterative preparative thin layer chromatography. Interestingly, the $^{1}$H NMR spectrum of the crude reaction mixture after removal of the $Cu^{+}$ template only indicated the presence of rotaxane and free axle (**Figure 2.14**), with apparently no unreacted macrocycle. This suggested an impressive 100% conversion with respect to the macrocycle. The hypothesis was corroborated by integration of the respective proton peaks in the $^{1}$H NMR spectrum of the crude mixture, which revealed a 1:2 molar ratio of rotaxane to axle (as expected, since the molar ratio employed was 1:1:3:3 Cu(I):macrocycle:stopper alkyne:stopper azide).

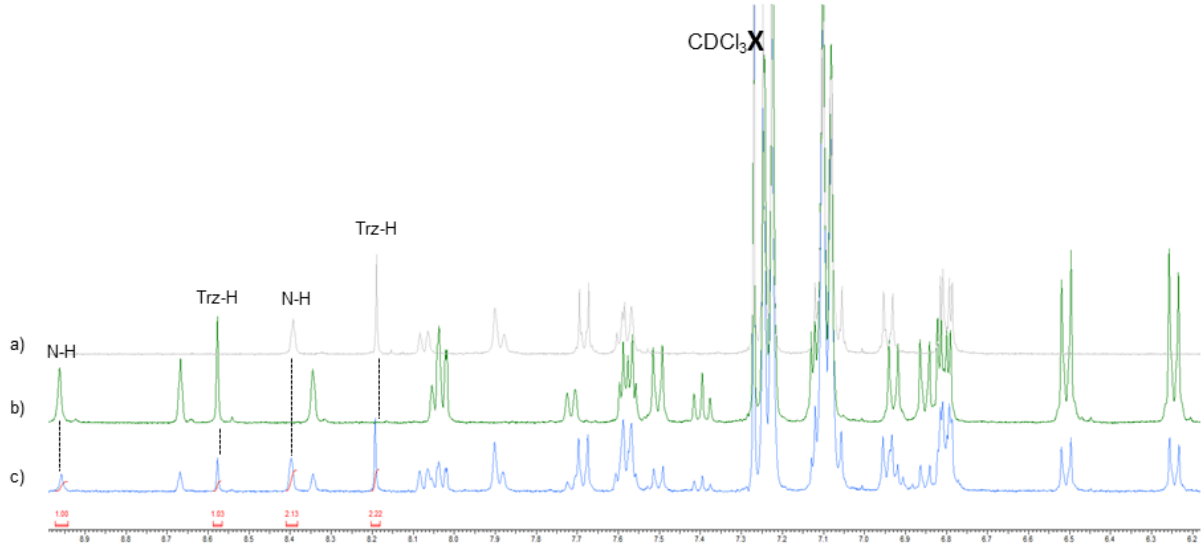



***Figure 2.14.*** *Overlay of truncated $^{1}$H NMR spectra of a) the axle component **2.37.HB.a**, b) amido-triazole HB rotaxane **2.37.HB**, and c) crude reaction mixture containing only **2.37.HB** and axle in a molar ratio of 1:2 ($CDCl_3$, 298 K, 400 MHz). N – H = amide signal, Trz-H = triazole signal.*

In the case of the formation of rotaxanes **2.38** and **2.39**, however, unreacted starting materials were detected in the $^{1}$H NMR spectra of the crude reaction mixtures, even when an excess of Cu(I) catalyst was used after 3 days. After iterative preparative TLC purification, the rotaxanes **2.38** and **2.39** were isolated in correspondingly lower yields of 30% and 17%, respectively. It is difficult to rationalise the rotaxane yield variation. Previous research in the Beer group showed that the rotaxane synthesis failed when the azide functional group was directly attached to the terphenyl stopper unit, [32] which suggests that steric hindrance at the macrocyclic metal binding site plays an important role in active metal templation. [29]

The three novel rotaxanes **2.37.HB**, **2.38**, and **2.39** were fully characterised by $^{1}$H NMR and $^{1}$H-$^{1}$H ROESY spectroscopy, as well as high-resolution electrospray mass spectrometry or MALDI in the case of **2.37.HB**. 2D ROESY spectroscopy further confirmed the interlocked nature of these rotaxanes (**Figures 2.16, 2.18** and **2.20**). Several inter-component couplings were observed between macrocycle and axle resonances, implying that in each case the macrocycle surrounds the triazole ring (which disrupts the hydroquinone π-stacking), with the triazole proton interacting with the pseudo-crown ether half of the macrocycle *via* hydrogen bonding.

Superimposing $^{1}$H NMR spectra of the rotaxane, axle (isolated as side-products from the reaction mixtures) and macrocycle for each of the three interlocked structures (**Figures 2.15, 2.17** and **2.19**) revealed that, upon formation of the mechanical bond, the chemical shifts of the axle and macrocycle proton signals were perturbed, with most of the aromatic protons being perturbed downfield whereas the majority of the alkyl protons shift upfield. In all cases, the hydroquinone resonances were observed to split and shift upfield, a characteristic $^{1}$H NMR signature of the interlocked rotaxane architectures which is attributed to overlap of the hydroquinone groups with the π electron clouds of the axle aromatic moieties.

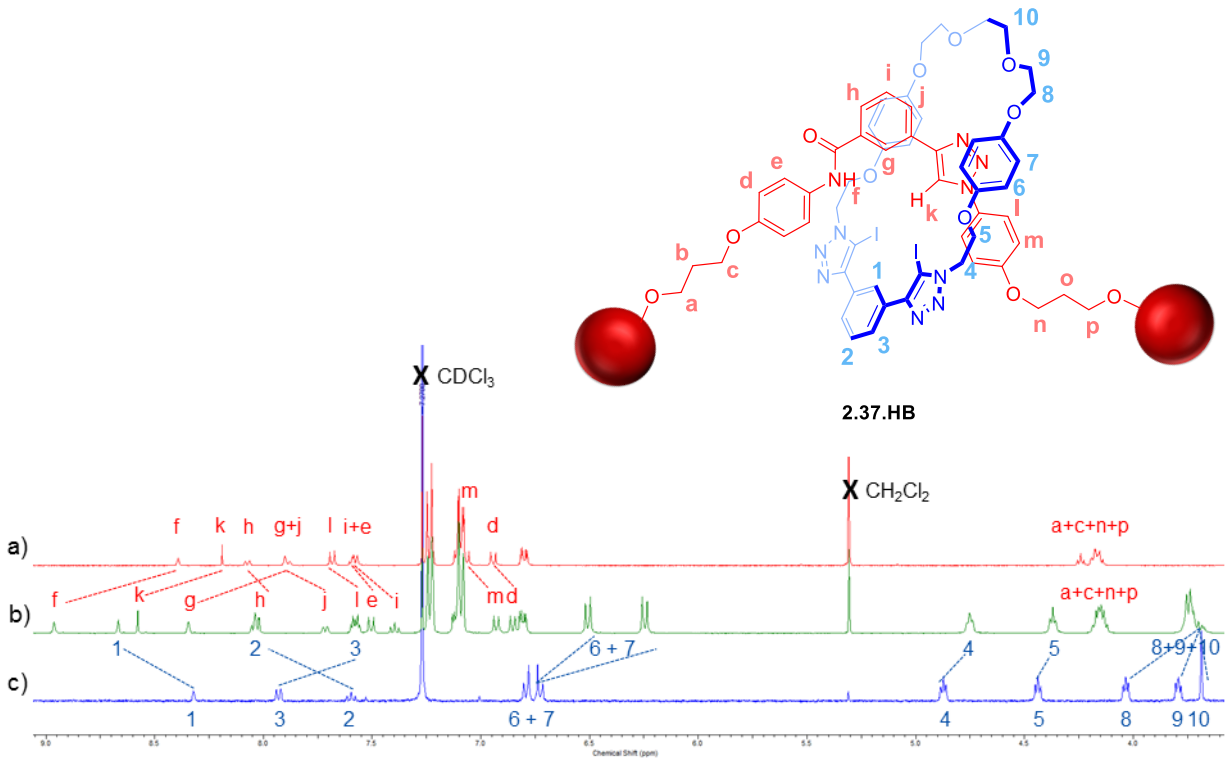



***Figure 2.15.*** *Overlay of truncated $^1$H NMR spectra of a) non-interlocked axle* ***2.37.HB.a****, b) rotaxane* ***2.37.HB*** *and c) non-interlocked macrocycle* ***2.35*** *($CDCl_3$, 298 K, 400 MHz).*

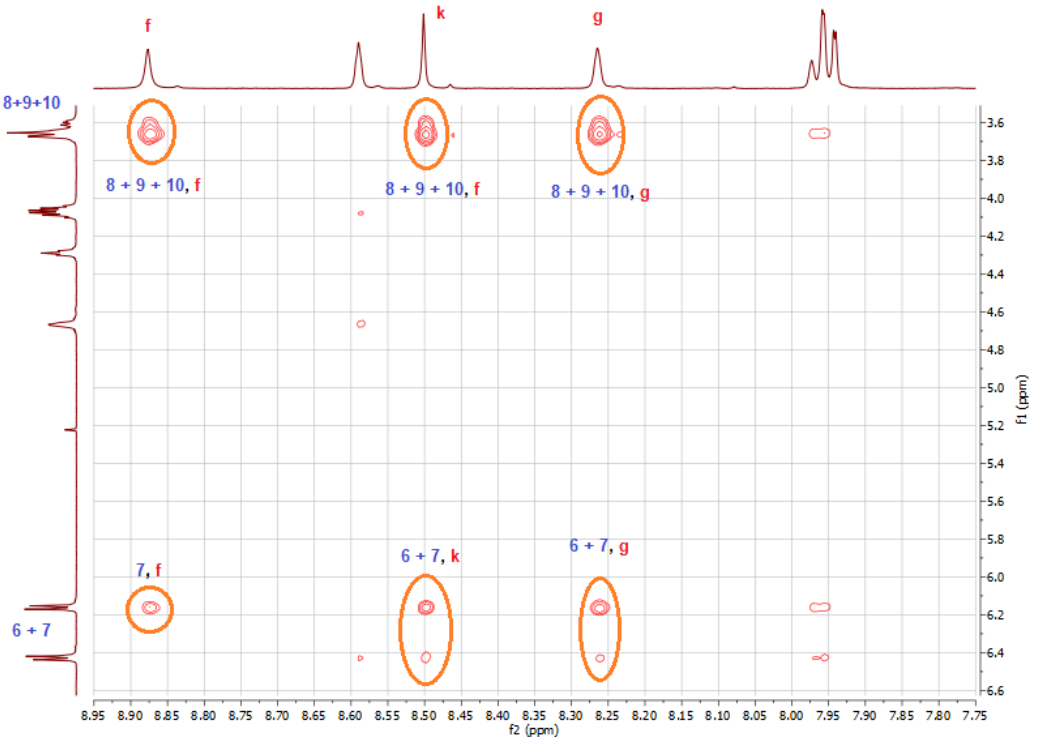



***Figure 2.16.*** *Truncated 2D ROESY spectrum of rotaxane* ***2.37.HB*** *showing relevant inter-component couplings ($CDCl_3$, 298 K).*

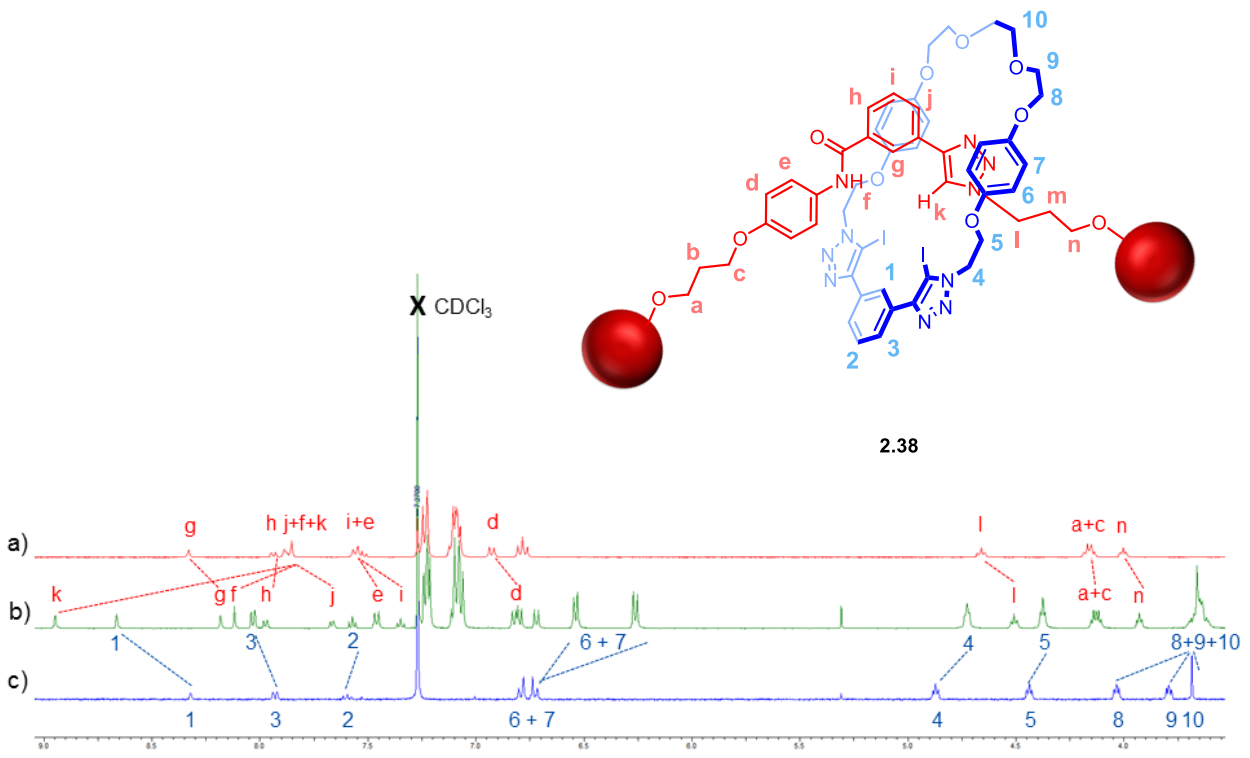



***Figure 2.17.*** *Overlay of truncated $^{1}$H NMR spectra of a) non-interlocked axle* ***2.38.a****, b) rotaxane* ***2.38*** *and c) non-interlocked macrocycle* ***2.35*** *($CDCl_3$, 298 K, 400 MHz).*

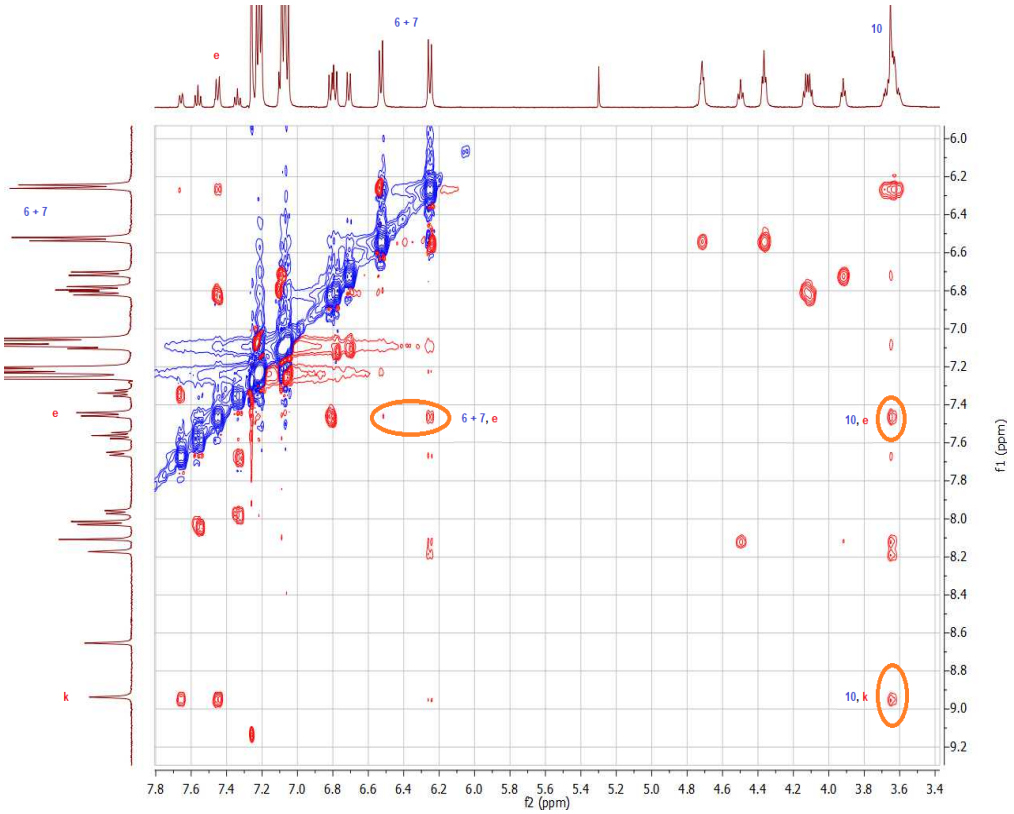



***Figure 2.18.*** *Truncated 2D ROESY spectrum of rotaxane* ***2.38*** *showing relevant inter-component couplings ($CDCl_3$, 298 K).*

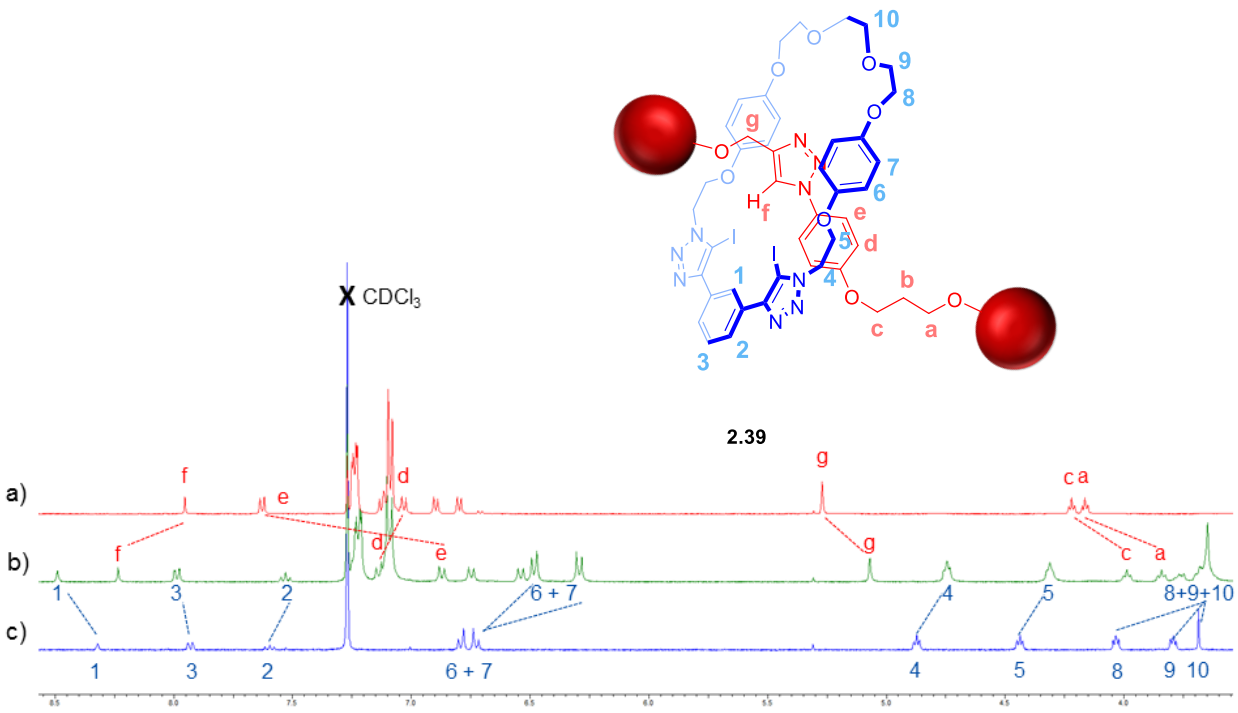



***Figure 2.19.*** *Overlay of truncated $^{1}$H NMR spectra of a) non-interlocked axle* ***2.39.a****, b) rotaxane* ***2.39*** *and c) non-interlocked macrocycle* ***2.35*** *($CDCl_3$, 298 K, 400 MHz).*

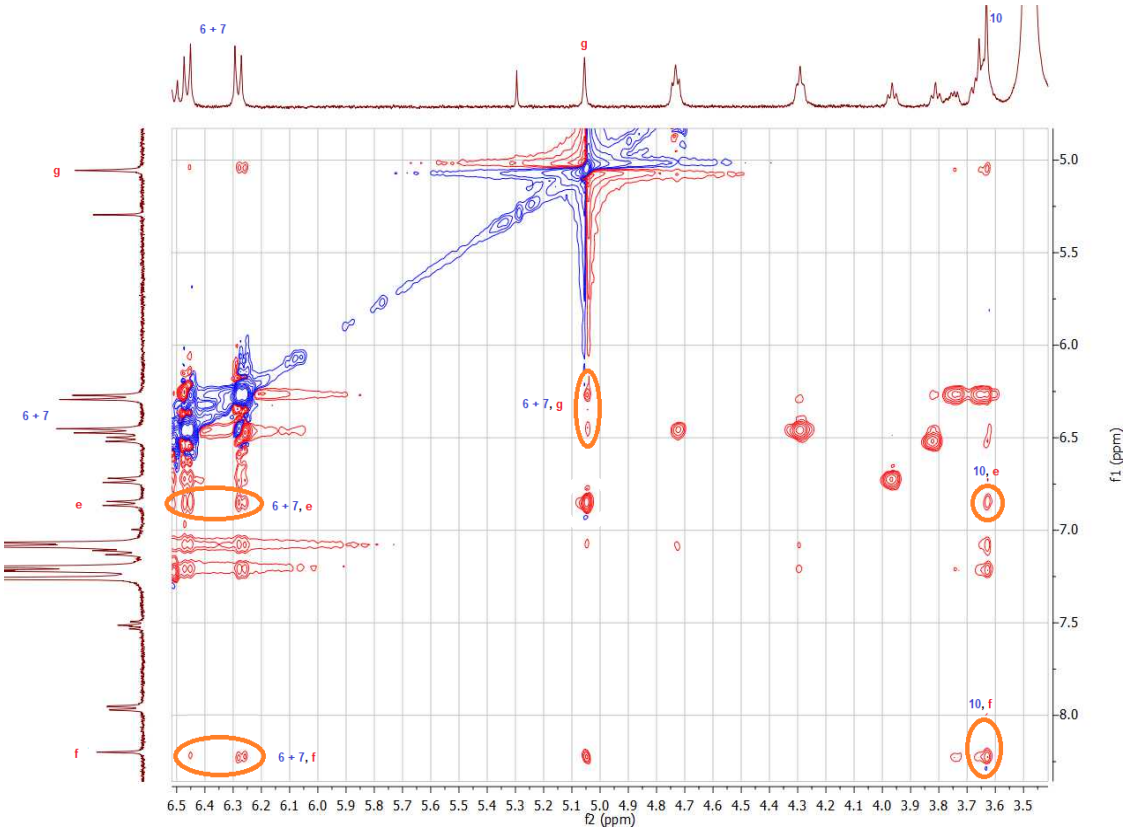



***Figure 2.20.*** *Truncated 2D ROESY spectrum of rotaxane* ***2.39*** *showing relevant inter-component couplings ($CDCl_3$, 298 K).*

### 2.4.4.2. Anion binding studies of neutral HB/XB rotaxanes

The anion recognition properties of **2.37.HB**, **2.38**, and **2.39** were determined via $^1$H NMR titration experiments in 2% or 5% $D_2O$ – acetone-$d_6$. Typically, upon addition of anions, the aromatic protons shifted downfield, with the notable exception of $I^-$, for which the majority of protons shifted upfield, indicating that the large halide anion binds outside the rotaxane cavity. As expected due to competitive anion hydration, the magnitude of change in chemical shift upon anion addition was smaller upon increasing the percentage of $D_2O$. In the case of **2.38**, the inner proton ***g*** shifted only slightly upfield, indicating that it did not participate in the binding process. Interestingly, for rotaxanes **2.37.HB** and **2.38**, the macrocycle alkyl resonances split into multiplets upon addition of halides, with a greater degree of splitting occurring with smaller halides (**Figure 2.21**).

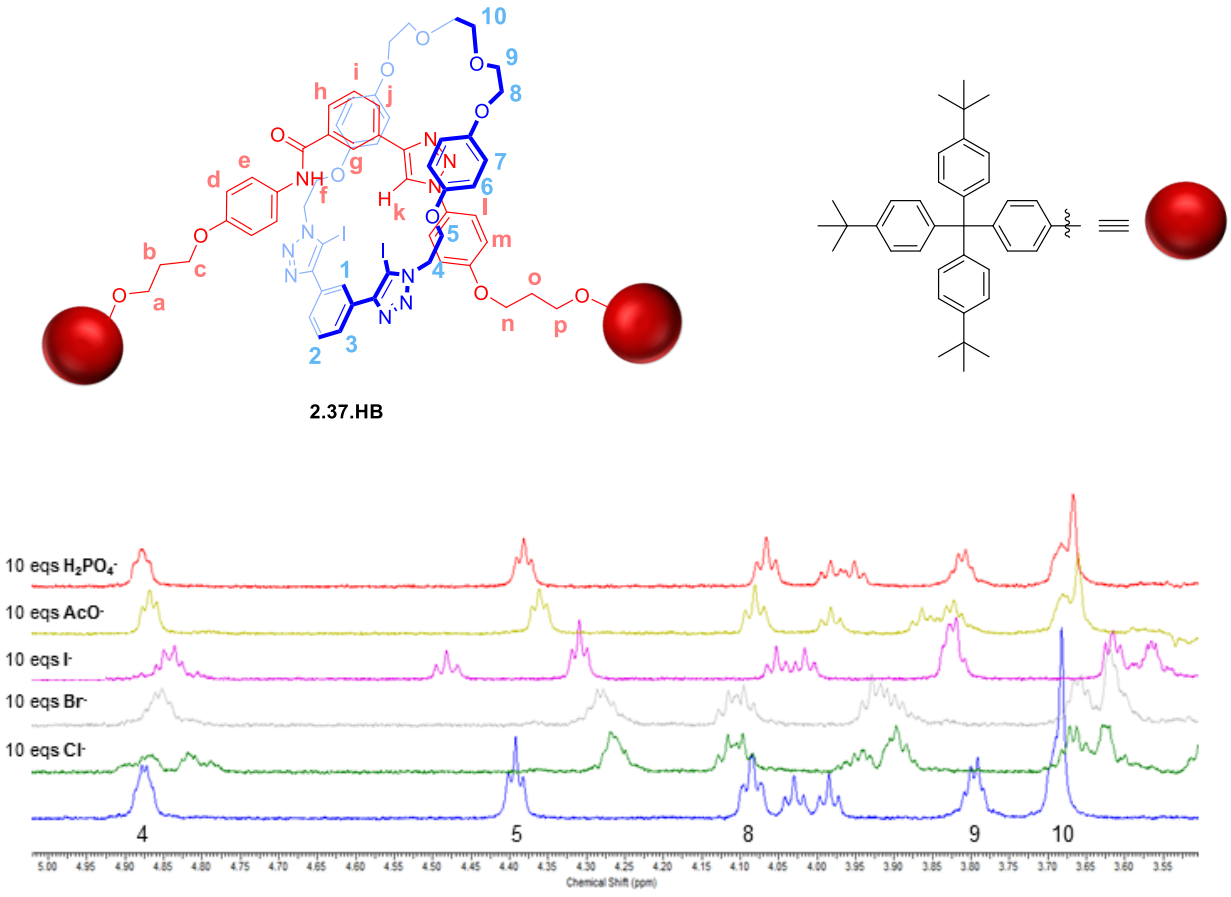


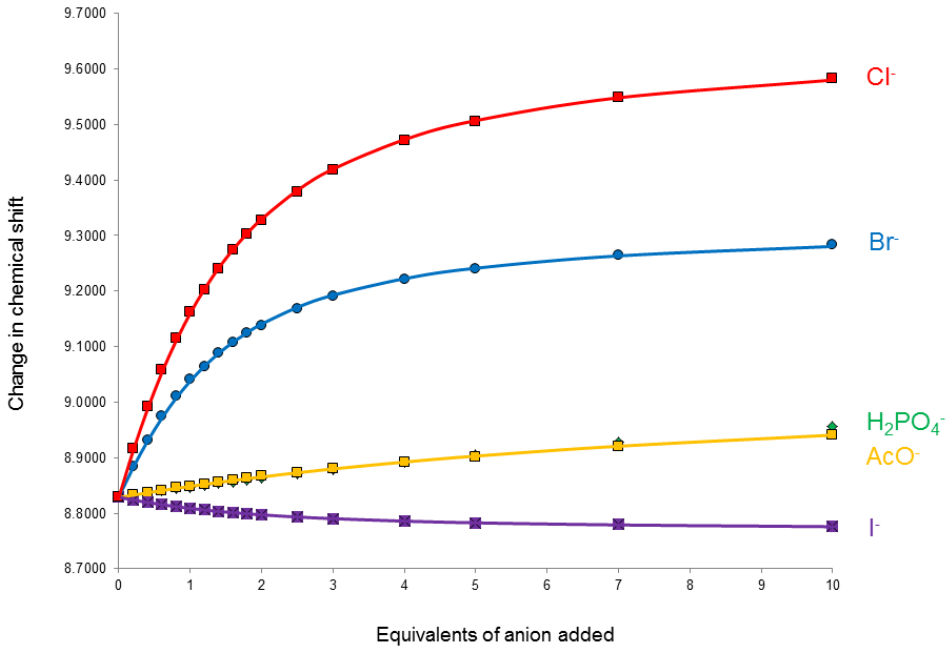

***Figure 2.21.*** *Superimposed truncated $^1$H NMR spectra of rotaxane **2.37.HB** obtained before and after the addition of 10 equivalents of anion in 2% $D_2O$ – acetone-$d_6$. Inset: structure of **2.37.HB**.*

Interestingly, a higher degree of splitting is favoured with decreasing size of the halide and decreasing percentage of $D_2O$, but is apparently independent of the binding affinity itself (see **Table 2.4** below). It can be assumed that the alkyl protons ***4***, ***5***, ***8***, ***9***, and ***10*** become diastereotopic upon incorporation into the rotaxane framework due to the asymmetry of the axles, as one of the mirror planes of the macrocycle is lost. This behaviour is not observed for the aromatic protons ***6*** and ***7*** as they can interchange their position through rotation of the hydroquinone groups around the C – O bonds.

It can be hypothesised that the splitting becomes more pronounced during the titration experiments due to a more locked conformation upon anion binding; alternatively, it is also possible that the difference in the chemical shifts of the diastereotopic protons becomes more exaggerated when an anion is bound. A slow exchange regime between the bound and unbound states of the rotaxanes can be ruled out as the majority of resonances do not split upon addition of anion.

Monitoring the axle triazole proton ***k*** upon anion addition, a representative set of binding isotherms is shown in **Figure 2.22**.

a)




b)

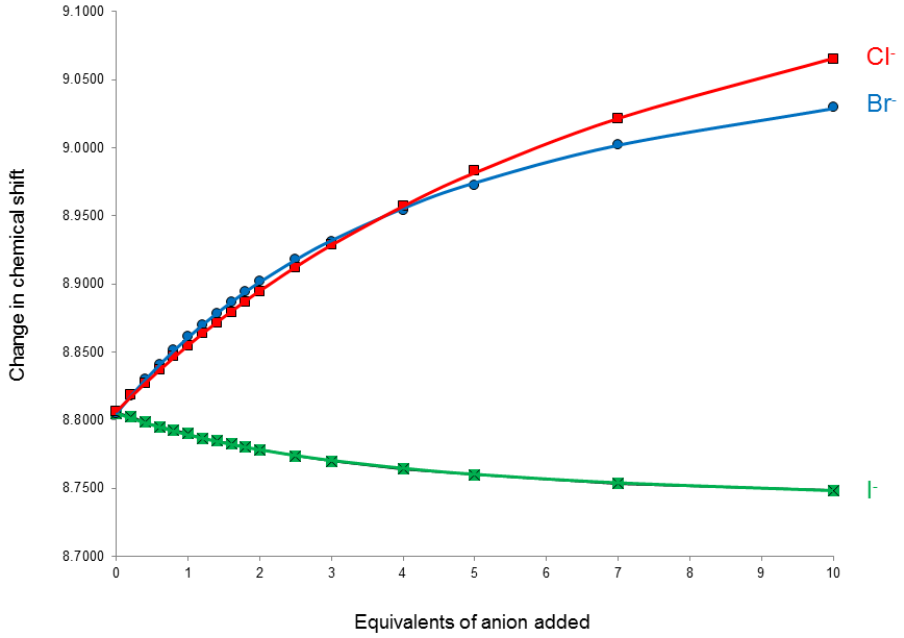



***Figure 2.22.*** *Plots of the changes in chemical shift of the triazole proton* ***k*** *against equivalents of anion added (as the TBA salt) for rotaxane* ***2.37.HB.*** *Top – 2% $D_2O$, bottom – 5% $D_2O$.*

BindFit [14,15] analysis of the titration data gave the 1:1 stoichiometric anion association constants summarised in **Table 2.4**, which were compared to those obtained for rotaxane **2.40** previously synthesised in the group.

***Table 2.4.*** *Anion association constants ($M^{-1}$) for neutral amido-triazole [2]rotaxanes at 298 K*

| **Anion**[a] | **Association constants ($K_a$/ $M^{-1}$)** [b,c] | | | | |
|---|---|---|---|---|---|
| | **2.37.HB** | **2.37.HB** | **2.38** | **2.39** | **2.40** [f] |
| | *2% $D_2O$* | *5% $D_2O$* | *2% $D_2O$* | *2% $D_2O$* | *2% $D_2O$* |
| $Cl^-$ | 1071 | 85 | 597 | 223 | 114 |
| $Br^-$ | 1245 | 214 | 742 | 707 | 371 |
| $I^-$ | 687 | 295 | 631 | 516 | 533 |
| $AcO^-$ | 81 | NB [d] | — [e] | — [e] | — [e] |
| $H_2PO_4^-$ | < 50 | NB [d] | — [e] | — [e] | — [e] |

*[a] Anions were added as their tetrabutylammonium (TBA) salts. [b] Calculated using BindFit [14,15] by monitoring the change in the chemical shift of the internal aromatic proton (labelled **b** in Figure 1). Errors < 10%. [c] Titrations were conducted in 2:98 or 5:95 $D_2O$/acetone-$d_6$ (v/v); the percentage of $D_2O$ employed is mentioned above each set of data. [d] NB = no binding. In all cases, the perturbations of the chemical shift were very small ($\Delta\delta \leq 0.05$ ppm), which indicates that the receptor does not interact significantly with the guest anion. [e] Titration not performed. [f] $K_a$ values for **2.40** were taken from reference **11.***

When comparing rotaxanes, it is noticeable that the incorporation of the aromatic amide motif into the axle component drastically increases the association constant magnitudes for the smaller halides by a factor of around 5 for $Cl^-$ and 2 for $Br^-$. This can be rationalised in terms of the strong hydrogen bond donor character of the amide proton, which favours interactions with harder anions. A comparison of rotaxanes **2.40** and **2.39** and rotaxanes **2.37.HB** and **2.38** reveals that introducing a single phenyl ring next to the nitrogen atom of the triazole unit increases the $K_a$ value for $Cl^-$ and $Br^-$ by approximately the same factor (around 1.8), whereas the affinity for iodide is largely the same. The aromatic ring decreases the electronic density on the triazole, which increases the polarisation of the triazole C – H bond in the anion binding site. Since these changes only affect HB donor groups on the interior of the three-dimensional cavity of the rotaxane, the affinity towards iodide, which binds on the periphery and is a less effective HB acceptor owing to its lower charge density, is mostly unchanged in this family of rotaxanes. A combination of the phenyl ring and the aromatic amide leads to further enhancement of the anion affinity, with **2.37.HB** displaying the strongest binding affinities for the smaller halides amongst the four rotaxanes studied.

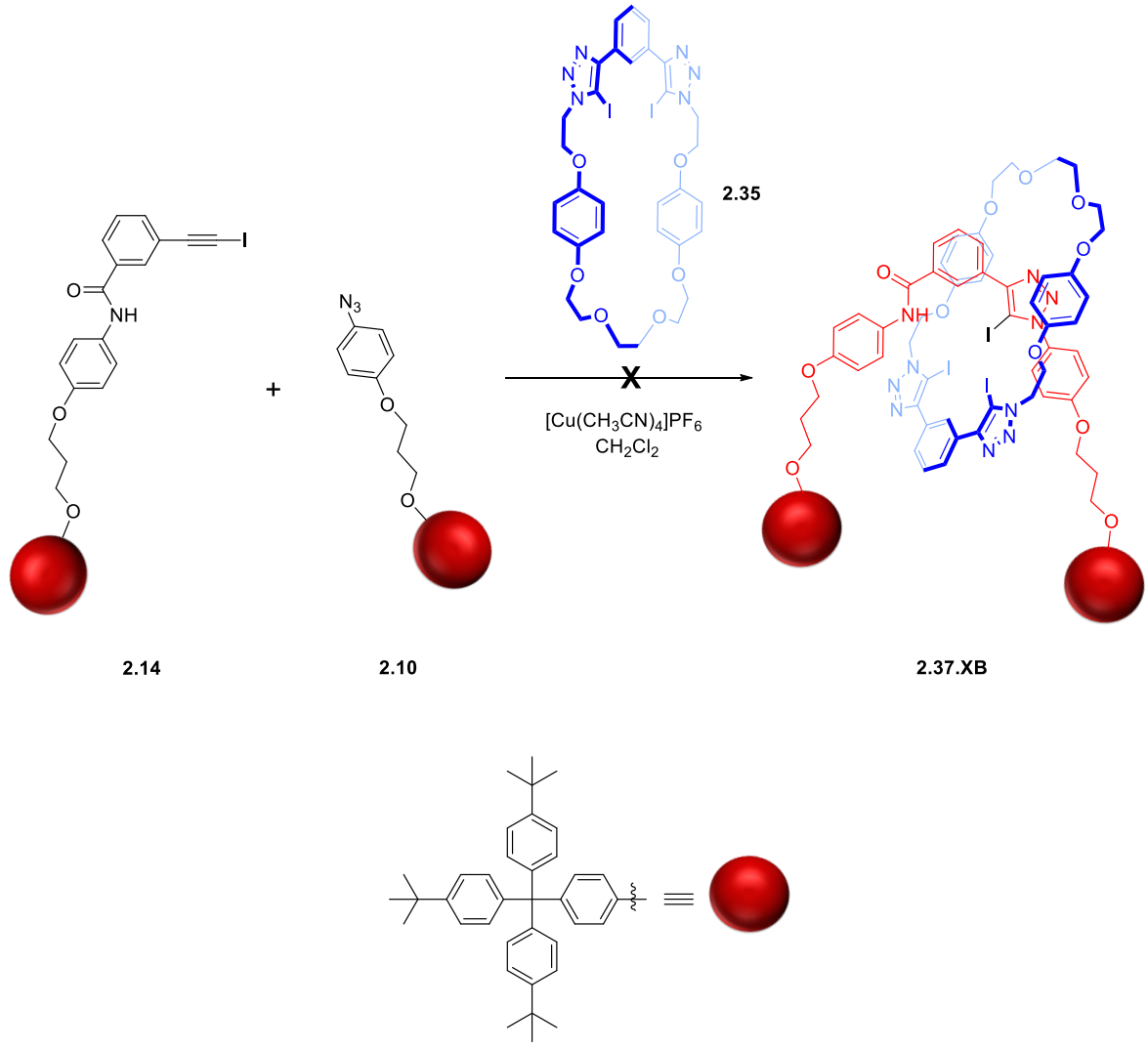
Notably, rotaxane **2.37.HB** binds bromide very strongly in 2% $D_2O$ – acetone-$d_6$, however, increasing the percentage of $D_2O$ to 5% significantly reduces $Cl^-$ binding strength, whose $K_a$ value decreases more than tenfold, and less so for bromide and iodide. This stems from a Hofmeister bias towards the binding of larger, less solvated anions in the

presence of a higher $D_2O$ percentage. All rotaxanes are selective for halides over oxoanions, which are too large to penetrate the interlocked binding site.

### 2.4.5. Synthesis of amido-iodotriazole [2]rotaxanes

#### 2.4.5.1. Neutral XB rotaxanes

Owing to the potency of XB donors, it was hypothesised that replacing the axle HB triazole motif of **2.37.HB** with an XB analogue could enhance the anion binding properties. A similar AMT protocol was sought out, employing the stopper iodoalkyne **2.14** instead of the protoalkyne analogue **2.13** (**Scheme 2.11**).

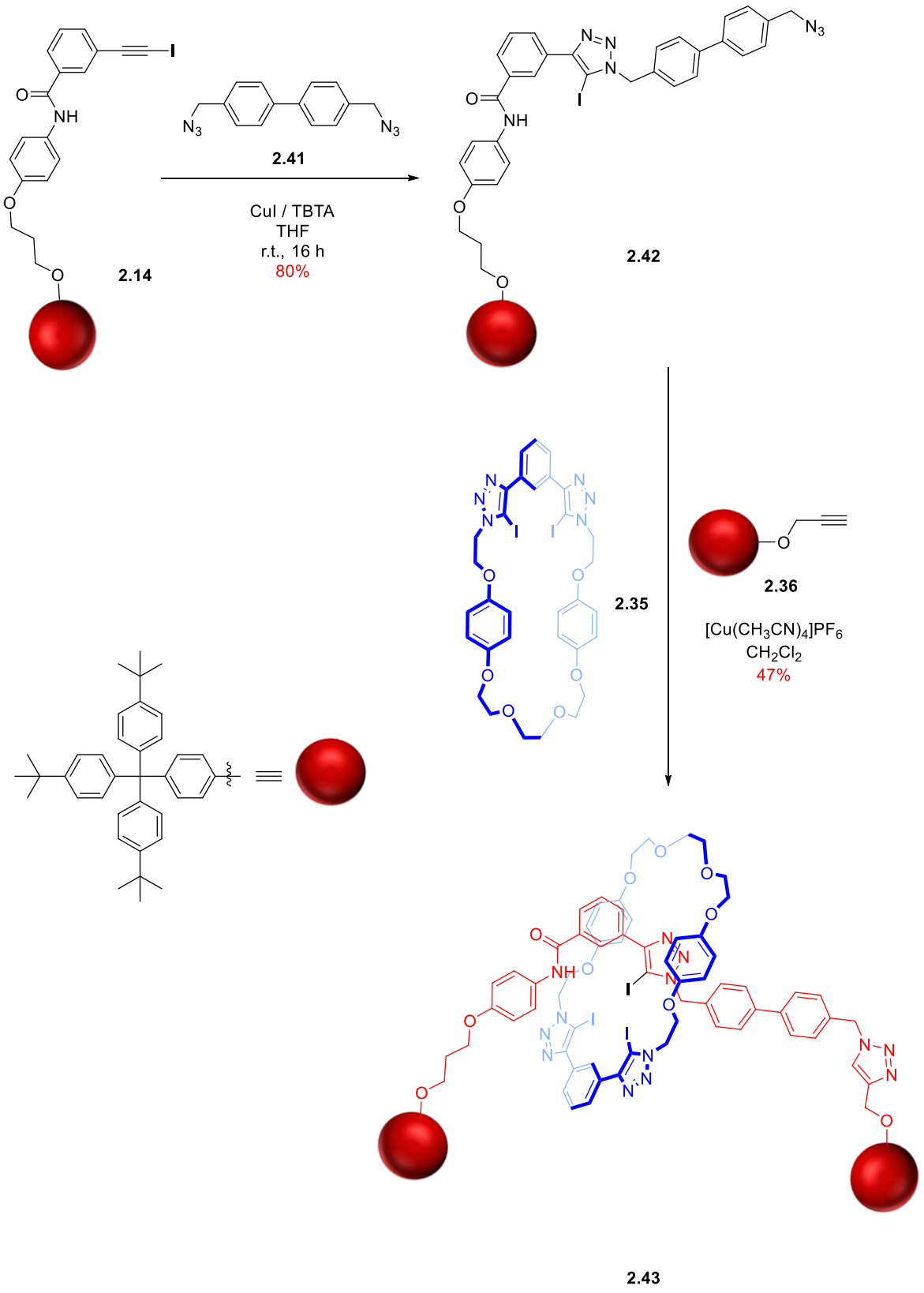



***Scheme 2.11.*** *Attempted AMT synthesis of a [2]rotaxane containing an amido-iodotriazole motif.*

Unfortunately, no click product was formed, with all starting materials fully recovered at the end of the reaction. Despite numerous attempts at optimisation, including employing microwave conditions, the same outcome was observed. This was attributed to the incompatibility of the azide and alkyne precursors with the AMT stoichiometric requirements. As noted in **Section 2.3.3.1**, the CuAAC reaction between **2.14** and **2.10** required high catalyst loadings and high concentrations, whereas the AMT protocol typically employs a 1:1:3:3 macrocycle:$Cu^{+}$:azide:alkyne stoichiometric ratio, with excess catalyst favouring axle formation over rotaxane formation. [30]

Since the iodotriazole formation under AMT conditions is highly challenging, an alternative pathway was designed in which the iodotriazole motif would be formed before the mechanical bond formation step; although the resulting [2]rotaxane would have a slightly different structure, it was assumed its binding properties could still be compared to those of **2.37.HB.**

The synthetic route towards the target amido-iodotriazole [2]rotaxane is outlined in **Scheme 2.12**. The iodoalkyne **2.14** was clicked with an excess of bis-azide **2.41** (prepared by a literature procedure [31] and kindly donated by Dr. Jessica Pancholi) in THF to give terminal azide **2.42** with a preformed amido-iodotriazole binding site in 80% yield. This was then subjected to a similar AMT protocol with the stopper alkyne **2.36** and macrocycle **2.35** to produce the desired rotaxane **2.43** in an impressive isolated yield of 47% after preparative TLC purification followed by size exclusion chromatography (**Scheme 2.12**).




***Scheme 2.12.*** *Synthesis of neutral amido-iodotriazole [2]rotaxane* ***2.43****.*

The novel rotaxane **2.43** was fully characterised by $^{1}$H NMR (**Figure 2.21**), $^{13}$C NMR, high resolution mass spectrometry, and $^{1}$H-$^{1}$H ROESY spectroscopy, which confirmed the existence of through-space cross-couplings between axle and macrocycle (**Figure 2.22**).

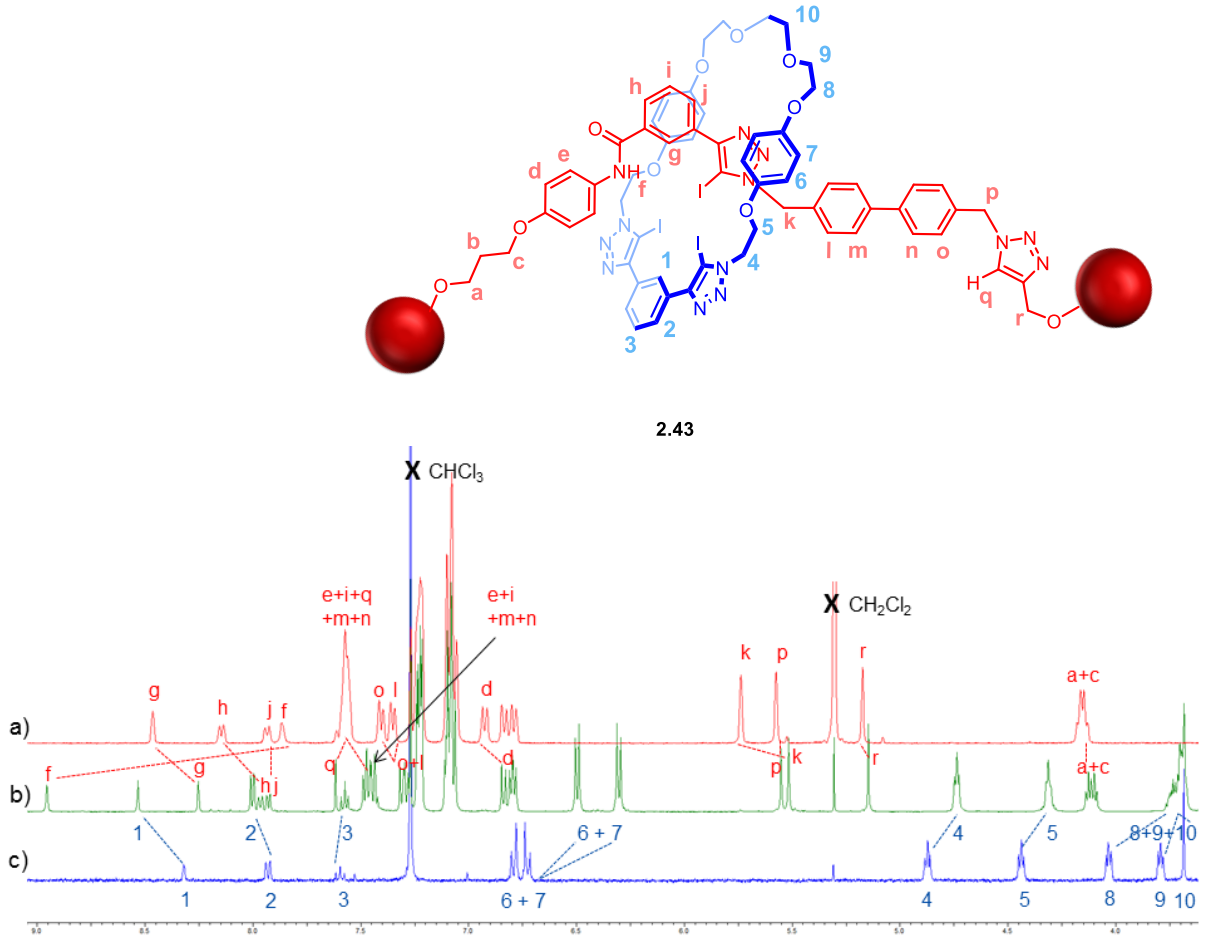



***Figure 2.21.*** *Overlay of truncated $^{1}$H NMR spectra of a) non-interlocked axle, b) rotaxane **2.43** and c) non-interlocked macrocycle **2.35** ($CDCl_3$, 298 K, 400 MHz).*

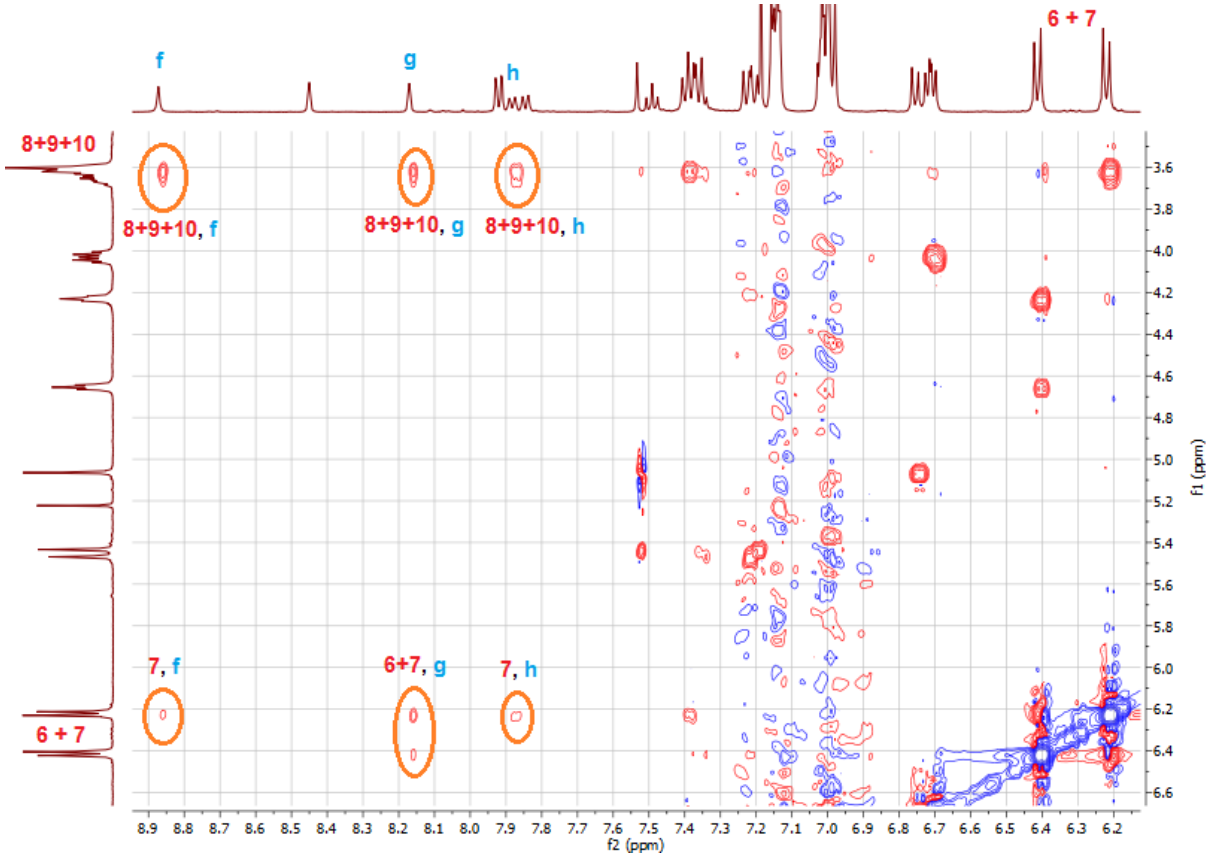



***Figure 2.22.*** *Truncated 2D ROESY spectrum of rotaxane* ***2.43*** *showing relevant inter-component couplings ($CDCl_3$, 298 K).*

#### 2.4.5.1.1. Anion binding studies of neutral XB rotaxane

The anion binding properties of the novel XB rotaxane were determined through $^1$H NMR titration experiments in 2:98 $D_2O$/acetone-$d_6$ (*v/v*). Upon addition of increasing amounts of halide anions, the majority of proton signals exhibited downfield shifts, with the notable exceptions of the hydroquinone protons and methylene signal ***p***, which shifted significantly upfield. Similarly to amido-triazole rotaxanes **2.37.HB** and **2.38**, diastereotopic splitting of the macrocycle alkyl protons was observed upon addition of anion, with a higher degree of splitting observed for smaller halides.

Unfortunately, in the case of **2.43**, there was no single suitable proton signal to monitor, as the chemical shifts of the cavity protons did not always change significantly during the course of titration experiments. Therefore, association constants were determined via global fitting of the protons that displayed sufficient change in chemical shift after the addition of 15 equivalents of anions. BindFit [14,15] analysis of the titration data gave the 1:1

stoichiometric host:guest association constants summarized in **Table 2.5**, which were compared to those obtained for the amido-triazole rotaxane **2.37.HB** (**Figure 2.23**).

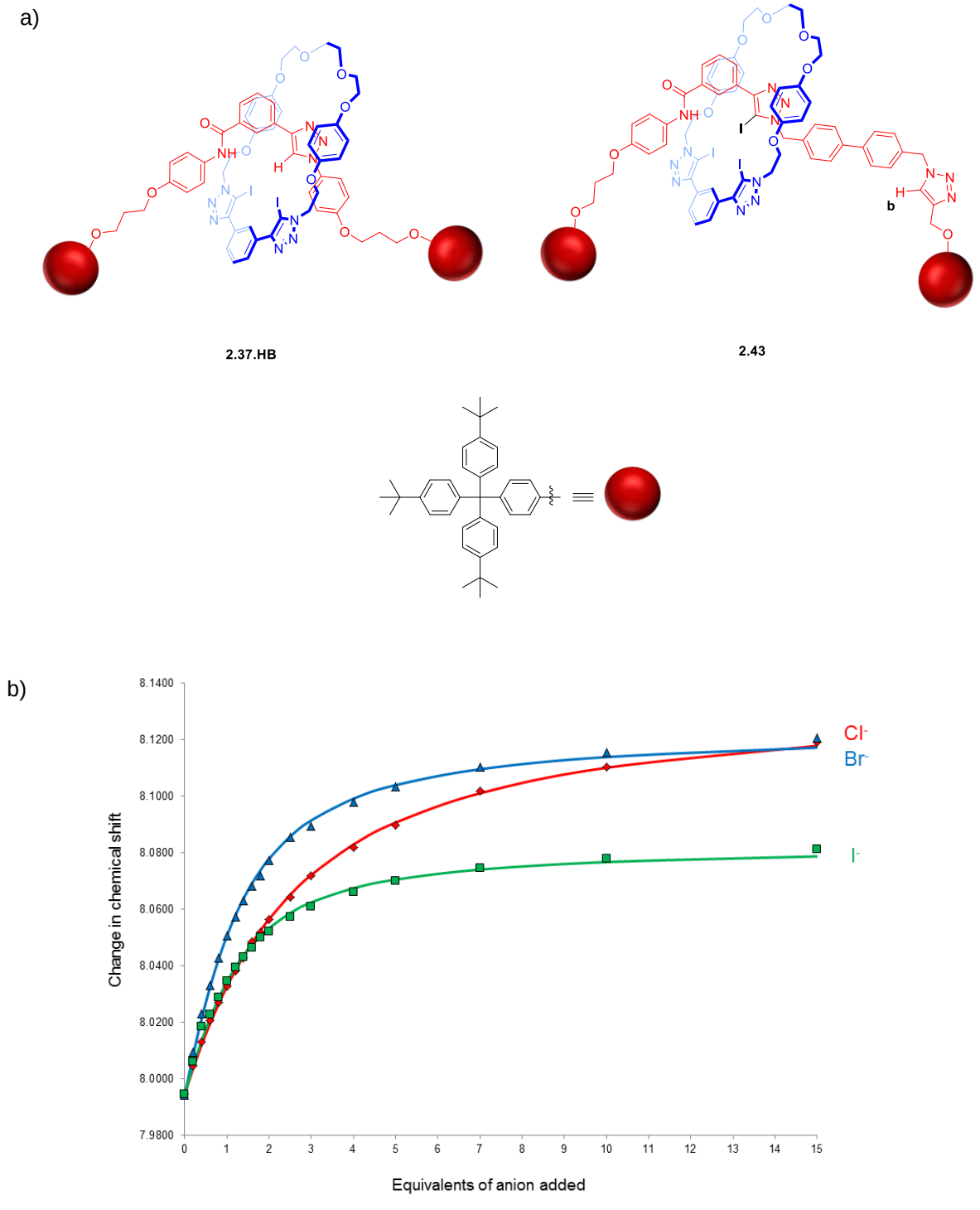



***Figure 2.23.*** *a) Structures of amido-triazole rotaxane* ***2.37.HB*** *(left) and amido-iodotriazole rotaxane* ***2.43*** *(right); b) Binding isotherms obtained by monitoring the chemical shifts of the axle triazole proton (labelled* ***b****) with increasing quantities of various anions (2:98 $D_2O$/acetone-$d_6$ (v/v), 298 K).*

***Table 2.5.*** *Anion association constants ($M^{-1}$) for neutral amido-triazole [2]rotaxanes in 2:98 $D_2O$/acetone-$d_6$ (v/v) at 298 K.*

| Anion[a] | Association constants ($K_a$/ $M^{-1}$) [b] | |
|---|---|---|
| | **2.37.HB** | **2.43** |
| $Cl^-$ | 1071 | 465 |
| $Br^-$ | 1245 | 1323 |
| $I^-$ | 687 | 1599 |
| $AcO^-$ | 81 | — [c] |
| $H_2PO_4^-$ | < 50 | — [c] |

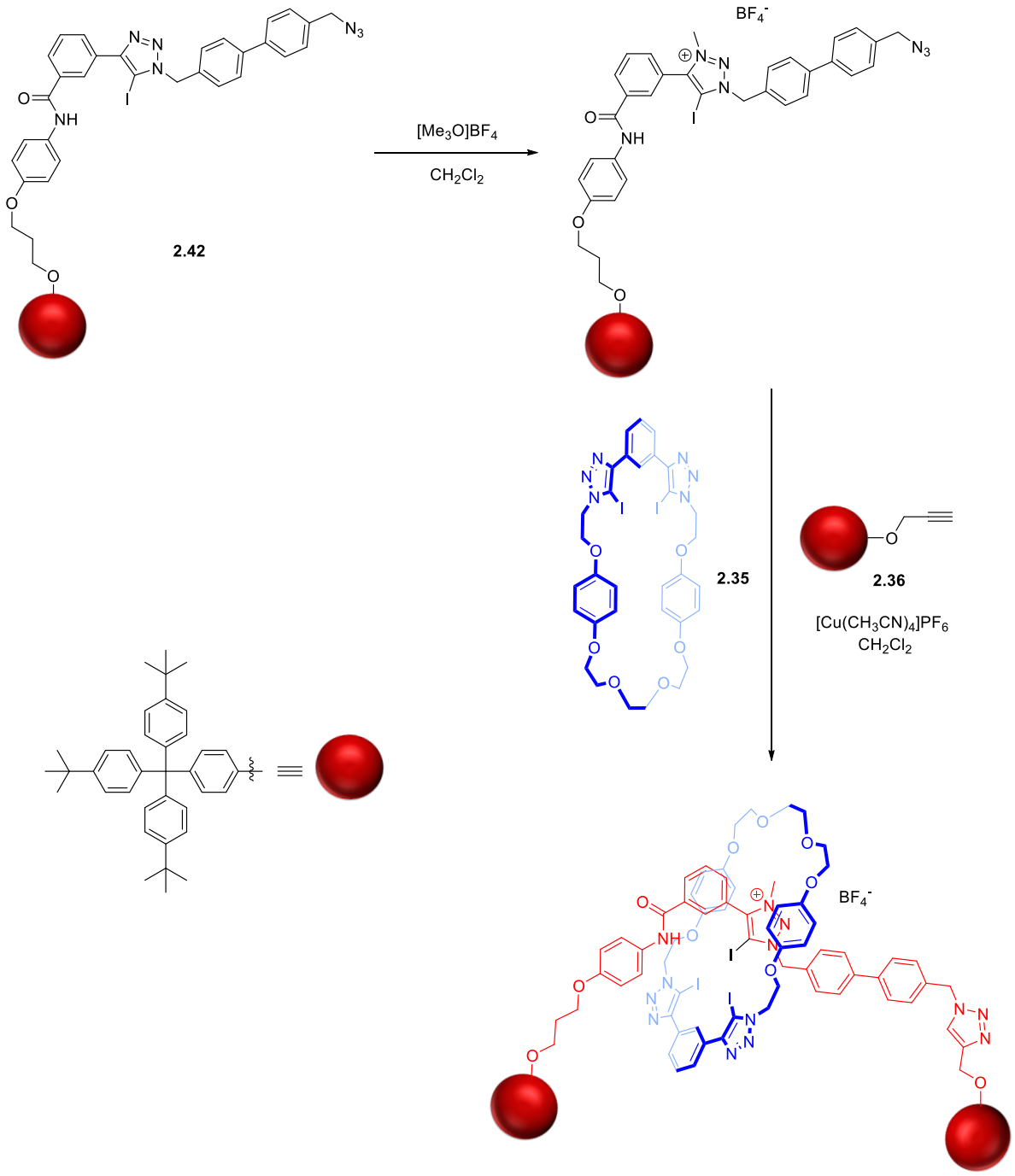
*[a] Anions were added as their tetrabutylammonium (TBA) salts. [b] Calculated using BindFit [14,15] by monitoring the change in the chemical shift of the triazole proton **a** in the case of **2.37.HB** or several axle protons in the case of **2.43**, as labelled in the inset above. Errors < 10%. [c] Titration not performed.*

The strength of binding of $I^-$ by the amido-iodotriazole axle-containing rotaxane **2.43** is increased significantly compared to the amido-triazole host **2.37.HB**. Iodide binding is enhanced by the presence of the additional XB donor, which favours soft-soft interactions due to the high degree of covalency of the halogen bonding interaction. [24] Conversely, **2.43** displays a significantly lower affinity for chloride, possibly due to the increased steric bulk of the additional iodotriazole group, which may disfavour convergent binding to the amide and other donor groups within the cavity. Overall, the rotaxane **2.43** displays high selectivity for $I^-$ over $Cl^-$ and a modest preference for $I^-$ over $Br^-$.

## 2.5. Conclusions and future work

In conclusion, a series of neutral and cationic acyclic and interlocked rotaxane anion receptors incorporating the amido-(iodo)triazole motif were constructed and their anion binding properties compared and contrasted. Cationic [2]rotaxanes were synthesised by chloride-templated ring-closing metathesis and the HB amido-triazolium receptor was shown to have superior binding affinities compared to an analogous, more rigid rotaxane in highly competitive media. A family of neutral [2]rotaxanes were synthesised by an active metal templation methodology; the HB amido-triazole host was proven to be a potent host for $Br^-$, whereas the XB amido-iodotriazole host displayed impressive affinity for $I^-$ in 2:98 $D_2O$/acetone-$d_6$ (*v/v*). Importantly, it was demonstrated that the integration of a XB donor motif into the axle or macrocycle component of a rotaxane structure dramatically influences the anion recognition properties of the interlocked host.

Future work could focus on exploiting the active metal templation strategy to synthesise an cationic amido-iodotriazolium analogue of [2]rotaxane **2.43**. Methylation of the triazole motif of **2.42** using $[Me_3O]BF_4$ would produce a novel azide-appended stopper, from which the novel [2]rotaxane could be produced in a single step via an AMT protocol with stopper alkyne **2.36** and macrocycle **2.35** (**Scheme 2.15**).




***Scheme 2.15.*** *Proposed synthesis of a cationic amido-iodotriazolium [2]rotaxane.*

Other future research avenues could focus on further tuning the anion binding properties of amido-triazole rotaxanes by incorporating electron-withdrawing perfluoroaryl motifs into an axle structure (**Figure 2.24.a**). Alternatively, a tripodal structure bearing three convergent amido-triazole motifs could be constructed based on a tris(2-aminoethyl)amine (*tren*) platform (**Figure 2.24.b**). Protonation of the basic tertiary amine would introduce a supplementary N – H donor and further enhance the anion binding affinities, whereas appending hydrophilic polyether chains could allow the host to function in aqueous media.

a)

b)

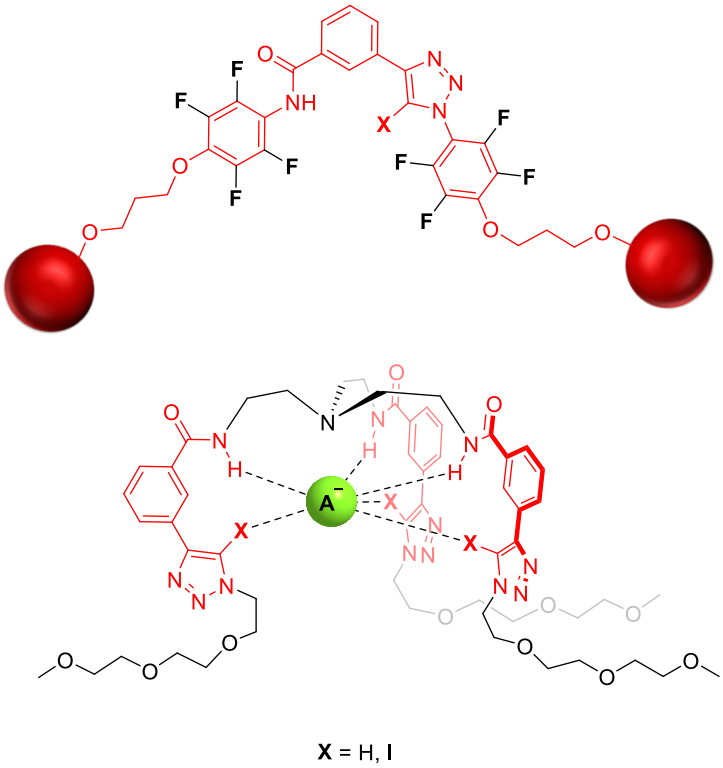



***Figure 2.24.*** *Target novel structures incorporating the amido-triazole motif: a) an axle component for incorporation into a [2]rotaxane; b) a tripodal receptor based on a tren platform.*

## 2.6. References


1. B. A. Moyer and R. P. Singh, *Fundamentals and Applications of Anion Separations*, Springer US, Boston, MA, **2004**.
2. J. L. Sessler, E. Katayev, G. D. Pantos and Y. A. Ustynyuk, *Chem. Commun.*, **2004**, 1276.
3. J. L. Sessler, E. Katayev, G. D. Pantos, P. Scherbakov, M. D. Reshetova, V. N. Khrustalev, V. M. Lynch and Y. A. Ustynyuk, *J. Am. Chem. Soc.*, **2005**, 127, 11442–11446.
4. R. Huisgen, G. Szeimies and L. Möbius, *Chem. Ber.*, **1967**, 100, 2494–2507.
5. V. V. Rostovtsev, L. G. Green, V. V. Fokin and K. B. Sharpless, *Angew. Chem. Int. Ed.*, **2002**, 41, 2596–2599.
6. C. W. Tornøe, C. Christensen and M. Meldal, *J. Org. Chem.*, **2002**, 67, 3057–3064.
7. J. E. Hein, J. C. Tripp, L. B. Krasnova, K. B. Sharpless and V. V. Fokin, *Angew. Chem. Int. Ed.*, **2009**, 48, 8018–8021.
8. W. S. Brotherton, R. J. Clark and L. Zhu, *J. Org. Chem.*, **2012**, 77, 6443–6455.
9. V. Haridas, S. Sahu and P. P. Praveen Kumar, *Tetrahedron Lett.*, **2011**, 52, 6930–6934.
10. Y.-J. Li, L. Xu, W.-L. Yang, H.-B. Liu, S.-W. Lai, C.-M. Che and Y.-L. Li, *Chem. - Eur. J.*, **2012**, 18, 4782–4790.
11. Y. Wang, J. Xiang and H. Jiang, *Chem. - Eur. J.*, **2011**, 17, 613–619.
12. L. C. Gilday, N. G. White and P. D. Beer, *Dalton Trans.*, **2013**, 42, 15766.
13. N. G. White, A. R. Colaço, I. Marques, V. Félix and P. D. Beer, *Org. Biomol. Chem*, **2014**, 12, 4924–4931.
14. P. Thordarson, *Chem. Soc. Rev*, **2011**, 40, 1305–1323.
15. D. B. Hibbert and P. Thordarson, *Chem. Commun.*, **2016**, 52, 12792–12805.
16. H. W. Gibson, S. H. Lee, P. T. Engen, P. Lecavalier, J. Sze, Y. X. Shen and M. Bheda, *J. Org. Chem.*, **1993**, 58, 3748–3756.
17. H. Zheng, W. Zhou, J. Lv, X. Yin, Y. Li, H. Liu and Y. Li, *Chem. - Eur. J.*, **2009**, 15, 13253–13262.
18. S. Forshaw, A. J. Matthews, T. J. Brown, L. J. Diorazio, L. Williams and M. Wills, *Org. Lett.*, **2017**, 19, 2789–2792.
19. D. J. Baek, N. MacRitchie, N. G. Anthony, S. P. Mackay, S. Pyne, N. J. Pyne and R. Bittman, *J. Med. Chem.*, **2013**, 56, 9310–9327.
20. C. J. Campbell, D. A. Leigh, I. J. Vitorica-Yrezabal and S. L. Woltering, *Angew. Chem. Int. Ed.*, **2014**, 53, 13771–13774.
21. M. R. Sambrook, P. D. Beer, M. D. Lankshear, R. F. Ludlow and J. A. Wisner, *Org. Biomol. Chem.*, **2006**, 4, 1529.
22. J. Y. C. Lim, T. Bunchuay and P. D. Beer, *Chem. - Eur. J.*, **2017**, 23, 4700–4707.
23. W.-T. Lee, D. A. Dickie, A. J. Metta-Magaña and J. M. Smith, *Inorg. Chem.*, **2013**, 52, 12842–12846.
24. S. W. Robinson, C. L. Mustoe, N. G. White, A. Brown, A. L. Thompson, P. Kennepohl and P. D. Beer, *J. Am. Chem. Soc.*, **2015**, 137, 499–507.
25. J. Y. C. Lim and P. D. Beer, *Chem. Commun.*, **2015**, 51, 3686–3688.
26. J. Y. C. Lim, I. Marques, A. L. Thompson, K. E. Christensen, V. Félix and P. D. Beer, *J. Am. Chem. Soc.*, **2017**, 139, 3122–3133.
27. F. Friscourt, C. J. Fahrni and G.-J. Boons, *J. Am. Chem. Soc.*, **2012**, 134, 18809–18815.
28. V. Aucagne, K. D. Hänni, D. A. Leigh, P. J. Lusby and D. B. Walker, *J. Am. Chem. Soc.*, **2006**, 128, 2186–2187.
29. M. Denis and S. M. Goldup, *Nat. Rev. Chem.*, **2017**, 1, 0061.
30. J. D. Crowley, S. M. Goldup, A.-L. Lee, D. A. Leigh and R. T. McBurney, *Chem. Soc. Rev.*, **2009**, 38, 1530.
31. J. R. Thomas, X. Liu and P. J. Hergenrother, *J. Am. Chem. Soc.*, **2005**, 127, 12434–12435.
32. J. Y. C. Lim, *DPhil thesis.*

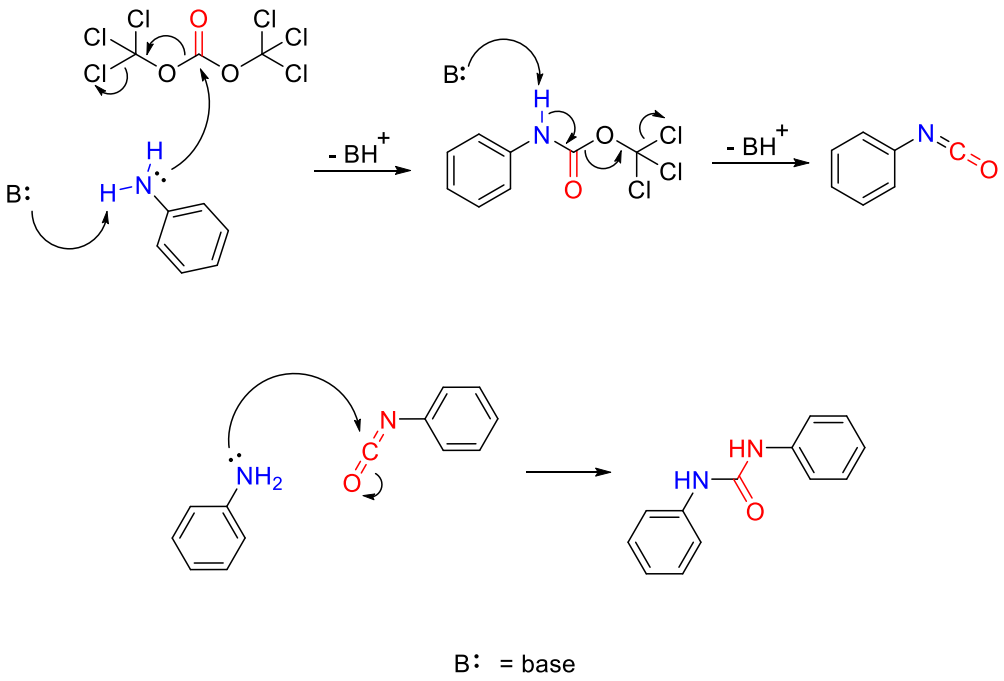
# Chapter 3

## Urea and thiourea-based (iodo)triazole structures for anion binding

# Chapter 3: Urea and thiourea-based (iodo)triazole structures for anion binding

## 3.1. Introduction

Urea and thiourea functional groups have been successfully and widely employed for anion recognition purposes due to their potent HB donor ability (see **Chapter 1, Section 1.2.5.2.2**). [1,2] They can be readily synthesised through the reaction of a primary amine with a (thio)carbonyl donor such as triphosgene, thiophosgene or the milder 1,1'-(thio)carbonyldiimidazole, followed by reacting the resulting iso(thio)cyanate with a further equivalent of amine (**Scheme 3.1**). By varying the nature of the two amines, a wide variety of *N,N'*-disubstituted (thio)ureas can thus be obtained and incorporated into anion receptor scaffolds.




***Scheme 3.1.*** *Synthesis of N,N'-disubstituted ureas from amines and triphosgene: a) formation of the isocyanate intermediate; b) reaction of the isocyanate with another equivalent of amine.*

### 3.1.1. The (thio)urea-triazole motifs in anion binding

Supplementing (thio)urea donors with 1,2,3-triazole motifs for increasing anion affinities is underexploited in the literature; in particular, there is a single reported example of exploiting iodotriazoles in conjunction with ureas for enhanced phosphate binding, [3] which highlights the unexplored promise of the urea/XB combination. Dehaen and co-workers have designed a family of structurally related hosts incorporating two 1,2,3-triazole motifs along with additional N – H donors such as amides, ureas, and thioureas. These receptors were shown to display strong variations in halide binding strength and selectivity (**Figure 3.1**). [4]

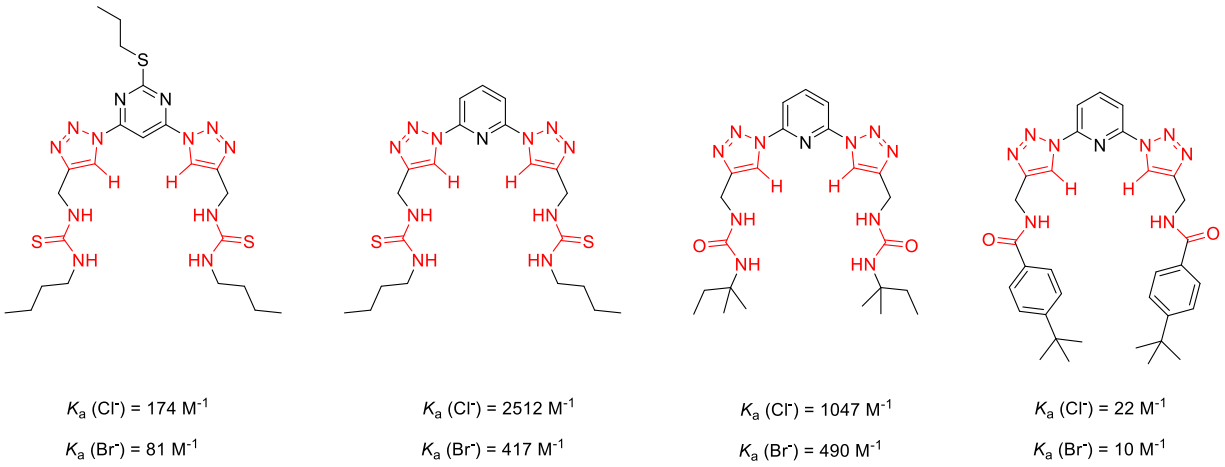



***Figure 3.1.*** *A series of structurally related receptors incorporating triazole and amide or (thio)urea motifs, each exhibiting different anion binding properties ($CD_3CN$).*

The application of the urea-triazole motif to anion binding has also been recently extended to interlocked structures. A [2]rotaxane bearing a urea and a triazole motif separated by a methylene spacer has been constructed by Goldup and co-workers (**Figure 3.2**), which exhibited significant enhancement of anion binding properties in 1:1 $CD_3CN/CDCl_3$ (*v/v*) upon protonation of the macrocycle bipyridine moiety. [5]

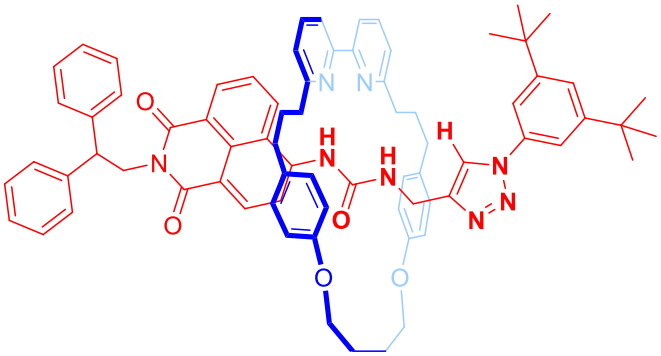


***Figure 3.2.*** *Goldup's [2]rotaxane incorporating a urea-triazole motif for anion binding.*

### 3.2. Chapter aims

The research aim of this chapter focuses on the synthesis of novel HB/XB acyclic and interlocked structures incorporating (thio)ureas and (iodo)triazoles for halide and oxoanion recognition. In particular, this chapter will explore two main avenues:

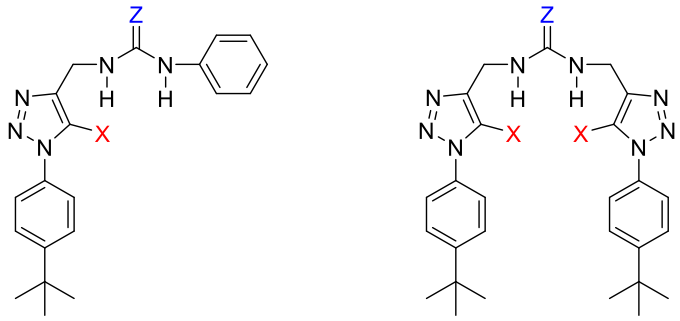
1) A series of acyclic (thio)urea-(iodo)triazole hosts are synthesised and the effect of structural modifications such as spacer identity, donor nature, and number of donors on anion binding properties is explored and rationalised. Construction of a urea-triazole fluorescent sensor for dicarboxylate anions is also attempted.

2) Numerous attempts to incorporate urea-(iodo)triazole motifs into interlocked structures are undertaken via active metal templation or anion-templated ring-closing metathesis protocols. Synthesis of an analogous macrocycle is similarly investigated.

## 3.3. Acyclic HB/XB (thio)urea-triazole structures for anion recognition

### 3.3.1. Design of target acyclic hosts

Building on literature precedent, [4–6] a library of anion receptors was designed, incorporating convergent (iodo)triazole and (thio)urea donors separated by a methylene spacer (**Figure 3.3**). The following sections describe the synthesis, characterisation and anion binding properties of the novel urea-triazole host structures.




**3.1.HB.O** X = H, Z = O
**3.1.XB.O** X = I, Z = O
**3.1.HB.S** X = H, Z = S
**3.1.XB.S** X = I, Z = S

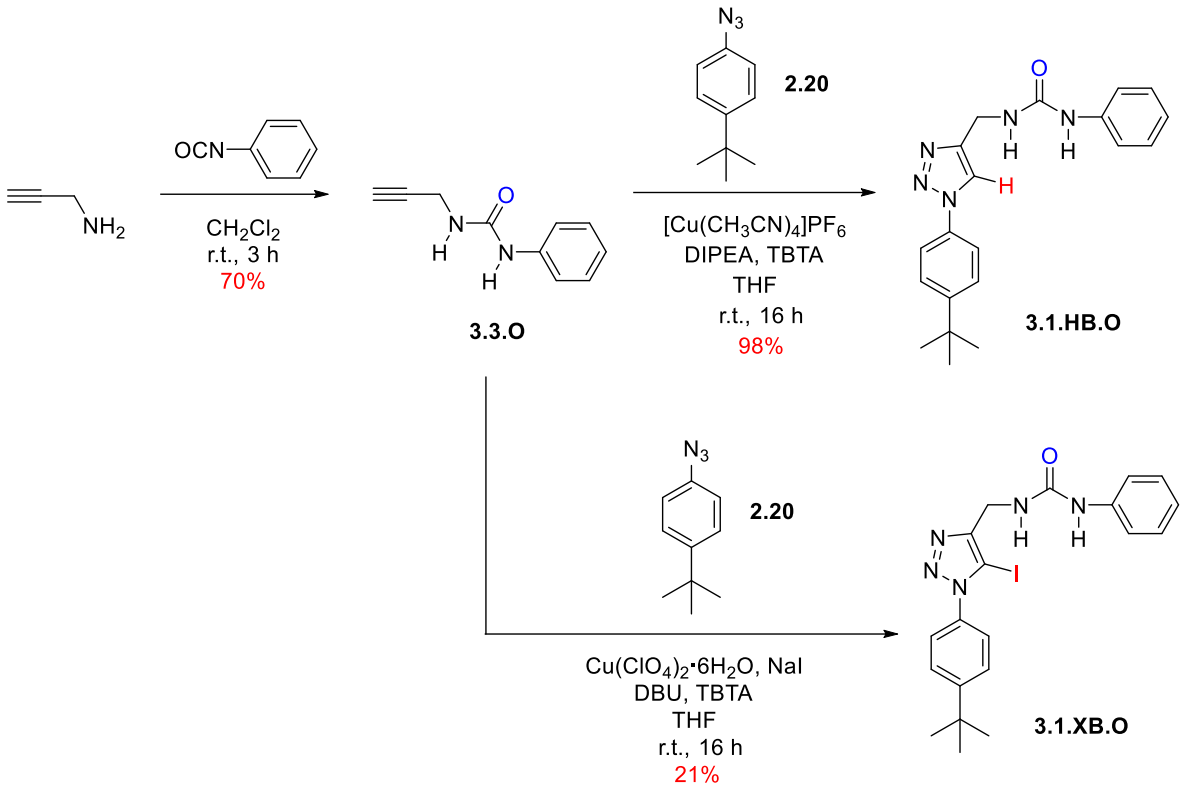
**3.2.HB.O** X = H, Z = O
**3.2.XB.O** X = I, Z = O
**3.2.HB.S** X = H, Z = S
**3.2.XB.S** X = I, Z = S

***Figure 3.3.*** *Structures of the target acyclic (thio)urea-triazole receptors with a flexible methylene spacer.*

### 3.3.2. Flexible (thio)urea-triazole receptors

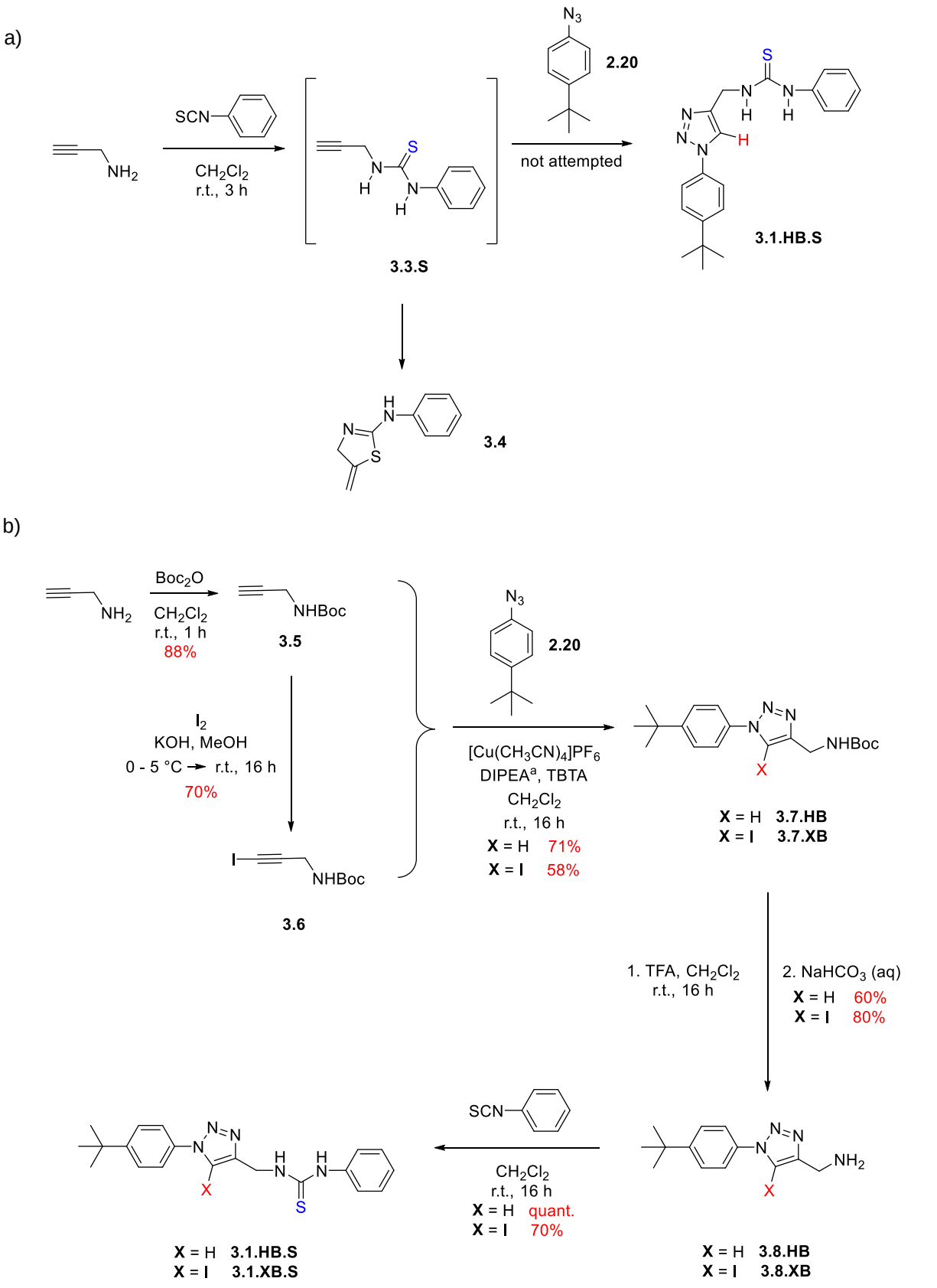
#### 3.3.2.1. Synthesis of (thio)urea-monotriazole receptors incorporating a methylene spacer

Firstly, acyclic urea and thiourea-based receptors incorporating a single additional triazole motif were synthesised through a combination of literature and novel procedures (**Scheme 3.2**). Commercially available propargylamine was reacted with phenyl isocyanate to afford alkyne-appended urea **3.3.O**, [7] which was subsequently reacted with 4-(tert-butyl)phenyl azide **2.20** under proto-click CuAAC conditions to afford **3.1.HB.O** in a near-quantitative yield and under one-pot iodo-click CuAAC conditions to afford the halogen bonding analogue **3.1.XB.O** in a lower yield of 21%.




***Scheme 3.2.*** *Synthesis of the neutral monotriazole-urea receptors.*

In order to synthesise the thiourea hosts, an analogous method was sought (**Scheme 3.3.a**); however, the reaction between propargylamine and phenyl isothiocyanate afforded a heterocyclic isomer **3.4** of the desired alkyne-appended thiourea **3.3.S.** An alternative pathway was therefore employed (**Scheme 3.3.b**), which required propargylamine to be first Boc-protected to give the proto-alkyne *N*-Boc-propargylamine **3.5**, [8] and then converted to its iodo-alkyne analogue **3.6** with molecular $I_2$ under basic conditions in MeOH. [9] Each of these alkynes was reacted separately with 4-(tert-butyl)phenyl azide **2.20** under CuAAC conditions to give *N*-Boc-aminotriazoles **3.7.HB** and **3.7.XB** in 71% and 58% yields, respectively, which were deprotected with trifluoroacetic acid to afford aminotriazoles **3.8.HB** and **3.8.XB**. In the final step, each aminotriazole was reacted with phenyl isothiocyanate in $CH_2Cl_2$ to produce the target monotriazole-thiourea hosts **3.1.HB.S** and **3.1.XB.S**.




***Scheme 3.3.*** *Failed (**a**) and successful (**b**) syntheses of the neutral monotriazole-thiourea receptors.*

*[a] DIPEA was not added for **X** = I.*

### 3.3.2.2. Preliminary anion binding studies

The affinities of monotriazole-(thio)urea receptors for various anions were probed via $^{1}$H NMR titration experiments in the mildly competitive 2:98 $D_2O$/acetone-$d_6$ (*v/v*) solvent system. Upon anion addition, the largest downfield chemical shifts were observed for the triazole proton (0.12 – 0.42 ppm) and the phenyl proton *meta* to the urea motif (0.05 – 0.49 ppm); however, for consistency reasons and to allow direct comparison with analogous bistriazole receptors (see **Section 3.3.2.4**), the chemical shift of the phenyl proton proximal to the triazole motif (labelled ***c*** in **Figure 3.4**) was monitored instead. The anion-induced shifts were plotted against the equivalents of anion added and the resulting binding isotherms were analysed with BindFit [10,11] to give the association constants for 1:1 stoichiometric binding summarised in **Table 3.1**.

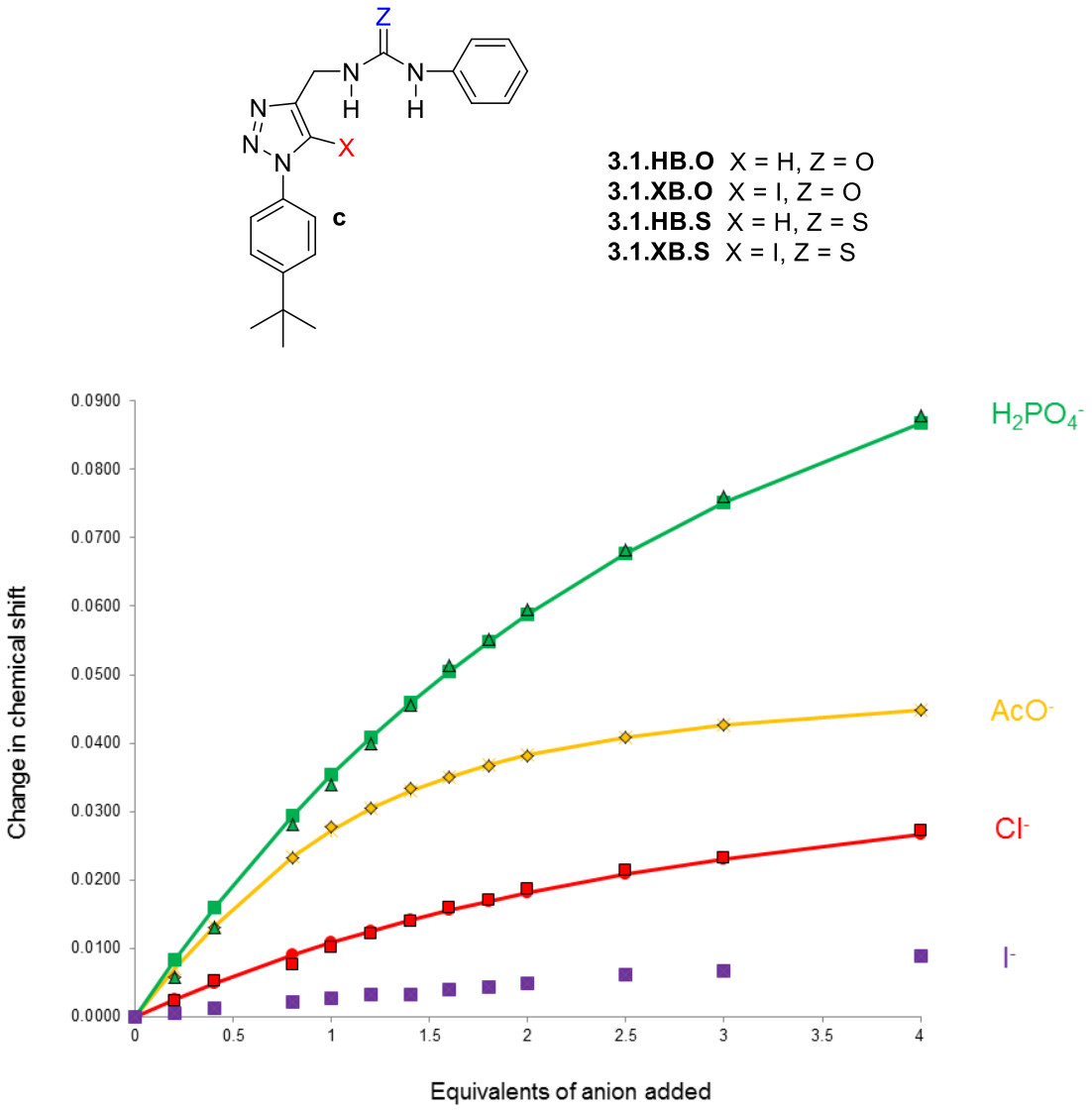



***Figure 3.4.*** *Partial comparative plots of the change in chemical shift of the proton* ***c*** *(ppm) against equivalents of anion added for the acyclic monotriazole-urea receptor* ***3.1.HB.O*** *(2:98 $D_2O$/acetone-$d_6$ (v/v), 298 K). Observed data is represented as solid points, whereas fitted isotherms are represented as lines. Inset: Generic structure of receptors* ***3.1****.*

***Table 3.1.*** *Anion association constants ($K_a$/ $M^{-1}$) for monotriazole-(thio)urea receptors in 2:98 $D_2O$/acetone-$d_6$ (v/v) at 298 K.*

| Anion[a] | Association constants ($K_a$/ $M^{-1}$) [b] | | | |
|---|---|---|---|---|
| | **3.1.HB.O** | **3.1.XB.O** | **3.1.HB.S** | **3.1.XB.S** |
| $AcO^-$ | 1240 | NB [c] | 1381 | NB [c] |
| $H_2PO_4^-$ | 176 | NB [c] | 269 | NB [c] |
| $Cl^-$ | 182 | NB [c] | 536 | NB [c] |
| $I^-$ | NB [c] | NB [c] | NB [c] | NB [c] |

*[a] Anions were added as their tetrabutylammonium (TBA) salts. [b] Calculated using BindFit [10,11] by monitoring the change in the chemical shift of the phenyl proton proximal to the triazole (labelled **c** in **Figure 3.4**). Errors < 5%. [c] NB = no binding. In all cases, the perturbations of the chemical shift were very small (Δδ ≤ 0.05 ppm), which indicates that the receptor does not interact significantly with the guest anion.*

Both HB receptors bind in the order $AcO^- > Cl^- > H_2PO_4^- > I^-$. The acetate selectivity is reflective of its strong basicity, as well as the geometric complementarity between this oxoanion and the urea moiety. Although thiourea is expected to be more acidic and therefore a more potent HB donor than urea, **3.1.HB.S** and **3.1.HB.O** have very similar $AcO^-$ and $H_2PO_4^-$ affinities; only $Cl^-$ is bound significantly more strongly by **3.1.HB.S.** Surprisingly, the halogen bonding hosts do not appear to interact with any of the anions studied. This may indicate formation of intramolecular 7-membered rings via halogen bonding to the oxygen or sulfur atom of the (thio)urea group (**Figure 3.5**), which would inhibit the participation of the XB iodotriazole donor in the anion binding process.

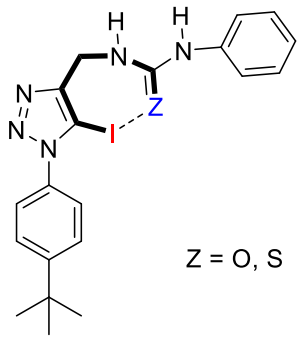
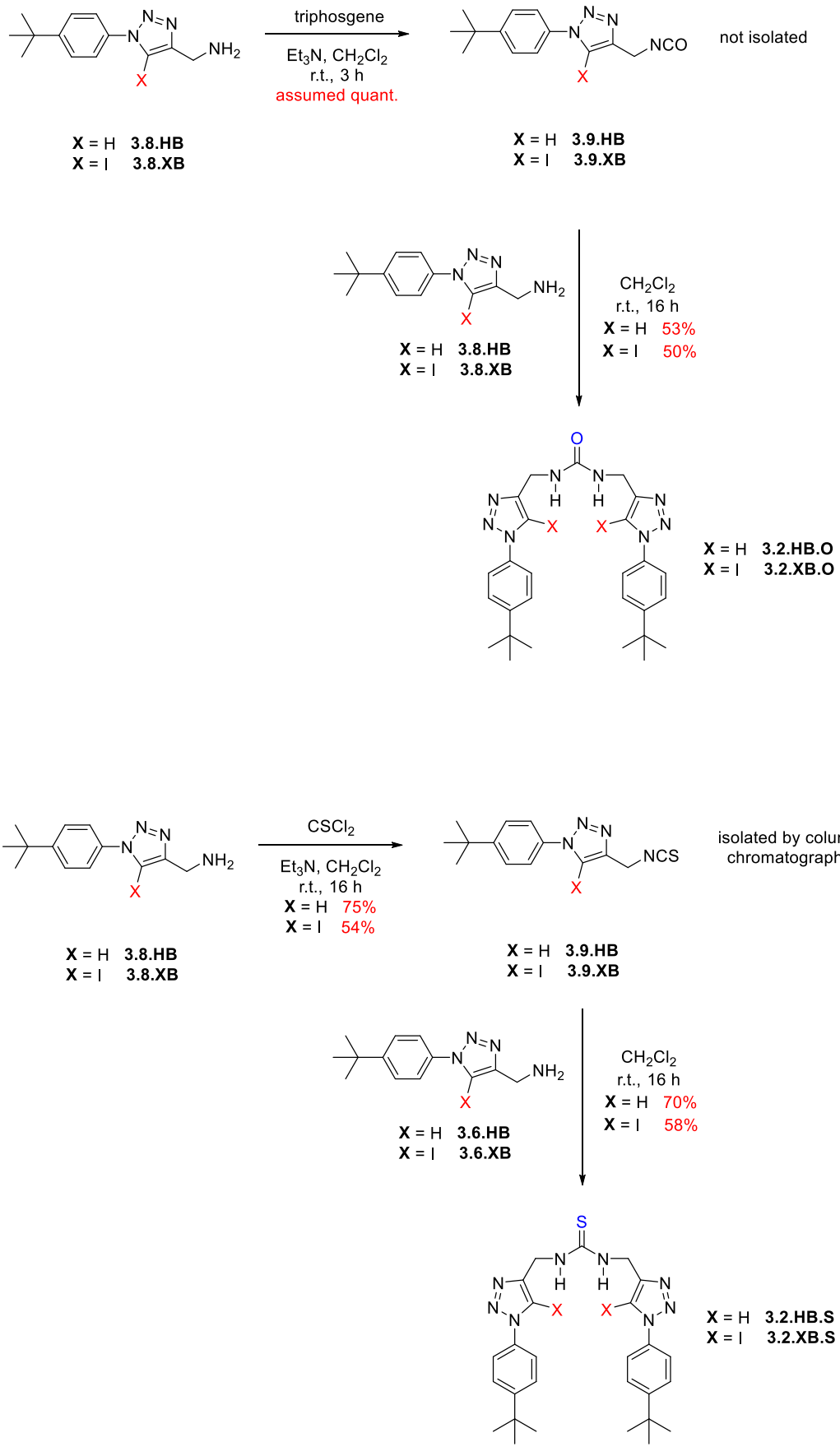



***Figure 3.5.*** *Suggested conformation of hosts **3.1.XB.O** and **3.1.XB.S** in solution, highlighting the intramolecular XB structure.*

### 3.3.2.3. Synthesis of (thio)urea-bistriazole receptors incorporating a methylene spacer

Having studied the anion binding properties of the monotriazole-(thio)urea receptor, an analogous family of hosts were constructed bearing an additional triazole motif (**Scheme 3.4**). The aminotriazoles **3.8.HB** and **3.8.XB** were converted to their corresponding isocyanates in situ through reaction with triphosgene. Subsequent reaction of the isocyanate intermediates with a further equivalent of aminotriazole produced symmetric urea hosts **3.2.HB.O** and **3.2.XB.O** in moderate yields. The thiourea analogues **3.2.HB.S** and **3.2.XB.S** were synthesised through a similar pathway, with the isothiocyanate intermediates being isolated via flash column chromatography.




***Scheme 3.4.*** *Synthesis of the neutral bistriazole-(thio)urea receptors.*

### 3.3.2.4. Preliminary anion binding studies

The affinities of the bistriazole-(thio)urea receptors for various anions were probed via $^{1}$H NMR titration experiments in the same, mildly competitive 2:98 $D_2O$/acetone-$d_6$ (*v/v*) solvent system. Upon anion addition, the largest downfield chemical shifts were observed for the triazole proton (0.08 – 0.37 ppm); however, to allow direct comparison with analogous monotriazole receptors (see **Section 3.3.2.2**), the chemical shift of the phenyl proton proximal to the triazole motif (labelled ***c*** in **Figure 3.6**) was monitored instead. BindFit [10,11] analysis of the titration data determined 1:1 stoichiometric association constants shown in **Table 3.2**.

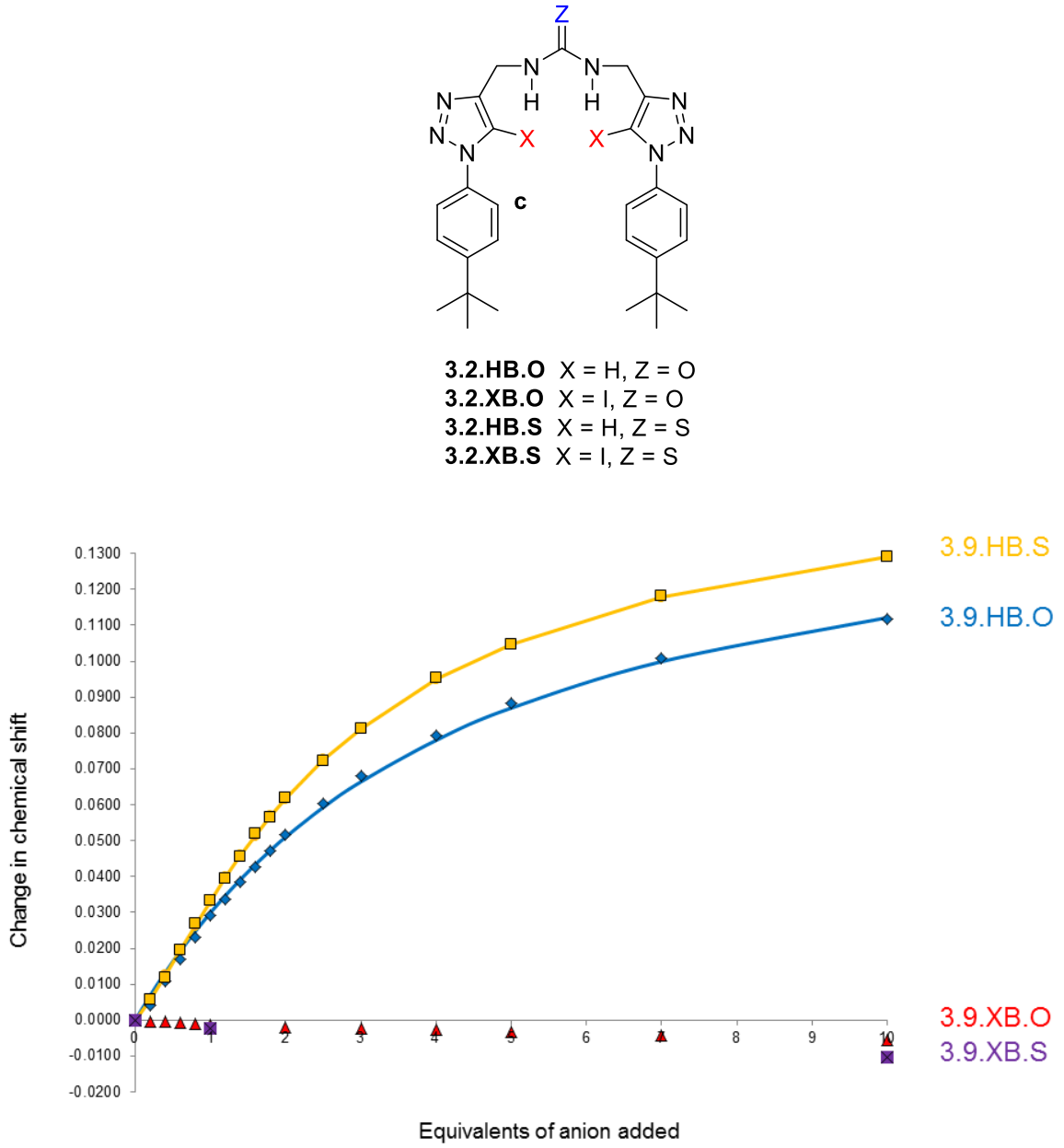



***Figure 3.6.*** *Comparative plots of the change in chemical shift of the proton* ***c*** *(ppm) against equivalents of* $H_2PO_4^-$ *added for the acyclic bistriazole-(thio)urea receptors (2:98* $D_2O$*/acetone-*$d_6$ *(v/v), 298 K). Observed data is represented as solid points, whereas fitted isotherms are represented as lines. Inset: Structure of bistriazole-(thio)urea hosts.*

***Table 3.2.*** *Anion association constants ($K_a$/ $M^{-1}$) for bistriazole-(thio)urea receptors in 2:98 $D_2O$/acetone-$d_6$ (v/v) at 298 K.*

| Anion[a] | Association constants ($K_a$/ $M^{-1}$) [b] | | | |
|---|---|---|---|---|
| | **3.2.HB.O** | **3.2.XB.O** | **3.2.HB.S** | **3.2.XB.S** |
| $AcO^-$ | 316 | NB [c] | 317 | NB [c] |
| $H_2PO_4^-$ | 130 | NB [c] | $K_1$ = 412, $K_2$ = 74 [d] | NB [c] |
| $Cl^-$ | 176 | NB [c] | 334 | NB [c] |
| $I^-$ | NB [c] | NB [c] | NB [c] | NB [c] |

*[a] Anions were added as their tetrabutylammonium (TBA) salts. [b] Calculated using BindFit [10,11] by monitoring the change in the chemical shift of the phenyl proton proximal to the triazole (labelled **c** in **Figure 3.6**). Errors < 5%. [c] NB = no binding. In all cases, the perturbations of the chemical shift were very small (Δδ ≤ 0.05 ppm), which indicates that the receptor does not interact significantly with the guest anion. [d] Stepwise constants for a 2:1 host:guest binding mode.*

It becomes immediately apparent that the bistriazole receptors have markedly lower anion binding affinities than their monotriazole analogues. Again, the XB hosts **3.2.XB.O** and **3.2.XB.S** do not seem to bind any of the anions investigated. Both HB analogues display a similar affinity towards acetate, however, the thiourea **3.2.HB.S** binds chloride and dihydrogen phosphate more strongly than the urea analogue **3.2.HB.O** – a trend that mirrors the one for asymmetric receptors **3.1.HB.S** and **3.1.HB.O**.

An attempt to rationalise the behaviour of these receptors towards anions was made through $^1$H NMR dilution studies, as urea and thiourea-based molecules have been reported to display a tendency to aggregate in solution through the formation of intermolecular hydrogen bonds, [12] which may decrease their propensity to interact with anions.

Firstly, 2 mM solutions of each receptor in the titration solvent (2% $D_2O$ – acetone-$d_6$) were prepared and their $^1$H NMR spectra recorded. Secondly, a volume of pure solvent mixture equal to the total volume of anion solution added over the course of a single titration (200 μL) was added to each solution of receptor and the $^1$H NMR spectra recorded again, in order to determine how the chemical shift of each proton in each receptor varies within the concentration range employed during the titration experiment. Overall, the changes in chemical shift upon dilution were relatively small for most receptors, indicating that self-association was negligible over the 1.5 mM – 2 mM concentration range.

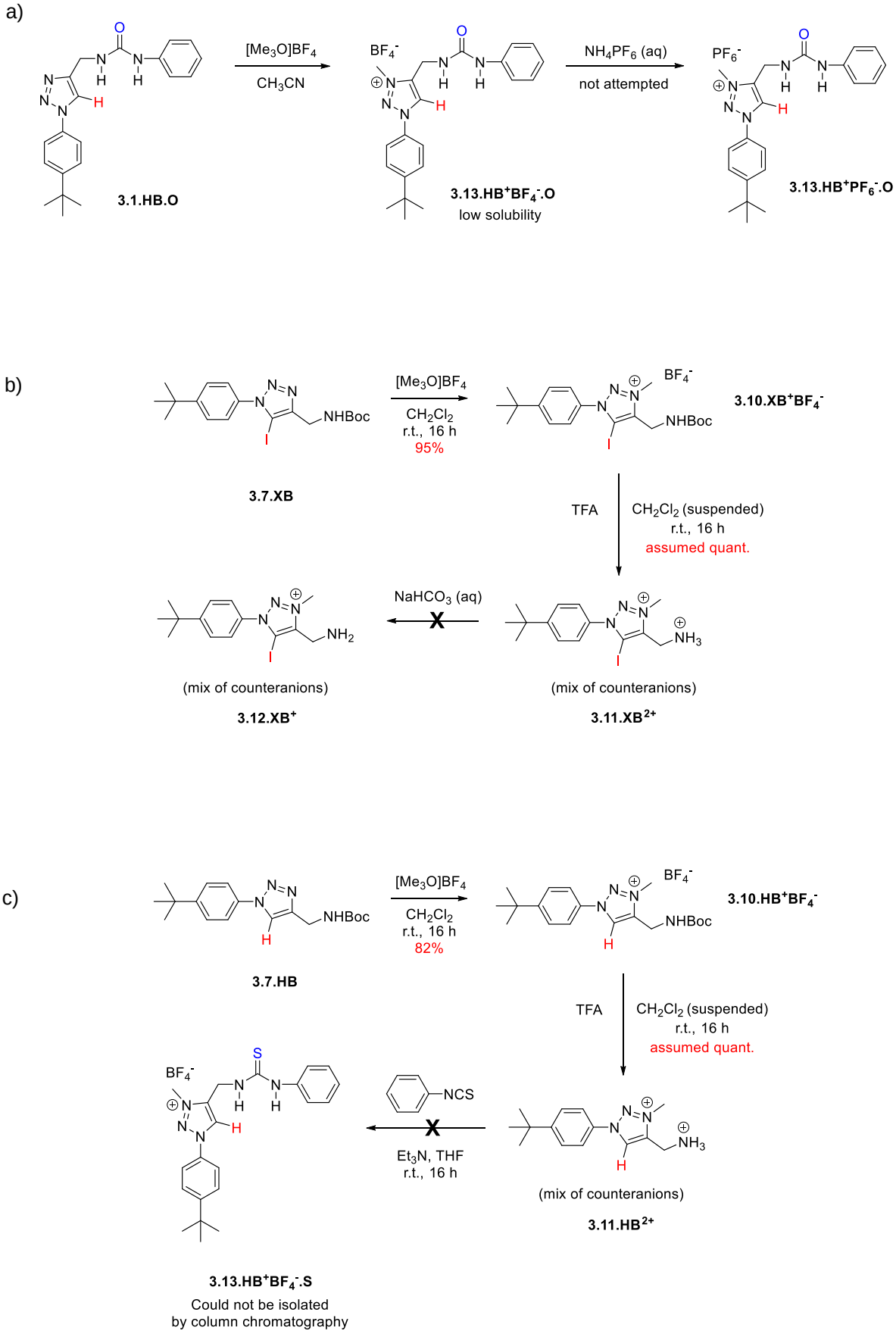
### 3.3.2.5. Towards cationic (thio)urea-triazole receptors

It was envisaged that increasing the charge on the triazole motif would enhance the modest anion binding properties of the neutral (thio)urea-triazole receptors studied so far. Several synthetic approaches towards these target cationic receptors were undertaken, as outlined below.

Initially, the neutral host **3.1.HB.O** was directly methylated in the presence of $[Me_3O]BF_4$ to give the cationic structure **3.13.HB$^+$BF$_4^-$.O** (**Scheme 3.5.a**); unfortunately, the product was poorly soluble in common organic solvents and the yield could not be determined accurately.

Next, *N*-Boc-aminotriazole **3.7.XB** was alkylated with $[Me_3O]BF_4$ in $CH_2Cl_2$ to give **3.10.XB$^+$BF$_4^-$** in 95% yield (**Scheme 3.5.b**). Subsequently, the amine motif was deprotected with trifluoroacetic acid for reaction with an iso(thio)cyanate. Unfortunately, the free amine could not be extracted with organic solvents after the aqueous workup, presumably due to its positive charge and low hydrophobicity.

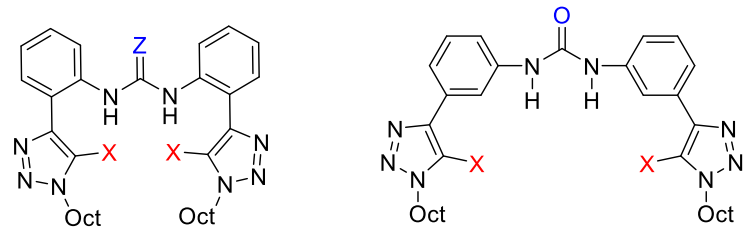
Finally, **3.7.HB** was methylated with $[Me_3O]BF_4$ to give **3.10.HB$^+$BF$_4^-$** in 82% yield (**Scheme 3.5.c**). After removal of the Boc group, the resulting ammonium salt was reacted in situ with phenyl isothiocyanate under basic conditions. The formation of product **3.13.HB$^+$BF$_4^-$.S** was observed by mass spectrometry; however, disappointingly, it could not be isolated by column chromatography.




***Scheme 3.5.*** *Attempted syntheses of the cationic monotriazolium-(thio)urea receptors.*

### 3.3.3. Rigid (thio)urea-triazole receptors

In order to examine the effect of greater rigidity and preorganisation on the anion binding properties, a series of novel acyclic hosts were targeted based on the design of previous (thio)urea-triazole receptors by replacing the methylene spacer with a rigid 1,2- or 1,3-phenylene spacer (**Figure 3.7**).




**3.20.HB.O** X = H, Z = O
**3.20.XB.O** X = I, Z = O
**3.20.HB.S** X = H, Z = S
**3.20.XB.S** X = I, Z = S

**3.26.HB** X = H
**3.26.XB** X = I

***Figure 3.7.*** *Structures of the target acyclic (thio)urea-triazole receptors with a rigid phenylene spacer (oct = n-$C_8H_{17}$).*

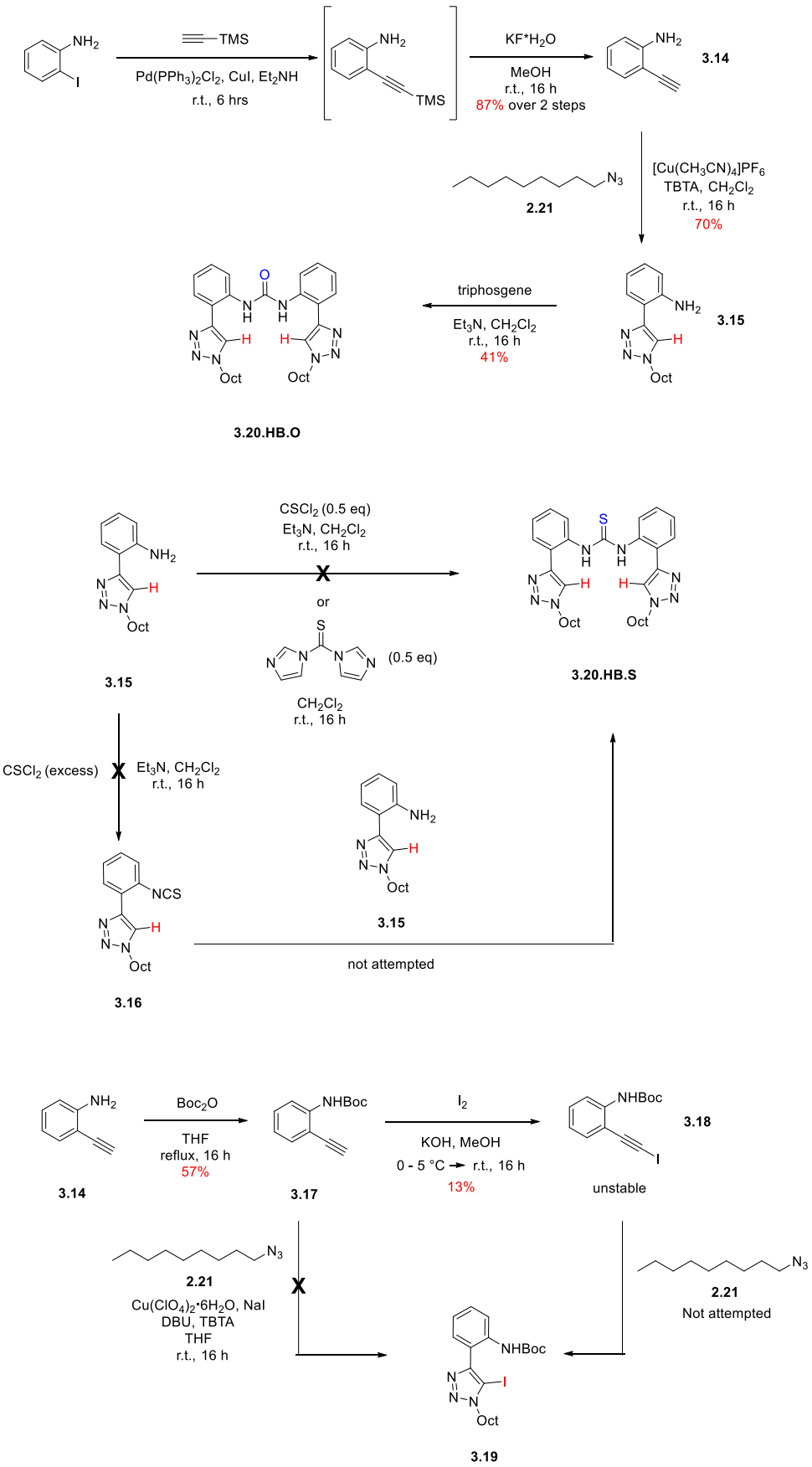
#### 3.3.3.1. Synthesis of (thio)urea-triazole receptors incorporating a 1,2-phenylene spacer

The synthetic approaches towards integrating a 1,2-phenylene spacer into (thio)urea-triazole receptors are outlined in **Scheme 3.6** below.

Commercially available 2-iodoaniline was converted to 2-ethynylaniline **3.14** via a Sonogashira reaction with TMS-protected acetylene followed by cleavage of the trimethylsilyl group with KF in MeOH. [13] The resulting alkyne was then reacted with octyl azide to give aminotriazole **3.15**, which was finally subjected to a reaction with triphosgene to afford receptor **3.20.HB.O** in a 41% yield. Compound **3.14** was also reacted with 0.5 equivalents of thiophosgene or 1,1'-thiocarbonyldiimidazole or excess thiophosgene, however, neither the target thiourea receptor **3.20.HB.S** nor the thiocyanate intermediate could be isolated.

In order to obtain the halogen bonding analogues, 2-ethynylaniline **3.14** was *N*-Boc-protected to give alkyne **3.17** in a 57% yield. [14] A two-pronged approach was sought to obtain target iodotriazole **3.19**. Initially, **3.17** was directly subjected to a one-pot iodo-CuAAC reaction with octyl azide, which failed to afford any product. Alternatively,

protoalkyne **3.17** was converted to iodoalkyne **3.18**; disappointingly, the product was found to be unstable over time, which likely contributed to the low isolated yield of 13%. As a consequence, further reaction of iodoalkyne **3.18** with octyl azide **2.21** was not attempted.

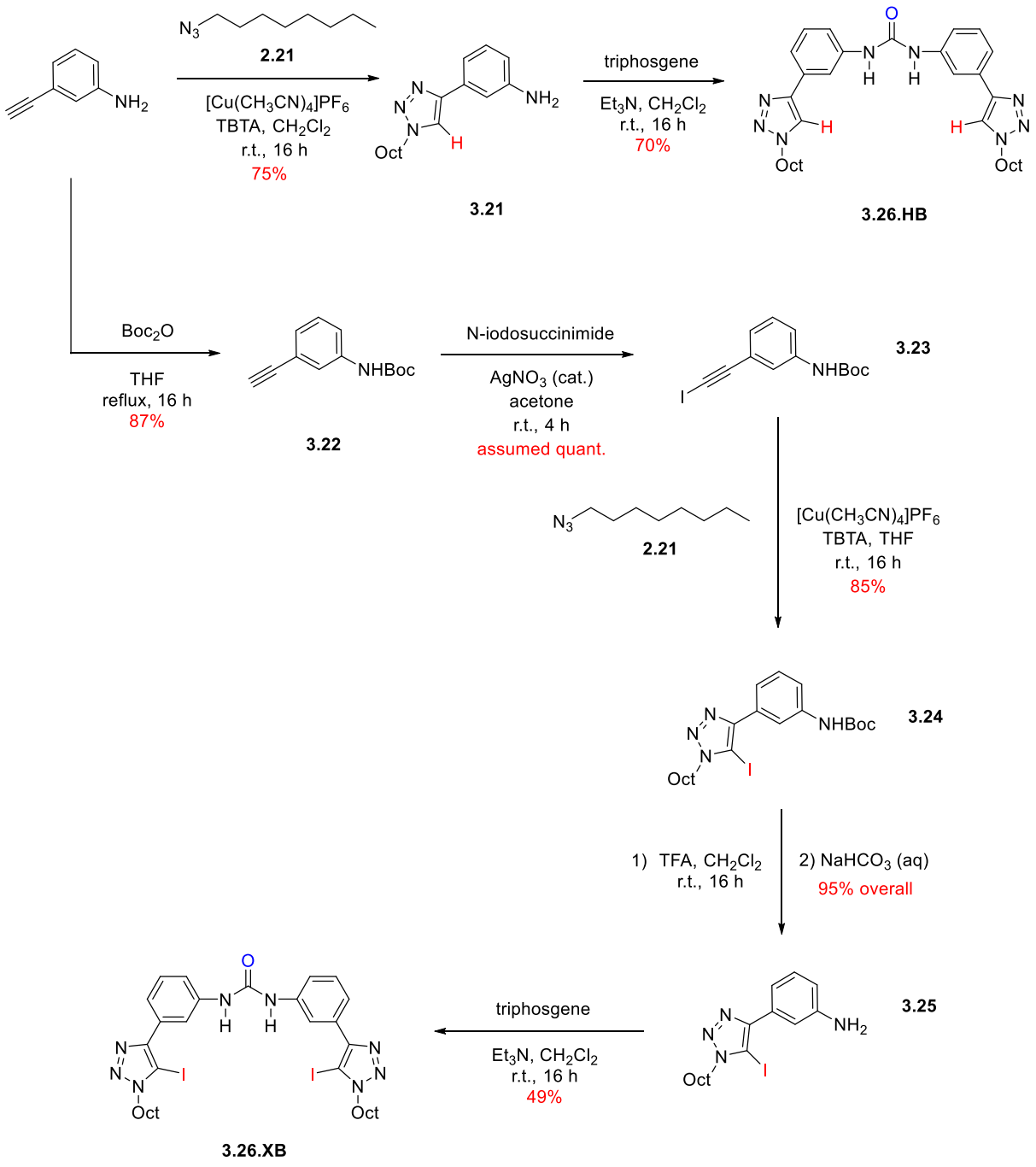



***Scheme 3.6.*** *Synthetic approaches towards rigid bistriazole-(thio)urea receptors with a 1,2-phenylene spacer.*

### 3.3.3.2. Synthesis of urea-triazole receptors incorporating a 1,3-phenylene spacer

Due to the challenging nature of the synthesis of (thio)urea-triazole receptors with a 1,2-phenylene spacer, the incorporation of 1,3-phenylene spacers was undertaken instead (**Scheme 3.7**).

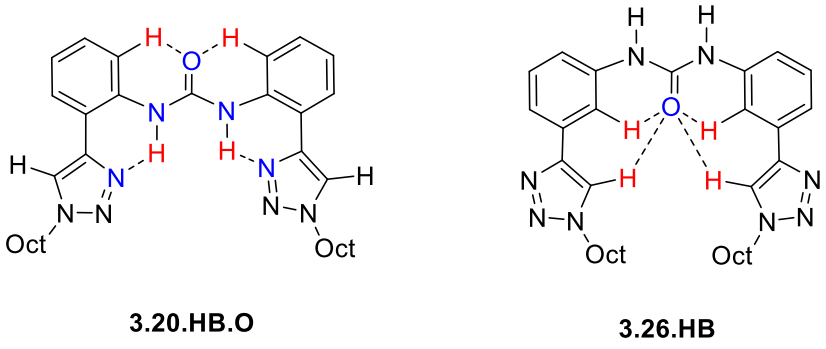
3-Ethynylaniline was reacted with octyl azide under CuAAC conditions to afford amino-triazole **3.21**, which was then reacted with triphosgene in $CH_2Cl_2$ to give target urea host **3.26.HB** in a 70% yield. In order to obtain the halogen bonding analogue **3.26.XB**, 3-ethynylaniline was first *N*-Boc-protected to give protoalkyne **3.22**, [15] then converted to iodoalkyne **3.23**. A reaction of **3.23** with octyl azide afforded intermediate **3.24** which was subsequently almost quantitatively deprotected under acidic conditions to give amino-iodotriazole **3.25**. Finally, **3.26.XB** was obtained through reacting **3.25** with triphosgene in a moderate yield of 49%.




***Scheme 3.7.*** *Synthesis of rigid bistriazole-urea receptors with a 1,3-phenylene spacer.*

### 3.3.3.3. Preliminary chloride binding studies

The chloride binding properties of receptors **3.20.HB.O** and **3.26.HB** were investigated through $^{1}$H NMR titration experiments in 1:9 MeOD:$CDCl_3$ (*v/v*) due to the limited solubility of the receptors in pure chloroform. Unfortunately, partial precipitation of the receptors during the addition of the halide anion prevented the determination of accurate values of the association constants. The binding was therefore analysed qualitatively through monitoring the change in chemical shift (Δδ) of various proton signals after the addition of 1 equivalent of $Cl^-$, 10 equivalents of $Cl^-$ (200 µL of solution), and 200 µL of pure solvent mixture, respectively. The anion-induced shifts were very small (<0.06 ppm and typically <0.01 ppm for most signals), suggesting limited anion binding in solution. Dilution effects were also found to be negligible (<0.01 ppm), indicating either no significant aggregation or the presence of strong intramolecular hydrogen bonds which are not significantly perturbed over the 1.5 – 2 mM concentration range (**Figure 3.8**).



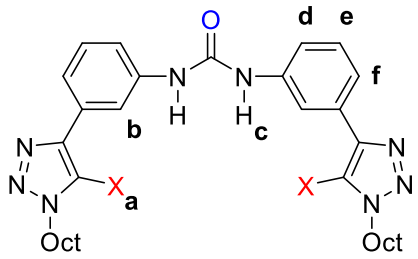

**3.20.HB.O** **3.26.HB**

***Figure 3.8.*** *Suggested conformations of hosts **3.20.HB.O** and **3.26.HB** in solution, highlighting the intramolecular hydrogen bond networks.*

Due to solubility problems and apparent low affinity towards $Cl^-$ in MeOD/$CDCl_3$, the chloride binding properties were studied for the 1,3-phenylene receptors **3.26.HB** and **3.26.XB** in $CDCl_3$/DMSO-$d_6$ mixtures of various compositions. Upon chloride addition, the largest changes in chemical shift by far were observed for the urea protons ***c*** for both hosts (> 1 ppm). The second largest downfield shifts, however, were observed for the adjacent aromatic protons ***d*** (host **3.26.HB**, >0.08 ppm) and ***b***, respectively (host **3.26.XB**, >0.23 ppm); surprisingly, very small downfield shifts were observed for the triazole proton in the case of **3.26.HB** (<0.02 ppm).

The anion-induced shifts of the urea N – H protons (labelled ***c*** in **Figure 3.9**) were plotted against the equivalents of $Cl^-$ added and BindFit [10,11] analysis of the titration data

determined the 1:1 stoichiometric host:guest association constants summarised in **Table 3.3.**




**X** = H **3.26.HB**
**X** = I **3.26.XB**

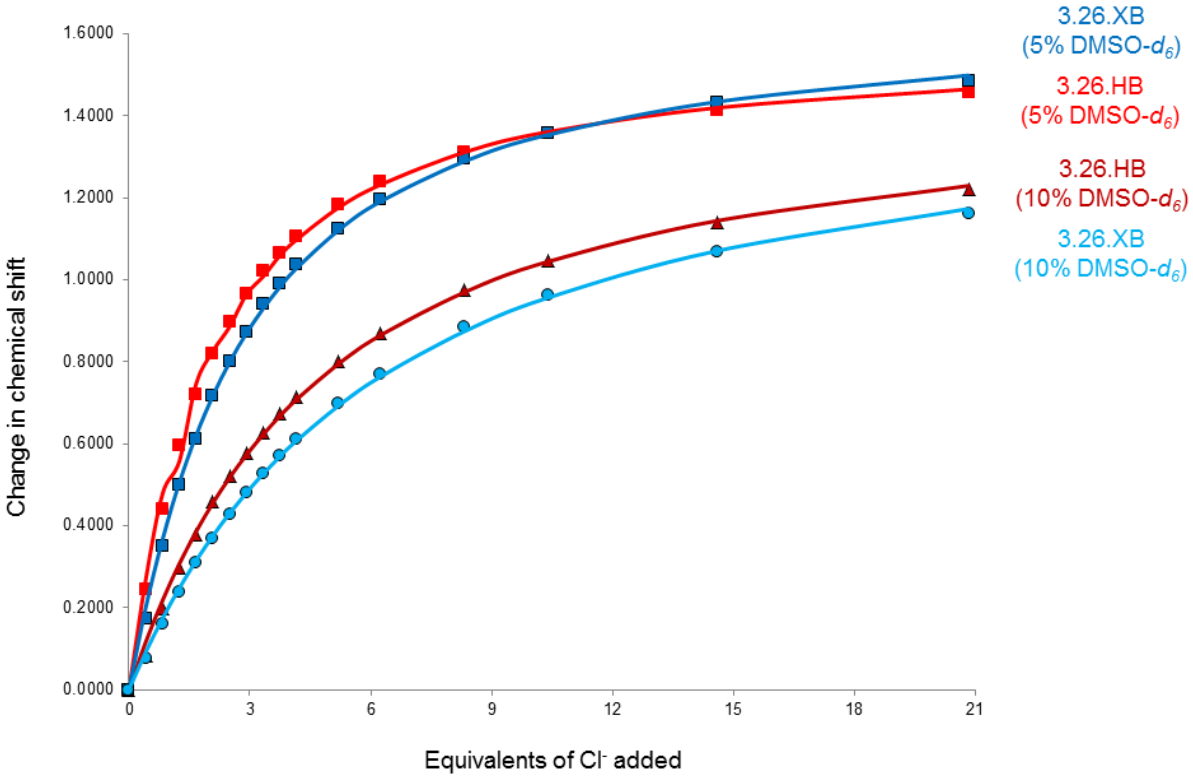



***Figure 3.9.*** *Comparative plots of the change in chemical shift of the proton* ***c*** *(ppm) against equivalents of* $Cl^-$ *added for the acyclic 1,3-phenylene-based bistriazole-urea receptors (*$CDCl_3$*/DMSO-*$d_6$ *mixtures, 298 K). Observed data is represented as solid points, whereas fitted isotherms are represented as lines. Inset: Structure of 1,3-phenylene-based bistriazole-urea receptors.*

***Table 3.3.*** *Chloride association constants ($K_a$/ $M^{-1}$) for triazole-urea receptors **3.26.HB** and **3.26.XB** in $CDCl_3$/DMSO-$d_6$ mixtures at 298 K.*

| Percentage of DMSO-$d_6$ by volume | Association constants ($K_a$/ $M^{-1}$) [a,b] | |
|---|---|---|
| | **3.26.HB** | **3.26.XB** |
| 5% | 644 | 450 |
| 7.5% | 438 | 283 |
| 10% | 246 | 171 |

*[a] Chloride was added as its tetrabutylammonium (TBA) salt. [b] Calculated using BindFit [10,11] by monitoring the change in the chemical shift of the urea N – H proton (labelled **c** in **Figure 3.9**). Errors < 5%.*

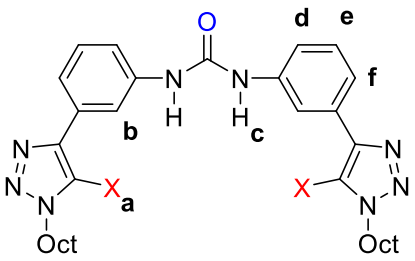
The hydrogen-bonding receptor **3.26.HB** forms a stronger chloride complex than the XB receptor in all solvent mixtures studied. As expected, the association constant magnitudes decreased with increasing percentage of the more competitive solvent DMSO. Moreover, the binding of chloride by **3.26.HB** was notably weaker when employing MeOD instead of DMSO. This can be related to the superior anion solvation properties of the protic solvent methanol.

### 3.3.3.4. Dicarboxylate binding studies

It was hypothesised that, due to the rigidity of the 1,3-phenylene spacer, **3.26.HB** and **3.26.XB** may possess an optimal bite size for dicarboxylate anions. Thus $^1$H NMR titration experiments were undertaken to probe the affinities of these receptors for a series of aliphatic dicarboxylates in 1:9 DMSO-$d_6$/$CDCl_3$ (*v/v*).

Upon dicarboxylate anion addition, the largest changes in chemical shift were observed in the vicinity of the binding site, notably for the urea protons ***c*** for both hosts (approximately 3 ppm). The second largest downfield shifts were observed for the triazole protons (host **3.26.HB**, 0.1 – 0.32 ppm) and aromatic protons, of particular interest being the inner proton ***b*** flanked by the urea and triazole motifs (0.12 – 0.14 ppm for host **3.26.HB**, 0.31 – 0.37 ppm for host **3.26.XB**).

BindFit [10,11] analysis of the aromatic proton ***b*** titration data determined 1:1 stoichiometric host-guest association constants (**Table 3.4**).




**X** = H **3.26.HB**
**X** = I **3.26.XB**

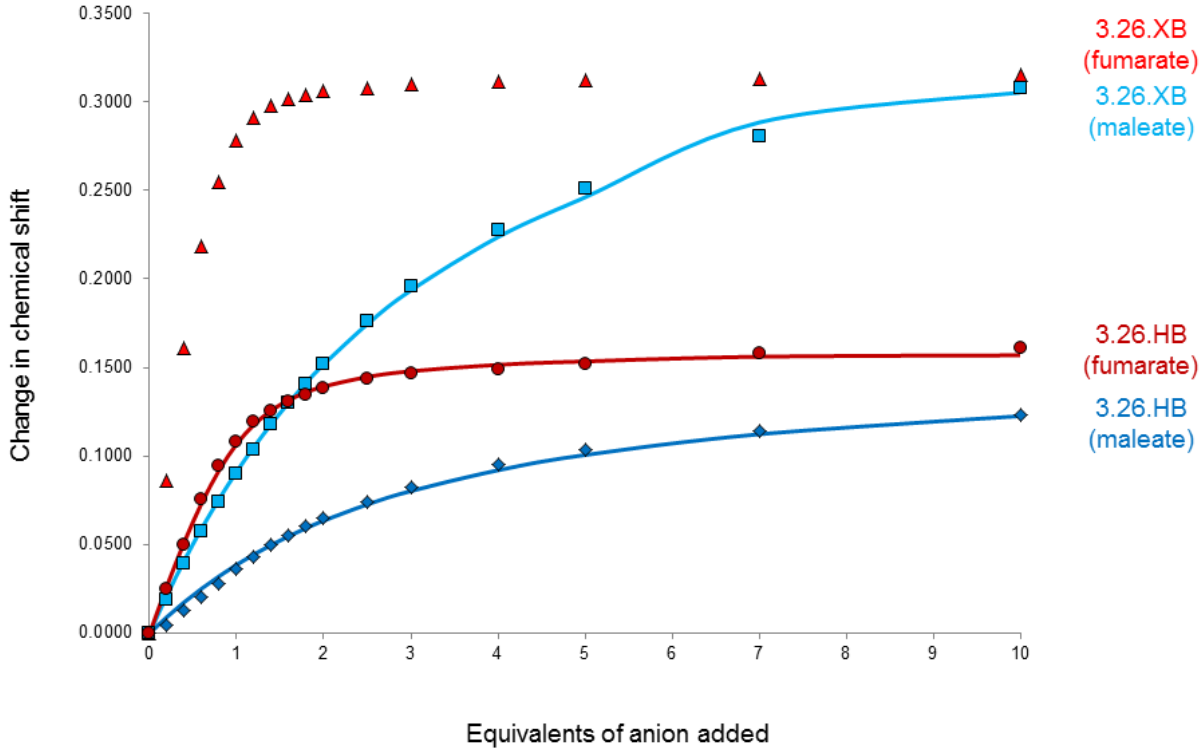
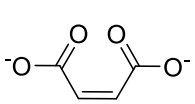
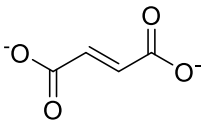



***Figure 3.10.*** *Comparative plots of the change in chemical shift (ppm) of the monitored proton against equivalents of maleate or fumarate added for the rigid 1,3-phenylene urea receptors (1:9 DMSO-$d_6$/$CDCl_3$ (v/v), 298 K). Proton **b** was monitored in all cases, with the exception of **3.26.HB** with fumarate, where the triazole proton signal **a** was followed.*

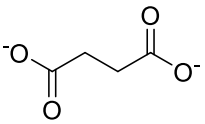
***Table 3.4.*** *Dicarboxylate association constants ($K_a$/ $M^{-1}$) of 1,3-disubstituted receptors* ***3.26.HB*** *and* ***3.26.XB*** *in 1:9 DMSO-$d_6$/$CDCl_3$ mixtures at 298 K.*



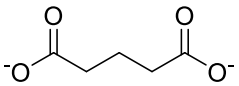
maleate



fumarate



succinate



glutarate

| Anion [a] | p$K_a$ of conjugate acid in water [16] | Association constants ($K_a$/ $M^{-1}$) [b] | |
|---|---|---|---|
| | | 3.26.HB | 3.26.XB |
| Maleate | 6.07 | 411 | 355 |
| Fumarate | 4.44 | 6137 | > $10^4$ [c] |
| Succinate | 5.6 | 328 | 1085 |
| Glutarate | 5.4 | 2133 | 2487 |

*[a] Anions were added as their tetrabutylammonium (TBA) salts. [b] Calculated using BindFit [10,11] by monitoring the change in the chemical shift of the inner aromatic proton (labelled* ***b*** *in* ***Figure 3.10****). Errors < 10%. [c] The value of the association constant was too high to be accurately determined. A lower value of $10^4$ $M^{-1}$ could be estimated.*

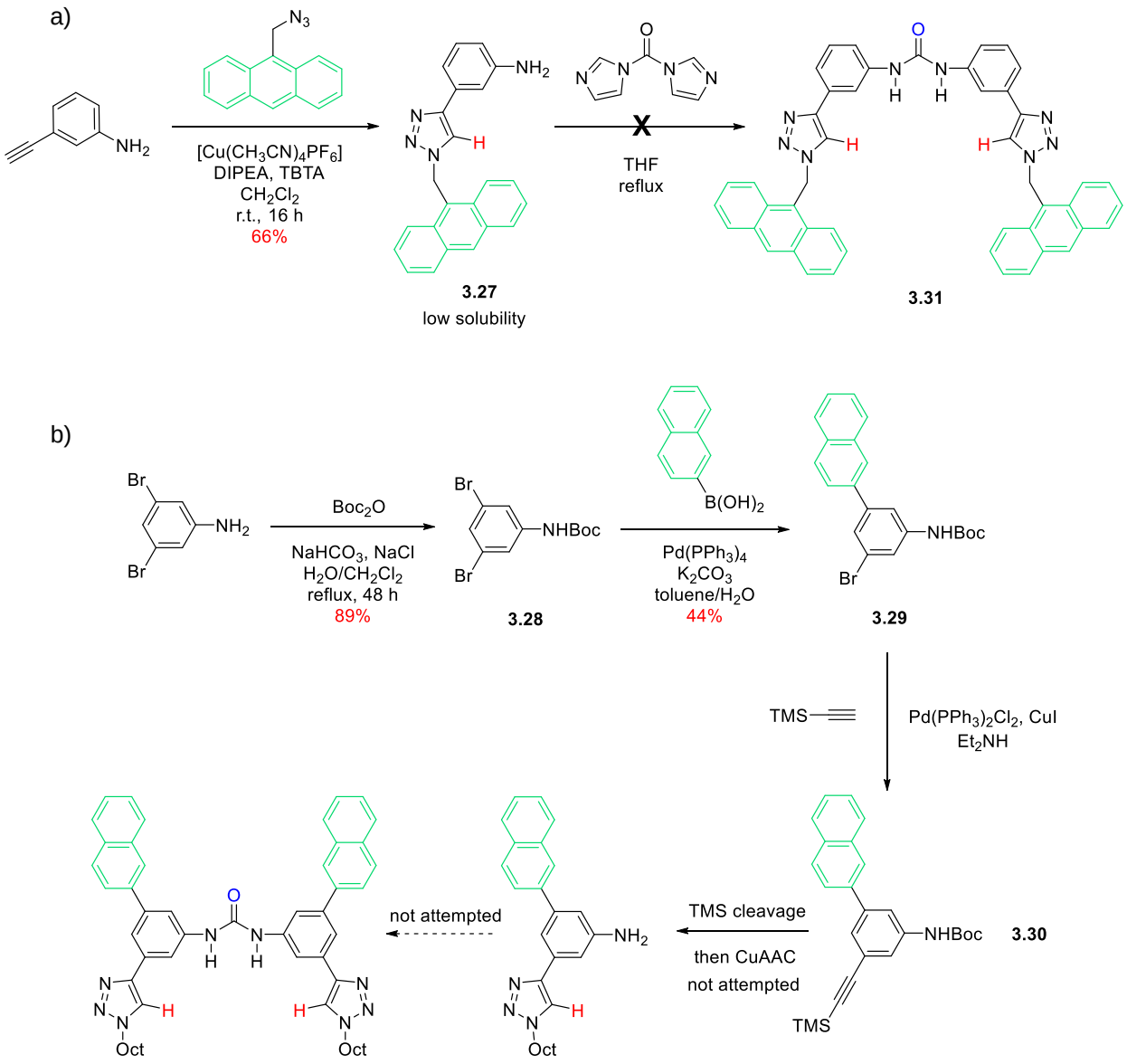
Interestingly, the binding trend in the case of **3.26.HB** appears to be independent of the basicity of the dicarboxylate; in fact, the least basic, fumarate, is bound the strongest, whereas the association constants for maleate and succinate are of similar magnitude to that of chloride despite the double negative charge. However, there is evident correlation between binding strength and dicarboxylate anion geometry. The (Z)-alkene fumarate is bound significantly more strongly than the (E)-alkene maleate due to its geometric complementarity to the binding pocket of **3.26.HB** and also more strongly than its saturated analogue succinate due to the rigidity of the C=C bond which reduces the loss of entropy upon binding. The introduction of a saturated, flexible propylene spacer increases the binding affinity of glutarate compared to succinate, however, glutarate is bound with a lower $K_a$ than fumarate due to the rigidity of the latter. Notably, the introduction of XB donors leads to an increase in affinity towards most dicarboxylates, with the exception of maleate, due to the strength and directionality of the halogen bond. This also leads to an increase in the degree of selectivity for fumarate over maleate.

### 3.3.3.5. Towards a fluorescent dicarboxylate sensor based on the urea-triazole motif

Due to the high potency of receptors **3.26.HB** and **3.26.XB** towards fumarate in particular, attempts to incorporate a fluorescent reporter group proximal to the binding site for dicarboxylate sensing applications were undertaken.

Initially, attachment of an anthracene motif to the triazole unit was investigated (**Scheme 3.8.a**). For this purpose, aniline **3.27** was prepared in a 66% yield through a CuAAC reaction of 3-ethynylaniline and 9-(azidomethyl)anthracene (prepared by a literature procedure [17] and kindly donated by Dr. Xiaoxiong Li). This was further subjected to a reaction with 1,1'-carbonyldiimidazole (CDI), however, the limited solubility of both **3.27** and target **3.31** made purification highly challenging.

Hence, an alternative sensor was designed, with naphthalene motifs attached to the phenyl rings (**Scheme 3.8.b**). Commercial 3,5-dibromoaniline was *N*-Boc-protected to afford **3.28** in 89% yield, [18] after which the naphthalene fluorophore was covalently attached to the phenyl ring via a Suzuki coupling with 2-naphthaleneboronic acid. After challenging separation by column chromatography, the product **3.29** was isolated in a 44% yield. A TMS-protected alkyne was introduced onto the scaffold through a Sonogashira reaction to give **3.30**. Disappointingly, the TMS group of **3.30** could not be cleaved even after a variety of deprotection conditions were tried, and repeating the synthesis of **3.30** itself proved surprisingly difficult, which negated any further investigations into sensing applications for these receptors.

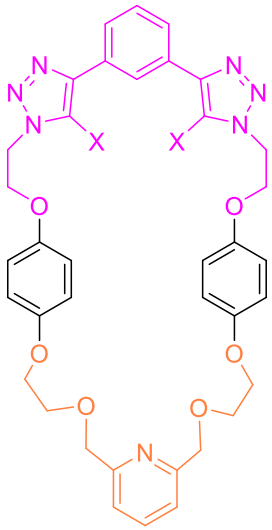



***Scheme 3.8.*** *Attempted syntheses of fluorescent rigid HB and XB bistriazole-urea receptors.*

## 3.4. Interlocked HB/XB urea-triazole structures for anion recognition

### 3.4.1. Neutral urea-monotriazole [2]rotaxanes incorporating a methylene spacer

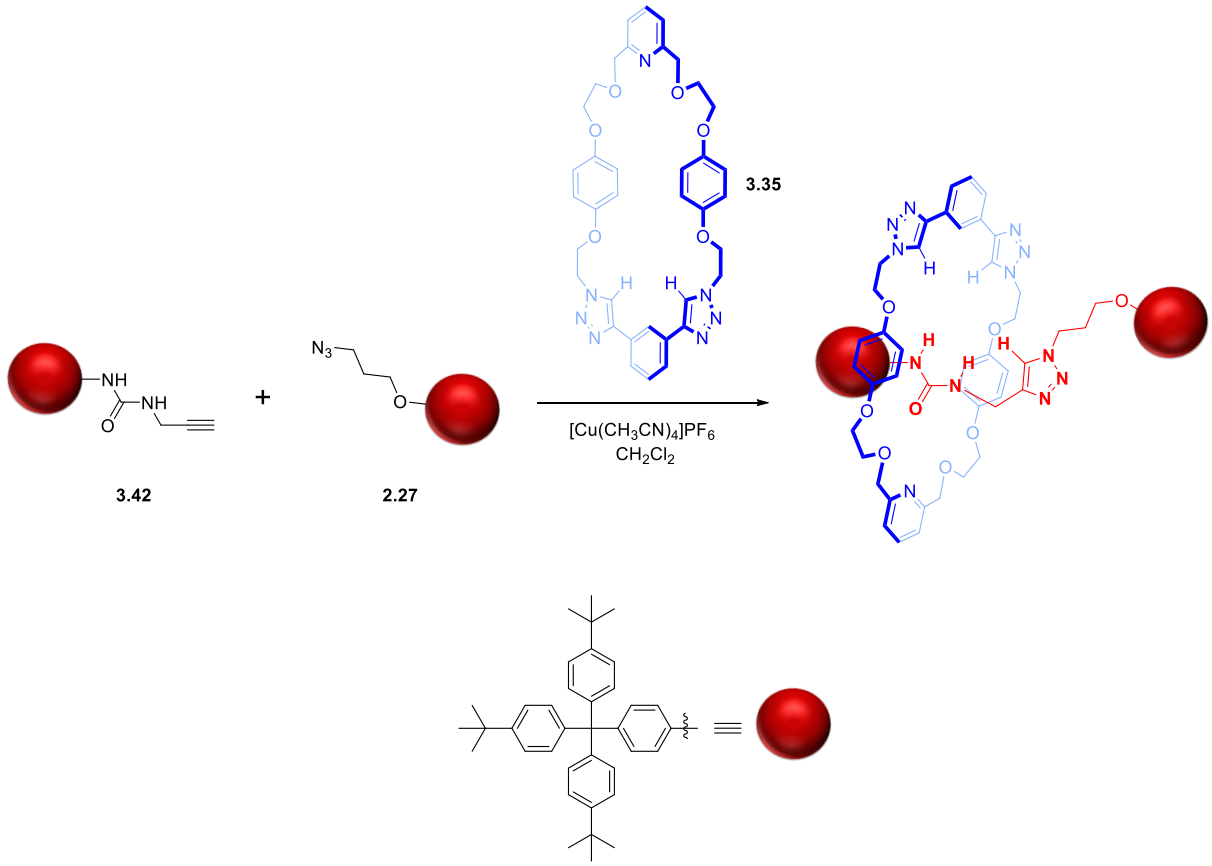
Capitalising on previous work in the Beer group, [19–21] a novel macrocycle for the active metal template (AMT) synthesis of interlocked rotaxane host structures containing HB/XB urea-triazole axle components for anion recognition was designed (**Figure 3.11**). It was envisaged that the pyridyl nitrogen atom of the target macrocyclic species **3.35** would coordinate a Cu(I) cation endotopically, as previously reported in the literature, [22] and thus favour AMT synthesis of a urea-triazole [2]rotaxane (**Scheme 3.9**), while the macrocycle component's bistriazole motif would enhance the anion binding properties of the resulting interlocked structure.



**3.35**

**X** = H, I

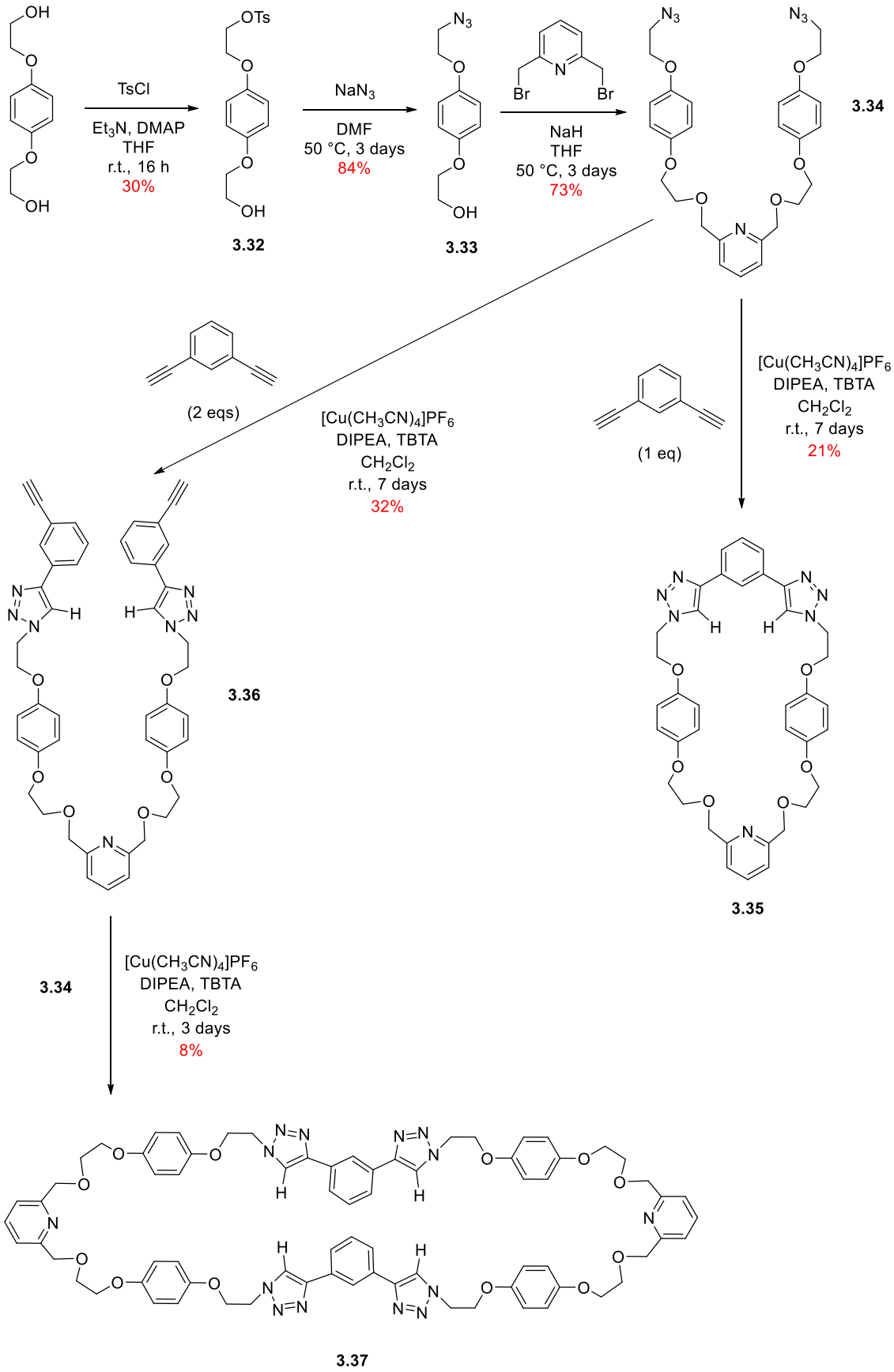
***Figure 3.11.*** *Structure of target marocycle* ***3.32*** *for AMT [2]rotaxane synthesis.*




***Scheme 3.9.*** *Proposed AMT synthesis of a monotriazole-urea axle containing rotaxane.*

### 3.4.1.1. Synthesis of a bis(triazole)-pyridyl macrocycle

The target HB macrocyclic structure was synthesised as shown in **Scheme 3.10**. Initially, hydroquinone bis(2-hydroxyethyl) ether was converted to its monotosylate **3.32** in a 30% yield, [23] after which it was subjected to a $S_N2$ reaction with $NaN_3$ in DMF to afford azide **3.33** [24] and subsequently reacted with 2,6-bis(bromomethyl)pyridine in THF in the presence of NaH to give versatile bis-azide **3.34**. [24] A CuAAC reaction of **3.34** with commercially available 1,3-diethynylbenzene under high dilution conditions afforded the desired macrocycle **3.35** in 21% yield when employing a 1:1 azide:alkyne stoichiometric ratio, as well as side-product **3.36** in 32% yield when employing 2 equivalents of alkyne. The resulting bis-alkyne **3.36** was further subjected to a CuAAC reaction with starting bis-azide **3.34** to give extended macrocycle **3.37**, albeit in a low yield, which shows promise in the synthesis of higher order interlocked structures such as [3]rotaxanes and [3]catenanes.

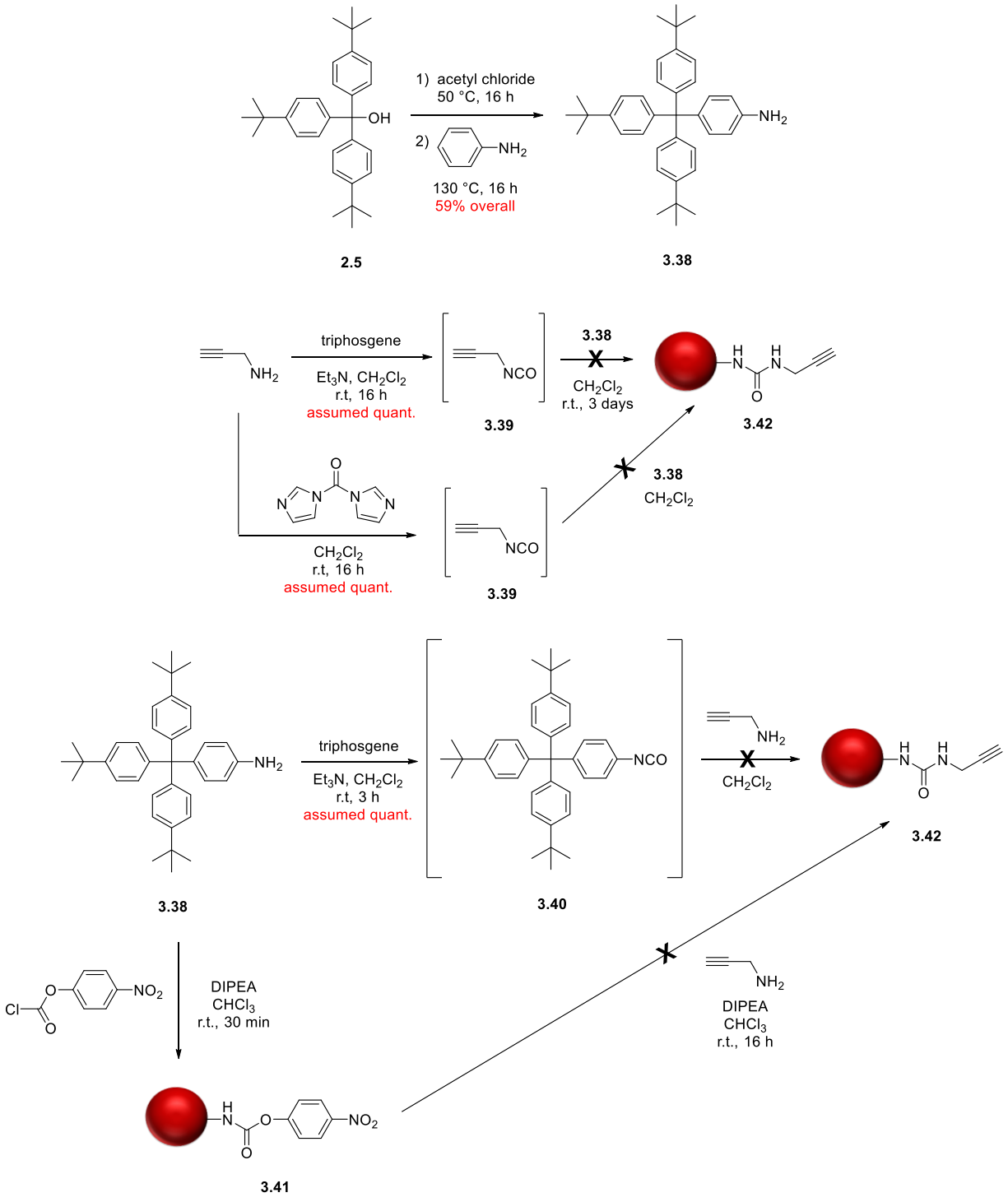



***Scheme 3.10.*** *Synthesis of two ditopic pyridyl macrocycles incorporating triazole motifs.*

### 3.4.1.2. Synthesis of an alkyne-appended stopper incorporating a urea motif

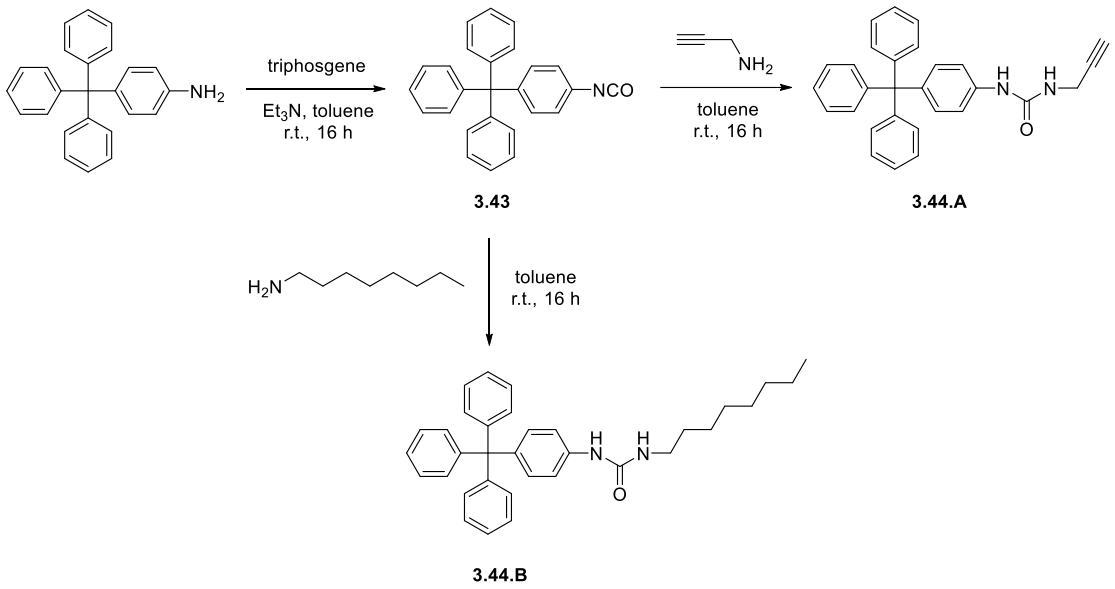
A synthesis of the target alkyne-functionalised urea terphenyl stopper **3.42** was attempted according to **Scheme 3.11**. Tertiary alcohol compound **2.5** was reacted with acetyl chloride followed by aniline at 130 °C to give aromatic amine **3.38** [25] and subsequently condensed with propargyl isocyanate **3.39**, formed in situ from propargyl amine and triphosgene. Unfortunately, the synthesis was unexpectedly low yielding and the purification highly challenging. Formation of the target stopper was subsequently attempted by either forming propargyl isocyanate **3.39** with triphosgene or CDI, followed by reaction with the aromatic amine **3.38**, or forming aromatic isocyanate **3.40** in situ, followed by a reaction with propargylamine. Although the presence of **3.42** in the crude reaction mixtures was confirmed by mass spectrometry, all attempts to isolate the desired product failed.

Consequently, an alternative route was designed by adapting a literature procedure, [26] which involved the formation of a 4-nitrophenyl carbamate intermediate **3.41** from the reaction of stopper amine **3.39** and 4-nitrophenyl chloroformate, followed by a reaction with propargylamine. Disappointingly, no product could be isolated by this procedure either.




***Scheme 3.11.*** *Synthetic attempts towards a urea-based alkyne stopper.*

In order to investigate the apparent lack of stability of stopper alkyne **3.42**, two test reactions were run in parallel on model aromatic urea compounds, one bearing an alkyne motif in the vicinity of the urea and the other bearing a simple octyl chain (**Scheme 3.12**). To this extent, commercially available 4-tritylaniline was converted to isocyanate **3.43**, which was reacted in situ separately with propargylamine and octylamine.




***Scheme 3.12.*** *Control reactions of two model aromatic ureas.*

The reaction progress was monitored by mass spectrometry. For the formation of **3.44.A**, no mass signal corresponding to the product was observed, with notable peaks being present at *m/z* 243.3 (trityl cation) and an unassignable peak at 165.0. In the case of the formation of **3.44.B**, a small mass peak at m/z 489.2 (very close to to the *m/z* of [**3.44.B**+H]$^+$ at 491.3) was present; however, the spectrum was dominated by the trityl cation peak and the same unassignable signal at 165.0.

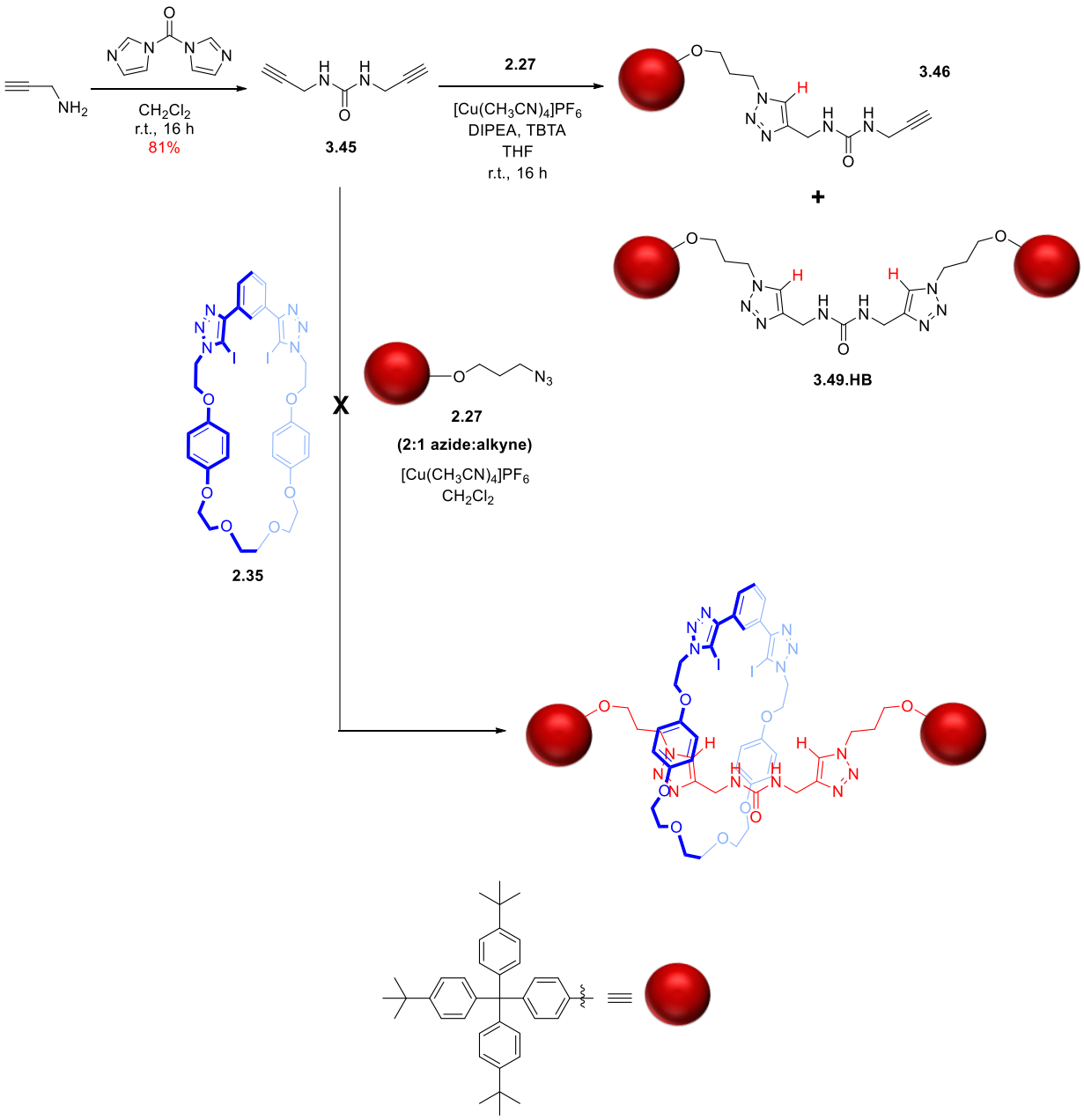
Comparative $^1$H NMR analysis of the crude reaction mixtures revealed that in both cases the aromatic backbone was intact (two doublets in the 7 ppm region) whereas the amine moiety (broad singlet around 3.6 ppm) had disappeared, which was consistent with its conversion to another functional group. Unfortunately, the alkyl regions were dominated by superimposing multiplets which were not part of the aliphatic amine backbone, strongly suggesting that decomposition and/or multiple side reactions had occured in both cases. From this evidence, it could be concluded that 4-tritylanilines are intrinsically not stable towards urea formation.

### 3.4.2. Neutral urea-bistriazole [2]rotaxanes incorporating a methylene spacer

#### 3.4.2.1. Attempted synthesis of a [2]rotaxane

It was envisaged that a symmetric, bistriazole-urea [2]rotaxane might be more synthetically accessible than the monotriazole analogue. To this extent, a synthetic pathway towards the target symmetrical [2]rotaxane was designed, as outlined in **Scheme 3.13** below.

Propargylamine was first reacted with CDI to afford bis-alkyne urea **3.45** in an 81% yield, [7] after which it was subjected to a CuAAC reaction with one equivalent of stopper azide **2.27**. Unfortunately, axle **3.49.HB** was also formed along with the target stopper alkyne **3.46** and the two could not be separated, even after iterative column chromatography. An alternative pathway was sought, in which bis-alkyne **3.45** was directly subjected to an AMT protocol with two equivalents of stopper azide **2.27** and macrocycle **2.35**. Unfortunately, this also failed to afford the target [2]rotaxane.



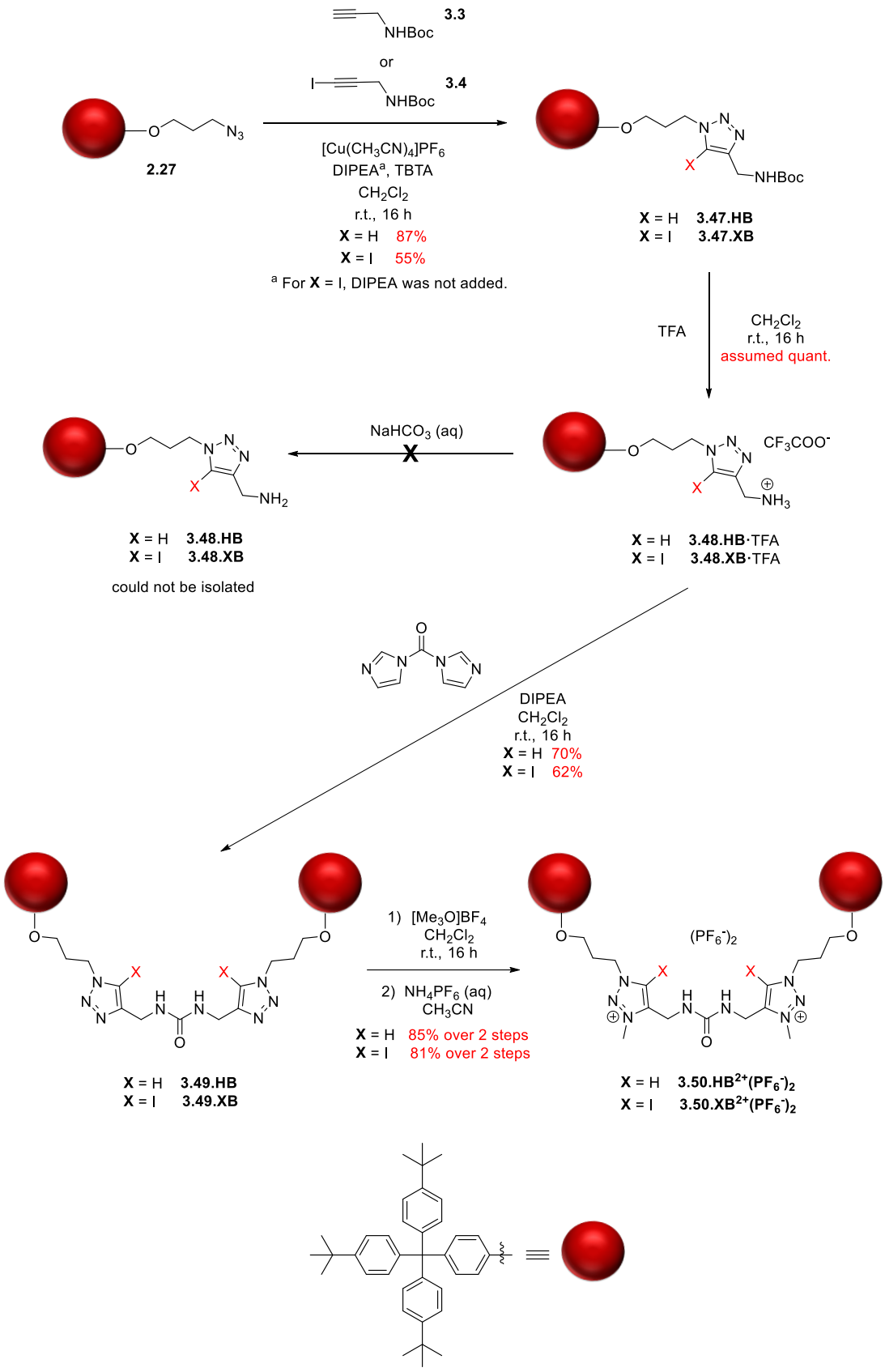

***Scheme 3.13.*** *Proposed synthetic pathways towards a neutral bistriazole-urea [2]rotaxane.*

### 3.4.3. Cationic urea-bistriazolium [2]rotaxanes incorporating a methylene spacer

Due to the challenging synthesis of neutral urea-based rotaxanes by active metal templation and of monotriazole-urea synthons in particular, investigations into cationic bis-urea [2]rotaxanes were undertaken. Firstly, two dicationic axle components incorporating a bis(iodo)triazolium-urea motif were prepared, after which integration into interlocked rotaxane structures was sought by anion-templated ring closing metathesis.

### 3.4.3.1. Synthesis of a cationic urea-bistriazolium axle

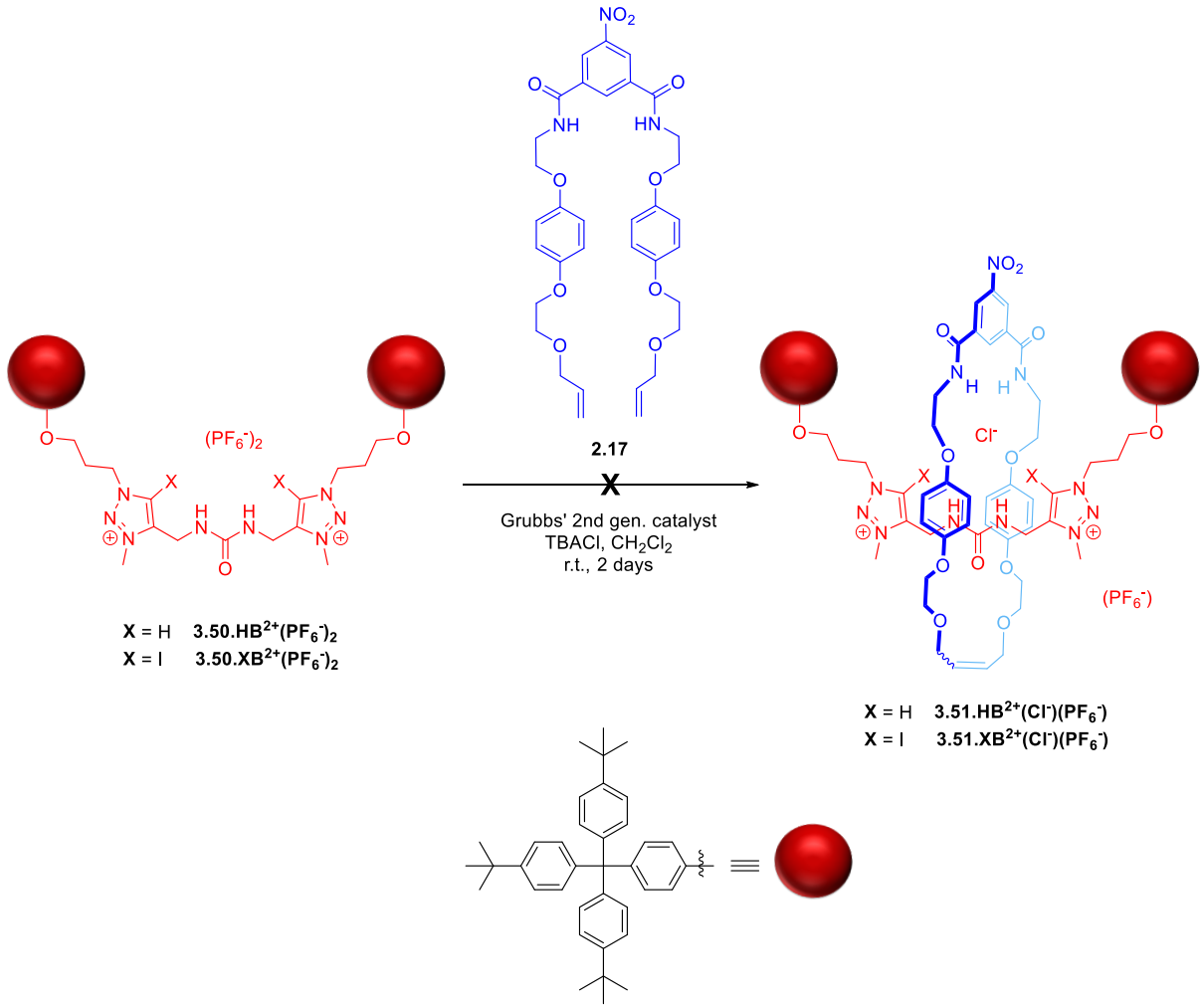
The novel dicationic axles were synthesised as outlined in **Scheme 3.14**. A CuAAC reaction of azide stopper **2.27** and *N*-Boc-propargylamine or *N*-Boc-iodopropargylamine afforded *N*-Boc-protected aminotriazoles **3.47.HB** and **3.47.XB** in 87% and 55% yields, respectively. Subsequent cleavage of the protecting group under acidic conditions gave amino-triazoles **3.48.HB** and **3.48.XB** as their trifluoroacetate salts; however, the free base forms could not be isolated after aqueous workup with $NaHCO_3$. Hence, **3.48.HB·TFA** and **3.48.XB·TFA** were reacted in situ with 1,1'-carbonyldiimidazole under basic conditions, which afforded the target neutral axles **3.49.HB** and **3.49.XB** in yields of 70% and 62%, respectively. The dicationic axles were obtained by methylation of **3.49.HB** and **3.49.XB** with $[Me_3O]BF_4$, followed by anion exchange through dissolving the resulting tetrafluoroborate salts in $CH_3CN$ and precipitation of the $PF_6^-$ salts with an aqueous solution of $NH_4PF_6$.




***Scheme 3.14.*** *Synthesis of bis(iodo)triazolium-urea axle components.*

### 3.4.3.2. Attempted anion template synthesis of cationic [2]rotaxanes

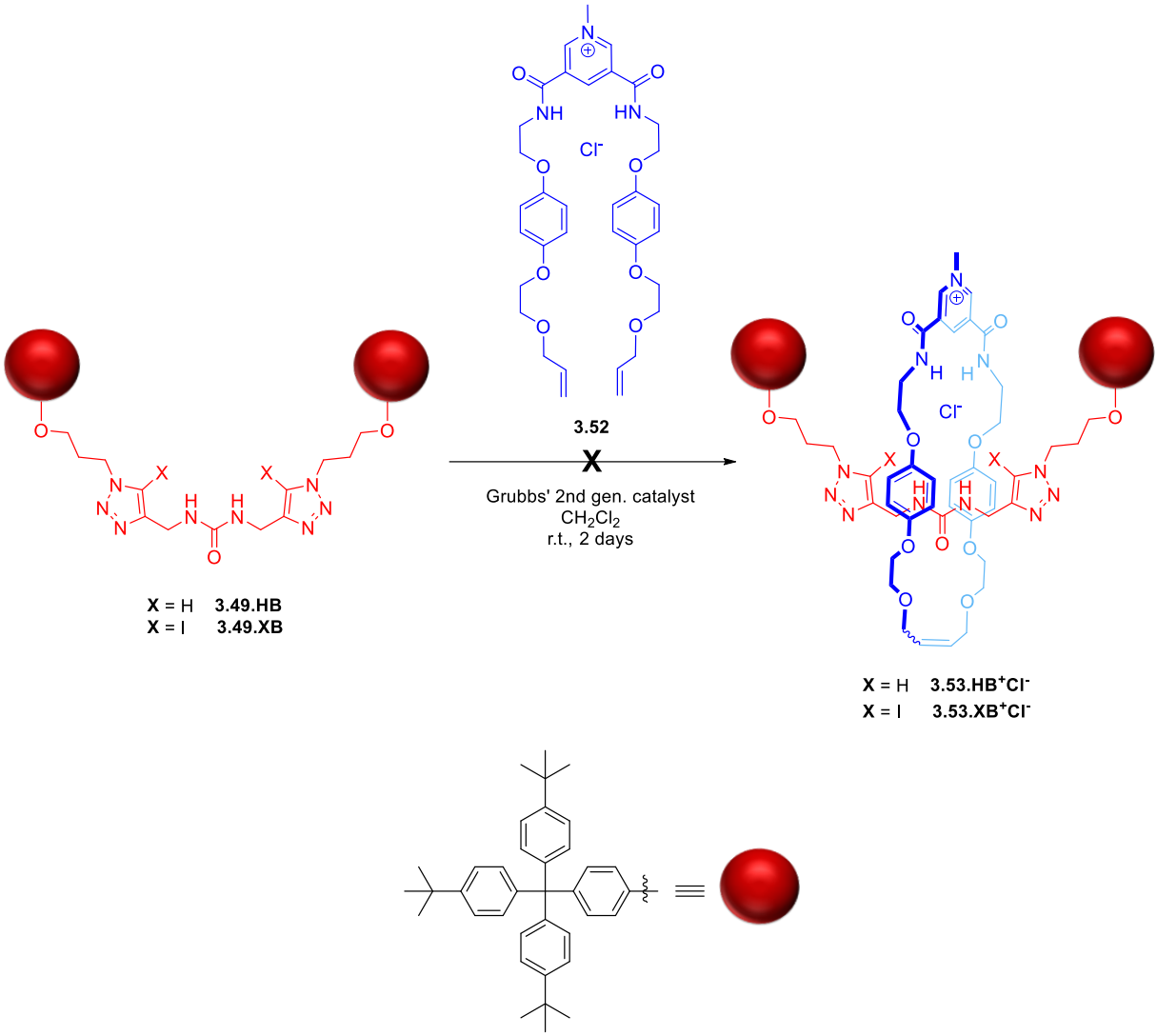
The dicationic axles **3.50.HB$^{2+}$(PF$_6^-$)$_2$** and **3.50.XB$^{2+}$(PF$_6^-$)$_2$** were dissolved separately in $CH_2Cl_2$ along with one equivalent of TBACl and a slight excess of nitroisophthalamide bis-alkene **2.17**. After stirring for 20 minutes, Grubbs' 2$^{nd}$ generation catalyst was added and the mixture stirred for a further 2 days at room temperature (**Scheme 3.15**). Unfortunately, only the ring-closed macrocycle could be detected through $^1$H NMR analysis of the crude reaction mixture.




***Scheme 3.15.*** *Attempted synthesis of a bis(iodo)triazolium-urea [2]rotaxane by chloride-templated ring-closing metathesis.*

### 3.4.3.3. Attempted synthesis of cationic [2]rotaxanes incorporating a neutral bistriazole-urea axle

Due to the challenges posed by the dicationic axles, it was envisaged that a neutral bistriazole-urea axle could be employed instead with a positively charged pyridinium bis-alkene macrocycle precursor. For this purpose, neutral axles **3.49.HB** and **3.49.XB** were separately reacted with pyridinium bis-alkene **3.52** as its chloride salt (prepared according to a literature procedure [27] and kindly donated by Dr. Asha Brown) under ring-closing metathesis conditions, however, no traces of rotaxane **3.53.HB$^+$** or **3.53.XB$^+$** could be detected by mass spectrometry or $^1$H NMR, only the macrocycle byproduct (**Scheme 3.16**).

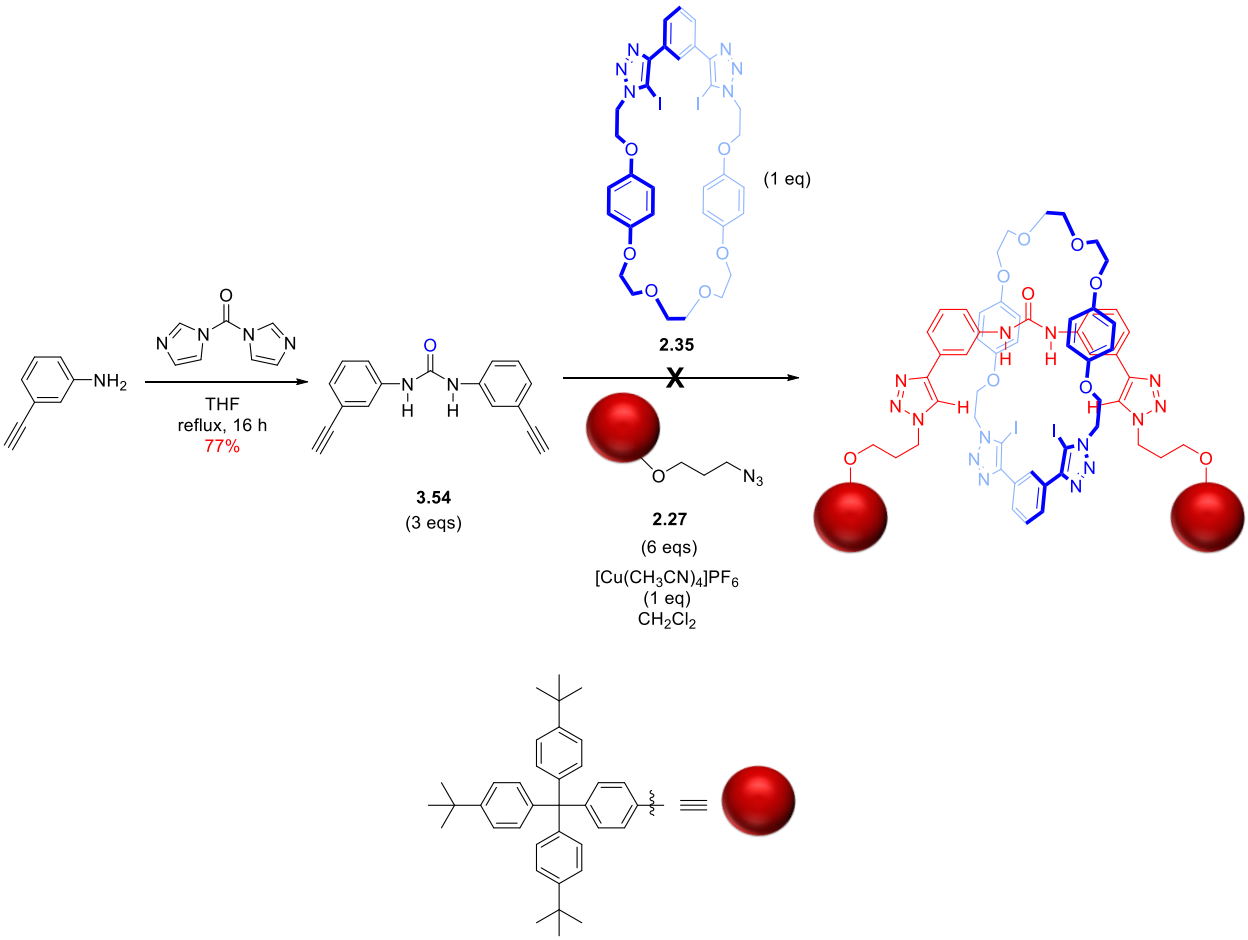



***Scheme 3.16.*** *Attempted synthesis of a bis(iodo)triazole-urea [2]rotaxane with a cationic macrocycle component by chloride-templated ring-closing metathesis.*

### 3.4.4. Neutral urea-bistriazole [2]rotaxanes incorporating a 1,3-phenylene spacer

#### 3.4.4.1. Attempted synthesis of a neutral [2]rotaxane

Due to the challenging nature of cationic urea-triazole rotaxanes, a simple synthesis of a neutral analogue incorporating the 1,3-phenylene spacer was undertaken. 3-Ethynylaniline was converted to bis-alkyne **3.54** by reaction with CDI in refluxing THF in a 77% yield [28] and then directly reacted with macrocycle **2.35** and 6 equivalents of stopper azide **2.27** under AMT conditions (**Scheme 3.17**). Disappointingly, no traces of interlocked product or axle could be detected by $^{1}$H NMR or mass spectrometry.




***Scheme 3.17.*** *Attempted synthesis of a neutral bistriazole-urea [2]rotaxane with 1,3-phenylene spacers.*

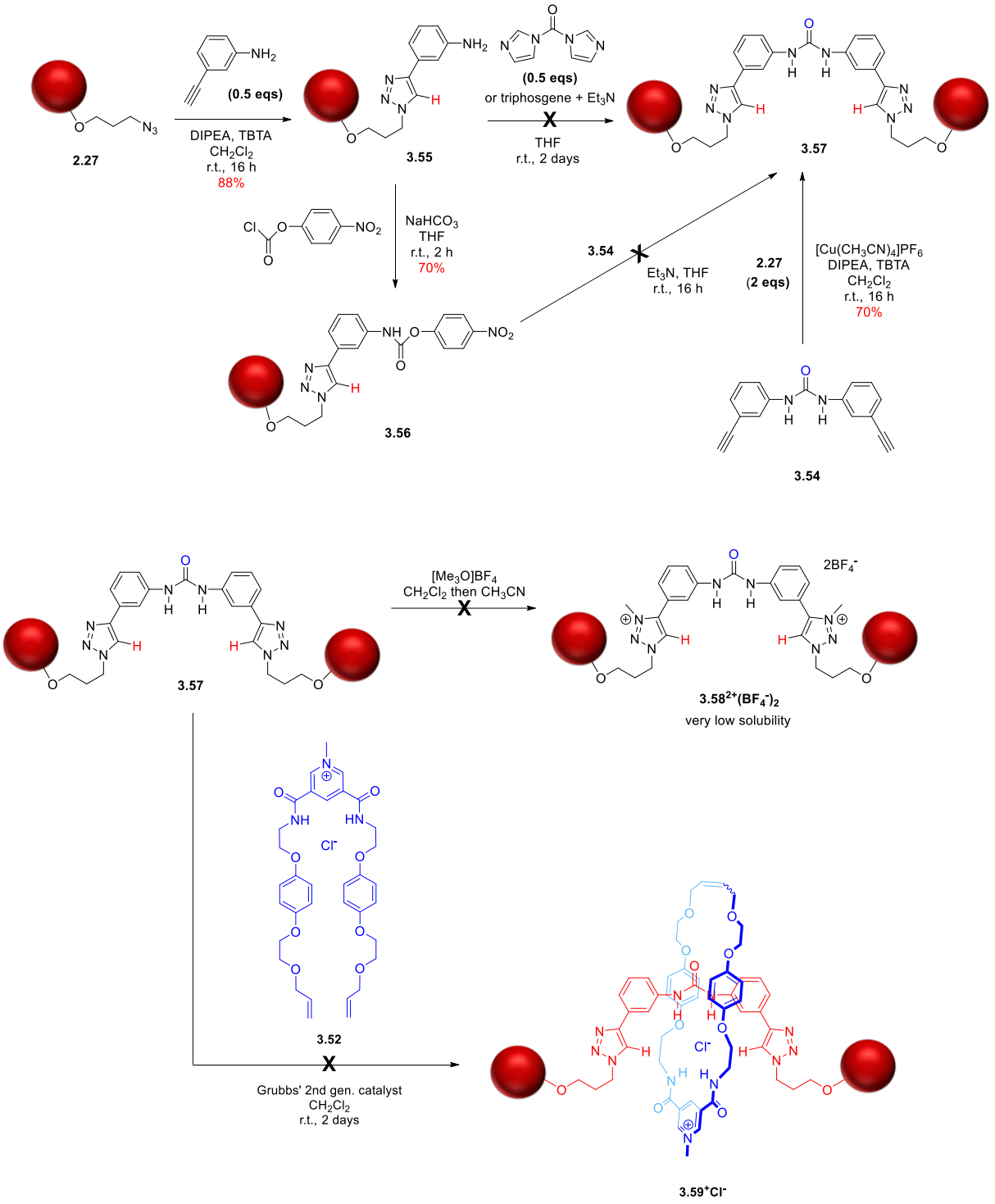
### 3.4.5. Cationic urea-bistriazolium [2]rotaxanes incorporating a 1,3-phenylene spacer

#### 3.4.5.1. Attempted syntheses of cationic [2]rotaxanes

Attempts to produce positively charged [2]rotaxanes containing a bistriazole-urea axle component with a 1,3-phenylene spacer were undertaken via an anion template approach (**Scheme 3.18**).

Triazole-amine **3.55** was obtained via a CuAAC reaction of azide stopper **2.27** and 3-ethynylaniline in 88% yield. Formation of the corresponding axle was attempted directly from **3.55** with either CDI or triphosgene; however, both attempts failed to produce the target urea axle **3.57**. Alternatively, the amine **3.55** was converted to its nitrophenyl carbamate analogue **3.54** [29] and this synthon reacted with a further equivalent of **3.65** but no product was detected. The axle was successfully synthesised in a 70% yield through a CuAAC reaction of bis-alkyne **3.54** with two equivalents of azide stopper **2.27**.

The reaction of pyridinium chloride bis-alkene **3.52** with axle **3.57** and Grubbs' 2$^{nd}$ generation catalyst disappointingly failed to produce the target rotaxane. Finally, in order to obtain a cationic [2]rotaxane, the neutral component **3.57** was reacted with $[Me_3O]BF_4$ in $CH_2Cl_2$, resulting in a mixture of sparingly soluble mono- and dialkylated axles. To promote full dialkylation of the mixture, this was redissolved in $CH_3CN$ and a further portion of $[Me_3O]BF_4$ was added, leading to the formation of $\mathbf{3.58^{2+}(BF_4^-)_2}$. Unfortunately, the limited solubility of the product negated the possibility for incorporation into a rotaxane.



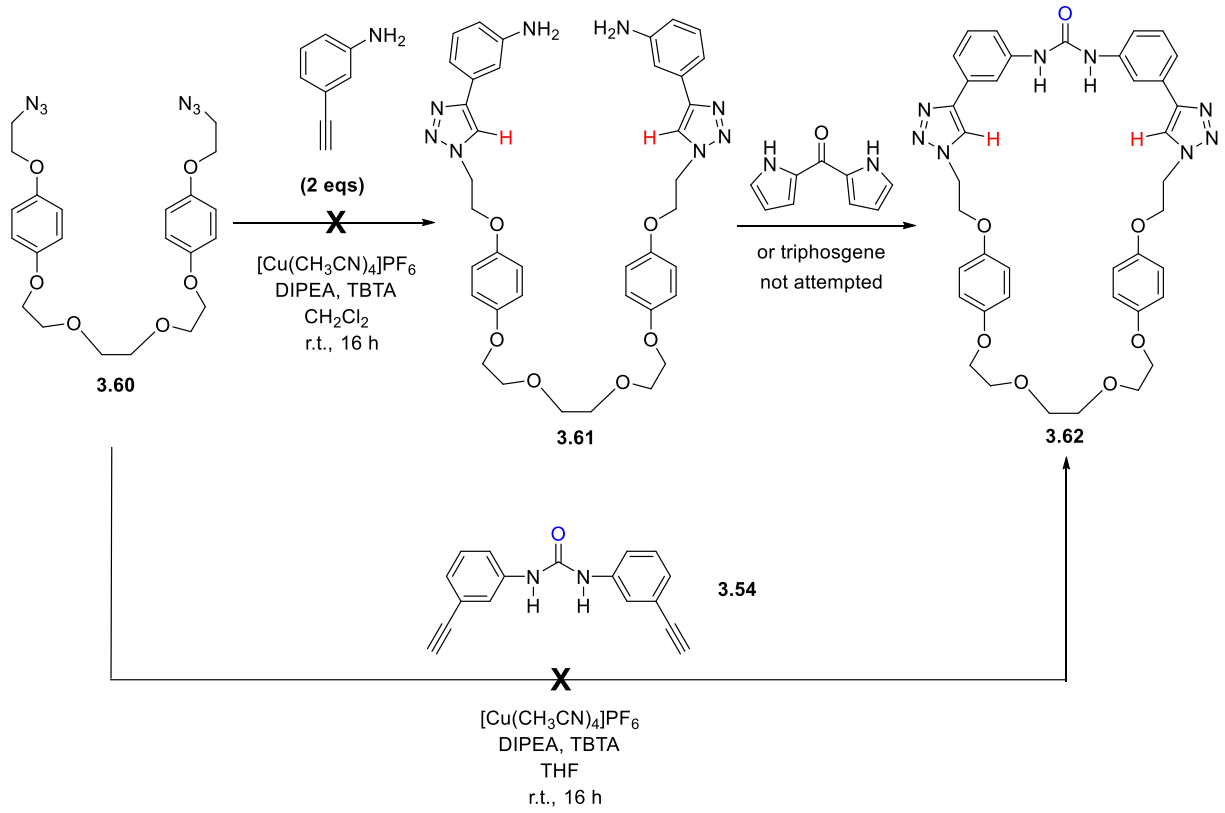

***Scheme 3.18.*** *Attempted synthesis of cationic bistriazole-urea [2]rotaxanes with 1,3-phenylene spacers.*

## 3.5. Macrocyclic urea-triazole structures for anion recognition

### 3.5.1. Attempted synthesis of a urea-triazole macrocycle

Given the difficulties encountered with the synthesis of the [2]rotaxane architectures, a macrocyclic receptor structure incorporating a bistriazole-urea motif was designed (**Scheme 3.19**).

Bis-azide **3.60** (kindly donated by Sam Sutton) was subjected to a CuAAC reaction with two equivalents of 3-ethynylaniline to afford bisamine **3.61**. Disappointingly, the low solubility of the product in common organic solvents precluded its further use in a macrocyclisation reaction. Hence, the formation of this intermediate was avoided by directly reacting **3.60** with bis-alkyne **3.54** under high dilution conditions. The formation of macrocycle **3.62** was observed by mass spectrometry, however, all chromatographic attempts to isolate the macrocycle failed.



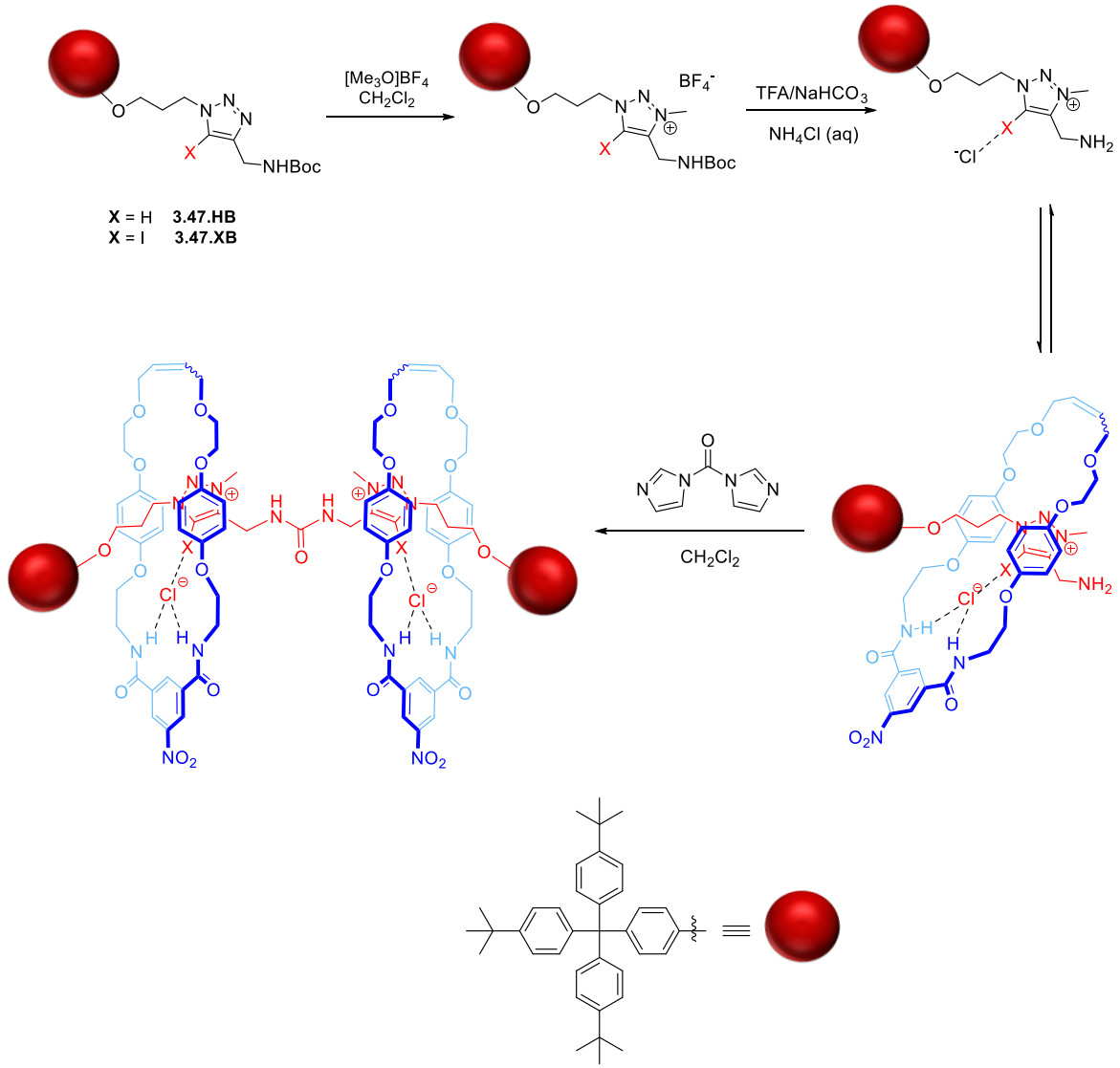

***Scheme 3.19.*** *Attempted synthesis of a bistriazole-urea macrocycle with 1,3-phenylene spacers.*

### 3.6. Conclusions and future work

To conclude, a number of XB/HB acyclic anion hosts incorporating urea or thiourea and (iodo)triazole motifs were successfully synthesised. Their anion binding properties have been assessed and the influence of a range of parameters such as number and nature of XB/HB donors, rigidity of the spacer, and bite angle on strength and selectivity trends rationalised. Importantly, integration of two XB donors into a rigid urea framework with a 1,3-phenylene spacer generated a receptor that was highly selective for the dicarboxylate fumarate over its geometric isomer maleate in 1:9 DMSO-$d_6$/$CDCl_3$ (v/v).

Numerous attempts to integrate these acyclic motifs as axle components of [2]rotaxane structural frameworks were undertaken with either an active metal template or anion template protocols; however, every attempt failed to afford an isolable interlocked product.

Future research avenues could focus on exploiting the advantages of amine reactions with carbonyl donors to synthesise higher-order structures such as [3]rotaxanes via anion templation (**Scheme 3.20**). Condensation between two amine-appended, chloride template assembled pseudorotaxanes with CDI could afford a symmetrical homo[3]rotaxane or asymmetric hetero[3]rotaxanes.




***Scheme 3.20.*** *Proposed synthesis of a bis(iodo)triazole-urea [2]rotaxane with a cationic macrocycle component by chloride-templated ring-closing metathesis.*

### 3.7. References


1. D. E. Gómez, L. Fabbrizzi, M. Licchelli and E. Monzani, *Org. Biomol. Chem*, **2005**, 3, 1495–1500.
2. V. Blažek Bregović, N. Basarić and K. Mlinarić-Majerski, *Coord. Chem. Rev.*, **2015**, 295, 80–124.
3. T. K. Ghosh, S. Mondal, S. Bej, M. Nandi and P. Ghosh, *Dalton Trans.*, **2019**, 48, 4538–4546.
4. T. Merckx, P. Verwilst and W. Dehaen, *Tetrahedron Lett.*, **2013**, 54, 4237–4240.
5. M. Denis, L. Qin, P. Turner, K. A. Jolliffe and S. M. Goldup, *Angew. Chem. Int. Ed.*, **2018**, 57, 5315–5319.
6. O. Ozay, M. Yildirim and H. Ozay, *Phosphorus Sulfur Silicon Relat. Elem.*, **2017**, 192, 307–315.
7. J. Budhathoki-Uprety, P. V. Jena, D. Roxbury and D. A. Heller, *J. Am. Chem. Soc.*, **2014**, 136, 15545–15550.
8. H. Chachignon, N. Scalacci, E. Petricci and D. Castagnolo, *J. Org. Chem.*, **2015**, 80, 5287–5295.
9. K. Yamamoto, T. Bruun, J. Y. Kim, L. Zhang and M. Lautens, *Org. Lett.*, **2016**, 18, 2644–2647.
10. P. Thordarson, *Chem. Soc. Rev*, **2011**, 40, 1305–1323.
11. D. B. Hibbert and P. Thordarson, *Chem. Commun.*, **2016**, 52, 12792–12805.
12. M. Obrzud, M. Rospenk and A. Koll, *Phys. Chem. Chem. Phys.*, **2014**, 16, 3209.
13. N. Sakai, K. Tamura, K. Shimamura, R. Ikeda and T. Konakahara, *Org. Lett.*, **2012**, 14, 836–839.
14. C. P. Allen, T. Benkovics, A. K. Turek and T. P. Yoon, *J. Am. Chem. Soc.*, **2009**, 131, 12560–12561.
15. A. Lilienkampf, M. Pieroni, B. Wan, Y. Wang, S. G. Franzblau and A. P. Kozikowski, *J. Med. Chem.*, **2010**, 53, 678–688.
16. E. Lide, *Handbook of chemistry and physics: a ready-reference book of chemical and physical data*, CRC Press, Boca Raton, Florida, **1993**.
17. V. V. S. Mummidivarapu, V. K. Hinge, K. Tabbasum, R. G. Gonnade and C. P. Rao, *J. Org. Chem.*, **2013**, 78, 3570–3576.
18. L. Schweighauser, M. A. Strauss, S. Bellotto and H. A. Wegner, *Angew. Chem. Int. Ed.*, **2015**, 54, 13436–13439.
19. J. Y. C. Lim, T. Bunchuay and P. D. Beer, *Chem. - Eur. J.*, **2017**, 23, 4700–4707.
20. J. Y. C. Lim, I. Marques, A. L. Thompson, K. E. Christensen, V. Félix and P. D. Beer, *J. Am. Chem. Soc.*, **2017**, 139, 3122–3133.
21. L. C. Gilday, T. Lang, A. Caballero, P. J. Costa, V. Félix and P. D. Beer, *Angew. Chem. Int. Ed.*, **2013**, 52, 4356–4360.
22. V. Aucagne, K. D. Hänni, D. A. Leigh, P. J. Lusby and D. B. Walker, *J. Am. Chem. Soc.*, **2006**, 128, 2186–2187.
23. M. D. Lankshear, N. H. Evans, S. R. Bayly and P. D. Beer, *Chem. - Eur. J.*, **2007**, 13, 3861–3870.
24. A. Brown, T. Lang, K. M. Mullen and P. D. Beer, *Org. Biomol. Chem.*, **2017**, 15, 4587–4594.
25. C. J. Serpell, R. Chall, A. L. Thompson and P. D. Beer, *Dalton Trans.*, **2011**, 40, 12052 - 12055.
26. N. H. Evans, C. J. Serpell, K. E. Christensen and P. D. Beer, *Eur. J. Inorg. Chem.*, **2012**, 2012, 939–944.
27. M. R. Sambrook, P. D. Beer, J. A. Wisner, R. L. Paul and A. R. Cowley, *J. Am. Chem. Soc.*, **2004**, 126, 15364–15365.
28. W. C. Drewe and S. Neidle, *Chem. Commun.*, **2008**, 5295 - 5297.
29. R. K. Sankar, R. S. Kumbhare, A. T. Dharmaraja and H. Chakrapani, *Chem Commun*, **2014**, 50, 15323–15326.

# Chapter 4

## Perfluoroaryl-based carbazole-(iodo)triazole structures for anion recognition

# Chapter 4: Perfluoroaryl-based carbazole-(iodo)triazole structures for anion recognition

## 4.1. Introduction

Carbazole is a rigid, highly conjugated heterocyclic framework featuring a highly acidic NH hydrogen bond donor (see **Chapter 1**, **Section 1.2.5.2.2**), with well-known optical and electronic properties such as an intense, deep blue fluorescence and efficient hole-transporting properties. [1,2] It is readily functionalised at the 1, 3, 6, 8, and 9*H* positions (**Figure 4.1**) [3] and thus can be modified with appropriate electrophiles, which makes it highly attractive for incorporation into anion receptor structures.

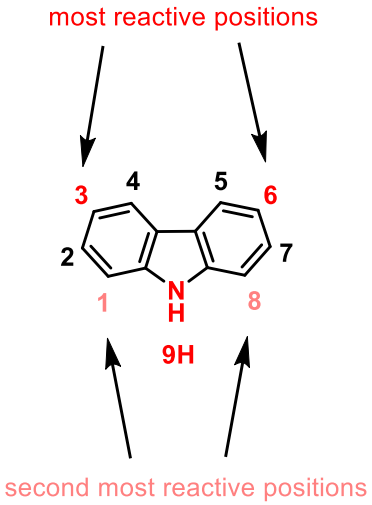



***Figure 4.1.*** *Standard numbering of the carbazole framework, with the varying reactivities of different positions highlighted.*

There is a precedent for the introduction of carbazole motifs into anion host frameworks; however, they are mostly employed in conjunction with other N – H donors such as ureas and amides. Kim and co-workers prepared a carbazole-bisurea receptor which exhibited different combinations of UV-Vis and fluorescent responses for a number of anions, thus allowing them to be differentiated via a 2D analysis by plotting fluorescence emission as a function of absorbance (**Figure 4.2.a**). [4] A carbazole-bisamide host has been synthesised by Chmielewski and co-workers which was shown to selectively sense $SO_4^{2-}$ even in highly competitive $D_2O$ – DMSO-$d_6$ solvent mixtures (**Figure 4.2.b**). [5]

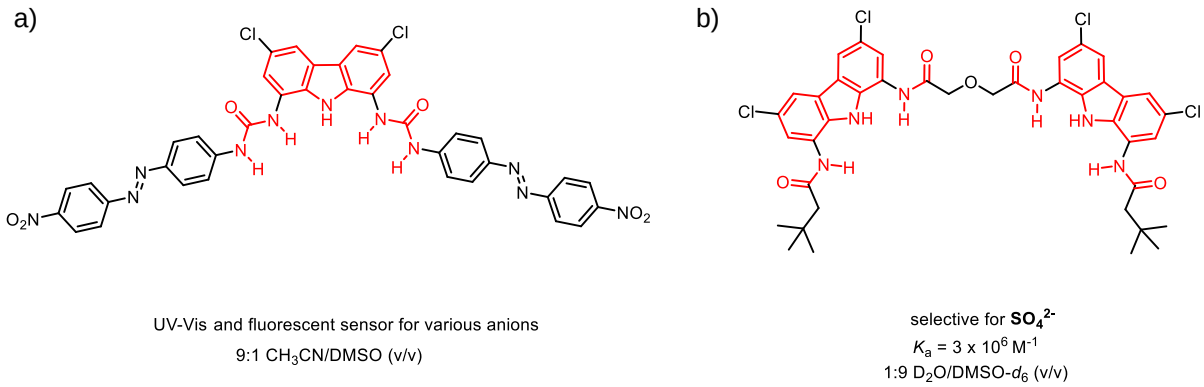



***Figure 4.2.*** *Structures of two carbazole-based anion receptors: a) Kim's carbazole-bisurea host exhibiting dual fluorescent and UV-Vis sensing; b) Chmielewski's carbazole-bisamide host which chelates sulfate.*

### 4.1.1. The carbazole-triazole motif in anion binding

Receptor structures incorporating 1,2,3-triazole motifs directly conjugated to a carbazole framework have been reported in the literature, however, they are typically employed for the chelation of metal cations such as $Co^{3+}$, $Pt^{2+}$, $Ru^{2+}$ or $Au^{+}$. [6–9] Interestingly, one such example (**Figure 4.3**) was shown to be capable of detecting $CN^-$ at sub-micromolar concentrations through displacement of a $ClO_4^-$ ligand and subsequent demetallation. [10]

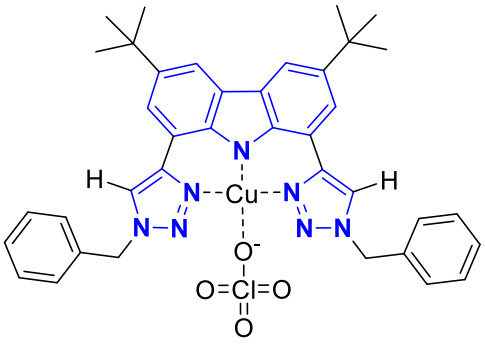



***Figure 4.3.*** *A fluorescent sensor for cyanide based on a carbazole-bistriazole motif.*

Examples incorporating halogen bond donors are even less common (**Figure 4.4**). Schubert and co-workers recently appended iodotriazoles onto a carbazole scaffold to achieve $Cl^-$ selectivity in THF, [11] whereas Beer and co-workers synthesised a [2]rotaxane incorporating a carbazole-bisiodotriazolium unit which proved capable of strong and selective sensing of $Br^-$ over $Cl^-$ and $I^-$ in the competitive 45:45:10 $CDCl_3$:$CD_3OD$:$D_2O$ solvent mixture. [12]

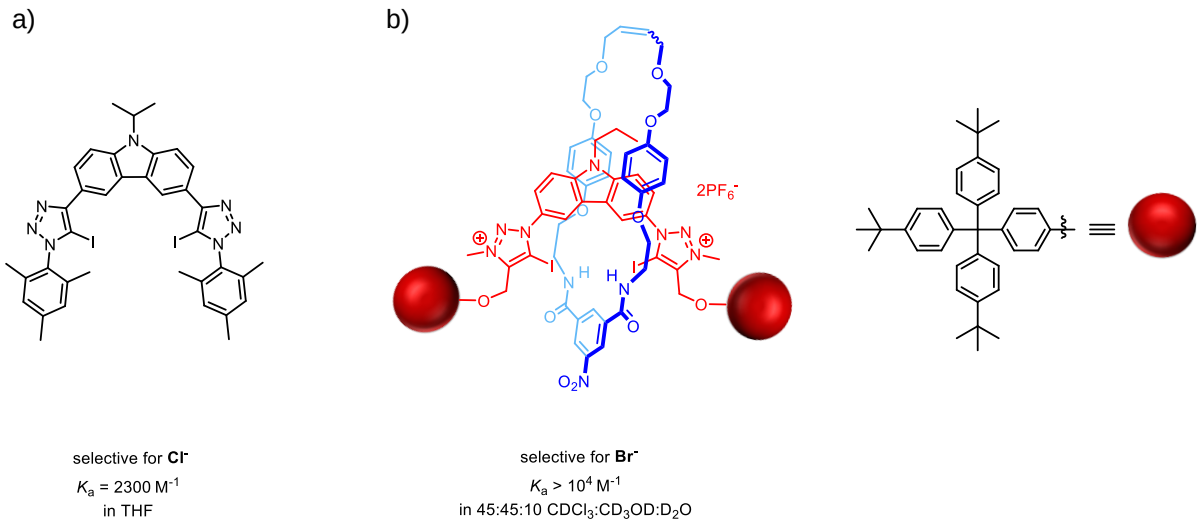



***Figure 4.4.*** *Structures of carbazole-based anion receptors incorporating XB donors: a) Schubert's carbazole-iodotriazole chloride-selective host; b) Beer's carbazole-iodotriazolium [2]rotaxane.*

## 4.2. Chapter Aims

This chapter describes the development of neutral HB/XB carbazole-triazole structures for anion recognition and sensing in organic media. More specifically, a family of acyclic 1,8-carbazole-bis(iodo)triazole receptors was synthesised. Extensive $^1$H NMR, UV-Vis and fluorescence experiments determined the effect of replacing octyl chains with electron-withdrawing perfluoroaryl motifs on the binding properties for a wide range of anions. Moreover, several attempts to incorporate the 1,8-carbazole-bis(iodo)triazole motif into analogous macrocyclic and interlocked structures such as [2]rotaxanes were undertaken through active metal templation.

## 4.3. Acyclic HB/XB carbazole-triazole structures for anion recognition

### 4.3.1. Design of target acyclic hosts

As highlighted in **Section 4.1.1**, there is precedent for carbazole frameworks functionalised at the 3 and 6 positions with triazole motifs being incorporated into anion receptor structures; however, the anion binding properties of 1,8-carbazolebistriazole analogues have not been studied. The latter benefits from the presence of the N – H atom as an additional, highly acidic HB donor which could assist the existing triazole donors in convergently binding an anion.

The strength of anion complexation by a receptor can typically be further enhanced by covalent attachment of an electron withdrawing group. In recent published work, Beer and co-workers described the superior anion binding properties of perfluoroaryl-appended pyridinium-bisiodotriazole acyclic and interlocked receptors over alkyl- and aryl-appended analogues, which was attributed to the highly electron withdrawing nature of the perfluoroaryl analogue, as well as its rigidity and hydrophobicity (**Figure 4.5**). [13] This highlights the suitability of perfluoroaryls as novel synthons for incorporation into architectures for anion recognition.

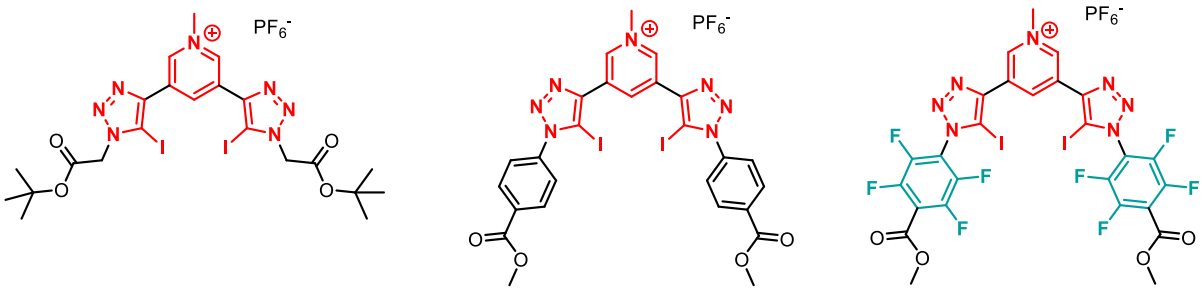
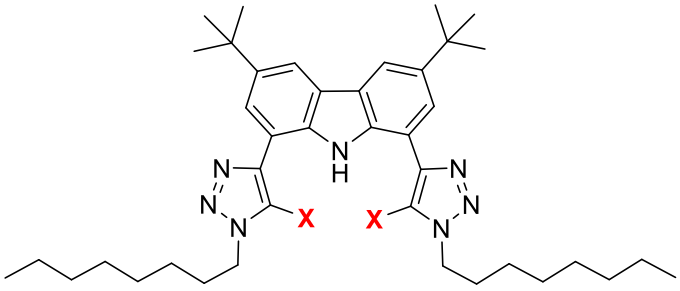
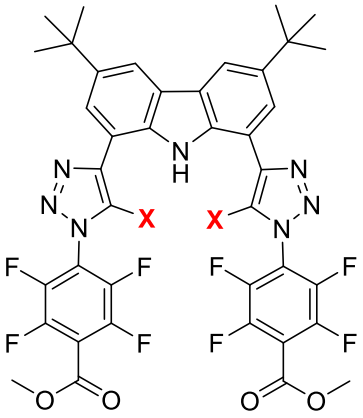



***Figure 4.5.*** *Beer's acyclic pyridinium-bisiodotriazole receptors with different groups attached to the triazole motifs. Association constants were determined in DMSO-$d_6$ at 298 K.*

Building on these results, a series of 1,8-carbazole-bis(iodo)triazole receptors was designed, with either octyl or perfluoroaryl groups attached to the triazole motifs (**Figure 4.6**). Neutral hosts were targeted with the aim of potentially achieving selectivity for softer anions such as $I^-$.



**X** = H **4.1.HB**
**X** = I **4.1.XB**



**X** = H **4.2.HB**
**X** = I **4.2.XB**

***Figure 4.6.*** *Structures of the target acyclic carbazole-triazole receptors with either octyl or perfluoroaryl pendant groups.*

### 4.3.2. Carbazole-triazole receptors with octyl chains

#### 4.3.2.1. Synthesis of HB/XB carbazole-triazole receptors with octyl chains

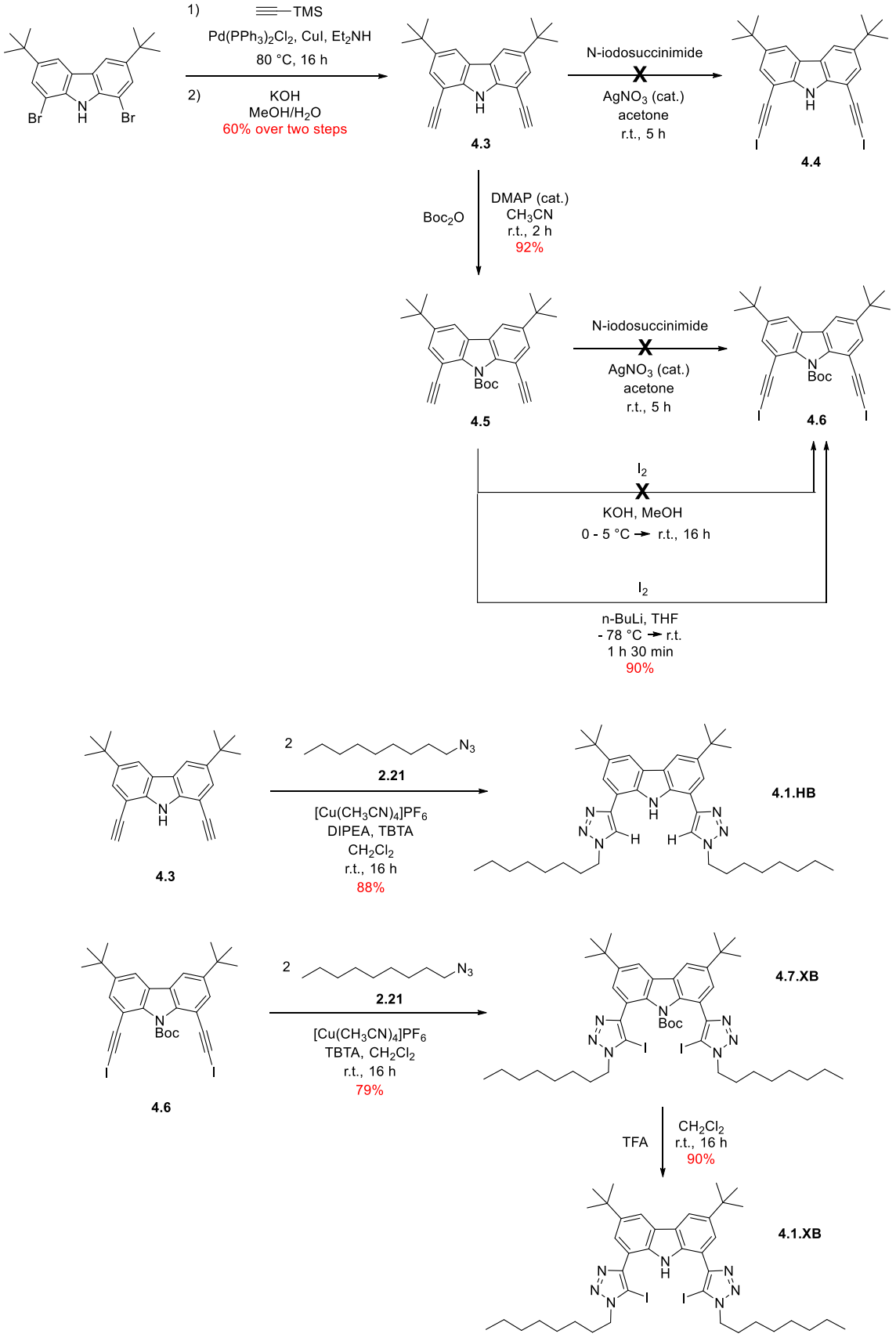
The synthetic approach towards octyl-appended carbazole receptors is outlined in **Scheme 4.1.**

Firstly, 1,8-dibromo-3,6-di(tert-butyl)-carbazole (prepared according to a literature procedure [14] and kindly donated by Dr. Ben Mullaney) was converted to the trimethylsilyl (TMS)-protected bis-alkyne via a Sonogashira reaction and subsequently deprotected under basic conditions in MeOH to give carbazole bis-alkyne **4.3** in an overall 60% yield. [6]

The synthesis of the bis-iodoalkyne analogue **4.4** proved significantly more challenging. Direct iodination with *N*-iodosuccinimide led to substantial decomposition of the starting material; hence, **4.3** was first *N*-Boc-protected in $CH_3CN$ to afford intermediate **4.5** in a near-quantitative yield. [15] Iodination of **4.5** with either *N*-iodosuccinimide or $I_2$ / KOH failed to give the desired product, however, deprotonation of **4.5** with n-BuLi in THF at – 78 °C followed by addition of molecular $I_2$ cleanly afforded *N*-Boc-protected bis-iodoalkyne **4.6** in a 90% yield.

Each of the alkyne synthons **4.3** and **4.6** was reacted separately with two equivalents of octyl azide **2.21** under CuAAC conditions to afford carbazole-bistriazole receptor **4.1.HB**

and *N*-Boc-protected carbazole-bisiodotriazole receptor **4.7.XB**, respectively. **4.7.XB** was finally deprotected with TFA in $CH_2Cl_2$ to give target carbazole-bistriazole receptor **4.1.XB** in a 90% yield.




***Scheme 4.1.*** *Synthesis of acyclic HB/XB carbazole-triazole receptors with octyl pendant groups.*

### 4.3.2.2. Preliminary anion binding studies

$^1$H NMR titration experiments in acetone-$d_6$ were undertaken to probe the affinities of octyl carbazole-bistriazole receptors **4.1.HB** and **4.1.XB** towards a wide range of anions. Surprisingly, in the case of **4.1.HB**, the anion-induced shifts after the addition of 10 equivalents of anion were very small (<0.02 ppm for the triazole proton and <0.01 ppm for both carbazole protons), the notable exception being benzoate (0.05 ppm for the triazole proton), implying that the anion complexation is negligible. For its halogen bonding analogue **4.1.XB**, the overall perturbations were only marginally larger (0.05 – 0.07 ppm with $Cl^-$ and 0.03 – 0.05 ppm with $Br^-$, <0.01 ppm for other anions tested) (**Figure 4.7**). The N – H proton could not be consistently monitored, as it broadened or faded into the baseline during several of the titration experiments. Only in the case of $Cl^-$ and **4.1.XB** was a stoichiometric 1:1 host-guest association constant of 124 $M^{-1}$ determined through BindFit [16,17] analysis .

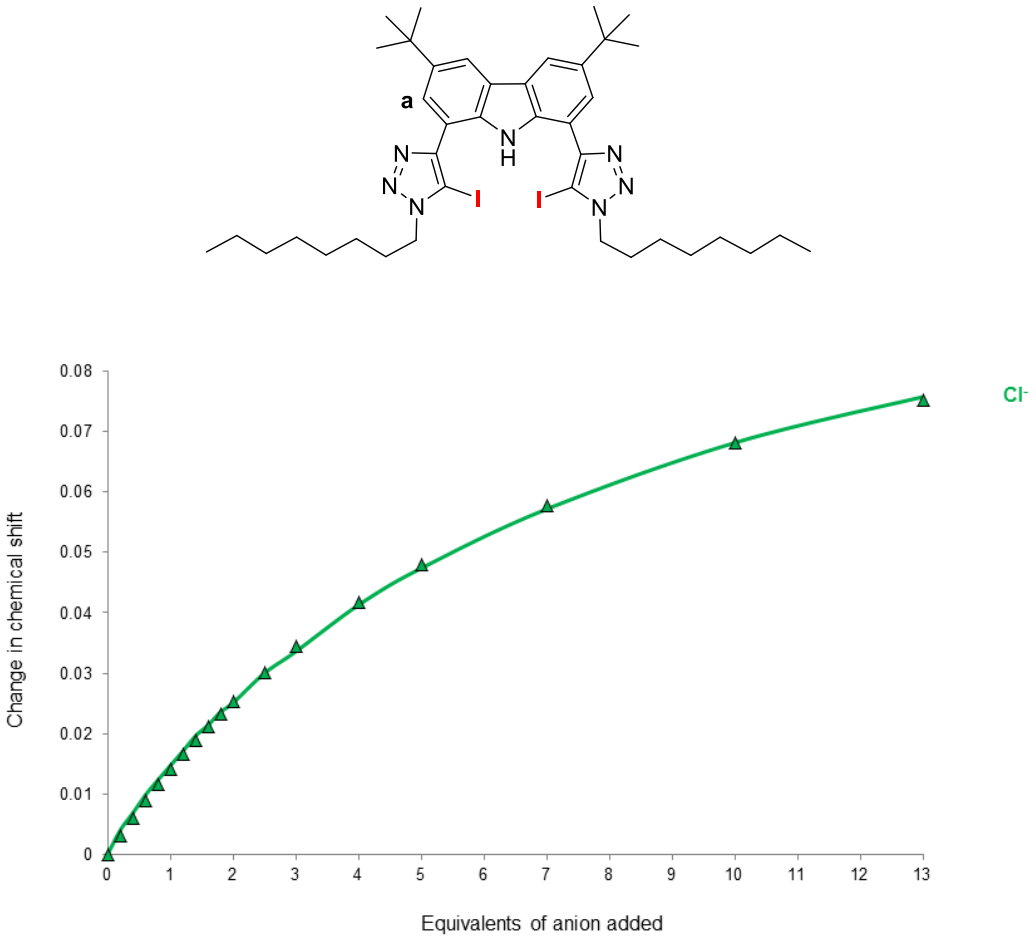



***Figure 4.7.*** *Comparative plots of the change in chemical shift of the proton* ***a*** *(ppm) against equivalents of* $Cl^-$ *added for the acyclic carbazole-bistriazole receptor* ***4.1.XB*** (*acetone-*$d_6$*, 298 K*).

In the case of **4.1.HB**, the addition of $CN^-$ led to an immediate change in the colour of the solution from colourless to yellow, which was correlated in the $^1H$ NMR spectrum with a disappearance of the carbazole N – H signal and significant broadening of the remaining aromatic signals. Presumably, the highly basic cyanide anion is capable of deprotonating the acidic carbazole N – H, which leads to decomposition of the receptor. Given that **4.1.HB** does not interact significantly with any of the other anions tested, it could serve as an selective optical chemodosimeter for cyanide. Disappointingly, **4.1.XB** displayed similarly limited anion binding capabilities, with the sole exception of the $Cl^-$ which bound with a moderate $K_a$ of 124 $M^{-1}$.

The limited anion binding capabilities of these receptors could be tentatively explained through inspection of crystal structure data previously obtained in the Beer group (**Figure 4.8**). [32] In the solid state, the N – H ⋯ N distance was shown to be less than the sum of the van der Waals radii, suggesting the existence of intramolecular HB interactions between the pyrrolic N – H proton and the electron-rich N atoms on the triazole motifs. Additionally, this interaction forces the triazole C – H protons to point in opposite directions and away from the binding cavity.

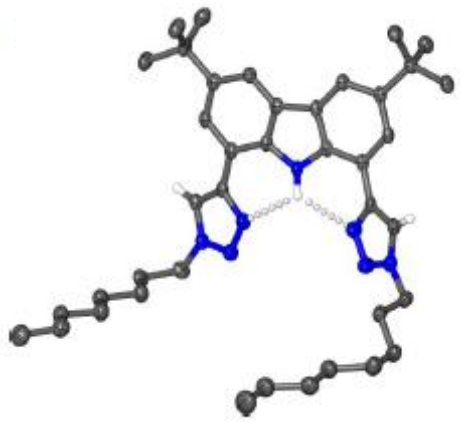


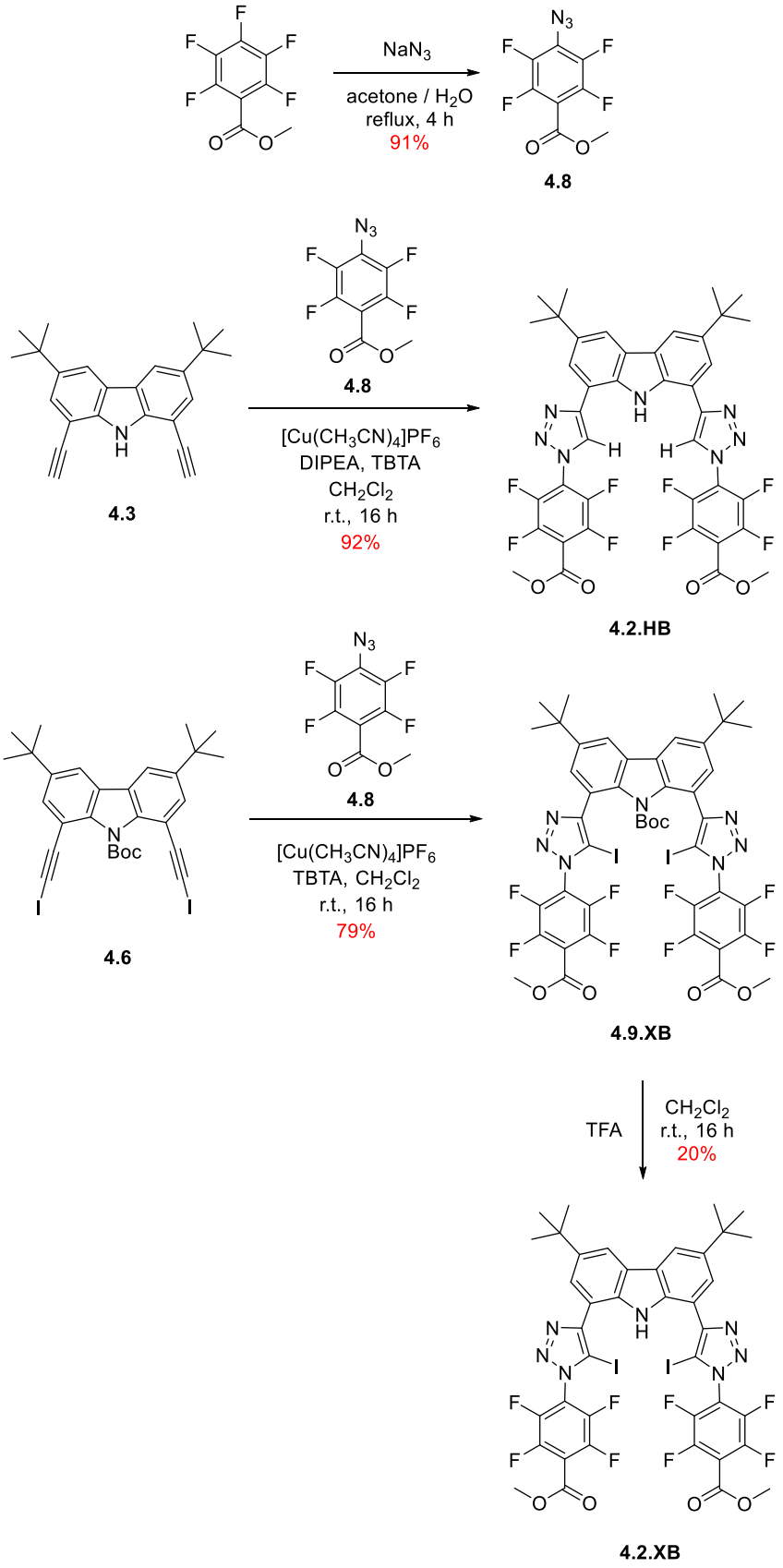
***Figure 4.8.*** *The solid state structure of* ***4.1.HB****, as determined through single crystal X-ray diffraction. Non-acidic protons were omitted for clarity.*

### 4.3.3. Carbazole-triazole receptors with perfluorobenzene motifs

#### 4.3.3.1. Synthesis of HB/XB carbazole-triazole receptors with perfluorobenzene motifs

In order to study the effect of the perfluoroaryl motif on anion binding properties, the analogous perfluoroaryl-based carbazole-triazole hosts were subsequently targeted (**Scheme 4.2**).

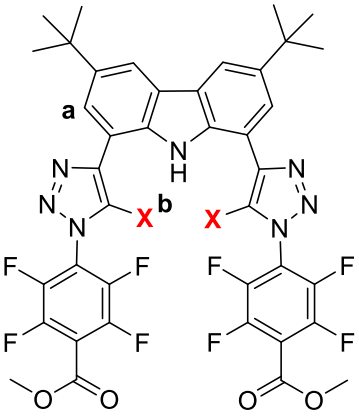
Commercially available methyl perfluorobenzoate was converted to the versatile perfluoro-azide synthon **4.8** through an $S_NAr$ reaction with $NaN_3$ in refluxing aqueous acetone. [18] This was reacted with either protoalkyne **4.3** or *N*-Boc-protected iodoalkyne **4.6** under CuAAC conditions in $CH_2Cl_2$ to give receptor **4.2.HB** in a 92% yield and *N*-Boc-protected receptor **4.9.XB** in a 79% yield, respectively. The target host **4.2.XB** was obtained via deprotection of **4.9** under acidic conditions in a 20% yield after iterative preparative thin layer chromatography.




***Scheme 4.2.*** *Synthesis of the acyclic HB/XB carbazole-triazole receptors with perfluoroaryl pendant groups.*

### 4.3.3.2. Preliminary anion binding studies

Having investigated the binding behaviour of the octyl-based hosts, the anion binding properties of the analogous perfluoroaryl-based hosts were similarly assessed via $^1$H NMR titration experiments in acetone-$d_6$ (**Figure 4.9**, **Table 4.1**).




**X** = H **4.2.HB**
**X** = I **4.2.XB**

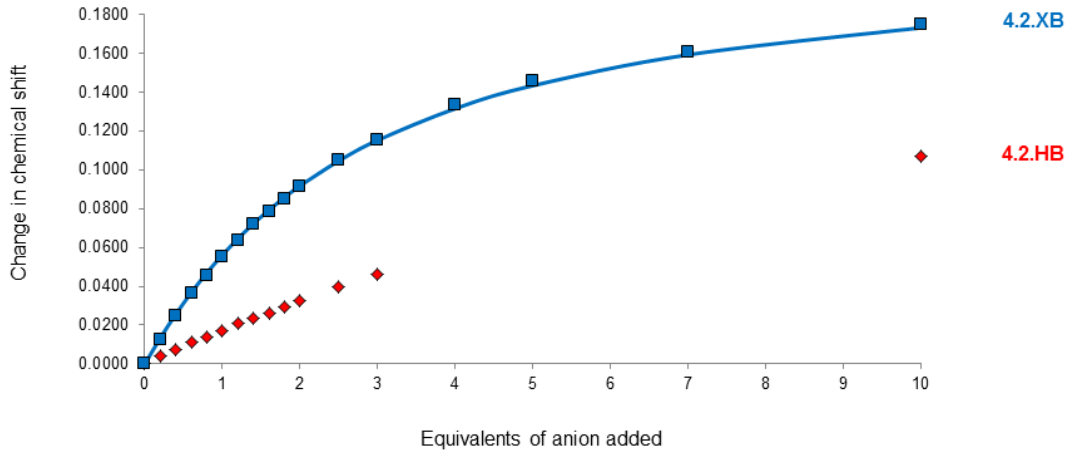



***Figure 4.9.*** *Comparative plots of the change in chemical shift of the proton* ***a*** *(ppm) against equivalents of chloride added for the acyclic carbazole-bistriazole receptors* ***4.2.HB*** *and* ***4.2.XB*** *(acetone-$d_6$, 298 K). Inset: Structure of receptors* ***4.2.HB*** *and* ***4.2.XB****.*

***Table 4.1.*** *Anion association constants ($K_a$/ $M^{-1}$) for carbazole-bistriazole receptors bearing perfluoroaryl groups in acetone-$d_6$ at 298 K.*

| Anion[a] | Association constants ($K_a$/ $M^{-1}$) [b] | |
|---|---|---|
| | **4.2.HB** | **4.2.XB** |
| $Cl^-$ | NB [c] | 445 |
| $Br^-$ | NB [c] | 214 |
| $I^-$ | NB [c] | 79 |
| $NO_2^-$ | NB [c] | 76 |
| $NO_3^-$ | NB [c] | NB [c] |
| $ClO_4^-$ | NB [c] | NB [c] |
| $AcO^-$ | — [d] | — [d] |
| $H_2PO_4^-$ | NB [c] | — [d] |
| $N_3^-$ | — [d] | — [d] |
| $CN^-$ | — [d] | — [d] |
| $SCN^-$ | NB [c] | NB [c] |
| $SO_4^{2-}$ | — [d] | — [d] |
| $PhCOO^-$ | 214 | — [d] |

*[a] Anions were added as their tetrabutylammonium (TBA) salts. [b] Calculated using BindFit [16,17] by monitoring the change in the chemical shift of the triazole proton (labelled **b** in **Figure 4.9**) for **4.2.HB** or the carbazole C - H proton proximal to the triazole (labelled **a** in **Figure 4.9**) for **4.2.XB**. Errors < 5%. [c] NB = no binding. In all cases, the perturbations of the chemical shift were very small (Δδ ≤ 0.05 ppm), which indicates that the receptor does not interact significantly with the guest anion. [d] Decomposition was observed upon anion addition.*

In the case of **4.2.HB**, the N – H and carbazole protons exhibited a negligible change in chemical shift upon addition of anion (< 0.02 ppm), whilst the shift of the triazole proton was significant (0.11 ppm). Contrastingly, the addition of benzoate imparted significantly larger downfield shifts throughout the receptor (0.22 ppm for the N – H, 0.59 ppm for the triazole, 0.04 – 0.12 ppm for the carbazole protons). This was also the sole anion for which the binding process could be quantified (214 $M^{-1}$), which is notable given that **4.2.HB** does not appreciably bind smaller anions of similar basicity such as $NO_2^-$ and $SCN^-$. The stark contrast between the binding behaviours of **4.2.HB** and **4.1.HB** towards benzoate may indicate that aromatic donor-acceptor interactions between the two electron-poor perfluoroaryl rings and the electron-rich benzoate are a major contributor for the enhanced affinity of the former towards benzoate (**Figure 4.10**).

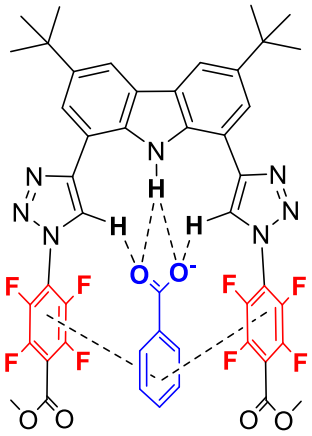


***Figure 4.10.*** *Suggested interaction mode between* ***4.2.HB*** *and a benzoate anion.*

For the halogen bonding analogue **4.2.XB**, the anion-induced shifts were pronounced only for the halides and $NO_2^-$ (0.06 – 0.17 ppm for the carbazole N – H proton and 0.05 – 0.19 ppm for the carbazole C – H protons), with very small shifts (<0.01 ppm) in the case of $NO_3^-$, $ClO_4^-$, and $SCN^-$ and substantial decomposition upon addition of other basic anions. While **4.2.XB** is arguably the most potent halide receptor among the four carbazole hosts studied so far, it is also the most susceptible to decomposition either through abstraction of the N – H proton or via an $S_NAr$ attack by nucleophilic species.

### 4.3.4. Optical properties

Following the quantitative anion binding studies, a series of qualitative UV-Vis and fluorescence studies were undertaken in order to probe any changes in the carbazole absorption or emission properties upon anion addition. Although the analogous $^1$H NMR binding studies were performed in acetone-$d_6$, optical studies were undertaken in acetonitrile due to its lower UV cutoff (190 nm compared to 330 nm for acetone), similar polar aprotic nature and Gutmann donor-acceptor numbers. However, it should be noted that acetonitrile has both a higher dielectric constant and dipole moment. [19]

#### 4.3.4.1. UV-Vis absorption studies

Preliminary absorbance investigations were undertaken by analysing the spectral features of all four receptors **4.1** – **4.2** along with the parent alkyne precursor **4.3** under similar conditions (**Figure 4.11, Table 4.2**).

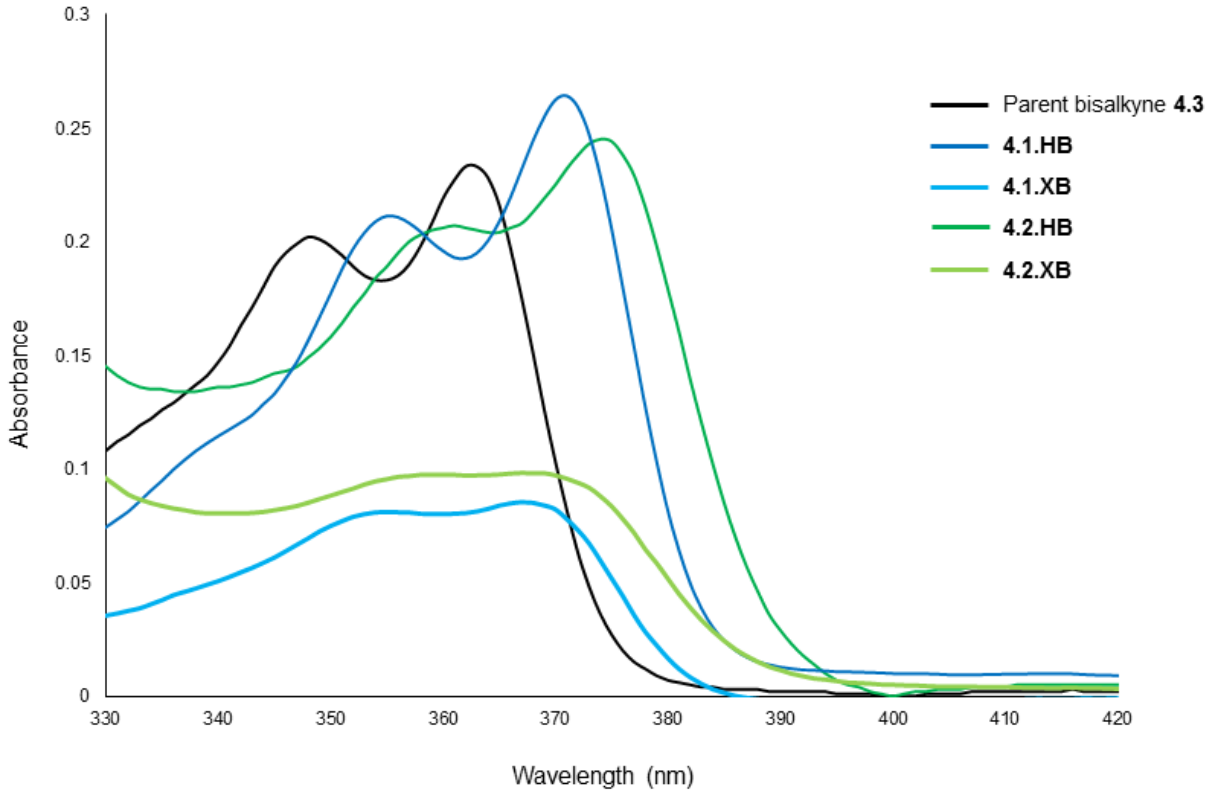



***Figure 4.11.*** *Superimposed truncated UV-Vis spectra for parent bisalkyne* ***4.3*** *and all four receptors* ***4.1*** *–* ***4.2*** *(30 μM, $CH_3CN$, 298 K).*

***Table 4.2.*** *UV-Vis absorption parameters for precursor bis-alkyne* ***4.3*** *and receptors* ***4.1*** *–* ***4.2****, measured for the $S_0 \rightarrow S_1$ band.*

| Property | Precursor | Receptor | | | |
|---|---|---|---|---|---|
| | **4.3** | **4.1.HB** | **4.1.XB** | **4.2.HB** | **4.2.XB** |
| $\lambda_{max}$ (nm) | 363 | 371 | 368 | 374 | 369 |
| $\varepsilon_{max}$ ($M^{-1}$ x $cm^{-1}$) | 7.8 x $10^3$ | 8.8 x $10^3$ | 2.8 x $10^3$ | 8.2 x $10^3$ | 3.2 x $10^3$ |

Compared to the bis-alkyne **4.3**, all receptors display small bathochromic shifts of the main $S_0 \rightarrow S_1$ band (6 – 11 nm), consistent with increasing conjugation. Interestingly, the HB receptors show a slight increase in the absorption coefficient (hyperchromic shift), whereas both XB hosts display significant hypochromic shifts, which may be attributed to a loss of planarity in the latter case due to steric effects. [20]

Qualitative studies were undertaken by adding a large excess of various anions as their TBA salts in their solid form to a solution of each receptor in $CH_3CN$ (**Figures 4.12** – **4.13**).

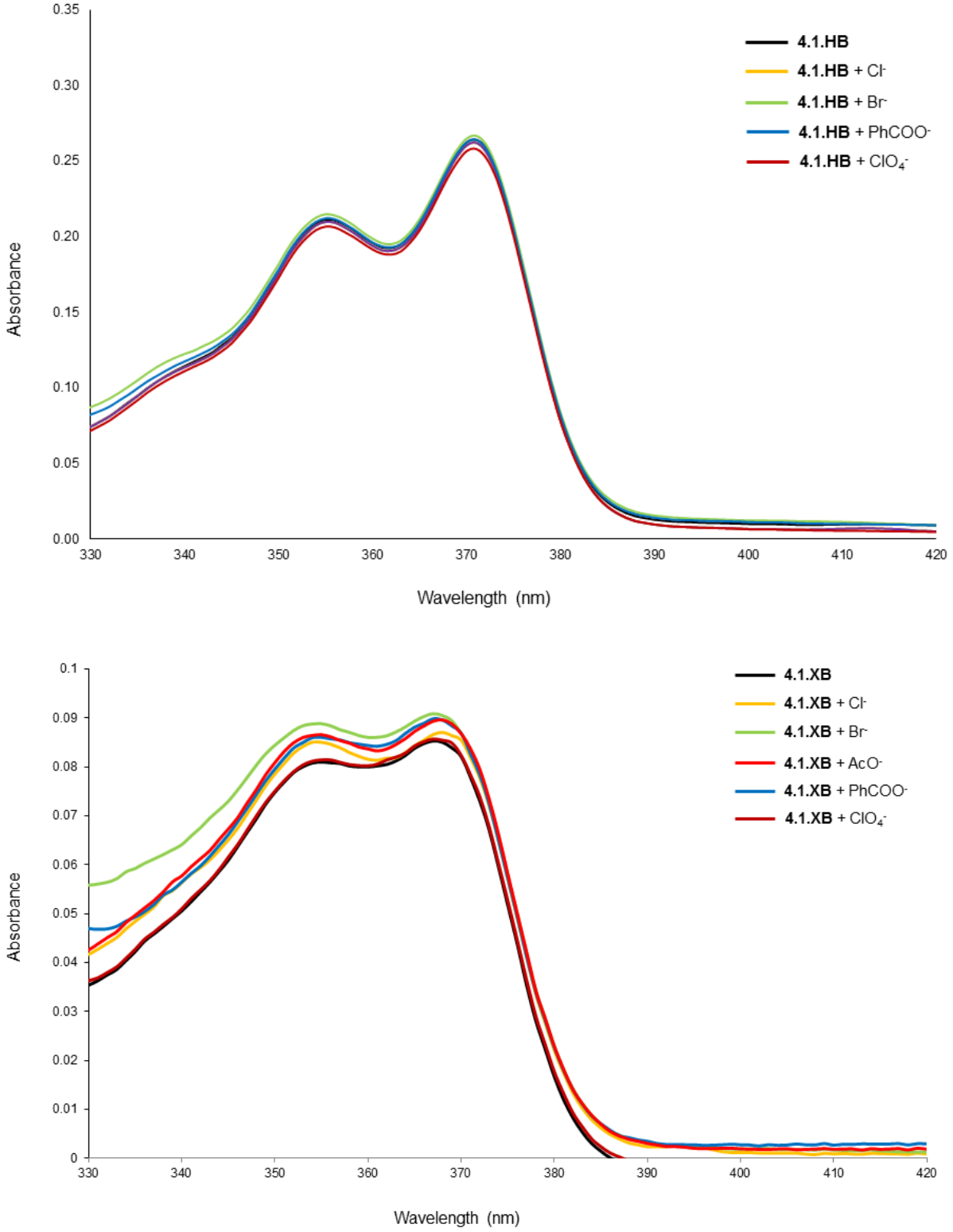



***Figure 4.12.*** *Superimposed truncated UV-Vis spectra obtained before and after addition of a large excess of various anions to 30 μM solutions of octyl-appended receptors* ***4.1.HB*** *(above) or* ***4.1.XB*** *(below) in $CH_3CN$ at 298 K (final anion concentration ~ 50 mM, > 1000 eqs).*

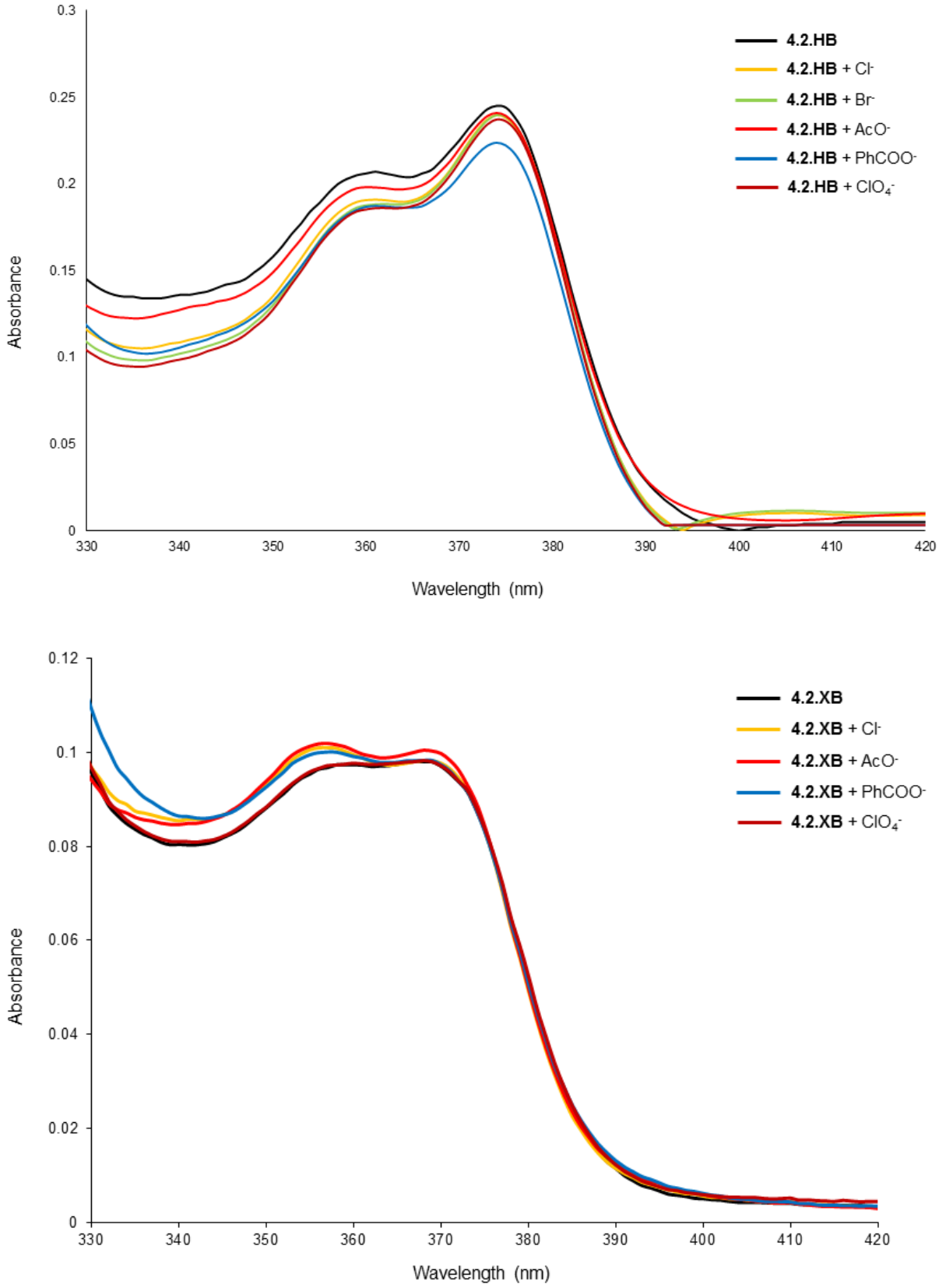



***Figure 4.13.*** *Superimposed truncated UV-Vis spectra obtained before and after addition of a large excess of various anions to 30 μM solutions of perfluoroaryl-appended receptors* ***4.2.HB*** *(above) or* ***4.2.XB*** *(below) in $CH_3CN$ at 298 K (final anion concentration ~ 50 mM, > 1000 eqs).*

In all cases, the addition of a large excess of a range of anions elicited very small changes in the absorption spectrum, which correlates with the negligible binding measured by $^{1}H$ NMR spectroscopy. Even in the case of the most strongly interacting pair (**4.2.XB** and $Cl^-$), addition of more than 1000 equivalents of chloride only induced a 9% decrease in absorbance, which may indicate that the carbazole chromophore is not strongly involved in the anion binding process.

#### 4.3.4.1. Fluorescence emission behaviour

Similarly, qualitative fluorescence studies were undertaken by adding a large excess of various anions as their TBA salts in their solid form to a solution of each receptor in $CH_3CN$, exciting the sample at the maximum absorption wavelength and recording the resulting emission spectra (**Figures 4.14** – **4.15**).

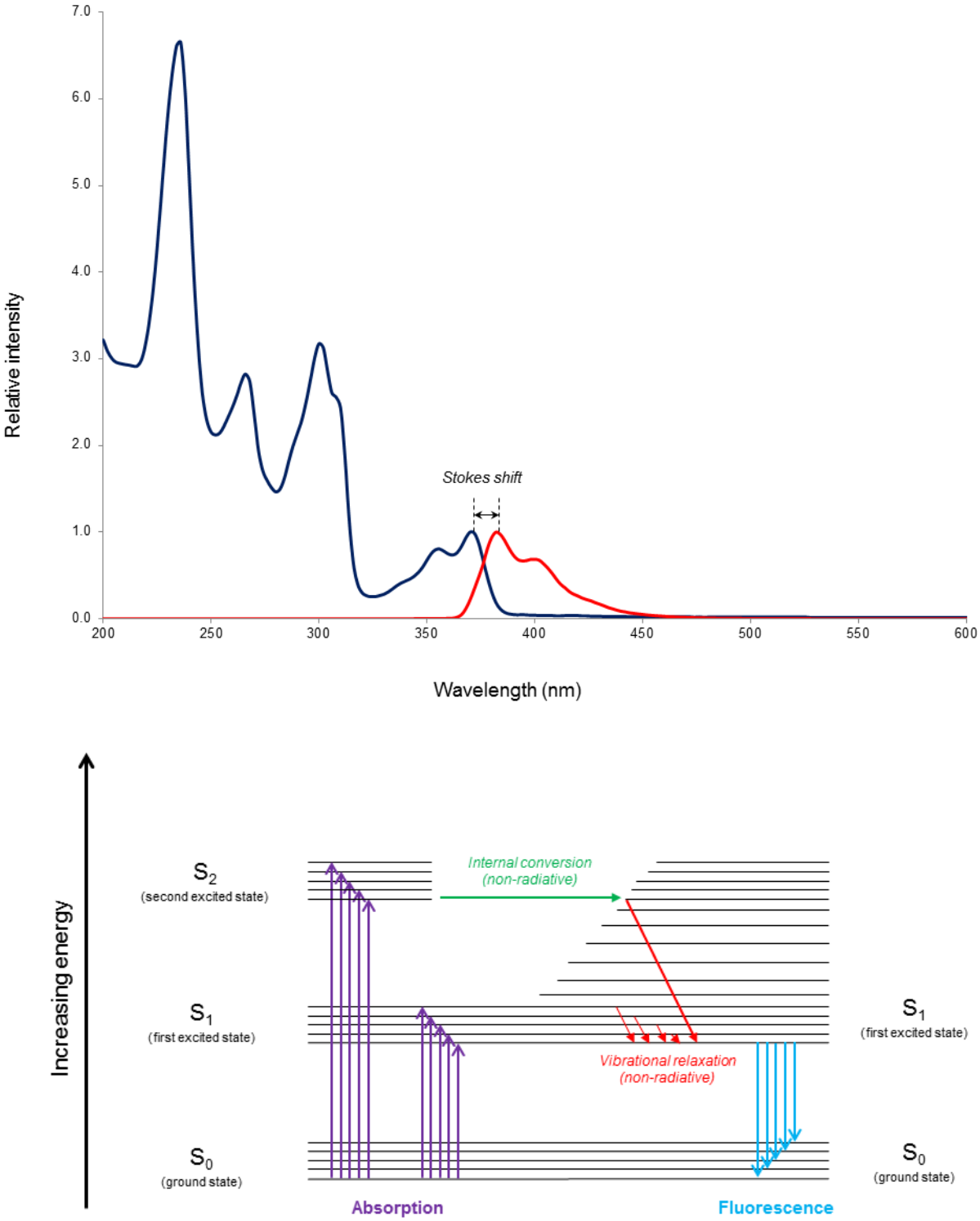



***Figure 4.14.*** *a) Superimposed UV-Vis (dark blue) and fluorescence (red) spectra for* ***4.1.HB*** *in $CH_3CN$ at normalised absorption/emission intensities. UV-Vis:* ***[4.1.HB] =*** *30 μM, fluorescence:* ***[4.1.HB] =*** *2.4 μM, $\lambda_{ex}$ = 371 nm. b) Simplified Jablonski diagram illustrating the main excitation and emission transitions, as well as non-radiative pathways. Carbazole compounds absorb purple light (thus appearing yellow in colour) and emit blue light.*

Direct comparison of the UV-Vis and fluorescence spectra of **4.1.HB** at normalised intensities (**Figure 4.15**) confirmed that the emission spectrum is the mirror image of the $S_0 \rightarrow S_1$ transition in the absorption spectrum, along with the presence of a small Stokes shift of 11 nm.

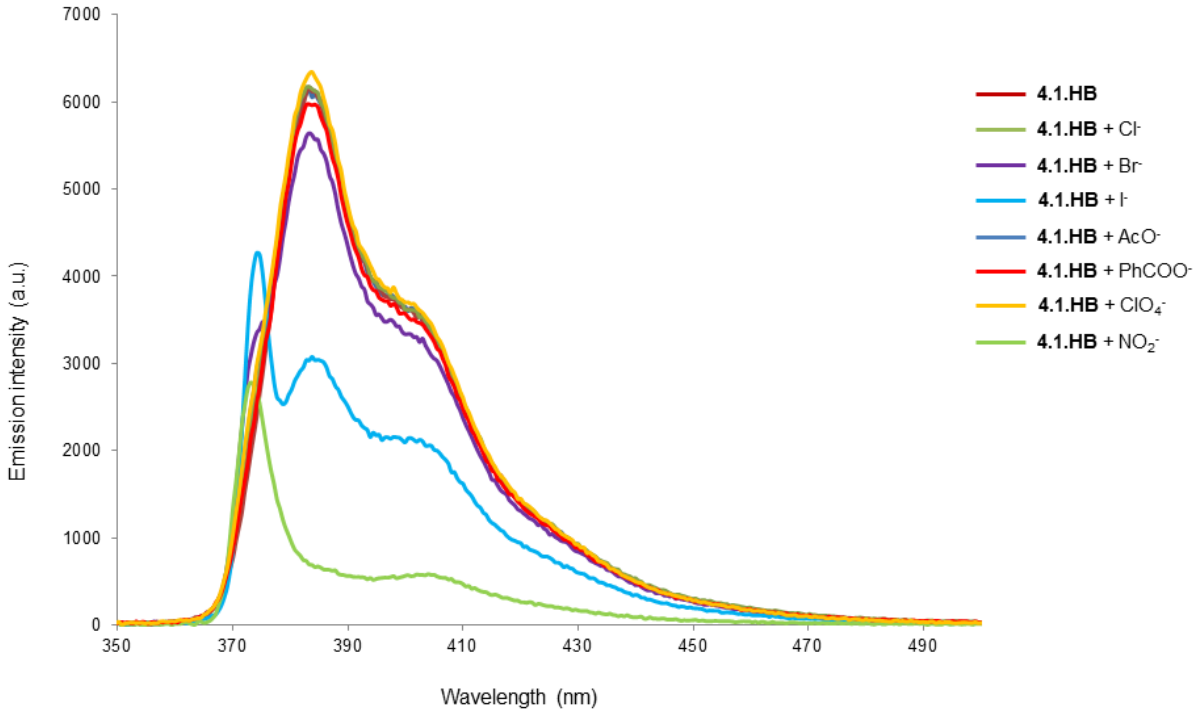



***Figure 4.15.*** *Superimposed truncated fluorescence emission spectra obtained before and after addition of a large excess of various anions to a 2.4 μM solution of octyl-appended receptor* ***4.1.HB*** *in $CH_3CN$ at 298 K ($\lambda_{ex}$ = 371 nm, final anion concentration ~ 50 mM, > 1000 eqs).*

As expected, the emission spectra of **4.1.HB** remained largely unchanged upon addition of several anions, with the notable exceptions of $I^-$ and $NO_2^-$ which induce significant fluorescence quenching, as well as the presence of a new, distinct peak around 373 – 374 nm. This can be attributed to a significant absorption of their TBA salts in the emission region of **4.1.HB**.

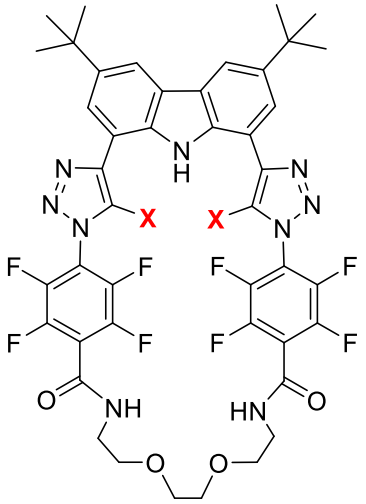
The other receptors **4.1.XB, 4.2.HB** and **4.2.XB** exhibited negligible fluorescence emission in $CH_3CN$, even upon addition of excess anion ($Cl^-$, $Br^-$, $I^-$, $NO_2^-$, $AcO^-$, $PhCOO^-$, or $ClO_4^-$). This can be attributed to the highly electron-withdrawing nature of the perfluoroaryl motifs and the internal heavy atom quenching effect, which favours non-radiative transitions such as intersystem crossing through increased spin-orbit coupling. [21]

## 4.4. Towards macrocyclic HB/XB carbazole-triazole structures

### 4.4.1. Design of initial target macrocyclic hosts

Given that acyclic perfluroaryl host **4.2.XB** showed the most promising anion recognition properties of the four receptors tested, an analogous macrocycle incorporating this motif was designed (**Figure 4.16**). It was envisaged that incorporation into a more preorganised, macrocyclic structure could further augment its anion binding and optical sensing properties, with a view to later constructing three-dimensional rotaxane and catenane binding cavities.

The synthetic attempts towards **4.16.HB** and **4.16.XB** are outlined below.




**X** = H **4.16.HB**
**X** = I **4.16.XB**

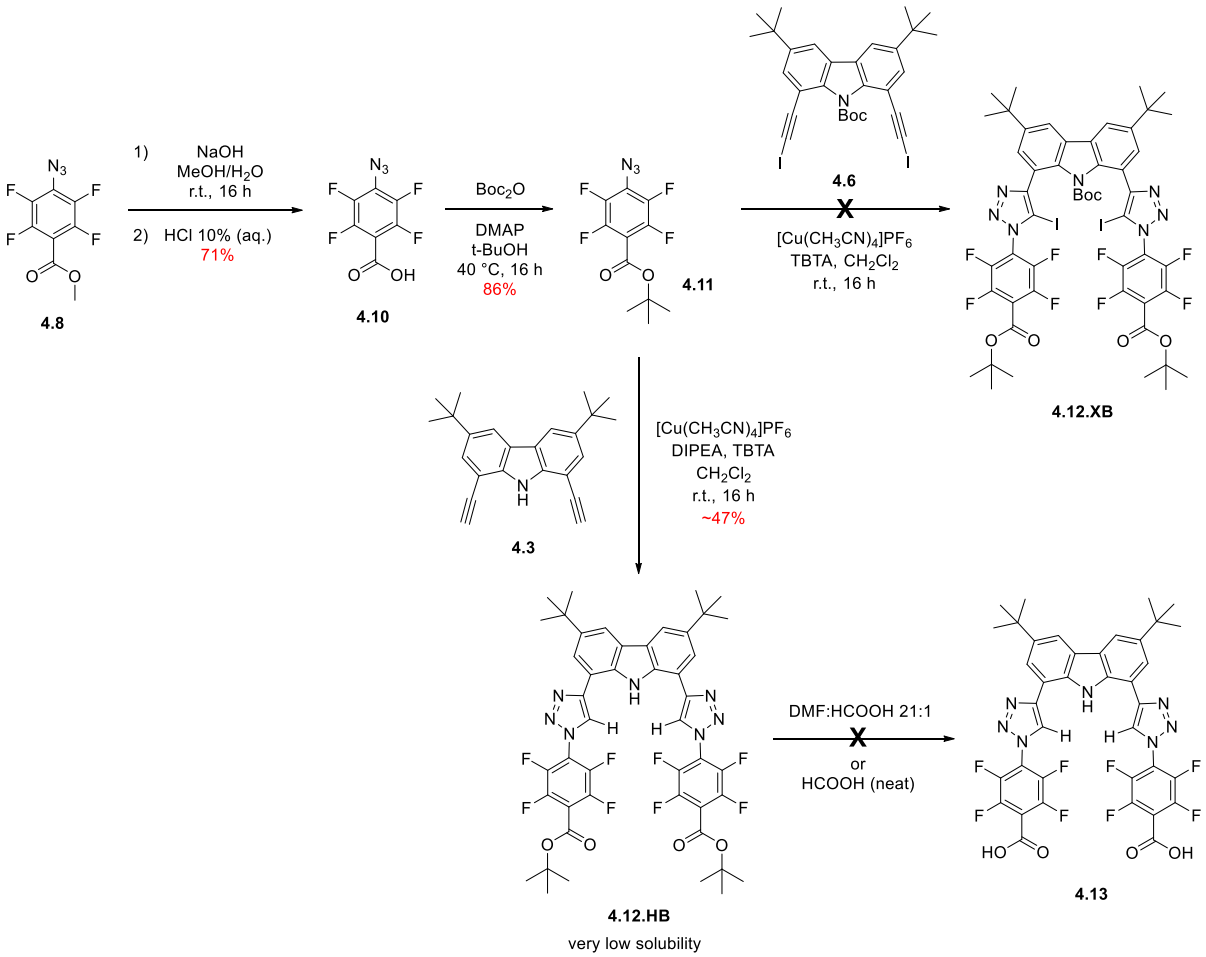
***Figure 4.16.*** *Structures of the target carbazole-triazole macrocyclic structures.*

#### 4.4.1.1. Synthetic attempts towards initial target macrocyclic hosts

It was envisaged that the macrocyclic receptors **4.16.HB** and **4.16.XB** could be synthesised from a condensation between commercially available 2,2′-(ethylenedioxy)bis(ethylamine) and the appropriate bis-acids (**Scheme 4.3**).

For this purpose, perfluoro-azide methyl ester **4.8** was converted to its tert-butyl ester analogue **4.11** through deprotection under basic conditions [22] followed by esterification of the resulting acid **4.10** with $Boc_2O$ in tert-butanol. A CuAAC reaction of **4.11** with the bis-

iodoalkyne **4.6** failed to afford the target **4.12.XB** host, with only the bis(prototriazole) and monoproto-monoiodotriazole derivatives being recovered from the reaction mixture. The analogous reaction of **4.11** with bis-protoalkyne **4.3** gave the desired bis-ester product **4.12.HB**; however, it proved to be surprisingly insoluble in most common organic solvents, to such an extent that $^{1}$H NMR characterisation data could only be obtained in pyridine-$d_5$. Expecting that the bis-acid **4.13** would be sufficiently soluble for further manipulation, several attempts to deprotect the two tert-butyl ester motifs were undertaken. Suspending **4.13** in neat HCOOH failed to afford any product, hence an alternative method was sought wherein **4.12.HB** was first dissolved in a large excess of hot DMF and subsequently formic acid was added. Disappointingly, after a short period of time, the starting material precipitated almost quantitatively from the reaction mixture.

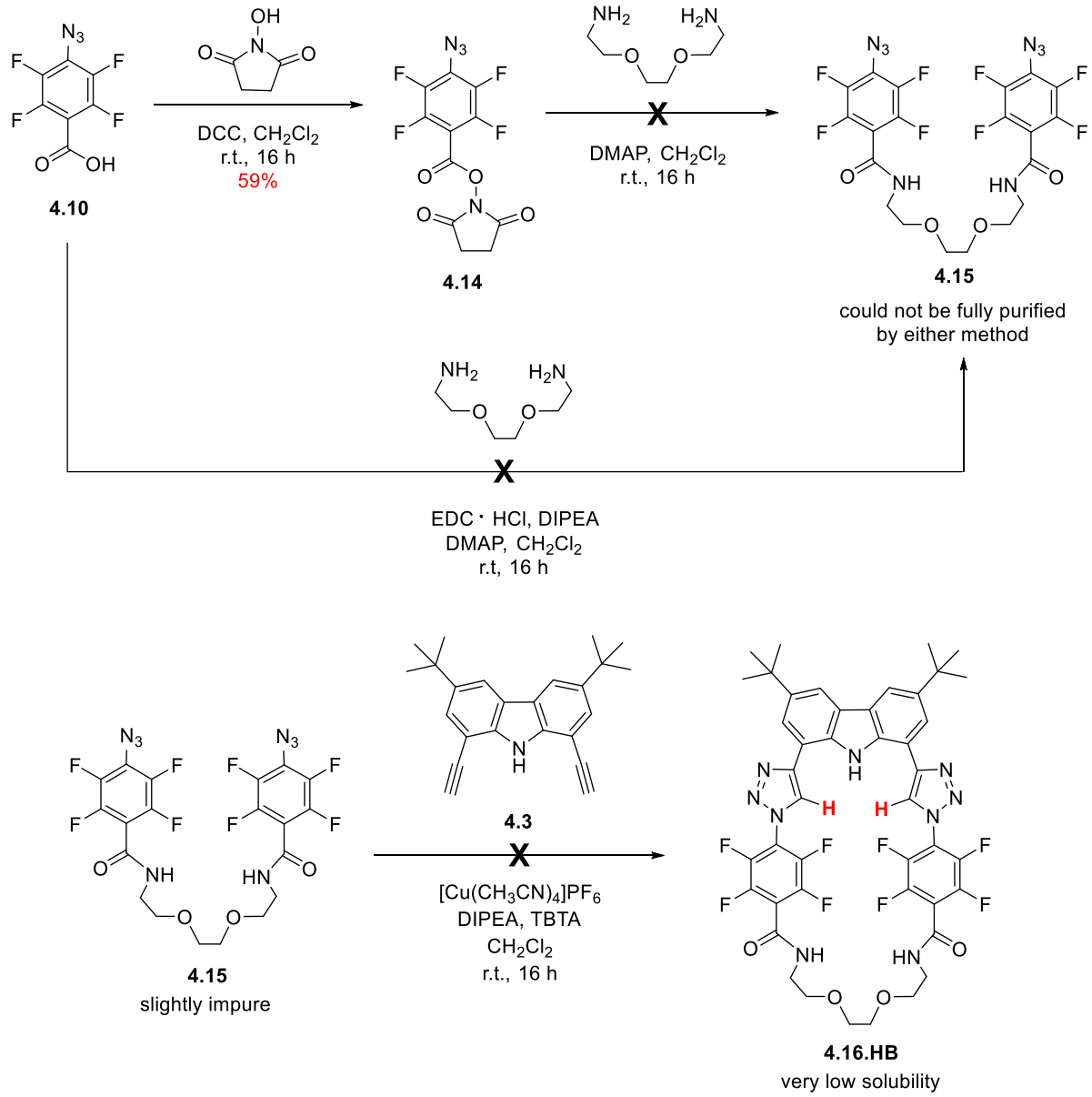



***Scheme 4.3.*** *Synthetic pathways towards target carbazole bis-acid synthons.*

In light of these solubility limitations, a different synthetic approach towards **4.16.HB** and **4.16.XB** had to be designed, which involved a CuAAC reaction between a carbazole bis-alkyne and a suitable bis-azide as the ring-closing step (**Scheme 4.4**).

Previously synthesised acid **4.10** was first converted to the labile ester **4.14** through a DCC-mediated reaction with *N*-hydroxysuccinimide in $CH_2Cl_2$ in a 59% yield. [22] Commercial 2,2′-(ethylenedioxy)bis(ethylamine) was condensed separately with both **4.10** and **4.14**, however, both attempts produced an impure bis-azide **4.15**, which could not be fully purified even by iterative column chromatography. Inspection of the $^{19}F$ spectrum of crude **4.15** revealed the presence of several minor peaks alongside the two expected $^{19}F$ signals for the pure product, which may indicate that the perfluoroaryl motif is susceptible towards nucleophilic attack from the highly reactive DMAP catalyst.

Given that the intermediate **4.15** contained only minor impurities, a test CuAAC reaction with carbazole bis-alkyne **4.3** was undertaken. The macrocycle **4.16.HB** was detected by mass spectrometry and was separated from the reaction mixture by filtration, along with structurally related impurities; unfortunately, the limited solubility of both product and contaminants meant that even after repeated attempts at purification, only trace amounts of **4.16.HB** could be recovered.




***Scheme 4.4.*** *Synthesis of intermediate perfluoroaryl-bisazide* ***4.15*** *and carbazole-bistriazole macrocycle* ***4.16.HB.***

### 4.4.2. Design of modified target macrocyclic hosts

Due to the challenging synthesis of **4.16.HB** and **4.16.XB**, the design of the macrocycle was slightly altered, with an alkene metathesis as the ring-closing step and a variety of functional groups bridging the perfluoroaryl motifs and the polyether bottom part (**Figure 4.17.a**). For each functional group, the corresponding azide-based synthon was identified and targeted (**Figure 4.17.b**).

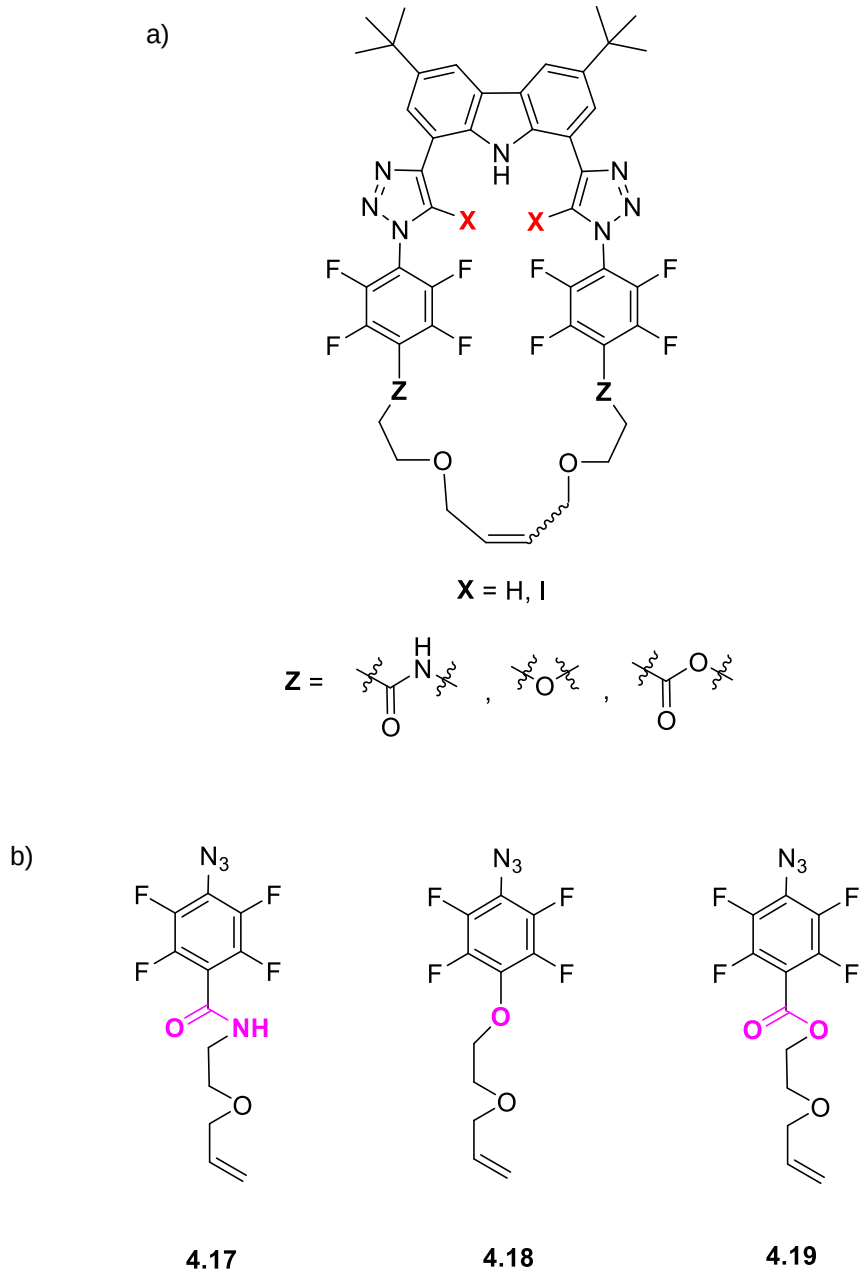


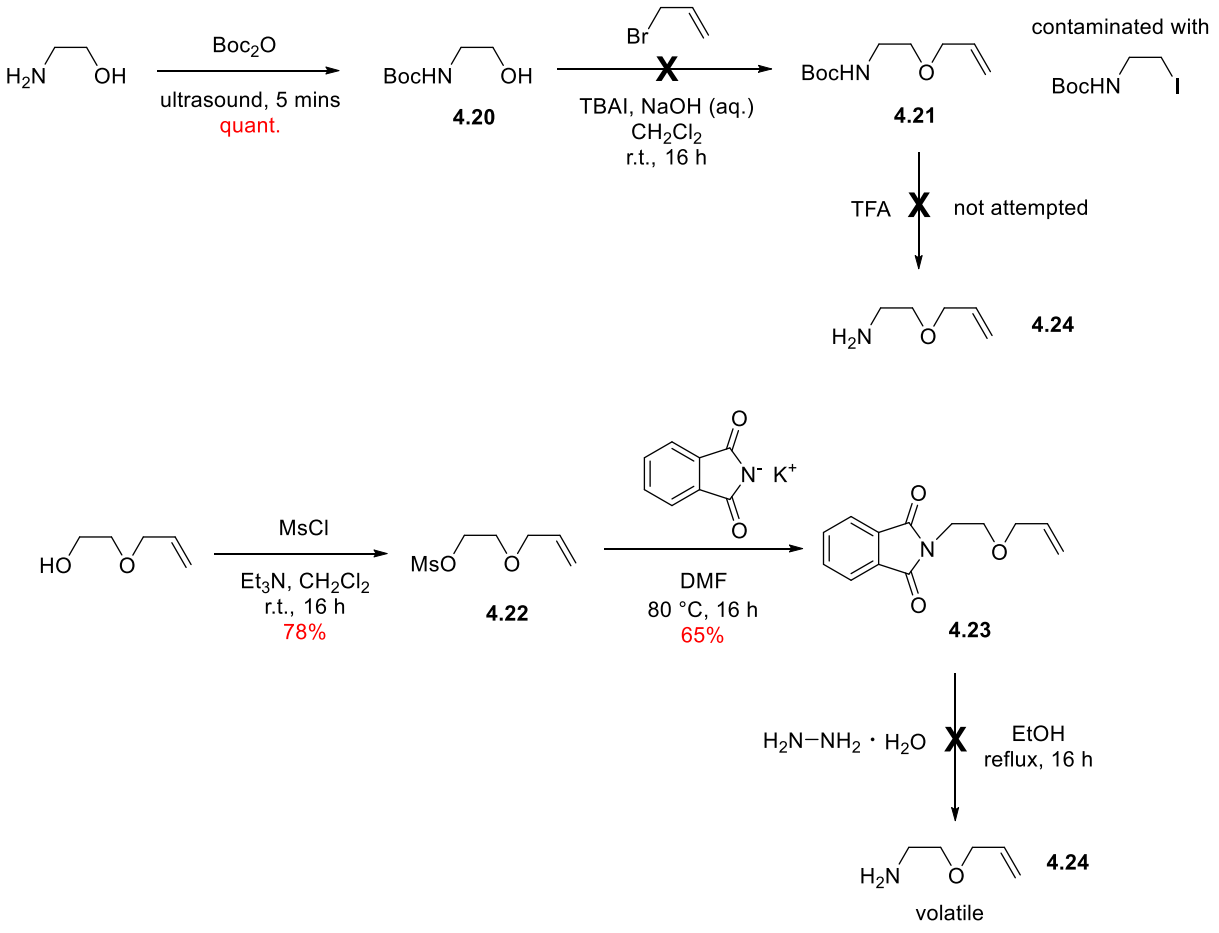

***Figure 4.17.*** *a) General structures of the novel target carbazole-triazole macrocyclic hosts. b) The three identified target azide synthons.*

### 4.4.1.1. Synthetic attempts towards novel target macrocyclic hosts

Initially, the amide-linked azide synthon **4.17** was approached, which first necessitated the synthesis of a suitable amine (**Scheme 4.5**).

2-Aminoethanol was sonicated in the presence of $Boc_2O$ to quantitatively afford the *N*-Boc-protected synthon **4.20**, [23] which was then reacted with allyl bromide in the presence of TBAI and NaOH according to a literature procedure. [24] The desired product **4.21** was found to be contaminated with *N*-Boc-2-iodoethanamine and highly challenging to purify.

It was subsequently envisaged that a Gabriel synthesis might be better suited for the target amine synthon. Firstly, 2-allyloxyethanol was converted to the mesylate **4.22** in a 78% yield through a reaction with methanesulfonyl chloride in $CH_2Cl_2$ [25] and then reacted with potassium phthalimide in DMF at 80 °C to afford alkene-appended product **4.23**. Subsequent cleavage of the phthalimide with hydrazine in refluxing ethanol was successful in affording the desired amine **4.24**; however, this was discovered to be surprisingly volatile and difficult to separate from the high boiling solvent.

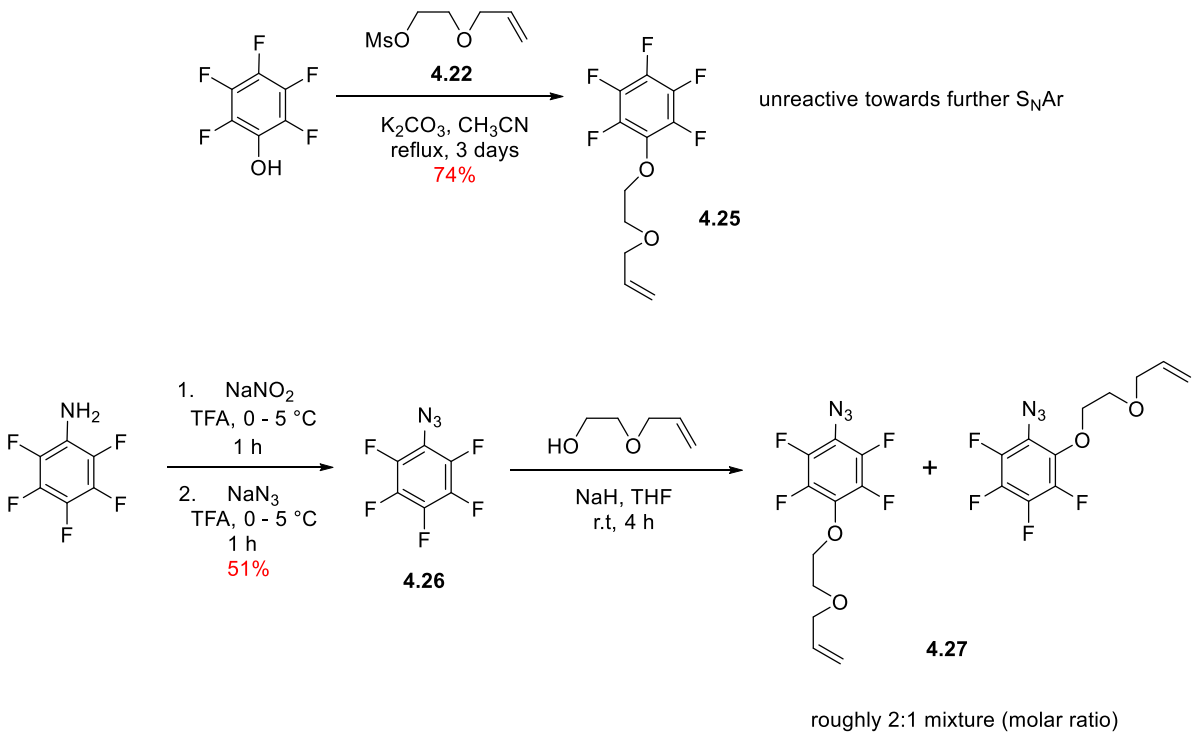



***Scheme 4.5.*** *Synthetic attempts towards an amine-appended alkene.*

Consequently, the synthesis the ether-linked azide synthon **4.18** was targeted (**Scheme 4.6**).

Initially, the allyl-appended ether group was introduced first into the perfluoroaryl ring through a reaction of pentafluorophenol with 2-allyloxyethanol mesylate **4.22** in refluxing $CH_3CN$, which gave the product **4.25** in a 74% yield. Unfortunately, insertion of the electron-donating ether substituent was found to have made the perfluoroaryl ring highly unreactive towards any further $S_NAr$, which implied that the azide group had to be introduced before the ether.

For that purpose, pentafluoroaniline was converted to the analogous perfluoroazide **4.26** in a 51% yield via diazotisation in neat TFA followed by a reaction with $NaN_3$. [26] A reaction of **4.26** with allyloxyethanol in the presence of NaH (adapted from a literature procedure) [27] afforded a mixture of ortho- and para-disubstituted isomers in roughly a 2:1 molar ratio, which could not be further separated.

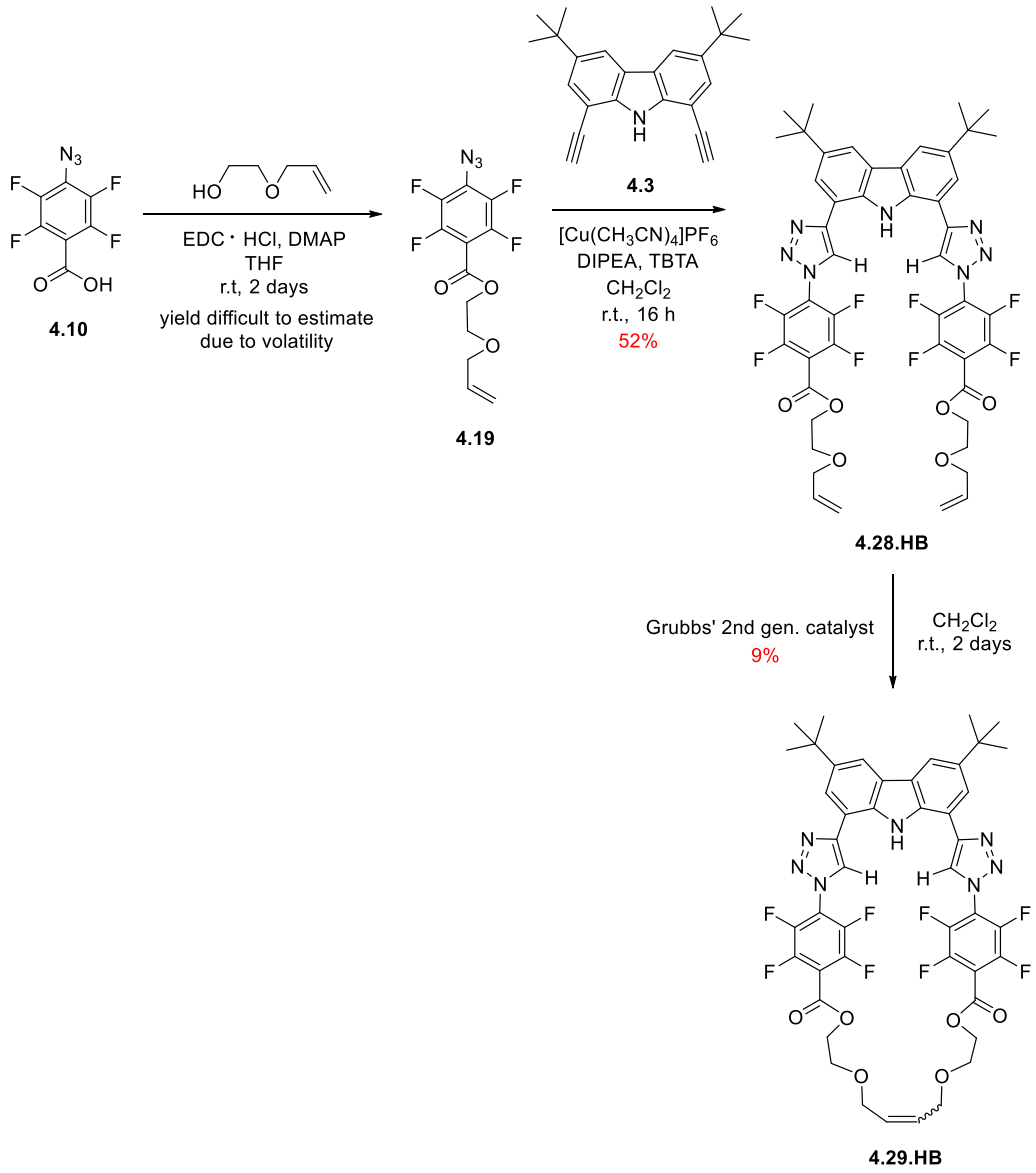



***Scheme 4.6.*** *Synthetic attempts towards a perfluoroaryl azide-appended alkene.*

Given the challenging nature of the syntheses of both amide- and ether-based intermediates **4.17** and **4.18**, a more accessible, ester-linked azide synthon was sought (**Scheme 4.7**).

Perfluoroaryl acid **4.10** was esterified with 2-allyloxyethanol in THF to give alkene-appended azide **4.19,** which was purified by column chromatography without any

previous work-up or removal of solvent due to its high volatility. A subsequent CuAAC reaction with carbazole bis-alkyne **4.3** afforded target bis-alkene **4.28.HB** in a moderate 52% yield, which was finally subjected to a ring-closing metathesis reaction in the presence of Grubbs' 2nd generation catalyst in $CH_2Cl_2$. Iterative preparative thin layer chromatography afforded a very small amount of pure macrocycle **4.29.HB**, which sufficed for characterisation (**Figure 4.18**).




***Scheme 4.7.*** *Synthesis of a perfluoroaryl carbazole-bistriazole bis-alkene and its corresponding macrocycle.*

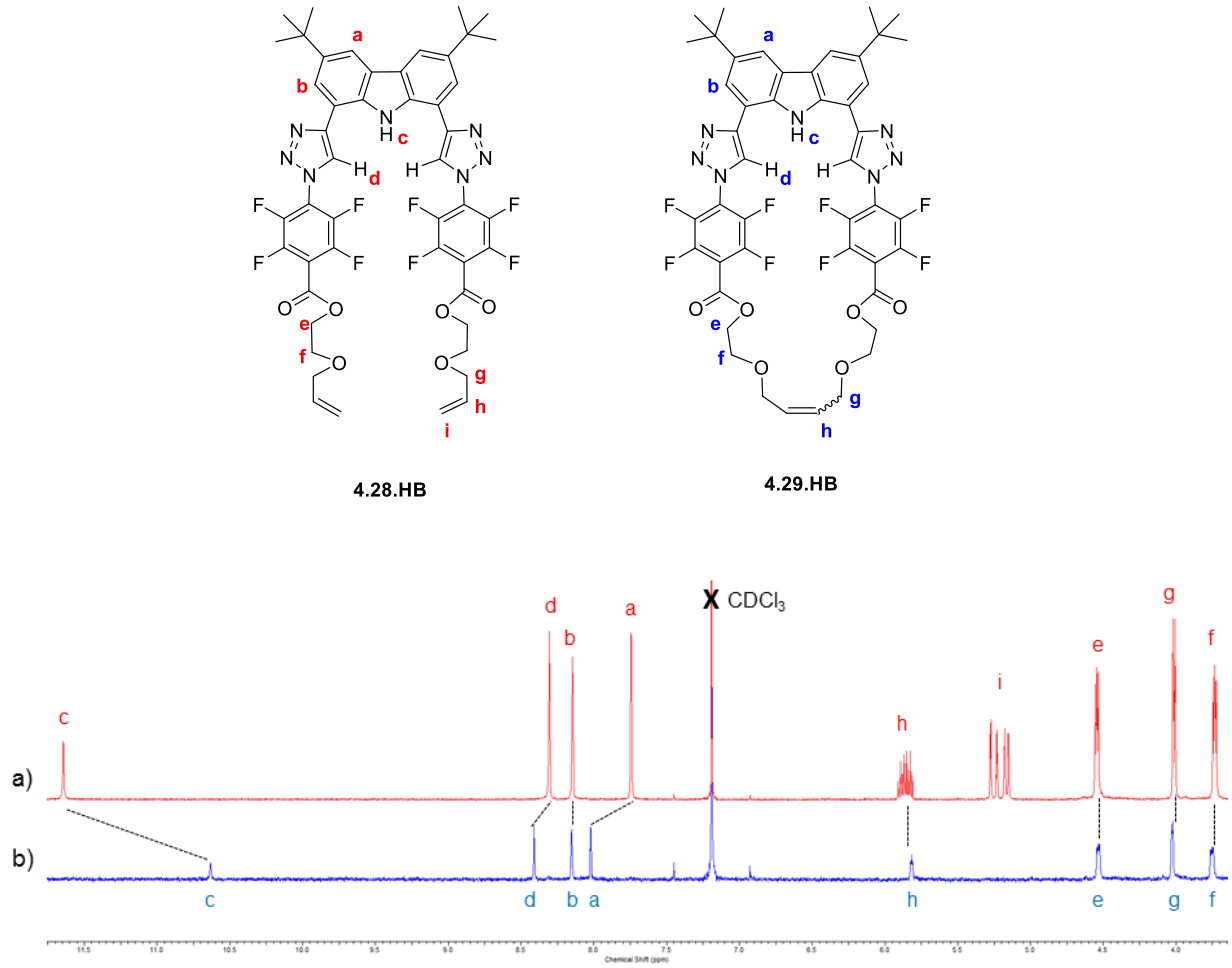



***Figure 4.18.*** *Overlay of truncated $^{1}$H NMR spectra of a) acyclic carbazole bis-alkene* ***4.28.HB*** *and b) carbazole macrocycle* ***4.29.HB*** *($CDCl_3$, 298 K, 500 MHz).*

Upon ring-closing, the carbazole N – H signal shifted significantly upfield, while conversely, the triazole C – H shifted downfield, perhaps due to the disruption of the intramolecular hydrogen bond between these two motifs as a consequence of the increased rigidity of the macrocycle compared to the acyclic bis-alkene. As expected, peaks in the alkyl region exhibited similar chemical shifts, with the notable exceptions of **i** which fully disappears (being eliminated as ethene) and ***h***, which simplified due to the loss of a coupling partner.

### 4.4.3. Attempts to increase the solubility of perfluoroaryl receptors

It was envisaged that the solubility difficulties with the conjugated, rigid perfluoroaryl carbazole-triazole motifs could be circumvented by appending bulky groups in the 3,6 positions of the carbazole ring, which would then reduce the degree of intermolecular self-association (**Figure 4.19**). After careful analysis, suitable candidates for such groups were chosen as trityl and adamantyl.

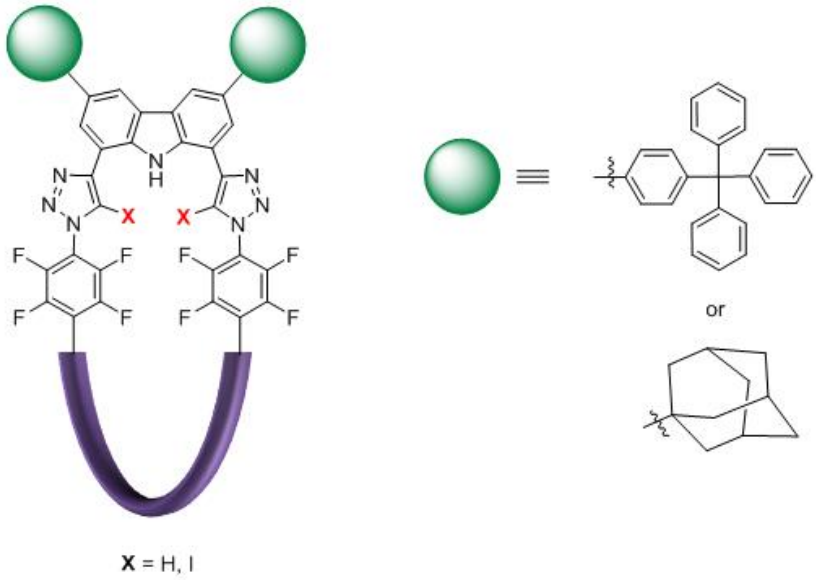



***Figure 4.19.*** *Generic structure of the novel target carbazole-triazole macrocyclic structures with bulky groups appended.*

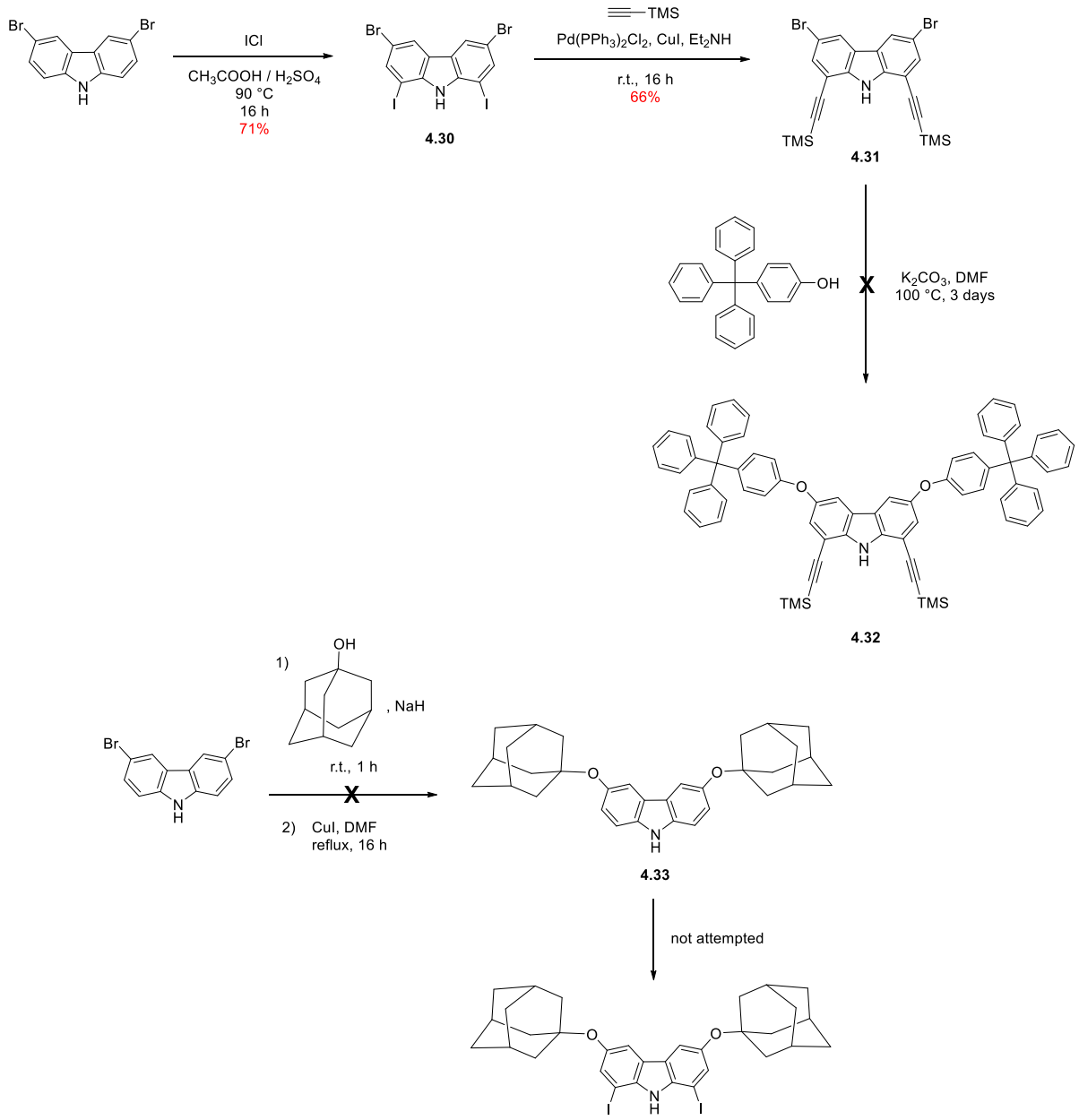
#### 4.4.3.1. Synthetic attempts to introduce bulky groups

Appending the carbazole motif with bulky groups was sought as shown in **Scheme 4.8** below, starting from a carbazole motif already functionalised at the 3 and 6 positions with bromine groups.

For trityl motifs, reaction of this synthon with ICl in an acetic acid / sulfuric acid mixture introduced the more reactive iodine group in the 1 and 8 positions on the carbazole scaffold to give halogenated intermediate **4.30**. [28] This was cleanly converted to the TMS-protected bis-alkyne **4.31** through a Sonogashira reaction with TMS acetylene. A catalyst-free Ullmann coupling [29] of **4.31** with 4-tritylphenol was subsequently attempted because of possible interaction of the Cu catalyst with the alkyne groups. Unfortunately, the

reaction mixture proved sufficiently basic to cleave the TMS groups, which ultimately led to significant decomposition of the substrate.

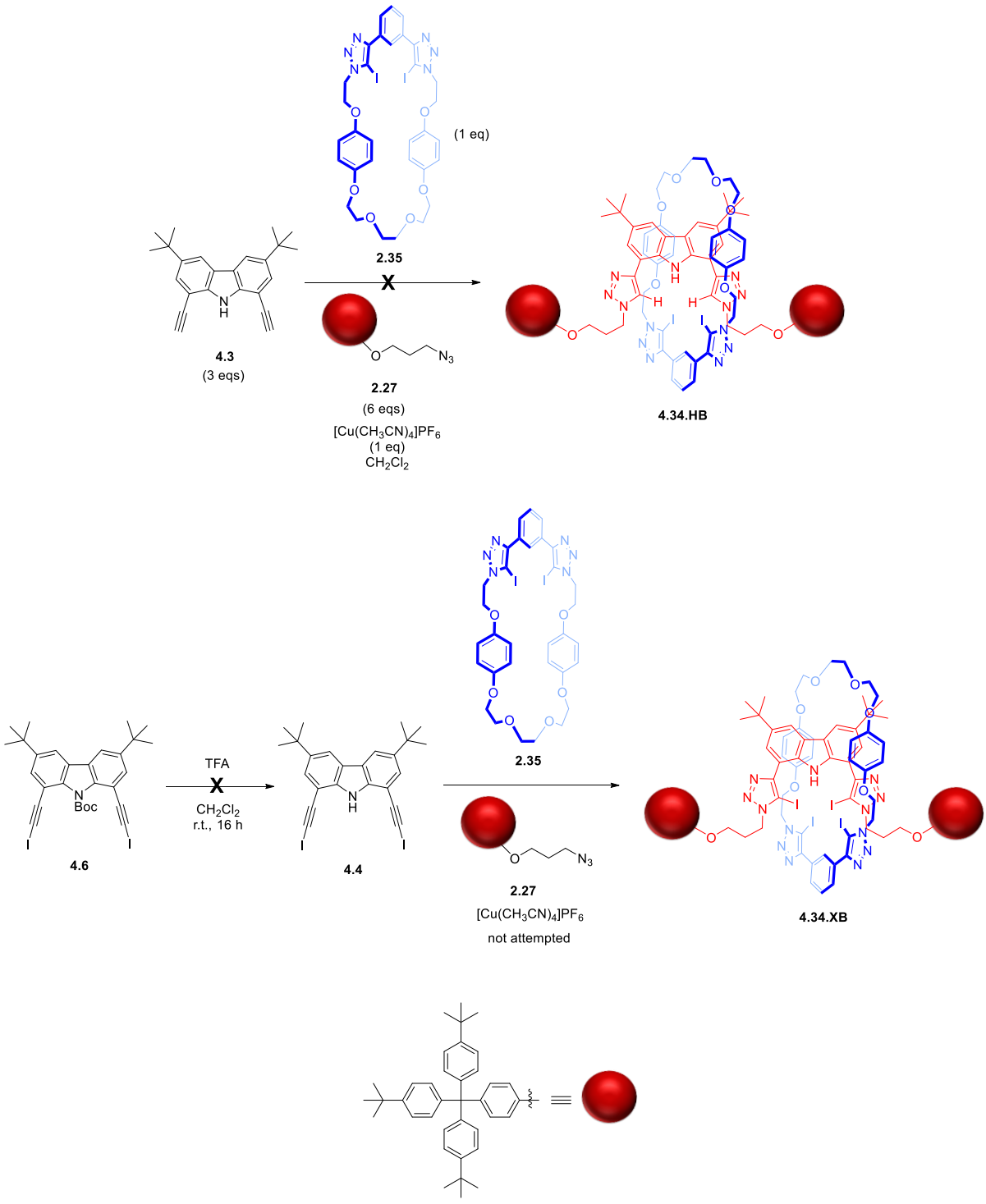
For adamantyl motifs, the same starting reagent was subjected to a standard Cu-catalysed Ullmann coupling with 1-adamantol [30] with the intention of subsequently introducing iodine substituents in the 1 and 8 positions; however, the reaction was very slow and only the formation of 3-bromo-6-iodocarbazole could be observed by mass spectrometry.




***Scheme 4.8.*** *Attempts towards insertion of bulky trityl and adamantyl groups onto a carbazole scaffold.*

### 4.5. Towards interlocked HB/XB carbazole-triazole [2]rotaxane structures

Attempts were also made to incorporate the carbazole-bistriazole motif into a [2]rotaxane, which would also most likely circumvent the solubility limitations. For this purpose, protoalkyne **4.3** was reacted with macrocycle **2.35** and 6 equivalents of stopper azide **2.27** under AMT conditions (**Scheme 4.8**). Unfortunately, no traces of interlocked product or axle could be detected by $^{1}$H NMR or mass spectrometry. For the AMT synthesis of the XB analogue, **4.6** was first subjected to a deprotection of *N*-Boc-protected iodoalkyne **4.6** with TFA in $CH_2Cl_2$, however, significant decomposition was observed and neither starting material nor the target product **4.4** could be recovered.




***Scheme 4.8.*** *Attempted AMT syntheses of carbazole-bistriazole [2]rotaxanes.*

### 4.6. Conclusions and future work

To summarise, a family of carbazole-based acyclic receptors was synthesised. Replacing a HB donor with a XB donor and appending electron-withdrawing perfluoroaryl motifs resulted in an increase in anion affinities, with the HB perfluoroaryl receptors selectively binding benzoate and the XB analogue binding $Cl^-$ the strongest amongst all hosts studied. Qualitative UV-Vis absorption and fluorescence emission studies were undertaken, with very small spectral changes being observed. Numerous attempts to incorporate this motif into macrocycles and rotaxanes were undertaken, however, due to limited solubility, only small amounts of two carbazole-triazole based macrocycles could be obtained.

The work in this chapter could be further developed by covalently attaching polyether groups to the receptor scaffold (**Figure 4.20**), in order to increase its solubility in aqueous media and exploit the potential of the hydrophobic effect, which has been previously reported to impart exceptional iodide selectivity in charge neutral systems. [31]

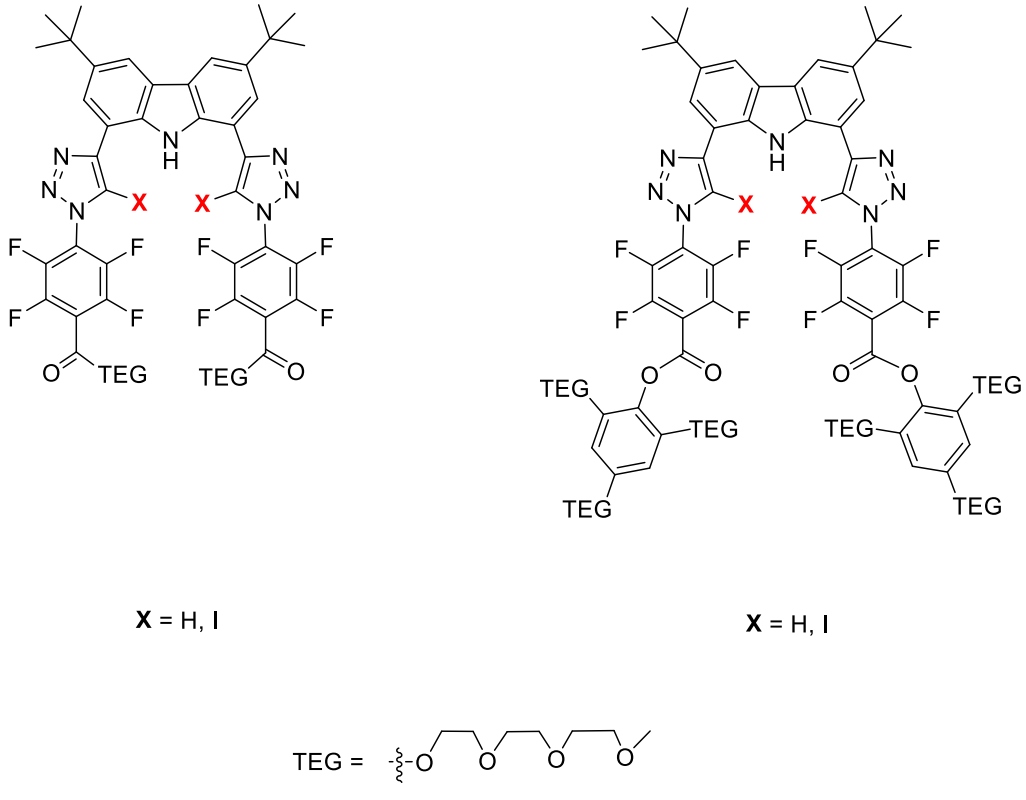



***Figure 4.20.*** *Generic structure of the target water-soluble polyether-appended systems.*

### 4.7. References


1. M. Reig, J. Puigdollers and D. Velasco, *J. Mater. Chem. C*, **2015**, 3, 506–513.
2. J.-X. Yang, X.-T. Tao, C. X. Yuan, Y. X. Yan, L. Wang, Z. Liu, Y. Ren and M. H. Jiang, *J. Am. Chem. Soc.*, **2005**, 127, 3278–3279.
3. J. A. Joule, in *Advances in Heterocyclic Chemistry*, Elsevier, **1984**, vol. 35, pp. 83–198.
4. T. D. Thangadurai, N. J. Singh, I.-C. Hwang, J. W. Lee, R. P. Chandran and K. S. Kim, *J. Org. Chem.*, **2007**, 72, 5461–5464.
5. K. M. Bąk, K. Masłowska and M. J. Chmielewski, *Org. Biomol. Chem.*, **2017**, 15, 5968–5975.
6. M. S. Bennington, H. L. C. Feltham, Z. J. Buxton, N. G. White and S. Brooker, *Dalton Trans.*, **2017**, 46, 4696–4710.
7. B. Schulze, C. Friebe, M. Jäger, H. Görls, E. Birckner, A. Winter and U. S. Schubert, *Organometallics*, **2018**, 37, 145–155.
8. G. Kleinhans, G. Guisado-Barrios, E. Peris and D. I. Bezuidenhout, *Polyhedron*, **2018**, 143, 43–48.
9. G. Kleinhans, M. M. Hansmann, G. Guisado-Barrios, D. C. Liles, G. Bertrand and D. I. Bezuidenhout, *J. Am. Chem. Soc.*, **2016**, 138, 15873–15876.
10. H.-C. Gee, C.-H. Lee, Y.-H. Jeong and W.-D. Jang, *Chem. Commun.*, **2011**, 47, 11963 - 11965.
11. R. Tepper, B. Schulze, H. Görls, P. Bellstedt, M. Jäger and U. S. Schubert, *Org. Lett.*, **2015**, 17, 5740–5743.
12. B. R. Mullaney, B. E. Partridge and P. D. Beer, *Chem. - Eur. J.*, **2015**, 21, 1660–1665.
13. T. Bunchuay, A. Docker, A. J. Martinez-Martinez and P. D. Beer, *Angew. Chem. Int. Ed.*, **2019**.
14. V. C. Gibson, S. K. Spitzmesser, A. J. P. White and D. J. Williams, *Dalton Trans.*, **2003**, 2718.
15. V. Diep, J. J. Dannenberg and R. W. Franck, *J. Org. Chem.*, **2003**, 68, 7907–7910.
16. P. Thordarson, *Chem. Soc. Rev*, **2011**, 40, 1305–1323.
17. D. B. Hibbert and P. Thordarson, *Chem. Commun.*, **2016**, 52, 12792–12805.
18. J. F. W. Keana and S. X. Cai, *J. Org. Chem.*, **1990**, 55, 3640–3647.
19. J. Y. C. Lim, J. Y. Liew and P. D. Beer, *Chem. - Eur. J.*, **2018**, 24, 14560–14566.
20. H. H. Jaffé and M. Orchin, *J. Chem. Soc*, **1960**, 0, 1078–1087.
21. B. Valeur and I. John Wiley & Sons, *Molecular Fluorescence*, Wiley-VCH, Weinheim, **2002**.
22. A. Welle, F. Billard and J. Marchand-Brynaert, *Synthesis*, **2012**, 44, 2249–2254.
23. A. Amira, H. K'tir, M. Berredjem and N.-E. Aouf, *Monatshefte Für Chem. - Chem. Mon.*, **2014**, 145, 509–515.
24. S. Fustero, D. Jiménez, J. Moscardó, S. Catalán and C. del Pozo, *Org. Lett.*, **2007**, 9, 5283–5286.
25. K. Bala and H. C. Hailes, *Synthesis*, **2005**, 3423–3427.
26. L.-M. Jin, X. Xu, H. Lu, X. Cui, L. Wojtas and X. P. Zhang, *Angew. Chem. Int. Ed.*, **2013**, 52, 5309–5313.
27. L. Maugeri, J. Asencio-Hernández, T. Lébl, D. B. Cordes, A. M. Z. Slawin, M.-A. Delsuc and D. Philp, *Chem. Sci.*, **2016**, 7, 6422–6428.
28. C. Maeda and N. Yoshioka, *Org. Biomol. Chem.*, **2012**, 10, 5182 - 5185.
29. F. Li, Q. Wang, Z. Ding and F. Tao, *Org. Lett.*, **2003**, 5, 2169–2171.
30. F. R. P. Limberg, A. Miasojedovas, P. Pingel, F. Reisbeck, S. Janietz, A. P. Monkman and H. Krüger, *RSC Adv.*, **2015**, 5, 83122–83128.
31. A. Borissov, I. Marques, J. Y. C. Lim, V. Félix, M. D. Smith and P. D. Beer, *J. Am. Chem. Soc.*, **2019**, 141, 4119–4129.
32. Benjamin Mullaney, *DPhil thesis*.

# Chapter 5

Conclusions

# Chapter 5: Conclusions

The work in this thesis focused on the synthesis of acyclic and interlocked host structures incorporating various combinations of (iodo)triazole and N – H donors such as amides (**Chapter 1**), (thio)ureas (**Chapter 2**), and carbazoles (**Chapter 3**), as well as the study of their host-guest interactions with anions, followed by comparison and contrast of the observed binding trends. Conclusive experimental evidence established halogen bonding as a powerful tool for anion receptor design, especially when incorporated into the unique three – dimensional cavities of [2]rotaxane structures.

**Chapter 2** revealed the potency of the amido – (iodo)triazole motif for anion recognition in aqueous organic media. A family of cationic and neutral [2]rotaxanes bearing this motif were constructed by employing either anion – templated ring – closing metathesis or active metal templation protocols. Counterintuitively, the cationic [2]rotaxane was shown to be a more potent host than a rigid host with a similar binding cavity. By changing the number of donors flanking the cavity, exchanging a HB donor for a XB analogue, and altering the percentage of water in the solvent mixture, the selectivity of such a host could be fine-tuned for a particular halide (**Figure 5.1**).

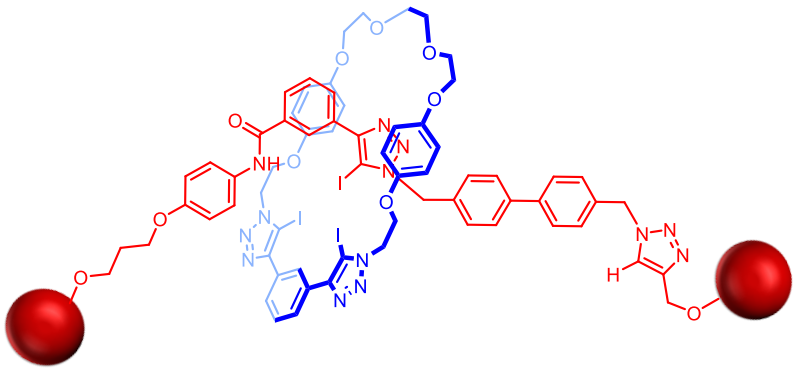


***Figure 5.1.*** *A neutral [2]rotaxane flanked with one N – H donor and three XB iodotriazole donors which is capable of highly strong iodide binding in aqueous organic media.*

In **Chapter 3**, a series of acyclic receptors incorporating one or two (iodo)triazole donors appended to a urea or thiourea scaffold were prepared. Unexpectedly, extensive $^{1}$H NMR studies revealed that, overall, the binding strength was inversely correlated to the

number of triazole donors and moreover, iodotriazole-bearing hosts performed very poorly compared to their HB analogues. However, it was established that employing a more rigid 1,3 – phenylene spacer resulted in significant dicarboxylate binding. An impressive selectivity for fumarate over its geometric isomer maleate was also observed, with the XB receptor exhibiting a higher degree of discrimination (**Figure 5.2**).

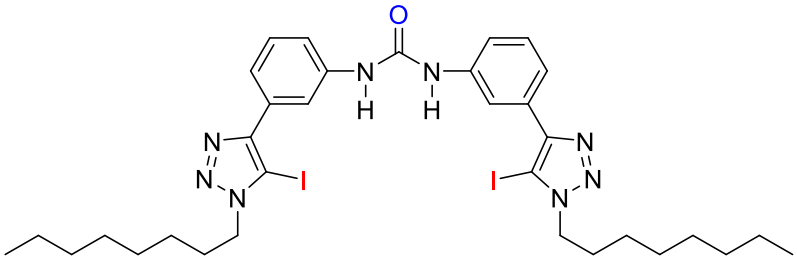



***Figure 5.2.*** *A rigid urea – based receptor incorporating two XB iodotriazole donors, which exhibits significant geometric isomer discrimination.*

**Chapter 4** described a family of neutral carbazole – bis(triazole) anion hosts. Integration of rigid, electron-withdrawing perfluoroaryl motifs was found to significantly enhance anion affinities, particularly when combined with XB donors such as iodotriazoles. The distinctive electronic properties of perfluoroaryls induced additional binding modes via donor – acceptor aromatic interactions, with one such receptor exhibiting notable selectivity for benzoate over all other anions studied (**Figure 5.3**). Despite solubility limitations, this motif was successfully incorporated into an analogous macrocyclic structure through alkene metathesis mediated by Grubbs' 2$^{nd}$ generation catalyst.

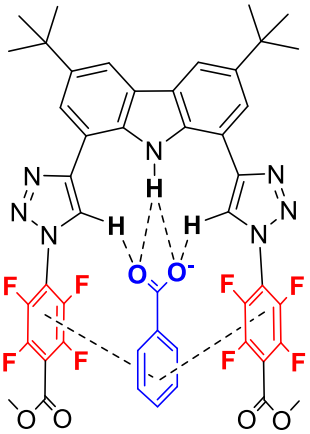


***Figure 5.3.*** *A carbazole – bistriazole receptor which selectively complexes benzoate anions through aromatic stacking interactions between electron – poor perfluoroaryl substituents and electron – rich benzoate.*

To summarise, the work described in this thesis offered compelling evidence for the potency of complementary halogen- and hydrogen bonding interactions for anion recognition applications, especially when incorporated into the three-dimensional cavities of interlocked structures such as [2]rotaxanes. Careful fine – tuning of the receptor structure can efficiently augment the binding strength and selectivity for a particular anionic guest, which paves the way for novel generations of hosts for future anion recognition and sensing applications, particularly in aqueous media.

# Chapter 5

Experimental

# Chapter 6: Experimental

## 6.1. General considerations

### 6.1.1. Chemicals and solvents

All solvents and reagents employed in this thesis were purchased from commercial suppliers and used without further purification, with the exception of triethylamine, which was distilled and stored over potassium hydroxide. Anhydrous solvents were obtained by purging with $N_2$ and then passing through an MBraun MPSP-800 column. Deionised water was obtained from a Milli-$Q_r$ Millipore machine. Tetrabutylammonium salts, Grubbs' 2$^{nd}$ generation catalyst, and $[Cu(CH_3CN)_4]PF_6$ were stored in a vacuum desiccator containing phosphorus pentoxide prior to use. Brine refers to a saturated aqueous solution of NaCl, while the basic EDTA solution employed is an aqueous solution containing 20 mM EDTA and 1% $NH_3$.

Thin layer chromatography was undertaken on Merck silica Kieselgel 60 F254 0.25 mm plates, which were subsequently visualised under UV light (254 or 365 nm) or, if necessary, by staining with $I_2$ or a basic $KMnO_4$ solution. Column chromatography was carried out on silicagel (particle size 40 – 63 µm) and preparative thin layer chromatography was performed on silicagel-coated 20×20 cm plates (1 mm thickness). Size exclusion chromatography was undertaken in a glass column packed with styrene-divinylbenzene beads (3% crosslinkage, 40–80 µm bead size) using $CHCl_3$ as an eluent, with the column being washed with fresh $CHCl_3$ several times before use.

### 6.1.2. Instrumentation

NMR spectra were recorded on a Bruker AVIII HD 400, a Bruker AVIII HD 500, or a Bruker AVII 500. $^1$H NMR titration experiments were performed on a Bruker AVIII HD 400 or a Bruker AVIII HD 500. Chemical shifts are quoted in ppm (parts per million) relative to the residual solvent signal or the signal of the solvent with the greatest number of deuterons for mixed solvent systems (nearest 0.01 ppm). Signal splittings are denoted as singlet (s), doublet (d), triplet (t), quartet (quart.), quintet (quint.), and multiplet (m). Mass spectra were carried out on a Waters LCT premier (low resolution) or a Bruker microTOF spectrometer (high resolution). Fluorescence and UV-Vis spectra were recorded on a Horiba Duetta™

dual absorbance and fluorescence spectrometer using quartz cuvettes with a path length of 1 cm. All spectra were recorded at 298 K.

### 6.1.3. $^{1}$H-NMR titration protocols

In a typical $^{1}$H NMR titration experiment, to a 1.0 mM solution of host (initial volume 0.60 mL) were added aliquots of a 30 mM solution of anionic guest as its tetrabutylammonium salt. After each addition, the samples were thoroughly shaken and then the spectra recorded at 0, 0.2, 0.4, 0.6, 0.8, 1.0, 1.2, 1.4, 1.6, 1.8, 2.0, 2.5, 3.0, 4.0, 5.0, 7.0 and 10 equivalents of anion. In all cases, the bound and unbound hosts were found to be in fast exchange on the NMR timescale. The observed chemical shift for relevant protons were monitored after each addition and the resulting data processed through BindFit using a non-linear regression model to give an estimated association constant.

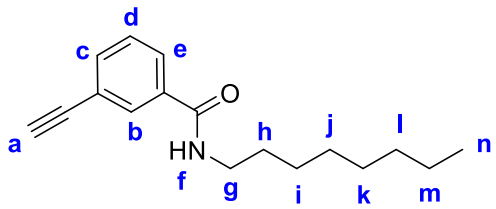
### 6.1.4. Qualitative optical anion binding protocols

In the case of UV-Vis studies, a 30 mM solution of host in HPLC-grade $CH_3CN$ was prepared and subsequently diluted until $A_{max} < 0.5$. For each anion under study, a large excess of guest as its tetrabutylammonium salt (one spatula tip) was added to 1 mL of this solution, which was thoroughly shaken and then the UV-Vis spectrum was recorded between 200 and 800 nm.

In the case of fluorescence studies, a 30 mM solution of host in HPLC-grade $CH_3CN$ was diluted to a μM level concentration. For each anion under study, a large excess of guest as its tetrabutylammonium salt (one spatula tip) was added to 1 mL of this solution. The solution was thoroughly shaken, then it was excited at the wavelength of maximum absorbance ($\lambda_{max}$) and the fluorescence emission spectrum was recorded between 200 and 800 nm.

## 6.2. Synthetic procedures and characterisation of compounds in Chapter 2

### 3-Ethynylbenzamide 2.1




3-Ethynylbenzoic acid (300 mg, 2.05 mmol) was suspended in anhydrous $CH_2Cl_2$ (5 mL). Oxalyl chloride (0.26 mL, 3.08 mmol, 1.5 eqs) was added dropwise, followed by 1 – 2 drops of DMF. The reaction mixture was stirred at room temperature for 3 h, after which the volatile components were removed under reduced pressure to afford an intense orange solid. This was subsequently redissolved in anhydrous $CH_2Cl_2$ (5 mL) and cooled to 0 °C in an ice bath, followed by slow addition of $Et_3N$ (0.57 mL, 4.11 mmol, 2 eqs) and octylamine (0.51 mL, 3.08 mmol, 1.5 eqs). The mixture was allowed to warm to room temperature and stirred for 16 h, after which it was quenched with a 3 M HCl solution (5 mL), further diluted with $CH_2Cl_2$ (5 mL) and water (5 mL) and the product extracted with $CH_2Cl_2$ (3 x 5 mL). The combined organic phases were washed with a saturated $NaHCO_3$ solution (10 mL) and brine (10 mL), dried over $MgSO_4$, then filtered and the filtrate concentrated under reduced pressure to afford **2.1** as an orange solid.

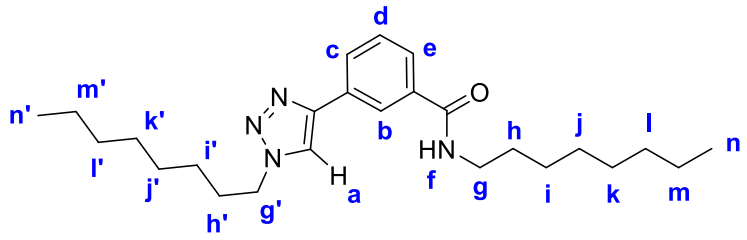
Yield: 423 mg (80%)

**$^1$H-NMR** (400 MHz, $CDCl_3$) $\delta$ = 7.85 (1 H, s, $\mathbf{H_b}$), 7.76 (1 H, d, *J*=7.8 Hz, $\mathbf{H_c}$), 7.60 (1 H, d, *J*=7.7 Hz, $\mathbf{H_e}$), 7.40 (1 H, m, $\mathbf{H_d}$), 6.17 (1 H, br. s., $\mathbf{H_f}$), 3.44 (2 H, q, *J*=6.6 Hz, $\mathbf{H_g}$), 3.12 (1 H, s, $\mathbf{H_a}$), 1.61 (2 H, quin, *J*=6.8 Hz, $\mathbf{H_h}$) 1.32 (10 H, m, $\mathbf{H_{i-m}}$), 0.89 (3 H, m, $\mathbf{H_n}$).

**$^{13}$C-NMR** (101 MHz, $CDCl_3$) $\delta$ = 166.55, 135.18, 134.73, 130.31, 128.71, 127.39, 122.60, 82.71, 78.16, 40.21, 31.80, 29.64, 29.28, 29.20, 26.99, 22.64, 14.09.

**HRMS** (ESI+ve) m/z: 258.18525 ($[M+H]^+$, $C_{17}H_{24}NO^+$ requires 258.18524).

**Amido-triazole acyclic precursor 2.3.HB**




Alkyne **2.1** (73.6 mg, 0.29 mmol), octyl azide **2.21** (44.4 mg, 0.29 mmol, 1 eq), DIPEA (0.08 mL, 0.46 mmol, 1.58 eqs), and TBTA (7.59 mg, 0.01 mmol, 0.05 eqs) were dissolved in anhydrous $CH_2Cl_2$ (5 mL). The mixture was degassed, after which $[Cu(CH_3CN)_4]PF_6$ (5.33 mg, 0.01 mmol, 0.05 eqs) was added and the reaction mixture stirred at room temperature for 16 h. After completion, a 0.1 M aqueous solution of EDTA (10 mL) was added and the resulting organic phase washed with brine (10 mL), dried over $MgSO_4$ and filtered. The filtrate was concentrated under reduced pressure and purified by column chromatography ($CH_2Cl_2$, followed by 1% MeOH - $CH_2Cl_2$) to afford **2.3.HB** as a white solid.

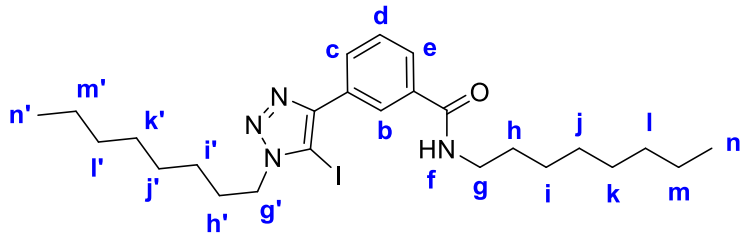
Yield: 109 mg (92%)

**$^1$H-NMR** (400 MHz, $CDCl_3$) $\delta$ = 8.22 (1 H, s, $\mathbf{H_b}$), 7.97 (1 H, d, *J*=7.7 Hz, $\mathbf{H_c}$), 7.83 (1 H, s, $\mathbf{H_a}$), 7.75 (1 H, d, *J*=7.7 Hz, $\mathbf{H_e}$), 7.50 (1 H, t, *J*=7.7 Hz, $\mathbf{H_d}$), 6.27 (1 H, br. s., $\mathbf{H_f}$), 4.42 (2 H, t, *J*=7.2 Hz, $\mathbf{H_{g'}}$), 3.48 (2 H, q, *J*=6.8 Hz, $\mathbf{H_g}$), 1.95 (2 H, m, *J*=6.7 Hz, $\mathbf{H_{h'}}$), 1.63 (2 H, m, $\mathbf{H_h}$), 1.32 (20 H, m, $\mathbf{H_{i\text{-}m}}$ + $\mathbf{H_{i'\text{-}m'}}$), 0.88 (6 H, m, $\mathbf{H_n}$ + $\mathbf{H_{n'}}$).

**$^{13}$C-NMR** (101 MHz, $CDCl_3$) $\delta$ = 167.10, 146.92, 135.40, 131.11, 129.16, 128.36, 126.56, 123.91, 119.85, 50.56, 40.23, 31.81, 31.71, 30.33, 29.70, 29.30, 29.21, 29.05, 28.98, 27.03, 26.50, 22.65, 22.60, 14.09, 14.06.

**HRMS** (ESI+ve) m/z: 413.32766 ($[M+H]^+$, $C_{25}H_{41}N_4O^+$ requires 413.32749).

**Amido-iodotriazole acyclic precursor 2.3.XB**




Alkyne **2.1** (57.6 mg, 0.22 mmol), *N*-iodosuccinimide (60.4 mg, 0.27 mmol, 1.2 eqs), and acetone (2 mL) were added to a round-bottomed flask. An aqueous solution of $AgNO_3$ (3.8 mg, 0.02 mmol, 0.1 eqs) was added and the mixture was stirred in the dark at room temperature for 3 h. The iodoalkyne intermediate **2.2** was extracted with $CH_2Cl_2$ (3 x 7 mL), after which the combined organic phases were washed with water (10 mL) and brine (10 mL), dried over $MgSO_4$, filtered and the filtrate concentrated under reduced pressure to afford a yellow solid.

Iodoalkyne **2.2** was immediately redissolved in anhydrous, degassed THF (5 mL). To this solution, octyl azide **2.21** (38.2 mg, 0.25 mmol, 1.1 eqs), TBTA (5.94 mg, 0.01 mmol, 0.05 eqs), and $[Cu(CH_3CN)_4]PF_6$ (4.17 mg, 0.01 mmol, 0.05 eqs) were added and the reaction mixture stirred at room temperature for 16 h. The solvent was removed under reduced pressure and the resulting solid redissolved in $CH_2Cl_2$ (6 mL), washed with 0.1 M EDTA (5 mL) and brine (10 mL), dried over $MgSO_4$, filtered and the filtrate concentrated under reduced pressure. The crude solid was purified by column chromatography (30% EtOAc – hexanes) to afford **2.3.XB** as an off-white solid.

Yield: 96.5 mg (80%)

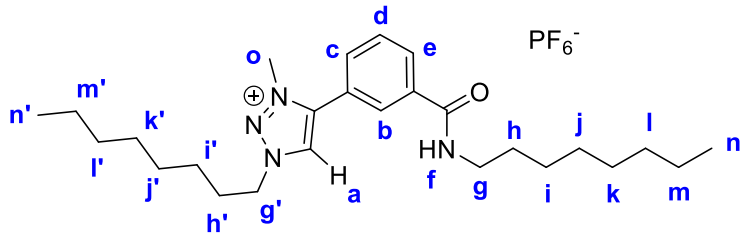
**$^1$H-NMR** (400 MHz, $CDCl_3$) $\delta$ = 8.32 (1 H, s, $\mathbf{H_b}$), 8.09 (1 H, d, *J*=7.1 Hz, $\mathbf{H_c}$), 7.86 (1 H, d, *J*=7.3 Hz, $\mathbf{H_e}$), 7.55 (1 H, t, *J*=8.2 Hz, $\mathbf{H_d}$), 6.22 (1 H, br. s., $\mathbf{H_f}$), 4.46 (2 H, t, *J*=7.6 Hz, $\mathbf{H_{g'}}$), 3.48 (2 H, q, *J*=6.8 Hz, $\mathbf{H_g}$), 1.97 (2 H, quin, *J*=7.3 Hz, $\mathbf{H_{h'}}$), 1.64 (2 H, m, $\mathbf{H_h}$), 1.34 (20 H, m, $\mathbf{H_{i\text{-}m}}$ + $\mathbf{H_{i'\text{-}m'}}$), 0.88 (6 H, m, $\mathbf{H_n}$ + $\mathbf{H_{n'}}$).

**$^{13}$C-NMR** (101 MHz, $CDCl_3$) $\delta$ = 167.03, 135.28, 130.66, 129.96, 128.90, 127.31, 125.48, 51.07, 40.18, 31.79, 31.71, 29.92, 29.66, 29.28, 29.20, 29.05, 28.97, 27.01, 26.40, 22.63, 22.60, 14.08.

There were fewer $^{13}$C signals than anticipated due to coincidence.

**HRMS** (ESI+ve) m/z: 539.22393 ($[M+H]^+$, $C_{25}H_{40}IN_4O^+$ requires 539.22413).

**Amido-triazolium acyclic receptor 2.4.HB$^+$PF$_6^-$**




Amido-triazole acyclic precursor **2.3.HB** (72.5 mg, 0.18 mmol) was dissolved in anhydrous $CH_2Cl_2$ (3 mL), after which $[Me_3O]BF_4$ (33.8 mg, 0.23 mmol, 1.3 eqs) was added in one portion. The reaction mixture was stirred at room temperature for 16 h, after which MeOH (3 mL) was added to quench the alkylating agent and the volatiles were removed under reduced pressure. The crude solid was purified by column chromatography (2% MeOH – $CHCl_3$, followed by 10% MeOH – $CHCl_3$) to afford **2.4.HB$^+$BF$_4^-$**, which was redissolved in $CH_2Cl_2$ (10 mL) and repeatedly washed with a 0.1 M solution of $NH_4PF_6$ (7 x 10 mL) to give **2.4.HB$^+$PF$_6^-$** as a white solid.

Yield: 101 mg (95%)

**$^1$H-NMR** (500 MHz, 1:1 $CD_3OD$:$CDCl_3$) $\delta$ = 8.84 (1 H, s, **H$_a$**), 8.08 (1 H, d, *J*=9.3 Hz, **H$_c$**), 8.05 (1 H, s, **H$_b$**), 7.76 (1 H, d, *J*=7.6 Hz, **H$_e$**), 7.70 (1 H, m, *J*=7.8 Hz, **H$_d$**), 4.32 (3H, s, **H$_o$**), 3.39 (2 H, t, *J*=7.2 Hz, **H$_g$**), 2.08 (1 H, dt, *J*=14.6, 7.2 Hz, **H$_{h'}$**), 1.62 (1 H, dt, *J*=14.6, 7.3 Hz, **H$_h$**), 1.33 (20 H, m, **H$_{i\text{-}m}$** + **H$_{i'\text{-}m'}$**), 0.82 (6 H, m, **H$_n$** + **H$_{n'}$**).

**H$_{g'}$** was obscured by the solvent signal.

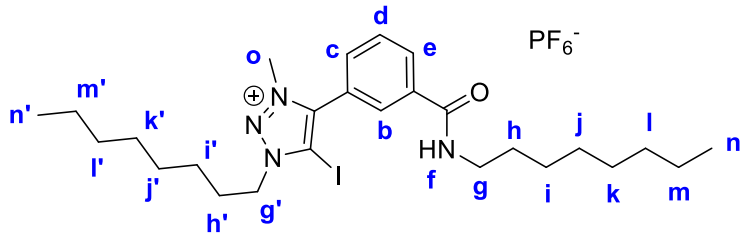
**$^{19}$F-NMR** (377 MHz, $CDCl_3$) $\delta$ = -72.69 (6 F, d)

**$^{13}$C-NMR** (101 MHz, $CDCl_3$) $\delta$ = 165.60, 142.82, 136.43, 131.18, 129.88, 128.57, 127.71, 121.75, 54.42, 40.46, 38.40, 31.80, 31.63, 29.25, 29.22, 28.99, 28.89, 28.72, 26.98, 26.12, 22.62, 22.55, 14.07, 14.02.

There were fewer $^{13}$C signals than anticipated due to coincidence.

**HRMS** (ESI+ve) m/z: 427.34336 ([M+H]$^+$, $C_{26}H_{43}N_4O^+$ requires 427.34314).

**Amido-iodotriazolium acyclic receptor 2.4.XB$^{+}$PF$_6^{-}$**




Amido-triazole acyclic precursor **2.3.XB** (81.0 mg, 0.15 mmol) was dissolved in anhydrous $CH_2Cl_2$ (5 mL), after which $[Me_3O]BF_4$ (28.9 mg, 0.20 mmol, 1.3 eqs) was added in one portion. The reaction mixture was stirred at room temperature for 16 h, after which MeOH (4 mL) was added to quench the alkylating agent and the volatiles were removed under reduced pressure. The crude solid was purified by column chromatography (1% MeOH – $CHCl_3$ to 10% MeOH – $CHCl_3$) to afford **2.4.XB$^{+}$BF$_4^{-}$**, which was redissolved in $CH_2Cl_2$ (10 mL) and repeatedly washed with a 0.1 M solution of $NH_4PF_6$ (7 x 10 mL) to give **2.4.XB$^{+}$PF$_6^{-}$** as a white solid.

Yield: 94.6 mg (90%)

**$^{1}$H-NMR** (500 MHz, 1:1 $CD_3OD$:$CDCl_3$) $\delta$ = 8.10 (1 H, d, *J*=7.8 Hz, **H$_c$**), 8.00 (1 H, s, **H$_b$**), 7.71 (2 H, m, **H$_d$** + **H$_e$**), 4.23 (3H, s, **H$_o$**), 3.40 (2 H, t, *J*=7.5 Hz, **H$_g$**), 2.08 (2 H, dt, *J*=14.3, 7.0 Hz, **H$_{h'}$**), 1.62 (2 H, m, **H$_h$**), 1.35 (20 H, m, **H$_{i\text{-}m}$** + **H$_{i'\text{-}m'}$**), 0.86 (6 H, m, **H$_n$** + **H$_{n'}$**).

**H$_{g'}$** was obscured by the solvent signal.

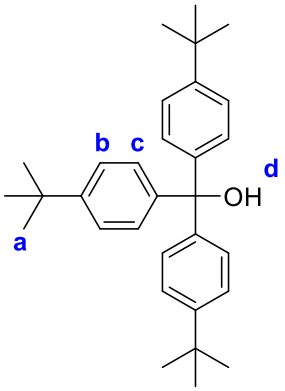
**$^{19}$F-NMR** (377 MHz, $CDCl_3$) $\delta$ = -71.74, - 73.63.

**$^{13}$C-NMR** (101 MHz, $CDCl_3$) $\delta$ = 165.61, 136.55, 132.03, 131.59, 130.01, 128.47, 122.13, 87.07, 55.30, 40.55, 39.17, 31.80, 31.66, 29.23, 29.21, 28.91, 28.76, 28.70, 26.97, 26.18, 22.62, 22.56, 14.08, 14.05.

There were fewer $^{13}$C signals than anticipated due to coincidence.

**HRMS** (ESI+ve) m/z: 553.23931 ([M+H]$^{+}$, $C_{26}H_{42}IN_4O^{+}$ requires 553.23978).

**Terphenyl alcohol stopper 2.5** [1]

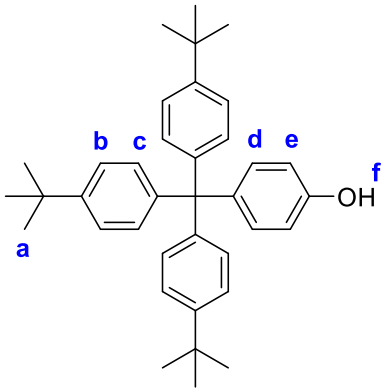



Mg turnings (1.84 g, 76.7 mmol, 3.66 eqs) were placed in a round-bottomed flask, washed with small amounts of anhydrous THF and heated at 100 °C for 40 mins, after which they were allowed to cool to room temperature. Anhydrous THF (25 mL) and a few crystals of $I_2$ were then added. Separately, 1-bromo-4-tert-butylbenzene (12 mL, 69.8 mmol, 3.33 eqs) was dissolved in anhydrous THF (15 mL); three quarters of this solution by volume were added to the Mg suspension under a $N_2$ atmosphere, after which the remainder was added dropwise. The reaction mixture was heated to reflux for 1 hour, following which a solution of diethyl carbonate (2.52 mL, 21.0 mmol) in anhydrous THF (6 mL) was added dropwise and the mixture heated to reflux for a further 1 hour. This was subsequently allowed to cool to room temperature and then neutralised with a 10% HCl solution in an ice bath. Ice-cold water was added to the solution and the resulting precipitate was collected by filtration under reduced pressure and washed with hexane to afford **2.5** as a white solid.

Yield: 7.02 g (79%)

**$^1$H-NMR** (400 MHz, $CDCl_3$) $\delta$ = 7.32 (6 H, d, *J*=4.6 Hz, $\mathbf{H_c}$), 7.20 (6 H, d, *J*=4.6 Hz, $\mathbf{H_b}$), 2.72 (1 H, s, $\mathbf{H_d}$) 1.32 (27 H, s, $\mathbf{H_a}$).

**Phenol stopper 2.6** [1]

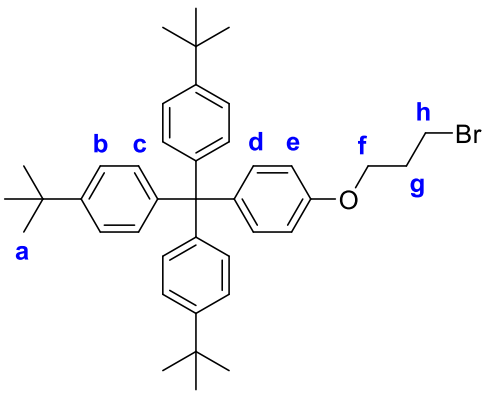



Terphenyl alcohol stopper **2.5** (3.46 g, 8.10 mmol) was dissolved in molten phenol (17.3 g), after which a 37% HCl solution (0.64 mL) was added and the reaction mixture heated at 160 °C for 16 h. After completion, it was allowed to cool to room temperature, after which toluene (50 mL) was added and the resulting solution washed sequentially with dilute NaOH (50 mL), dilute HCl (50 mL), water (50 mL), and brine (50 mL). The organic phase was dried over $MgSO_4$, filtered and then concentrated under reduced pressure, after which the crude solid was repeatedly triturated with hexane to afford **2.6** as a pale yellow solid.

Yield: 3.11 g (76%)

**$^1$H-NMR** (400 MHz, $CDCl_3$) $\delta$ = 7.24 (6 H, d, *J*=4.8 Hz, $\mathbf{H_b}$), 7.07 (8 H, m, $\mathbf{H_c}$ + $\mathbf{H_d}$), 6.71 (2 H, d, *J*=8.8 Hz, $\mathbf{H_e}$), 4.60 (1 H, s, $\mathbf{H_f}$), 1.31 (27 H, s, $\mathbf{H_a}$).

**Bromide stopper 2.7** [2]



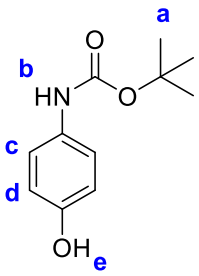

Phenol stopper **2.6** (3.09 g, 6.12 mmol) and 1,3-dibromopropane (6.20 mL, 61.2 mmol, 10 eqs) were suspended in anhydrous $CH_3CN$ (33 mL), after which $K_2CO_3$ (2.50 g, 18.4 mmol,

3 eqs) was added in one portion. The reaction mixture was heated to 80 °C under a $N_2$ atmosphere for 2 days, after which it was allowed to cool to room temperature. The solids were filtered, washed with distilled water and subsequently dissolved in $CH_2Cl_2$ (25 mL). The resulting solution was dried over $MgSO_4$, filtered and then concentrated under reduced pressure to afford **2.7** as a white solid.

Yield: 3.41 g (89%)

**$^1$H-NMR** (400 MHz, $CDCl_3$) $\delta$ = 7.24 (6 H, d, *J*=8.7 Hz, $\mathbf{H_b}$), 7.10 (8 H, m, $\mathbf{H_c}$ + $\mathbf{H_d}$), 6.78 (2 H, d, *J*=8.9 Hz, $\mathbf{H_e}$), 4.09 (2 H, t, *J*=5.7 Hz, $\mathbf{H_f}$), 3.61 (2 H, t, *J*=6.5 Hz, $\mathbf{H_h}$), 2.31 (2 H, quin, *J*=6.1 Hz, $\mathbf{H_g}$), 1.31 (27 H, s, $\mathbf{H_a}$).

**_N_-Boc-4-aminophenol 2.8** [3]

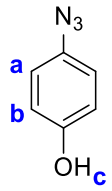



4-Aminophenol (1.00 g, 9.17 mmol) and $Boc_2O$ (2.00 g, 9.17 mmol, 1 eq) were dissolved in anhydrous THF (5 mL) and the reaction mixture was stirred at room temperature for 2 h. The volatile components were removed under reduced pressure, after which water was added (7 mL) and the product extracted with $Et_2O$ (3 x 10 mL). The combined organic extracts were washed with brine (15 mL), dried over $MgSO_4$, filtered and then concentrated under reduced pressure to give **2.8** as a light brown solid.

Yield: 1.92 g (quantitative)

**$^1$H-NMR** (400 MHz, $CDCl_3$) $\delta$ = 7.23 (2 H, d, *J*=8.4 Hz, $\mathbf{H_c}$), 6.78 (2 H, d, *J*=8.8 Hz, $\mathbf{H_d}$), 6.33 (1 H, br. s., $\mathbf{H_b}$), 4.72 (1 H, br. s., $\mathbf{H_e}$), 1.53 (9 H, s, $\mathbf{H_a}$).

**4-Azidophenol 2.9** [4]

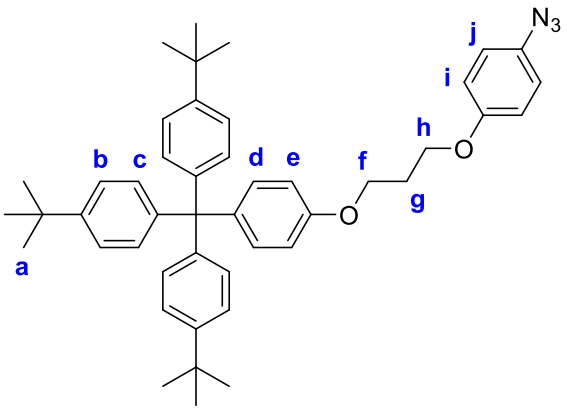



4-Aminophenol (500 mg, 4.58 mmol) was dissolved in 10% HCl (10 mL). To this, a solution of $NaNO_2$ (474 mg, 6.87 mmol, 1.5 eqs) in water (5 mL) was added in an ice bath and the mixture stirred for 30 minutes at 0 °C. Subsequently, a solution of $NaN_3$ (447 mg, 6.87 mmol, 1.5 eqs) in water (5 mL) was added in small portions, after which the reaction mixture was allowed to warm to room temperature and stirred for a further 2 h. The product was extracted with EtOAc (3 x 20 mL) and the combined organic layers washed with water (20 mL) and brine (20 mL), dried over $MgSO_4$, filtered and then concentrated under reduced pressure to give **2.9** as a dark red oil.

Yield: 124.4 mg (20%)

**$^1$H-NMR** (400 MHz, $CDCl_3$) $\delta$ = 6.92 (2 H, m, **$H_a$**), 6.83 (2 H, m, **$H_b$**), 4.75 (1 H, s, **$H_c$**).

**Aromatic azide stopper 2.10**




4-azidophenol **2.9** (428 mg, 3.17 mmol, 2.5 eqs) and $Cs_2CO_3$ (1.03 g, 3.17 mmol, 2.5 eqs) were suspended in acetone (30 mL) and the suspension stirred at room temperature for 5 minutes. Subsequently, bromide stopper **2.7** (793 mg, 1.27 mmol) was added in one portion and the reaction mixture heated at reflux for 16 h. The suspension was allowed to cool to room temperature, after which the solvent was evaporated under reduced pressure and the

crude solid partitioned between water (15 mL) and $CHCl_3$ (3 x 30 mL). The combined organic layers were dried over $MgSO_4$, filtered and then concentrated under reduced pressure. The resulting crude solid was purified by column chromatography (50% $CH_2Cl_2$ – hexanes, followed by 90% $CH_2Cl_2$ – hexanes) to give **2.10** as a yellow solid.

Yield: 503 mg (58%)

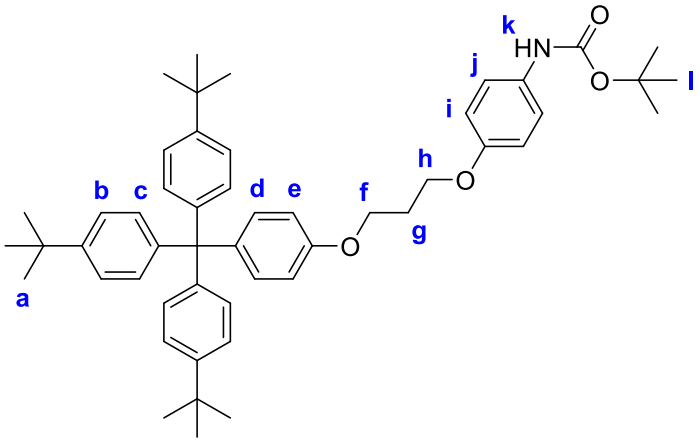
**$^1$H-NMR** (400 MHz, $CDCl_3$) $\delta$ = 7.24 (6 H, d, *J*=8.6 Hz, $\mathbf{H_b}$), 7.09 (8 H, m, $\mathbf{H_c}$ + $\mathbf{H_d}$), 6.92 (4 H, m, $\mathbf{H_i}$ + $\mathbf{H_j}$), 6.78 (2 H, m, $\mathbf{H_e}$), 4.14 (4 H, t, *J*=6.1 Hz, $\mathbf{H_f}$ + $\mathbf{H_h}$), 2.25 (2 H, quin, *J*=6.1 Hz, $\mathbf{H_g}$), 1.31 (27 H, s, $\mathbf{H_a}$).

**$^{13}$C-NMR** (101 MHz, $CDCl_3$) $\delta$ = 148.33, 144.13, 132.28, 130.72, 124.04, 119.99, 115.76, 112.96, 64.90, 64.09, 63.05, 34.29, 31.38, 29.34.

There were fewer $^{13}$C signals than anticipated due to coincidence.

**HRMS** (ESI+ve) m/z: 697.44753 ($[M+NH_4]^+$, $C_{46}H_{57}N_4O_2^+$ requires 697.44760).

***N*-Boc-aniline stopper 2.11** [5]



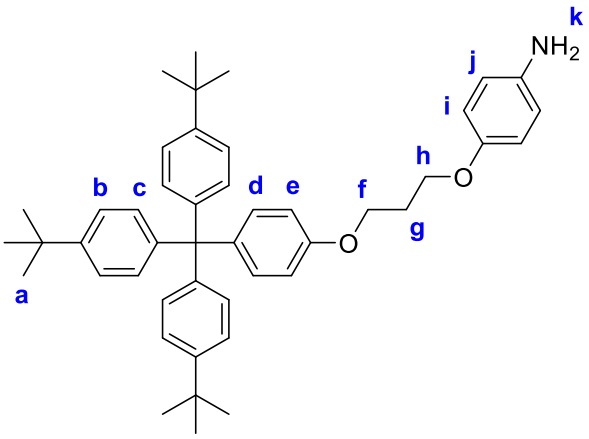

*N*-Boc-4-aminophenol **2.8** (522 mg, 2.49 mmol, 3.5 eqs) and $Cs_2CO_3$ (811 mg, 2.49 mmol, 3.5 eqs) were suspended in acetone (10 mL) and the suspension stirred at room temperature for 5 minutes. Subsequently, bromide stopper **2.7** (446 mg, 0.71 mmol) was added in one portion and the reaction mixture heated at reflux for 16 h. The suspension was allowed to cool to room temperature, after which the solvent was evaporated under reduced pressure and the crude solid partitioned between water (15 mL) and $CHCl_3$ (3 x 15 mL). The combined organic layers were dried over $MgSO_4$, filtered and then concentrated under

reduced pressure. The resulting crude solid was purified by column chromatography (50% $CH_2Cl_2$ – hexanes, followed by 75% $CH_2Cl_2$ – hexanes) to give **2.11** as a white solid.

Yield: 382 mg (71%)

**$^1$H-NMR** (400 MHz, $CDCl_3$) $\delta$ = 7.15 (8 H, d, *J*=8.6 Hz, $\mathbf{H_b}$ + $\mathbf{H_j}$), 7.00 (8 H, d, *J*=8.6 Hz, $\mathbf{H_c}$ + $\mathbf{H_d}$), 6.76 (2 H, d, *J*=8.9 Hz, $\mathbf{H_e}$), 6.70 (2 H, d, *J*=8.8 Hz, $\mathbf{H_i}$), 6.24 (1 H, br. s., $\mathbf{H_k}$), 4.04 (4 H, m, $\mathbf{H_f}$ + $\mathbf{H_h}$), 2.15 (2 H, quin, *J*=6.0 Hz, $\mathbf{H_g}$), 1.43 (9 H, s, $\mathbf{H_l}$), 1.22 (27 H, s, $\mathbf{H_a}$).

**Aniline stopper 2.12** [5]

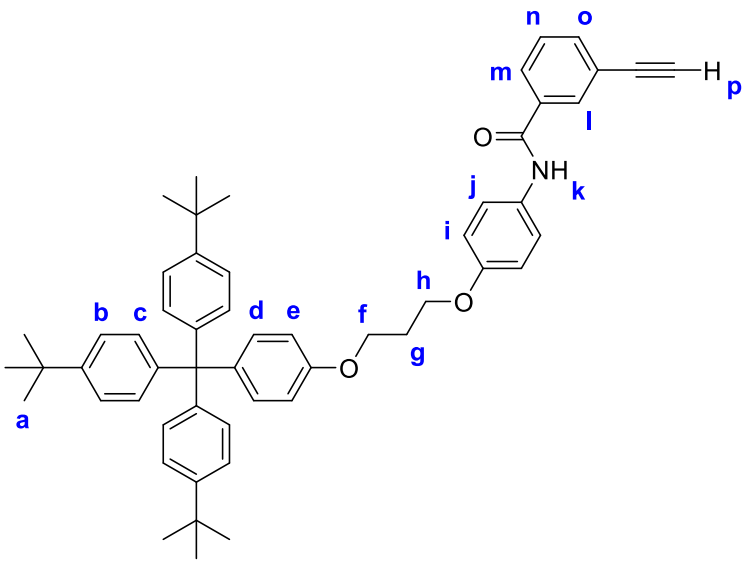



*N*-Boc-aniline stopper **2.11** (381 mg, 0.5 mmol) was dissolved in anhydrous $CH_2Cl_2$ (5 mL), after which TFA (10 mL) was added and the reaction mixture stirred at room temperature for 30 minutes. Subsequently, $CH_2Cl_2$ (3 mL) was added and the solution washed with a saturated $NaHCO_3$ solution (15 mL) and water (10 mL), dried over $MgSO_4$, filtered and then concentrated under reduced pressure to afford **2.12** as a pale orange solid.

Yield: 305 mg (92%)

**$^1$H-NMR** (400 MHz, $CDCl_3$) $\delta$ = 7.24 (6 H, m, $\mathbf{H_b}$), 7.09 (8 H, m, $\mathbf{H_c}$ + $\mathbf{H_d}$), 6.77 (4 H, m, $\mathbf{H_e}$ + $\mathbf{H_j}$), 6.65 (2 H, m, $\mathbf{H_i}$), 4.13 (2 H, t, *J*=6.1 Hz, $\mathbf{H_f}$), 4.08 (2 H, t, *J*=6.2 Hz, $\mathbf{H_h}$), 2.21 (2 H, quin, *J*=6.1 Hz, $\mathbf{H_g}$), 1.31 (27 H, s, $\mathbf{H_a}$).

**Aromatic alkyne stopper 2.13**




Aniline stopper **2.12** (85.1 mg, 0.13 mmol), 3-ethynylbenzoic acid (19.0 mg, 0.13 mmol, 1 eq), and DMAP (cat.) were suspended in anhydrous $CH_2Cl_2$ (5 mL). To this suspension EDC·HCl (30 mg, 0.16 mmol, 1.2 eqs) was added and the reaction mixture stirred at reflux for 16 h. After completion, the resulting solution was washed with a saturated $NaHCO_3$ solution (15 mL), water (10 mL), and brine (10 mL), dried over $MgSO_4$, filtered and the filtrate concentrated under reduced pressure. The crude solid was purified by column chromatography (50% $CH_2Cl_2$ – hexanes, followed by $CH_2Cl_2$) to afford **2.13** as a white solid.

Yield: 77.6 mg (76%)

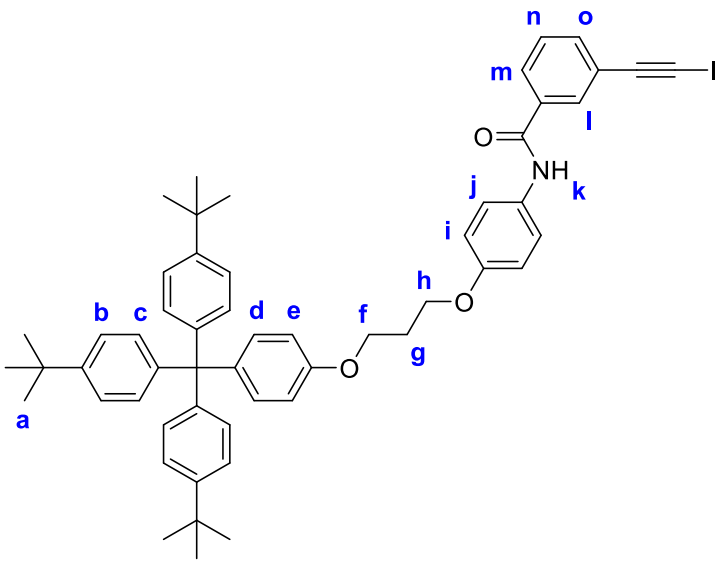
**$^1$H-NMR** (400 MHz, $CDCl_3$) $\delta$ = 7.96 (1 H, s, **$H_l$**), 7.86 (1 H, d, *J*=7.8 Hz, **$H_m$**), 7.70 (1 H, br. s., **$H_k$**), 7.66 (1 H, d, *J*=7.7 Hz, **$H_o$**), 7.52 (2 H, d, *J*=8.9 Hz, **$H_j$**), 7.46 (1 H, t, *J*=7.8 Hz, **$H_n$**), 7.24 (6 H, m, **$H_b$**), 7.10 (8 H, m, **$H_c$** + **$H_d$**), 6.92 (2 H, d, *J*=9.0 Hz, **$H_i$**), 6.79 (2 H, d, *J*=8.9 Hz, **$H_e$**), 4.16 (4 H, m, **$H_f$** + **$H_h$**), 3.16 (1 H, s, **$H_p$**), 2.26 (2 H, quin, *J*=6.1 Hz, **$H_g$**), 1.31 (27 H, s, **$H_a$**).

**$^{13}$C-NMR** (126 MHz, $CDCl_3$) $\delta$ = 164.60, 156.61, 156.07, 148.28, 144.13, 139.67, 135.34, 135.05, 132.25, 130.70, 130.40, 128.89, 127.49, 124.02, 122.81, 122.10, 114.91, 112.95, 82.55, 78.43, 64.79, 64.15, 63.03, 34.27, 31.37, 29.34.

There were fewer $^{13}$C signals than anticipated due to coincidence.

**HRMS** (ESI+ve) m/z: 780.44236 ([M-H]$^-$, $C_{55}H_{58}NO_3^+$ requires 780.44222).

**Aromatic iodoalkyne stopper 2.14**



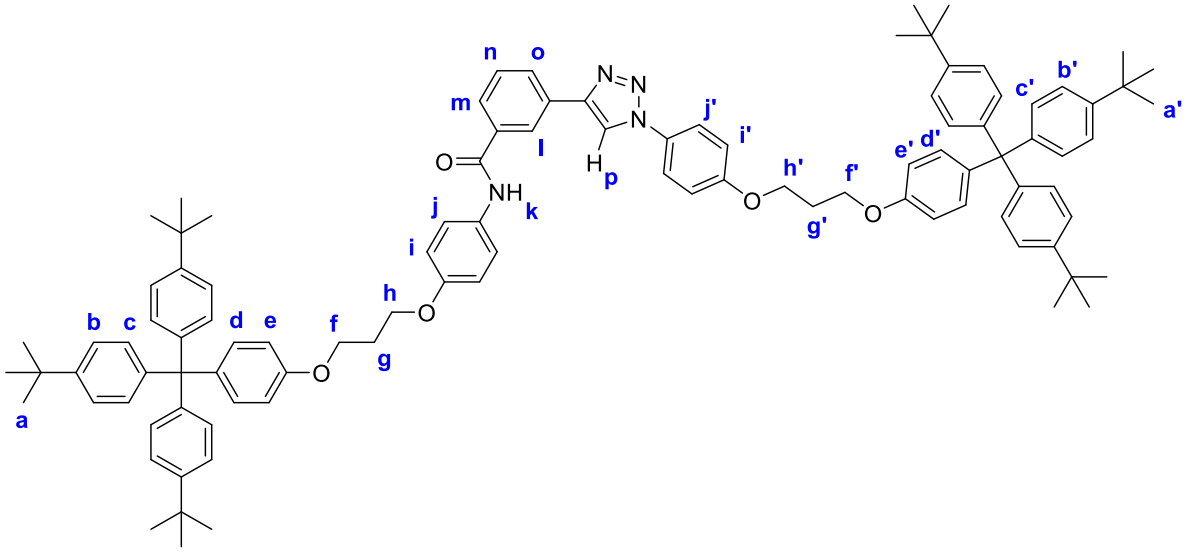

Aromatic alkyne stopper **2.13** (131 mg, 0.17 mmol), *N*-iodosuccinimide (45.3 mg, 0.20 mmol, 1.2 eqs), and acetone (4 mL) were added to a round-bottomed flask. An aqueous solution of $AgNO_3$ (2.94 mg, 0.02 mmol, 0.1 eqs) was added and the mixture was stirred in the dark at room temperature for 3 h. The product was extracted with $CH_2Cl_2$ (3 x 8 mL), after which the combined organic phases were washed with water (10 mL) and brine (10 mL), dried over $MgSO_4$, filtered and the filtrate concentrated under reduced pressure to afford a yellow solid.

Yield: 143 mg (94%)

**$^1$H-NMR** (400 MHz, $CDCl_3$) $\delta$ = 7.89 (1 H, s, $\mathbf{H_l}$), 7.84 (1 H, d, *J*=7.8 Hz, $\mathbf{H_m}$), 7.69 (1 H, br. s., $\mathbf{H_k}$), 7.59 (1 H, d, *J*=7.7 Hz, $\mathbf{H_o}$), 7.52 (2 H, d, *J*=8.8 Hz, $\mathbf{H_j}$), 7.45 (1 H, m, $\mathbf{H_n}$), 7.24 (6 H, d, *J*=8.4 Hz, $\mathbf{H_b}$), 7.09 (8 H, d, *J*=8.4 Hz, $\mathbf{H_c}$ + $\mathbf{H_d}$), 6.92 (2 H, d, *J*=8.9 Hz, $\mathbf{H_i}$), 6.79 (2 H, d, *J*=8.9 Hz, $\mathbf{H_e}$), 4.16 (4 H, m, $\mathbf{H_f}$ + $\mathbf{H_h}$), 2.26 (2 H, quin, *J*=6.0 Hz, $\mathbf{H_g}$), 1.31 (27 H, s, $\mathbf{H_a}$).

This compound was used immediately after isolation, hence no other characterisation data was obtained.

**Neutral amido-triazole HB axle 2.15.HB**




Aromatic azide stopper **2.10** (53.6 mg, 0.08 mmol), aromatic alkyne stopper **2.13** (61.7 mg, 0.08 mmol, 1 eq), DIPEA (0.03 mL, 0.17 mmol, 2.15 eqs), and TBTA (2.09 mg, 0.004 mmol, 0.05 eqs) were dissolved in anhydrous $CH_2Cl_2$ (10 mL). The mixture was degassed, after which $[Cu(CH_3CN)_4]PF_6$ (1.47 mg, 0.004 mmol, 0.05 eqs) was added and the reaction mixture stirred at room temperature for 16 h. After completion, a 0.1 M aqueous solution of EDTA was added (5 mL) and the resulting organic phase washed with brine (10 mL), dried over $MgSO_4$ and filtered. The filtrate was concentrated under reduced pressure and purified by column chromatography ($CH_2Cl_2$, followed by 1% MeOH - $CH_2Cl_2$) to afford **2.15.HB** as a white solid.

Yield: 81.9 mg (71%)

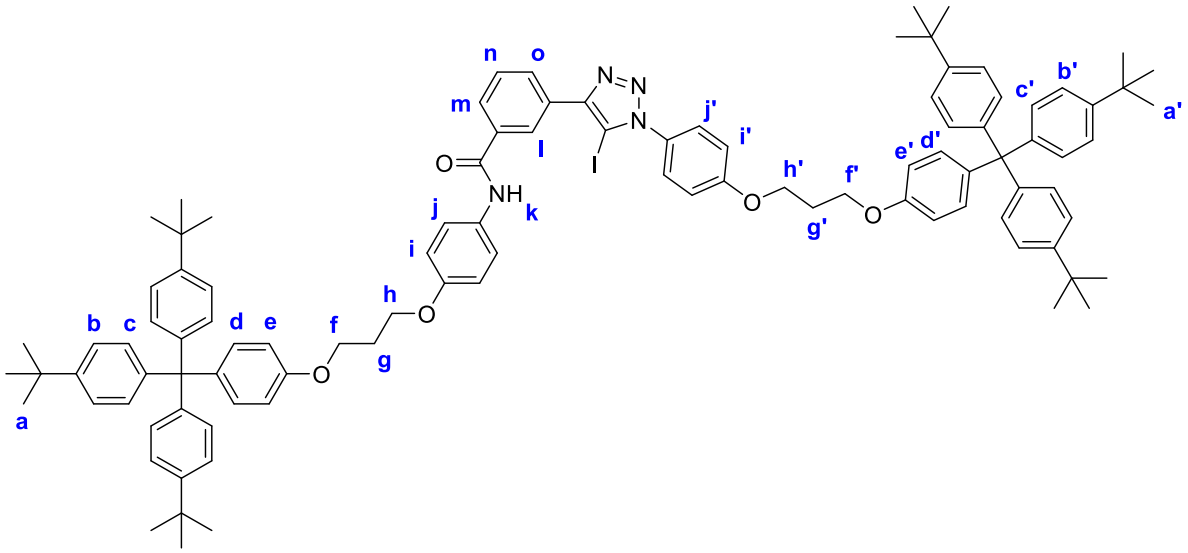
**$^1$H-NMR** (400 MHz, $CDCl_3$) $\delta$ = 8.39 (1 H, s, $\mathbf{H_k}$), 8.19 (1 H, s, $\mathbf{H_p}$), 8.07 (1 H, d, *J*=7.8 Hz, $\mathbf{H_m}$), 7.89 (2 H, m, $\mathbf{H_l}$ + $\mathbf{H_o}$), 7.69 (2 H, m, $\mathbf{H_{j'}}$), 7.58 (3 H, m, $\mathbf{H_n}$ + $\mathbf{H_j}$), 7.24 (12 H, m, $\mathbf{H_b}$ + $\mathbf{H_{b'}}$), 7.09 (18 H, m, $\mathbf{H_c}$ + $\mathbf{H_d}$ + $\mathbf{H_{c'}}$ + $\mathbf{H_{d'}}$+ $\mathbf{H_{i'}}$), 6.94 (2 H, d, *J*=8.9 Hz, $\mathbf{H_i}$), 6.79 (4 H, m, $\mathbf{H_e}$ + $\mathbf{H_{e'}}$), 4.25 (2 H, t, d, *J*=6.1 Hz, $\mathbf{H_{h'}}$), 4.15 (6 H, m, $\mathbf{H_f}$ + $\mathbf{H_h}$ + $\mathbf{H_{f'}}$), 2.29 (4 H, m, $\mathbf{H_g}$ + $\mathbf{H_{g'}}$), 1.30 (54 H, s, $\mathbf{H_a}$ + $\mathbf{H_{a'}}$).

**$^{13}$C-NMR** (101 MHz, $CDCl_3$) $\delta$ = 159.34, 156.63, 156.54, 156.00, 148.33, 148.27, 147.25, 144.14, 144.10, 139.81, 139.66, 132.29, 132.25, 130.97, 130.70, 129.46, 128.83, 127.00, 124.03, 122.19, 122.12, 118.33, 115.41, 114.91, 112.97, 112.95, 64.99, 64.79, 64.18, 63.95, 63.09, 34.27, 31.37.

There were fewer $^{13}$C signals than anticipated due to coincidence.

**HRMS** (ESI+ve) m/z: 1461.86805 ([M+H]$^+$, $C_{101}H_{113}N_4O_5^+$ requires 1461.87055).

**Neutral amido-iodotriazole XB axle 2.15.XB**



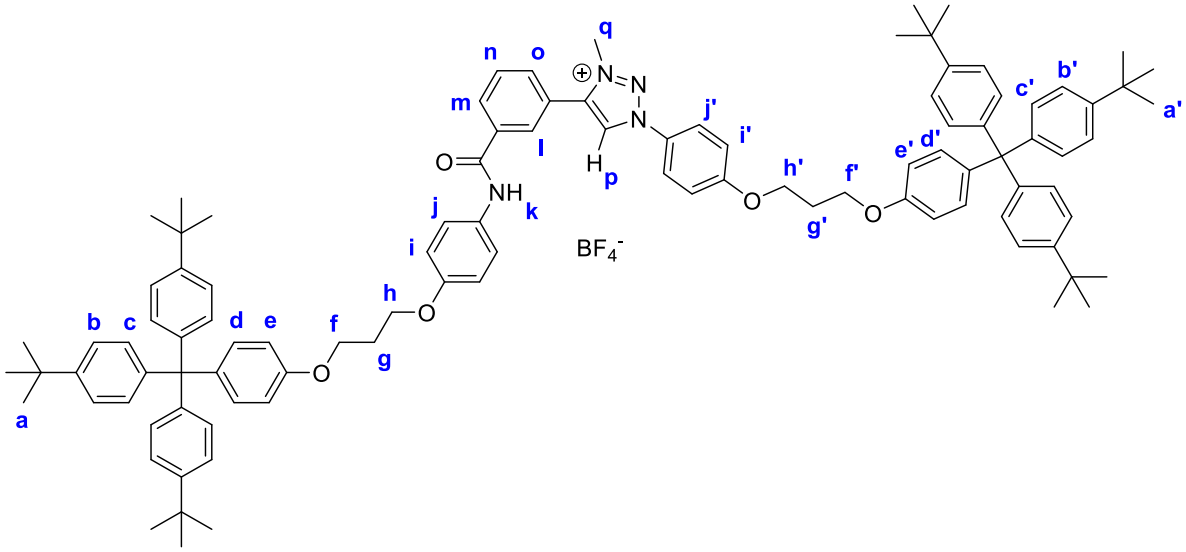

Aromatic azide stopper **2.10** (35.1 mg, 0.04 mmol), aromatic iodoalkyne stopper **2.14** (26.3 mg, 0.04 mmol, 1 eq), and TBTA (6 mg, 0.011 mmol, 0.29 eqs) were dissolved in anhydrous $CH_2Cl_2$ (1 mL). The mixture was degassed, after which $[Cu(CH_3CN)_4]PF_6$ (5.00 mg, 0.013 mmol, 0.35 eqs) was added and the reaction mixture stirred at room temperature for 16 h. After completion, a 0.1 M aqueous solution of EDTA was added (5 mL) and the resulting organic phase washed with brine (10 mL), dried over $MgSO_4$ and filtered. The filtrate was concentrated under reduced pressure and purified by column chromatography ($CH_2Cl_2$, followed by 0.5% MeOH - $CH_2Cl_2$) to afford **2.15.XB** as a yellow solid.

Yield: 44.8 mg (73%)

**$^1$H-NMR** (400 MHz, $CDCl_3$) $\delta$ = 8.52 (1 H, s, $\mathbf{H_k}$), 8.22 (1 H, d, *J*=7.6 Hz, $\mathbf{H_o}$), 7.98 (1 H, d, *J*=7.8 Hz, $\mathbf{H_m}$), 7.89 (1 H, s, $\mathbf{H_l}$), 7.64 (1 H, t, *J*=7.8 Hz, $\mathbf{H_n}$), 7.58 (2 H, d, *J*=8.9 Hz, $\mathbf{H_j}$), 7.46 (2 H, d, *J*=8.8 Hz, $\mathbf{H_{j'}}$), 7.24 (12 H, d, *J*=8.4 Hz, $\mathbf{H_b} + \mathbf{H_{b'}}$), 7.09 (18 H, m, $\mathbf{H_c} + \mathbf{H_d} + \mathbf{H_{c'}} + \mathbf{H_{d'}} + \mathbf{H_{i'}}$), 6.94 (2 H, d, *J*=8.9 Hz, $\mathbf{H_i}$), 6.80 (4 H, m, $\mathbf{H_e} + \mathbf{H_{e'}}$), 4.25 (2 H, t, d, *J*=6.1 Hz, $\mathbf{H_{h'}}$), 4.15 (6 H, m, $\mathbf{H_f} + \mathbf{H_h} + \mathbf{H_{f'}}$), 2.29 (4 H, m, $\mathbf{H_g} + \mathbf{H_{g'}}$), 1.30 (m, 54 H, $\mathbf{H_a} + \mathbf{H_{a'}}$).

**HRMS** (ESI+ve) m/z: 1587.76733 ([M+H]$^+$, $C_{101}H_{112}IN_4O_5^+$ requires 1587.76719).

**Cationic amido-triazolium HB axle 2.16.HB$^{+}$BF$_4^{-}$**




Neutral amido-triazole HB axle **2.15.HB** (66.5 mg, 0.05 mmol) was dissolved in anhydrous $CH_2Cl_2$ (5 mL), after which $[Me_3O]BF_4$ (8.75 mg, 0.06 mmol, 1.3 eqs) was added in one portion. The reaction mixture was stirred at room temperature for 16 h, after which MeOH (4 mL) was added to quench the alkylating agent and the volatiles were removed under reduced pressure. The crude solid was purified by column chromatography (3% MeOH – $CH_2Cl_2$, followed by 10% MeOH - $CH_2Cl_2$) to afford **2.15.HB$^{+}$BF$_4^{-}$** as a white solid.

Yield: 67.6 mg (95%)

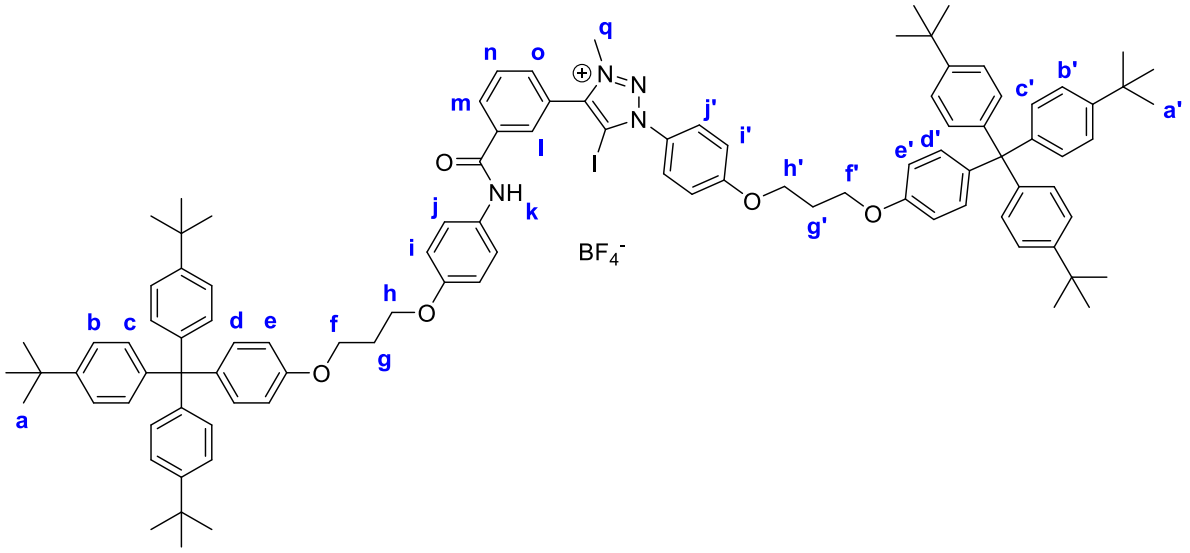
**$^{1}$H-NMR** (400 MHz, $CDCl_3$) $\delta$ = 9.03 (1 H, s, **H$_k$**), 8.99 (1 H, s, **H$_p$**), 8.16 (1 H, s, **H$_l$**), 8.12 (1 H, d, *J*=7.8 Hz, **H$_o$**), 7.76 (4 H, m, **H$_j$** + **H$_{j'}$**), 7.65 (1 H, d, *J*=7.8 Hz, **H$_m$**), 7.53 (1 H, m, **H$_n$**), 7.22 (12 H, d, *J*=7.5 Hz, **H$_b$** + **H$_{b'}$**), 7.09 (16 H, m, **H$_c$** + **H$_d$** + **H$_{c'}$** + **H$_{d'}$**), 7.00 (2 H, d, *J*=9.0 Hz, **H$_i$**), 6.88 (2 H, d, *J*=9.0 Hz, **H$_{i'}$**), 6.79 (4 H, m, **H$_e$** + **H$_{e'}$**), 4.30 (3 H, s, **H$_q$**), 4.21 (2 H, t, *J*=6.1 Hz, **H$_{h'}$**), 4.13 (6 H, m, **H$_f$** + **H$_h$** + **H$_{f'}$**), 2.25 (4 H, m, **H$_g$** + **H$_{g'}$**), 1.30 (54 H, s, **H$_a$** + **H$_{a'}$**).

**$^{13}$C-NMR** (101 MHz, $CDCl_3$) $\delta$ = 163.60, 161.59, 156.64, 156.49, 155.62, 148.31, 148.31, 148.23, 144.15, 144.11, 143.55, 139.83, 139.61, 132.31, 132.24, 131.71, 130.71, 129.86, 127.86, 127.66, 127.41, 125.93, 124.02, 122.72, 121.77, 121.20, 115.88, 114.63, 112.96, 65.84, 65.25, 64.70, 64.25, 63.80, 63.03, 38.73, 34.27, 31.37, 29.69, 29.35, 29.09, 15.26.

There were fewer $^{13}$C signals than anticipated due to coincidence.

**HRMS** (ESI+ve) m/z: 1475.88620 ([M-BF$_4^{-}$]$^{+}$, $C_{102}H_{115}N_4O_5^{+}$ requires 1475.88620).

**Cationic amido-iodotriazolium XB axle 2.16.XB$^{+}$BF$_4^{-}$**




Neutral amido-iodotriazole XB axle **2.15.XB** (75.2 mg, 0.05 mmol) was dissolved in anhydrous $CH_2Cl_2$ (5 mL), after which $[Me_3O]BF_4$ (9.11 mg, 0.06 mmol, 1.3 eqs) was added in one portion. The reaction mixture was stirred at room temperature for 16 h, after which MeOH was added to quench the alkylating agent and the volatiles were removed under reduced pressure. The crude solid was purified by column chromatography ($CH_2Cl_2$, followed by 0.5% MeOH – $CH_2Cl_2$, and 10% MeOH - $CH_2Cl_2$) to afford **2.16.XB$^{+}$BF$_4^{-}$** as a white solid.

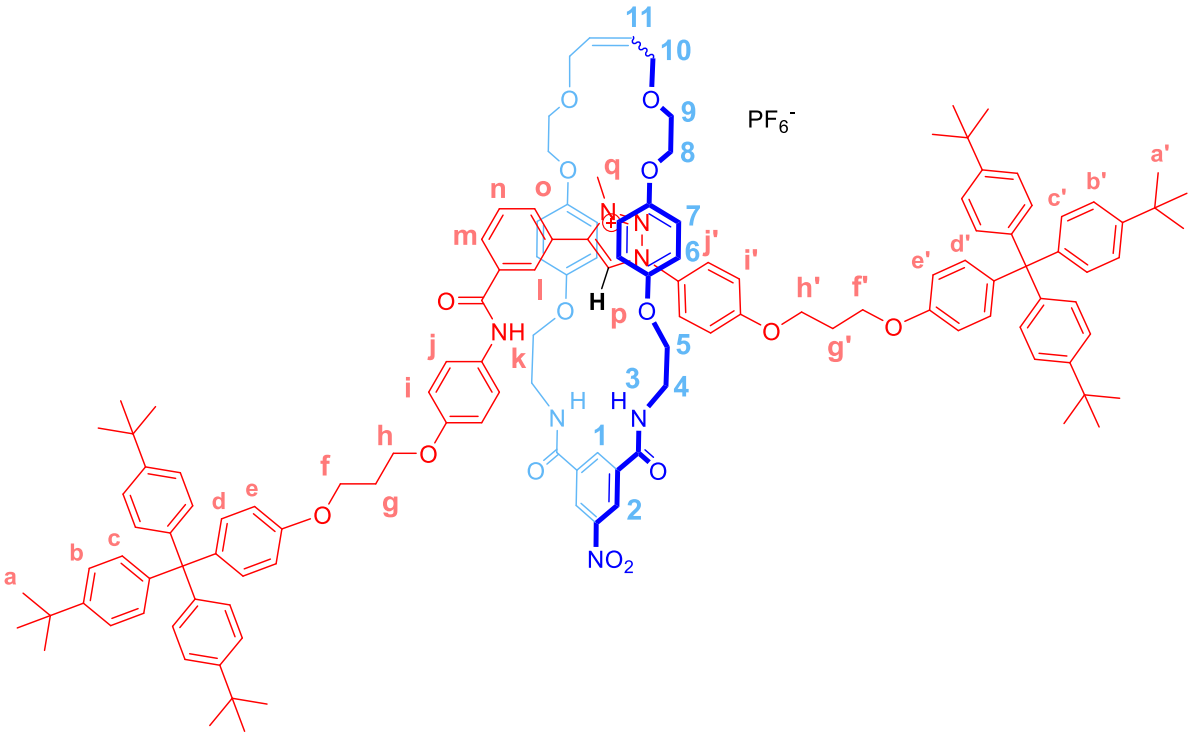
Yield: 76.7 mg (96%)

**$^{1}$H-NMR** (400 MHz, $CDCl_3$) $\delta$ = 8.99 (1 H, s, **H$_l$**), 8.42 (1 H, s, **H$_k$**), 8.39 (1 H, d, *J*=8.3 Hz, **H$_o$**), 7.77 (3 H, m, **H$_n$** + **H$_{j'}$**), 7.62 (3 H, m, **H$_j$** + **H$_m$**), 7.23 (12 H, d, *J*=8.6 Hz, **H$_b$** + **H$_{b'}$**), 7.09 (18 H, m, **H$_c$** + **H$_d$** + **H$_{c'}$** + **H$_{d'}$**+ **H$_i$**), 6.90 (2 H, d, *J*=9.1 Hz, **H$_{i'}$**), 6.79 (4 H, m, **H$_e$** + **H$_{e'}$**), 4.33 (3 H, s, **H$_q$**), 4.28 (2 H, t, *J*=6.1 Hz, **H$_{h'}$**), 4.15 (6 H, m, **H$_f$** + **H$_h$** + **H$_{f'}$**), 2.29 (4 H, m, **H$_g$** + **H$_{g'}$**), 1.30 (54 H, s, **H$_a$** + **H$_{a'}$**).

**$^{19}$F-NMR** (377 MHz, $CDCl_3$) $\delta$ = - 152.41.

**HRMS** (ESI+ve) m/z: 1601.77917 ($[M\text{-}BF_4^-]^+$, $C_{102}H_{114}IN_4O_5^+$ requires 1601.78284).

**Amido-triazolium HB [2]rotaxane 2.18.HB$^+$PF$_6^-$**



Cationic amido-triazolium HB axle **2.16.HB$^+$BF$_4^-$** (58.2 mg, 0.037 mmol), nitroisophthalamide bis-alkene **2.17** (29.0 mg, 0.045 mmol, 1.2 eqs), and tetrabutylammonium chloride (10.3 mg, 0.037 mmol, 1 eq) were dissolved in anhydrous $CH_2Cl_2$ (11 mL) and stirred for 20 minutes. After complex formation, Grubbs' 2$^{nd}$ generation catalyst (2.90 mg, 10% w/w) was added and the mixture allowed to stir at room temperature for 16 h, after which a subsequent portion of catalyst was added and the mixture stirred for a further 16 h. Iterative preparative thin layer chromatography (50% EtOAc - $CHCl_3$) afforded **2.16.HB$^+$Cl$^-$** as a white solid, which was redissolved in $CH_2Cl_2$ (4 mL) and repeatedly washed with 0.1 M $NH_4PF_6$ (10 x 5 mL) to give **2.16.HB$^+$PF$_6^-$** as a white solid.

Yield: 22.1 mg (26%)

**$^1$H-NMR** (400 MHz, 1:1 $CD_3OD$:$CDCl_3$) $\delta$ = 9.29 (1 H, s, **H$_p$**), 8.85 (3 H, m, **H$_1$** + **H$_2$**), 8.09 (1 H, d, *J*=7.7 Hz, **H$_o$**), 7.85 (1 H, s, **H$_l$**), 7.75 (2 H, d, *J*=9.0 Hz, **H$_j$**), 7.64 (1 H, m, **H$_n$**), 7.21 (12 H, m, **H$_b$** + **H$_{b'}$**), 7.06 (16 H, m, **H$_c$** + **H$_d$** + **H$_{c'}$** + **H$_{d'}$**), 6.90 (2 H, d, *J*=9.0 Hz, **H$_i$**), 6.81 (6 H, m, **H$_e$** + **H$_{e'}$** + **H$_{i'}$**), 6.40 (4 H, m, **H$_6$**), 6.29 (4 H, m, **H$_7$**), 5.91 (2 H, m, **H$_{11}$**), 4.24 (3 H, m, **H$_q$**), 3.83 (24 H, m, **H$_f$** + **H$_h$** + **H$_{f'}$** + **H$_{h'}$** + **H$_4$** + **H$_5$**), 2.21 (4 H, m, **H$_g$** + **H$_{g'}$**), 1.79 (12 H, m, **H$_{8\text{-}10}$**), 1.27 (54 H, s, **H$_a$** + **H$_{a'}$**).

**H$_m$** and **H$_{j'}$** were obscured by the solvent signal.

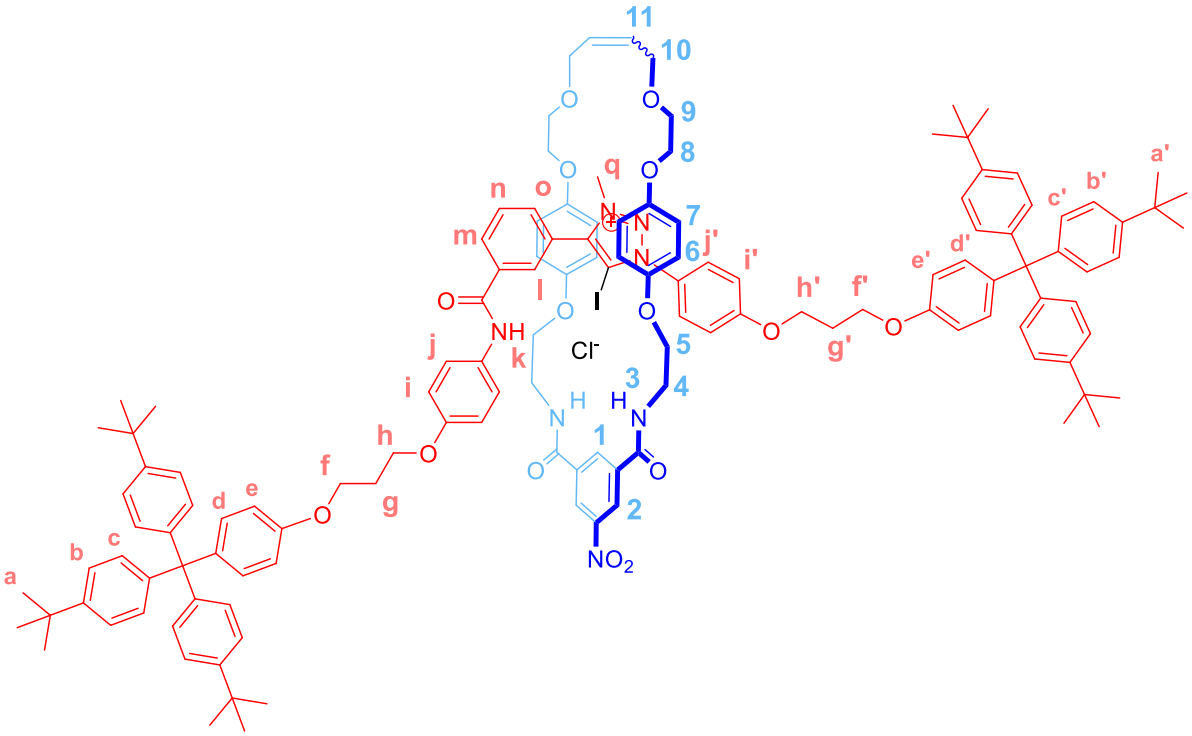
**$^{19}$F-NMR** (377 MHz, $CDCl_3$) $\delta$ = - 68.77 (6 F, d)

**$^{13}$C-NMR** (101 MHz, 1:1 $CD_3OD$:$CDCl_3$) $\delta$ = 166.10, 162.40, 157.45, 157.37, 157.02, 153.48, 153.21, 149.39, 149.06, 149.04, 145.03, 145.01, 143.33, 140.65, 140.51, 136.83, 136.63, 133.00, 132.95, 131.62, 131.58, 131.46, 130.39, 130.22, 129.66, 128.19, 126.81, 126.16, 124.77, 123.71, 123.09, 122.69, 116.53, 115.60, 115.33, 115.20, 113.81, 71.53, 69.93, 68.51, 66.87, 65.95, 65.54, 65.06, 64.59, 63.82, 40.83, 40.23, 34.88, 32.85, 31.82.

There were fewer $^{13}$C signals than anticipated due to coincidence.

**HRMS** (ESI+ve) m/z: 2098.11807 ([M-$BF_4^-$]$^+$, $C_{134}H_{150}N_7O_{15}^+$ requires 2098.12180).

**Amido-iodotriazolium XB [2]rotaxane 2.18.XB$^+$Cl$^-$**




Cationic amido-iodotriazolium XB axle **2.16.XB$^+$BF$_4^-$** (40.6 mg, 0.024 mmol), nitroisophthalamide bis-alkene **2.17** (18.7 mg, 0.029 mmol, 1.2 eqs), and tetrabutylammonium chloride (6.68 mg, 0.024 mmol, 1 eq) were dissolved in anhydrous $CH_2Cl_2$ (7.25 mL) and stirred for 20 minutes. After complex formation, Grubbs' 2$^{nd}$ generation catalyst (1.87 mg, 10% w/w) was added and the mixture allowed to stir at room temperature for 16 h, after which a subsequent portion of catalyst was added and the mixture stirred for a further 16 h. Iterative preparative thin layer chromatography (2% MeOH – $CHCl_3$) afforded **2.16.XB$^+$Cl$^-$** as a white solid.

Yield: 2.85 mg (5%)

**$^{1}$H-NMR** (400 MHz, 1:1 $CD_3OD$:$CDCl_3$) $\delta$ = 9.19 (1 H, s, $\mathbf{H_l}$), 9.11 (2 H, s, $\mathbf{H_2}$), 8.85 (1 H, s, $\mathbf{H_1}$), 8.65 (2 H, m, $\mathbf{H_3}$), 8.31 (1 H, d, *J*=4.8 Hz, $\mathbf{H_o}$), 7.80 (1 H, br. s., $\mathbf{H_k}$), 7.65 (3 H, m, $\mathbf{H_n}$ + $\mathbf{H_{j'}}$), 7.42 (2 H, d, *J*=8.2 Hz, $\mathbf{H_j}$), 7.24 (12 H, m, $\mathbf{H_b}$ + $\mathbf{H_{b'}}$), 7.09 (16 H, m, $\mathbf{H_c}$ + $\mathbf{H_d}$ + $\mathbf{H_{c'}}$ + $\mathbf{H_{d'}}$), 6.97 (2 H, d, *J*=8.7 Hz, $\mathbf{H_{i'}}$), 6.80 (4 H, m, $\mathbf{H_e}$ + $\mathbf{H_{e'}}$), 6.74 (2 H, m, $\mathbf{H_i}$), 6.53 (4 H, d, *J*=9.2 Hz, $\mathbf{H_6}$), 6.30 (4 H, d, *J*=8.9 Hz, $\mathbf{H_7}$), 5.80 (2 H, m, $\mathbf{H_{11}}$), 4.31 (3 H, s, $\mathbf{H_q}$), 4.22 – 3.37 (28 H, m, $\mathbf{H_f}$ + $\mathbf{H_h}$ + $\mathbf{H_{f'}}$ + $\mathbf{H_{h'}}$ + $\mathbf{H_4}$ + $\mathbf{H_5}$ + $\mathbf{H_{8\text{-}10}}$), 2.22 (4 H, m, $\mathbf{H_g}$ + $\mathbf{H_{g'}}$), 1.31 (54 H, s, $\mathbf{H_a}$ + $\mathbf{H_{a'}}$).

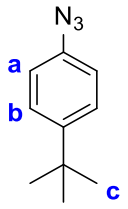
$\mathbf{H_m}$ was obscured by the solvent signal.

**$^{13}$C-NMR** (126 MHz, $CDCl_3$) $\delta$ = 164.60, 163.81, 161.16, 156.58, 156.36, 153.14, 151.05, 148.82, 148.32, 148.23, 144.17, 144.09, 139.76, 139.63, 135.98, 135.31, 132.29, 132.26, 130.73, 130.69, 130.37, 128.97, 127.37, 127.12, 126.45, 126.23, 124.04, 123.05, 121.91, 70.31, 68.71, 67.14, 66.93, 65.32, 64.71, 64.05, 63.67, 63.03, 40.48, 39.21, 34.28, 31.92, 31.37, 30.93, 29.70, 29.35, 29.34, 28.85, 22.69.

There were fewer $^{13}$C signals than anticipated due to coincidence.

**HRMS** (ESI+ve) m/z: 2223.01465 ($[M\text{-}Cl^-]^+$, $C_{134}H_{149}IN_7O_{15}^+$ requires 2223.01509).

**4-(*tert*-Butyl)phenyl azide 2.20** [6]

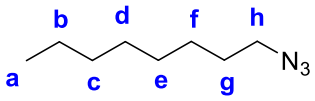



4-(*tert*-Butyl)aniline (1 mL, 6.28 mmol) was added to an aqueous 17% HCl solution (40 mL), after which EtOH (25 mL) was added and the mixture heated. After dissolution of all solids, the flask was cooled to 0 °C in an ice bath. $NaNO_2$ (866 mg, 12.5 mmol, 2 eqs) was then added portionwise and the mixture left to stir at 0 °C for 45 minutes. Subsequently, $NaN_3$ (816 mg, 12.5 mmol, 2 eqs) was added portionwise and the reaction mixture allowed to warm to room temperature and stirred for 16 h. Water (40 mL) was then added and the product extracted with $Et_2O$ (3 x 40 mL). The combined organic phases were washed with a saturated solution of $NaHCO_3$ (3 x 40 mL) and brine (40 mL), dried over $MgSO_4$, filtered and the filtrate concentrated under reduced pressure to afford an orange-red liquid.

Yield: 1.05 g (95%)

**$^1$H-NMR** (400 MHz, $CDCl_3$) $\delta$ = 7.38 (2 H, d, *J*=8.7 Hz, $\mathbf{H_b}$), 6.98 (2 H, d, *J*=8.7 Hz, $\mathbf{H_a}$), 1.32 (9 H, s, $\mathbf{H_c}$).

**Octyl azide 2.21** [7]

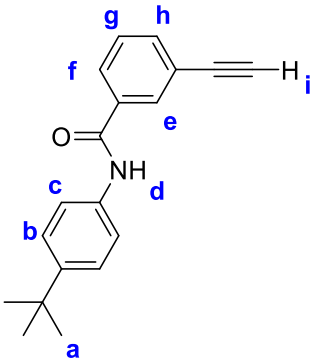



Octyl bromide (1.8 mL, 10.4 mmol) and $NaN_3$ (793 mg, 12.2 mmol, 1.17 eqs) were dissolved in DMSO (30 mL). The reaction mixture was stirred at room temperature for 16 h, after which it was diluted with water (50 mL) and the product extracted with $Et_2O$ (3 x 60 mL). The combined organic layers were washed with water (50 mL) and brine (50 mL), dried over $MgSO_4$, filtered and the filtrate concentrated under reduced pressure to afford a pale yellow liquid.

Yield: 1.46 g (90%)

**$^1$H-NMR** (400 MHz, $CDCl_3$) $\delta$ = 3.26 (2 H, t, *J*=7.0 Hz, $\mathbf{H_h}$), 1.60 (2 H, quin, *J*=7.2 Hz, $\mathbf{H_g}$), 1.35 (10 H, m, $\mathbf{H_{b\text{-}f}}$), 0.89 (3 H, m, $\mathbf{H_a}$).

**Aromatic alkyne 2.22**




4-(tert-butyl)aniline (0.1 mL, 0.63 mmol), 3-ethynylbenzoic acid (91.8 mg, 0.63 mmol, 1 eq), and DMAP (cat.) were suspended in anhydrous $CH_2Cl_2$ (4 mL). To this suspension EDC·HCl (145 mg, 0.76 mmol, 1.2 eqs) was added and the reaction mixture stirred at reflux for 16 h.

After completion, the resulting solution was washed sequentially with dilute HCl (10 mL), saturated $NaHCO_3$ (10 mL), water (10 mL), and brine (15 mL), dried over $MgSO_4$, filtered and the filtrate concentrated under reduced pressure to afford a yellow solid.

Yield: 126 mg (73%)

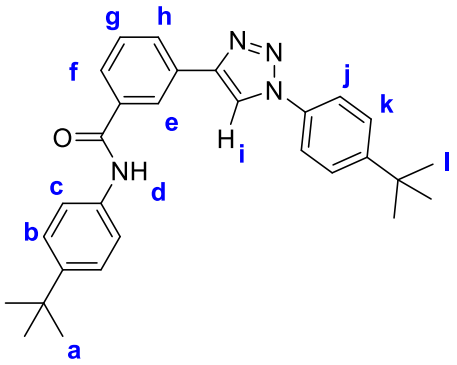
**$^1$H-NMR** (400 MHz, $CDCl_3$) $\delta$ = 7.96 (1 H, s, **$H_e$**), 7.91 (1 H, br. s., **$H_d$**), 7.85 (1 H, d, *J*=7.8 Hz, **$H_f$**), 7.64 (1 H, d, *J*=7.7 Hz, **$H_h$**), 7.55 (2 H, d, *J*=8.6 Hz, **$H_c$**), 7.43 (1 H, t, *J*=8.1 Hz, **$H_g$**), 7.39 (2 H, d, *J*=8.6 Hz, **$H_b$**), 3.15 (1 H, s, **$H_i$**), 1.33 (9 H, s, **$H_a$**).

**$^{13}$C-NMR** (126 MHz, $CDCl_3$) $\delta$ = 147.85, 135.42, 135.13, 135.01, 130.41, 128.94, 127.50, 125.98, 122.89, 120.04, 82.54, 78.47, 34.44, 31.35.

There were fewer $^{13}$C signals than anticipated due to coincidence.

**HRMS** (ESI+ve) m/z: 278.15387 ($[M+H]^+$, $C_{19}H_{20}NO^+$ requires 278.15394).

**Aromatic amido-triazole receptor 2.23**




Aromatic alkyne **2.22** (40.1 mg, 0.14 mmol), 4-(tert-butyl)phenyl azide **2.20** (51.0 mg, 0.29 mmol, 2 eqs), DIPEA (0.04 mL, 0.22 mmol, 1.5 eqs), and TBTA (3.7 mg, 0.007 mmol, 0.05 eqs) were dissolved in anhydrous $CH_2Cl_2$ (3 mL). The mixture was degassed, after which $[Cu(CH_3CN)_4]PF_6$ (2.60 mg, 0.007 mmol, 0.05 eqs) was added and the reaction mixture stirred at room temperature for 16 h. After completion, a 0.1 M aqueous solution of EDTA (5 mL) was added and the resulting organic phase washed with brine (10 mL), dried over $MgSO_4$ and filtered. The filtrate was concentrated under reduced pressure and purified by column chromatography ($CH_2Cl_2$) to afford **2.25** as a white solid.

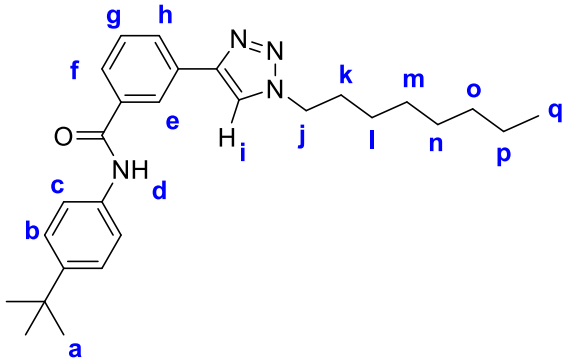
Yield: 51.1 mg (78%)

**$^{1}$H-NMR** (400 MHz, $CDCl_3$) δ = 8.41 (1 H, s, $\mathbf{H_e}$), 8.27 (1 H, s, $\mathbf{H_i}$), 8.10 (1 H, d, *J*=7.7 Hz, $\mathbf{H_h}$), 8.02 (1 H, s, $\mathbf{H_d}$), 7.89 (1 H, d, *J*=7.9 Hz, $\mathbf{H_f}$), 7.72 (2 H, d, *J*=8.8 Hz, $\mathbf{H_j}$), 7.60 (5 H, m, $\mathbf{H_c}$ + $\mathbf{H_g}$ + $\mathbf{H_k}$), 7.42 (2 H, d, *J*=8.7 Hz, $\mathbf{H_b}$), 1.39 (9 H, s, $\mathbf{H_a}$), 1.34 (9 H, s, $\mathbf{H_l}$).

**$^{13}$C-NMR** (126 MHz, $CDCl_3$) δ = 152.42, 147.71, 147.30, 135.73, 135.21, 134.50, 131.01, 129.48, 128.93, 126.98, 126.75, 125.96, 124.17, 120.27, 120.08, 118.16, 34.84, 34.44, 31.37, 31.26.

**HRMS** (ESI+ve) m/z: 453.26486 ($[M+H]^+$, $C_{29}H_{33}N_4O^+$ requires 453.26489).

**Aliphatic amido-triazole receptor 2.24**




Aromatic alkyne **2.22** (22.3 mg, 0.08 mmol), octyl azide **2.21** (25.0 mg, 0.16 mmol, 2 eqs), DIPEA (0.02 mL, 0.12 mmol, 1.5 eqs), and TBTA (2.10 mg, 0.004 mmol, 0.05 eqs) were dissolved in anhydrous $CH_2Cl_2$ (1 mL). The mixture was degassed, after which $[Cu(CH_3CN)_4]PF_6$ (1.50 mg, 0.004 mmol, 0.05 eqs) was added and the reaction mixture stirred at room temperature for 16 h. After completion, a 0.1 M aqueous solution of EDTA (5 mL) was added and the resulting organic phase washed with brine (10 mL), dried over $MgSO_4$ and filtered. The filtrate was concentrated under reduced pressure and purified by column chromatography ($CH_2Cl_2$) to afford **2.25** as a white solid.

Yield: 25.5 mg (74%)

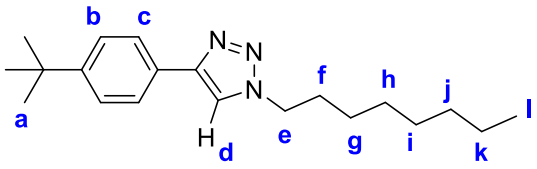
**$^{1}$H-NMR** (500 MHz, $CDCl_3$) δ = 8.31 (1 H, s, $\mathbf{H_e}$), 8.07 (1 H, br. s., $\mathbf{H_d}$), 8.00 (1 H, d, *J*=7.8 Hz, $\mathbf{H_h}$), 7.84 (2 H, m, $\mathbf{H_f}$ + $\mathbf{H_i}$), 7.61 (2 H, d, *J*=8.5 Hz, $\mathbf{H_c}$), 7.53 (1 H, m, $\mathbf{H_g}$), 7.40 (2 H, d, *J*=8.5 Hz, $\mathbf{H_b}$), 4.41 (2 H, t, *J*=7.2 Hz, $\mathbf{H_j}$), 1.94 (2 H, m, $\mathbf{H_k}$), 1.32 (19 H, m, $\mathbf{H_a}$ + $\mathbf{H_{l\text{-}p}}$), 0.88 (3 H, t, *J*=6.9 Hz, $\mathbf{H_q}$).

**$^{13}$C-NMR** (126 MHz, $CDCl_3$) δ = 147.85, 135.42, 135.13, 135.01, 130.41, 128.94, 127.50, 125.98, 122.89, 120.04, 82.54, 78.47, 34.44, 31.35.

There were fewer $^{13}$C signals than anticipated due to coincidence.

**HRMS** (ESI+ve) m/z: 433.29596 ([M+H]$^+$, $C_{27}H_{37}NO_4^+$ requires 433.29619).

**Mixed aliphatic – aromatic triazole receptor 2.25**




1-Decyne (0.05 mL, 0.28 mmol), 4-(*tert*-butyl)phenyl azide **2.20** (97.0 mg, 0.55 mmol, 2 eqs), DIPEA (0.07 mL, 0.42 mmol, 1.5 eqs), and TBTA (7.00 mg, 0.01 mmol, 0.05 eqs) were dissolved in anhydrous $CH_2Cl_2$ (3 mL). The mixture was degassed, after which $[Cu(CH_3CN)_4]PF_6$ (5.00 mg, 0.01 mmol, 0.05 eqs) was added and the reaction mixture stirred at room temperature for 16 h. After completion, a 0.1 M aqueous solution of EDTA (6 mL) was added and the resulting organic phase washed with brine (10 mL), dried over $MgSO_4$ and filtered. The filtrate was concentrated under reduced pressure and purified by column chromatography ($CH_2Cl_2$) to afford **2.25** as a white solid.

Yield: 70.1 mg (81%)

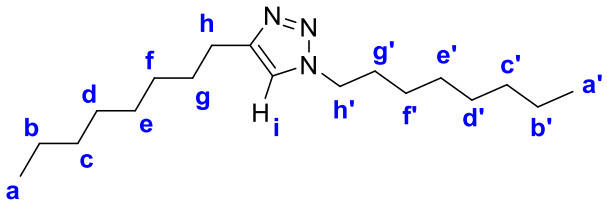
**$^1$H-NMR** (400 MHz, $CDCl_3$) δ = 7.69 (1 H, s, **$H_d$**), 7.64 (2 H, d, *J*=8.7 Hz, **$H_c$**), 7.51 (2 H, d, *J*=8.7 Hz, **$H_b$**), 2.79 (2 H, t, *J*=7.7 Hz, **$H_e$**), 1.73 (2 H, quin, *J*=7.5 Hz, **$H_f$**), 1.34 (19 H, m, **$H_a$** + **$H_{g-k}$**), 0.88 (3 H, t, *J*=6.7 Hz, **$H_l$**).

**$^{13}$C-NMR** (126 MHz, $CDCl_3$) δ = 151.66, 149.00, 134.87, 126.47, 120.07, 118.73, 34.70, 31.82, 31.24, 29.40, 29.32, 29.25, 29.19, 25.67, 22.62, 14.06.

There were fewer $^{13}$C signals than anticipated due to coincidence.

**HRMS** (ESI+ve) m/z: 314.25891 ([M+H]$^+$, $C_{20}H_{32}N_3^+$ requires 314.25907).

**Fully aliphatic triazole receptor 2.26**




Octyl azide **2.21** (58.0 mg, 0.37 mmol), 1-decyne (0.13 mL, 0.75 mmol, 2 eqs), DIPEA (0.2 mL, 1.11 mmol, 3 eqs), and TBTA (10.0 mg, 0.04 mmol, 0.05 eqs) were dissolved in anhydrous $CH_2Cl_2$ (2 mL). The mixture was degassed, after which $[Cu(CH_3CN)_4]PF_6$ (14.0 mg, 0.04 mmol, 0.1 eqs) was added and the reaction mixture stirred at room temperature for 16 h. After completion, a 0.1 M aqueous solution of EDTA (10 mL) was added and the resulting organic phase washed with brine (10 mL), dried over $MgSO_4$ and filtered. The filtrate was concentrated under reduced pressure and purified by column chromatography ($CH_2Cl_2$) to afford **2.25** as a white solid.

Yield: 82.8 mg (76%)

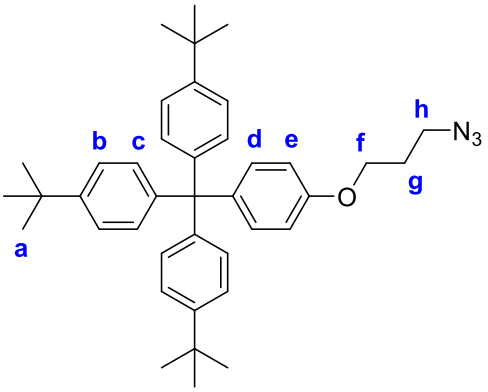
**$^1$H-NMR** (400 MHz, $CDCl_3$) $\delta$ = 7.24 (1 H, s, $\mathbf{H_i}$), 4.30 (2 H, t, *J*=7.2 Hz, $\mathbf{H_h}$), 2.70 (2 H, t, *J*=7.8 Hz, $\mathbf{H_{h'}}$), 1.89 (2 H, m, $\mathbf{H_g}$), 1.66 (2 H, quin, *J*=7.4 Hz, $\mathbf{H_{g'}}$), 1.29 (20 H, m, $\mathbf{H_{b\text{-}f}} + \mathbf{H_{b'\text{-}f'}}$), 0.88 (6 H, t, *J*=6.7 Hz, $\mathbf{H_a} + \mathbf{H_{a'}}$).

**$^{13}$C-NMR** (101 MHz, $CDCl_3$) $\delta$ = 148.42, 120.28, 50.15, 31.84, 31.69, 30.91, 30.34, 29.49, 29.33, 29.26, 29.20, 29.03, 28.96, 26.50, 25.70, 22.64, 22.58, 14.08, 14.04.

An extra $^{13}$C signal was observed.

**HRMS** (ESI+ve) m/z: 294.29093 ($[M+H]^+$, $C_{18}H_{36}N_3^+$ requires 294.29037).

**Aliphatic azide stopper 2.27** [2]

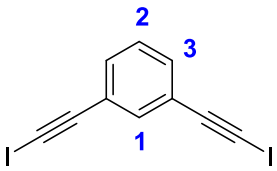



Bromide stopper **2.7** (1.71 g, 2.73 mmol) and $NaN_3$ (1.07 g, 16.5 mmol, 6 eqs) were suspended in anhydrous DMF (25 mL) and the reaction mixture was stirred at 80 °C for 16 h. This was subsequently allowed to cool to room temperature, after which water (50 mL) was added and the resulting precipitate separated through filtration under reduced pressure and washed with water. The crude solid was purified by column chromatography (25% $CH_2Cl_2$ - hexanes) to afford **2.27** as a white solid.

Yield: 801 mg (50%)

**$^1$H-NMR** (400 MHz, $CDCl_3$) $\delta$ = 7.24 (6 H, d, *J*=8.6 Hz, $\mathbf{H_b}$), 7.10 (8 H, m, $\mathbf{H_c}$ + $\mathbf{H_d}$), 6.77 (2 H, d, *J*=8.9 Hz, $\mathbf{H_e}$), 4.04 (2 H, t, *J*=5.9 Hz, $\mathbf{H_f}$), 3.52 (2 H, t, *J*=6.7 Hz, $\mathbf{H_h}$), 2.05 (2 H, quin, *J*=6.3 Hz, $\mathbf{H_g}$), 1.31 (27 H, s, $\mathbf{H_a}$).

**1,3-Bis(iodoethynyl)benzene 2.28** [8]



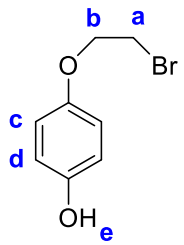

1,3-Diethynylbenzene (0.3 mL, 2.26 mmol) was dissolved in anhydrous THF (5 mL) and cooled to -78 °C. A 2.5 M solution of n-BuLi in hexanes (4.5 mL, 5 eqs) was added dropwise, then the mixture was stirred for 30 minutes. Subsequently, a solution of $I_2$ (2.86 g, 11.3 mmol) in anhydrous THF (15 mL) was added dropwise, then the mixture was stirred for a further 60 minutes. This was allowed to slowly warm to room temperature, after which it was poured onto a saturated aqueous solution of $Na_2S_2O_3$ (50 mL) and the product extracted

with $CH_2Cl_2$ (3 x 50 mL). The organic layer was washed with water (50 mL) and brine (50 mL), dried over $MgSO_4$ and filtered. The filtrate was concentrated under reduced pressure and purified by column chromatography ($CH_2Cl_2$) to afford **2.28** as orange-brown crystals.

Yield: 773 mg (91%)

**$^1$H-NMR** (400 MHz, $CDCl_3$) $\delta$ = 7.50 (1 H, s, **$H_1$**), 7.39 (2 H, d, *J*=7.7 Hz, **$H_3$**), 7.27 (1 H, m, **$H_3$**).

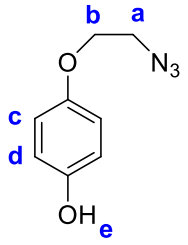
**Bromo-phenol 2.29** [9]




Hydroquinone (2.12 g, 19.3 mmol) and finely powdered KOH (1.08 g, 19.3 mmol, 1 eq) were dissolved in degassed MeOH (50 ml) and the mixture was stirred at room temperature for 30 minutes under an atmosphere of $N_2$. Subsequently, 1,2-dibromoethane (2 mL, 34.7 mmol, 1.20 eqs) was added dropwise, after which the reaction mixture was heated to reflux and stirred over 2 days. The volatiles were removed under reduced pressure and the resulting solid suspended in $CHCl_3$ (50 mL), filtered and the filtrate concentrated under reduced pressure to give **2.29** (contaminated with hydroquinone) as a light brown solid. This was used without further purification.

**$^1$H-NMR** (400 MHz, $CDCl_3$) $\delta$ = 6.79 (4 H, m, **$H_c$** + **$H_d$**), 4.55 (1 H, s, **$H_e$**), 4.24 (2 H, m, **$H_b$**), 3.62 (2 H, m, **$H_a$**).

**Azido-phenol 2.30** [9]

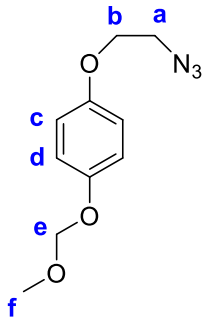



To a solution of crude bromo-phenol **2.29** (825 mg, ~ 3.78 mmol) in DMSO (5 mL) was added $NaN_3$ (494 mg, 7.60 mmol, 2 eqs) portionwise. The reaction mixture was stirred at room temperature for 16 h, after which water (25 mL) was added and the product extracted repeatedly with $Et_2O$ (5 x 20 mL). The combined organic layers were washed with brine (25 mL), dried over $MgSO_4$ and filtered. The filtrate was concentrated under reduced pressure and purified by column chromatography ($CH_2Cl_2$) to afford **2.30** as a pale yellow liquid which solidified on standing to give a yellow solid.

Yield: 485 mg (~ 71%)

**$^1$H-NMR** (400 MHz, $CDCl_3$) $\delta$ = 6.80 (4 H, m, $\mathbf{H_c}$ + $\mathbf{H_d}$), 4.73 (1 H, s, $\mathbf{H_e}$), 4.10 (2 H, t, *J*=5.0 Hz, $\mathbf{H_b}$), 3.57 (2 H, t, *J*=5.0 Hz, $\mathbf{H_a}$).

**MOM-protected azido-phenol 2.31** [10]



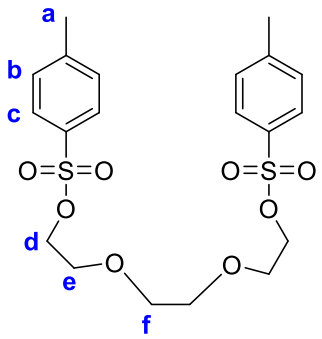

Azido-phenol **2.30** (485 mg, 2.71 mmol) and DIPEA (0.71 mL, 4.06 mmol, 1.5 eqs) were dissolved in anhydrous $CH_2Cl_2$ (10 mL) and cooled to 0 °C in an ice bath, after which chloromethyl methyl chloride (0.31 mL, 4.06 mmol, 1.5 eqs) was added dropwise under an atmosphere of $N_2$. The reaction mixture was allowed to warm to room temperature and stirred for 16 h, following which water (10 mL) was added and the two layers separated. The organic phase was washed with water (10 mL) and saturated $NaHCO_3$ (15 mL), dried over

$MgSO_4$ and filtered. The filtrate was concentrated under reduced pressure and purified by column chromatography ($CH_2Cl_2$) to afford **2.31** as a very pale green liquid.

Yield: 439 mg (66%)

**$^1$H-NMR** (400 MHz, $CDCl_3$) $\delta$ = 6.99 (2 H, m, $\mathbf{H_d}$), 6.87 (2 H, m, $\mathbf{H_c}$), 5.12 (2 H, s, $\mathbf{H_e}$), 4.12 (2 H, m, $\mathbf{H_b}$), 3.58 (2 H, t, *J*=5.0 Hz, $\mathbf{H_a}$), 3.49 (3 H, s, $\mathbf{H_f}$).

**Triethylene glycol bistosylate 2.32** [11]

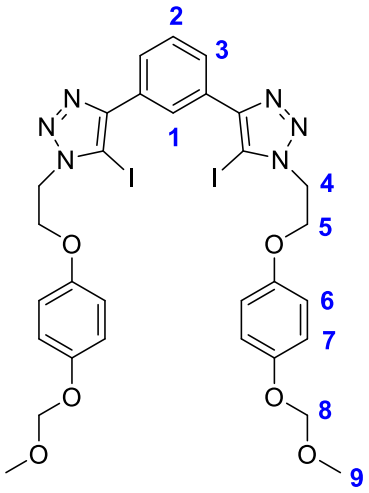



Triethylene glycol (2.50 mL, 18.7 mmol) was added portionwise to a suspension of p-toluenesulfonyl chloride (7.13 g, 37.4 mmol, 2 eqs) in anhydrous $CH_2Cl_2$ (30 mL), after which the reaction mixture was cooled to 0 °C in an ice bath and powdered KOH (8.40 g, 150 mmol, 8 eqs) was added portionwise. The reaction mixture was stirred at 0 °C for 1 hour, then it was allowed to warm to room temperature and stirred for a further 16 h. Subsequently, the mixture was partitioned between $CH_2Cl_2$ (50 mL) and water (50 mL) and the aqueous layer extracted with $CHCl_3$ (4 x 50 mL). The combined organic layers were dried over $MgSO_4$ and filtered, after which the filtrate was concentrated under reduced pressure and the resulting solid purified by column chromatography (50% EtOAc - petroleum ether) to afford **2.32** as a white solid.

Yield: 7.29 g (85%)

**$^1$H-NMR** (400 MHz, $CDCl_3$) $\delta$ = 7.80 (4 H, d, *J*=8.3 Hz, $\mathbf{H_c}$), 7.35 (4 H, d, *J*=8.1 Hz, $\mathbf{H_b}$), 4.15 (4 H, m, $\mathbf{H_d}$), 3.66 (4 H, m, $\mathbf{H_e}$), 3.53 (4 H, s, $\mathbf{H_f}$), 2.45 (6 H, s, $\mathbf{H_a}$).

**MOM-protected iodotriazole – bisphenol 2.33** [10]

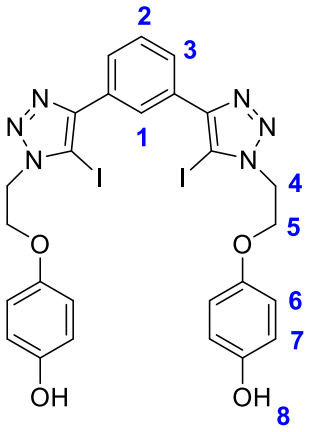



$[Cu(CH_3CN)_4]PF_6$ (15.0 mg, 0.04 mmol, 0.1 eqs) and TBTA (21.2 mg, 0.04 mmol, 0.1 eqs) were stirred together for 20 minutes in anhydrous, degassed THF (4 mL). The resulting solution was added to MOM-protected azido-phenol **2.31** (207 mg, 0.84 mmol, 2.1 eqs) in a round-bottomed flask, followed by 1,3-bis(iodoethynyl)benzene **2.28** (152 mg, 0.40 mmol). The flask was covered with foil and the reaction mixture stirred at room temperature for 16 h, following which the solvent was removed under reduced pressure. The resulting crude solid was redissolved in $CH_2Cl_2$ (5 mL) and washed with 0.1 M EDTA (6 mL) and brine (5 mL), dried over $MgSO_4$ and filtered. The filtrate was concentrated under reduced pressure and purified by column chromatography ($CH_2Cl_2$, followed by 1% MeOH - $CH_2Cl_2$) to afford **2.33** as a white solid.

Yield: 285 mg (86%)

**$^1$H-NMR** (400 MHz, $CDCl_3$) $\delta$ = 8.54 (1 H, s, **$H_1$**), 8.00 (2 H, dd, *J*=7.8, 1.5 Hz, **$H_3$**), 7.59 (1 H, t, *J*=7.9 Hz, **$H_2$**), 6.97 (4 H, d, *J*=9.0 Hz, **$H_6$**), 6.83 (4 H, d, *J*=9.2 Hz, **$H_7$**), 5.10 (4 H, s, **$H_8$**), 4.87 (4 H, t, *J*=5.7 Hz, **$H_4$**), 4.46 (4 H, t, *J*=5.7 Hz, **$H_5$**), 3.47 (6 H, s, **$H_9$**).

**Iodotriazole – bisphenol 2.34** [10]

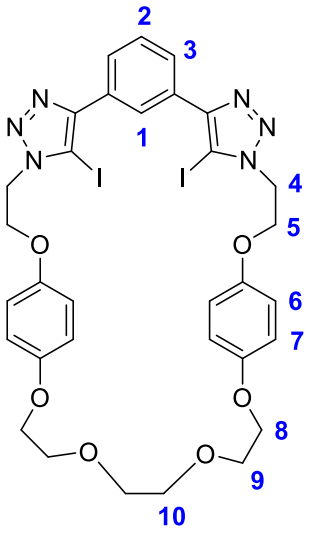



Acetyl chloride (0.79 mL, 11.0 mmol, 32 eqs) was added to MeOH (2 mL) in an ice bath and stirred for 5 minutes at 0 °C, after which it was allowed to warm to room temperature and stirred for a further 15 minutes. To this, a solution of MOM-protected iodotriazole – bisphenol **2.33** (285 mg, 0.35 mmol) in $CH_2Cl_2$ (2 mL) was added dropwise and the resulting mixture stirred for 2 h. The solvent was subsequently removed under reduced pressure and the solid washed with water to give **2.34** as an off-white solid.

Yield: 227 mg (90%)

**$^1$H-NMR** (400 MHz, acetone-$d_6$) $\delta$ = 8.66 (1 H, s, **$H_1$**), 8.04 (2 H, dd, *J*=7.8, 1.4 Hz, **$H_3$**), 7.64 (1 H, s, **$H_2$**), 6.77 (8 H, m, **$H_6$** + **$H_7$**), 4.91 (4 H, t, *J*=5.3 Hz, **$H_4$**), 4.50 (4 H, t, *J*=5.4 Hz, **$H_5$**).

**Bis(iodotriazole) macrocycle 2.35** [10]

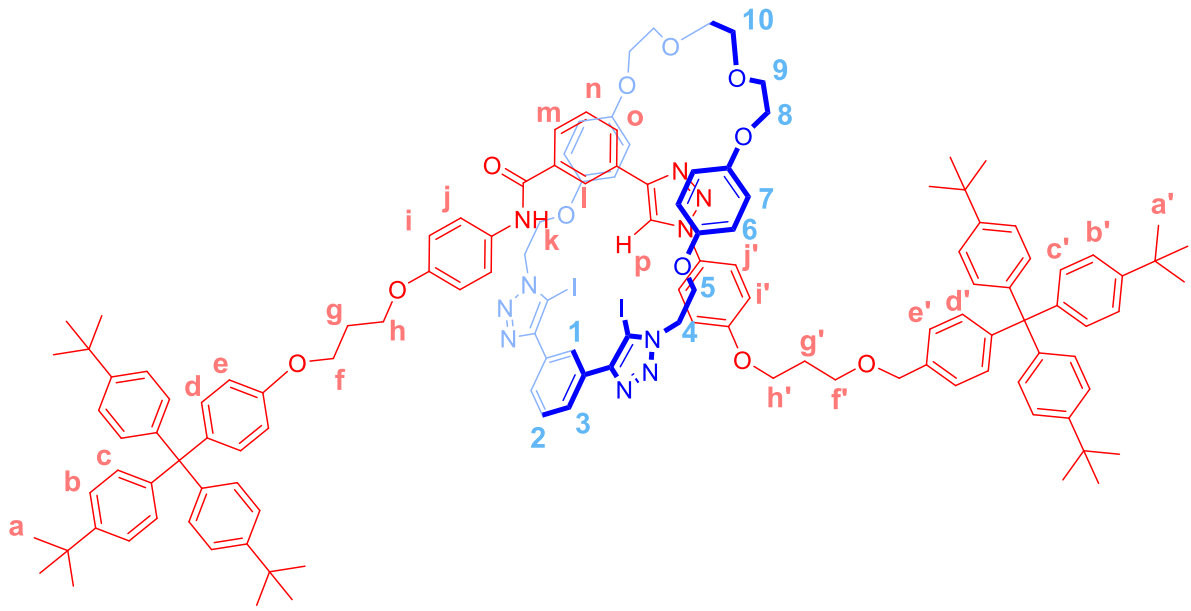



Bisphenol **2.34** (212 mg, 0.29 mmol) and bistosylate **2.32** (132 mg, 0.29 mmol, 1 eq) were added to a round-bottomed flask. Anhydrous, degassed DMF (90 mL) was added and the mixture stirred under a $N_2$ atmosphere until both solids dissolved. Subsequently, $Cs_2CO_3$ (376 mg, 1.15 mmol, 4 eqs) was added in one portion and the reaction mixture heated at 70 °C for 16 h. The solvent was removed under reduced pressure and the resulting solids stirred in 1:1 water/$CHCl_3$ (*v/v*, 50 mL) for 30 minutes. The layers were then separated and the aqueous layer extracted with $CHCl_3$ (4 x 25 mL) after which the combined organic extracts were washed with brine (50 mL), dried over $MgSO_4$ and filtered. The filtrate was concentrated under reduced pressure and purified by column chromatography (1% MeOH - $CH_2Cl_2$) to afford **2.35** as an off-white solid.

Yield: 119 mg (49%)

**$^1$H-NMR** (400 MHz, $CDCl_3$) $\delta$ = 8.32 (1 H, s, $\mathbf{H_1}$), 7.93 (2 H, d, *J*=7.5 Hz, $\mathbf{H_3}$), 7.60 (1 H, t, *J*=7.4 Hz, $\mathbf{H_2}$), 6.79 (2 H, m, $\mathbf{H_6}$), 6.73 (2 H, m, $\mathbf{H_7}$), 4.87 (4 H, t, *J*=4.7 Hz, $\mathbf{H_4}$), 4.44 (4 H, t, *J*=4.7 Hz, $\mathbf{H_5}$), 4.03 (4 H, t, *J*=4.8 Hz, $\mathbf{H_8}$), 3.79 (4 H, t, *J*=4.5 Hz, $\mathbf{H_8}$), 3.69 (4 H, s, $\mathbf{H_{10}}$).

**Neutral amido-triazole rotaxane 2.37.HB**



Bis(iodotriazole) macrocycle **2.35** (24.6 mg, 0.029 mmol) and $[Cu(CH_3CN)_4]PF_6$ (10.8 mg, 0.029 mmol, 1 eq) were dissolved in anhydrous, degassed $CH_2Cl_2$ (2.9 mL) and stirred together for 20 minutes. Subsequently, aromatic azide stopper **2.10** (58.9 mg, 0.087 mmol, 3 eqs) and aromatic alkyne stopper **2.13** (67.8 mg, 0.087 mmol, 3 eqs) were added, after which the reaction mixture was degassed and stirred at room temperature for 16 h. A further portion of $[Cu(CH_3CN)_4]PF_6$ was added to ensure full conversion of the stopper components, after which the reaction mixture was washed with 0.1 M EDTA (10 mL) and brine (15 mL), dried over $MgSO_4$, filtered and the filtrate concentrated under reduced pressure. The crude solid was purified by iterative preparative thin layer chromatography ($CH_2Cl_2$, followed by 2% MeOH – $CH_2Cl_2$) to afford **2.37.HB** as a white solid.

Yield: 36.65 mg (55%)

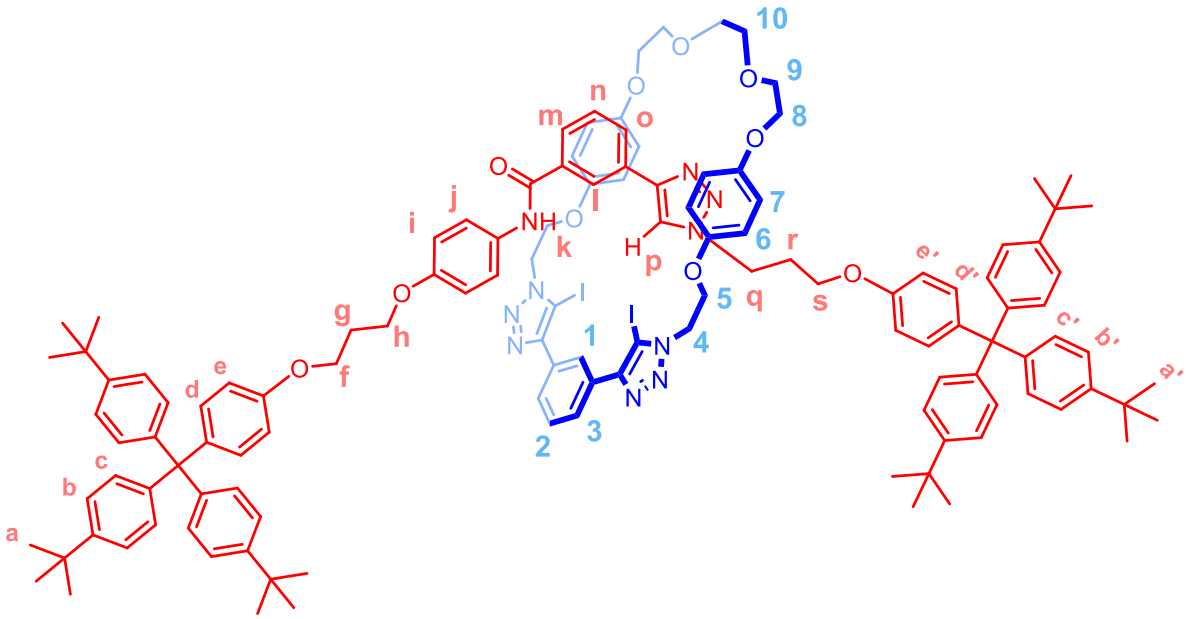
**$^1$H-NMR** (400 MHz, $CDCl_3$) $\delta$ = 8.96 (1 H, s, $\mathbf{H_k}$), 8.67 (1 H, s, $\mathbf{H_1}$), 8.58 (1 H, s, $\mathbf{H_p}$), 8.34 (1 H, s, $\mathbf{H_l}$), 8.03 (2 H, m, $\mathbf{H_m}$ + $\mathbf{H_2}$), 7.72 (1 H, d, *J*=7.6 Hz, $\mathbf{H_o}$), 7.58 (4 H, m, $\mathbf{H_{j'}}$ + $\mathbf{H_3}$), 7.50 (2 H, d, *J*=8.9 Hz, $\mathbf{H_j}$), 7.40 (1 H, t, *J*=7.8 Hz, $\mathbf{H_n}$), 7.23 (12 H, d, *J*=8.1 Hz, $\mathbf{H_b}$ + $\mathbf{H_{b'}}$), 7.11 (16 H, m, $\mathbf{H_c}$ + $\mathbf{H_d}$ + $\mathbf{H_{c'}}$ + $\mathbf{H_{d'}}$), 6.93 (2 H, d, *J*=8.9 Hz, $\mathbf{H_{i'}}$), 6.85 (2 H, d, *J*=8.9 Hz, $\mathbf{H_i}$), 6.79 (4 H, m, $\mathbf{H_e}$ + $\mathbf{H_{e'}}$), 6.51 (4 H, d, *J*=9.0 Hz, $\mathbf{H_6}$), 6.25 (4 H, d, *J*=9.0 Hz, $\mathbf{H_7}$), 4.75 (4 H, t, *J*=5.1 Hz, $\mathbf{H_4}$), 4.37 (4 H, t, *J*=5.3 Hz, $\mathbf{H_5}$), 4.15 (8 H, m, $\mathbf{H_f}$ + $\mathbf{H_h}$ + $\mathbf{H_{f'}}$ + $\mathbf{H_{h'}}$), 3.75 (12 H, m, $\mathbf{H_{8\text{-}10}}$), 2.26 (4 H, m, $\mathbf{H_g}$ + $\mathbf{H_{g'}}$), 1.30 (54 H, s, $\mathbf{H_a}$ + $\mathbf{H_{a'}}$).

**$^{13}$C-NMR** (101 MHz, $CDCl_3$) δ = 165.38, 158.93, 156.64, 156.58, 155.56, 152.57, 151.75, 149.46, 148.34, 148.30, 147.10, 144.12, 144.10, 139.83, 139.72, 135.37, 132.30, 132.28, 131.65, 130.70, 130.35, 130.24, 129.16, 128.96, 128.29, 127.93, 127.79, 125.51, 124.42, 124.04, 122.37, 121.48, 119.29, 115.77, 115.20, 114.61, 112.94, 80.29, 70.84, 69.99, 67.02, 66.95, 64.87, 64.67, 64.19, 63.97, 63.04, 49.11, 34.28, 31.37, 29.69, 29.36, 29.24.

There were fewer $^{13}$C signals than anticipated due to coincidence.

**HRMS** (ESI+ve) m/z: 2311.91919 ([M+H]$^+$, $C_{133}H_{145}I_2N_{10}O_{11}^+$ requires 2311.91782).

**Neutral aliphatic amido-triazole rotaxane 2.38**



Bis(iodotriazole) macrocycle **2.35** (20.8 mg, 0.024 mmol) and $[Cu(CH_3CN)_4]PF_6$ (9.18 mg, 0.024 mmol, 1 eq) were dissolved in anhydrous, degassed $CH_2Cl_2$ (2.4 mL) and stirred together for 20 minutes. Subsequently, aliphatic azide stopper **2.27** (43.1 mg, 0.073 mmol, 3 eqs) and aromatic alkyne stopper **2.13** (57.4 mg, 0.073 mmol, 3 eqs) were added, after which the reaction mixture was degassed and stirred at room temperature for 16 h. A further portion of $[Cu(CH_3CN)_4]PF_6$ was added to ensure full conversion of the stopper components, after which the reaction mixture was washed with 0.1 M EDTA (10 mL) and brine (10 mL), dried over $MgSO_4$, filtered and the filtrate concentrated under reduced pressure. The crude solid was purified by iterative preparative thin layer chromatography (1% MeOH – $CH_2Cl_2$, followed by 2% MeOH – $CH_2Cl_2$) to afford **2.38** as a white solid.

Yield: 16.54 mg (30%)

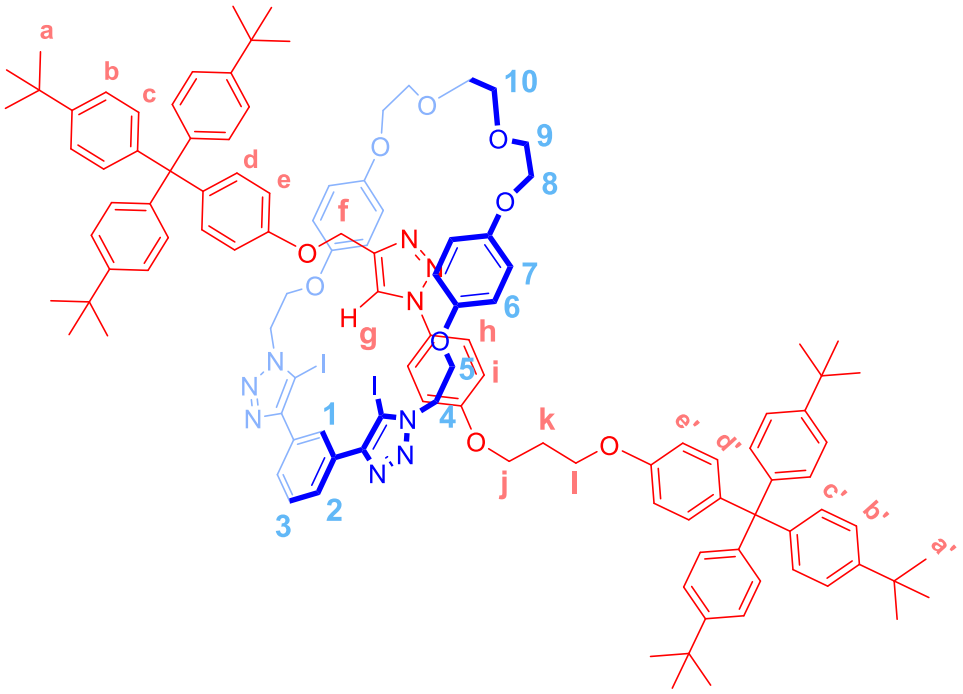
**$^{1}$H-NMR** (500 MHz, $CDCl_3$) $\delta$ = 8.95 (1 H, s, $\mathbf{H_p}$), 8.66 (1 H, s, $\mathbf{H_1}$), 8.18 (1 H, s, $\mathbf{H_l}$), 8.12 (1 H, s, $\mathbf{H_k}$), 8.03 (2 H, dd, *J*=7.8, 1.5 Hz, $\mathbf{H_3}$), 7.97 (1 H, d, *J*=7.9 Hz, $\mathbf{H_m}$), 7.67 (1 H, d, *J*=7.8 Hz, $\mathbf{H_o}$), 7.57 (1 H, t, *J*=7.8 Hz, $\mathbf{H_2}$), 7.46 (2 H, d, *J*=8.9 Hz, $\mathbf{H_j}$), 7.35 (1 H, t, *J*=7.8 Hz, $\mathbf{H_n}$), 7.23 (12 H, m, $\mathbf{H_b}$ + $\mathbf{H_{b'}}$), 7.09 (16 H, m, $\mathbf{H_c}$ + $\mathbf{H_d}$ + $\mathbf{H_{c'}}$ + $\mathbf{H_{d'}}$), 6.81 (4 H, m, $\mathbf{H_e}$ + $\mathbf{H_i}$), 6.72 (2 H, d, *J*=9.0 Hz, $\mathbf{H_{e'}}$), 6.54 (4 H, d, *J*=9.0 Hz, $\mathbf{H_6}$), 6.26 (2 H, d, *J*=9.0 Hz, $\mathbf{H_7}$), 4.73 (4 H, m, $\mathbf{H_4}$), 4.51 (2 H, t, *J*=6.9 Hz, $\mathbf{H_q}$), 4.38 (4 H, t, *J*=5.1 Hz, $\mathbf{H_5}$), 4.13 (4 H, m, $\mathbf{H_f}$ + $\mathbf{H_h}$), 3.93 (2 H, t, *J*=5.7 Hz, $\mathbf{H_s}$), 3.66 (12 H, m, $\mathbf{H_{8\text{-}10}}$), 2.35 (2 H, quin, *J*=6.2 Hz, $\mathbf{H_r}$), 2.24 (2 H, quin, *J*=6.1 Hz, $\mathbf{H_g}$), 1.30 (54 H, s, $\mathbf{H_a}$ + $\mathbf{H_{a'}}$).

**$^{13}$C-NMR** (126 MHz, $CDCl_3$) $\delta$ = 165.34, 156.62, 156.20, 155.47, 152.66, 151.69, 149.39, 148.37, 148.30, 146.84, 144.11, 144.01, 140.14, 139.71, 135.32, 132.32, 132.27, 131.68, 130.69, 130.64, 130.35, 129.19, 128.74, 128.22, 127.75, 125.36, 124.57, 124.08, 124.04, 122.38, 121.48, 121.48, 115.92, 114.71, 114.47, 112.93, 80.43, 70.69, 69.91, 67.00, 66.84, 64.63, 64.19, 63.84, 63.03, 48.94, 47.13, 34.27, 31.36, 30.93, 29.89, 29.69, 29.35.

There were fewer $^{13}$C signals than anticipated due to coincidence.

**HRMS** (ESI+ve) m/z: 2219.88940 ($[M+H]^+$, $C_{127}H_{141}I_2N_{10}O_{10}^+$ requires 2219.89160).

**Neutral mixed aliphatic – aromatic triazole rotaxane 2.39**



Bis(iodotriazole) macrocycle **2.35** (16.9 mg, 0.020 mmol) and $[Cu(CH_3CN)_4]PF_6$ (7.43 mg, 0.020 mmol, 1 eq) were dissolved in anhydrous, degassed $CH_2Cl_2$ (2.0 mL) and stirred together for 20 minutes. Subsequently, aromatic azide stopper **2.10** (40.6 mg, 0.060 mmol, 3 eqs) and aliphatic alkyne stopper **2.36** (32.5 mg, 0.060 mmol, 3 eqs) were added, after which the reaction mixture was degassed and stirred at room temperature for 16 h. A further portion of $[Cu(CH_3CN)_4]PF_6$ was added to ensure full conversion of the stopper components, after which the reaction mixture was washed with 0.1 M EDTA (9 mL) and brine (10 mL), dried over $MgSO_4$, filtered and the filtrate concentrated under reduced pressure. The crude solid was purified by iterative preparative thin layer chromatography (1% MeOH – $CH_2Cl_2$, followed by 2% MeOH – $CH_2Cl_2$) to afford **2.39** as a white solid.

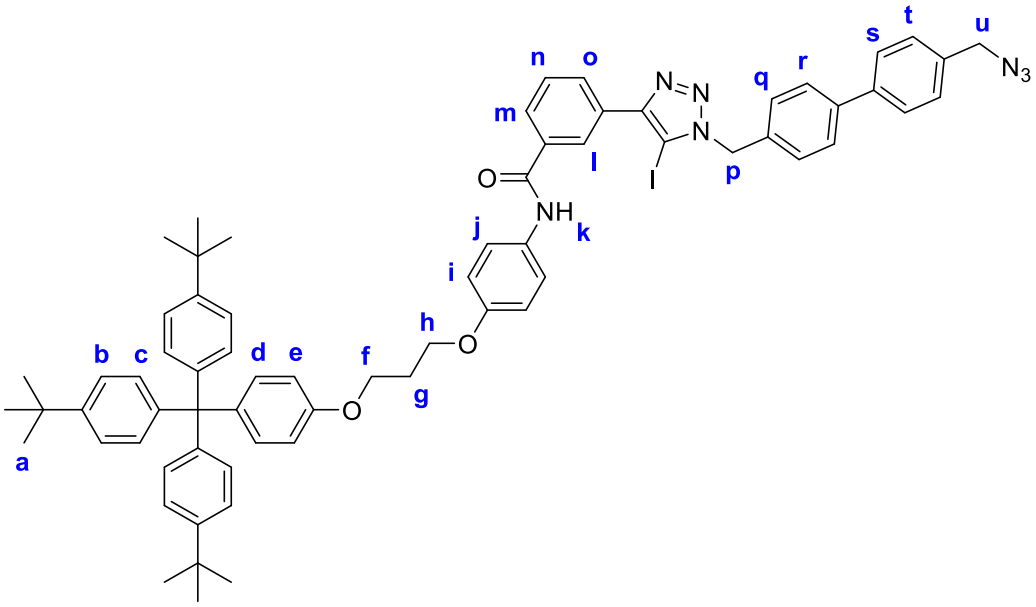
Yield: 7.00 mg (17%)

**$^1$H-NMR** (400 MHz, $CDCl_3$) $\delta$ = 8.49 (1 H, s, $\mathbf{H_1}$), 8.23 (1 H, s, $\mathbf{H_g}$), 7.99 (2 H, dd, *J*=7.9, 1.5 Hz, $\mathbf{H_3}$), 7.53 (1 H, t, *J*=7.8 Hz, $\mathbf{H_2}$), 7.23 (12 H, m, *J*=8.6 Hz, 12 H, m, $\mathbf{H_b} + \mathbf{H_{b'}}$), 7.11 (18 H, m, $\mathbf{H_c} + \mathbf{H_d} + \mathbf{H_{c'}} + \mathbf{H_{d'}} + \mathbf{H_i}$), 6.87 (2 H, d, *J*=8.9 Hz, $\mathbf{H_h}$), 6.75 (2 H, d, *J*=8.8 Hz, $\mathbf{H_{e'}}$), 6.54 (2 H, d, *J*=8.9 Hz, $\mathbf{H_e}$), 6.48 (4 H, d, *J*=9.0 Hz, $\mathbf{H_6}$), 6.29 (4 H, d, *J*=9.0 Hz, $\mathbf{H_7}$), 5.07 (2 H, s, $\mathbf{H_f}$), 4.75 (4 H, t, *J*=5.1 Hz, $\mathbf{H_4}$), 4.31 (4 H, t, *J*=3.8 Hz, $\mathbf{H_5}$), 3.99 (1 H, t, *J*=5.6 Hz, $\mathbf{H_j}$), 3.84 (1 H, t, *J*=5.4 Hz, $\mathbf{H_l}$), 3.66 (12 H, m, $\mathbf{H_{8\text{-}10}}$), 2.05 (2 H, m, $\mathbf{H_k}$), 1.30 (54 H, s, $\mathbf{H_a} + \mathbf{H_{a'}}$).

**$^{13}$C-NMR** (126 MHz, $CDCl_3$) δ = 158.53, 156.58, 156.27, 152.85, 151.69, 149.38, 148.34, 148.30, 144.13, 144.07, 143.69, 140.07, 139.66, 132.30, 132.26, 130.68, 130.57, 129.91, 129.06, 129.03, 128.22, 127.70, 125.69, 125.28, 124.05, 122.69, 121.82, 115.53, 114.80, 114.53, 113.29, 112.96, 79.77, 70.77, 69.78, 67.33, 67.00, 64.53, 67.00, 64.53, 63.95, 63.06, 63.03, 61.06, 49.41, 34.28, 31.37, 29.69, 29.04.

**HRMS** (ESI+ve) m/z: 2072.82373 ($[M+H]^+$, $C_{118}H_{132}I_2N_9O_9^+$ requires 2072.82319).

**Amido-iodotriazole azide 2.42**




Iodoalkyne **2.14** (67.5 mg, 0.07 mmol), bis-azide **2.41** (293 mg, 1.1 mmol, 16 eqs), and TBTA (19.7 mg, 0.04 mmol, 0.5 eqs) were dissolved in anhydrous, degassed THF (10 mL), after which CuI (7.10 mg, 0.04 mmol, 0.5 eqs) was added. The reaction mixture was stirred at room temperature for 16 h. The solvent was then removed under reduced pressure and the resulting solid redissolved in $CH_2Cl_2$, washed with 0.1 M EDTA (10 mL) and brine (10 mL), dried over $MgSO_4$, filtered and the filtrate concentrated under reduced pressure. The crude solid was purified by column chromatography ($CH_2Cl_2$, followed by 2% MeOH – $CH_2Cl_2$) to afford **2.42** as an off-white solid.

Yield: 69.94 mg (80%)

**$^1$H-NMR** (400 MHz, $CDCl_3$) δ = 8.46 (1 H, s, $\mathbf{H_k}$), 8.14 (1 H, d, *J*=7.7 Hz, $\mathbf{H_o}$), 7.93 (2 H, m, $\mathbf{H_l}$ + $\mathbf{H_m}$), 7.58 (7 H, m, $\mathbf{H_j}$ + $\mathbf{H_n}$ + $\mathbf{H_r}$ + $\mathbf{H_s}$), 7.41 (4 H, m, $\mathbf{H_q}$ + $\mathbf{H_t}$), 7.25 (6 H, m, $\mathbf{H_b}$), 7.09 (8 H, d,

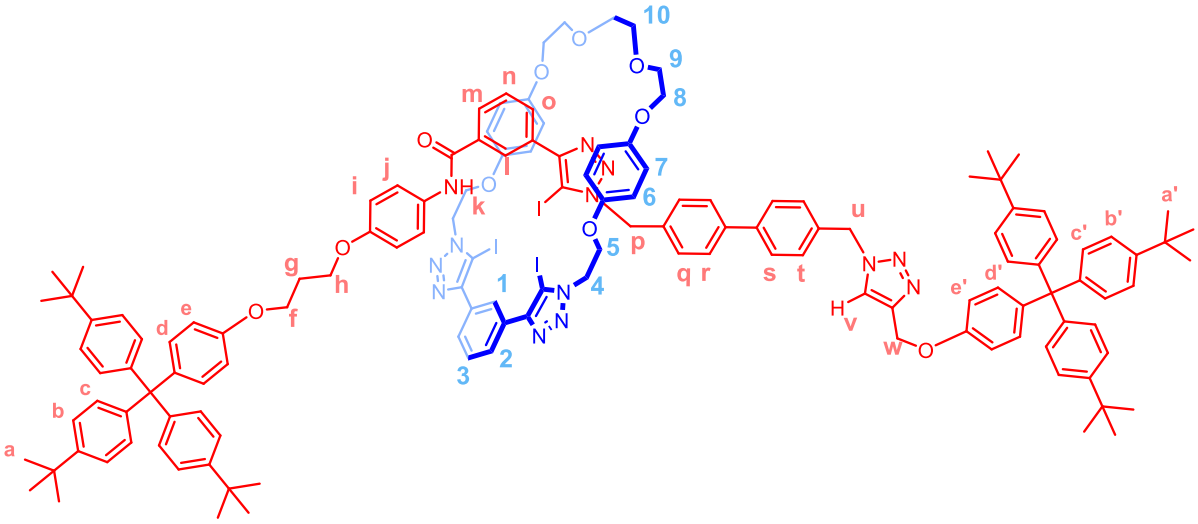
*J*=7.8 Hz, **H$_c$** + **H$_d$**), 6.92 (2 H, d, *J*=7.8 Hz, **H$_i$**), 6.79 (2 H, d, *J*=7.8 Hz, **H$_e$**), 5.74 (2 H, s, **H$_p$**), 4.39 (2 H, s, **H$_u$**), 4.15 (4 H, m, **H$_f$** + **H$_h$**), 2.25 (2 H, m, **H$_g$**), 1.31 (27 H, s, **H$_a$**).

**$^{13}$C-NMR** (126 MHz, $CDCl_3$) δ = 165.06, 156.63, 155.96, 149.32, 148.28, 144.14, 140.88, 140.27, 139.66, 135.47, 134.79, 133.29, 132.25, 130.99, 130.71, 130.67, 130.27, 129.13, 128.72, 128.38, 127.63, 127.50, 125.60, 124.02, 64.80, 64.20, 63.03, 54.46, 54.22, 34.27, 31.37, 29.68, 29.34.

There were fewer $^{13}$C signals than anticipated due to coincidence.

**HRMS** (ESI+ve) m/z: 1172.46619 ([M+H]$^+$, $C_{69}H_{71}IN_7O_3^+$ requires 1172.46576).

**Amido-iodotriazole rotaxane 2.43**



Bis(iodotriazole) macrocycle **2.35** (7.98 mg, 0.009 mmol) and $[Cu(CH_3CN)_4]PF_6$ (3.50 mg, 0.009 mmol, 1 eq) were dissolved in anhydrous, degassed $CH_2Cl_2$ (0.9 mL) and stirred together for 20 minutes. Subsequently, amido-iodotriazole azide **2.42** (33.0 mg, 0.028 mmol, 3 eqs) and aliphatic alkyne stopper **2.36** (15.3 mg, 0.028 mmol, 3 eqs) were added, after which the reaction mixture was degassed and stirred at room temperature for 3 days. A further portion of $[Cu(CH_3CN)_4]PF_6$ was added to ensure full conversion of the stopper components, after which the reaction mixture was washed with 0.1 M EDTA (6 mL) and brine (9 mL), dried over $MgSO_4$, filtered and the filtrate concentrated under reduced pressure. The crude solid was purified by iterative preparative thin layer chromatography (2% MeOH – $CH_2Cl_2$) followed by size exclusion chromatography to afford **2.43** as a white solid.

Yield: 11.3 mg (47%)

**$^{1}$H-NMR** (400 MHz, $CDCl_3$) δ = 8.96 (1 H, s, **$H_k$**), 8.54 (1 H, s, **$H_1$**), 8.25 (1 H, s, **$H_l$**), 8.01 (2 H, m, **$H_2$**), 7.92 (2 H, m, **$H_m$** + **$H_o$**), 7.62 (1 H, s, **$H_v$**), 7.58 (1 H, t, *J*=7.8 Hz, **$H_3$**), 7.47 (7 H, m, **$H_j$** + **$H_n$** + **$H_r$** + **$H_s$**), 7.31 (4 H, m, **$H_q$** + **$H_t$**), 7.23 (12-15 H, m, **$H_b$** + **$H_{b'}$**), 7.08 (17-20 H, m, **$H_c$** + **$H_d$** + **$H_{c'}$** + **$H_{d'}$**), 6.81 (6 H, m, **$H_e$** + **$H_{e'}$** + **$H_i$**), 6.50 (4 H, d, *J*=9.0 Hz, **$H_6$**), 6.30 (4 H, d, *J*=9.0 Hz, **$H_7$**), 5.55 (2 H, s, **$H_u$**), 5.52 (2 H, s, **$H_p$**), 5.15 (2 H, s, **$H_w$**), 4.74 (4 H, t, *J*=5.1 Hz, **$H_4$**), 4.32 (4 H, m, **$H_5$**), 4.11 (4 H, m, **$H_f$** + **$H_h$**), 3.69 (12 H, m, **$H_{8\text{-}10}$**), 2.22 (2 H, m, **$H_g$**), 1.30 (54 H, s, **$H_a$** + **$H_{a'}$**).

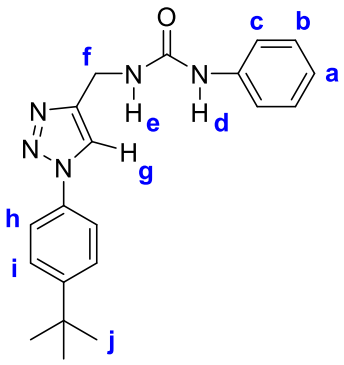
**$^{13}$C-NMR** (126 MHz, $CDCl_3$) δ = 164.91, 156.63, 156.10, 155.43, 152.87, 151.56, 149.48, 149.37, 148.33, 148.29, 144.73, 144.11, 144.03, 140.71, 140.35, 140.18, 139.69, 135.34, 133.75, 133.61, 132.30, 132.26, 131.70, 130.69, 130.18, 129.95, 129.13, 128.60, 128.49, 128.21, 128.02, 127.84, 127.68, 127.45, 126.54, 125.72, 124.03, 122.82, 122.50, 115.71, 114.90, 114.35, 113.21, 112.95, 80.11, 70.65, 69.83, 66.99, 64.63, 64.22, 63.03, 61.98, 53.92, 53.81, 49.13, 34.27, 31.37, 29.68, 29.34.

There were fewer $^{13}$C signals than anticipated due to coincidence.

**HRMS** (ESI+ve) m/z: 2564.86768 ($[M+H]^+$, $C_{141}H_{149}I_3N_{13}O_{10}^+$ requires 2564.86789).

### 6.3. Synthetic procedures and characterisation of compounds in Chapter 3

**Monotriazole-urea receptor 3.1.HB.O**




Alkyne-appended urea **3.3.O** (84.7 mg, 0.49 mmol), 4-(*tert*-butyl)phenyl azide **2.20** (85.3 mg, 0.49 mmol, 1 eq), DIPEA (0.13 mL, 0.75 mmol, 1.52 eqs), and TBTA (51.6 mg, 0.10 mmol, 0.2 eqs) were dissolved in anhydrous $CH_2Cl_2$ (5 mL). The mixture was degassed, after which $[Cu(CH_3CN)_4]PF_6$ (36.3 mg, 0.10 mmol, 0.2 eqs) was added and the reaction mixture stirred

at room temperature for 2 days. After completion, a 0.1 M aqueous solution of EDTA (20 mL) was added and the resulting organic phase washed with brine (20 mL), dried over $MgSO_4$ and filtered. The filtrate was concentrated under reduced pressure and purified by column chromatography (EtOAc) followed by trituration with $Et_2O$ to afford **3.1.HB.O** as a white solid.

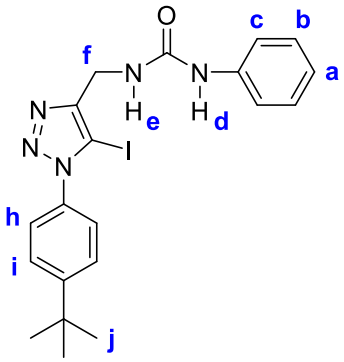
Yield: 167 mg (98%)

**$^1$H-NMR** (400 MHz, DMSO-$d_6$) $\delta$ = 8.61 (1 H, s, **$H_g$**), 8.57 (1 H, s, **$H_d$**), 7.80 (2 H, d, *J*=8.7 Hz, **$H_h$**), 7.59 (2 H, d, *J*=8.7 Hz, **$H_i$**), 7.40 (2 H, d, *J*=7.8 Hz, **$H_c$**), 7.22 (2 H, t, *J*=7.9 Hz, **$H_b$**), 6.89 (1 H, t, *J*=7.3 Hz, **$H_a$**), 6.65 (1 H, t, *J*=5.6 Hz, **$H_e$**), 4.43 (2 H, d, *J*=4.9 Hz, **$H_f$**), 1.32 (9 H, s, **$H_j$**).

**$^{13}$C-NMR** (101 MHz, $CD_3OD$) $\delta$ = 140.92, 129.96, 127.97, 123.81, 123.78, 121.37, 120.48, 120.46, 72.06, 36.28, 35.80, 31.77, 30.24.

**HRMS** (ESI+ve) m/z: 350.19784 ($[M+H]^+$, $C_{20}H_{24}N_5O^+$ requires 350.19754).

**Monoiodotriazole-urea receptor 3.1.XB.O**




NaI (177 mg, 1.20 mmol, 4 eqs) was suspended in anhydrous THF (2 mL) and vigorously stirred, after which $Cu(ClO_4)_2 \cdot 6H_2O$ (220 mg, 0.60 mmol, 2 eqs) was added and the suspension stirred for a further 5 minutes under a $N_2$ atmosphere. Subsequently, 4-(tert-butyl)phenyl azide **2.20** (52.0 mg, 0.30 mmol), TBTA (7.87 mg, 0.015 mmol, 0.05 eqs), DBU (0.044 mL, 0.30 mmol, 1 eq), and alkyne-appended urea **3.3.O** (51.7 mg, 0.30 mmol, 1 eq) were successively added. The reaction mixture was diluted with anhydrous THF (2 mL) and vigorously stirred in the dark at room temperature for 7 days. After completion, the solvent was removed under reduced pressure and the resulting solid redissolved in EtOAc (10 mL) and washed with 10% $NH_3$ (25 mL) and brine (15 mL), dried over $MgSO_4$ and filtered. The filtrate was concentrated under reduced pressure and purified by column chromatography (25% EtOAc – $CH_2Cl_2$) to afford **3.1.XB.O** as an off-white solid.

Yield: 29.9 mg (21%)

**$^1$H-NMR** (400 MHz, $CDCl_3$) $\delta$ = 7.57 (2 H, d, *J*=8.6 Hz, $\mathbf{H_h}$), 7.45 (2 H, d, *J*=8.7 Hz, $\mathbf{H_i}$), 7.34 (2 H, m, $\mathbf{H_c}$), 7.12 (1 H, br. s., $\mathbf{H_d}$), 7.04 (1 H, m, $\mathbf{H_a}$), 6.06 (1 H, br. s., $\mathbf{H_e}$), 4.64 (2 H, d, *J*=5.5 Hz, $\mathbf{H_f}$), 1.40 (9 H, s, $\mathbf{H_j}$).

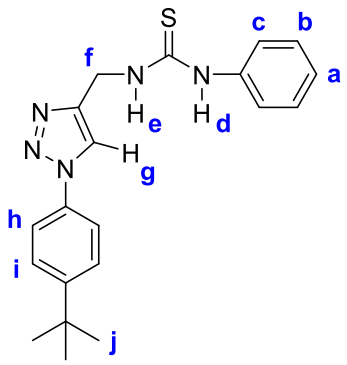
$\mathbf{H_b}$ was obscured by the solvent signal.

**$^{13}$C-NMR** (101 MHz, $CDCl_3$) $\delta$ = 155.51, 153.73, 149.82, 138.87, 134.02, 129.03, 126.36, 125.50, 123.25, 120.29, 79.89, 36.17, 34.99, 31.25.

There were fewer $^{13}$C signals than anticipated due to coincidence.

**HRMS** (ESI+ve) m/z: 476.09404 ($[M+H]^+$, $C_{20}H_{23}IN_5O^+$ requires 476.09418).

**Monotriazole-thiourea receptor 3.1.HB.S**




Phenyl isothiocyanate (0.01 mL, 0.08 mmol) was dissolved in anhydrous $CH_2Cl_2$ (0.5 mL), after which a solution of aminotriazole **3.8.HB** (29.9 mg, 0.13 mmol, 1.54 eqs) in anhydrous $CH_2Cl_2$ (0.5 mL) was added. The reaction mixture was stirred at room temperature for 16 h, following which the solvent was removed under reduced pressure. The crude solid was purified by column chromatography ($CH_2Cl_2$, followed by 1% MeOH – $CH_2Cl_2$) to afford **3.1.HB.S** as a pale yellow oil.

Yield: 31.0 mg (100%)

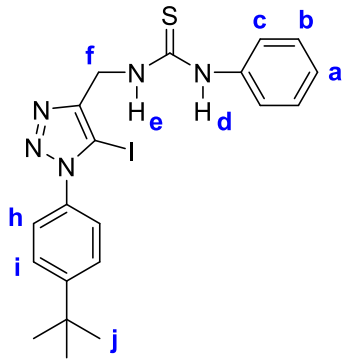
**$^1$H-NMR** (400 MHz, $CDCl_3$) $\delta$ = 8.16 (1 H, s, $\mathbf{H_g}$), 7.99 (1 H, br. s., $\mathbf{H_d}$), 7.63 (2 H, m, $\mathbf{H_h}$), 7.52 (2 H, m, $\mathbf{H_i}$), 7.42 (2 H, m, $\mathbf{H_b}$), 7.24 (2 H, m, $\mathbf{H_c}$), 6.93 (1 H, br. s., $\mathbf{H_e}$), 5.01 (2 H, d, *J*=5.7 Hz, $\mathbf{H_f}$), 1.37 (9 H, s, $\mathbf{H_j}$).

$\mathbf{H_a}$ was obscured by the solvent signal.

**$^{13}$C-NMR** (101 MHz, $CDCl_3$) δ = 180.73, 152.23, 144.43, 136.15, 134.40, 130.00, 127.15, 126.56, 125.10, 121.13, 120.23, 40.10, 34.73, 31.20.

**HRMS** (ESI+ve) m/z: 366.17428 ($[M+H]^+$, $C_{20}H_{24}N_5S^+$ requires 366.17469).

**Monoiodotriazole-thiourea receptor 3.1.XB.S**




Phenyl isothiocyanate (0.01 mL, 0.08 mmol) was dissolved in anhydrous $CH_2Cl_2$ (0.5 mL), after which a solution of aminoiodotriazole **3.8.XB** (40.9 mg, 0.11 mmol, 1.38 eqs) in anhydrous $CH_2Cl_2$ (0.5 mL) was added. The reaction mixture was stirred at room temperature for 16 h, following which the solvent was removed under reduced pressure. The crude solid was purified by column chromatography (1% MeOH – $CH_2Cl_2$) to afford **3.1.XB.S** as a white solid.

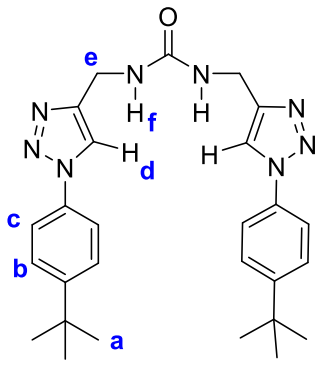
Yield: 38.8 mg (70%)

**$^1$H-NMR** (400 MHz, $CDCl_3$) δ = 7.95 (1 H, br. s., $\mathbf{H_d}$), 7.56 (2 H, d, *J*=8.6 Hz, $\mathbf{H_h}$), 7.44 (4 H, m, $\mathbf{H_i}$ + $\mathbf{H_c}$), 7.32 (3 H, m, $\mathbf{H_a}$ + $\mathbf{H_b}$), 6.91 (1 H, br. s., $\mathbf{H_e}$), 4.98 (2 H, d, *J*=4.9 Hz, $\mathbf{H_f}$), 1.38 (m, 9 H, $\mathbf{H_j}$).

**$^{13}$C-NMR** (101 MHz, $CDCl_3$) δ = 180.62, 153.52, 148.08, 136.27, 133.97, 130.00, 127.04, 126.25, 125.32, 124.96, 80.07, 41.36, 34.91, 31.19.

**HRMS** (ESI+ve) m/z: 492.07141 ($[M+H]^+$, $C_{20}H_{23}IN_5S^+$ requires 492.07134).

**Bisprototriazole-urea receptor 3.2.HB.O**




Aminotriazole **3.8.HB** (36.5 mg, 0.16 mmol) was dissolved in anhydrous $CH_2Cl_2$ (1 mL), after which triphosgene (15.5 mg, 0.05 mmol, 0.33 eqs) was added at 0 °C, followed by $Et_3N$ (0.04 mL, 0.31 mmol, 2 eqs). The reaction mixture was stirred at room temperature for 3 h, after which a solution of aminotriazole **3.8.HB** (36.5 mg, 0.16 mmol, 1 eq) in anhydrous $CH_2Cl_2$ (1 mL) was added and the mixture stirred at room temperature for a further 16 h. The residual solids were removed by filtration; the filtrate was concentrated and purified by column chromatography (EtOAc) to afford **3.2.HB.O** as a white solid.

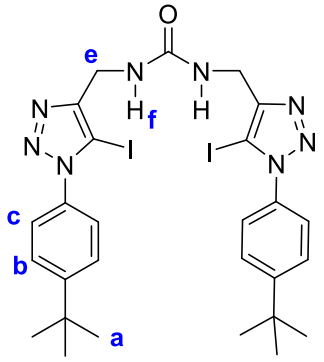
Yield: 40.4 mg (53%)

**$^1$H-NMR** (400 MHz, $CDCl_3$) $\delta$ = 7.98 (2 H, s, $\mathbf{H_d}$), 7.58 (4 H, m, $\mathbf{H_c}$), 7.48 (4 H, m, $\mathbf{H_b}$), 6.16 (2 H, br. s., $\mathbf{H_f}$), 4.59 (4 H, d, *J*=5.9 Hz, $\mathbf{H_e}$), 1.34 (18 H, s, $\mathbf{H_a}$).

**$^{13}$C-NMR** (101 MHz, $CDCl_3$) $\delta$ = 158.50, 151.93, 146.84, 134.43, 126.51, 120.36, 120.01, 35.54, 34.67, 31.18.

**HRMS** (ESI+ve) m/z: 487.29294 ($[M+H]^+$, $C_{27}H_{35}N_8O^+$ requires 487.29283).

**Bisiodotriazole-urea receptor 3.2.XB.O**




Aminoiodotriazole **3.8.XB** (41.0 mg, 0.11 mmol) was dissolved in anhydrous $CH_2Cl_2$ (1 mL), after which triphosgene (11.4 mg, 0.04 mmol, 0.33 eqs) was added at 0 °C, followed by $Et_3N$ (0.025 mL, 0.17 mmol, 1.45 eqs). The reaction mixture was stirred at room temperature for 2 h, after which a solution of aminotriazole **3.8.XB** (41.0 mg, 0.11 mmol, 1 eq) and $Et_3N$ (0.025 mL, 0.17 mmol, 1.45 eqs) in anhydrous $CH_2Cl_2$ (1 mL) was added and the mixture stirred at room temperature for a further 16 h. The solvent was removed under reduced pressure and the crude solid purified by column chromatography (25% EtOAc – $CH_2Cl_2$ to 50% EtOAc – $CH_2Cl_2$) to afford **3.2.XB.O** as a white solid.

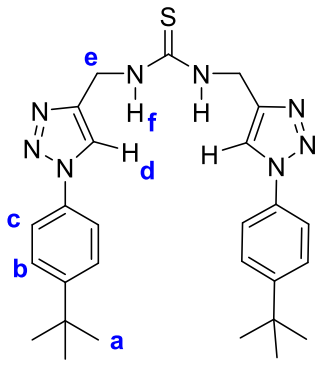
Yield: 42.5 mg (50%)

**$^1$H-NMR** (400 MHz, acetone-$d_6$) $\delta$ = 7.69 (4 H, m, **$H_c$**), 7.52 (4 H, m, **$H_b$**), 6.10 (2 H, br. s., **$H_f$**), 4.51 (4 H, d, *J*=5.4 Hz, **$H_e$**), 1.40 (18 H, s, **$H_a$**).

**$^{13}$C-NMR** (126 MHz, DMSO-$d_6$) $\delta$ = 152.77, 148.36, 134.27, 126.93, 126.31, 125.61, 122.63, 84.78, 34.71, 31.01.

**HRMS** (ESI+ve) m/z: 739.08530 ($[M+H]^+$, $C_{27}H_{33}I_2N_8O^+$ requires 739.08612).

**Bisprototriazole-thiourea receptor 3.2.HB.S**




Aminotriazole **3.8.HB** (75.0 mg, 0.33 mmol) and $Et_3N$ (0.36 mL, 2.61 mmol, 8 eqs) were dissolved in anhydrous $CH_2Cl_2$ (2 mL), after which thiophosgene (0.10 mL, 1.30 mmol, 4 eqs) was added at 0 °C. The reaction mixture was allowed to warm to room temperature and stirred for 16 h, after which the volatiles were removed under reduced pressure and the residual solid purified by flash column chromatography ($CH_2Cl_2$) to give the intermediate isothiocyanate **3.9.HB**.

A portion of **3.9.HB** (66.2 mg, 0.24 mmol) was immediately redissolved in anhydrous $CH_2Cl_2$ (4 mL) along with another portion of the starting aminotriazole **3.8.HB** (56.0 mg, 0.24 mmol, 1 eq). The reaction mixture was stirred at room temperature for 16 h, after which the resulting precipitate was collected by filtration under reduced pressure and washed with small amounts of $CH_2Cl_2$ to give **3.2.HB.S** as a white solid.

Yield: 82.0 mg (70%)

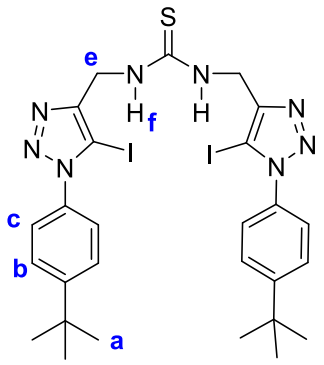
**$^1$H-NMR** (400 MHz, acetone-$d_6$) $\delta$ = 8.45 (2 H, s, **$H_d$**), 7.79 (4 H, m, **$H_c$**), 7.62 (6 H, m, **$H_b$** + **$H_f$**), 4.92 (4 H, d, *J*=4.9 Hz, **$H_e$**), 1.37 (18 H, s, **$H_a$**).

**$^{13}$C-NMR** (101 MHz, 1:1 $CD_3OD$:$CDCl_3$) $\delta$ = 153.11, 146.35, 135.23, 127.36, 122.10, 120.89, 40.06, 35.37, 31.66.

There were fewer $^{13}$C signals than anticipated due to coincidence.

**HRMS** (ESI+ve) m/z: 503.26972 ($[M+H]^+$, $C_{27}H_{35}N_8S^+$ requires 503.26999).

**Bisiodotriazole-thiourea receptor 3.2.XB.S**




Aminoiodotriazole **3.8.XB** (92.9 mg, 0.26 mmol) and $Et_3N$ (0.29 mL, 2.08 mmol, 8 eqs) were dissolved in anhydrous $CH_2Cl_2$ (2 mL), after which thiophosgene (0.08 mL, 1.04 mmol, 4 eqs) was added at 0 °C. The reaction mixture was allowed to warm to room temperature and stirred for 16 h, after which the volatiles were removed under reduced pressure and the residual solid purified by flash column chromatography (50% EtOAc - cyclohexane) to give the intermediate isothiocyanate **3.9.XB**.

A portion of **3.9.XB** (52.9 mg, 0.13 mmol) was immediately redissolved in anhydrous $CH_2Cl_2$ (5 mL) along with another portion of the starting aminoiodotriazole **3.8.XB** (47.1 mg, 0.13 mmol, 1 eq). The reaction mixture was stirred at room temperature for 16 h, after which the resulting precipitate was collected by filtration under reduced pressure and washed with small amounts of $CH_2Cl_2$ to give **3.2.XB.S** as a white solid.

Yield: 58.1 mg (58%)

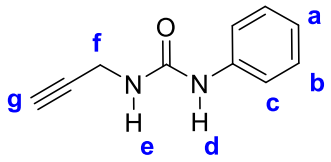
**$^1$H-NMR** (400 MHz, acetone-$d_6$) $\delta$ = 7.69 (4 H, m, $\mathbf{H_c}$), 7.53 (6 H, m, $\mathbf{H_b}$ + $\mathbf{H_f}$), 4.91 (4 H, d, $J$=4.6 Hz, $\mathbf{H_e}$), 1.40 (18 H, s, $\mathbf{H_a}$).

**$^{13}$C-NMR** (101 MHz, DMSO-$d_6$) $\delta$ = 152.76, 148.36, 134.26, 126.30, 125.60, 84.70, 34.69, 30.98.

There were fewer $^{13}$C signals than anticipated due to coincidence.

**HRMS** (ESI+ve) m/z: 755.06287 ($[M+H]^+$, $C_{27}H_{33}I_2N_8S^+$ requires 755.06328).

**Alkyne-appended urea 3.3.O** [12]

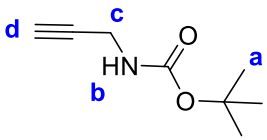



Phenyl isocyanate (0.15 mL, 1.38 mmol) was dissolved in anhydrous $CH_2Cl_2$ (5 mL) and cooled to 0 °C. To this, a solution of propargyl amine (0.1 mL, 1.56 mmol, 1.13 eqs) in anhydrous $CH_2Cl_2$ (5 mL) was added. The reaction mixture was allowed to warm to room temperature and stirred for a further 3 hours, after which the resulting precipitate was collected by filtration under reduced pressure to afford **3.3.O** as a white solid.

Yield: 169 mg (70%)

**$^1$H-NMR** (400 MHz, DMSO-$d_6$) $\delta$ = 8.55 (1 H, s, H, **$H_d$**), 7.38 (2 H, d, *J*=7.6 Hz, **$H_c$**), 7.22 (2 H, t, *J*=7.9 Hz, **$H_b$**), 6.90 (1 H, t, *J*=7.3 Hz, **$H_a$**), 6.43 (1 H, t, *J*=5.6 Hz, **$H_e$**), 3.88 (2 H, dd, *J*=5.7, 2.4 Hz, **$H_f$**), 3.10 (1 H, t, *J*=2.4 Hz, **$H_g$**).

***N*-Boc-protected propargyl amine 3.5** [13]

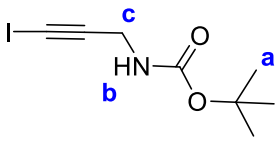



Propargyl amine (0.20 mL, 3.12 mmol) was dissolved in anhydrous $CH_2Cl_2$ (5 mL) and cooled to 0 °C. To this, a solution of Boc anhydride (681 mg, 3.12 mmol, 1 eq) in anhydrous $CH_2Cl_2$ (5 mL) was added. The reaction mixture was allowed to warm to room temperature and stirred for a further 1 hour, after which the volatiles were removed under reduced pressure to afford **3.5** as a yellow oil which solidified under high vacuum.

Yield: 425 mg (88%)

**$^1$H-NMR** (400 MHz, $CDCl_3$) $\delta$ = 4.70 (1 H, br. s., **$H_b$**), 3.93 (2 H, m, **$H_c$**), 2.22 (1 H, d, *J*=2.5 Hz, **$H_d$**), 1.46 (9 H, s, **$H_a$**).

**_N_-Boc-protected iodopropargyl amine 3.6** [14]

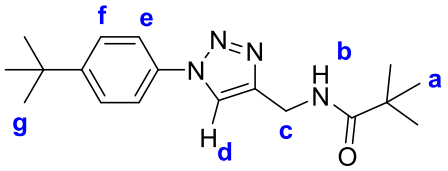



_N_-Boc-protected propargyl amine **3.5** (438 mg, 2.82 mmol) was dissolved in MeOH (5 mL) and cooled to 0 °C. To this, an aqueous solution of KOH (396 mg, 7.05 mmol, 2.5 eqs) was added and the mixture stirred at 0 °C for 10 mins. Subsequently, $I_2$ (787 mg, 3.10 mmol, 1.1 eqs) was added in one portion and the reaction mixture was allowed to warm to room temperature and stirred for 16 h. Water was added (10 mL) and the product was extracted with $Et_2O$ (3 x 15 mL), then the combined organic layers were washed with a saturated $Na_2S_2O_3$ solution (25 mL) and brine (25 mL), dried over $MgSO_4$ and filtered. The filtrate was concentrated under reduced pressure to afford **3.6** as a yellow solid.

Yield: 555 mg (70%)

**$^1$H-NMR** (400 MHz, $CDCl_3$) $\delta$ = 4.74 (1 H, br. s., **$H_b$**), 4.08 (2 H, d, _J_=4.3 Hz, **$H_c$**), 1.45 (9 H, m, **$H_a$**).

**_N_-Boc-protected aminotriazole 3.7.HB**




_N_-Boc-protected propargyl amine **3.5** (99.1 mg, 0.64 mmol), 4-(*tert*-butyl)phenyl azide **2.20** (111.9 mg, 0.64 mmol, 1 eq), DIPEA (0.16 mL, 0.92 mmol, 1.44 eqs), and TBTA (67.8 mg, 0.13 mmol, 0.2 eqs) were dissolved in anhydrous $CH_2Cl_2$ (5 mL). The mixture was degassed, after which $[Cu(CH_3CN)_4]PF_6$ (47.6 mg, 0.13 mmol, 0.2 eqs) was added and the reaction mixture stirred at room temperature for 16 h. After completion, a 0.1 M aqueous solution of EDTA (50 mL) was added and the resulting organic phase washed with brine (40 mL), dried over $MgSO_4$ and filtered. The filtrate was concentrated under reduced pressure

and purified by column chromatography (10% EtOAc - $CH_2Cl_2$, followed by 20% EtOAc - $CH_2Cl_2$) to afford **3.7.HB** as a yellow-white solid.

Yield: 149 mg (71%)

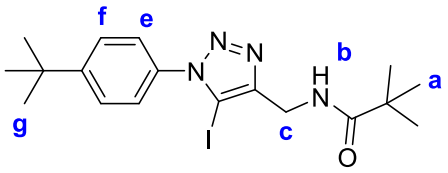
**$^1$H-NMR** (400 MHz, $CDCl_3$) $\delta$ = 7.94 (1 H, s, **$H_d$**), 7.63 (2 H, d, *J*=8.6 Hz, **$H_e$**), 7.52 (2 H, m, **$H_f$**), 5.23 (1 H, br. s., **$H_b$**), 4.47 (2 H, d, *J*=6.0 Hz, **$H_c$**), 1.46 (9 H, s, **$H_a$**), 1.36 (9 H, s, **$H_g$**).

**$^{13}$C-NMR** (101 MHz, $CDCl_3$) $\delta$ = 152.12, 134.61, 126.60, 120.23, 36.12, 34.78, 31.25, 28.38.

There were fewer $^{13}$C signals than anticipated due to coincidence.

**HRMS** (ESI+ve) m/z: 331.21379 ($[M+H]^+$, $C_{18}H_{27}N_4O_2^+$ requires 331.21285).

***N*-Boc-protected aminoiodotriazole 3.7.XB**




*N*-Boc-protected iodopropargyl amine **3.6** (235 mg, 0.83 mmol), 4-(*tert*-butyl)phenyl azide **2.20** (146 mg, 0.83 mmol, 1 eq), and TBTA (88.6 mg, 0.17 mmol, 0.2 eqs) were dissolved in anhydrous $CH_2Cl_2$ (10 mL). The mixture was degassed, after which $[Cu(CH_3CN)_4]PF_6$ (62.2 mg, 0.17 mmol, 0.2 eqs) was added and the reaction mixture stirred at room temperature for 48 h. After completion, a 0.1 M aqueous solution of EDTA (50 mL) was added and the resulting organic phase washed with brine (50 mL), dried over $MgSO_4$ and filtered. The filtrate was concentrated under reduced pressure and purified by column chromatography (5% EtOAc - $CH_2Cl_2$) to afford **3.7.XB** as a a colourless oil, which solidified under high vacuum to give a yellow wax.

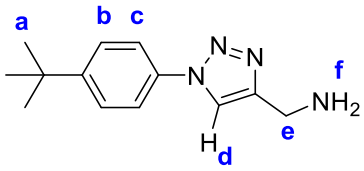
Yield: 221 mg (58%)

**$^1$H-NMR** (400 MHz, $CDCl_3$) $\delta$ = 7.56 (2 H, m, **$H_e$**), 7.44 (2 H, m, **$H_f$**), 5.18 (1 H, br. s., **$H_b$**), 4.48 (2 H, d, *J*=5.5 Hz, **$H_c$**), 1.48 (9 H, s, **$H_a$**), 1.38 (9 H, m, **$H_g$**).

**$^{13}$C-NMR** (101 MHz, $CDCl_3$) $\delta$ = 155.55, 153.45, 149.04, 134.13, 126.24, 125.41, 79.65, 79.12, 36.76, 34.91, 31.21, 28.37.

**HRMS** (ESI+ve) m/z: 457.10899 ([M+H]$^+$, $C_{18}H_{26}IN_4O_2^+$ requires 457.10950).

**Aminotriazole 3.8.HB**




*N*-Boc-protected aminotriazole **3.7.HB** (72.3 mg, 0.22 mmol) was dissolved in anhydrous $CH_2Cl_2$ (1 mL), after which TFA (0.27 mL, 3.53 mmol, 16 eqs) was added and the reaction mixture stirred at room temperature for 16 h. Subsequently, $CH_2Cl_2$ (5 mL) was added and the solution washed with a saturated $NaHCO_3$ solution (10 mL) and water (10 mL), dried over $MgSO_4$, filtered and then concentrated under reduced pressure to afford **3.8.HB** as a yellow-orange oil.

Yield: 31.8 mg (60%)

**$^1$H-NMR** (400 MHz, $CDCl_3$) $\delta$ = 7.93 (1 H, br. s., **$H_d$**), 7.63 (2 H, d, *J*=8.4 Hz, **$H_c$**), 7.52 (2 H, d, *J*=8.4 Hz, **$H_b$**), 1.35 (9 H, s, **$H_a$**).

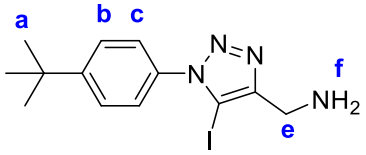
No resonance could be found for **$H_e$**; however, it does appear upon conversion of the amine to a different functional group.

**$^{13}$C-NMR** (101 MHz, $CDCl_3$) $\delta$ = 151.95, 134.75, 126.56, 120.14, 119.59, 34.71, 31.19.

There were fewer $^{13}$C signals than anticipated due to coincidence.

**HRMS** (ESI+ve) m/z: 231.16071 ([M+H]$^+$, $C_{13}H_{19}N_4^+$ requires 231.16042).

**Aminoiodotriazole 3.8.XB**




*N*-Boc-protected aminoiodotriazole **3.7.XB** (85.7 mg, 0.19 mmol) was dissolved in anhydrous $CH_2Cl_2$ (1 mL), after which TFA (0.25 mL, 3.26 mmol, 17.2 eqs) was added and the reaction mixture stirred at room temperature for 16 h. Subsequently, $CH_2Cl_2$ (5 mL) was added and the solution washed with a saturated $NaHCO_3$ solution (10 mL) and water (10 mL), dried over $MgSO_4$, filtered and then concentrated under reduced pressure to afford **3.8.XB** as a yellow oil.

Yield: 54.8 mg (80%)

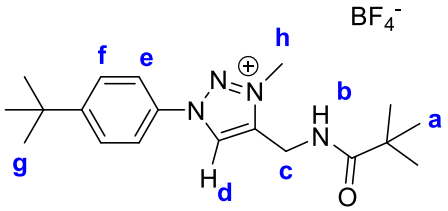
**$^1$H-NMR** (400 MHz, $CDCl_3$) $\delta$ = 7.57 (2 H, m, **$H_c$**), 7.45 (2 H, m, **$H_b$**), 3.91 (2 H, br. s., **$H_e$**), 1.39 (9 H, s, **$H_a$**).

**$^{13}$C-NMR** (101 MHz, $CDCl_3$) $\delta$ = 153.28, 134.17, 126.18, 125.35, 78.67, 34.85, 31.18.

There were fewer $^{13}$C signals than anticipated due to coincidence.

**HRMS** (ESI+ve) m/z: 357.05676 ($[M+H]^+$, $C_{13}H_{18}IN_4^+$ requires 357.05707).

***N*-Boc-protected aminoiodotriazolium 3.10.HB$^+$BF$_4^-$**




*N*-Boc-protected aminotriazole **3.7.HB** (33.3 mg, 0.1 mmol) was dissolved in anhydrous $CH_2Cl_2$ (0.5 mL), after which $[Me_3O]BF_4$ (14.91 mg, 0.1 mmol, 1 eq) was added in one portion. The reaction mixture was stirred at room temperature for 16 h, after which MeOH (3 mL) was added to quench the alkylating agent and the volatiles were removed under

reduced pressure. The crude solid was purified by column chromatography ($CH_2Cl_2$, followed by 2% MeOH - $CH_2Cl_2$) to afford **3.10.HB$^+$BF$_4^-$** as an off-white solid.

Yield: 35.9 mg (82%)

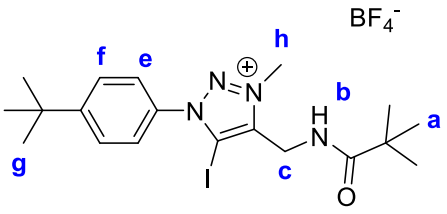
**$^1$H-NMR** (400 MHz, $CDCl_3$) $\delta$ = 8.84 (1 H, s, **H$_d$**), 7.74 (2 H, d, *J*=8.8 Hz, **H$_e$**), 7.60 (2 H, d, *J*=8.7 Hz, **H$_f$**), 6.11 (1 H, br. s., **H$_b$**), 4.60 (2 H, d, *J*=6.0 Hz, **H$_c$**), 4.45 (3 H, s, **H$_h$**), 1.41 (9 H, s, **H$_a$**), 1.36 (9 H, s, **H$_g$**).

**$^{19}$F-NMR** (377 MHz, $CDCl_3$) $\delta$ = - 152.34.

**$^{13}$C-NMR** (101 MHz, $CDCl_3$) $\delta$ = 156.33, 155.71, 143.78, 132.29, 127.59, 127.35, 120.99, 80.49, 38.38, 35.08, 33.43, 31.06, 28.21.

**HRMS** (ESI+ve) m/z: 345.22870 ([M-$BF_4^-$]$^+$, $C_{19}H_{29}N_4O_2^+$ requires 345.22850).

***N*-Boc-protected aminoiodotriazolium 3.10.XB$^+$BF$_4^-$**




*N*-Boc-protected aminoiodotriazole **3.7.XB** (31.9 mg, 0.07 mmol) was dissolved in anhydrous $CH_2Cl_2$ (1 mL), after which $[Me_3O]BF_4$ (10.34 mg, 0.07 mmol, 1 eq) was added in one portion. The reaction mixture was stirred at room temperature for 16 h, after which MeOH (4 mL) was added to quench the alkylating agent and the volatiles were removed under reduced pressure. The crude solid was purified by column chromatography (1% MeOH – $CH_2Cl_2$, followed by 2%, 3%, and 5% MeOH - $CH_2Cl_2$) to afford **3.10.XB$^+$BF$_4^-$** as a white solid.

Yield: 37.0 mg (95%)

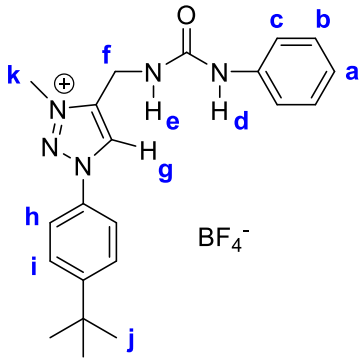
**$^1$H-NMR** (400 MHz, $CDCl_3$) $\delta$ = 7.59 (4 H, m, **H$_e$** + **H$_f$**), 6.11 (1 H, br. s., **H$_b$**), 4.65 (2 H, d, *J*=5.6 Hz, **H$_c$**), 4.47 (3 H, s, **H$_h$**), 1.45 (9 H, s, **H$_a$**), 1.39 (9 H, s, **H$_g$**).

**$^{19}$F-NMR** (377 MHz, $CDCl_3$) $\delta$ = – 154.99.

**$^{13}$C-NMR** (101 MHz, $CD_3OD$) δ = 158.14, 157.43, 146.26, 134.25, 128.15, 127.21, 92.46, 81.48, 39.55, 36.18, 35.79, 31.63, 28.76.

**HRMS** (ESI+ve) m/z: 471.12523 ([M-$BF_4^-$]$^+$, $C_{19}H_{28}IN_4O_2^+$ requires 471.12515).

**Monotriazolium-urea receptor 3.13.HB$^+$BF$_4^-$.O**




Monotriazole-urea receptor **3.1.HB.O** (59.4 mg, 0.17 mmol) was dissolved in anhydrous $CH_3CN$ (2 mL), after which $[Me_3O]BF_4$ (25.14 mg, 0.17 mmol, 1 eq) was added in one portion. The reaction mixture was stirred at room temperature for 3 days, after which MeOH (5 mL) was added to quench the alkylating agent and the volatiles were removed under reduced pressure. The crude solid was purified by column chromatography (5% MeOH - $CH_2Cl_2$) to afford **3.10.HB$^+$BF$_4^-$** as a colourless oil that partly solidified under high vacuum.

The product was too poorly soluble in most common organic solvents and the yield could not be determined accurately.

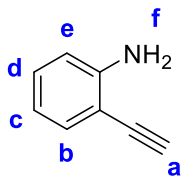
**$^1$H-NMR** (400 MHz, $CD_3OD$) δ = 7.88 (2 H, d, *J*=8.8 Hz, **$H_h$**), 7.74 (2 H, d, *J*=8.8 Hz, **$H_i$**), 7.38 (2 H, d, *J*=7.7 Hz, **$H_c$**), 7.26 (2 H, t, *J*=7.9 Hz, **$H_b$**), 7.01 (1 H, t, *J*=7.3 Hz, **$H_a$**), 4.71 (2 H, s, **$H_f$**), 4.47 (3 H, s, **$H_k$**), 1.39 (9 H, s, **$H_j$**).

**$^{19}$F-NMR** (377 MHz, $CD_3OD$) δ = - 150.44.

**$^{13}$C-NMR** (101 MHz, $CD_3OD$) δ = 157.97, 157.03, 145.18, 140.47, 134.21, 129.99, 128.61, 124.18, 122.37, 120.69, 38.94, 36.14, 34.39, 31.60.

There were fewer $^{13}$C signals than anticipated due to coincidence.

**2-Ethynylaniline 3.14** [15]




**1)** Preparation of the TMS-alkyne

2-Iodoaniline (1.39 g, 6.36 mmol) was dissolved in diethylamine (10 mL) in a vial, after which $Pd(PPh_3)_2Cl_2$ (89.3 mg, 0.13 mmol, 0.02 eqs) and CuI (48.5 mg, 0.25 mmol, 0.04 eqs) were added. The vial was capped and the mixture was degassed for 5 minutes, following which TMS acetylene (1.77 mL, 12.7 mmol, 2 eqs) was added via a syringe. The reaction mixture was stirred at room temperature for 16 h, after which 1 M HCl (20 mL) was added and the product extracted with EtOAc (3 x 30 mL), the combined organic layers washed with brine (50 mL), dried over $MgSO_4$ and filtered. The filtrate was concentrated under reduced pressure to afford the TMS-protected intermediate as a red solid.

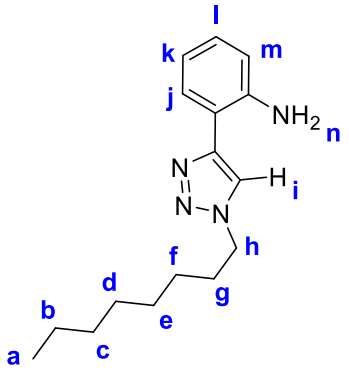
**2)** Deprotection of the TMS group

The TMS-protected intermediate was subsequently redissolved in MeOH (10 mL), to which $KF{\cdot}2H_2O$ (1.80 g, 19.1 mmol, 3 eqs) was added and the reaction mixture was allowed to stir at room temperature for 16 h. Subsequently, water (10 mL) was added and the final product was extracted with EtOAc (3 x 30 mL); the combined organic layers were dried over $MgSO_4$ and filtered, after which the filtrate was concentrated under reduced pressure and purified by column chromatography (hexanes, followed by 10% EtOAc - hexanes) to afford **3.14** as a brown liquid.

Yield: 647 mg (87%)

**$^1$H-NMR** (400 MHz, $CDCl_3$) $\delta$ = 7.34 (1 H, dd, *J*=7.6, 1.3 Hz, $\mathbf{H_e}$), 7.16 (1 H, m, $\mathbf{H_c}$), 6.69 (2 H, m, $\mathbf{H_b} + \mathbf{H_d}$), 4.26 (2 H, br. s., $\mathbf{H_f}$), 3.40 (1 H, s, $\mathbf{H_a}$).

**2-triazolylaniline 3.15**




2-Ethynylaniline **3.14** (57.3 mg, 0.49 mmol), octyl azide **2.21** (75.9 mg, 0.49 mmol, 1 eq), and TBTA (13.0 mg, 0.02 mmol, 0.05 eqs) were dissolved in anhydrous $CH_2Cl_2$ (5 mL). The mixture was degassed, after which $[Cu(CH_3CN)_4]PF_6$ (9.11 mg, 0.02 mmol, 0.05 eqs) was added and the reaction mixture stirred at room temperature for 16 h. After completion, a 0.1 M aqueous solution of EDTA (10 mL) was added and the resulting organic phase washed with brine (15 mL), dried over $MgSO_4$ and filtered. The filtrate was concentrated under reduced pressure and purified by column chromatography ($CH_2Cl_2$) to afford **3.15** as a yellow oil which solidified under high vacuum to give a brown solid.

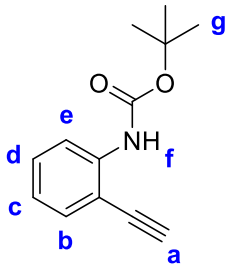
Yield: 93.4 mg (70%)

**$^1$H-NMR** (400 MHz, $CDCl_3$) $\delta$ = 7.75 (1 H, s, $\mathbf{H_i}$), 7.36 (1 H, dd, *J*=7.7, 1.3 Hz, $\mathbf{H_m}$), 7.13 (1 H, m, $\mathbf{H_k}$), 6.78 (1 H, dd, *J*=8.1, 0.9 Hz, $\mathbf{H_j}$), 6.73 (1 H, td, *J*=7.5, 1.2 Hz, $\mathbf{H_l}$), 5.52 (2 H, br. s., $\mathbf{H_n}$), 4.41 (2 H, t, *J*=7.2 Hz, $\mathbf{H_h}$), 1.96 (2 H, t, *J*=7.1 Hz, $\mathbf{H_g}$), 1.31 (10 H, m, $\mathbf{H_{b\text{-}f}}$), 0.89 (3 H, m, $\mathbf{H_a}$).

**$^{13}$C-NMR** (101 MHz, $CDCl_3$) $\delta$ = 148.32, 145.07, 128.87, 127.59, 119.56, 117.19, 116.65, 113.68, 50.38, 31.66, 30.26, 28.99, 28.92, 26.44, 22.54, 14.01.

**HRMS** (ESI+ve) m/z: 273.20732 ($[M+H]^+$, $C_{16}H_{25}N_4^+$ requires 273.20737).

**_N_-Boc-protected 2-ethynylaniline 3.17** [16]

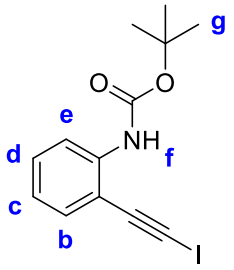



2-Ethynylaniline **3.14** (222 mg, 1.90 mmol) was dissolved in anhydrous THF (5 mL), to which $Boc_2O$ was added (621 mg, 2.85 mmol, 1.5 eqs). The reaction mixture was stirred at reflux for 16 h, after which the volatiles were removed under reduced pressure. The resulting solid was redissolved in $Et_2O$ (10 mL), washed with 0.1 M KOH (10 mL), dried over $MgSO_4$ and filtered. The filtrate was concentrated under reduced pressure and purified by column chromatography (15% EtOAc – hexanes) to afford **3.17** as a yellow liquid.

Yield: 234 mg (57%)

**$^1$H-NMR** (400 MHz, $CDCl_3$) $\delta$ = 8.16 (1 H, d, *J*=8.4 Hz, **$H_e$**), 7.43 (1 H, dd, *J*=7.7, 1.5 Hz, **$H_b$**), 7.33 (1 H, m, **$H_c$**), 6.97 (1 H, td, *J*=7.6, 1.1 Hz, **$H_d$**), 3.48 (1 H, s, **$H_a$**), 1.54 (9 H, s, **$H_g$**).

**_N_-Boc-protected 2-iodoethynylaniline 3.18**




*N*-Boc-protected 2-ethynylaniline **3.17** (93.5 mg, 0.43 mmol) was dissolved in MeOH (5 mL) and cooled to 0 °C. To this, an aqueous solution of KOH (121 mg, 2.15 mmol, 5 eqs) was added and the mixture stirred at 0 °C for 15 mins. Subsequently, $I_2$ (273 mg, 1.08 mmol, 2.5 eqs) was added in one portion and the reaction mixture was allowed to warm to room temperature and stirred for 16 h. Water was added (10 mL) and the resulting precipitate was separated by filtration under reduced pressure to give **3.18** as a light orange solid.

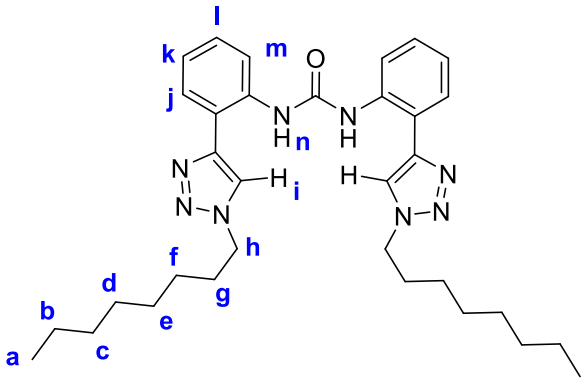
Yield: 19.2 mg (13%)

**$^1$H-NMR** (400 MHz, $CDCl_3$) $\delta$ = 8.14 (1 H, d, *J*=8.3 Hz, $\mathbf{H_e}$), 7.37 (1 H, d, *J*=7.7 Hz, $\mathbf{H_b}$), 7.15 (1 H, br. s., $\mathbf{H_f}$), 6.96 (1 H, m, $\mathbf{H_d}$), 1.56 (9 H, s, $\mathbf{H_g}$).

$\mathbf{H_c}$ was obscured by the solvent signal.

The product was not stable enough to allow for further characterisation data to be obtained.

**1,2-Phenylene bistriazole-urea receptor 3.20.HB.O**




2-Triazolylaniline **3.15** (46.6 mg, 0.17 mmol) and triethylamine (0.03 mL, 0.22 mmol, 1.27 eqs) were dissolved in anhydrous $CH_2Cl_2$ (2 mL), after which triphosgene (8.46 mg, 0.03 mmol, 0.17 eqs) was added and the reaction mixture was stirred at room temperature for 16 h. The resulting precipitate was collected by filtration under reduced pressure to afford **3.20.HB.O** as an off-white solid.

Yield: 20.0 mg (41%)

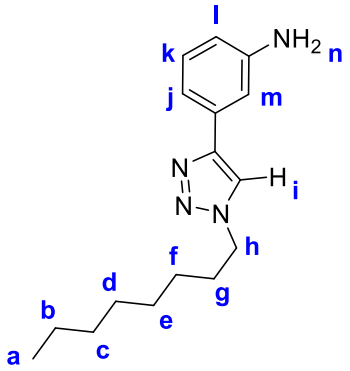
**$^1$H-NMR** (400 MHz, DMSO-$d_6$) $\delta$ = 13.36 (2 H, br. s., $\mathbf{H_n}$), 9.83 (2 H, s, $\mathbf{H_i}$), 8.26 (2 H, d, *J*=7.9 Hz, $\mathbf{H_m}$), 7.81 (2 H, m, $\mathbf{H_k}$), 7.55 (4 H, m, $\mathbf{H_j}$ + $\mathbf{H_l}$), 4.92 (4 H, t, *J*=7.0 Hz, $\mathbf{H_h}$), 2.03 (4 H, m, $\mathbf{H_g}$), 1.26 (20 H, m, $\mathbf{H_{b\text{-}f}}$), 0.86 (6 H, m, $\mathbf{H_a}$).

**$^{13}$C-NMR** (101 MHz, 1:1 $CD_3OD$:$CDCl_3$) $\delta$ = 140.83, 136.57, 135.28, 126.47, 126.38, 117.75, 108.96, 56.55, 32.37, 30.27, 29.66, 29.54, 26.86, 23.23, 14.38.

There were fewer $^{13}$C signals than anticipated due to coincidence.

**HRMS** (ESI+ve) m/z: 571.38679 ($[M+H]^+$, $C_{33}H_{47}N_4O^+$ requires 571.38673).

**3-Triazolylaniline 3.21**




3-Ethynylaniline (0.1 mL, 0.96 mmol), octyl azide **2.21** (148 mg, 0.96 mmol, 1 eq), and TBTA (25.4 mg, 0.05 mmol, 0.05 eqs) were dissolved in anhydrous $CH_2Cl_2$ (5 mL). The mixture was degassed, after which $[Cu(CH_3CN)_4]PF_6$ (17.8 mg, 0.05 mmol, 0.05 eqs) was added and the reaction mixture stirred at room temperature for 16 h. After completion, a 0.1 M aqueous solution of EDTA (15 mL) was added and the resulting organic phase washed with brine (20 mL), dried over $MgSO_4$ and filtered. The filtrate was concentrated under reduced pressure and purified by column chromatography ($CH_2Cl_2$, followed by 25%, 50%, and 75% EtOAc - $CH_2Cl_2$) to afford **3.21** as a dark brown oil.

Yield: 195 mg (75%)

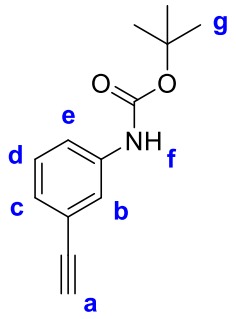
**$^1$H-NMR** (400 MHz, $CDCl_3$) $\delta$ = 7.70 (1 H, s, $\mathbf{H_i}$), 7.21 (1 H, m, $\mathbf{H_k}$), 7.14 (1 H, m, $\mathbf{H_j}$), 6.67 (1 H, dd, *J*=7.8, 1.2 Hz, $\mathbf{H_m}$), 4.39 (2 H, t, *J*=7.3 Hz, $\mathbf{H_h}$), 3.75 (2 H, br. s., $\mathbf{H_n}$), 1.94 (2 H, quin, *J*=7.1 Hz, $\mathbf{H_g}$), 1.31 (10 H, m, $\mathbf{H_{b\text{-}f}}$), 0.88 (3 H, t, *J*=6.7 Hz, $\mathbf{H_a}$).

$\mathbf{H_l}$ was obscured by the solvent signal.

**$^{13}$C-NMR** (126 MHz, $CDCl_3$) $\delta$ = 147.71, 146.87, 131.58, 129.66, 119.40, 115.88, 114.77, 112.13, 50.33, 31.64, 30.28, 28.99, 28.91, 26.43, 22.53, 14.00.

**HRMS** (ESI+ve) m/z: 273.20733 ($[M+H]^+$, $C_{16}H_{25}N_4^+$ requires 273.20737).

**_N_-Boc-protected 3-ethynylaniline 3.22** [17]

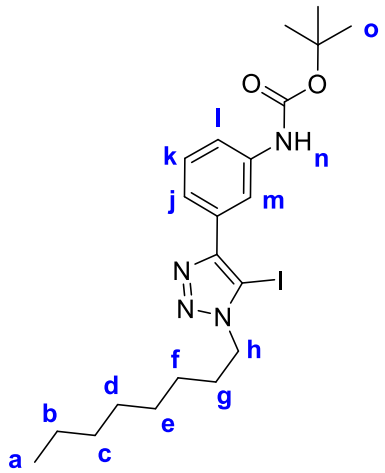



3-Ethynylaniline (0.3 mL, 2.87 mmol) was dissolved in anhydrous THF (10 mL), to which $Boc_2O$ was added (1.25 g, 5.74 mmol, 2 eqs). The reaction mixture was stirred at reflux for 16 h, after which the volatiles were removed under reduced pressure. The resulting solid was redissolved in $Et_2O$ (10 mL), washed with water (10 mL) and brine (15 mL), dried over $MgSO_4$ and filtered. The filtrate was concentrated under reduced pressure and purified by flash column chromatography (50% $CH_2Cl_2$ – hexanes) to afford **3.22** as an off-white solid.

Yield: 545 mg (87%)

**$^1$H-NMR** (400 MHz, $CDCl_3$) $\delta$ = 7.54 (1 H, s, $\mathbf{H_b}$), 7.35 (1 H, d, *J*=7.9 Hz, $\mathbf{H_e}$), 7.22 (1 H, t, *J*=7.8 Hz, $\mathbf{H_d}$), 7.15 (1 H, m, $\mathbf{H_c}$), 6.61 (1 H, br. s., $\mathbf{H_f}$), 3.05 (1H, s, $\mathbf{H_a}$), 1.52 (9 H, m, $\mathbf{H_g}$).

**_N_-Boc-protected 3-iodotriazolylaniline 3.24**




*N*-Boc-protected 3-ethynylaniline **3.22** (283 mg, 1.3 mmol), *N*-iodosuccinimide (351 mg, 1.56 mmol, 1.2 eqs), and acetone (10 mL) were added to a round-bottomed flask. An aqueous

solution of $AgNO_3$ (22.1 mg, 0.13 mmol, 0.1 eqs) was added and the mixture was stirred in the dark at room temperature for 4 h. The iodoalkyne intermediate **3.23** was extracted with $CH_2Cl_2$ (3 x 20 mL), after which the combined organic phases were washed with water (20 mL) and brine (25 mL), dried over $MgSO_4$, filtered and the filtrate concentrated under reduced pressure to afford a red solid.

Iodoalkyne intermediate **3.23** was immediately redissolved in anhydrous, degassed THF (10 mL). To this solution, octyl azide **2.21** (222 mg, 1.43 mmol, 1.1 eqs), TBTA (35.0 mg, 0.07 mmol, 0.05 eqs), and $[Cu(CH_3CN)_4]PF_6$ (24.3 mg, 0.01 mmol, 0.05 eqs) were added and the reaction mixture stirred at room temperature for 16 h. The solvent was removed under reduced pressure and the resulting solid redissolved in $CH_2Cl_2$ (10 mL) washed with 0.1 M EDTA (20 mL) and brine (25 mL), dried over $MgSO_4$, filtered and the filtrate concentrated under reduced pressure. The crude solid was purified by column chromatography ($CH_2Cl_2$, followed by 15% EtOAc – $CH_2Cl_2$) to afford **3.24** as an intense yellow oil, which solidified under high vacuum to give a yellow solid.

Yield: 551 mg (85%)

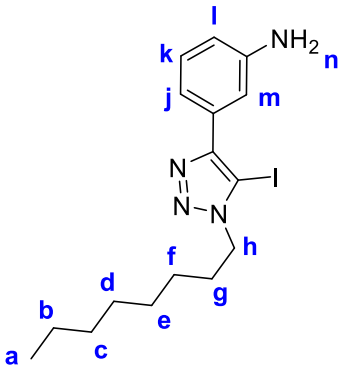
**$^1$H-NMR** (400 MHz, $CDCl_3$) $\delta$ = 7.85 (1 H, s, $\mathbf{H_m}$), 7.61 (1 H, d, *J*=7.7 Hz, $\mathbf{H_j}$), 7.52 (1 H, d, *J*=7.7 Hz, $\mathbf{H_l}$), 7.39 (1 H, m, $\mathbf{H_k}$), 6.56 (1 H, br. s., $\mathbf{H_n}$), 4.44 (2 H, t, *J*=7.4 Hz, $\mathbf{H_h}$), 1.95 (2 H, quin, *J*=7.1 Hz, $\mathbf{H_g}$), 1.54 (9 H, s, $\mathbf{H_o}$), 1.31 (10 H, m, $\mathbf{H_{b\text{-}f}}$), 0.89 (3 H, t, *J*=6.7 Hz, $\mathbf{H_a}$).

**$^{13}$C-NMR** (126 MHz, $CDCl_3$) $\delta$ = 152.64, 149.30, 138.62, 131.04, 129.14, 122.01, 118.61, 117.52, 80.53, 76.25, 50.91, 31.67, 29.88, 28.92, 28.30, 26.36, 22.56, 14.03.

An extra $^{13}$C signal was observed.

**HRMS** (ESI+ve) m/z: 499.15642 ($[M+H]^+$, $C_{21}H_{32}IN_4O_2^+$ requires 499.15645).

**3-Iodotriazolylaniline 3.25**




*N*-Boc-protected 3-iodotriazolylaniline **3.24** (326 mg, 0.65 mmol) was dissolved in anhydrous $CH_2Cl_2$ (5 mL) after which TFA (0.8 mL, 10.5 mmol, 16 eqs) was added and the reaction mixture stirred at room temperature for 16 h. Subsequently, volatiles were removed under reduced pressure, after which the resulting solid was redissolved in $CH_2Cl_2$ (7 mL) and the solution washed with a saturated $NaHCO_3$ solution (10 mL) and brine (15 mL), dried over $MgSO_4$, filtered and then concentrated under reduced pressure to afford **3.25** as an off-white solid.

Yield: 247 mg (95%)

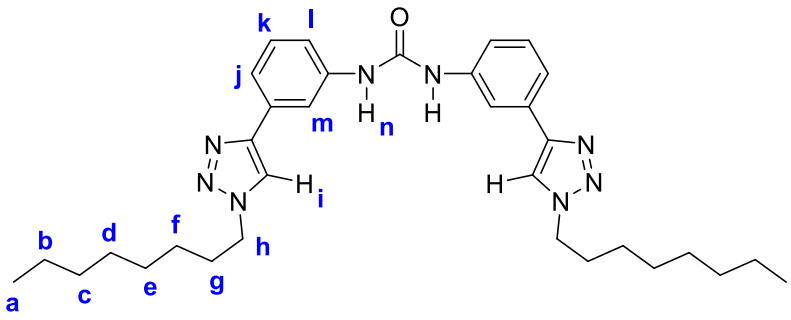
**$^1$H-NMR** (400 MHz, $CDCl_3$) $\delta$ = 7.33 (1 H, m, $\mathbf{H_l}$), 6.72 (1 H, d, *J*=7.9 Hz, $\mathbf{H_j}$), 4.43 (2 H, t, *J*=7.4 Hz, $\mathbf{H_h}$), 3.77 (1 H, br. s., $\mathbf{H_n}$), 1.94 (2 H, m, $\mathbf{H_g}$), 1.33 (10 H, m, $\mathbf{H_{b\text{-}f}}$), 0.89 (3 H, m, $\mathbf{H_a}$).

$\mathbf{H_k}$ and $\mathbf{H_m}$ were obscured by the solvent signal.

**$^{13}$C-NMR** (126 MHz, $CDCl_3$) $\delta$ = 149.61, 146.59, 131.22, 129.33, 117.57, 115.22, 114.06, 76.10, 50.88, 31.66, 29.88, 29.00, 28.92, 26.36, 22.56, 14.03.

**HRMS** (ESI+ve) m/z: 399.10439 ($[M+H]^+$, $C_{16}H_{24}IN_4^+$ requires 399.10402).

**1,3-Phenylene bistriazole-urea receptor 3.26.HB**




3-Triazolylaniline **3.21** (166 mg, 0.61 mmol) and triethylamine (0.1 mL, 2.35 mmol, 1.18 eqs) were dissolved in anhydrous $CH_2Cl_2$ (5 mL), after which triphosgene (30.3 mg, 0.10 mmol, 0.17 eqs) was added and the reaction mixture was stirred at room temperature for 16 h. The resulting precipitate was collected by filtration under reduced pressure and then washed with small amounts of $CH_2Cl_2$ to afford **3.26.HB** as an off-white solid.

Yield: 122 mg (70%)

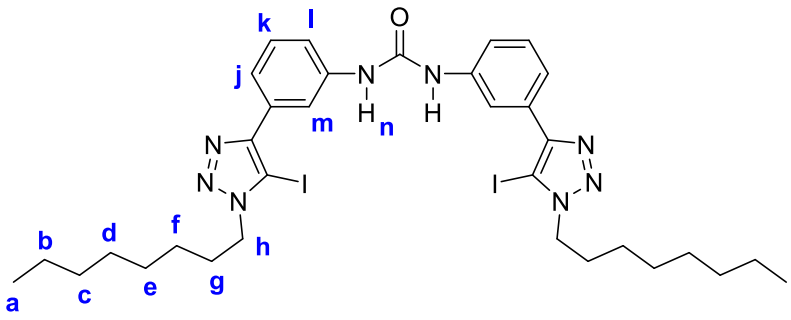
**$^1$H-NMR** (400 MHz, DMSO-$d_6$) $\delta$ = 8.82 (2 H, s, $\mathbf{H_n}$), 8.55 (2 H, s, $\mathbf{H_i}$), 8.08 (2 H, s, $\mathbf{H_m}$), 7.38 (6 H, m, $\mathbf{H_{j-l}}$), 4.39 (4 H, t, $J$=7.0 Hz, $\mathbf{H_h}$), 1.85 (4 H, m, $\mathbf{H_g}$), 1.26 (20 H, m, $\mathbf{H_{b-f}}$), 0.84 (6 H, t, $J$=6.4 Hz, $\mathbf{H_a}$).

**$^{13}$C-NMR** (126 MHz, DMSO-$d_6$) $\delta$ = 206.87, 152.54, 146.30, 140.21, 131.43, 129.36, 121.31, 118.89, 117.66, 114.79, 49.50, 31.19, 29.63, 28.53, 28.36, 25.86, 22.06, 13.95.

An extra $^{13}$C signal was observed.

**HRMS** (ESI+ve) m/z: 571.38694 ([M+H]$^+$, $C_{33}H_{47}N_4O^+$ requires 571.38673).

**1,3-Phenylene bis(iodotriazole)-urea receptor 3.26.XB**




3-Iodotriazolylaniline **3.25** (186 mg, 0.47 mmol) and triethylamine (0.08 mL, 0.57 mmol, 1.23 eqs) were dissolved in anhydrous $CH_2Cl_2$ (5 mL), after which triphosgene (23.1 mg, 0.08 mmol, 0.17 eqs) was added and the reaction mixture was stirred at room temperature for 16 h. The triethylamine hydrochloride side product was collected by filtration under reduced pressure and the filtrate was then washed with 1 M HCl (15 mL) and a saturated $NaHCO_3$ solution (15 mL), dried over $MgSO_4$, filtered and then concentrated under reduced pressure. The resulting crude solid was purified by column chromatography (10% EtOAc – $CH_2Cl_2$) to afford **3.26.XB** as a white solid.

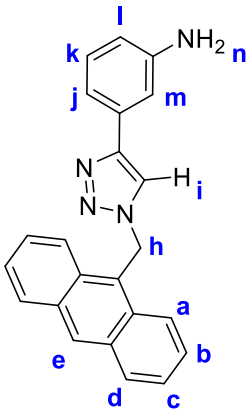
Yield: 94.6 mg (49%)

**$^1$H-NMR** (400 MHz, $CDCl_3$) $\delta$ = 7.82 (1 H, s, $\mathbf{H_n}$), 7.69 (1 H, s, $\mathbf{H_m}$), 7.62 (2 H, m, $\mathbf{H_j}$ + $\mathbf{H_l}$), 7.38 (1 H, t, *J*=7.9 Hz, $\mathbf{H_k}$), 4.46 (2 H, t, *J*=7.3 Hz, $\mathbf{H_h}$), 1.95 (2 H, quin, *J*=6.9 Hz, $\mathbf{H_g}$), 1.31 (10 H, m, $\mathbf{H_{b\text{-}f}}$), 0.88 (3 H, s, $\mathbf{H_a}$).

**$^{13}$C-NMR** (101 MHz, 1:1 $CD_3OD$:$CDCl_3$) $\delta$ = 154.55, 150.48, 140.19, 131.55, 129.89, 122.72, 120.21, 120.21, 118.98, 51.86, 32.43, 30.58, 29.77, 29.66, 27.07, 23.27, 14.43.

**HRMS** (ESI+ve) m/z: 823.18012 ($[M+H]^+$, $C_{33}H_{45}I_2N_8O^+$ requires 823.18002).

**Anthracene-appended 3-triazolylaniline 3.27**




9-(Azidomethyl)anthracene (26.3 mg, 0.11 mmol), 3-ethynylaniline (50.0 mg, 0.43 mmol, 3.9 eqs), DIPEA (0.11 mL, 0.64 mmol, 1.58 eqs), and TBTA (5.8 mg, 0.01 mmol, 0.1 eqs) were dissolved in anhydrous $CH_2Cl_2$ (2 mL). The mixture was degassed, after which $[Cu(CH_3CN)_4]PF_6$ (4.00 mg, 0.01 mmol, 0.1 eqs) was added and the reaction mixture stirred at room temperature for 16 h. After completion, a 0.1 M aqueous solution of EDTA (6 mL) was added and the resulting organic phase washed with brine (10 mL), dried over $MgSO_4$ and filtered. The filtrate was concentrated under reduced pressure and purified by column chromatography (10% EtOAc - $CH_2Cl_2$, followed by 30%, then 50% EtOAc - $CH_2Cl_2$) to afford **3.27** as a pale yellow solid.

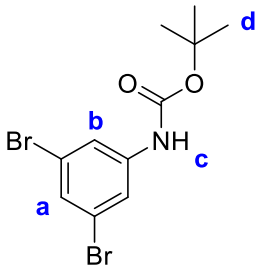
Yield: 26.0 mg (66%)

**$^1$H-NMR** (400 MHz, $CDCl_3$) $\delta$ = 8.62 (1 H, s, $\mathbf{H_e}$), 8.35 (2 H, d, *J*=8.7 Hz, $\mathbf{H_d}$), 8.11 (2 H, d, *J*=8.2 Hz, $\mathbf{H_a}$), 7.62 (2 H, m, $\mathbf{H_c}$), 7.55 (2 H, m, $\mathbf{H_b}$), 7.24 (1 H, s, $\mathbf{H_i}$), 7.05 (2 H, m, $\mathbf{H_m}$ + $\mathbf{H_k}$), 6.92 (1 H, d, *J*=7.9 Hz, $\mathbf{H_j}$), 6.59 (2 H, s, $\mathbf{H_h}$), 6.55 (1 H, d, *J*=8.1 Hz, $\mathbf{H_l}$), 3.63 (2 H, br. s., $\mathbf{H_n}$).

**$^{13}$C-NMR** (101 MHz, $CDCl_3$) $\delta$ = 147.89, 146.68, 131.45, 131.32, 130.84, 129.89, 129.54, 129.48, 127.72, 125.45, 123.74, 123.00, 119.12, 115.89, 114.77, 112.05, 46.48.

**HRMS** (ESI+ve) m/z: 351.16037 ($[M+H]^+$, $C_{23}H_{19}N_4^+$ requires 351.16042).

**_N_-Boc-protected 2,5-dibromoaniline 3.28** [18]

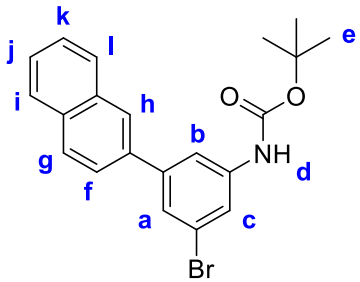



3,5-Dibromoaniline (600 mg, 2.4 mmol) was dissolved in $CHCl_3$ (4 mL). To this, a solution of $NaHCO_3$ (605 mg, 7.2 mmol, 3 eqs) in water (8 mL) was added, along with NaCl (420 mg, 3 eqs) and $Boc_2O$ (1.34 g, 6 mmol, 2.5 eqs). The reaction mixture was stirred at reflux for 2 days, after which water (10 mL) was added, the layers separated and the aqueous layer extracted with $CH_2Cl_2$ (3 x 20 mL). The combined organic phases were washed with water (30 mL) and brine (30 mL), dried over $MgSO_4$, filtered and the filtrate concentrated under reduced pressure. Subsequently, the resulting solid was dissolved in a small amount of $Et_2O$ and purified by precipitation with water to give **3.28** as a white solid.

Yield: 751 mg (89%)

**$^1$H-NMR** (400 MHz, $CDCl_3$) $\delta$ = 7.52 (2 H, s, **$H_b$**), 7.32 (1 H, s, **$H_a$**), 6.45 (1 H, br. s., **$H_c$**), 1.52 (9 H, s, **$H_d$**).

**Naphthalene-appended _N_-Boc-protected bromoaniline 3.29**




_N_-Boc-protected 2,5-dibromoaniline **3.28** (375 mg, 1.07 mmol) and 2-naphthaleneboronic acid (331 mg, 1.93 mmol,1.8 eqs) were dissolved in toluene (8 mL) in a vial. The mixture was degassed, after which $Pd(PPh_3)_4$ (62.0 mg, 0.05 mmol, 0.05 eqs) was added and the reaction mixture was heated to reflux for 3 days. Subsequently, it was allowed to cool to

room temperature, after which water (10 mL) was added and the product extracted with $CH_2Cl_2$ (3 x 30 mL).The combined organic phases were washed with water (20 mL) and brine (25 mL), dried over $MgSO_4$, filtered and the filtrate concentrated under reduced pressure. The crude solid was purified by column chromatography (25% $CH_2Cl_2$ – hexanes, followed by 30% $CH_2Cl_2$ – hexanes) to afford **3.29** as a white solid.

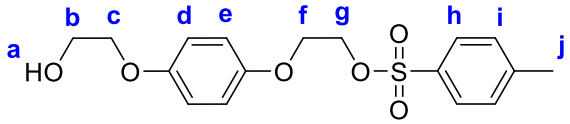
Yield: 186.95 mg (44%)

**$^1$H-NMR** (400 MHz, $CDCl_3$) $\delta$ = 8.01 (1 H, s, $\mathbf{H_c}$), 7.89 (3 H, m, $\mathbf{H_f}$ + $\mathbf{H_g}$ + $\mathbf{H_l}$), 7.69 (1 H, dd, *J*=8.5, 1.8 Hz, $\mathbf{H_h}$), 7.65 (1 H, s, $\mathbf{H_b}$), 7.61 (1 H, s, $\mathbf{H_a}$), 7.52 (3 H, m, $\mathbf{H_i}$ + $\mathbf{H_j}$ + $\mathbf{H_k}$), 6.60 (1 H, br. s., $\mathbf{H_d}$), 1.56 (9 H, s, $\mathbf{H_e}$).

**$^{13}$C-NMR** (126 MHz, $CDCl_3$) $\delta$ = 152.44, 143.54, 139.97, 136.72, 133.44, 132.84, 128.51, 128.23, 127.59, 126.40, 126.24, 125.99, 125.11, 124.90, 123.09, 120.03, 115.93, 81.06, 28.28.

**HRMS** (ESI+ve) m/z: 420.05693 ($[M+Na]^+$, $C_{21}H_{20}BrNO_2Na^+$ requires 420.05696).

**Hydroquinone-based monotosylate 3.32** [19]

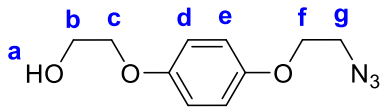



Hydroquinone bis(2-hydroxyethyl)ether (1.00 g, 5.05 mmol), triethylamine (0.92 mL), and DMAP (10 mg, 0.08 mmol, 0.016 eqs) was dissolved in anhydrous THF (25 mL) with stirring. *p*-Toluenesulfonyl chloride (1.01 g, 5.30 mmol, 1 eq) was added to the previous solution and the reaction mixture was stirred under a $N_2$ atmosphere for 16 h. The resulting white suspension was filtered and the filtrate was concentrated under reduced pressure to give a crude yellow material, which was purified by column chromatography (20% EtOAc – hexanes, followed by 30%, 40%, and 50% EtOAc – hexanes) to give **3.32** as a colourless oil.

Yield: 553.6 mg (30%)

**$^1$H-NMR** (400 MHz, $CDCl_3$) $\delta$ = 7.83 (2 H, d, *J*=8.3 Hz, $\mathbf{H_h}$), 7.35 (2 H, d, *J*=7.8 Hz, $\mathbf{H_i}$), 6.83 (2 H, m, $\mathbf{H_e}$), 6.74 (2 H, m, $\mathbf{H_d}$), 4.35 (2 H, m, $\mathbf{H_g}$), 4.11 (2 H, m, $\mathbf{H_f}$), 4.04 (2 H, m, $\mathbf{H_c}$), 3.95 (2 H, m, $\mathbf{H_b}$), 2.46 (3 H, s, $\mathbf{H_j}$), 2.01 (1 H, t, *J*=6.2 Hz, $\mathbf{H_a}$).

**Hydroquinone-based monoazide 3.33** [20]

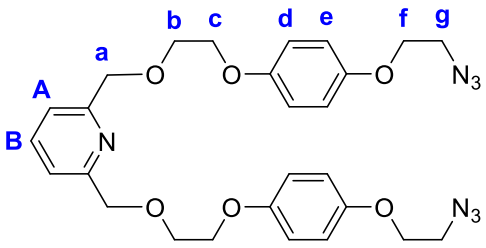



Hydroquinone-based monotosylate **3.1** (500 mg, 1.42 mmol) and $NaN_3$ (92.3 mg, 1.42 mmol, 1 eq) were suspended in anhydrous DMF (10 mL) and the mixture was stirred under a $N_2$ atmosphere at 50 °C for 3 days. The solvent was then removed under reduced pressure, the resulting solid suspended in $CHCl_3$ (30 mL) and the suspension filtered. The filtrate was concentrated under reduced pressure to afford **3.33** as a yellow oil that solidified upon standing.

Yield: 267 mg (84%)

**$^1$H-NMR** (400 MHz, $CDCl_3$) $\delta$ = 6.88 (4 H, s, $\mathbf{H_d}$ + $\mathbf{H_e}$), 4.12 (2 H, t, *J*=5.0 Hz, $\mathbf{H_f}$), 4.05 (2 H, m, $\mathbf{H_c}$), 3.95 (2 H, m, $\mathbf{H_b}$), 3.58 (2 H, t, *J*=5.0 Hz, $\mathbf{H_g}$), 2.00 (1 H, t, *J*=6.2 Hz, $\mathbf{H_a}$).

**Bisazide precursor 3.34** [20]

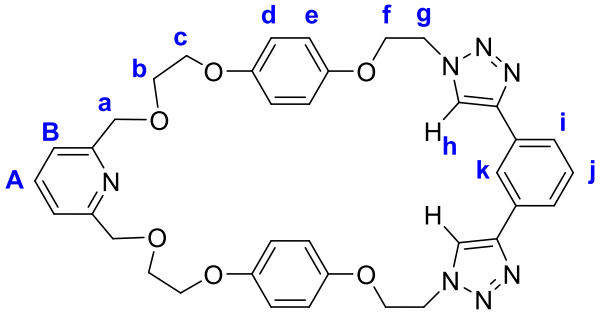



NaH (54.0 mg suspension 60% in mineral oil, 1.35 mmol, 3 eqs) was suspended in anhydrous THF (17 mL), after which hydroquinone-based monoazide **3.33** (200 mg, 0.9 mmol, 2 eqs) was added and the reaction mixture was stirred for 20 minutes. Subsequently, 2,6-bis(bromomethyl)pyridine (119 mg, 0.45 mmol) was added at the mixture heated at 50 °C for 5 days. The solvent was then removed under reduced pressure, the resulting solid dissolved in $CH_2Cl_2$ (6 mL) and washed with water (5 mL) and brine (5 mL), dried over $MgSO_4$, filtered and the filtrate concentrated under reduced pressure to afford **3.34** as an orange oil.

Yield: 183.5 mg (73%)

**$^1$H-NMR** (400 MHz, $CDCl_3$) δ = 7.71 (1 H, m, **$H_B$**), 7.40 (2 H, d, *J*=7.7 Hz, **$H_A$**), 6.87 (8 H, m, **$H_d$** + **$H_e$**), 4.74 (4 H, s, **$H_a$**), 4.14 (4 H, m, **$H_f$**), 4.09 (4 H, t, *J*=5.0 Hz, **$H_c$**), 3.91 (4 H, m, **$H_b$**), 3.56 (4 H, t, *J*=4.9 Hz, **$H_g$**).

**Pyridyl-bistriazole macrocycle 3.35**




Bisazide precursor **3.34** (57.9 mg, 0.11 mmol), 1,3-diethynylbenzene (25 µL, 0.188 mmol, 1 eq), DIPEA (28 µL, 0.16 mmol, 1.53 eqs), and TBTA (5.60 mg, 0.011 mmol, 0.06 eqs) were dissolved in anhydrous $CH_2Cl_2$ (250 mL). The mixture was degassed, after which $[Cu(CH_3CN)_4]PF_6$ (7.85 mg, 0.02 mmol, 0.2 eqs) was added and the reaction mixture stirred at room temperature for 16 h. After completion, a 0.1 M aqueous solution of EDTA was added (10 mL) and the resulting organic phase washed with brine (15 mL), dried over $MgSO_4$ and filtered. The filtrate was concentrated under reduced pressure and purified by preparative plate chromatography (2% MeOH - $CH_2Cl_2$) to afford **3.35** as a white solid.

Yield: 14.9 mg (21%)

**$^1$H-NMR** (400 MHz, $CDCl_3$) δ = 8.15 (1 H, s, **$H_k$**), 8.04 (2 H, s, **$H_h$**), 7.89 (2 H, d, *J*=7.8 Hz, **$H_i$**), 7.58 (1 H, m, **$H_j$**), 7.51 (1 H, m, **$H_A$**), 6.77 (8 H, m, **$H_d$** + **$H_e$**), 4.80 (4 H, t, *J*=4.7 Hz, **$H_g$**), 4.67 (4 H, s, **$H_a$**), 4.34 (4 H, t, *J*=4.8 Hz, **$H_f$**), 4.10 (4 H, m, **$H_c$**), 3.87 (4 H, m, **$H_b$**).

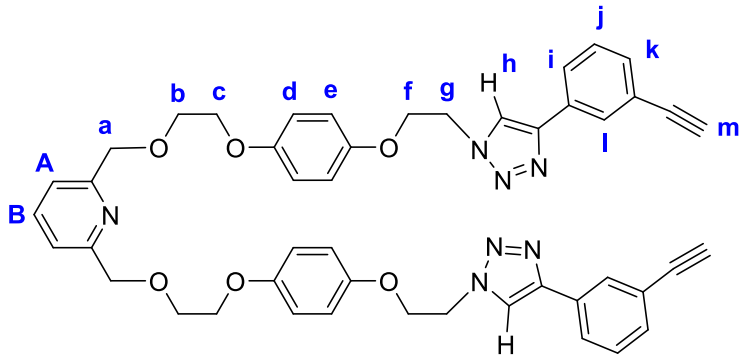
**$H_B$** was obscured by the solvent signal.

**$^{13}$C-NMR** (101 MHz, $CDCl_3$) δ = 157.68, 153.61, 152.24, 147.55, 137.20, 131.17, 129.48, 125.50, 123.04, 121.27, 121.27, 120.34, 115.93, 115.74, 74.09, 69.33, 68.14, 67.55, 50.24, 30.93.

There were fewer $^{13}$C signals than anticipated due to coincidence.

**HRMS** (ESI+ve) m/z: 676.28842 ($[M+H]^+$, $C_{37}H_{38}N_7O_6^+$ requires 676.28781).

**Pyridyl-bistriazole bisalkyne 3.36**



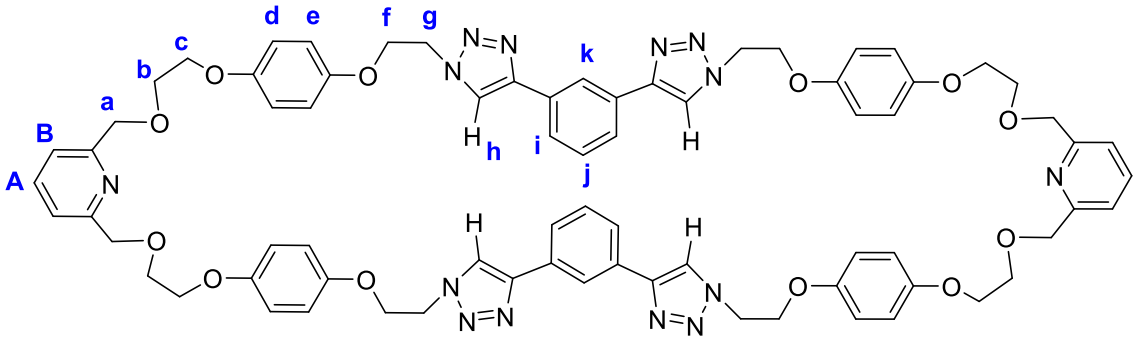

1,3-Diethynylbenzene (0.02 mL, 0.15 mmol, 2 eqs), DIPEA (0.02 mL, 0.115 mmol, 1.53 eqs), TBTA (5.99 mg, 0.011 mmol, 0.15 eqs), and $[Cu(CH_3CN)_4]PF_6$ (5.61 mg, 0.015 mmol, 0.20 eqs) were dissolved in anhydrous, degassed $CH_2Cl_2$ (50 mL). A solution of bisazide precursor **3.34** (41.3 mg, 0.075 mmol) in a small amount of $CH_2Cl_2$ was added dropwise, after which the mixture was stirred at room temperature for 7 days. After completion, a 0.1 M aqueous solution of EDTA (10 mL) was added and the resulting organic phase washed with brine (20 mL), dried over $MgSO_4$ and filtered. The filtrate was concentrated under reduced pressure and purified by preparative plate chromatography (2% MeOH - $CH_2Cl_2$) to afford **3.36** as a white solid.

Yield: 19.3 mg (32%)

**$^1$H-NMR** (400 MHz, $CDCl_3$) $\delta$ = 7.98 (2 H, s, $\mathbf{H_h}$), 7.95 (2 H, s, $\mathbf{H_l}$), 7.87 (2 H, d, *J*=8.1 Hz, $\mathbf{H_A}$), 7.69 (1 H, m, $\mathbf{H_B}$), 7.46 (2 H, m, $\mathbf{H_i}$), 7.39 (4 H, m, $\mathbf{H_j}$ + $\mathbf{H_k}$), 6.85 (8 H, m, $\mathbf{H_d}$ + $\mathbf{H_e}$), 4.79 (4 H, t, *J*=4.8 Hz, $\mathbf{H_g}$), 4.73 (4 H, s, $\mathbf{H_a}$), 4.36 (4 H, t, *J*=4.9 Hz, $\mathbf{H_f}$), 4.13 (4 H, m, $\mathbf{H_c}$), 3.90 (4 H, t, *J*=4.6 Hz, $\mathbf{H_b}$), 3.11 ppm (2 H, s, $\mathbf{H_m}$).

**HRMS** (ESI+ve) m/z: 802.33434 ($[M+H]^+$, $C_{47}H_{44}N_7O_6^+$ requires 802.33476).

**Bispyridyl-tetrakistriazole macrocycle 3.37**




Bisazide precursor **3.34** (10.5 mg, 0.019 mmol), pyridyl-bistriazole bisalkyne **3.36** (15.4 mg, 0.019 mmol, 1 eq), DIPEA (5 µL, 0.029 mmol, 1.53 eqs), and TBTA (15.23 mg, 0.003 mmol, 0.15 eqs) were dissolved in anhydrous $CH_2Cl_2$ (100 mL). The mixture was degassed, after which $[Cu(CH_3CN)_4]PF_6$ (1.43 mg, 0.004 mmol, 0.20 eqs) was added and the reaction mixture stirred at room temperature for 3 days. Afterwards, the majority of the solvent was removed under reduced pressure, a 0.1 M aqueous solution of EDTA was added (6 mL) and the resulting organic phase washed with brine (6 mL), dried over $MgSO_4$ and filtered. The filtrate was concentrated under reduced pressure and purified by preparative plate chromatography (2% MeOH - $CH_2Cl_2$) to afford **3.37** as a white solid.

Yield: 2.10 mg (8%)

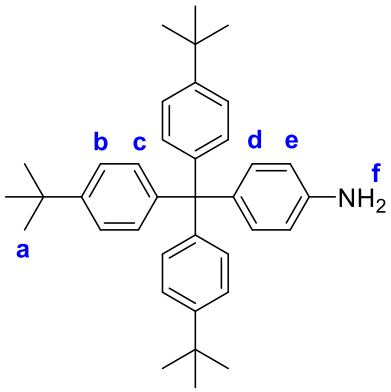
**$^1$H-NMR** (500 MHz, $CDCl_3$) $\delta$ = 8.26 (2 H, m, $\mathbf{H_k}$), 8.04 (4 H, m, $\mathbf{H_h}$), 7.84 (4 H, m, $\mathbf{H_i}$), 7.66 (2 H, m, $\mathbf{H_j}$), 7.49 (2 H, m, $\mathbf{H_A}$), 7.35 (4 H, m, $\mathbf{H_B}$), 6.82 (16 H, m, $\mathbf{H_d}$ + $\mathbf{H_e}$), 4.79 (8 H, m, $\mathbf{H_g}$), 4.70 (8 H, m, $\mathbf{H_a}$), 4.35 (8 H, m, $\mathbf{H_f}$), 4.11 (8 H, m, $\mathbf{H_c}$), 3.87 (8 H, m, $\mathbf{H_b}$).

**$^{13}$C-NMR** (127 MHz, $CDCl_3$) $\delta$ = 157.71, 153.68, 152.16, 147.55, 137.28, 131.17, 129.43, 125.47, 122.99, 121.12, 120.15, 115.76. 74.13, 69.41, 68.00, 67.28, 50.04.

There were fewer $^{13}$C signals than anticipated due to coincidence.

**HRMS** (ESI+ve) m/z: 1351.56920 ($[M+H]^+$, $C_{74}H_{75}N_{14}O_{12}^+$ requires 1351.56834).

**Aniline stopper 3.38** [21]

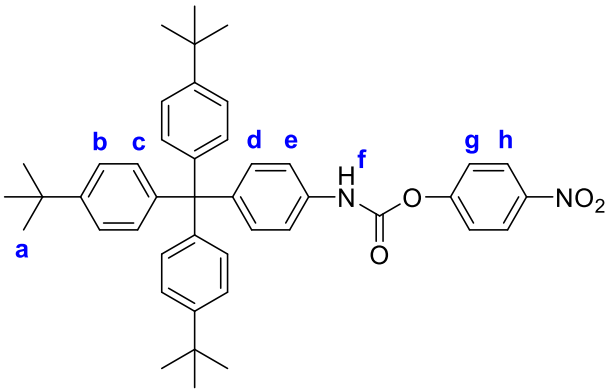



Terphenyl alcohol stopper **2.5** (926 mg, 2.17 mmol) was suspended in acetyl chloride (7 mL) and heated at 60 °C under a $N_2$ atmosphere for 16 hours. Subsequently, the volatiles were removed under reduced pressure and the crude residue immediately re-dissolved in aniline (7 mL). The reaction mixture was heated at 130 °C under a $N_2$ atmosphere for 16 hours, after which it was allowed to cool to room temperature and poured onto 10% HCl (26 mL) and stirred for 30 mins. The mixture was extracted with $CH_2Cl_2$ (4 x 30 mL) and the combined organic layers were washed with 10% HCl (13 mL), followed by a saturated $Na_2CO_3$ solution (2 x 13 mL), water (2 x 30 mL), then dried over $MgSO_4$, filtered and the filtrate concentrated under reduced pressure. The crude solid was purified by column chromatography ($CH_2Cl_2$) followed by repeated recrystallisations (30% toluene - hexane) to afford **3.38** as a pale yellow solid.

Yield: 645 mg (59%)

**$^1$H-NMR** (400 MHz, $CDCl_3$) $\delta$ = 7.23 (6 H, d, *J*=8.7 Hz, $\mathbf{H_b}$), 7.09 (6 H, m, $\mathbf{H_c}$), 6.96 (2 H, d, *J*=8.7 Hz, $\mathbf{H_d}$), 6.58 (2 H, d, *J*=8.6 Hz, $\mathbf{H_e}$), 3.59 (2 H, s, $\mathbf{H_f}$), 1.31 (27 H, s, $\mathbf{H_a}$).

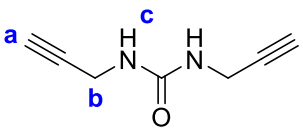
**Stopper 4-nitrophenyl carbamate 3.41** [22]




Aniline stopper **3.38** (202 mg, 0.4 mmol) and DIPEA (0.08 mL, 0.44 mmol, 1.1 eqs) were dissolved in $CHCl_3$ (3 mL), after which 4-nitrophenyl chloroformate (88.9 mg, 0.44 mmol, 1.1 eqs) was added. The reaction mixture was stirred at room temperature for 30 mins, after which hexane (10 mL) was added and the resulting precipitate collected by filtration under reduced pressure to afford **3.41** as an impure, off-white solid. This was used without further purification.

Yield: 62.4 mg

**Aliphatic urea bis-alkyne 3.45** [12]

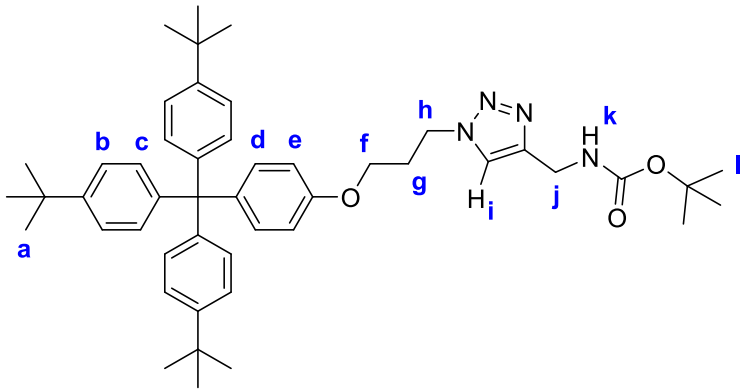



Propargyl amine (0.3 mL, 4.68 mmol) was dissolved in anhydrous $CH_2Cl_2$ (2 mL) at 0 °C, after which CDI (380 mg, 2.34 mmol, 0.5 eqs) was added and the reaction mixture stirred at room temperature for 16 h. The resulting precipitate was separated by filtration under reduced pressure and washed with small amounts of $CH_2Cl_2$ to afford **3.45** as a white solid.

Yield: 258 mg (81%)

**$^1$H-NMR** (400 MHz, acetone-$d_6$) $\delta$ = 5.86 (2 H, br. s., $\mathbf{H_c}$), 3.94 (4 H, dd, $J$=5.7, 2.5 Hz, $\mathbf{H_b}$), 2.59 (2 H, t, $J$=2.5 Hz, $\mathbf{H_a}$).

***N*-Boc-protected aminotriazole stopper 3.47.HB**




Aliphatic azide stopper **2.27** (316 mg, 0.54 mmol), *N*-Boc-protected propargyl amine **3.5** (83.5 mg, 0.54 mmol, 1 eq), DIPEA (0.14 mL, 0.81 mmol, 1.5 eqs), and TBTA (14.3 mg, 0.03 mmol, 0.05 eqs) were dissolved in anhydrous $CH_2Cl_2$ (10 mL). The mixture was degassed, after which $[Cu(CH_3CN)_4]PF_6$ (10.0 mg, 0.03 mmol, 0.05 eqs) was added and the reaction mixture stirred at room temperature for 16 h. After completion, a 0.1 M aqueous solution of EDTA (10 mL) was added and the resulting organic phase washed with brine (15 mL), dried over $MgSO_4$ and filtered. The filtrate was concentrated under reduced pressure and purified by column chromatography (30% EtOAc - hexanes) to afford **3.47.HB** as an off-white solid.

Yield: 349 mg (87%)

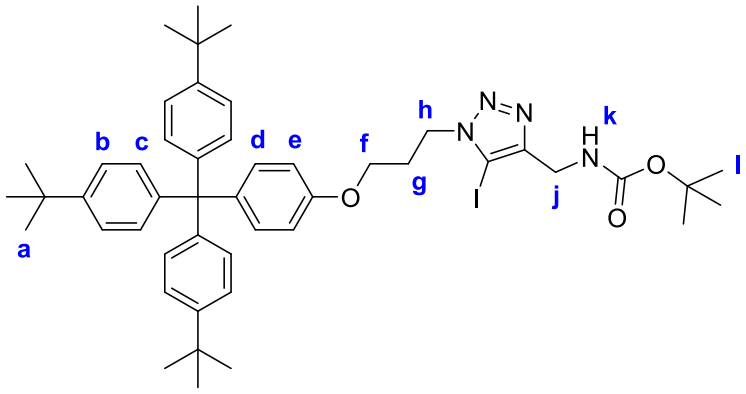
**$^1$H-NMR** (400 MHz, $CDCl_3$) $\delta$ = 7.54 (1 H, s, $\mathbf{H_i}$), 7.24 (6 H, d, *J*=8.4 Hz, $\mathbf{H_b}$), 7.09 (8 H, m, $\mathbf{H_c}$ + $\mathbf{H_d}$), 6.75 (2 H, d, *J*=8.7 Hz, $\mathbf{H_e}$), 5.07 (1 H, m, $\mathbf{H_k}$), 4.56 (2 H, t, *J*=6.8 Hz, $\mathbf{H_h}$), 4.39 (2 H, d, *J*=6.0 Hz, $\mathbf{H_j}$), 3.96 (2 H, t, *J*=5.7 Hz, $\mathbf{H_f}$), 2.38 (2 H, quin, *J*=6.3 Hz, $\mathbf{H_g}$), 1.43 (9 H, s, $\mathbf{H_l}$), 1.31 (27 H, s, $\mathbf{H_a}$).

**$^{13}$C-NMR** (126 MHz, $CDCl_3$) $\delta$ = 156.19, 148.34, 144.04, 140.14, 132.34, 130.70, 124.05, 112.91, 63.86, 63.04, 47.19, 34.28, 31.37, 30.07, 28.37.

There were fewer $^{13}$C signals than anticipated due to coincidence.

**HRMS** (ESI+ve) m/z: 743.48927 ($[M+H]^+$, $C_{48}H_{63}N_4O_3^+$ requires 743.48947).

**_N_-Boc-protected aminoiodotriazole stopper 3.47.XB**




Aliphatic azide stopper **2.27** (386 mg, 0.66 mmol), *N*-Boc-protected iodopropargyl amine **3.6** (184 mg, 0.66 mmol, 1 eq), and TBTA (34.8 mg, 0.07 mmol, 0.10 eqs) were dissolved in anhydrous $CH_2Cl_2$ (10 mL). The mixture was degassed, after which $[Cu(CH_3CN)_4]PF_6$ (24.5 mg, 0.07 mmol, 0.10 eqs) was added and the reaction mixture stirred at room temperature for 16 h. After completion, a 0.1 M aqueous solution of EDTA (20 mL) was added and the resulting organic phase washed with brine (30 mL), dried over $MgSO_4$ and filtered. The filtrate was concentrated under reduced pressure and purified by column chromatography (5% EtOAc – $CH_2Cl_2$) to afford **3.47.XB** as a white solid.

Yield: 315 mg (55%)

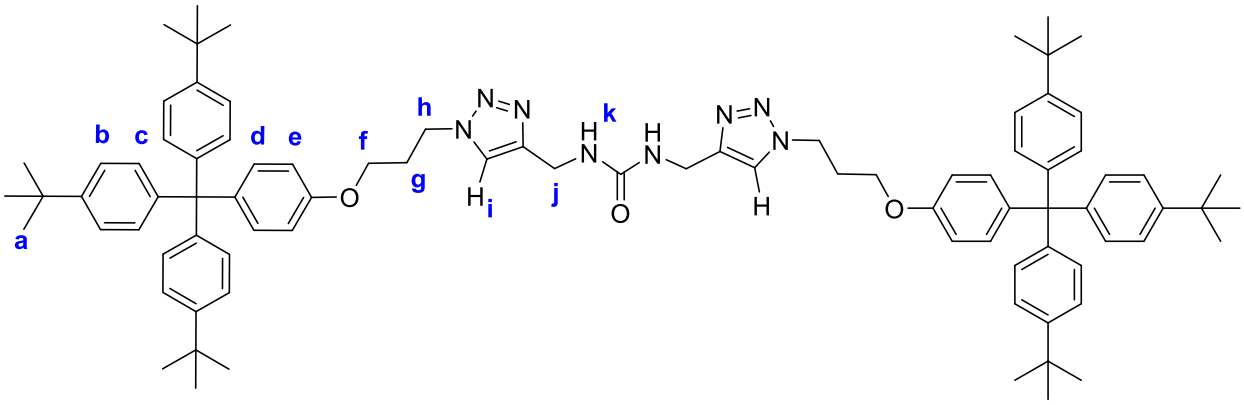
**$^1$H-NMR** (400 MHz, $CDCl_3$) $\delta$ = 7.24 (6 H, m, $\mathbf{H_b}$), 7.09 (8 H, m, $\mathbf{H_c}$ + $\mathbf{H_d}$), 6.76 (2 H, d, *J*=8.9 Hz, $\mathbf{H_e}$), 5.09 (1 H, br. s., $\mathbf{H_k}$), 4.58 (2 H, t, *J*=7.0 Hz, $\mathbf{H_h}$), 4.38 (2 H, d, *J*=5.5 Hz, $\mathbf{H_j}$), 4.00 (2 H, t, *J*=5.8 Hz, $\mathbf{H_f}$), 2.39 (2 H, quin, *J*=6.4 Hz, $\mathbf{H_g}$), 1.46 (9 H, s, $\mathbf{H_l}$), 1.31 (27 H, s, $\mathbf{H_a}$).

**$^{13}$C-NMR** (126 MHz, $CDCl_3$) $\delta$ = 156.17, 148.64, 148.33, 144.06, 140.08, 132.29, 130.70, 124.05, 113.04, 63.88, 63.05, 47.77, 36.60, 34.28, 31.37, 29.65, 28.39.

There were fewer $^{13}$C signals than anticipated due to coincidence.

**HRMS** (ESI+ve) m/z: 869.38604 ($[M+H]^+$, $C_{48}H_{62}IN_4O_3^+$ requires 869.38611).

**Neutral bistriazole-urea axle with methylene bridges 3.49.HB**



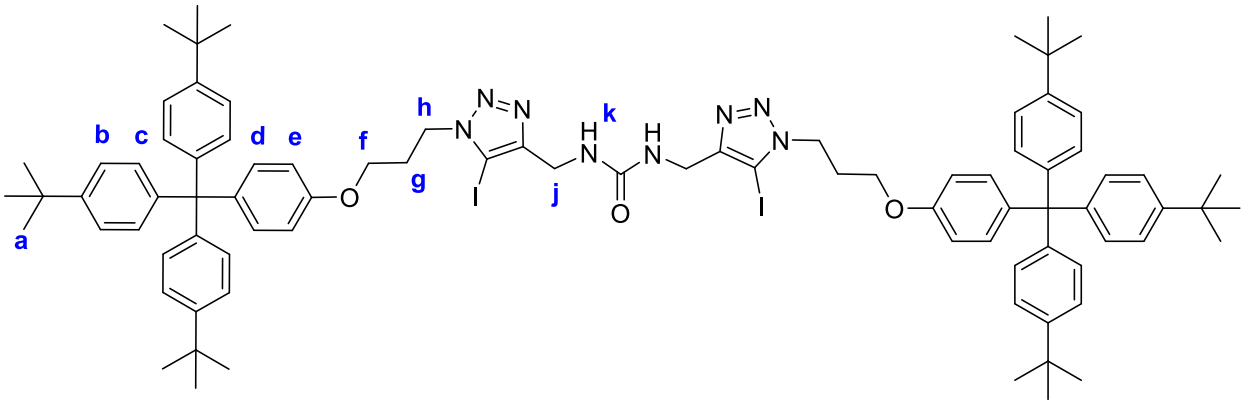

*N*-Boc-protected aminotriazole stopper **3.47.HB** (484 mg, 0.65 mmol) was dissolved in anhydrous $CH_2Cl_2$ (5 mL) after which TFA (0.8 mL, 10.4 mmol, 16 eqs) was added and the reaction mixture stirred at room temperature for 16 h. Excess TFA was removed under reduced pressure and the residue subsequently redissolved in anhydrous $CH_2Cl_2$ (5 mL). To this solution, DIPEA (0.23 mL, 1.3 mmol, 2 eqs) and CDI (70.3 mg, 0.43 mmol, 0.67 eqs) were added and the reaction mixture stirred at room temperature for a further 16 h. The solvent was removed under reduced pressure and the resulting solid purified by column chromatography (2% MeOH – $CH_2Cl_2$, followed by 3.5% MeOH – $CH_2Cl_2$ and 5% MeOH – $CH_2Cl_2$) to afford **3.49.HB** as a white solid.

Yield: 299 mg (70%)

**$^1$H-NMR** (400 MHz, $CDCl_3$) $\delta$ = 7.52 (1 H, s, $\mathbf{H_i}$), 7.23 (6 H, d, *J*=8.3 Hz, $\mathbf{H_b}$), 7.07 (8 H, d, *J*=7.8 Hz, $\mathbf{H_c}$ + $\mathbf{H_d}$), 6.72 (2 H, d, *J*=8.3 Hz, $\mathbf{H_e}$), 5.59 (1 H, br. s., $\mathbf{H_k}$), 4.51 (2 H, m, $\mathbf{H_h}$), 4.42 (2 H, d, *J*=5.6 Hz, $\mathbf{H_j}$), 3.93 (2 H, t, *J*=4.9 Hz, $\mathbf{H_f}$), 2.34 (2 H, quin, *J*=6.3 Hz, $\mathbf{H_g}$), 1.30 (27 H, s, $\mathbf{H_a}$).

**HRMS** (ESI+ve) m/z: 1311.84738 ($[M+H]^+$, $C_{87}H_{107}N_8O_3^+$ requires 1311.84607).

**Neutral bisiodotriazole-urea axle with methylene bridges 3.49.XB**



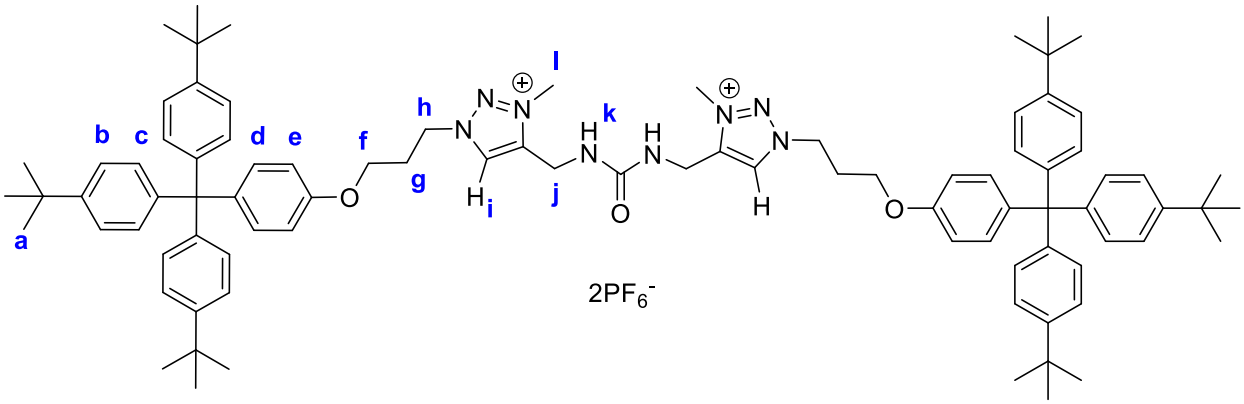

*N*-Boc-protected aminoiodotriazole stopper **3.47.XB** (284 mg, 0.33 mmol) was dissolved in anhydrous $CH_2Cl_2$ (7 mL), after which TFA (0.4 mL, 5.22 mmol, 16 eqs) was added and the reaction mixture stirred at room temperature for 16 h. Excess TFA was removed under reduced pressure and the residue subsequently redissolved in anhydrous $CH_2Cl_2$ (7 mL) To this solution, DIPEA (0.11 mL, 0.65 mmol, 2 eqs) and CDI (35.3 mg, 0.22 mmol, 0.67 eqs) were added and the reaction mixture stirred at room temperature for a further 16 h. The solvent was removed under reduced pressure and the resulting solid purified by column chromatography (10% EtOAc – $CH_2Cl_2$, followed by 70% EtOAc – $CH_2Cl_2$) to afford **3.49.XB** as a white solid.

Yield: 317 mg (62%)

**$^1$H-NMR** (400 MHz, $CDCl_3$) $\delta$ = 7.23 (6 H, m, $\mathbf{H_b}$), 7.08 (8 H, m, $\mathbf{H_c}$ + $\mathbf{H_d}$), 6.75 (2 H, d, *J*=9.0 Hz, $\mathbf{H_e}$), 5.25 (1 H, t, *J*=5.3 Hz, $\mathbf{H_k}$), 4.56 (2 H, t, *J*=7.0 Hz, $\mathbf{H_h}$), 4.44 (2 H, d, *J*=5.4 Hz, $\mathbf{H_j}$), 3.99 (2 H, t, *J*=5.7 Hz, $\mathbf{H_f}$), 2.37 (2 H, m, $\mathbf{H_g}$), 1.30 (27 H, s, $\mathbf{H_a}$).

**HRMS** (ESI+ve) m/z: 1563.63576 ($[M+H]^+$, $C_{87}H_{105}I_2N_8O_3^+$ requires 1563.63935).

**Cationic bistriazolium-urea axle with methylene bridges 3.50.HB$^{2+}$(PF$_6^-$)$_2$**




Neutral bistriazole-urea axle with methylene bridges **3.49.HB** (299 mg, 0.23 mmol) was suspended in anhydrous $CH_3CN$ (75 mL) and the suspension was slowly heated using a heat gun until all the solid dissolved, after which the solution was allowed to cool to room temperature. Subsequently, $[Me_3O]BF_4$ (101 mg, 0.34 mmol, 2 eqs) was added in one portion and the reaction mixture stirred at room temperature for 16 h. The excess alkylating reagent was quenched with MeOH (10 mL), after which the solvent was removed under reduced pressure and the resulting solid redissolved in warm $CH_3CN$ (25 mL). The solution was allowed to cool to room temperature, following which 0.1 M $NH_4PF_6$ (100 mL) was added and the resulting precipitate separated by filtration under reduced pressure and washed with distilled water to afford **3.50.HB$^{2+}$(PF$_6^-$)$_2$** as a white solid.

Yield: 293 mg (85%)

**$^1$H-NMR** (400 MHz, DMSO-*d*$_6$) δ = 8.77 (2 H, s, **H$_i$**), 7.28 (12 H, m, **H$_b$**), 7.13 (2 H, t, *J*=5.6 Hz, **H$_k$**), 7.03 (16 H, m, **H$_c$** + **H$_d$**), 6.74 (4 H, d, *J*=8.9 Hz, **H$_e$**), 4.72 (4 H, t, *J*=6.5 Hz, **H$_h$**), 4.43 (4 H, d, *J*=5.4 Hz, **H$_j$**), 4.15 (6 H, s, **H$_l$**), 4.00 (4 H, m, **H$_f$**), 2.33 (4 H, m, **H$_g$**), 1.24 (54 H, s, **H$_a$**).

**$^{13}$C-NMR** (126 MHz, DMSO-*d*$_6$) δ = 155.73, 147.81, 143.93, 139.28, 131.46, 129.96, 129.21, 124.37, 113.27, 62.57, 34.06, 31.13, 30.71.

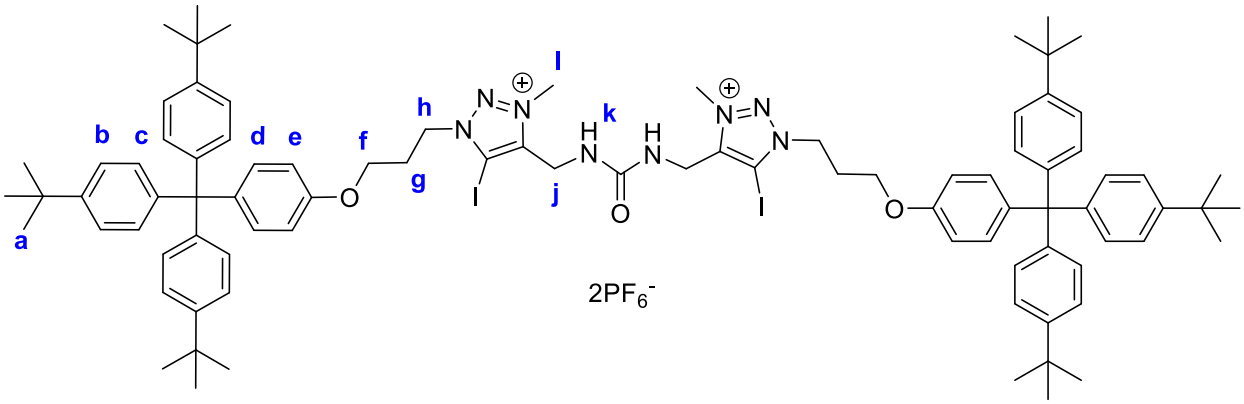
There were fewer $^{13}$C signals than anticipated due to coincidence.

**$^{19}$F-NMR** (470 MHz, DMSO-*d*$_6$) δ = - 70.15 (12 F, d)

**$^{31}$P-NMR** (202 MHz, DMSO-*d*$_6$) δ = -144.21 (2 P, quin)

**HRMS** (ESI+ve) m/z: 670.44239 ([M-2BF$_4^-$]$^{2+}$, $C_{89}H_{112}N_8O_3^{2+}$ requires 670.44232).

**Cationic bisiodotriazolium-urea axle with methylene bridges 3.50.XB$^{2+}$(PF$_6^-$)$_2$**




Neutral bisiodotriazole-urea axle with methylene bridges **3.49.XB** (159 mg, 0.10 mmol) was suspended in anhydrous $CH_2Cl_2$ (10 mL), after which $[Me_3O]BF_4$ (45.2 mg, 0.30 mmol, 3 eqs) was added in one portion and the reaction mixture stirred at room temperature for 16 h. The excess alkylating reagent was quenched with MeOH (6 mL), after which the solvent was removed under reduced pressure and the resulting solid redissolved in warm $CH_3CN$ (20 mL). The solution was allowed to cool to room temperature, following which 0.1 M $NH_4PF_6$ (100 mL) was added and the resulting precipitate separated by filtration under reduced pressure and washed with distilled water to afford **3.50.XB$^{2+}$(PF$_6^-$)$_2$** as a white solid.

Yield: 146 mg (81%)

**$^1$H-NMR** (400 MHz, DMSO-*d*$_6$) $\delta$ = 7.28 (12 H, d, *J*=8.6 Hz, **H$_b$**), 7.13 (2 H, t, *J*=5.5 Hz, **H$_k$**), 7.02 (16 H, m, **H$_c$** + **H$_d$**), 6.72 (4 H, d, *J*=8.9 Hz, **H$_e$**), 4.69 (4 H, t, *J*=6.5 Hz, **H$_h$**), 4.35 (4 H, d, *J*=5.3 Hz, **H$_j$**), 4.17 (6 H, s, **H$_l$**), 4.03 (4 H, t, *J*=5.4 Hz, **H$_f$**), 2.32 (4 H, m, **H$_g$**), 1.24 (54 H, s, **H$_a$**).

**$^{13}$C-NMR** (101 MHz, DMSO-*d*$_6$) $\delta$ = 157.58, 155.67, 147.81, 144.83, 143.92, 139.25, 131.46, 129.98, 124.35, 113.27, 91.97, 64.10, 62.59, 51.53, 38.36, 34.05, 33.52, 31.14, 27.94.

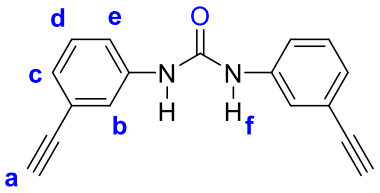
There were fewer $^{13}$C signals than anticipated due to coincidence.

**$^{19}$F-NMR** (470 MHz, DMSO-*d*$_6$) $\delta$ = - 70.15 (12 F, d)

**$^{31}$P-NMR** (202 MHz, DMSO-*d*$_6$) $\delta$ = -144.21 (2 P, quin)

**HRMS** (ESI+ve) m/z: 796.33670 ([M-2BF$_4^-$]$^{2+}$, $C_{89}H_{110}I_2N_8O_3^{2+}$ requires 796.33896).

**Aromatic urea bis-alkyne 3.54** [23]

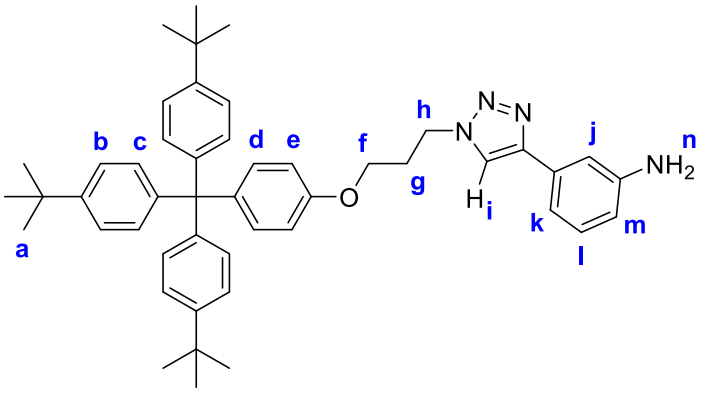



3-Ethynylaniline (243 mg, 2.07 mmol) was dissolved in anhydrous THF (3 mL), to which CDI (202 mg, 1.24 mmol, 0.6 eqs) was added and the reaction mixture was heated at reflux for 16 h. The solvent was removed under reduced pressure and the resulting solid redissolved in EtOAc (5 mL) and washed with 1 M HCl (10 mL) and brine (10 mL), dried over $MgSO_4$ and filtered. The filtrate was concentrated under reduced pressure to afford **3.54** as a light brown solid.

Yield: 206 mg (77%)

**$^1$H-NMR** (400 MHz, DMSO-$d_6$) $\delta$ = 8.84 (2 H, s, **$H_f$**), 7.66 (2 H, s, **$H_b$**), 7.40 (2 H, d, *J*=9.2 Hz, **$H_e$**), 7.29 (2 H, t, *J*=7.9 Hz, **$H_d$**), 7.08 (2 H, d, *J*=7.5 Hz, **$H_c$**), 4.16 (2 H, s, **$H_a$**).

**Aromatic aminotriazole stopper 3.55**




Aliphatic azide stopper **2.27** (153 mg, 0.26 mmol), 3-ethynylaniline (30.4 mg, 0.26 mmol, 1 eq), DIPEA (0.07 mL, 0.40 mmol, 1.55 eqs), and TBTA (6.89 mg, 0.013 mmol, 0.05 eqs) were dissolved in anhydrous $CH_2Cl_2$ (5 mL). The mixture was degassed, after which $[Cu(CH_3CN)_4]PF_6$ (4.84 mg, 0.013 mmol, 0.05 eqs) was added and the reaction mixture stirred at room temperature for 16 h. After completion, a 0.1 M aqueous solution of EDTA (8

mL) was added and the resulting organic phase washed with brine (10 mL), dried over $MgSO_4$ and filtered. The filtrate was concentrated under reduced pressure and purified by column chromatography (2% MeOH - $CH_2Cl_2$, followed by 5% MeOH - $CH_2Cl_2$) to afford **3.55** as a light orange solid.

Yield: 161 mg (88%)

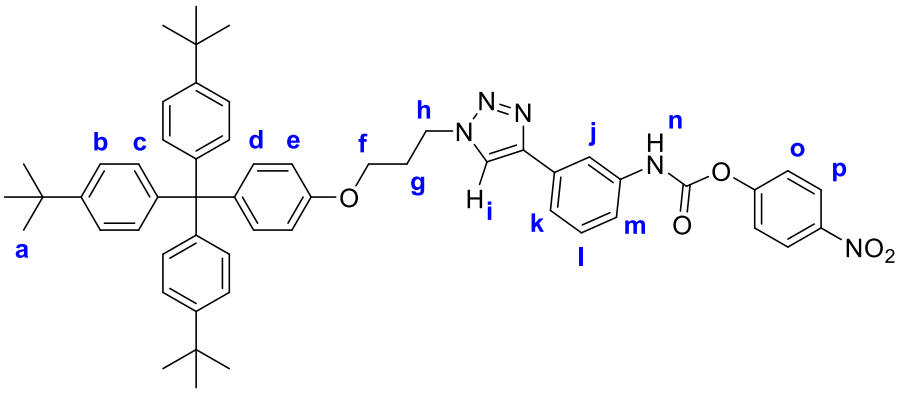
**$^1$H-NMR** (400 MHz, $CDCl_3$) $\delta$ = 7.72 (1 H, s, $\mathbf{H_i}$), 7.24 (7 H, d, *J*=7.8 Hz, $\mathbf{H_b}$ + $\mathbf{H_j}$), 7.18 (1 H, m, $\mathbf{H_l}$), 7.10 (9 H, m, $\mathbf{H_c}$ + $\mathbf{H_d}$ + $\mathbf{H_k}$), 6.77 (2 H, d, *J*=8.6 Hz, $\mathbf{H_e}$), 6.66 (1 H, d, *J*=7.9 Hz, $\mathbf{H_m}$), 4.63 (2 H, t, *J*=6.7 Hz, $\mathbf{H_h}$), 3.98 (2 H, t, *J*=5.5 Hz, $\mathbf{H_f}$), 3.70 (2 H, br. s., $\mathbf{H_n}$), 2.43 (2 H, m, $\mathbf{H_g}$), 1.31 (27 H, s, $\mathbf{H_a}$).

**$^{13}$C-NMR** (101 MHz, $CDCl_3$) $\delta$ = 156.22, 148.35, 147.78, 146.87, 144.04, 140.14, 132.37, 131.48, 130.69, 129.75, 124.05, 120.20, 116.00, 114.86, 112.95, 112.19, 63.81, 63.03, 47.13, 34.28, 31.36, 30.01.

An extra $^{13}$C signal was observed.

**HRMS** (ESI+ve) m/z: 705.45221 ($[M+H]^+$, $C_{48}H_{57}N_4O^+$ requires 705.45269).

**Stopper triazole 4-nitrophenyl carbamate 3.56**




Aromatic aminotriazole stopper **3.55** (51.4 mg, 0.07 mmol) and 4-nitrophenyl chloroformate (17.6 mg, 0.09 mmol, 1.2 eqs) were dissolved in anhydrous THF (1 mL), after which $NaHCO_3$ (7.35 mg, 0.09 mmol, 1.2 eqs) was added at 0 °C. The reaction mixture was allowed to warm to room temperature and stirred for a further 2 h. Subsequently, water (5 mL) was added and the mixture was extracted with $CH_2Cl_2$ (3 x 10 mL). The combined organic layers were dried over $MgSO_4$ and filtered, after which the filtrate was concentrated under reduced pressure to afford **3.56** as an off-white solid.

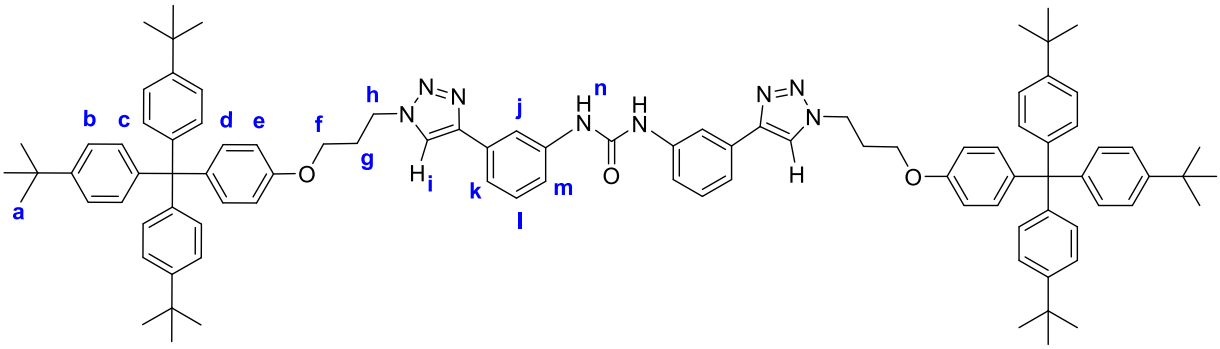
Yield: 44.4 mg (70%)

**$^1$H-NMR** (400 MHz, $CDCl_3$) $\delta$ = 8.28 (2 H, d, *J*=9.2 Hz, $\mathbf{H_p}$), 7.91 (1 H, s, $\mathbf{H_n}$), 7.81 (1 H, s, $\mathbf{H_i}$), 7.56 (2 H, m, $\mathbf{H_k}$ + $\mathbf{H_m}$), 7.38 (2 H, m, $\mathbf{H_o}$), 7.23 (6 H, m, $\mathbf{H_b}$), 7.09 (8 H, m, $\mathbf{H_c}$ + $\mathbf{H_d}$), 6.92 (1 H, m, $\mathbf{H_j}$), 6.76 (2 H, d, *J*=8.9 Hz, $\mathbf{H_e}$), 4.65 (2 H, m, $\mathbf{H_h}$), 3.99 (2 H, t, *J*=5.7 Hz, $\mathbf{H_f}$), 2.44 (2 H, m, $\mathbf{H_g}$), 1.30 (54 H, m, $\mathbf{H_a}$).

$\mathbf{H_n}$ was obscured by the solvent signal.

This compound was used immediately after isolation, hence no other characterisation data was obtained.

**Neutral bistriazole-urea axle with phenylene bridges 3.57**




Aromatic urea bis-alkyne **3.54** (12.4 mg, 0.05 mmol), aliphatic azide stopper **2.27** (64.4 mg, 0.11 mmol, 2.3 eq), DIPEA (0.03 mL, 0.15 mmol, 3 eqs), and TBTA (2.65 mg, 0.005 mmol, 0.1 eqs) were dissolved in anhydrous $CH_2Cl_2$ (2 mL). The mixture was degassed, after which $[Cu(CH_3CN)_4]PF_6$ (1.80 mg, 0.005 mmol, 0.1 eqs) was added and the reaction mixture stirred at room temperature for 16 h. After completion, a 0.1 M aqueous solution of EDTA (5 mL) was added and the resulting organic phase washed with brine (10 mL), dried over $MgSO_4$ and filtered. The filtrate was concentrated under reduced pressure and purified by column chromatography ($CH_2Cl_2$, followed by 50% EtOAc - $CH_2Cl_2$) to afford **3.57** as a slightly off-white solid.

Yield: 47.9 mg (70%)

**$^1$H-NMR** (400 MHz, $CDCl_3$) $\delta$ = 7.87 (2 H, br. s., $\mathbf{H_n}$), 7.74 (2 H, s, $\mathbf{H_j}$), 7.70 (2 H, s, $\mathbf{H_i}$), 7.64 (2 H, d, *J*=8.1 Hz, $\mathbf{H_k}$), 7.35 (2 H, m, $\mathbf{H_m}$), 7.22 (12 H, d, *J*=8.6 Hz, $\mathbf{H_b}$), 7.08 (16 H, m, $\mathbf{H_c}$ + $\mathbf{H_d}$), 6.71 (4 H, d, *J*=8.9 Hz, $\mathbf{H_e}$), 4.61 (4 H, t, *J*=6.8 Hz, $\mathbf{H_h}$), 3.94 (4 H, t, *J*=5.6 Hz, $\mathbf{H_f}$), 2.38 (4 H, quin, *J*=6.1 Hz, $\mathbf{H_g}$), 1.28 (54 H, s, $\mathbf{H_a}$).

$\mathbf{H_l}$ was obscured by the solvent signal.

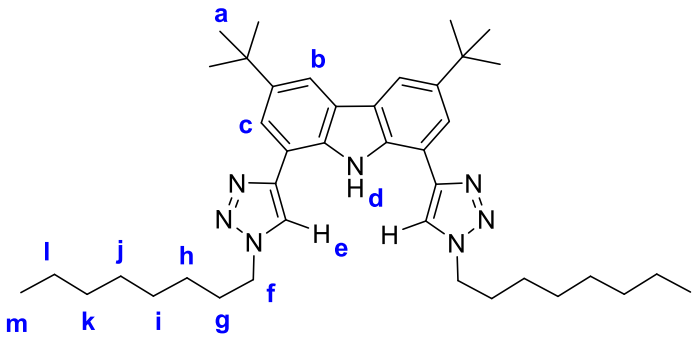
**$^{13}$C-NMR** (126 MHz, $CDCl_3$) $\delta$ = 156.22, 153.01, 148.34, 147.60, 144.08, 140.00, 139.68, 132.32, 130.83, 130.68, 129.60, 124.08, 120.75, 120.29, 119.68, 116.58, 112.95, 63.92, 63.03, 47.47, 34.26, 31.36, 30.93, 30.02.

Several extra $^{13}$C signals were observed.

**HRMS** (ESI+ve) m/z: 1435.87769 ($[M+H]^+$, $C_{97}H_{111}N_8O_3^+$ requires 1435.87737).

### 6.4. Synthetic procedures and characterisation of compounds in Chapter 4

**Octyl carbazole-triazole host 4.1.HB**




Carbazole bis-alkyne **4.3** (33.5 mg, 0.10 mmol), octyl azide **2.21** (16 mg, 0.30 mmol, 3 eqs), DIPEA (0.05 mL, 0.3 mmol, 3 eqs), and TBTA (5.3 mg, 0.01 mmol, 0.1 eqs) were dissolved in anhydrous $CH_2Cl_2$ (2 mL). The mixture was degassed, after which $[Cu(CH_3CN)_4]PF_6$ (3.7 mg, 0.01 mmol, 0.1 eqs) was added and the reaction mixture stirred at room temperature for 16 h. After completion, a 0.1 M aqueous solution of EDTA (5 mL) was added and the resulting organic phase washed with brine (10 mL), dried over $MgSO_4$ and filtered. The filtrate was concentrated under reduced pressure and purified by column chromatography ($CH_2Cl_2$, followed by 1% MeOH – $CH_2Cl_2$) to afford **4.1.HB** as a yellow solid.

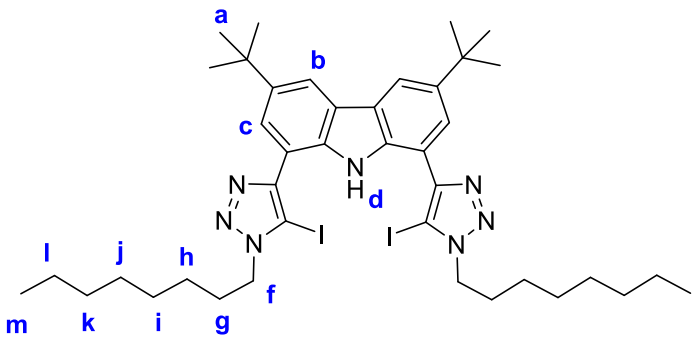
Yield: 57.4 mg (88%)

**$^1$H-NMR** (400 MHz, $CDCl_3$) $\delta$ = 11.64 (1 H, s, $\mathbf{H_d}$), 8.13 (2 H, s, $\mathbf{H_c}$), 8.02 (2 H, s, $\mathbf{H_e}$), 7.76 (2 H, d, *J*=1.0 Hz, $\mathbf{H_b}$), 4.48 (4 H, t, *J*=7.2 Hz, $\mathbf{H_f}$), 2.02 (4 H, quin, *J*=7.0 Hz, $\mathbf{H_g}$), 1.52 (18 H, s, $\mathbf{H_a}$), 1.33 (20 H, m, $\mathbf{H_{h\text{-}l}}$), 0.88 (6 H, t, *J*=6.7 Hz, $\mathbf{H_m}$).

**$^{13}$C-NMR** (101 MHz, $CDCl_3$) $\delta$ = 141.76, 135.73, 123.87, 120.22, 119.09, 116.23, 112.94, 50.52, 34.72, 32.11, 31.72, 30.75, 30.41, 29.03, 29.00, 26.55, 22.58, 14.03.

**HRMS** (ESI+ve) m/z: 638.48935 ($[M+H]^+$, $C_{40}H_{60}N_7^+$ requires 638.49047).

**Octyl carbazole-iodotriazole host 4.1.XB**




*N*-Boc-protected octyl carbazole-iodotriazole host **4.7.XB** (20 mg, 0.02 mmol) was dissolved in anhydrous $CH_2Cl_2$ (2 mL) after which TFA (0.5 mL, excess) was added and the reaction mixture stirred at room temperature for 16 h. Subsequently, volatiles were removed under reduced pressure, after which the resulting solid was redissolved in $CH_2Cl_2$ (5 mL) and the solution washed with a saturated $NaHCO_3$ solution (2 x 8 mL) and brine (10 mL), dried over $MgSO_4$, filtered and then concentrated under reduced pressure to afford **4.1.XB** as a yellow solid.

Yield: 16.0 mg (90%)

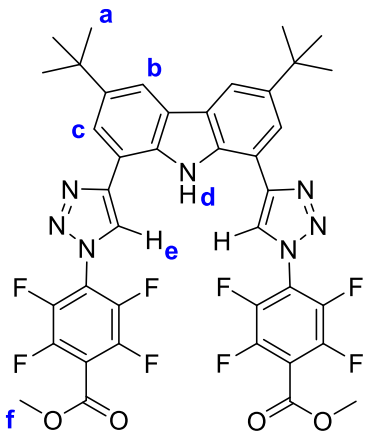
**$^1$H-NMR** (500 MHz, $CDCl_3$) $\delta$ = 11.33 (1 H, s, $\mathbf{H_d}$), 8.28 (2 H, d, *J*=1.7 Hz, $\mathbf{H_c}$), 8.17 (2 H, d, *J*=1.4 Hz, $\mathbf{H_b}$), 4.52 (4 H, t, *J*=7.5 Hz, $\mathbf{H_f}$), 2.02 (4 H, quin, *J*=7.3 Hz, $\mathbf{H_g}$), 1.54 (18 H, s, $\mathbf{H_a}$), 1.36 (20 H, m, $\mathbf{H_{h\text{-}l}}$), 0.90 (6 H, t, *J*=6.9 Hz, $\mathbf{H_m}$).

**$^{13}$C-NMR** (126 MHz, $CDCl_3$) $\delta$ = 148.33, 141.25, 136.26, 123.78, 121.56, 116.75, 112.45, 75.01, 51.00, 35.05, 32.13, 31.76, 29.95, 29.08, 26.51, 22.62, 14.09.

There were fewer $^{13}$C signals than anticipated due to coincidence.

**HRMS** (ESI+ve) m/z: 890.28411 ($[M+H]^+$, $C_{40}H_{58}I_2N_7^+$ requires 890.28376).

**Perfluoroaryl carbazole-triazole host 4.2.HB**




Carbazole bis-alkyne **4.3** (40 mg, 0.12 mmol), methyl perfluorobenzoate azide (70 mg, 0.28 mmol, 2.3 eqs), DIPEA (0.06 mL, 0.37 mmol, 3 eqs), and TBTA (6.48 mg, 0.01 mmol, 0.1 eqs) were dissolved in anhydrous $CH_2Cl_2$ (5 mL). The mixture was degassed, after which $[Cu(CH_3CN)_4]PF_6$ (5 mg, 0.01 mmol, 0.05 eqs) was added and the reaction mixture stirred at room temperature for 16 h. After completion, a 0.1 M aqueous solution of EDTA (8 mL) was added and the resulting organic phase washed with brine (10 mL), dried over $MgSO_4$ and filtered. The filtrate was concentrated under reduced pressure and purified by column chromatography ($CH_2Cl_2$) to afford **4.2.HB** as a yellow solid.

Yield: 92.6 mg (92%)

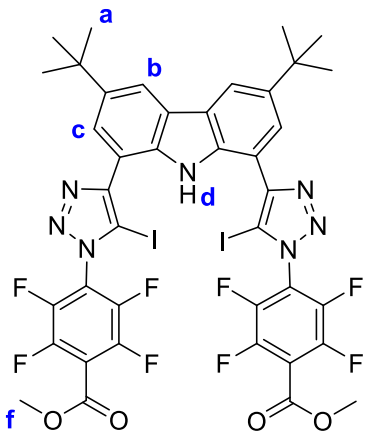
**$^1$H-NMR** (400 MHz, $CDCl_3$) $\delta$ = 11.73 (1 H, s, H, **$H_d$**), 8.39 (2 H, s, **$H_e$**), 8.23 (2 H, d, *J*=1.6 Hz, **$H_c$**), 7.82 (2 H, d, *J*=1.7 Hz, **$H_b$**), 4.07 (6 H, s, **$H_f$**), 1.54 (18 H, s, **$H_a$**).

**$^{19}$F-NMR** (377 MHz, $CDCl_3$) $\delta$ = - 136.65, - 144.61.

$^{13}$C-NMR data could not be obtained due to low solubility.

**HRMS** (ESI+ve) m/z: 826.23852 ($[M+H]^+$, $C_{40}H_{32}F_8N_7O_4^+$ requires 826.23825).

**Perfluoroaryl carbazole-iodotriazole host 4.2.XB**




*N*-Boc-protected perfluoroaryl carbazole-iodotriazole host **4.9.XB** (63.9 mg, 0.05 mmol) was dissolved in anhydrous $CH_2Cl_2$ (1 mL) after which TFA (0.07 mL, 0.87 mmol, 16 eqs) was added and the reaction mixture stirred at room temperature for 16 h. Subsequently, volatiles were removed under reduced pressure, after which the resulting solid was redissolved in $CH_2Cl_2$ (5 mL) and the solution washed with a saturated $NaHCO_3$ solution (2 x 5 mL) and brine (10 mL), dried over $MgSO_4$, filtered and then concentrated under reduced pressure. The crude solid was purified by column chromatography ($CH_2Cl_2$) followed by iterative preparative thin layer chromatography ($CH_2Cl_2$, followed by 50% hexane – $CH_2Cl_2$) to afford **4.2.XB** as an orange solid.

Yield: 12.0 mg (20%)

**$^1$H-NMR** (400 MHz, $CDCl_3$) $\delta$ = 11.58 (1 H, s, $\mathbf{H_d}$), 8.43 (2 H, d, *J*=1.8 Hz, $\mathbf{H_c}$), 8.27 (2 H, d, *J*=1.6 Hz, $\mathbf{H_b}$), 4.09 (6 H, s, $\mathbf{H_f}$), 1.55 (18 H, s, $\mathbf{H_a}$).

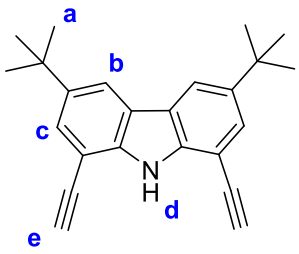
**$^{19}$F-NMR** (377 MHz, $CDCl_3$) $\delta$ = - 136.86, - 141.04.

**$^{13}$C-NMR** (126 MHz, $CDCl_3$) $\delta$ = 159.09, 149.35, 144.67, 143.08, 141.78, 136.20, 124.08, 121.58, 118.80, 117.81, 115.61, 111.10, 77.96, 53.88, 35.14, 32.11.

There were fewer $^{13}$C signals than anticipated due to coincidence.

**HRMS** (ESI+ve) m/z: 1078.03175 ($[M+H]^+$, $C_{40}H_{30}F_8I_2N_7O_4^+$ requires 1078.03154).

**Carbazole bis-alkyne 4.3** [24]

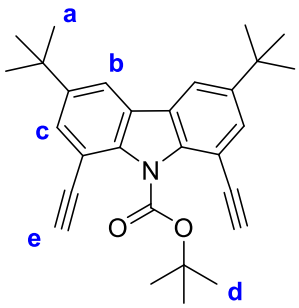



1,8-Dibromo-3,6-di(tert-butyl)-carbazole (2.00 g, 4.57 mmol), $Pd(PPh_3)_2Cl_2$ (128 mg, 0.18 mmol, 0.04 eqs) and CuI (70 mg, 0.37 mmol, 0.08 eqs) were added to a round-bottomed flask which was subsequently purged with $N_2$. Anhydrous, degassed $Et_3N$ (40 mL) was added, followed by TMS acetylene (3.8 mL, 27.5 mmol, 6 eqs). The reaction mixture was stirred at 80 °C for 16 h, after which it was allowed to cool to room temperature and hexane (40 mL) was added. The solids were removed by filtration and the filtrate concentrated under reduced pressure and passed through a silica pad (hexane). The resulting crude solid was suspended in MeOH (27 mL) after which KOH (1.54 g, 27.5 mmol, 6 eqs) was added and the mixture was stirred at room temperature for 1 h. Subsequently, water (25 mL) was added and the product extracted with hexane (3 x 30 mL). The combined organic layers were dried over $MgSO_4$, filtered and then concentrated under reduced pressure. The crude solid was purified by column chromatography (hexane) to give **4.3** as a yellow solid.

Yield: 904 mg (60%)

**$^1$H-NMR** (400 MHz, $CDCl_3$) $\delta$ = 8.46 (1 H, br. s., $\mathbf{H_d}$), 8.09 (2 H, d, *J*=1.3 Hz, $\mathbf{H_c}$), 7.65 (2 H, d, *J*=1.7 Hz, $\mathbf{H_b}$), 3.47 (2 H, s, $\mathbf{H_e}$), 1.45 (18 H, s, $\mathbf{H_a}$).

**_N_-Boc-protected carbazole bis-alkyne 4.5**




Carbazole bis-alkyne **4.5** (103 mg, 0.31 mmol) was dissolved in anhydrous $CH_3CN$ (3 mL), after which $Boc_2O$ (205 mg, 0.94 mmol, 3 eqs) and DMAP (38.3 mg, 0.31 mmol, 1 eq) were added. The reaction mixture was stirred at room temperature for 2 h, after which the volatiles were removed under reduced pressure. The resulting solid was redissolved in $CH_2Cl_2$ and passed through a silica plug ($CH_2Cl_2$) to afford **4.5** as a white - yellow solid.

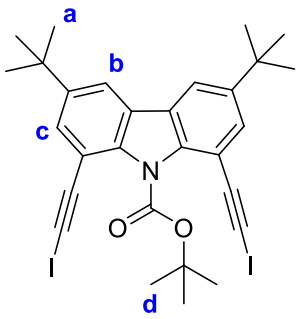
Yield: 124 mg (92%)

**$^1$H-NMR** (400 MHz, $CDCl_3$) $\delta$ = 7.97 (2 H, d, *J*=2.0 Hz, **$H_c$**), 7.68 (2 H, d, *J*=2.0 Hz, **$H_b$**), 3.37 (2 H, s, **$H_e$**), 1.69 (9 H, s, **$H_d$**), 1.44 (18 H, s, **$H_a$**).

**$^{13}$C-NMR** (126 MHz, $CDCl_3$) $\delta$ = 150.59, 145.32, 137.85, 131.30, 125.91, 117.22, 108.25, 85.96, 82.37, 81.91, 34.60, 31.63, 28.18.

**HRMS** (ESI+ve) m/z: 450.24048 ($[M+Na]^+$, $C_{29}H_{33}NO_2Na^+$ requires 450.24035).

**_N_-Boc-protected carbazole bis-iodoalkyne 4.6**



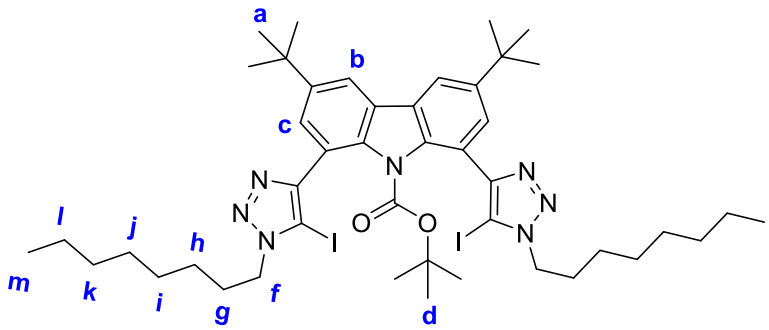

_N_-Boc-protected carbazole bis-alkyne **4.5** (83.9 mg, 0.20 mmol) was dissolved in anhydrous THF (3 mL) and cooled to -78 °C. A 2.5 M solution of n-BuLi in hexanes (0.8 mL, 2.0 mmol, 10 eqs) was added dropwise, then the mixture was stirred for 30 minutes. Subsequently, a solution of $I_2$ (498 mg, 2 mmol, 10 eqs) in anhydrous THF (2 mL) was added dropwise, then the mixture was stirred for a further 60 minutes. This was allowed to slowly warm to room temperature, after which it was poured onto a saturated aqueous solution of $Na_2S_2O_3$ (25 mL) and the product extracted with $CH_2Cl_2$ (3 x 30 mL). The organic layer was washed with water (30 mL) and brine (30 mL), dried over $MgSO_4$ and filtered. The filtrate was concentrated under reduced pressure to afford **4.6** as a yellow solid.

Yield: 120 mg (90%)

**$^1$H-NMR** (500 MHz, $CDCl_3$) $\delta$ = 7.93 (2 H, d, *J*=2.0 Hz, $\mathbf{H_c}$), 7.62 (2 H, d, *J*=2.0 Hz, $\mathbf{H_b}$), 1.68 (9 H, s, $\mathbf{H_d}$), 1.43 (18 H, s, $\mathbf{H_a}$).

This compound was used immediately after isolation, hence no other characterisation data was obtained.

**_N_-Boc-protected octyl carbazole-iodotriazole host 4.7.XB**




_N_-Boc-protected carbazole bis-iodoalkyne **4.6** (33.2 mg, 0.05 mmol), octyl azide **2.21** (30 mg, 0.20 mmol, 4 eqs), and TBTA (5.3 mg, 0.01 mmol, 0.20 eqs) were dissolved in anhydrous $CH_2Cl_2$ (2 mL). The mixture was degassed, after which $[Cu(CH_3CN)_4]PF_6$ (3.6 mg, 0.01 mmol, 0.2 eqs) was added and the reaction mixture stirred at room temperature for 16 h. After completion, a 0.1 M aqueous solution of EDTA (7 mL) was added and the resulting organic phase washed with brine (10 mL), dried over $MgSO_4$ and filtered. The filtrate was concentrated under reduced pressure and purified by column chromatography (2% MeOH – $CH_2Cl_2$) to afford **4.7.XB** as a white solid.

Yield: 39.1 mg (79%)

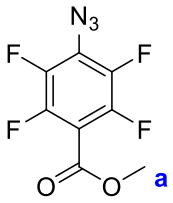
**$^1$H-NMR** (400 MHz, $CDCl_3$) $\delta$ = 8.01 (2 H, s, $\mathbf{H_c}$), 7.66 (2 H, s, $\mathbf{H_b}$), 4.45 (4 H, t, $J$=7.2 Hz, $\mathbf{H_f}$), 1.98 (4 H, m, $\mathbf{H_g}$), 1.39 (38 H, m, $\mathbf{H_a}$ + $\mathbf{H_{h\text{-}l}}$), 0.91 (15 H, m, $\mathbf{H_d}$ + $\mathbf{H_m}$).

**$^{13}$C-NMR** (126 MHz, $CDCl_3$) $\delta$ = 152.48, 150.36, 146.79, 137.14, 129.01, 128.07, 119.96, 116.36, 82.67, 79.23, 50.88, 34.87, 31.76, 31.68, 30.08, 29.08, 29.02, 27.43, 26.50, 22.62.

There were fewer $^{13}$C signals than anticipated due to coincidence.

**HRMS** (ESI+ve) m/z: 990.33572 ($[M+Na]^+$, $C_{45}H_{66}I_2N_7O_2Na^+$ requires 990.33619).

**Methyl perfluorobenzoate azide 4.8** [25]



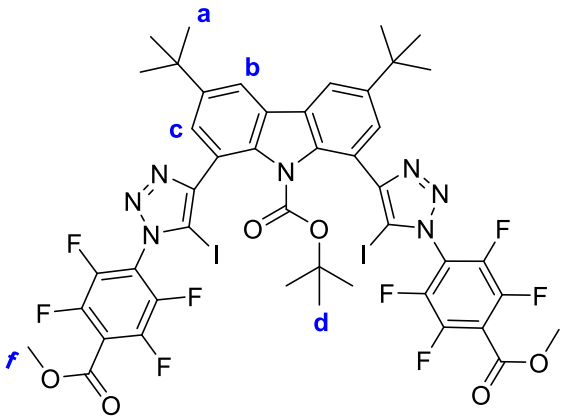

Methyl perfluorobenzoate (1 mL, 6.78 mmol) and $NaN_3$ (580 mg, 8.80 mmol, 1.3 eqs) were dissolved in 2:1 acetone/water (*v/v*, 15 mL) and the reaction mixture was heated to reflux for 4 hours. Subsequently, it was allowed to cool to room temperature, then diluted with water (20 mL) and extracted with $Et_2O$ (3 x 20 mL). The combined organic layers were dried over $MgSO_4$, filtered and the solvent removed under reduced pressure to afford **4.8** as a yellow solid.

Yield: 1.53 g (91%)

**$^1$H-NMR** (400 MHz, $CDCl_3$) $\delta$ = 3.98 (3 H, s, **$H_a$**).

**$^{19}$F-NMR** (377 MHz, $CDCl_3$) $\delta$ = - 138.63, - 150.91.

***N*-Boc-protected perfluoroaryl carbazole-iodotriazole host 4.9.XB**




*N*-Boc-protected carbazole bis-iodoalkyne **4.6** (73.8 mg, 0.11 mmol), methyl perfluorobenzoate azide **4.8** (62.2 mg, 0.25 mmol, 2.3 eqs), and TBTA (5.8 mg, 0.01 mmol, 0.10 eqs) were dissolved in anhydrous $CH_2Cl_2$ (2 mL). The mixture was degassed, after which $[Cu(CH_3CN)_4]PF_6$ (4 mg, 0.01 mmol, 0.10 eqs) was added and the reaction mixture

stirred at room temperature for 16 h. After completion, a 0.1 M aqueous solution of EDTA (5 mL) was added and the resulting organic phase washed with brine (10 mL), dried over $MgSO_4$ and filtered. The filtrate was concentrated under reduced pressure and purified by column chromatography ($CH_2Cl_2$, followed by 1% MeOH – $CH_2Cl_2$) to afford **4.9.XB** as a yellow solid.

Yield: 102 mg (79%)

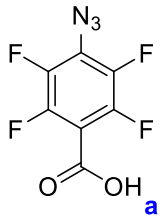
**$^1$H-NMR** (400 MHz, $CDCl_3$) $\delta$ = 8.08 (2 H, d, *J*=2.0 Hz, **$H_c$**), 7.81 (2 H, d, *J*=1.8 Hz, **$H_b$**), 4.08 (6 H, s, **$H_f$**), 1.52 (18 H, s, **$H_a$**).

**$^{19}$F-NMR** (377 MHz, $CDCl_3$) $\delta$ = - 137.11, - 141.01.

**$^{13}$C-NMR** (126 MHz, $CDCl_3$) $\delta$ = 159.11, 153.68, 150.27, 147.28, 144.68, 143.03, 137.36, 129.50, 127.83, 119.36, 119.03, 117.05, 115.27, 83.66, 82.03, 53.84, 35.02, 31.70, 27.36.

**HRMS** (ESI+ve) m/z: 1200.06265 ($[M+Na]^+$, $C_{45}H_{37}F_8I_2N_7O_6Na^+$ requires 1200.06591).

**Perfluorobenzoic acid azide 4.10** [26]

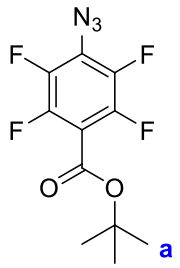



Methyl perfluorobenzoate azide **4.8** (597 mg, 2.4 mmol) was dissolved in MeOH (10 mL), after which 20% NaOH (0.8 mL) was added and the reaction mixture was stirred at room temperature for 16 h. The mixture was acidified to pH < 1 with 10% HCl, then water (10 mL) was added and the product extracted with $CHCl_3$ (3 x 20 mL). The combined organic layers were dried over $MgSO_4$, filtered and the solvent removed under reduced pressure to afford **4.10** as a white solid.

Yield: 402 mg (71%)

**$^{19}$F-NMR** (377 MHz, $CDCl_3$) $\delta$ = - 136.86, - 150.63.

**Tert-butyl perfluorobenzoate azide 4.11**




Perfluorobenzoic acid azide **4.10** (308 mg, 1.31 mmol) was dissolved in tert-butanol (4 mL), after which DMAP (16 mg, 0.13 mmol, 0.1 eqs) and $Boc_2O$ (571 mg, 2.62 mmol, 2 eqs) were added. The reaction mixture was heated to 40 °C for 16 h, following which it was allowed to cool down to room temperature and 1 M HCl (3 mL) was added. The product was extracted with EtOAc (3 x 10 mL) and the combined organic layers were washed with saturated $Na_2CO_3$ (3 x 20 mL) and brine (20 mL), then dried over $MgSO_4$, filtered and the solvent removed under reduced pressure to afford **4.11** as an orange solid.

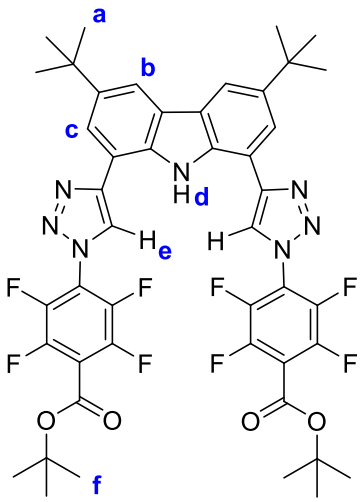
Yield: 326 mg (86%)

**$^{1}$H-NMR** (400 MHz, $CDCl_3$) $\delta$ = 1.59 (9 H, s, **$H_a$**).

**$^{19}$F-NMR** (377 MHz, $CDCl_3$) $\delta$ = - 140.26, - 151.27.

$^{13}$C data could not be obtained.

**Perfluoroaryl tert-butyl ester 4.12.HB**




Carbazole bis-alkyne **4.3** (80.2 mg, 0.25 mmol), tert-butyl perfluorobenzoate azide **4.11** (164 mg, 0.56 mmol, 2.3 eqs), DIPEA (0.13 mL, 0.73 mmol, 3 eqs), and TBTA (13.3 mg, 0.025 mmol, 0.1 eqs) were dissolved in anhydrous $CH_2Cl_2$ (3 mL). The mixture was degassed, after which $[Cu(CH_3CN)_4]PF_6$ (9.3 mg, 0.025 mmol, 0.1 eqs) was added and the reaction mixture stirred at room temperature for 16 h. After completion, the mixture was filtered and the solid washed with small amounts of $CH_2Cl_2$ to afford **4.12.HB** as a pale yellow solid.

Yield: ~105 mg (~47%)

**$^1$H-NMR** (400 MHz, pyridine-$d_5$) $\delta$ = 12.85 (1 H, s, **$H_d$**), 9.72 (2 H, s, **$H_e$**), 8.26 (2 H, d, *J*=1.8 Hz, **$H_c$**), 1.61 (18 H, m, **$H_f$**), 1.49 (18 H, s, **$H_a$**).

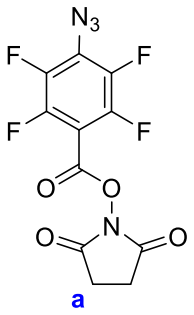
**$H_b$** was obscured by the solvent signal.

**$^{19}$F-NMR** (377 MHz, pyridine-$d_5$) $\delta$ = - 139.45, - 145.91.

$^{13}$C-NMR data could not be obtained due to low solubility.

**HRMS** (ESI-ve) m/z: 908.31818 ($[M-H]^-$, $C_{46}H_{42}F_8N_7O_4^-$ requires 908.31760).

**Perfluorobenzoic acid azide, *N*-hydroxysuccinimide ester 4.14** [25]



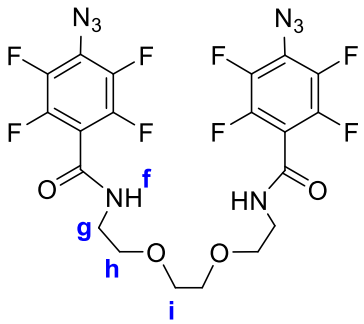

Perfluorobenzoic acid azide **4.10** (182 mg, 0.77 mmol) and *N*-hydroxysuccinimide (89.1 mg, 0.77 mmol, 1 eq) were dissolved in $CH_2Cl_2$ (3 mL), after which DCC (163 mg, 0.79 mmol, 1.02 eqs) was added portionwise. The reaction mixture was stirred at room temperature for 16 h, following which the solids were removed by filtration and the filtrate concentrated under reduced pressure to give **4.14** as a white solid.

Yield: 151 mg (59%)

**$^1$H-NMR** (400 MHz, $CDCl_3$) $\delta$ = 2.92 (4 H, s, **$H_a$**).

**$^{19}$F-NMR** (377 MHz, $CDCl_3$) $\delta$ = - 133.51, - 149.84.

**Perfluoroaryl bis-azide 4.15**




Perfluorobenzoic acid azide **4.10** (323 mg, 1.37 mmol), EDC·HCl (263 mg, 1.37 mmol, 1 eq), DIPEA (0.24 mL, 1.37 mmol, 1 eq), and DMAP (cat.) were dissolved in anhydrous $CH_2Cl_2$ (10 mL), after which 2,2′-(ethylenedioxy)bis(ethylamine) (0.08 mL, 0.55 mmol, 0.4 eqs) was added dropwise and the reaction allowed to stir at room temperature for 16 h. Subsequently,

this was washed with 1 M HCl (20 mL), followed by saturated $NaHCO_3$ (20 mL), water (30 mL), and brine (20 mL). The organic layer was dried over $MgSO_4$ and filtered, after which the filtrate was concentrated under reduced pressure and purified by column chromatography (1% MeOH – $CH_2Cl_2$, followed by 3% MeOH – $CH_2Cl_2$) to afford slighly impure **4.15** as a pale yellow solid.

Yield: 63.5 mg (~20%)

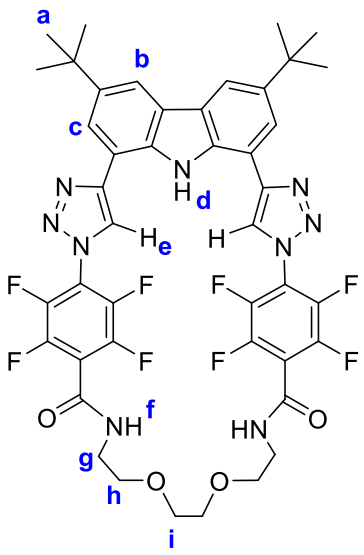
**$^1$H-NMR** (400 MHz, $CDCl_3$) $\delta$ = 6.58 (2 H, br. s., **$H_f$**), 3.66 (12 H, m, **$H_{g\text{-}i}$**).

**$^{19}$F-NMR** (377 MHz, $CDCl_3$) $\delta$ = - 141.20, - 150.65.

The sample was not considered pure enough for $^{13}$C NMR analysis.

**HRMS** (ESI+ve) m/z: 583.10821 ($[M+H]^+$, $C_{20}H_{14}F_8N_8O_4^+$ requires 583.10830).

**Carbazole perfluoroaryl-amide macrocycle 4.16.HB**




Carbazole bis-alkyne **4.3** (11.7 mg, 0.036 mmol), perfluoroaryl bis-azide **4.15** (20.9 mg, ~0.036 mmol, 1 eq), DIPEA (0.02 mL, 0.107 mmol, 3 eqs), and TBTA (4.80 mg, 0.009 mmol, 0.25 eqs) were dissolved in anhydrous $CH_2Cl_2$ (12 mL). The mixture was degassed, after which $[Cu(CH_3CN)_4]PF_6$ (6.7 mg, 0.018 mmol, 0.50 eqs) was added and the reaction mixture stirred at room temperature for 16 h. After completion, the mixture was filtered and the solid washed with small amounts of $CH_2Cl_2$ to afford slightly impure **4.16.HB** as a white solid.

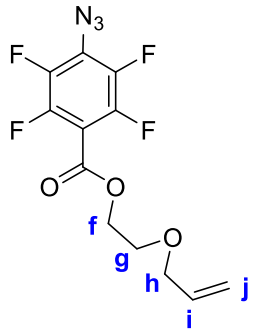
Yield: ~15 mg (~46%)

**$^{1}$H NMR** (400 MHz, DMSO-$d_6$) $\delta$ = 11.88 (1 H, br. s., **$H_d$**), 9.58 (2 H, m, **$H_e$**), 9.21 (2 H, m, **$H_c$**), 8.34 (2 H, m, **$H_b$**), 7.99 (2 H, m, **$H_f$**), 3.62 (12 H, m, **$H_{g-i}$**), 1.49 (18 H, s, **$H_a$**).

The sample was not considered pure enough for $^{13}$C NMR analysis.

**HRMS** (ESI+ve) m/z: ([M+]$^+$, $C_{44}H_{39}F_8N_9O_4^+$ requires).

**2-Allyloxyethyl perfluorobenzoate azide 4.19**



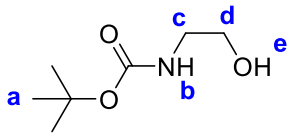

Perfluorobenzoic acid azide **4.10** (229 mg, 0.98 mmol), 2-allyloxyethanol (0.13 mL, 1.18 mmol, 1.2 eqs), and EDC·HCl (280 mg, 1.47 mmol, 1.5 eq) were dissolved in anhydrous THF (3 mL), after which a catalytic amount of DMAP was added and the reaction allowed to stir at room temperature for 16 h. The solvent was removed under reduced pressure and the crude solid purified by column chromatography ($CH_2Cl_2$) without any aqueous workup to give **4.19** as a colourless liquid. The yield was difficult to estimate due to the volatility of the product.

**$^{1}$H-NMR** (400 MHz, $CDCl_3$) $\delta$ = 5.91 (1 H, m, **$H_i$**), 5.27 (2 H, m, **$H_j$**), 4.52 (2 H, m, **$H_f$**), 4.06 (2 H, d, *J*=5.6 Hz, **$H_h$**), 3.76 (2 H, m, **$H_g$**).

**$^{19}$F-NMR** (377 MHz, $CDCl_3$) $\delta$ = - 138.42, - 150.95.

This compound was used immediately after isolation, hence no other characterisation data was obtained.

**_N_-Boc-protected 2-aminoethanol 4.20** [27]

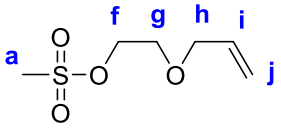



Ethanolamine (1 mL, 16.6 mmol) was added to a round-bottomed flask, followed by $Boc_2O$ (4 g, 18.2 mmol, 1.1 eqs). The mixture was sonicated for 5 minutes, after which the volatiles were removed under reduced pressure to afford **4.20** as a yellow liquid.

Yield: 2.67 g (100%)

**$^1$H-NMR** (400 MHz, $CDCl_3$) $\delta$ = 4.97 (1 H, br. s., $\mathbf{H_b}$), 3.70 (2 H, q, *J*=5.0 Hz, $\mathbf{H_c}$), 3.30 (2 H, m, $\mathbf{H_d}$), 2.47 (1 H, br. s., $\mathbf{H_e}$), 1.45 (9 H, s, $\mathbf{H_a}$).

**2-Allyloxyethanol mesylate 4.22** [28]

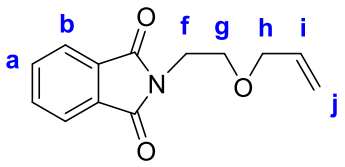



2-Allyloxyethanol (3.2 mL, 30 mmol) was dissolved in anhydrous $CH_2Cl_2$ (25 mL), after which methanesulfonyl chloride (2.32 mL, 30 mmol, 1 eq) and $Et_3N$ (4.17 mL, 30 mmol, 1 eq) were added dropwise. The reaction mixture was stirred at room temperature for 16 h, following which the precipitate was separated by filtration. Water (25 mL) was added to the filtrate and the organic phase was washed with saturated $NaHCO_3$ (2 x 20 mL) and brine (30 mL) then dried over $MgSO_4$ and filtered. The filtrate was concentrated under reduced pressure to afford **4.22** as a yellow liquid.

Yield: 4.23 g (78%)

**$^1$H-NMR** (300 MHz, $CDCl_3$) $\delta$ = 5.88 (1H, m, $\mathbf{H_i}$), 5.25 (2H, m, $\mathbf{H_j}$), 4.37 (2 H, t, *J* = 4.6 Hz, $\mathbf{H_f}$), 4.03 (2 H, dt, *J* = 5.6, 1.6 Hz, $\mathbf{H_h}$), 3.70 (2H, m, $\mathbf{H_g}$), 3.05 (3H, s, $\mathbf{H_a}$).

**2-Allyloxyethaneamine phthalimide 4.23**




2-Allyloxyethanol mesylate 4.22 (2.22 g, 12.3 mmol) and potassium phthalimide (5.46 g, 29.6 mmol, 2.4 eqs) were dissolved in anhydrous DMF (25 mL) and the reaction mixture was stirred at 80 °C for 16 h. This was allowed to cool to room temperature, after which the solids were removed by filtration and the filtrate concentrated under reduced pressure. The resulting solid was redissolved in $CH_2Cl_2$ (20 mL) and the solution washed with a saturated $Na_2CO_3$ solution (20 mL), water (20 mL), and brine (25 mL), then dried over $MgSO_4$ and filtered. The filtrate was concentrated under reduced pressure to afford **4.23** as a yellow solid.

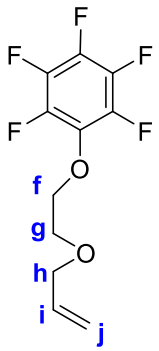
Yield: 1.86 g (65%)

**$^1$H-NMR** (400 MHz, $CDCl_3$) $\delta$ = 7.86 (2 H, m, $\mathbf{H_b}$), 7.73 (2 H, m, $\mathbf{H_a}$), 5.85 (1 H, m, $\mathbf{H_i}$), 5.20 (2 H, m, $\mathbf{H_j}$), 4.01 (2 H, dt, *J*=5.6, 1.4 Hz, $\mathbf{H_h}$), 3.92 (2 H, t, *J*=5.8 Hz, $\mathbf{H_f}$), 3.70 (2 H, t, *J*=5.9 Hz, $\mathbf{H_g}$).

**$^{13}$C-NMR** (126 MHz, $CDCl_3$) $\delta$ = 168.22, 134.32, 133.86, 132.06, 123.20, 117.12, 71.58, 66.70, 37.41.

**HRMS** (ESI+ve) m/z: 232.09702 ($[M+H]^+$, $C_{13}H_{14}NO_3^+$ requires 232.09682).

**Pentafluorophenyl 2-allyloxyethyl ether 4.25**



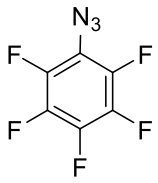

Pentafluorophenol (95.7 mg, 0.52 mmol) and 2-allyloxyethanol mesylate (141 mg, 0.78 mmol, 1.5 eqs) were dissolved in anhydrous $CH_3CN$ (5 mL), after which $K_2CO_3$ (144 mg, 1.04 mmol, 2 eqs) was added and the reaction mixture heated to reflux for 3 days. The solvent was removed under reduced pressure, after which $CH_2Cl_2$ was added (10 mL), the insoluble solids separated by filtration, and the filtrate concentrated under reduced pressure. The resulting crude solid was purified by column chromatography ($CH_2Cl_2$) to give **4.25** as a colourless liquid.

Yield: 103 mg (74%)

**$^1$H-NMR** (400 MHz, $CDCl_3$) $\delta$ = 5.89 (1 H, m, $\mathbf{H_i}$), 5.23 (2 H, m, $\mathbf{H_j}$), 4.33 (2 H, m, $\mathbf{H_f}$), 4.04 (2 H, dt, *J*=5.7, 1.4 Hz, $\mathbf{H_h}$), 3.77 (2 H, m, $\mathbf{H_g}$).

**$^{19}$F-NMR** (377 MHz, $CDCl_3$) $\delta$ = - 156.68, - 163.69.

**Pentafluorophenyl azide 4.26** [29]

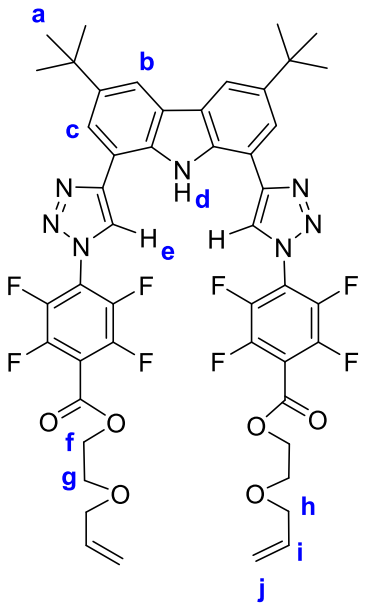



Pentafluoroaniline (180 mg, 1 mmol, 1 eqs) was dissolved in TFA (2.5 mL) and the solution was cooled to 0 °C, after which $NaNO_2$ (82.8 mg, 1.2 mmol, 1.2 eqs) was added portionwise and the mixture was allowed to stir at 0 °C. After 1 h, $NaN_3$ (97.5 mg, 1.5 mmol, 1.5 eqs) was added portionwise and the mixture was allowed to stir at 0 °C for a further 1 h. Subsequently, $Et_2O$ (5 mL) was added and the organic phase washed with water (3 x 20 mL) and saturated $NaHCO_3$ (20 mL), then dried over $MgSO_4$ and filtered. The filtrate was concentrated under reduced pressure and purified by flash column chromatography (hexane) to afford **4.26** as a colourless liquid.

Yield: 105 mg (51%)

**$^{19}$F-NMR** (377 MHz, $CDCl_3$) $\delta$ = - 151.47, - 159.73, - 161.55.

**Perfluoroaryl carbazole-triazole bis-alkene 4.28.HB**




Carbazole bis-alkyne **4.3** (53.0 mg, 0.16 mmol), 2-allyloxyethyl perfluorobenzoate azide **4.19** (120 mg, 0.38 mmol, 2.3 eqs), DIPEA (0.04 mL, 0.24 mmol, 1.5 eqs), and TBTA (8.5 mg, 0.2 mmol, 0.1 eqs) were dissolved in anhydrous $CH_2Cl_2$ (2 mL). The mixture was degassed, after which $[Cu(CH_3CN)_4]PF_6$ (6 mg, 0.2 mmol, 0.1 eqs) was added and the reaction mixture stirred at room temperature for 16 h. After completion, a 0.1 M aqueous solution of EDTA (8 mL) was added and the resulting organic phase washed with brine (10 mL), dried over $MgSO_4$ and filtered. The filtrate was concentrated under reduced pressure and purified by column chromatography (1% EtOAc - $CH_2Cl_2$) to afford **4.28.HB** as a yellow solid.

Yield: 80.5 mg (52%)

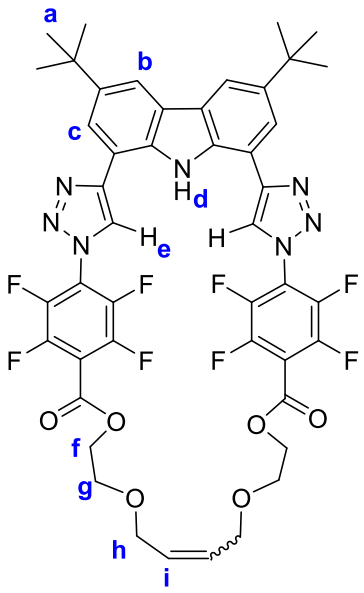
**$^1$H-NMR** (400 MHz, $CDCl_3$) $\delta$ = 11.73 (1 H, s, $\mathbf{H_d}$), 8.38 (2 H, s, $\mathbf{H_e}$), 8.23 (2 H, s, $\mathbf{H_c}$), 7.82 (2 H, s, $\mathbf{H_b}$), 5.92 (2 H, m, $\mathbf{H_i}$), 5.31 (4 H, m, $\mathbf{H_j}$), 4.63 (4 H, m, *J*=9.4 Hz, $\mathbf{H_f}$), 4.10 (4 H, d, *J*=5.9 Hz, $\mathbf{H_h}$), 3.82 (4 H, m, $\mathbf{H_g}$), 1.54 (18 H, s, $\mathbf{H_a}$).

**$^{19}$F-NMR** (377 MHz, $CDCl_3$) $\delta$ = - 136.55, - 144.64.

**HRMS** (ESI+ve) m/z: 966.32227 ($[M+H]^+$, $C_{48}H_{43}F_8N_7O_6^+$ requires 966.32198).

$^{13}$C NMR data could not be obtained.

**Carbazole perfluoroaryl-ester macrocycle 4.29.HB**




Perfluoroaryl carbazole-triazole bis-alkene **4.28.HB** (57.7 mg, 0.06 mmol) was dissolved in anhydrous $CH_2Cl_2$ (10 mL), after which Grubbs' 2$^{nd}$ generation catalyst (5.77 mg, 10% w/w) was added and the mixture allowed to stir at room temperature for 16 h, after which a subsequent portion of catalyst was added and the mixture stirred for a further 16 h. Iterative preparative thin layer chromatography (5% EtOAc – $CH_2Cl_2$, followed by 1% MeOH – $CH_2Cl_2$) afforded **4.29.HB** as a white solid.

Yield: 5.04 mg (9%)

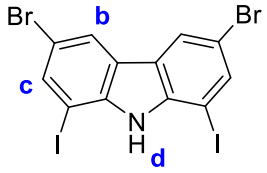
**$^{1}$H-NMR** (400 MHz, $CDCl_3$) $\delta$ = 10.72 (1 H, s, **$H_d$**), 8.49 (2 H, s, **$H_e$**), 8.23 (2 H, d, *J*=1.6 Hz, **$H_c$**), 8.10 (2 H, d, *J*=1.7 Hz, **$H_b$**), 5.90 (2 H, m, **$H_i$**), 4.60 (4 H, m, **$H_f$**), 4.10 (4 H, m, **$H_h$**), 3.82 (4 H, m, **$H_g$**), 1.56 (18 H, s, **$H_a$**).

**$^{19}$F-NMR** (377 MHz, $CDCl_3$) $\delta$ = - 136.49, - 144.60.

**HRMS** (ESI+ve) m/z: 938.29089 ($[M+H]^+$, $C_{46}H_{40}F_8N_7O_6^+$ requires 938.29068).

$^{13}$C NMR data could not be obtained.

**3,6-Dibromo-1,8-diiodocarbazole 4.30** [30]

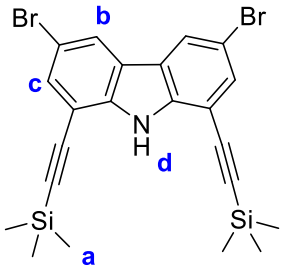



3,6-Dibromocarbazole (500 mg, 1,54 mmol) was suspended in a mixture of $CH_3COOH$ (12.5 mL) and concentrated $H_2SO_4$ (0.25 mL). ICl (0.33 mL, 6.62 mmol, 4.3 eqs) was subsequently added and the reaction mixture heated at 90 °C for 16 h. This was allowed to cool to room temperature, after which water (50 mL) was slowly added. The solids were filtered off, dissolved in a small amount of DMSO and re-precipitated with a saturated $Na_2S_2O_3$ solution (30 mL) to give **4.30** as a white solid.

Yield: 630 mg (71%)

**$^1$H-NMR** (400 MHz, DMSO-$d_6$) $\delta$ = 10.44 (1 H, s, **$H_d$**), 8.49 (2 H, s, **$H_c$**), 7.99 (2 H, s, **$H_b$**).

**TMS-protected 3,6-dibromo-1,8-diethynylcarbazole 4.31** [30]




3,6-Dibromo-1,8-diiodocarbazole (256 mg, 0.44 mmol), $Pd(PPh_3)_2Cl_2$ (6.20 mg, 0.01 mmol, 0.02 eqs) and CuI (3.4 mg, 0.02 mmol, 0.04 eqs) were added to a round-bottomed flask which was subsequently purged with $N_2$. Anhydrous, degassed THF (2 mL) and triethylamine (0.6 mL) were added, followed by TMS acetylene (0.36 mL, 2.62 mmol, 5.9 eqs). The reaction mixture was stirred at room temperature for 16 h, after which the solids were removed by filtration and the filtrate concentrated under reduced pressure. The resulting crude solid was purified by column chromatography (hexane, followed by 10% $CH_2Cl_2$ – hexane) to give **4.32** as a yellow solid.

Yield: 152 mg (66%)

**$^1$H-NMR** (400 MHz, $CDCl_3$) $\delta$ = 8.47 (1 H, s, $\mathbf{H_d}$), 8.00 (2 H, m, $\mathbf{H_c}$), 7.65 (2 H, d, *J*=1.6 Hz, $\mathbf{H_b}$), 0.36 (18 H, s, $\mathbf{H_a}$).

### 5.5. References


1. H. W. Gibson, S. H. Lee, P. T. Engen, P. Lecavalier, J. Sze, Y. X. Shen and M. Bheda, *J. Org. Chem.*, **1993**, 58, 3748–3756.
2. H. Zheng, W. Zhou, J. Lv, X. Yin, Y. Li, H. Liu and Y. Li, *Chem. - Eur. J.*, **2009**, 15, 13253–13262.
3. S. Forshaw, A. J. Matthews, T. J. Brown, L. J. Diorazio, L. Williams and M. Wills, *Org. Lett.*, **2017**, 19, 2789–2792.
4. D. J. Baek, N. MacRitchie, N. G. Anthony, S. P. Mackay, S. Pyne, N. J. Pyne and R. Bittman, *J. Med. Chem.*, **2013**, 56, 9310–9327.
5. C. J. Campbell, D. A. Leigh, I. J. Vitorica-Yrezabal and S. L. Woltering, *Angew. Chem. Int. Ed.*, **2014**, 53, 13771–13774.
6. W.-T. Lee, D. A. Dickie, A. J. Metta-Magaña and J. M. Smith, *Inorg. Chem.*, **2013**, 52, 12842–12846.
7. S. W. Robinson, C. L. Mustoe, N. G. White, A. Brown, A. L. Thompson, P. Kennepohl and P. D. Beer, *J. Am. Chem. Soc.*, **2015**, 137, 499–507.
8. J. Y. C. Lim and P. D. Beer, *Chem. Commun.*, **2015**, 51, 3686–3688.
9. J. Y. C. Lim, I. Marques, A. L. Thompson, K. E. Christensen, V. Félix and P. D. Beer, *J. Am. Chem. Soc.*, **2017**, 139, 3122–3133.
10. J. Y. C. Lim, T. Bunchuay and P. D. Beer, *Chem. - Eur. J.*, **2017**, 23, 4700–4707.
11. F. Friscourt, C. J. Fahrni and G.-J. Boons, *J. Am. Chem. Soc.*, **2012**, 134, 18809–18815.
12. J. Budhathoki-Uprety, P. V. Jena, D. Roxbury and D. A. Heller, *J. Am. Chem. Soc.*, **2014**, 136, 15545–15550.
13. H. Chachignon, N. Scalacci, E. Petricci and D. Castagnolo, *J. Org. Chem.*, **2015**, 80, 5287–5295.
14. K. Yamamoto, T. Bruun, J. Y. Kim, L. Zhang and M. Lautens, *Org. Lett.*, **2016**, 18, 2644–2647.
15. N. Sakai, K. Tamura, K. Shimamura, R. Ikeda and T. Konakahara, *Org. Lett.*, **2012**, 14, 836–839.
16. C. P. Allen, T. Benkovics, A. K. Turek and T. P. Yoon, *J. Am. Chem. Soc.*, **2009**, 131, 12560–12561.
17. A. Lilienkampf, M. Pieroni, B. Wan, Y. Wang, S. G. Franzblau and A. P. Kozikowski, *J. Med. Chem.*, **2010**, 53, 678–688.
18. L. Schweighauser, M. A. Strauss, S. Bellotto and H. A. Wegner, *Angew. Chem. Int. Ed.*, **2015**, 54, 13436–13439.
19. M. D. Lankshear, N. H. Evans, S. R. Bayly and P. D. Beer, *Chem. - Eur. J.*, **2007**, 13, 3861–3870.
20. A. Brown, T. Lang, K. M. Mullen and P. D. Beer, *Org. Biomol. Chem.*, **2017**, 15, 4587–4594.
21. C. J. Serpell, R. Chall, A. L. Thompson and P. D. Beer, *Dalton Trans.*, **2011**, 40, 12052.
22. M. R. Sambrook, P. D. Beer, J. A. Wisner, R. L. Paul and A. R. Cowley, *J. Am. Chem. Soc.*, **2004**, 126, 15364–15365.
23. W. C. Drewe and S. Neidle, *Chem. Commun.*, **2008**, 5295.
24. M. S. Bennington, H. L. C. Feltham, Z. J. Buxton, N. G. White and S. Brooker, *Dalton Trans.*, **2017**, 46, 4696–4710.
25. J. F. W. Keana and S. X. Cai, *J. Org. Chem.*, **1990**, 55, 3640–3647.
26. A. Welle, F. Billard and J. Marchand-Brynaert, *Synthesis*, **2012**, 44, 2249–2254.
27. A. Amira, H. K'tir, M. Berredjem and N.-E. Aouf, *Monatshefte Für Chem. - Chem. Mon.*, **2014**, 145, 509–515.
28. K. Bala and H. C. Hailes, *Synthesis*, **2005**, 3423–3427.
29. L.-M. Jin, X. Xu, H. Lu, X. Cui, L. Wojtas and X. P. Zhang, *Angew. Chem. Int. Ed.*, **2013**, 52, 5309–5313.
30. C. Maeda and N. Yoshioka, *Org. Biomol. Chem.*, **2012**, 10, 5182.